

TALLINN UNIVERSITY OF TECHNOLOGY
DOCTORAL THESIS
63/2019

Stability of Compressed Steel Elements in Fire Conditions: A Probabilistic Approach

ANDREI KERVALIŠVILI



TALLINN UNIVERSITY OF TECHNOLOGY

School of Engineering

Department of Civil Engineering and Architecture

This dissertation was accepted for the defence of the degree 28/11/2019

Supervisor: Associate Professor Ivar Talvik
School of Engineering
Tallinn University of Technology
Tallinn, Estonia

Opponents: Professor František Wald
Department of Steel and Timber Structures
Czech Technical University
Prague, Czech Republic

Professor Mikko Malaska
Tampere University of Technology
Tampere, Finland

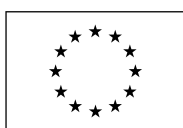
Defence of the thesis: 19/12/2019, Tallinn

Declaration:

Hereby I declare that this doctoral thesis, my original investigation and achievement, submitted for the doctoral degree at Tallinn University of Technology, has not been previously submitted for doctoral or equivalent academic degree.

Andrei Kervališvili

.....
signature



European Union
European Regional
Development Fund



Investing
in your future

Copyright: Andrei Kervališvili, 2019

ISSN 2585-6898 (publication)

ISBN 978-9949-83-514-0 (publication)

ISSN 2585-6901 (PDF)

ISBN 978-9949-83-515-7 (PDF)

TALLINNA TEHNIKAÜLIKOOL
DOKTORITÖÖ
63/2019

Surutud teraselementide stabiilsus tulekahju olukorras: tõenäosuslik käsitus

ANDREI KERVALIŠVILI



Contents

List of publications	7
Abbreviations	8
Symbols	9
1 Introduction	13
1.1 Background	13
1.2 Aim and objectives	14
1.3 Outline of chapters	14
2 State-of-the-art	16
2.1 Overview	16
2.2 Axially loaded column stability – origins of research	16
2.3 The Eurocode design method in fire	17
2.3.1 Thermal analysis	17
2.3.2 The Eurocode method for the buckling problem in fire	18
2.4 Alternative methods for the buckling problem in fire	19
2.5 Probabilistic analysis	22
2.6 Knowledge gap	24
3 Methodology of mechanical analysis	25
3.1 Overview	25
3.2 Numerical modelling	25
3.2.1 Finite element dimensionality	25
3.2.2 Meshing	25
3.2.3 Geometrical model and boundary conditions	27
3.2.4 Loading history	27
3.2.5 Thermal elongation and axial restraint	28
3.2.6 Local buckling	31
3.2.7 Procedure of finite element method	35
3.3 Material models	37
3.3.1 Strain rate and thermal creep	37
3.3.2 Eurocode material model	38
3.3.3 ECCS material model	39
3.3.4 Lie material model	39
3.3.5 Poh material model	41
3.3.6 Comparison of the different material models	42
3.3.7 Thermal properties	44
3.4 Residual stresses	45
3.5 Summary	46
4 Methodology of probabilistic analysis	47
4.1 Overview	47
4.2 Reliability analysis	47
4.3 Target reliability level and probability of fire	50
4.4 Parameter uncertainties	54
4.4.1 Resistance uncertainties	54
4.4.2 Loading uncertainties	54
4.4.3 Temperature related uncertainties	55
4.5 Safety concepts	57

4.6	Sensitivity analysis	59
4.7	Polynomial and spline approximation.....	60
4.8	Summary	61
5	Results of mechanical response	62
5.1	Overview	62
5.2	Numerical program	62
5.3	Dependence of bending stiffness on stress state	62
5.4	Column shape	66
5.5	Stresses	67
5.6	Residual stresses	76
5.7	Buckling factors	76
5.8	Proposed design method – Method C	83
5.9	Example.....	96
5.10	Validation against tests	99
5.11	Summary	102
6	Results of probabilistic analysis	103
6.1	Overview	103
6.2	Results of sensitivity analysis	103
6.3	Temperature distributions	105
6.4	Resistance distributions	106
6.5	Reliability analysis in fire conditions	112
6.5.1	Reliability analysis scheme.....	112
6.5.2	Failure probability in fire conditions	116
6.5.3	Ranking system of failure probability	118
6.5.4	Influence of the fire temperature model on the failure probability	123
6.6	Reliability based design method	126
6.6.1	Derivation of the method	126
6.6.2	Implementation of the method	129
6.6.3	Example.....	131
6.6.4	Validation of the proposed method.....	132
6.6.5	Comparison with the current Eurocode design methodology	133
6.7	Summary	136
7	Conclusions and further research	139
7.1	Conclusions	139
7.2	Further research	140
	Annexes.....	141
	List of figures.....	204
	List of tabels	207
	References	209
	Acknowledgements.....	214
	Abstract.....	215
	Lühikokkuvõte.....	216
	Curriculum vitae.....	217
	Elulookirjeldus.....	218

List of publications

- I A. Kervalishvili and I. Talvik, Alternative approach to buckling of square hollow section steel columns in fire, *Journal of Constructional Steel Research*, 96, 140-150, 2014
- II A. Kervalishvili and I. Talvik, Influence of residual stress on the stability of steel columns at elevated temperatures, *Journal of Civil Engineering and Management*, 23, 292-299, 2015
- III A. Kervalishvili and I. Talvik, Modified procedure for buckling of steel columns at elevated temperatures, *Journal of Constructional Steel Research*, 127, 108-119, 2016
- IV A. Kervalishvili and I. Talvik, Reliability based buckling capacity calculation method of the axially compressed steel column in fire conditions, *Journal of Structural Fire Engineering*, accepted, 2019

Abbreviations

CFD	–	computational fluid dynamics
COV	–	coefficient of variation
EC	–	Eurocode
EC1	–	Eurocode Parametric Fire Curve Method
FEM	–	finite element method
MC	–	Monte-Carlo
MCS	–	Monte-Carlo Simulation
NFSC	–	Natural Fire Safety Concept
RS	–	residual stress
ULS	–	ultimate limit state

Symbols

Latin capital letters

A	– section area	$[\text{mm}^2]$
A_{fi}	– compartment floor area	$[\text{m}^2]$
A_i	– idealized section area	$[\text{mm}^2]$
A_p/V	– section factor	$[\text{m}^{-1}]$
E	– action effect	
$E_{a,20^\circ\text{C}}$	– tangent modulus of steel in elastic range	$[\text{N/mm}^2]$
$E_{a,\theta}$	– tangent modulus of steel in elastic range	$[\text{N/mm}^2]$
El	– elastic bending stiffness	$[\text{Nmm}^2]$
El	– bending stiffness accounting for material property dependence on stress state	$[\text{Nmm}^2]$
El_0	– initial bending stiffness at zero stress state	$[\text{Nmm}^2]$
El_{fi}	– bending stiffness in fire accounting for effect of temperature and stress state on material properties	$[\text{Nmm}^2]$
$El_{fi,0}$	– bending stiffness in fire accounting effect of temperature on material properties (zero stress state)	$[\text{Nmm}^2]$
E_s	– tangent modulus of steel in elastic range	$[\text{N/mm}^2]$
$E_{s,fi}$	– secant modulus	$[\text{N/mm}^2]$
\mathbf{F}	– external force vector	$[\text{N}]$
G	– reliability margin variable	
$G(\mathbf{X})$	– non-linear performance function	
G_k	– characteristic value of permanent load	
H	– compartment height	$[\text{m}]$
\mathbf{K}_t	– tangent stiffness matrix	
L	– length of the column	$[\text{mm}]$
M	– acting bending moment	$[\text{Nmm}]$
M_E	– external bending moment	$[\text{Nmm}]$
M_{int}	– internal bending moment	$[\text{Nmm}]$
$M_{N,R}$	– internal bending moment	$[\text{Nmm}]$
$M_{pl,N,rd}$	– bending moment capacity for certain axial load level	$[\text{Nmm}]$
$M_{pl,N,rd,fi}$	– bending moment capacity in fire situation for a certain axial load level	$[\text{Nmm}]$
N	– acting axial load	$[\text{N}]$
$N_{b,fi,Rd,A}$	– buckling capacity according to the proposed Method A	$[\text{N}]$
$N_{b,fi,Rd,B}$	– buckling capacity according to the proposed Method B	$[\text{N}]$
$N_{b,fi,Rd,EC}$	– buckling capacity calculated using EC methodology	$[\text{N}]$
$N_{b,fi,Rd,FEM}$	– buckling capacity according to the FEM	$[\text{N}]$
$N_{b,fi,Rd,Rel}$	– buckling capacity according to the proposed reliability based method	$[\text{N}]$
$N_{b,fi,\theta,Rd}$	– stability capacity in fire conditions	$[\text{N}]$
N_{Cr}	– elastic critical force in ambient conditions	$[\text{N}]$
N_E	– external axial force	$[\text{N}]$
N_e	– external axial force	$[\text{N}]$
$N_{fi,Cr}$	– elastic critical force in fire conditions	$[\text{N}]$
$N_{fi,\theta,Rd}$	– section capacity in fire conditions	$[\text{N}]$
N_i	– section internal axial force	$[\text{N}]$
N_{int}	– internal axial force	$[\text{N}]$
$N_{pl,Rd}$	– section plastic capacity in ambient conditions	$[\text{N}]$
$N_{pl,rd}$	– section axial load capacity	$[\text{N}]$
$N_{pl,rd,fi}$	– section axial load capacity in fire situation	$[\text{N}]$
$N_{Rd,fi,ANSYS}$	– buckling capacity calculated using ANSYS	$[\text{N}]$
$N_{Rd,fi,beam}$	– buckling capacity calculated using beam finite elements	$[\text{N}]$
$N_{Rd,fi,FEM}$	– buckling capacity calculated using FEM	$[\text{N}]$
$N_{Rd,fi,pln}$	– buckling capacity calculated using polynomial approximation	$[\text{N}]$

$N_{Rd,fi,proc}$	– buckling capacity calculated using composed procedure	[N]
$N_{Rd,fi,shell}$	– buckling capacity calculated using shell finite elements	[N]
$N_{Rd,fi,spl}$	– buckling capacity calculated using spline	[N]
N_{st}	– stability capacity in ambient conditions	[N]
O	– opening factor	[mm ⁻¹]
P	– axial load	[N]
\mathbf{P}	– internal force vector	[N]
$P(.)$	– probability operator	
\mathbf{P}_{i,z^-}	– internal force vector of the element i for the backward perturbation of the degree of freedom z	
\mathbf{P}_{i,z^+}	– internal force vector of the element i for the forward perturbation of the degree of freedom z	
Q_k	– characteristic value of imposed load	[N]
R	– resistance of structure	[N]
$R_{fi,nom}$	– nominal resistance	[N]
S_i	– Sobol sensitivity index	
S_k	– characteristic value of snow load	[N]
U	– standardized random variable	
U_E	– deformation potential energy	[J]
V_{of}	– coefficient of variance for fire load density	
V_E	– work of the external force	[J]
V_i	– first order partial variance	
V_{ij}	– second order partial variance	
W_k	– characteristic value of wind load	[N]
X_i	– random variable	

Latin lower-case letters

a_{EC}	– Eurocode material model parameter	
a_i	– polynomial coefficient	
b	– section width	[mm]
b/t	– plate slenderness or width-to-thickness ratio	
b_{EC}	– Eurocode material model parameter	
b_{th}	– thermal inertia of enclosure	[J/(m ² s ^{0.5} K)]
c_a	– specific heat of steel	[J/kgK]
c_{EC}	– Eurocode material model parameter	
c_{fi}	– multiplier to the nominal resistance in the reliability calculations	
d_p	– thickness of an insulation material	[m]
d_p/λ_p	– thermal resistance parameter of an insulation material	[m ² sK/J]
e	– column top displacement due to bending	
e_0	– initial imperfection	[mm]
$f_{p,\theta}$	– proportionality limit stress at temperature θ	[N/mm ²]
f_y	– yield limit stress at ambient temperature	[N/mm ²]
$f_{y,20^\circ C}$	– yield limit stress at ambient temperature	[N/mm ²]
$f_{y,\theta}$	– yield limit stress at temperature θ	[N/mm ²]
g_i	– Method C model parameters	
h	– section height	[mm]
$k_{E,\theta}$	– reduction factor for elastic modulus of steel	
$k_{p,\theta}$	– reduction factor for proportionality limit stress of steel	
$k_{y,\theta}$	– reduction factor for effective yield strength of steel	
n	– number of all realization	
n_f	– number of realizations for which $G < 0$ (failure)	
p_1	– probability of severe fire	

p_2	– reduction factor depending on the fire brigade type and time between alarm and firemen intervention	
p_3	– reduction factor in case automatic fire detection and/or automatic transmission of the alarm are present	
p_4	– reduction factor for sprinkler system type and accounting for the probability of system failure	
p_f	– probability of failure	
$p_{f,fi}$	– failure probability in fire conditions	
$p_{f,fi,MCS}$	– failure probabilities obtained by performing MCS	
$p_{f,fi,Rel}$	– failure probability calculated using proposed reliability based method	
$p_{f,fi,t}$	– target failure probability in fire	
p_{fire}	– probability of fire emergence	
p_{fl}	– probability of flashover	
p_i, q_i	– model parameters for the proposed methods	
p_{ign}	– probability of fire ignition	
p_t	– target failure probability	
q_f	– fire load density	[MJ/m ²]
$q_{f,d}$	– design fire load density	[MJ/m ²]
$q_{f,k}$	– 80% fractile of the characteristic value of the fire load density	[MJ/m ²]
t	– plate thickness	[mm]
t_1	– wall thickness	[mm]
t_2	– flange thickness	[mm]
u	– displacement vector	
u_L	– uncertainty factor for loading model	
u_R	– uncertainty factor for resistance model	
w_0	– maximum initial imperfection	[mm]
$y_{0,mid}$	– maximum initial imperfection at the midheight of the element	[mm]
$y_{1,mid}$	– maximum displacement at the midheight of the element	[mm]
$y_{tot,mid}$	– total lateral displacement	[mm]
Δu^k	– incremental displacement vector	[mm]

Greek letters

μ_E	– mean action effect value
μ_G	– mean value of reliability margin G
μ_R	– mean resistance values
μ_X	– mean value of the random variable X
α	– factor describing relation between variable and permanent loads
α_1	– Method C model parameter
α_2	– Method C model parameter
β	– reliability index
β_1	– Method C model parameter
β_2	– Method C model parameter
$\beta_{f,fi,t}$	– reliability index in fire
$\beta_{f,fi,t}$	– target reliability index in fire
δ_{of}	– fire probability factor
$\Delta L/L$	– thermal elongation of steel
δ_n	– factor accounting for firefighting measures
δ_{q1}	– factor accounting for influence of compartment size
δ_{q2}	– factor accounting for type of occupancy
ε	– strain
$\varepsilon_1, \varepsilon_2$	– strains at section outermost points
ε_{fi}	– strain
$\varepsilon_{p,\theta}$	– proportionality limit strain at temperature θ

$\varepsilon_{y,\theta}$	–	yield limit strain at temperature θ	
η	–	Eurocode buckling model factor	
θ	–	temperature	[°C]
$\theta_{failure}$	–	failure temperature	[°C]
θ_{FEM}	–	calculated critical temperature	[°C]
θ_{nom}	–	nominal temperature of steel section	[°C]
θ_{test}	–	average temperature at failure according to test result	[°C]
$\lambda_{20^\circ C}$	–	slenderness	
λ_a	–	thermal conductivity of steel	[J/(msK)]
λ_p	–	thermal conductivity of an insulation material	[J/(msK)]
$\mu(\theta)$	–	calculated mean temperature of steel section	[°C]
σ	–	stress	[N/mm ²]
$\sigma_{0.2}$	–	material 0.2% proof stress	[N/mm ²]
σ_1	–	stress at section point 1	[N/mm ²]
σ_2	–	stress at section point 2	[N/mm ²]
σ_c	–	stress at section centroid	[N/mm ²]
σ_{cr}	–	the first buckling mode stress	[N/mm ²]
σ_E	–	standard deviation for action effect	
σ_{fi}	–	stress	[N/mm ²]
σ_G	–	standard deviation the reliability margin G	
σ_R	–	standard deviation for resistance	
σ_X	–	standard deviation of the random variable X	
Y_i	–	Method C model parameteres	
Φ^{-1}	–	inverse of the cumulative standard normal distribution	
χ	–	section curvature	
χ_{base}	–	buckling factor for a base group	
χ_{FEM}	–	buckling factor calculated using FEM	
χ_{fi}	–	buckling factor in fire conditions	
χ_{fi}	–	buckling factor in fire conditions	
$\chi_{fi,noRS}$	–	buckling factor of model without residual stress	
$\chi_{fi,RS}$	–	buckling factor of model with residual stress	
$\chi_{gr.mean}$	–	average buckling factor for a group	
χ_i	–	individual buckling factor	
χ_{Rel}	–	factor of the proposed reliability based design method	
χ_{test}	–	buckling factor according to the test result	
ψ_1	–	combination factor according to EN 1990	

1 Introduction

1.1 Background

Considerable effort of the ongoing research in structural engineering is dedicated to fire conditions. Various aspects of the performance of structures in fire are investigated: material behaviour, global structural response, fire modelling, fire probability and risk management etc.

The integrity of columns in a frame is vital considering progressive collapse – probability of the progressive collapse is higher in case of a column failure, compared to the failure of some other frame component.

Stability of a steel column is a common problem in structural design and buckling of axially loaded steel column is a substantial subgroup within the general column stability issues. Solution for an axially loaded column is often an important integrated part of some more general stability task. Axially loaded column in ambient temperature conditions has been extensively studied, both by analysis and experimentally. The respective current design methods show good correlation with test data. The situation is different in case of temperatures above 200°C i.e. in fire conditions. This is mainly due to the higher complexity, generated by the more complex stress-strain relationship of steel at elevated temperatures. In addition to that, the amount of experimental data is considerably limited compared to the data available for normal temperature conditions. At elevated temperatures the steel column buckling can be effectively solved using numerical methods.

An essential objective of engineering design is to produce a structural system that satisfies the accepted safety level, i.e. loads and actions do not exceed the resistance of the system. Obviously most of the load and strength parameters are random to some extent. In common code-based design procedures the uncertainties in the loads and structural response are taken into consideration by applying safety factors. Safety factors are easy to implement in prescriptive fire safety design, but the analysis does not always give specific information about the safety and risk level of the system. The mismatching of target safety levels by the semi-probabilistic approach of code-based framework has been reported for normal temperature conditions. It can be assumed that those tendencies are amplified in fire conditions.

Probabilistic response of structural elements in fire conditions is more complex compared to normal temperature conditions. Temperature of an element in fire conditions is defined by a number of parameters each having specific stochastic characteristic. As a result, thermal configurations having similar nominal temperature values can generate very different temperature distributions, which will lead to very different failure probability of a structural element.

Performance-based design is becoming more important in engineering design practice and has gained approval in fire safety design. Reliability analysis is the common format for quantifying the safety level in relation to the established target values. Benefiting from advanced numerical calculations and modelling of fire impact on structural behaviour, it is assumed in the performance-based design approach that the safety level can be explicitly determined in order to evaluate the adequacy of the design solution. The demand is building up for a practical method allowing to estimate the failure probability explicitly and without the rigid attachment to a certain safety framework.

1.2 Aim and objectives

The principal aim of this work is to study the impact of temperature distribution on the probabilistic response of a steel column in fire conditions and propose a user friendly practical method for estimating the failure probability.

To accomplish this aim the following objectives must be achieved:

1. Computationally efficient and sufficiently accurate model for prediction of buckling capacity is developed.
2. Large number of thermal configurations is analysed in order to generate temperature distributions database.
3. Sensitivity analysis is performed to analyse the influence of input variables on the stochastic performance of column buckling in fire.
4. Comprehensive reliability analysis of the axially compressed steel column in fire is performed for various slenderness values, steel grades and section types in order to produce database of failure probabilities.

The case of axial compression is used to demonstrate the methodology, which can be later adopted for other resistance problems of structural steel in fire conditions.

1.3 Outline of chapters

This work consists of 7 chapters:

Chapter 1: Introduction

Chapter 2: State-of-the art

Origins of the research dedicated to the buckling of columns are reported. The models of current Eurocode method are described for normal and elevated temperature conditions. Available alternative methods for the solution of the buckling problem in fire are presented. Current concepts of structural reliability are addressed and knowledge gaps are outlined.

Chapter 3: Methodology of mechanical analysis

Methodology of the mechanical analysis of steel column in fire conditions is presented in this section. Numerical modelling is addressed in the first place. Non-linear FEM procedure composed for the buckling analysis is described. Different material models of carbon steel in variable temperature conditions are investigated. Residual stresses are addressed.

Chapter 4: Methodology of probabilistic analysis

The aspects related to the reliability analysis are presented. Methodology of reliability analysis is described. Issues of target reliability levels and fire probability are discussed. Parameter uncertainties for resistance, loading and thermal variables are described. Existing structural safety concepts are described. Methodology of the sensitivity analysis is presented.

Chapter 5: Results of mechanical response

Results of the mechanical response of steel column in fire are presented. Numerical program is introduced and results in the form of buckling factors for various steel grades, different temperatures and section types are reported. Dependence of bending stiffness on temperature and stress-state is analysed. Distribution of normal stresses at failure for different temperatures and slenderness values is reported. The impact of initial residual stresses on the buckling capacity is demonstrated. Based on the results of numerical

simulations an original computationally efficient method for prediction of buckling capacity is proposed and validated.

Chapter 6: Results of probabilistic response

Extensive results of the probabilistic analysis of steel column in fire are reported. The impact of the variability of various input parameters on the stochastic performance is estimated using sensitivity analysis. A large set of temperature distributions is presented depending on the parameters like fire load, fire compartment geometry, passive protection solution etc. Stochastic thermal impact on the distribution of resistance function is demonstrated. Failure probabilities are reported for various steel grades, mean temperatures and slenderness values. Based on the results of the reliability analysis, method for failure probability prediction is proposed. The proposed method is validated and compared with the current Eurocode methodology. Implementation of the method is demonstrated by an example.

Chapter 7: Conclusions and further research

Results of the research are summarized. Proposition for the future research is made.

2 State-of-the-art

2.1 Overview

At first origins of the research dedicated to the buckling of columns are reported in this section. Then the models of current Eurocode method are described for normal and elevated temperature conditions. Available alternative methods for the solution of the buckling problem in fire are presented. Current concepts of structural reliability are addressed and knowledge gaps are outlined.

2.2 Axially loaded column stability – origins of research

Historical perspective of stability of steel columns in elevated temperature conditions cannot be separated from the research dedicated to column stability in general. As an introduction it is appropriate to recall shortly some historical moments of the research dedicated to the stability of axially compressed elements.

First achievements in the history of stability research have been relatively well documented. Hereby, based on overviews in [1], [2] and [3], only some most characteristic aspects are pointed out.

As generally accepted, the history of the buckling problem of compressed elements started in 1744, when Leonard Euler published his book on variational calculus. In the appendix of the book Euler presented his column formula, which is today known as the Euler's critical load formula. The initial form of the formula is given as equation (2-1):

$$P_{Euler} = \frac{\pi^2 E k^2}{L} \quad (2-1)$$

According to Euler, in the Equation (2-1) E stands for material strength related property and k stands for geometrical property of a column. E and k were both assumed to be defined experimentally. Euler's formula was widely criticized, because it did not perform well when applied in design practice to structural materials of its time: timber, iron, masonry. With the introduction of structural steel in construction practice (around 1850) the attitude to Euler's formula changed. It is especially easy to understand the initial criticism of the formula and the change of the attitude almost 100 years later – technological progress of that time had created more advanced material, which was closer to the theoretical ideal (elastic material).

The second turning point in the history of the column buckling research emerged in the year 1889 – first inelastic buckling formula was presented. In 1889 Armand Gabriel Considere published his work, where he reported test results on column buckling. He had noticed that stresses on the concave side of the deformed column increase with tangent modulus E_t , while on the opposite side the stresses decrease with elastic modulus E . Considere demonstrated, why Euler's equation (2-1) failed to adequately predict buckling in case of inelastic material. Considere also stated that the effective deformation modulus should be used, which must lie somewhere between E and E_t values. In the same year Freidreich Engesser published his work, where he suggested that Euler's formula must be modified – elastic modulus E should be replaced with tangent modulus E_t . In 1895 he once again presented his theory, which indicates that he was unaware of the Considere's work. Three month after that, Felix Jasinski has brought Considere's work to the attention of Engesser. One month later, Engesser has

acknowledged inaccuracy of his tangent modulus theory and presented updated version of his own – reduced modulus theory, which is today also referred to as Considere-Engesser theory. Engesser has pointed out, that reduced modulus was also dependent on section shape. The reduced modulus theory was presented again in 1908 and 1910 by Theodore von Karman. It is generally admitted, that von Karman produced his theory independently of the earlier researchers. Von Karman derived reduced modulus E_r for rectangular sections and idealized H-section. He also included influence of load eccentricity in the model.

Researchers were not completely satisfied with the reduced modulus theory – laboratory test showed that columns buckled and failed at or slightly above the tangent modulus load. Shanley referred to this paradox [4] and later solved it [5]. He also found that lateral deflections of an axially compressed column started very close to the load predicted by the tangent modulus theory, but additional load was carried until unloading started and the capacity predicted by the reduced modulus theory could never be reached.

In the current Eurocode system, the model for buckling capacity prediction in normal temperature conditions is based on the Ayrton & Perry approach, which assumes that resistance of a column with imperfection should be calculated regarding the first-yield criterion for the most compressed section fibre [6]. This approach was validated by experiments performed by Robertson in 1925 [7]. Ayrton & Perry – Robertson formula was adopted as the basis for the Eurocode buckling curves, which were introduced in 1970-ies as a result of extensive theoretical [8] and experimental [9] research programs. The reliability of the proposed model was validated by Strating and Vos implementing the Monte-Carlo method [10].

Until today researchers have continued further developing the analysis methods in order to improve models, which could provide sufficient accuracy with reasonable computational effort for practical design applications. A number of those works are referenced in the following chapters according to the context.

2.3 The Eurocode design method in fire

Present work is related to the framework of the Eurocode design codes: material models are adopted from Eurocode, thermal analysis is based on the corresponding Eurocode documents, buckling design method of Eurocode is discussed.

2.3.1 Thermal analysis

The dynamics of a real fire is very complex phenomenon and depends on a large number of parameters. The actual fire curve is very case-sensitive. A real fire in a worst-case scenario can be decomposed into five stages: ignition and smouldering, pre-flashover, flashover, post-flashover, decreasing phase [11]. Flashover is the rapid transition between localized fire and full scale fire, when the full compartment area is involved in fire. Depending whether flashover occurs, the real fires are sub-divided into two groups: local fires and post-flashover fires. Although post-flashover fires in general represent a worst-case scenario, this should not downsize the importance and the potential danger of the localized fires. The matter of modelling the evolution of temperature in fire has been in research focus for years and significant progress has been achieved and following method types have been proposed: methods based on empirical correlations (nominal and parameter fire curves [12], Lie correlations [13], Swedish curves [14]); zone models

(one-zone model [15], two-zone model [16], combined zone models [16]); computational fluid dynamics based methods (Fire Dynamics Simulator [17]).

Eurocode Parametric Fire Curve Method (EC1 method; [12]) is one of the available methods included in the Eurocode documents. Schleich et al [18] have analysed the performance of this method for the temperature evolution and demonstrated that the correlation coefficient for the EC1 method and test results to be 0.83. The method is described in Annex A1. The method has a number of limitations. It is valid in a certain range of enclosure thermal inertia b_{th} and opening factor O . The limits for those parameters correlate well with the limits for practical application. There are also strict limitations of the compartment geometry: compartment floor area $A_{fi} \leq 500 \text{ m}^2$ and compartment height $H \leq 4.0 \text{ m}$. These limitations have more serious impact on the practical applicability. In order to analyse fire gas temperatures for a wider set of cases, more advanced methods must be implemented, for example zone models or CFD based methods. Nowadays, an efficient tool to perform fire temperature analysis of the moderate complexity is OZone software package, based on the combined zone method. The tool is widely used in practice and research. The theory behind the OZone software and the zone methods can be found in [16]. Comparison between the test data and the software output can be found in [16] and [19]. OZone software has built-in possibility for the definition of the design fire load density in accordance with Annex E of the EN 1991-1-2. For both methods (EC1 and OZone) temperature evolution in a steel section is calculated in the similar way – the method of EN 1993-1-2 [20] is implemented as described in Annex A2.

2.3.2 The Eurocode method for the buckling problem in fire

The current Eurocode method for checking buckling capacity of columns in fire conditions is based on the extensive numerical investigation, performed by Talamona et al. [21] and experimental results [22]. Several authors like Knobloch et al. [23], Vila Real et al. [24], Toh et al. [25], Somaini et al. [26], Kervalisvili and Talvik [27] and [28], have referred to certain discrepancy between the present EN 1993-1-2 [20] design method and the results of experiments and numerical models for buckling resistance of steel columns in fire and proposed alternative procedures, which in general tend to be complex, not inherent to the common standard based approach and restricted to certain section type or parameter ranges.

EN 1993-1-2 [20] design method for axially compressed columns in elevated temperature conditions is in principle a modified version of the method for analogous problem in normal temperature conditions. It seems logical to start with the description of the design method in normal temperature conditions.

EN 1993-1-2 uses the Ayrton-Perry approach for buckling capacity estimation of axially compressed elements. It is generally accepted that Ayrton-Perry approach is one of the possibilities, which has been implemented in Eurocode. Ayrton-Perry approach itself is based on the analysis of an axially loaded column with initial curvature. Different formulations for this problem are available. In this document, formulation by the potential energy variation is used as was proposed by Timoshenko [29]. The initial shape of the beam-column element is presented in the form of a sinusoidal wave (2-2), where $y_{0,mid}$ is the maximum initial imperfection at the midheight of the element and is defined as a fraction of the length. The additional displacement due to compression of the element is defined as (2-3), where $y_{1,mid}$ is the maximum displacement at the midheight of the element. P is the axial load, EI is the elastic bending stiffness, L is the initial length of the column. The deformation potential energy U_E is defined in (2-4).

The column top displacement e due to bending is (2-5). The potential energy decrease due to the work of the external force V_E can be defined using (2-6). According to the potential energy variation principle regarding minor deviation from the equilibrium state the first variation of the total energy must be equal to zero (2-7). Then the column deformation can be defined as (2-8). The limit load can be derived from the second variation (2-9) of the total potential energy, reaching a well-known solution (2-10).

According to Ayrton-Perry approach, an initially curved column becomes unstable, if maximum compression stresses on the concave side in the mid-section of the column approach the yield limit value (2-11). Solution of (2-11) can be presented in the form of buckling factor (2-12) ... (2-15). Solution of this structure is used in Eurocode 3, with the following modification. Factor η formulation (2-14) is replaced with (2-16), which serves as a calibration parameter against test results. In case of elevated temperature, the following modifications have been introduced: formula of factor η (2-16) is replaced with (2-17) and relative slenderness (2-15) is replaced by (2-16). These modifications are based on the report by Schleich et al. [30]. The method of EN 1993-1-2 is presented in (2-18) ... (2-21), where notation corresponds to EN 1993-1-2. The matter of validation against the test results is addressed in the corresponding section 5.10. Nevertheless, the following aspects are worth to be mentioned here. Tests were performed in various time period from 1979 to 1994. In the report [30] data concerning material behaviour (stress-strain relationship) at different temperatures is not described in detail, which is essential if good correlation between numerical simulation and test results is to be expected. 35 test of total 38 axially loaded column tests correspond to the case of weak axis buckling. Tests were performed for H-shaped (IPE, HEA, HEB) hot rolled sections, which is consistent with the scope of the report. Despite of the limited scope of [30], the EN 1993-1-2 design model for prediction of axially loaded column buckling capacity in case of fire is still based on the model proposed in the report and is applied to all basic section types and buckling axes.

2.4 Alternative methods for the buckling problem in fire

One of the objectives of this work is to discuss the EN 1993-1-2 design method for axially compressed steel columns in fire conditions. Accordingly the short overview of the available alternative design methods for this problem is presented in this section.

Several works have proposed procedures for the buckling capacity prediction. Toh et al [25] have proposed the version of Rankine solution adopted for the case of fire conditions. The method has very simple analytical form, the performance of the method is not very different from the EN 1993-1-2 model. Neves et al [31] and Wang et al [32] have proposed design methods for the restrained steels column in fire. The methods predict the failure temperature of a restrained column.

Somaini [26] have proposed Von Karman type method for steel column stability in fire conditions. This method is presented here in detail, because buckling design method proposed in this work is also based on the von Karman solution. Von Karman type method deals with the equilibrium between external bending moment and internal bending moment in the critical section [33]. Consider an initially curved column in Figure 2.1. Initial imperfect shape of the column is approximated by sinusoidal half-wave, with the amplitude $y_{0.mid}$. With increasing axial load P , lateral displacement takes place and axial load eccentricity increases from $y_{0.mid}$ to $y_{tot.mid} = y_{0.mid} + y_{1.mid}$, which is obviously accompanied by the increase of external bending moment (2-22). The column remains

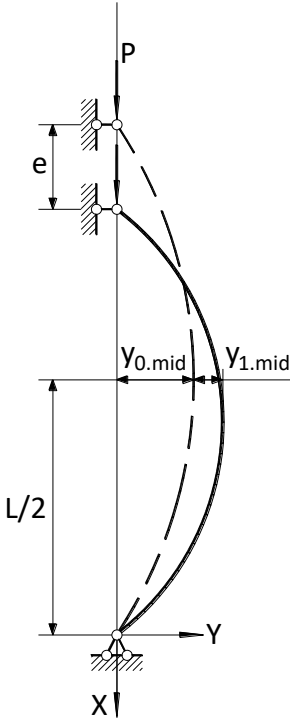


Figure 2.1: Column with imperfection

$$y_0 = y_{0.mid} \sin\left(\frac{\pi x}{L}\right) \quad (2-2)$$

$$y_1 = y_{1.mid} \sin\left(\frac{\pi x}{L}\right) \quad (2-3)$$

$$U_E = \int_0^L \frac{EI}{2} \left(\frac{d^2 y_1}{dx^2} \right)^2 dx = \frac{EI\pi^4}{4L^3} y_1^2 \quad (2-4)$$

$$\begin{aligned} e &= \int_0^L \left(\frac{d(y_0 + y_1)}{dx} \right)^2 dx \\ &\quad - \int_0^L \left(\frac{dy_0}{dx} \right)^2 dx \\ &= \frac{\pi^2}{2L} (y_1^2 + 2y_0 y_1) \end{aligned} \quad (2-5)$$

$$V_E = -\frac{1}{2} eP = -P \frac{\pi^2}{4L} (y_1^2 + 2y_0 y_1) \quad (2-6)$$

$$\Pi = U_E + V_E \rightarrow \delta \Pi = \delta U_E + \delta V_E = 0 \quad (2-7)$$

$$\begin{aligned} \delta U_E &= \frac{EI\pi^4}{2L^3} y_1 \quad \delta V_E = -P \frac{\pi^2}{2L} (y_1 + y_0) \\ &\rightarrow y_1 = \frac{EI\pi^2}{L^2 P} y_0 - 1 \end{aligned} \quad (2-8)$$

$$\delta^2 \Pi = \delta^2 U_E + \delta^2 V_E = 0 \quad (2-9)$$

$$\begin{aligned} \delta^2 U_E &= \frac{EI\pi^4}{2L^3} \quad \delta^2 V_E = -P \frac{\pi^2}{2L} \rightarrow P_{cr} \\ &= \frac{EI\pi^2}{L^2} \end{aligned} \quad (2-10)$$

$$\frac{P}{A} + \frac{P(y_1 + y_0)}{W_{el}} = f_y \quad (2-11)$$

$$\chi = \frac{1}{\Phi + \sqrt{\Phi^2 - \bar{\lambda}^2}} \quad (2-12)$$

$$\Phi = \frac{1}{2} (1 + \eta + \bar{\lambda}^2) \quad (2-13)$$

$$\eta = \frac{Aa_0}{W_e} \quad (2-14)$$

$$\bar{\lambda} = \sqrt{\frac{Af_y}{P_{cr}}} \quad (2-15)$$

$$\eta = \alpha(\bar{\lambda} - 0.2) \quad (2-16)$$

$$\eta = 0.65 \sqrt{235/f_y} \quad (2-17)$$

$$N_{b.fi.\theta.Rd} = \chi_{fi} A k_{y,\theta} f_y \quad (2-18)$$

$$\chi_{fi} = \frac{1}{\Phi_{\theta} + \sqrt{\Phi_{\theta}^2 - \bar{\lambda}_{\theta}^2}} \quad (2-19) \quad \Phi_{\theta} = \frac{1}{2} \left(1 + 0.65 \sqrt{235/f_y + \bar{\lambda}_{\theta}^2} \right) \quad (2-20)$$

$$\bar{\lambda}_{\theta} = \bar{\lambda} \sqrt{k_{y,\theta}/k_{E,\theta}} \quad (2-21)$$

$$M_E = N_E y_{tot,mid} \quad (2-22)$$

$$\frac{dM_E}{dy_{tot,mid}} \leq \frac{dM_{N,R}}{dy_{tot,mid}} \quad (2-23)$$

$$\chi = y_1 \left(\frac{\pi}{L} \right)^2 \quad (2-24)$$

$$\chi = \frac{\varepsilon_2 - \varepsilon_1}{h} \quad (2-25)$$

stable until the increase in external bending moment M_E is balanced by the corresponding increase in the inner bending moment $M_{N,R}$ and axial load N_E equals to internal axial force N_{int} . Mathematical formulation of the stability criteria could be presented in the form of (2-23). Internal bending moment M_{int} is in general a function of internal axial force N_{int} . M_{int} can be linked to $y_{tot,mid}$ via the section curvature χ . For column under consideration, middle section curvature and maximum lateral deflection are linked using equations (2-24) and (2-25), where ε_1 and ε_2 are strains at section outermost points and h is section height. If the strains are known, section inner forces can be easily calculated in elastic state, but this is not the case for steel with temperature higher than 100°C. Using equations (2-22), (2-23), (2-24) and having dependence of P_{int} and M_{int} on ε_1 and ε_2 one can calculate column buckling load. In case of steel in fire conditions the analytical model for P_{int} and M_{int} is not easy to compose, because of complicated nature of steel material law. Von-Karman method can be effectively used together with numerical methods implementing section discretization, but this approach although quite elegant is not much more effective than finite element modelling.

Somai's solution is actually a solution for the problem described above. He proposes to use approximation of the moment-curvature relationship. Internal bending moment as a function of section curvature χ for a given axial force N_E is approximated by (2-26). Tangent modulus for I-section strong axis and hollow sections is calculated using (2-30) and for I-section weak axis using (2-31).

$$M_{N,R} = M_{N,el} - a + \frac{b}{c} \sqrt{c^2 - (\chi_y - \chi)^2} \quad (2-26)$$

$$a = \frac{(M_{N,pl} - M_{N,el})^2}{(\chi_y - \chi_p) T_K I - 2(M_{N,pl} - M_{N,el})} \quad (2-27)$$

$$b = \sqrt{a(\chi_y - \chi_p) T_K I + a^2} \quad (2-28)$$

$$c = \sqrt{(\chi_y - \chi_p) \left(\chi_y - \chi_p + \frac{a}{T_K I} \right)} \quad (2-29)$$

$$T_{K,y} = \frac{2T_{\theta}E_{\theta}}{T_{\theta} + E_{\theta}} \quad (2-30)$$

$$T_{K,z} = \frac{4T_{\theta}E_{\theta}}{(\sqrt{T_{\theta}} + \sqrt{E_{\theta}})^2} \quad (2-31)$$

$$\chi_p = \frac{M_{N,el}}{T_k I} \quad (2-32)$$

$$M_{N,el} = W_{el} f_{p,\theta} \left(1 - \frac{N_E}{A f_{p,\theta}} \right) \geq 0 \quad (2-33)$$

$$\chi_y = \frac{M_{N,pl} - M_{N,el}}{S_k I} \frac{W_{pl}}{W_{el}} \geq \frac{3M_{N,pl} - M_{N,el}}{T_k I} \quad (2-34)$$

$$S_{\theta} = \frac{f_{y,\theta} - \sigma_N}{\varepsilon_{y,\theta} - \varepsilon_N} \leq \frac{f_{y,\theta} - f_{p,\theta}}{\varepsilon_{y,\theta} - \varepsilon_{p,\theta}} \quad (2-35)$$

External acting bending moment can be calculated using (2-36). Having expressions for external (2-36) and interior (2-26) bending moments for the given axial load level, two curves can be constructed as shown in Figure 2.2. Column equilibrium is obtained in the intersection point of two curves. M_E is a linear function in relation to curvature χ and axial force N_E , which is obviously not the case for $M_{N,R}$. As a result, a number of calculation cycles is needed (2-26) ... (2-35) to construct $M_{N,R}$ curve for a single given axial load level N_E . Buckling load capacity corresponds to the case where M_E curve is tangential to $M_{N,R}$ curve.

$$M_E = \left(e_0 + \chi \frac{L^2}{\pi^2} \right) N_E \quad (2-36)$$

Performance of the method against FEM models is presented in Figure 2.3 in the form of buckling factors comparison for different slenderness $\lambda_{20^\circ C}$ (5-1) values. Performance of the method against FEM is very good. The method can be implemented for the design of columns under combined compression and bending. The method has one disadvantage – its relative complexity. Considerable number of calculations is needed to calculate the buckling capacity making not a very effective to a non-linear FEM.

2.5 Probabilistic analysis

The main aim of structural design is to provide certain level of safety accounting for inherent uncertainties of structural system and actions with reasonable expenses. Currently available design approaches can be allocated into groups as follows: fully-deterministic, semi-probabilistic and fully-probabilistic. The approaches differ in the definition of safety concept. The deterministic approach implements global safety factor, which is often established based on experience of trial and error. A semi-probabilistic approach introduces partial safety factors concept. The design process remains deterministic, while the variability of the resistance and loading functions is accounted by calibration of corresponding safety factors with the aim to match the target failure probability. The fully-probabilistic approach imposes target failure probability for the performance function $R - E$, where R is the resistance function and E is the action function. The variability of all the variables and the model uncertainties are accounted

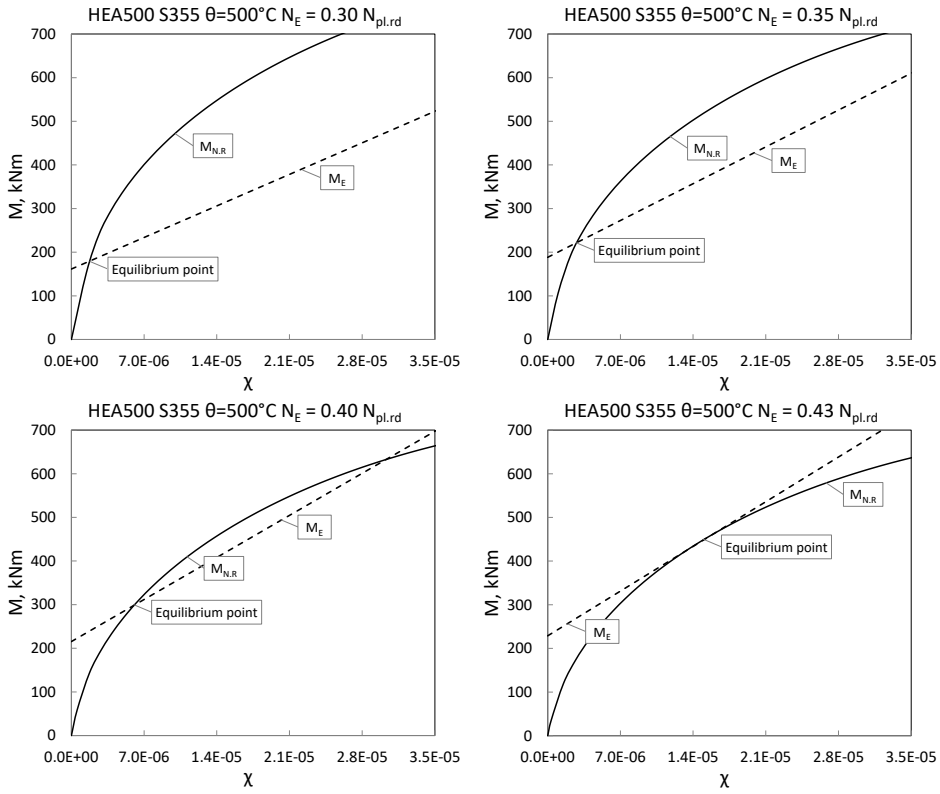


Figure 2.2: Graphical representation of the Somaini's methods

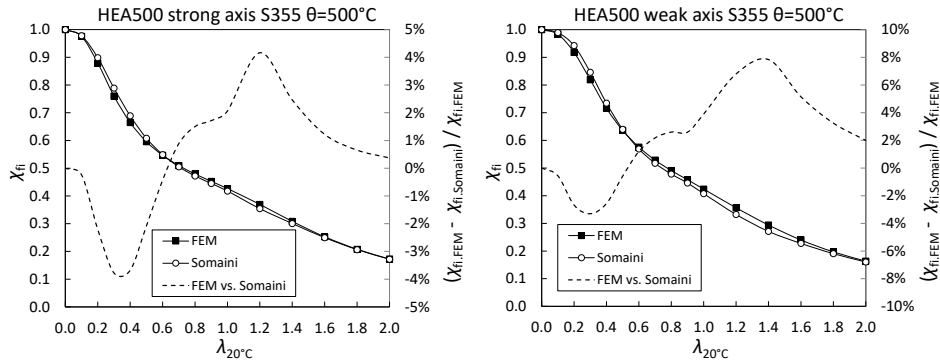


Figure 2.3: Performance of Somaini method vs. FEM

directly demanding considerable amount of specific probability calculations.

The current Eurocode framework is semi-probabilistic in its nature applying target failure probability in the form of target reliability index as stated in EN 1990 [34]. The semi-probabilistic approach has several limitations, which are therefore also valid for the present Eurocode system. In general the semi-probabilistic approach is expected to provide sufficient safety, but does not present safety level in explicit form. The approach is indifferent to the problem type (section capacity, global or local buckling etc.) and the composition of load combination (e.g. the fraction of imposed load in total load). For structural design in fire conditions an important stochastic characteristic is added – the probability of fire. Temperature itself is a stochastic property of fire

action, which has complex impact on resistance function. It is assumed, that for structural performance in fire conditions the focus should be shifted in the direction of fully-probabilistic approach.

Reliability analysis has been applied for a large number of problems in structural design: timber structures [35], reinforced and prestressed concrete structures [36], steel structures [37], fatigue [38] and stainless steel structures [39] to name only a few. Researchers have reported certain inconsistencies in the reliability estimations for structures designed according to Eurocode in ultimate limit state [37], [40] and in serviceability limit state [41], where they revealed that actual reliability indices calculated for certain steel and reinforced concrete elements do not match the stated target value.

Reliability analysis of structures in fire conditions has been applied by a number of researchers. One of the earliest reports on the subject was presented by Magnusson and Pettersson back in 1981 [42]. Later the issue of reliability has also received relevant attention in some fundamental works related to the performance of steel structures in fire and Natural Fire Safety Concept (NFSC) in general [18]. Nowadays reliability of structures in fire is being actively investigated. Guo has proposed framework to quantify the structural reliability level under fire in [43] and [44]. Steel columns in fire conditions with the emphasis on the intumescent coatings was investigated by Zhang in [45]. Heidari et al in [46] have performed probabilistic study of a reinforced concrete slab in fire. Van Coile has presented a framework for reliability-based decision making for concrete elements in fire conditions in [47]. Devaney in [48] has dealt with the development of software for reliability based design of steel structures in fire. Probability of fire plays significant role in the whole fire safety concept. A number of works has been published in recent years (e.g. [47], [49], [50]) dedicated to reliability of structures in fire, where authors have raised discussion concerning the approach to fire probability in general and in the context of the NFSC specifically, referring to the need for further studies due to the substantial influence of fire probability on safety evaluation. Criteria of structural safety are expressed as target values of reliability, which are commonly related to the structural system as a whole. As stated in [51], although probabilistic analysis is performed in most cases on the member level, the same target value as for the system may be used, provided that the particular member is dominant in the system failure. It is a common approach to study reliability in fire conditions on the member level (e.g. [46], [43], [52]).

2.6 Knowledge gap

Publications dedicated to the reliability of structures in fire conditions are usually built around a limited number of thermal configurations, which is explained by the computational challenges associated with the mechanical response of structures in fire. There is no sufficient data available to evaluate safety level for an arbitrary fire design case and check target reliability matching. Certain inconsistencies in the target failure probability matching by Eurocode methodology were reported for the normal temperature conditions. Due to uncertainties in thermal models, the mentioned inconsistencies are not expected to decrease in fire conditions. There is no user friendly procedure available for explicit estimation of failure probability of steel columns in fire conditions for practical applications. For the development of a user friendly method for the failure probability calculation comprehensive reliability calculations need to be performed. Consequently, computationally efficient and sufficiently accurate design method for buckling needs to be developed.

3 Methodology of mechanical analysis

3.1 Overview

Mechanical analysis is an important part of the reliability analysis. The computational demand of the mechanical response model defines the computational demand of the reliability analysis procedure. Consequently, computationally efficient and sufficiently accurate mechanical model is needed for the comprehensive reliability analysis program.

Methodology of the mechanical analysis of steel column in fire conditions is presented in this section. Numerical modelling is addressed in the first place. Non-linear FEM procedure composed for the buckling analysis is described. Different material models of carbon steel in variable temperature conditions are investigated. Residual stresses are addressed.

3.2 Numerical modelling

Finite element method (FEM) is widely used in this work, however, it is used purely as a tool and this research is not dedicated to FEM itself. Consequently, theory behind FEM is not included in this work and only major aspects specific to the problem are described. Non-linear FEM procedure is composed, which allows to implement different material models and automatically execute calculations for wide range of parameters.

3.2.1 Finite element dimensionality

The choice of element type for modelling is very important. It is agreed that generally the higher element dimensionality guarantees higher precision. The higher element dimensionality assumes thinner volume discretization, which results in higher computational costs. For steel profiles and axially compressed column buckling problem utilization of volumetric finite elements is excessive and is not practical. For the problem under consideration the choice usually lies between shell elements and beam elements. Initial calculations were performed using ANSYS finite element software package implementing beam element "BEAM188". 200 cases were randomly selected for validation against more accurate models composed of shell elements (element type "SHELL181"). Results of the statistical analysis for the comparative factor $N_{Rd,fi.beam}/N_{Rd,fi.shell}$ are presented in Table 3-1, where $N_{Rd,fi.beam}$ is the buckling capacity calculated using beam finite elements and $N_{Rd,fi.shell}$ is the buckling capacity calculated using shell finite elements. Results indicate high correlation between the models of different finite elements. The biggest discrepancies were observed for the cases of small slenderness and are associated with the local buckling in the support zone of the shell models. Based on the validation results it was concluded that utilization of beam finite elements is justified for the problem under consideration.

3.2.2 Meshing

Meshing is another important aspect of finite element modelling. Quality of meshing has considerable influence on the precision and effectiveness. Beam meshing is a fairly simple procedure. Due to non-linear stress-strain relationship for steel in elevated temperature, section meshing is needed to define section stiffness and inner forces.

Table 3-1: Descriptive statistics for beam vs. shell models

Parameter	Value
Mean	1.00042
Standard Error	0.00021
Standard Deviation	0.00554
Minimum	0.9884
Maximum	1.01258

Meshing along the column axis is straightforward – column is divided into integer number of finite elements. The influence of meshing density along the column axis is analysed in Figure 3.1. It can be concluded that the division into 10 elements along the column length is sufficient for the problem under consideration as the results for models composed of 10 elements and 20 elements basically coincide. If the column is divided into 4 elements the results are quite close to those achieved with much thinner mesh.

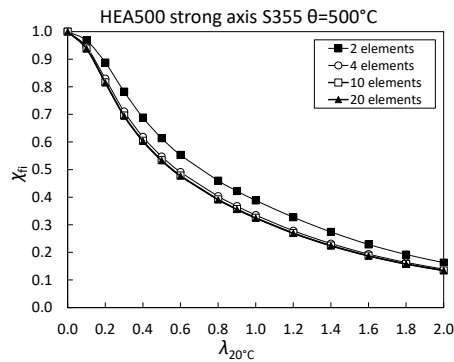


Figure 3.1: Meshing density along the column axis

Section meshing depends on the section topology (type). The analysis of section mesh density was performed for the I-section strong axis buckling. Mesh density for each section component must be chosen: flange in both directions, wall in both directions (Figure 3.2).

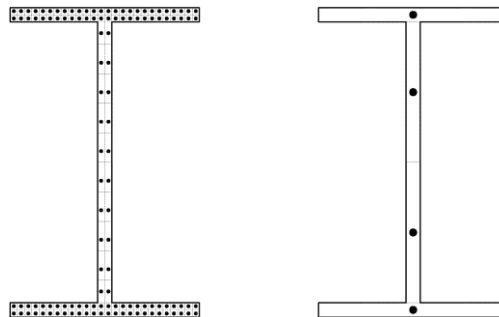


Figure 3.2: Section meshing

In order to estimate the influence of the mesh density on the buckling factor two sets of calculations were performed:

- The number of elements along the flange thickness is 10; the number of elements along the flange width is 10; the number of elements along the wall thickness is 2; the number of elements along the wall height is 20.

- b. The number of elements along the flange thickness is 1; the number of elements along the flange width is 1; the number of elements along the wall thickness is 1; the number of elements along the wall height is 2.

For the set *a* the meshing density is much higher. Comparison of buckling factors is presented in Figure 3.3. It is obvious that the buckling curves for both sets basically coincide (maximum difference was 0.36%). Although it is evident that relatively rough meshing could be utilized for the analysis, the situation is different in case residual stresses are included in the analysis.

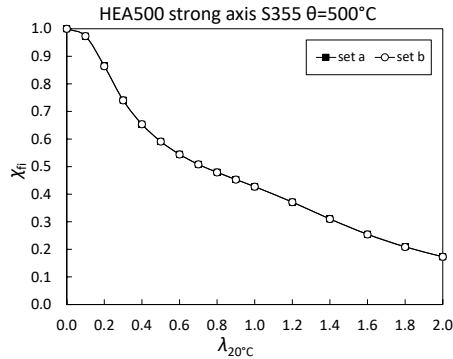


Figure 3.3: Influence of the section mesh density on the buckling factor

3.2.3 Geometrical model and boundary conditions

The chosen approach is consistent with the generally accepted practice. Column was assumed to have pinned boundary conditions allowing free rotation at both ends. The initial shape of the column was modelled as a sinusoid half wave with maximum initial imperfection in the middle of the column (Figure 2.1). Sinusoidal shape corresponds to the first buckling mode of an axially compressed elastic element. Maximum initial imperfection was chosen 1/1000 of column length based on [53], which is common practice for the analysis in case residual stresses are implied.

3.2.4 Loading history

Loading history modelling can in some cases be important. This concerns complicated structures for which configuration evolution during the construction stage cannot be ignored in the analysis (long-span bridges, tensile structures etc.). In case of modelling post-failure at elevated temperature the loading history should be also accounted for. Calculation in the temperature domain is closer to the real conditions: initially the structure is loaded at ambient temperature; then the temperature is changed, which leads to modification of material properties.

In the present research the influence of loading history was estimated. Results for models in resistance domain were compared with the results for models in temperature domain. At first the buckling factors were defined in the resistance domain for a given temperature. Calculations in temperature domain were performed as follows: column was loaded using buckling load value from the results of the calculations in the resistance domain as ambient temperature; temperature was risen until failure; failure temperature was compared to the temperature assumed for the resistance domain. Results are presented in Table 3-2, where χ_{fi} is the buckling factor and $\theta_{failure}$ is the failure temperature. Results indicate that the influence of the loading history is minimal.

3.2.5 Thermal elongation and axial restraint

The issue of thermal elongation and axial restraint has received considerable amount of attention by several researchers. The effect of axial restraint was described by Ali et al in [54] and Bennets et al in [55]. Neves et al [31] and Wang et al [32] have proposed methods for prediction of the failure temperature of a restrained steel column in fire. Franssen has presented his analysis of axial restraint in [56] effectively showing that the effect of axial restraint is much less severe phenomenon than it has sometimes been assumed, which is similar to the conclusion of Bennets et al [55].

Table 3-2: Influence of loading history (HEA500 S355 strong axis $\theta=500^{\circ}\text{C}$)

$\lambda_{20^{\circ}\text{C}}$	χ_{fi}	$\theta_{failure},$ $^{\circ}\text{C}$
0.1	0.975	500.29
0.2	0.878	500.28
0.3	0.757	499.57
0.4	0.662	500.38
0.5	0.593	500.18
0.6	0.545	500.30
0.7	0.509	500.44
0.8	0.479	499.92
0.9	0.453	499.95
1.0	0.427	500.45
1.2	0.371	500.35
1.4	0.309	500.35
1.6	0.254	499.72
1.8	0.209	499.89
2.0	0.173	500.13

Limited non-linear FEM analysis was performed to investigate the influence of axial restraint and validate FEM procedure. Material models from EN 1993-1-2 [20] were adopted. Model for elongation from the same document was used as described in section 3.3.7. The influence of thermal elongation was evaluated in the temperature domain, as was described in previous section. The procedure for the analysis was basically the same, with the only exception – thermal elongation was added to the material property set. Results of modelling are presented in Table 3-3 and Table 3-4.

It is validated that thermal elongation along has minor influence on the buckling stability of the unrestrained axially compressed column with initial imperfection. This brings us to the influence of restraint on the buckling capacity.

There is a number of questions, which have to be asked and answered when the restraint influence on the column buckling is addressed. The most crucial of those questions are:

- Which type of connection between the column and the horizontal elements of a frame is used? If pinned discontinuous connection is used, It is intuitive that column restraint can be expected to be minimal. In case beam/column connection is not pinned the connection rigidity has to be somehow estimated taking into consideration

the technical solution and thermal conditions of the connection which could be different from those of the column.

- b. Where is the heated column located within the fire zone? If all columns within one storey of a frame are heated similarly it can be expected that the restraint influence

Table 3-3: Influence of thermal elongation (HEA500 S355 strong axis $\theta=500^{\circ}\text{C}$)

$\lambda_{20^{\circ}\text{C}}$	χ_{fi}	$\theta_{failure},$ $^{\circ}\text{C}$
0.1	0.975	499.83
0.2	0.878	499.72
0.3	0.757	499.21
0.4	0.662	499.57
0.5	0.593	499.21
0.6	0.545	498.96
0.7	0.509	498.99
0.8	0.479	498.89
0.9	0.453	498.86
1.0	0.427	498.67
1.2	0.371	498.18
1.4	0.309	497.81
1.6	0.254	497.47
1.8	0.209	497.13
2.0	0.173	496.98

Table 3-4: Influence of thermal elongation (HEA500 S355 strong axis $\theta=900^{\circ}\text{C}$)

$\lambda_{20^{\circ}\text{C}}$	χ_{fi}	$\theta_{failure},$ $^{\circ}\text{C}$
0.1	0.971	899.85
0.2	0.871	899.51
0.3	0.775	899.29
0.4	0.712	898.90
0.5	0.672	898.92
0.6	0.644	899.12
0.7	0.621	899.26
0.8	0.601	899.30
0.9	0.580	899.15
1.0	0.557	899.61
1.2	0.499	899.03
1.4	0.428	898.63
1.6	0.358	898.02
1.8	0.297	897.83
2.0	0.248	897.23

is minimal. In case columns within a storey are heated differently, the restraint factor for a column under consideration depends on the heating scenario of columns and once again on the connection type between columns and horizontal elements.

- c. In which way heat transfer from one frame element to another via conduction is controlled? In case a frame element is heated the conduction will take place and temperature of other frame elements will change. This matter is case sensitive but it is clear that it is almost impossible to fully isolate frame elements thermally if the joint must transfer loads.

Answers to those questions imply that column under consideration must be placed into wider context. The column must be integrated into the frame for which heating and connection conditions are adequately modelled. Although these issues are outside the scope of the thesis, calculations were performed in order to roughly estimate the influence of the restraint on the column capacity. Two frames were analysed as presented in Figure 3.4 and Figure 3.5. Configuration of the frames and loading were chosen as follows: the maximum axial load for a middle column on the bottom floor must be 1 123 kN (axial buckling capacity around the strong axis of the C00 HEB200 S355 column with buckling length 4.0 m for 500°C temperature conditions). Column-beam connection was assumed pinned, the beams were assumed to be two-spanned, non-sway frame was assumed, initial column imperfection was taken as 1 / 1000 of its length. Analysis was performed in two stages: at first the frame was loaded in ambient temperature conditions; then the temperature rise was modelled and failure temperature was defined. Three options were considered:

- a. only middle column (C00) is heated;
- b. all bottom floor columns (C00, C01 and C02) are heated;
- c. all bottom floor structures (C00, C01, C02 and B0) are heated.

Results of the analysis are summarized in Table 3-5.

Table 3-5: Influence of the restraint

Analysis type	Failure temperature, °C	Maximum axial load during heating, kN	Axial load at 500°C, kN
Frame 1			
a.	476	1 167	---
b.	> 500	1 123	1 120
c.	> 500	1 123	1 119
Frame 2			
a.	479	1 178	---
b.	> 500	1 123	1 121
c.	> 500	1 123	1 120

It is evident, that axial restraint decreases the failure temperature only in case the column C00 is heated and temperature of other frame elements remains ambient. In this case the frame elements of 20°C have excessive capacity reserve and the failure of one column will not necessarily lead to the failure of the frame. For other heating scenarios the axial restraint does not have significant influence on the buckling capacity of the column. The axial restraint leads to the increase of load and has no direct influence on the capacity of the column. The axial restraint influence must be estimated in a separate procedure and if needed added to the design load.

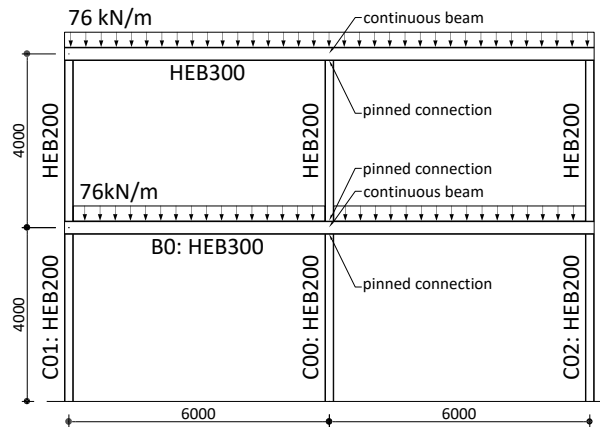


Figure 3.4: Restraint influence analysis – frame 1

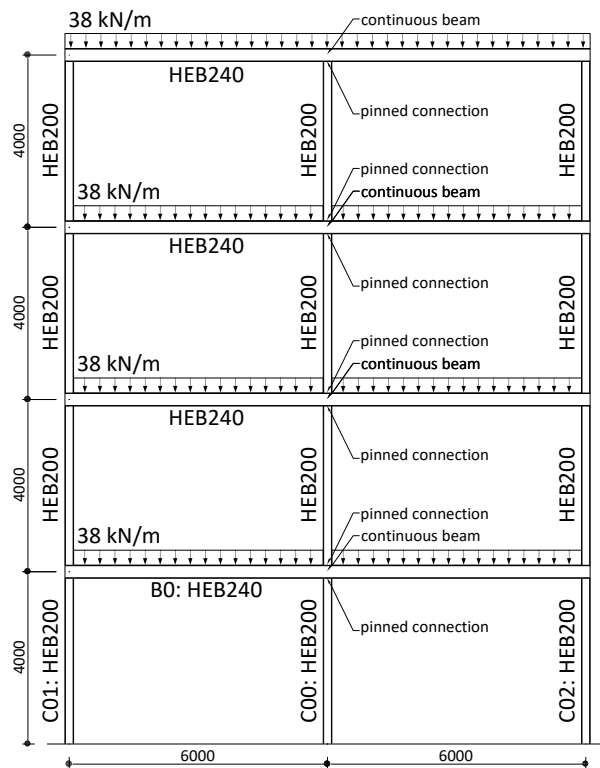


Figure 3.5: Restraint influence analysis – frame 2

3.2.6 Local buckling

In Eurocode 3 the issue of local buckling of an element is associated with section classification. In order to account for the risk of local buckling sections are divided into four classes and certain modifications and rules are implemented [57]. The differences between the section classes can be summarized as follows: class 1 and 2 sections are allowed to reach fully plastic state; for the class 3 section plastification is not allowed; for the class 4 effective geometrical properties must be reduced accounting for local

buckling effects (procedures from EN 1993-1-5 [58]). The limits of each class are defined by plate slenderness or width-to-thickness ratio b/t as presented in Table 3-6.

For normal temperature conditions parameter ε from Table 3-6 is defined as (3-1), while in fire conditions as (3-2).

Table 3-6: Section classification – b/t ratio limit values

Type / state	Class 1	Class 2	Class 3
Section flange in compressic	9ε	10ε	14ε
Section wall in compression	33ε	38ε	42ε

$$\varepsilon = \sqrt{\frac{235}{f_y}} \quad (3-1)$$

$$\varepsilon = \sqrt{\frac{k_{E,\theta}}{k_{y,\theta}}} \sqrt{\frac{235}{f_y}} \approx 0.85 \sqrt{\frac{235}{f_y}} \quad (3-2)$$

Approximate value of (3-2) is presented in order to show, that on average the section class in fire conditions is higher than the class for normal temperature conditions. For temperature higher than 850°C the ratio $k_{E,\theta}/k_{y,\theta}$ (section 3.3.2; [20]) is higher than 1.0 and section class in fire conditions can potentially become lower than in normal temperature conditions.

When dealing with local buckling one of the issues is the correct definition of maximum local imperfection. The tolerance standard EN 10034 prescribes [59] the out-of-plane tolerances as shown in Figure 3.6. Researchers [60], [61] implement Annex C of EN 1993-1-5 [58] which itself refers to the tolerances standard. According to EN 1993-1-5 the maximum imperfection must be taken as 1 / 200 of the panel length a or width b as sown in Figure 3.7.

During the research of buckling of stainless steel columns in fire, Gardner and Nethercot [62] have studied thoroughly the influence of local imperfections. Based on the actual measurement data they have proposed to use equation (3-3), where w_0 is the maximum initial imperfection, t is the plate thickness, $\sigma_{0.2}$ is the material 0.2% proof stress and σ_{cr} is the first buckling mode stress. For stub columns equation (3-3) can be approximated by 1% of the wall or flange thickness, which is in most cases much smaller value than 1/200 of the section width or height. Gardner and Nethercot have dealt with square and rectangular hollow sections which in many aspects are different from I and H sections. Pauli et al [63] have presented detailed report on steel column tests including data regarding local and global imperfections. According to the report the average local imperfection for HEA100 section is 0.18 mm, which is 0.03 of the wall thickness. For HEA500 the initial local imperfection for the section wall (12 mm) according to the tolerance standard is 2.4 mm, according to EN 1991-1-5 1.9 mm, according to the approach of Gardner and Nethercot 0.12 mm and according to Pauli can be expected to be 0.38 mm although this extrapolation can be questioned.

Example of the local buckling shape is presented in Figure 3.8, where the buckling shape of the column wall can be described by sinusoidal waves. In reality, the actual imperfect section shape (Figure 3.6) may remain constant along the column axis or with small number of waves. For example Figure 3.9 can be analysed (reproduced from Pauli [60]) as follows. Wall imperfections for HEA100 section of a 1800 mm long column are plotted for two cases. It is quite problematic to distinguish local and global imperfections from the diagrams.

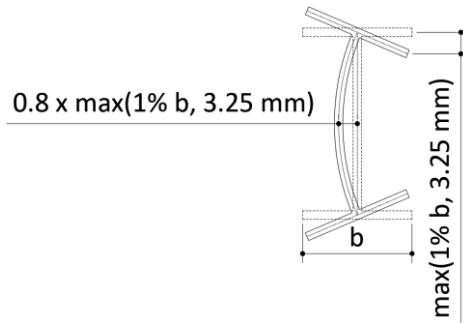


Figure 3.6: Local imperfection according to EN 10034

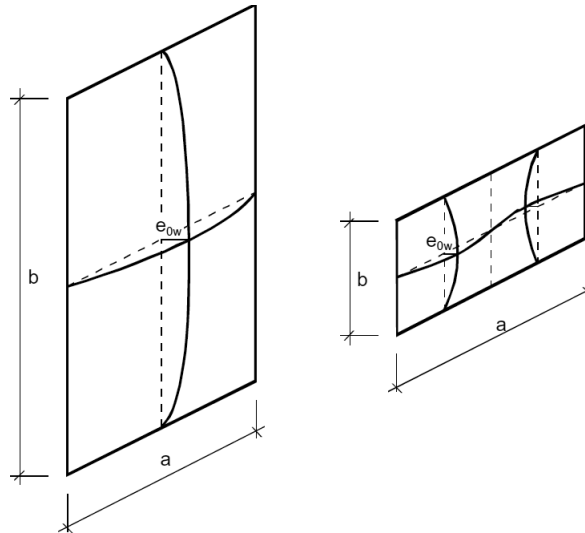


Figure 3.7: Local imperfection according to EN 1991-1-5 Annex C

$$w_0/t = 0.023(\sigma_{0.2}/\sigma_{cr}) \quad (3-3)$$

Several authors have reported the high importance of local buckling problem in fire conditions [23], [64]. Couto et al [64] has proposed to unite class 3 and class 4 into one category for the compression resistance calculations in fire conditions. According to his proposal the effective section area for class 3 must be calculated in accordance with the EN 1991-1-5 procedure.

In order to estimate the influence of local imperfections calculations have been performed for two sections HEA300 S355 (section class 3 in fire conditions) and HEA500 S355 (section class 4 in fire conditions) for five cases: C1 – without local imperfections; C2 – with local imperfections shape according to the buckling mode and EN 10034 (Figure 3.6); C3 – with local imperfections shape according to the buckling mode and maximum initial imperfection 0.03 of the plate thickness (extrapolated from the results by Pauli et al [63]); C4 – with constant local imperfection along the column axis in accordance with EN 10034 (Figure 3.6); C5 – with constant local imperfection along the column axis with maximum initial imperfection 0.03 of the plate thickness (extrapolated from the results by Pauli et al [63]). Beam finite elements are not suitable for this type of problem. Calculations were performed using ANSYS software implementing “SHELL181” finite

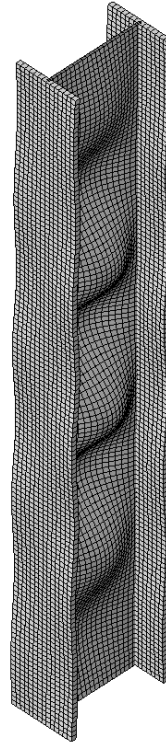


Figure 3.8: Local buckling shape example

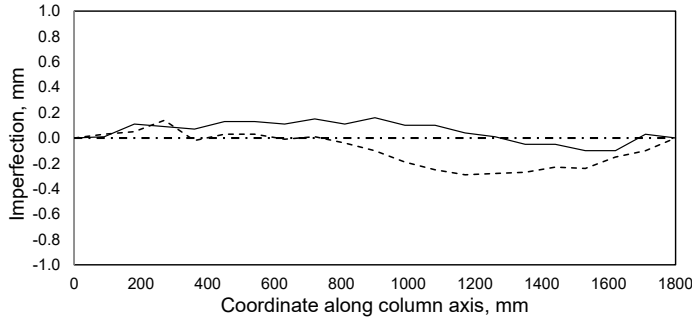


Figure 3.9: Wall imperfections along column length

element type in two stages as follows. At first linear buckling analysis with the purpose of acquiring global and local buckling shapes was performed. Then non-linear analysis with initial imperfections implementing Eurocode material models (section 3.3.2) was executed. Results of the calculations are presented in Figure 3.10. The buckling capacity is considerably influenced by the local imperfections for column length below 7 500 mm (low slenderness value). The effect of local imperfections on buckling capacity is strongly influenced by the way initial imperfections are integrated into the model. The biggest difference is observed for the minimum slenderness value (HEA300 column length 900 mm and HEA500 column length 1 500 mm) and initial imperfection scheme C2. The buckling capacity decreases by 21% and 19% correspondingly in relation to model without the local imperfection. In case initial imperfections are introduced in accordance with scheme C5, for minimum slenderness value the buckling capacity is decreased by 2.7%

(HEA300) and 4.9% (HEA500). Evidently the results for section class 3 (HEA300) are more sensitive to the initial imperfections.

Obviously, in order to make specific conclusions on the effect of local buckling on the buckling capacity in fire a more extensive research is needed. Considerable array of measurements is needed in order to make adequate judgement on absolute values and shape of the initial imperfections. Solution of this problem is outside of the

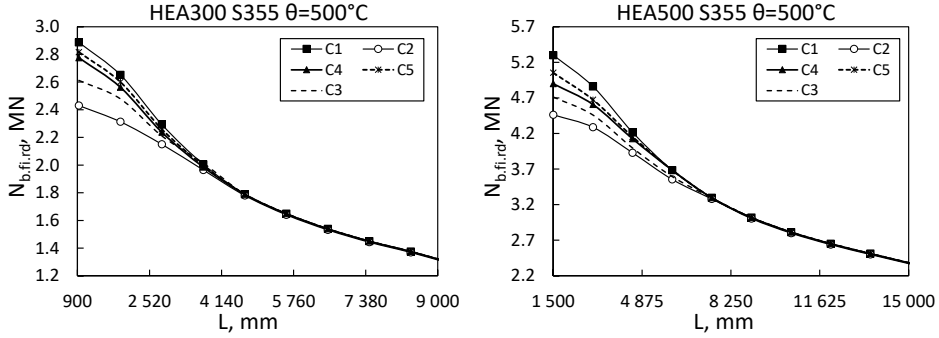


Figure 3.10: Influence of local imperfection on the buckling capacity

scope of this thesis. The results presented further in this work do not account for the local buckling effects and those effects must be considered separately.

3.2.7 Procedure of finite element method

Finite element procedure was composed using programming language Octave [65]. Major aspects of the procedure are shortly presented here.

The procedure is largely based on [66]. Beam model in two dimensional space is considered. Newton-Raphson method is implemented. The displacement vector \mathbf{u} is calculated iteratively. On each iteration step k updated displacement vector is defined using expression (3-4). Incremental displacement vector $\Delta \mathbf{u}^k$ can be found by solving (3-5), where \mathbf{F} stands for the external force (load) vector, \mathbf{P} for internal force vector (which is a function of displacement vector) and \mathbf{K}_t stands for tangent stiffness matrix (also a function of displacement vector). Tangent matrix is defined by the first variation of the internal force vector (3-6).

$$\mathbf{u}^{k+1} = \mathbf{u}^k + \Delta \mathbf{u}^k \quad (3-4) \quad \mathbf{K}_t^k \Delta \mathbf{u}^k = \mathbf{F} - \mathbf{P}(\mathbf{u}^k) \quad (3-5)$$

$$\mathbf{K}_t^k(\mathbf{u}^k) = \left(\frac{\partial \mathbf{P}}{\partial \mathbf{d}} \right)^k \quad (3-6) \quad \mathbf{K}_{i,z} = \frac{\mathbf{P}_{i,z}^+ - \mathbf{P}_{i,z}^-}{2\alpha} \quad (3-7)$$

$$N_i = \sum_{j=1}^n A_j \sigma_j(\varepsilon_j) \quad (3-8) \quad M_i = \sum_{j=1}^n A_j \sigma_j(\varepsilon_j) y_{loc,j} \quad (3-9)$$

$$V_i = 0.5 \gamma_i \sum_{j=1}^n A_j E(\varepsilon_j) \quad (3-10) \quad \varepsilon_i = \frac{c_\theta L_{c\psi} + s_\theta L_{s\psi}}{L_0} - 1 \quad (3-11)$$

$$\gamma_i = -\frac{s_\theta L_{c\psi} - c_\theta L_{s\psi}}{L_0} \quad (3-12) \quad \kappa_i = \frac{\theta_2 - \theta_1}{L_0} \quad (3-13)$$

$$\varepsilon_{i1} = \varepsilon_i - \kappa_i \frac{h}{2} \quad (3-14) \quad \varepsilon_{i2} = \varepsilon_i + \kappa_i \frac{h}{2} \quad (3-15)$$

$$\varepsilon_{ij} = \varepsilon_{i2} + \frac{(y_{loc,j} + 0.5h)}{h}(\varepsilon_{i1} - \varepsilon_{i2}) \quad (3-16) \quad X_{21} = x_{01} - x_{02} \quad (3-17)$$

$$Y_{21} = y_{01} - y_{02} \quad (3-18) \quad x_{21} = X_{21} + u_{x2} - u_{x1} \quad (3-19)$$

$$y_{21} = Y_{21} + u_{y2} - u_{y1} \quad (3-20) \quad L_0 = \sqrt{X_{21}^2 + Y_{21}^2} \quad (3-21)$$

$$L_{c\psi} = \frac{X_{21}x_{21} + Y_{21}y_{21}}{L_0} \quad (3-22) \quad L_{s\psi} = \frac{X_{21}y_{21} - Y_{21}x_{21}}{L_0} \quad (3-23)$$

$$\theta_m = \frac{\theta_1 + \theta_2}{2} \quad (3-24) \quad c_\theta = \cos(\theta_m) \quad (3-25)$$

$$s_\theta = \sin(\theta_m) \quad (3-26) \quad c_\phi = \frac{X_{21}}{L_0} \quad (3-27)$$

$$s_\phi = \frac{Y_{21}}{L_0} \quad (3-28) \quad c_m = c_\theta c_\phi - s_\theta s_\phi \quad (3-29)$$

$$s_m = c_\theta s_\phi + s_\theta c_\phi \quad (3-30) \quad \mathbf{P}_i = L_0 \mathbf{B}_m \begin{bmatrix} N_i \\ V_i \\ M_i \end{bmatrix} \quad (3-31)$$

$$\mathbf{B}_m = \frac{1}{L_0} \begin{bmatrix} -c_m & -s_m & \frac{L_0 \gamma_i}{2} & c_m & s_m & \frac{L_0 \gamma_i}{2} \\ s_m & -c_m & -\frac{L_0(1 + \varepsilon_i)}{2} & -s_m & c_m & -\frac{L_0(1 + \varepsilon_i)}{2} \\ 0 & 0 & -1 & 0 & 0 & 1 \end{bmatrix} \quad (3-32)$$

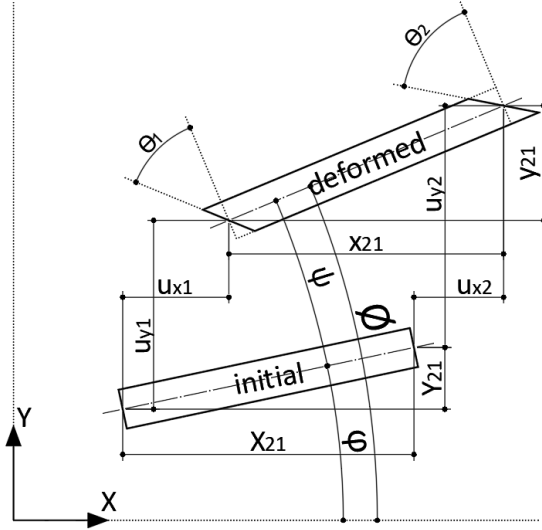


Figure 3.11: Beam element kinematics

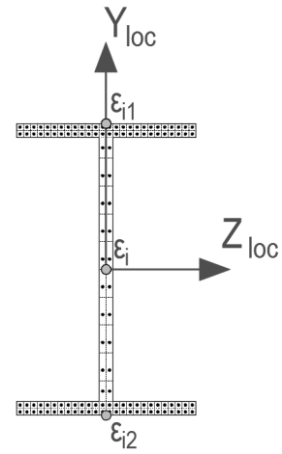


Figure 3.12: Beam section mesh

For the procedure the tangent stiffness matrix of an element was defined by the finite difference method (3-7): each degree of freedom is moved by a tiny amount α twice, forward (+) and backward (-); the element under consideration is denoted i , while the displaced degree of freedom is denoted by z ; internal force vector of the element i for the forward $\mathbf{P}_{i,z}^+$ and backward $\mathbf{P}_{i,z}^-$ perturbation of the degree of freedom z are then calculated; the z -th row of the element i tangent matrix can then be calculated using

(3-7). Element i tangent matrix is composed in the described way by perturbation of each degree of freedom (in 2D case the number of degrees of freedom is 6). Timoshenko type beam finite element using Total Lagrangian kinematic description and Green-Lagrange strain measure is implemented. Internal force vector for element i is defined as (3-31). Internal forces N_i (axial force), M_i (bending moment) and V_i (shear force) are calculated using (3-8), (3-9) and (3-10) accordingly. In all three cases the section mesh is used (Figure 3.12). For each individual section cell j axial strain can be defined using (3-16), which is itself defined by the beam element i extreme fibre strains (3-14) and (3-15). Axial mid-section strain of the element is defined by (3-11), section curvature is defined by (3-13) and shear strain by (3-12). Kinematical and geometrical parameters (3-17) ... (3-30) can be identified using Figure 3.11. Other procedures (nodes and elements numbering, global matrix composition, boundary conditions etc.) were implemented in the standard procedure [67] and are not described here. Results were validated against the results obtained by general purpose FEM software ANSYS for 1000 randomly chosen cases. Results of the statistical analysis for the comparative factor $N_{Rd,fi,proc}/N_{Rd,fi,ANSYS}$ are presented in Table 3-7, where $N_{Rd,fi,proc}$ is the buckling capacity calculated using procedure and $N_{Rd,fi,ANSYS}$ is the buckling capacity calculated using ANSYS.

Table 3-7: Descriptive statistics for composed procedure vs. ANSYS models

Parameter	Value
Mean	0.99989
Standard Error	0.00027
Standard Deviation	0.00852
Minimum	0.9854
Maximum	1.0152

3.3 Material models

Adequate material model is essential for any type of structural analysis. It is commonly accepted, that for normal temperature conditions ideal elasto-plastic material model can be effectively used for modelling carbon steel structures. It is also commonly agreed, that in case of elevated temperatures, carbon steel stress-strain relationship becomes much more complicated compared to the normal temperature conditions. Adequate material model is needed if high correlation between modelling and tests is expected. The main aim of this research was not to investigate the material model adequacy. Eurocode material model was used for the current research, but it seems still important and interesting to investigate the application of alternative material models and compare the results.

3.3.1 Strain rate and thermal creep

The comparison of material models starts with the study of the strain rate and the influence of thermal creep on the material response. Higher strain rate in general leads to the higher stress level, i.e. strength is increased [60], [68], [69], [70]. Real structures are in most cases loaded prior to the emergence of fire, so strain rate from loading can be expected to be minimal. Due to this reason, direct strain rate is ignored in this study. For the loaded structures the strain rate sensitivity of steel response is manifested in the form of thermal creep [71]. The importance of thermal creep has been reported by Twilt [72] and Hu et al [68]. Eurocode material model was based on the transient state test,

therefore it partly accounts for the thermal creep effects [73]. In this work the thermal creep is not explicitly accounted for and it is assumed that these effects are accounted by the stress-strain material model.

3.3.2 Eurocode material model

Material models from EN 1993-1-2 [20] were adopted in this work. Eurocode material model is based on the tests performed by Kirby and Preston [74]. Tests were performed in transient state meaning that the test specimen is preloaded, the load is held constant and the temperature is linearly increased until the engineering strain reaches its limit value of 0.02. According to the report by Twilt [75] the heating rate for the test was chosen as 10°C/min (for standard fire curve, heating rate is higher than 10°C/min during the first 15 minutes and is lower from 15 minutes and further). Material models are presented in Figure 3.13 and Figure 3.14, equations (3-33) – (3-40) and in Table 3-8. Notation used replicates the one used in Eurocode 3: ε is strain; $\varepsilon_{p,\theta}$ is proportionality limit strain at temperature θ ; $\varepsilon_{y,\theta}$ is yield limit strain at temperature θ ; σ is stress; $E_{a,\theta}$ is tangent modulus in elastic range; $f_{p,\theta}$ is proportionality limit stress at temperature θ ; $f_{y,\theta}$ is yield limit stress at temperature θ ; a_{EC} , b_{EC} and c_{EC} are for material model parameters.

Material model is obviously essential for predicting buckling capacity. As for each temperature value above 100°C there is a unique stress-strain curve, for each temperature value a unique buckling curve exists.

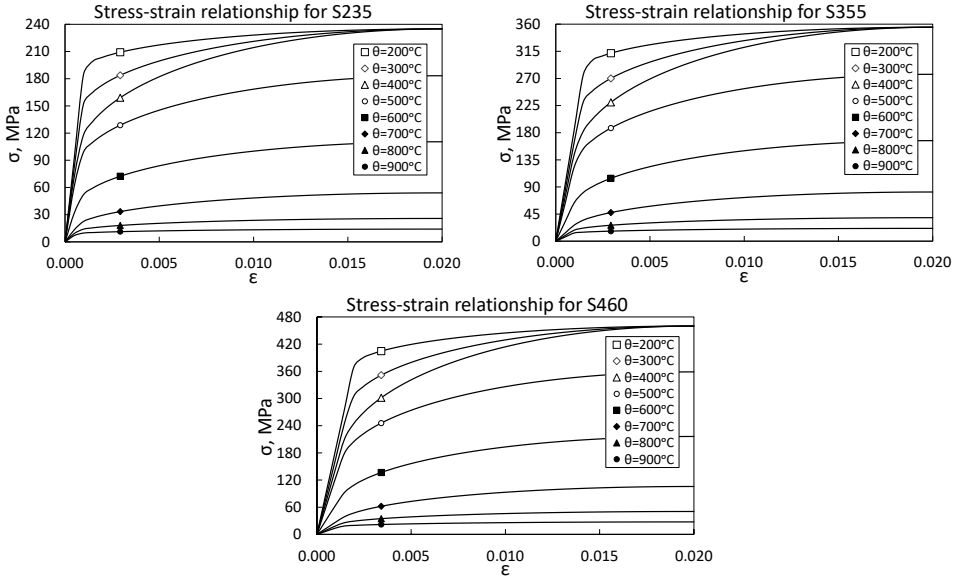


Figure 3.13: Eurocode 3 material models for carbon steel in elevated temperature conditions

$$\varepsilon \leq \varepsilon_{p,\theta}: \quad \sigma = \varepsilon E_{a,\theta} \quad (3-33)$$

$$\varepsilon_{p,\theta} < \varepsilon \leq \varepsilon_{y,\theta}: \quad (3-34)$$

$$\sigma = f_{p,\theta} - c_{EC} + \frac{b_{EC}}{a_{EC}} \sqrt{a_{EC}^2 - (\varepsilon_{y,\theta} - \varepsilon)^2} \quad (3-35)$$

$$\varepsilon_{y,\theta} \leq \varepsilon \leq \varepsilon_{t,\theta}: \quad \sigma = f_{y,\theta} \quad (3-36)$$

$$\varepsilon_{p,\theta} = \frac{f_{p,\theta}}{E_{a,\theta}} \quad \varepsilon_{y,\theta} = 0.02 \quad (3-37)$$

$$a_{EC}^2 = (\varepsilon_{y,\theta} - \varepsilon_{p,\theta}) \left(\varepsilon_{y,\theta} - \varepsilon_{p,\theta} + \frac{c_{EC}}{E_{a,\theta}} \right) \quad (3-38)$$

$$b^2 = c_{EC}(\varepsilon_{y,\theta} - \varepsilon_{p,\theta})E_{a,\theta} + c_{EC}^2 \quad (3-39)$$

$$c_{EC}^2 = \frac{(f_{y,\theta} - f_{p,\theta})^2}{(\varepsilon_{y,\theta} - \varepsilon_{p,\theta})E_{a,\theta} - 2(f_{y,\theta} - f_{p,\theta})} \quad (3-40)$$

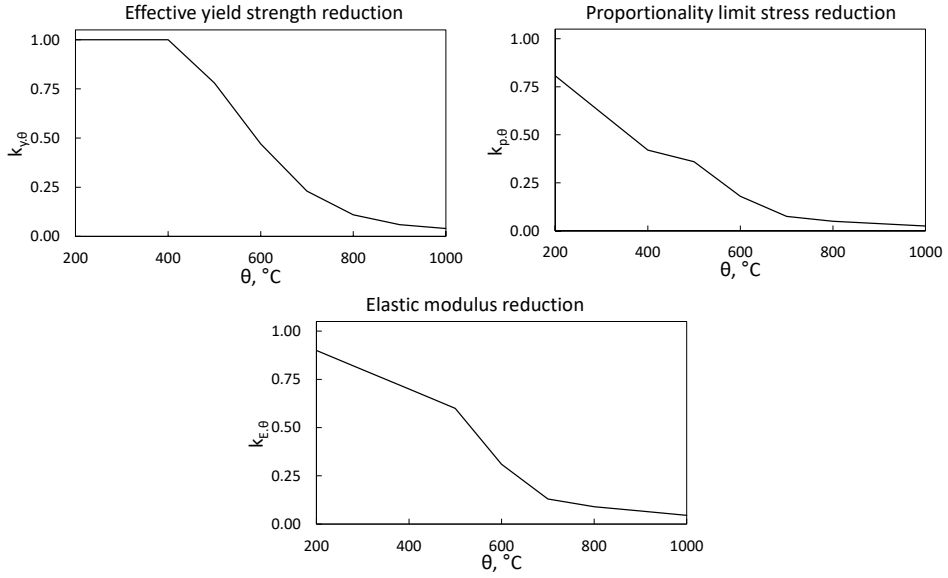


Figure 3.14: Eurocode 3 reduction coefficients for carbon steel in elevated temperature conditions

3.3.3 ECCS material model

The model was presented in the 1983 Technical Committee 3 report by The European Convention for Constructional Steelwork (ECCS) [76]. The model has not been widely used. The temperature range is limited by 600°C. In the report the model is presented in the form of diagrams and tabulated data. Material models are presented here in Figure 3.15 and Table 3-9 (notation is the same as for the Eurocode model).

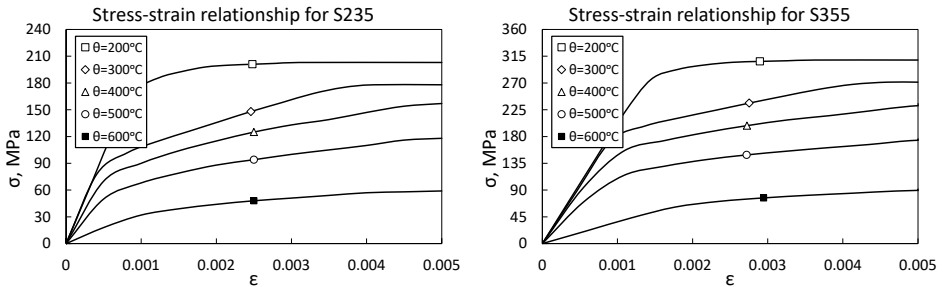


Figure 3.15: ECCS material model for carbon steel in elevated temperature conditions

3.3.4 Lie material model

Lie material model for steel in elevated temperature conditions was proposed in 1992 [77]. The model is quite compact compared to the Eurocode model. Lie material model is presented in Figure 3.16, equations (3-41) – (3-46) and Table 3-10 (notation is the same as for the Eurocode model).

Table 3-8: Eurocode 3 material model parameters for carbon steel in elevated temperature conditions

	$f_{p,\theta}$, MPa	$f_{y,\theta}$, MPa	$E_{a,\theta}$, MPa	$\epsilon_{p,\theta}$, %	a_{EC}	b_{EC}	c_{EC}	$f_{p,\theta}/f_{y,\theta}$	
S235	$\theta=200^{\circ}\text{C}$	190	235	189 000	0.1003%	0.01900	45.94	0.588	0.807
	$\theta=300^{\circ}\text{C}$	144	235	168 000	0.0857%	0.01915	93.67	2.726	0.613
	$\theta=400^{\circ}\text{C}$	99	235	147 000	0.0671%	0.01935	143.53	7.232	0.420
	$\theta=500^{\circ}\text{C}$	85	183	126 000	0.0671%	0.01935	103.05	4.353	0.462
	$\theta=600^{\circ}\text{C}$	42	110	65 100	0.0650%	0.01938	72.28	4.134	0.383
	$\theta=700^{\circ}\text{C}$	18	54	27 300	0.0646%	0.01941	39.34	2.913	0.326
	$\theta=800^{\circ}\text{C}$	12	26	18 900	0.0622%	0.01939	14.69	0.588	0.455
	$\theta=900^{\circ}\text{C}$	9	14	14 175	0.0622%	0.01938	5.39	0.106	0.625
S355	$\theta=200^{\circ}\text{C}$	286	355	189 000	0.1516%	0.01849	69.91	1.399	0.807
	$\theta=300^{\circ}\text{C}$	218	355	168 000	0.1295%	0.01872	143.97	6.582	0.613
	$\theta=400^{\circ}\text{C}$	149	355	147 000	0.1014%	0.01905	223.72	17.820	0.420
	$\theta=500^{\circ}\text{C}$	128	277	126 000	0.1014%	0.01903	159.72	10.616	0.462
	$\theta=600^{\circ}\text{C}$	64	167	65 100	0.0982%	0.01910	113.22	10.268	0.383
	$\theta=700^{\circ}\text{C}$	27	82	27 300	0.0975%	0.01916	62.42	7.397	0.326
	$\theta=800^{\circ}\text{C}$	18	39	18 900	0.0939%	0.01910	22.73	1.428	0.455
	$\theta=900^{\circ}\text{C}$	13	21	14 175	0.0939%	0.01907	8.24	0.251	0.625
S460	$\theta=200^{\circ}\text{C}$	371	460	189 000	0.1964%	0.01804	91.22	2.439	0.807
	$\theta=300^{\circ}\text{C}$	282	460	168 000	0.1678%	0.01836	189.66	11.643	0.613
	$\theta=400^{\circ}\text{C}$	193	460	147 000	0.1314%	0.01879	298.96	32.163	0.420
	$\theta=500^{\circ}\text{C}$	166	359	126 000	0.1314%	0.01876	212.17	18.967	0.462
	$\theta=600^{\circ}\text{C}$	83	216	65 100	0.1272%	0.01887	152.08	18.685	0.383
	$\theta=700^{\circ}\text{C}$	35	106	27 300	0.1264%	0.01899	85.08	13.781	0.326
	$\theta=800^{\circ}\text{C}$	23	51	18 900	0.1217%	0.01885	30.14	2.541	0.455
	$\theta=900^{\circ}\text{C}$	17	28	14 175	0.1217%	0.01880	10.79	0.436	0.625

Table 3-9: ECCS material model parametrs for carbon steel in elevated temperature conditions

	$f_{p,\theta}$, MPa	$f_{y,\theta}$, MPa	$E_{a,\theta}$, MPa	$\epsilon_{p,\theta}$, %	$f_{p,\theta}/f_{y,\theta}$	
S235	$\theta=200^{\circ}\text{C}$	148	203	200 000	0.0740%	0.729
	$\theta=300^{\circ}\text{C}$	78	178	190 244	0.0410%	0.438
	$\theta=400^{\circ}\text{C}$	70	157	140 000	0.0500%	0.446
	$\theta=500^{\circ}\text{C}$	50	118	100 000	0.0500%	0.424
	$\theta=600^{\circ}\text{C}$	18	59	36 000	0.0500%	0.305
S355	$\theta=200^{\circ}\text{C}$	73	309	202 210	0.0362%	0.237
	$\theta=300^{\circ}\text{C}$	88	271	192 375	0.0459%	0.325
	$\theta=400^{\circ}\text{C}$	94	198	172 294	0.0545%	0.474
	$\theta=500^{\circ}\text{C}$	70	149	127 757	0.0544%	0.466
	$\theta=600^{\circ}\text{C}$	21	77	36 333	0.0589%	0.279

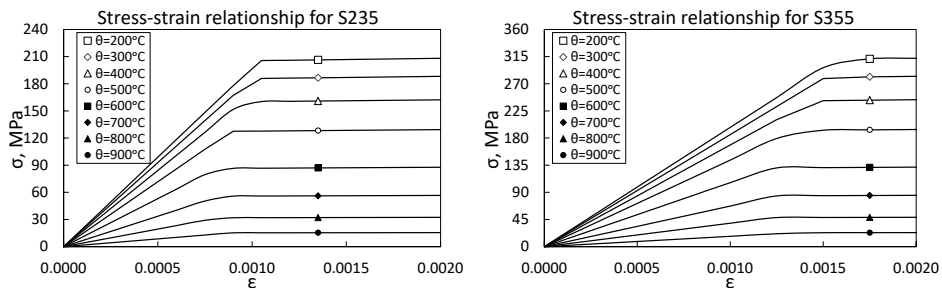


Figure 3.16: Lie material model for carbon steel in elevated temperature conditions

$$\theta \leq 600^{\circ}\text{C}: f_{y,\theta} = \left[1.0 + \frac{\theta}{900 \ln\left(\frac{\theta}{1750}\right)} \right] f_{y,20^{\circ}\text{C}} \quad (3-41)$$

$$600^{\circ}\text{C} < \theta \leq 1000^{\circ}\text{C}: f_{y,\theta} = \frac{340 - 0.34\theta}{\theta - 240} f_{y,20^{\circ}\text{C}} \quad (3-42)$$

$$\theta \leq 600^{\circ}\text{C}: E_{a,\theta} = \left[1.0 + \frac{\theta}{2000 \ln\left(\frac{\theta}{1100}\right)} \right] E_{20^{\circ}\text{C}} \quad (3-43)$$

$$600^{\circ}\text{C} < \theta \leq 1000^{\circ}\text{C}: E_{a,\theta} = \frac{690 - 0.69\theta}{\theta - 53.5} E_{20^{\circ}\text{C}} \quad (3-44)$$

$$\varepsilon_{p,\theta} = \frac{0.975 f_{y,\theta} - 12.5 f_{y,\theta}^2 / E_{a,\theta}}{E_{a,\theta} - 12.5 f_{y,\theta}^2} \quad f_{p,\theta} = \varepsilon_{p,\theta} E_{a,\theta} \quad (3-45)$$

$$\varepsilon \leq \varepsilon_{p,\theta}: \sigma = \varepsilon E_{a,\theta}$$

$$\varepsilon > \varepsilon_{p,\theta}: \sigma = (12.5\varepsilon + 0.975) - \frac{12.5 f_{y,\theta}^2}{E_{a,\theta}} \quad (3-46)$$

Table 3-10: Lie material models parametrs for carbon steel in elevated temperature conditions

	$f_{p,\theta}$, MPa	$f_{y,\theta}$, MPa	$E_{a,\theta}$, MPa	$\varepsilon_{p,\theta}$, %	$f_{p,\theta}/f_{y,\theta}$	
S235	$\theta=200^{\circ}\text{C}$	205.6	210.9	197 681	0.1040%	0.975
	$\theta=300^{\circ}\text{C}$	185.8	190.6	185 756	0.1000%	0.975
	$\theta=400^{\circ}\text{C}$	160.1	164.2	168 482	0.0950%	0.975
	$\theta=500^{\circ}\text{C}$	127.5	130.8	143 414	0.0889%	0.975
	$\theta=600^{\circ}\text{C}$	86.4	88.6	106 063	0.0815%	0.975
	$\theta=700^{\circ}\text{C}$	50.8	52.1	67 239	0.0755%	0.975
	$\theta=800^{\circ}\text{C}$	27.8	28.5	38 821	0.0717%	0.975
	$\theta=900^{\circ}\text{C}$	11.8	12.1	17 118	0.0689%	0.975
S355	$\theta=200^{\circ}\text{C}$	310.5	318.6	197 681	0.1571%	0.975
	$\theta=300^{\circ}\text{C}$	280.6	287.9	185 756	0.1510%	0.975
	$\theta=400^{\circ}\text{C}$	241.8	248.1	168 482	0.1435%	0.975
	$\theta=500^{\circ}\text{C}$	192.5	197.6	143 414	0.1343%	0.975
	$\theta=600^{\circ}\text{C}$	130.5	133.9	106 063	0.1230%	0.975
	$\theta=700^{\circ}\text{C}$	76.7	78.7	67 239	0.1141%	0.975
	$\theta=800^{\circ}\text{C}$	42.0	43.1	38 821	0.1082%	0.975
	$\theta=900^{\circ}\text{C}$	17.8	18.3	17 118	0.1041%	0.975

3.3.5 Poh material model

Poh material model was proposed in 1997 (general stress-strain equation) [78] and in 2001 (stress-strain-temperature equation) [79]. Poh material model is presented in Figure 3.17, equations (3-47) – (3-52) and Table 3-11 (notation is the same as for the Eurocode model).

$$E_{a,\theta} = \left[\frac{-1.4 * 10^{-3}\theta + 1.001}{(1 + |2.74 * 10^{-3}\theta - 1.959|^5)^{0.2}} + 0.493 \right] E_{20^{\circ}\text{C}} \quad (3-47)$$

$$f_{p,\theta} = \left[\frac{-1.25 * 10^{-3}\theta + 0.50625}{(1 + |3.175 * 10^{-3}\theta - 1.2875|^5)^{0.2}} - 2 * 10^{-4}\theta + 0.63425 \right] f_{y,20^{\circ}\text{C}} \quad (3-48)$$

$$\theta \leq 500^{\circ}\text{C}: \quad (3-49)$$

$$\beta_2 = \left[\frac{0.01334\theta + 7.6705}{(1 + |8 * 10^{-3}\theta - 4.6|^{5})^{0.2}} + 1.6 * 10^{-4}\theta - 1.6975 \right] E_{20^{\circ}\text{C}}$$

$$\beta_5 = \left[\frac{7.4 * 10^{-3}\theta - 0.925}{(1 + |0.0133\theta - 1.667|^{5})^{0.2}} - 2.4 * 10^{-3}\theta + 0.046 \right] f_{y,20^{\circ}\text{C}}$$

$$\theta > 500^{\circ}\text{C}: \quad \beta_2 = E_{a,\theta} \quad \beta_5 = f_{p,\theta} \quad (3-50)$$

$$\beta_3 = \left[\frac{-6.4 * 10^{-5}\theta + 0.03616}{(1 + |0.0222\theta - 12.556|^{5})^{0.2}} + 4 * 10^{-6}\theta - 3.8 * 10^{-4} \right] E_{20^{\circ}\text{C}} \quad (3-51)$$

$$E_{a,\theta} = \left[\frac{-1.4 * 10^{-3}\theta + 1.001}{(1 + |2.74 * 10^{-3}\theta - 1.959|^{5})^{0.2}} + 0.493 \right] E_{20^{\circ}\text{C}} \quad (3-52)$$

Table 3-11: Poh material models parametrs for carbon steel in elevated temperature conditions

	$f_{p,\theta}$, MPa	$f_{y,\theta}$, MPa	$E_{a,\theta}$, MPa	$\epsilon_{p,\theta}$, %	$f_{p,\theta}/f_{y,\theta}$	
S235	$\theta=200^{\circ}\text{C}$	199	220	207 364	0.0958%	0.904
	$\theta=300^{\circ}\text{C}$	166	207	202 137	0.0820%	0.799
	$\theta=400^{\circ}\text{C}$	132	228	189 171	0.0696%	0.578
	$\theta=500^{\circ}\text{C}$	98	191	165 880	0.0589%	0.511
	$\theta=600^{\circ}\text{C}$	65	120	137 319	0.0470%	0.536
	$\theta=700^{\circ}\text{C}$	38	72	107 940	0.0356%	0.534
	$\theta=800^{\circ}\text{C}$	24	46	78 543	0.0305%	0.516
	$\theta=900^{\circ}\text{C}$	16	33	49 497	0.0324%	0.489
S355	$\theta=200^{\circ}\text{C}$	300	324	207 364	0.1446%	0.925
	$\theta=300^{\circ}\text{C}$	250	305	202 137	0.1239%	0.820
	$\theta=400^{\circ}\text{C}$	199	334	189 171	0.1052%	0.596
	$\theta=500^{\circ}\text{C}$	148	273	165 880	0.0889%	0.540
	$\theta=600^{\circ}\text{C}$	98	179	137 319	0.0710%	0.545
	$\theta=700^{\circ}\text{C}$	58	109	107 940	0.0538%	0.534
	$\theta=800^{\circ}\text{C}$	36	70	78 543	0.0461%	0.517
	$\theta=900^{\circ}\text{C}$	24	49	49 497	0.0490%	0.497

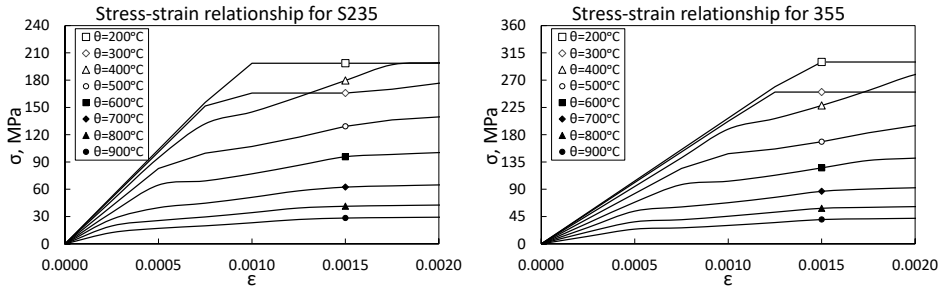


Figure 3.17: Poh material model for carbon steel in elevated temperature conditions

3.3.6 Comparison of the different material models

Differences between the presented material models are evident. In order to better visualize the differences the stress-strain curves for different models are plotted in one diagram for steel grade S355 and various temperatures (Figure 3.19). It is obvious that the ECCS model differs from others for temperatures higher than 200°C quite significantly. Although the other three models also show differences, it can be observed with certain level of abstraction that for temperatures below 700°C the stress-strain relationships are relatively similar.

In order to analyse the differences more deeply, the results of the buckling curves for different material models are presented in Figure 3.20. Calculations were performed only for the steel grade S355 and ECCS material model was ignored. It can be seen, that only for temperature 200°C all three material model give results close to each other. For other temperatures different material models produce mostly different results. The following tendencies can be observed: for temperatures below 700°C and for small column height (slenderness) values the results for all three material models produce relatively similar results; for all temperature values the shape of the curves corresponding to different material models is different; for medium to long columns, results of Lie and Poh models predict higher buckling capacity compared to Eurocode model and the discrepancy between the results is growing with rising temperature; for temperatures higher than 700°C the results for Poh material model predict higher buckling capacity compared to both Lie and Eurocode models.

Presented results have confirmed that buckling capacity is strongly dependent on the material model. The adequacy of the steel material model is still in the focus of researchers [70], [80]. Eurocode material model is sometimes criticized for lack of details behind the test data and model composition [70], [80]. On the other hand, Poh's material model is referred to as one based on a large set of experimental data and demonstrating better correlation with tests when used with high-temperature creep model [80]. Tests used for the basis of the Eurocode material model were performed in transient state and the thermal creep was at least partly accounted for [73]. This could explain the significant differences between the material models (Figure 3.19) and buckling curves (Figure 3.20) for temperature values above 500°C. During the research the choice was made in favour of Eurocode 3 material model. The main reasons behind this choice are as follows:

- utilization of Poh's material model would imply explicit implementation of thermal creep model, while Eurocode 3 material model partly takes thermal creep influence into account;
- in Figure 3.18 reduction coefficients for effective yield strength and elastic modulus are presented. Reduction coefficients values from different authors are compared with Eurocode (reproduced from [70]). Reduction coefficient values of Eurocode are generally on the safe side.

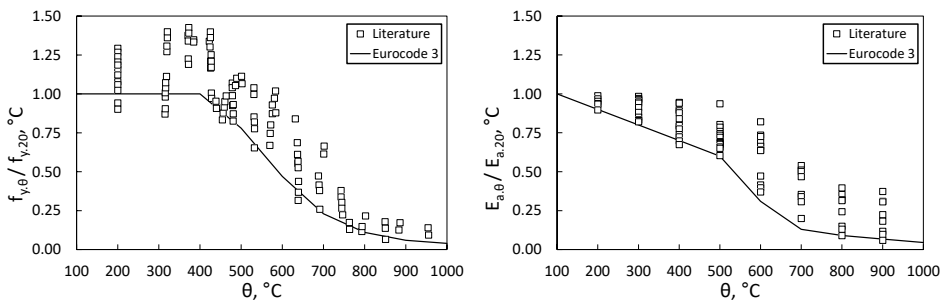


Figure 3.18: Variation of reduction coefficients for effective yield strength and elastic modulus

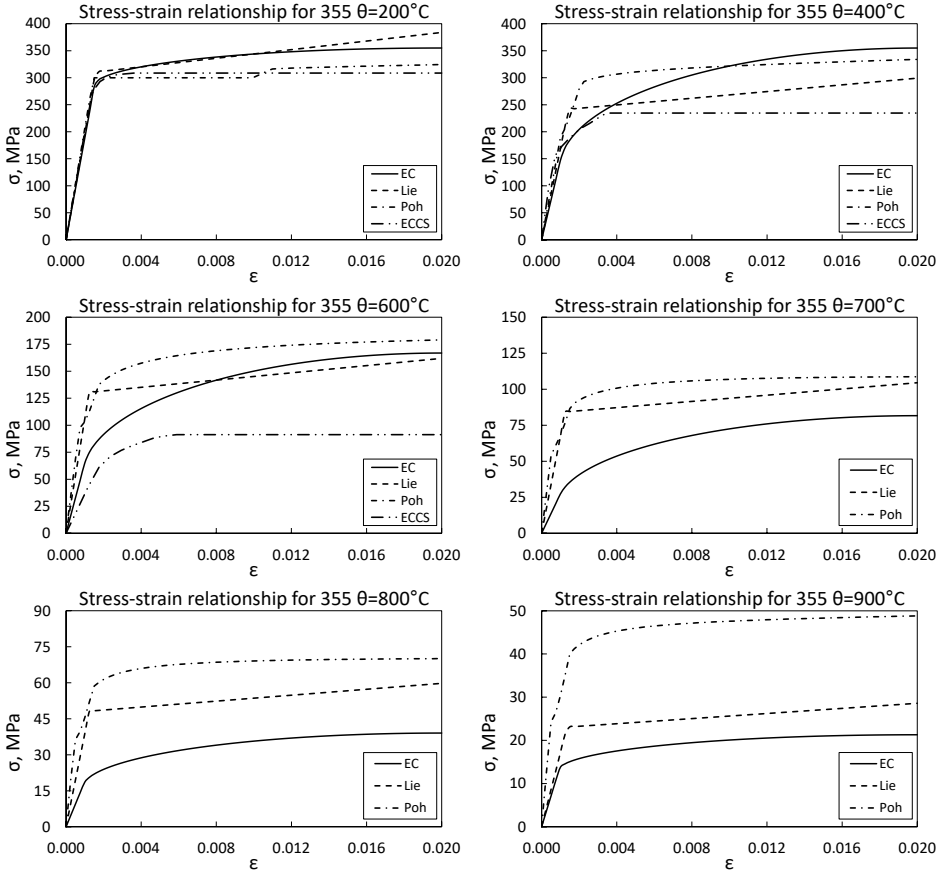


Figure 3.19: Comparison of the material models

3.3.7 Thermal properties

Models of thermal properties were adopted from EN 1993-1-2 [20]. In the context of this work three thermal properties are in the focus of interest: thermal elongation $\Delta L/L$, specific heat c_a and thermal conductivity λ_a . All thermal properties are temperature dependent. Dependence of thermal elongation on temperature is presented in (3-53). Dependence of specific heat on temperature is characterized by (3-54). Dependence of thermal conductivity on temperature is characterized by (3-55).

$$\begin{aligned} \theta < 750^\circ\text{C}: \quad \frac{\Delta L}{L} &= 1.2 \cdot 10^{-5} \theta + 0.4 \cdot 10^{-8} \theta^2 - 2.616 \cdot 10^{-4} \\ 750^\circ\text{C} \leq \theta < 860^\circ\text{C}: \quad \frac{\Delta L}{L} &= 1.1 \cdot 10^{-2} \end{aligned} \quad (3-53)$$

$$\begin{aligned} 860^\circ\text{C} \leq \theta < 1200^\circ\text{C}: \quad \frac{\Delta L}{L} &= 2 \cdot 10^{-5} \theta - 6.2 \cdot 10^{-3} \\ \theta < 600^\circ\text{C}: \quad c_a &= 425 + 7.73 \cdot 10^{-1} \theta - 1.69 \cdot 10^{-3} \theta^2 + 2.22 \cdot 10^{-6} \theta^3 \\ &\quad \text{J/kgK} \\ 600^\circ\text{C} \leq \theta < 735^\circ\text{C}: \quad c_a &= 666 + 13002/(738 - \theta) \text{ J/kgK} \\ 735^\circ\text{C} \leq \theta < 900^\circ\text{C}: \quad c_a &= 545 + 17820/(\theta - 731) \text{ J/kgK} \end{aligned} \quad (3-54)$$

$$900\text{ }^{\circ}\text{C} \leq \theta < 1200\text{ }^{\circ}\text{C}: c_a = 650\text{ J/kgK}$$

$$\theta < 800\text{ }^{\circ}\text{C}: \lambda_a = 54 - 3.73 \cdot 10^{-2} \theta\text{ W/mK}$$

$$800\text{ }^{\circ}\text{C} \leq \theta < 1200\text{ }^{\circ}\text{C}: \lambda_a = 27.3\text{ W/mK}$$

(3-55)

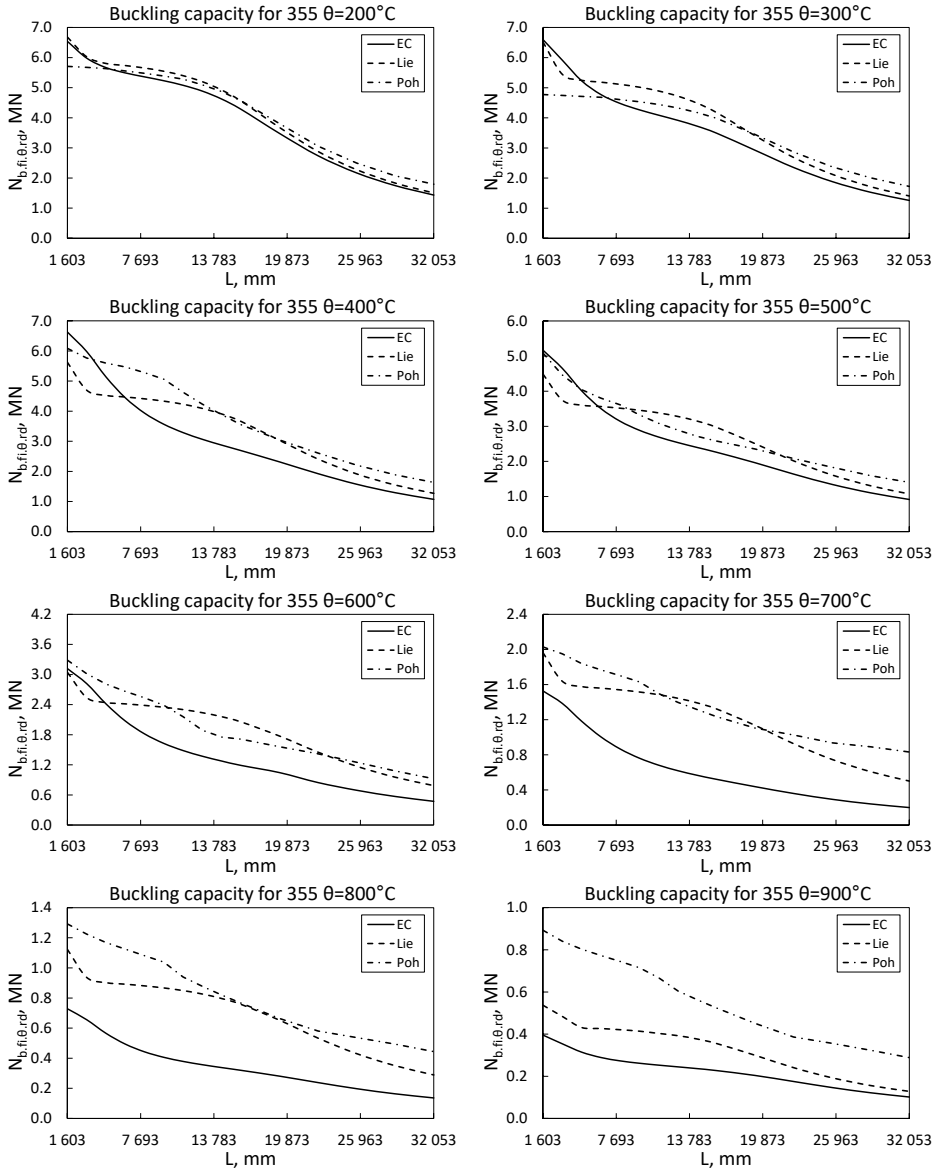


Figure 3.20: Buckling curves for different material models

3.4 Residual stresses

Residual stresses are known to have considerable influence on the stability of steel structural elements. Actual distribution patterns of residual stresses are complicated and vary with section topology and production technology (rolled or welded). A number of simplified distributions of residual stresses have been proposed and are nowadays

commonly used in structural modelling. Residual stresses do not influence section plastic capacity directly, but due to the residual stresses higher strains are needed to reach the fully plastic state of the section. Residual stresses impact column mechanical behaviour mostly by influencing its stiffness. It is generally acknowledged, that residual stresses have less influence on the column buckling capacity in elevated temperature conditions than in normal temperature conditions [81], [82].

In this work residual stresses are accounted for according to the patterns from one of the Eurocode 3 background documents [53] as is presented in Figure 3.21. Patterns used in this work are based on the assumption, that residual stresses are defined in relation to S235 steel class. It is expected, that influence of residual stress is lower for higher steel grades. In this research the influence of residual stresses on the buckling capacity of the axially loaded steel columns was estimated as follows. The results for models accounting for residual stresses are compared with the results for models without residual stresses as reported in section 5.6.

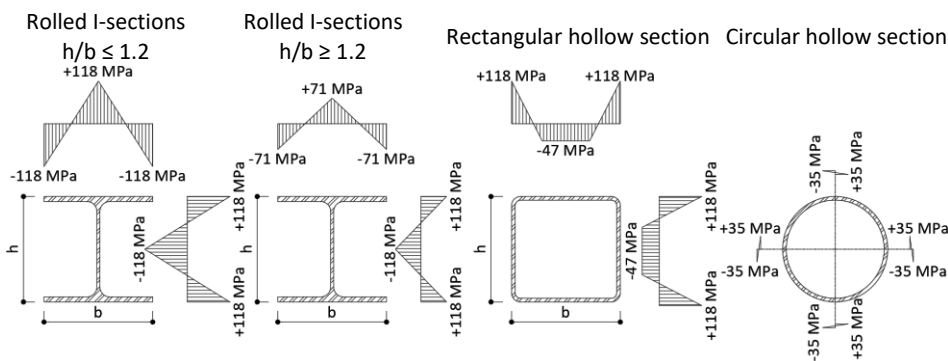


Figure 3.21: Residual stress distribution patterns

3.5 Summary

Aspects of mechanical modelling were investigated in this section. At first numerical modelling was addressed. The implementation of beam-type finite elements for the problem of steel column buckling in fire was justified. Geometrical model and boundary conditions were described. Impact of loading history, thermal elongation and restraint on the buckling capacity were estimated. It was concluded that loading history has no considerable effect. The effect of thermal elongation and restraint were concluded to be minor and will not be accounted for further in this work. Influence of local buckling was estimated. Although the influence of local buckling is in some cases quite significant, it was concluded that this influence will not be accounted for further in this work and the problem of local buckling must be addressed separately. Non-linear FEM procedure was described, which will be extensively used for numerical simulations further in this work.

Material models proposed by different researchers have been investigated. Eurocode material model was chosen because of its consistent format and the fact that it partially accounts for the effects of thermal creep.

The patterns of initial residual stresses commonly in the structural steel modelling have been described. Residual stresses will be accounted for further in this work.

4 Methodology of probabilistic analysis

4.1 Overview

Probabilistic approach to buckling resistance of steel column in fire is the core topic of this thesis. In this chapter the aspects related to the reliability analysis are presented. Methodology of reliability analysis is described. Issues of target reliability levels and fire probability are discussed. Parameter uncertainties for resistance, loading and thermal variables are described. Existing structural safety concepts are described. Methodology of the sensitivity analysis is presented.

The methodology enables to perform an extensive probabilistic analysis of a steel column in fire conditions, the results of which are used to compose reliability based design method.

4.2 Reliability analysis

The main principles of the reliability theory are shortly presented here according to Holický [83]. The fundamental principle of the reliability theory can be formulated as follows: the action effect E must not be greater than the resistance R of the structure.

$$E \leq R \quad (4-1)$$

In the real world of structures, both variables E and R are to a certain degree random. Due to the randomness of the variables, condition (4-1) cannot be expected to be fulfilled with the 100% probability, i.e. it has to be accepted that the probability of failure cannot be expected to be 0. The main objective of the reliability theory is to estimate the probability of failure p_f (4-2) and provide tools with the purpose of controlling the failure probability within certain limits.

$$p_f = P(E > R) \quad (4-2)$$

Random nature of the variables E and R implies that both variables have certain distribution. In most cases the distribution of action and resistance variables can be effectively approximated by one of the common distribution types (Normal Gaussian, Lognormal etc.), for which mathematical representation exists. In Figure 4.1 example distributions are presented: resistance distribution R is characterized by its mean value μ_R and standard deviation σ_R ; action (load) distribution E is characterized by its mean value μ_E and standard deviation σ_E . There is an overlapping zone between probability density functions for action and resistance. Within this zone, fulfilment of the condition $R > E$ cannot be guaranteed for all realizations of variables E and R . The fulfilment of the condition $\mu_R > \mu_E$ cannot itself guarantee, that the failure probability remains in the prescribed limits. In order to guarantee specific failure probability value, mean values and variances of both variables must be taken into consideration.

Random variable X is characterized by mean value μ_X and standard deviation σ_X with normal distribution and has the following probability density function:

$$\varphi_X = \frac{1}{\sigma_X \sqrt{2\pi}} e^{\left[-\frac{1}{2} \left(\frac{X - \mu_X}{\sigma_X} \right)^2 \right]} \quad (4-3)$$

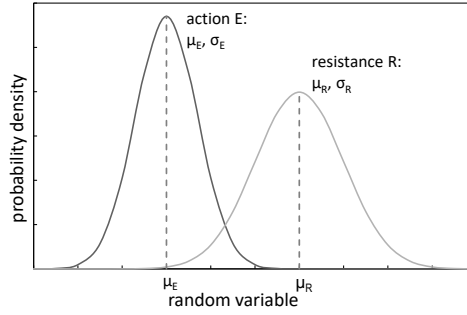


Figure 4.1: Schematic distributions of action E and resistance R

Probability can then be presented by means of a distribution function as follows:

$$\Phi_X(x) = P(X \leq x) = \int_{-\infty}^x \frac{1}{\sigma_X \sqrt{2\pi}} e^{\left[-\frac{1}{2} \left(\frac{x - \mu_X}{\sigma_X}\right)^2\right]} dx \quad (4-4)$$

The distribution function (4-4) for each given value x defines the probability that the random variable X value will be equal or lower than x . Integral (4-4) does not have an analytical solution. In practice, the integral can be solved numerically or precalculated tables can be used. In order to use precalculated tables, the random variable X must be replaced by the standardized variable U (4-5). Probability density function of the variable U can be presented as (4-6) and probability distribution function as (4-7).

$$U = \frac{X - \mu_X}{\sigma_X} \quad (4-5)$$

$$\varphi_U(u) = \frac{1}{\sqrt{2\pi}} e^{\left[-\frac{u^2}{2}\right]} \quad (4-6)$$

$$\Phi_U(u) = \frac{1}{\sqrt{2\pi}} \int_{-\infty}^u e^{\left[-\frac{t^2}{2}\right]} dt, \text{ where: } t = \frac{x - \mu_X}{\sigma_X} \quad (4-7)$$

If the two variables E and R are normally distributed, direct calculation of the failure probability using (4-4) is complicated. Effective solution can be found by introducing reliability margin variable G :

$$G = R - E \quad (4-8)$$

$$\mu_G = \mu_R - \mu_E \quad (4-9)$$

$$\sigma_G^2 = \sigma_R^2 + \sigma_E^2 \quad (4-10)$$

As both variables are assumed to have normal distribution, the mean value of G can be calculated using (4-9) and variance using (4-10). R and E are assumed to be mutually independent. Probability of failure can then be reformulated:

$$p_f = P(E > R) = P(G < 0) = \Phi_G(0) \quad (4-11)$$

Random variable G can be transformed to the standardized form using (4-5). U corresponding to $G = 0$ is denoted by u_0 :

$$u_0 = \frac{0 - \mu_G}{\sigma_G} = -\frac{\mu_G}{\sigma_G} \quad (4-12)$$

Probability of failure is given as follows:

$$p_f = \Phi_G(0) = \Phi_U(u_0) \quad (4-13)$$

The $-u_0$ value is commonly referred to as the reliability index and is denoted as β :

$$\beta = -u_0 = \frac{\mu_G}{\sigma_G} = \frac{\mu_R - \mu_E}{\sqrt{\sigma_R^2 + \sigma_E^2}} \quad (4-14)$$

Standard deviation σ_G multiplied by the reliability index β gives the distance between the mean value of G and 0 (Figure 4.2).

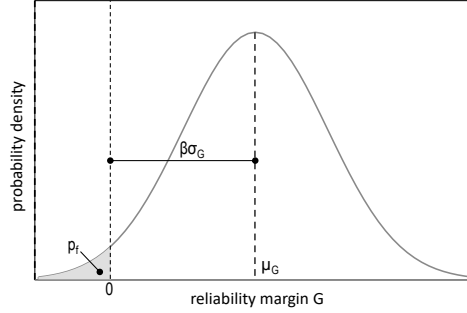


Figure 4.2: Reliability index

The case of two normally distributed variables is straightforward. In reality mostly and in case of axially compressed columns in fire particularly basic variables (E and R) are themselves functions of multiple random variables which have of the different distribution types. In addition to that the response function of the resistance variable is sometimes non-linear in relation to its input variables as it is definitely in case of buckling problem in fire. Therefore simple mathematical models (4-3) ... (4-7) cannot be used. Let $G(\mathbf{X})$ denote the non-linear performance function of the X_1, X_2, \dots, X_n random variables. Then the failure probability can be expressed as:

$$p_f = P(G(\mathbf{X}) < 0) = \int_{G(\mathbf{X}) \leq 0} \varphi(\mathbf{X}) d\mathbf{X} \quad (4-15)$$

For the problem under consideration the composition of the probability density function $\varphi(\mathbf{X})$ is problematic and numerical methods should be implemented. In this work Monte-Carlo (MC) method is applied. MC method is referred to as a zero-one indicator based method operating in the original space of variables \mathbf{X} . MC method is based on the assumption that an effective random number generator is available. Today available random number generators allow to generate effectively series of desired sample size and distribution type. The scheme for implementing MC method for the reliability analysis as follows:

- For each random variable $X_{1...m}$ a random series of size n is generated based on the given distribution parameters (distribution type, mean and standard deviation). As a result, the input matrix of n rows and m columns is formed.
- For each row in the input matrix, the reliability margin G is calculated.
- The number of all realization is n , the number of realizations for which $G < 0$ (failure) is denoted as n_f . The probability of failure is then calculated as:

$$p_f = \frac{n_f}{n} \quad (4-16)$$

The defined probability can be compared with the target level. The accuracy of the estimation of probability using (4-16) is growing with the growing number of realizations n .

A general rule for the specification of the minimal number of realizations n is as follows: if the expected order of probability is 10^{-k} , the number of realizations n must be equal to $k + 2$. For the problem which is addressed in this work, the required number of simulations is expected to be between 10^5 and 10^6 . The solution of one buckling capacity problem in fire conditions with non-linear FEM on average takes 2 seconds (3.60 GHz CPU 8 cores). It is clear, that the time consumption for the whole simulation process can become unacceptable which is one of the shortcomings of the MC method. A number of techniques is available to raise the speed of the MC method. This issue is addressed further in sections 4.6, 4.7 and 6.4.

4.3 Target reliability level and probability of fire

According to EN 1990 [34], reliability is measured and judged based by the reliability index β . Reliability index is an alternative representation of failure probability. Mathematical formulation of the reliability index β has already been given in (4-14). Reliability index is always represented by the probability distribution function of the standardized Normal Gauss distribution (4-13). According to EN 1990 [34] the target reliability index in general depends on the type of structure (consequence class) and reference period depending on structural life-time. Reliability index target values for 50 years reference period are presented in Table 4-1 [34].

Table 4-1: Target reliability index values according to EN 1990

Consequences Class / Reliability Class	Minimum value for β	Failure probability p_t
CC3 / RC3	4.3	8.540×10^{-6}
CC2 / RC2	3.8	7.235×10^{-5}
CC1 / RC1	3.3	4.834×10^{-4}

The presented values of target reliability index are related to the case of normal temperature conditions. The same target values for fire conditions are implemented [34]. It has been proposed to differentiate reliability target levels depending on the evacuation conditions has been made [19]. In fire conditions the target reliability level $\beta_t = 3.8$ is used for 50 years reference period corresponding to the target failure probability $p_t = 7.235 \times 10^{-5}$ [11].

An important aspect related to the reliability in fire conditions, is the fact that emergence of fire itself is a matter of probability. The condition for target probability can be presented as:

$$p_{f.fi} p_{fire} \leq p_t \quad (4-17)$$

, where $p_{f.fi}$ is the failure probability in fire conditions, p_{fire} is the probability of fire emergence and p_t is the target failure probability.

The target failure probability accounting for the probability of fire can be introduced as (4-18). In any particular case the actual failure probability $p_{f.fi}$ must remain smaller or equal to the target failure probability in fire $p_{f.fi.t}$.

$$p_{f.fi.t} = \frac{p_t}{p_{fire}} \quad (4-18)$$

Target reliability index accounting for the probability of fire can then be represented as:

$$\beta_{f.f.i.t} = \Phi^{-1}(p_{f.f.i.t}) = \Phi^{-1}\left(\frac{p_t}{p_{fire}}\right) = \Phi^{-1}\left(\frac{7.23 \cdot 10^{-5}}{p_{fire}}\right) \quad (4-19)$$

, where Φ^{-1} is the inverse of the cumulative standard normal distribution (4-7).

The data and the model for fire probability estimation can be taken from Scheich et al [19]. The probability of a severe fire per year is expressed as (4-20):

$$p_{fire} = p_1 p_2 p_3 p_4 A_{fi} \quad (4-20)$$

where p_1 is probability of severe fire (per 1 m² of a fire compartment area and per year); p_2 is reduction factor depending on the fire brigade type and time between alarm and firemen intervention; p_3 is reduction factor in case automatic fire detection and/or automatic transmission of the alarm are present; p_4 is reduction factor for sprinkler system type and accounting for the probability of system failure; A_{fi} is fire compartment area (m²).

Table 4-2: Probability of severe fire p_1

Occupancy type 10⁻⁷ / (m² x year)	
Office	2 -- 4
Dwelling	4 -- 9
Industrial	5 -- 10

Table 4-3: Reduction factor p_2

	Signal transfer time		
	≤ 10 min	10 min ≤ t ≤ 20 min	20 min ≤ t ≤ 30 min
Professional Firemen	0.05	0.10	0.20
Non-Professional Firemen	0.10	0.20	1.00

Table 4-4: Reduction factor p_3

Active measures	
Detection by Smoke	0.0625
Detection by Heat	0.2500
Automatic Alarm transmission to Fire Brigade	0.2500

Table 4-5: Reduction factor p_4

Type of sprinkler	
Normal (in accordance with regulations)	0.02
High standard	0.01 -- 0.005
Low standard	≥ 0.05

JCSS Model Code [84] presents another version of the fire probability model (4-21).

$$p_{fire} = p_{fi} p_{ign} A_{fi} \quad (4-21)$$

, where p_{ign} is the probability of fire ignition and p_{fi} is the probability of flashover.

Table 4-6: Probability of ignition p_{ign}

Occupancy type $10^6 / (m^2 \times \text{year})$	
Dwelling / School	0.5 -- 4
Shop / Office	1.0
Industrial	2 -- 10

Table 4-7: Probability of flashover p_{fl}

Protection method	
Public fire brigade	0.1
Sprinkler	0.01
Fire brigade + alarm system	0.001 to 0.01
Sprinkler + residential fire brigade	0.0001

Both presented models are a linear function of fire compartment area A_{fi} . Fire compartment area can vary in relatively broad limits. The fact that the fire probability increases with the area, in certain cases may lead to abnormally high probability of fire. For example for 10 000 m² industrial building with minimal fire-fighting measures the probability of fire for 50 years reference period is 50%. Obviously this value is unacceptably high and should not be tolerated. It is logical to assume that for compartments with big area and high basic fire probability certain measures will be implemented, which will bring the fire probability down.

In the Eurocode system the interaction between the target reliability level and the fire probability is addressed via design fire load density $q_{f,d}$ which is a function of factor δ_{af} (Annex E of EN 1991-1-2 [12]). This approach was proposed in [19]. Factor δ_{af} is defined as the relation between design fire load density $q_{f,d}$ and the 80% fractile of the characteristic value of the fire load density $q_{f,k}$ (4-22).

$$\delta_{af} = \frac{q_{f,d}}{q_{f,k}} = 1.05 \frac{1 - \frac{\sqrt{6}}{\pi} V_{af} [0.577 + \ln(-\ln(\Phi(0.9\beta_{f,fi,t})))]}{1 - \frac{\sqrt{6}}{\pi} V_{af} [0.577 + \ln(-\ln 0.8)]} \quad (4-22)$$

, where 1.05 is the safety factor for the model; V_{af} is the coefficient of variance for fire load density (0.3); $\beta_{f,fi}$ is the target reliability index in fire situation.

The relation between p_{fire} , $p_{f,fi,t}$, $\beta_{f,fi,t}$ and δ_{af} is presented in Figure 4.3.

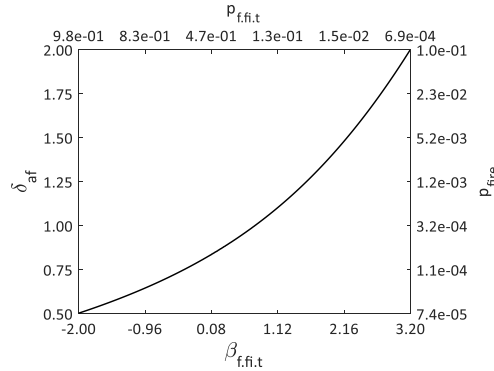


Figure 4.3: Relation between p_{fire} , $p_{f,fi,t}$, $\beta_{f,fi,t}$ and δ_{af} corresponding to the target failure probability $p_t = 7.235 \times 10^{-5}$

Factor δ_{af} is split into 3 factors (4-23) in order to account for influence of compartment size δ_{q1} , type of occupancy δ_{q2} and active firefighting measures δ_n on the fire probability p_{fire} .

$$\delta_{af} = \delta_{q1} \delta_{q2} \delta_n = \delta_{q1} \delta_{q2} \prod_{i=1}^{10} \delta_{ni} \quad (4-23)$$

Values of the factors are presented in Table 4-8, Table 4-9 and Table 4-10.

Table 4-8: Factor δ_{q1}

Fire compartment floor area A_f , m ²	Danger of fire activation δ_{q1}
25	1.10
250	1.50
2 500	1.90
5 000	2.00
10 000	2.13

Table 4-9: Factor δ_{q2}

Example of occupancies	Danger of fire activation δ_{q2}
artgallery, museum, swimming pool	0.78
offices, residence, hotel, paper industry	1.00
manufactory for machinery & engines	1.22
chemical laboratory, painting workshop	1.44
manufactory of fireworks or paints	1.66

Table 4-10: Factor δ_n

Active fire fighting measures δ_{ni}											
Automatic Fire Suppression				Automatic Fire Detection			Manual Fire Suppression				
Automatic Water Extinguishing System	Independent Water Supplies			Automatic fire Detection & Alarm		Automatic Alarm Transmission to Fire Brigade	Work Fire Brigade	Off Site Fire Brigade	Safe Access Routes	Fire Fighting Devices	Smoke Exhaust System
	0	1	2	by heat	by smoke						
δ_{n1}	δ_{n2}			δ_{n3}	δ_{n4}	δ_{n5}	δ_{n6}	δ_{n7}	δ_{n8}	δ_{n9}	δ_{n10}
0.61	1.00	0.87	0.70	0.87	0.73	0.87	0.61	0.78	0.9/1.0/ 1.5	1.0/1.5	1.0/1.5

After factor δ_{af} is calculated the design fire load can be determined as described above. Then the temperature evolution can be modelled using Eurocodes Parametric Fire Curve method, zone model or other methods (will be addressed in 4.4.3).

A number of works has been published in recent years ([47], [49], [50]) dedicated to the reliability of structures in fire, where authors have raised discussion concerning the approach to fire probability in general and in the context of the NFSC specifically, referring to the need for further studies due to the substantial influence of fire probability on safety evaluation. The present work is composed in compliance with the current safety framework of the Eurocode system and does not address the interpretation of the fire probability model.

4.4 Parameter uncertainties

Probabilistic approach assumes that the uncertainty characteristics of the model parameters are known. For further development of the procedure the parameters are allocated to resistance R parameters group and load E parameters group. In case of fire conditions, special attention should be given to temperature, which on the one hand belongs to the load parameter group as an action, but on the other hand has direct influence on the resistance properties of a structure. Therefore it was decided to consider temperature T as a separate group of uncertain parameters.

4.4.1 Resistance uncertainties

Resistance uncertainties and corresponding statistical parameters are presented in Table 4-11. Statistical characteristics for variables in Table 4-11 were obtained as follows: for geometric variables 1, 2, 3, 4 from Melcher *et al.* [85], for material resistance variables 5 and 6 from JCSS [86], for global imperfections from Kala [87], for maximum residual stress from Kala and Valeš [88] and model uncertainty variable 9 characteristics from Schleich and Cajot [18].

For yield limit stress three values are presented – corresponding to the 95% probability of the nominal yield limit for the steel classes S235, S355 and S460. For initial imperfection also two sets of values are presented, because the resistance model treats imperfection as an absolute value (does not account for “-” or “+” sign of the factual imperfection).

The variation of the reduction coefficients for steel mechanical properties in fire conditions ($k_{y,\theta}$, $k_{p,\theta}$, $k_{E,\theta}$ section 3.3.2) is not taken into account for the following reasons:

- It is assumed that the reduction factors values are dependent on the basic steel mechanical properties in normal temperature conditions ($f_{y,20^\circ\text{C}}$ and $E_{a,20^\circ\text{C}}$). The variability of the reduction factors is therefore at least partially accounted for by the variability of the $f_{y,20^\circ\text{C}}$ and $E_{a,20^\circ\text{C}}$;
- The data related to the variability of the reduction factors is scarce. The adequacy of the available data is questionable. As an example effective yield strength reduction coefficient variation is analysed as presented in Figure 3.18 (reproduced from [70]). According to the presented data, reduction coefficient value for the 200°C is higher than 1.0. This could be explained by the variability of the basic steel property – yield limit stress value in normal temperature. The situation with the availability of the data on the variability of the proportionality stress reduction factor is even worse, but proportionality limit stress is an important parameter of the Eurocode material model (section 3.3.2, [20]);
- Resistance model uncertainty factor should potentially offset the possible negative impact of the disregard of the variability of reduction factors.

4.4.2 Loading uncertainties

Load action is commonly a combination of two parts: permanent load (self-weight) and variable load (live load, snow load, wind load, etc.). For permanent load, the characteristic value G_k was taken as the mean value of Normal distribution with coefficient of variation (ratio of the variance to the mean value, further denoted as COV) being equal 0.1 [89]. The situation with variable load (imposed, snow, wind etc.) is more complicated, because of the time-variant nature of the load case under consideration. Combination of loads in fire is a challenging issue. Turkstra's approximation is used here to transform the time-variant domain to the time-invariant domain [90]. Fire effect

Table 4-11: Resistance uncertainties summary

ID	Description	Symbol	Density	Unit	Mean value (μ_i)	Std. deviation (σ_i)	Coefficient of variation (COV)
1	section height	h	Normal	mm	Nominal	--	0.0044
2	section width	b	Normal	mm	Nominal	--	0.0098
3	wall thickness	t ₁	Normal	mm	Nominal	--	0.0396
4	flange thickness	t ₂	Normal	mm	Nominal	--	0.0461
5	yield limit stress	f _y	Log-normal	MPa	264.20	18.494	0.0700
					399.50	27.965	
					517.50	36.225	
6	elasticity modulus	E _{a,20°C}	Normal	MPa	210 000	12 600	0.0300
7	global imperfection	e ₀	Normal	mm	0	0.000765 L	--
					0.000611 L	0.000461 L	0.7547
8	maximum residual stress	RS	Normal	MPa	90.0	18.0	0.2000
9	model uncertainty	--	Log-normal	--	1.0	0.15	0.1500

(temperature) is treated as the dominant action, which is fully justified when dealing with fire case related analysis as there is no point in treating fire effect as a secondary action in relation to variable loads. According to the Turkstra's combination rule the leading action (fire effect / temperature) is considered for the whole life time, the secondary actions are considered by the point-in-time value. Point-in-time values can themselves be approximated by the annual extremes for the wind and snow loads and 5-year extreme value for the imposed load [83]. The summary of the statistical characteristics of different types of variable loads are presented in Table 4-12, adopted from Holicky [83]. Statistical parameters for the 50-years reference period are presented for comparison. Gumbel Max distribution was adopted for the characteristic value of variable action in accordance with [90]. Statistical parameters of total load $V_k = G_k + Q_k$ depend on the fraction of each load type in the total load. In order to cover as wide spectrum of variable load actions as possible, factor α (4-24) is introduced, analogous to the approach proposed in [41]. Factor α can vary from 0 (only permanent load is applied) to 1.0 (only variable load is applied).

Load model uncertainties were accounted for in accordance with JCSS Model Code [91] applying uncertainty factor with mean factor value of 1.0 and COV 0.05.

$$\alpha = \frac{Q_k}{G_k + Q_k} \quad (4-24)$$

4.4.3 Temperature related uncertainties

Temperature has a fundamental influence on the buckling behaviour of a steel column in fire conditions, modifying mechanical properties of steel. In this sense temperature uncertainties could be related to the group of resistance uncertainties. On the other hand, the emergence of fire and the evolution of temperature and corresponding uncertainties are related to the external factors: compartment configuration, fire load,

Table 4-12: Statistical parameters of variable load

Load nature	Nominal load value symbol	Reference period	Mean value (μ)	Std. deviation (σ)	Coefficient of variation (COV)
Imposed	Q_k	5-years	0.20 Q_k	0.22 Q_k	1.10
		50-years	0.60 Q_k		0.37
Wind	W_k	1-year	0.30 W_k	0.25 W_k	0.83
		50-years	0.70 W_k		0.36
Snow	S_k	1-year	0.35 S_k	0.25 S_k	0.71
		50-years	1.10 S_k		0.23

protection system etc. The aspect has similarities with the load related uncertainties group.

Main variables and the source of uncertainty of the temperature evolution model are summarized in Table 4-13. Statistical characteristics of the temperature related parameters were obtained from references: mean values for the fire load q_f density from EN 1991-1-2 [12]; COV of enclosure thermal inertia b_{th} from Zhang [45]; opening factor O from JCSS Model Code [84]. Definition of enclosure thermal inertia b and opening factor O corresponds to the definition used in the Eurocode Parametric Fire Curve model (Annex A1). Thermal resistance parameter of an insulation material d_p/λ_p is defined as thermal insulation thickness d_p divided by the thermal conductivity λ_p . Due to the lack of statistical data regarding statistical properties of protection material approach used by Zhang [45] was adopted, where parameter d_p/λ_p is characterized by Log-normal distribution with mean value being equal to nominal parameter value and COV is 0.3. Statistical parameters of model uncertainty were taken as 1.0 for the mean factor value and corresponding COV 0.10. Geometrical parameters of the compartment and thermal properties of the steel material are assumed to be deterministic.

Eurocode Parametric Fire Curve Method (EC1 method; [12]) has been used in this work to model the gas temperature rise during fire. Schleich et al [18] have analysed the performance of this method for the temperature evolution and demonstrated that the

Table 4-13: Temperature uncertainties summary

ID	Description	Symbol	Density	Unit	Mean value (μ_i)	Coefficient of variation (COV)
1	fire load density	q_f	Log-normal	MJ/m ²	Nominal	0.30
2	compartment width	W	Deterministic	m	--	--
3	compartment length	L	Deterministic	m	--	--
4	compartment height	H	Deterministic	m	--	--
5	enclosure thermal inertia	b_{th}	Normal	J/(m ² s ^{0.5} K)	Nominal	0.09
6	opening factor	O	Log-normal	m ^{0.5}	0.8 Nominal	0.22
7	insulation material thermal resistance	d_p/λ_p	Log-normal	m ² K/J	Nominal	0.30
8	model uncertainty	--	Log-normal	--	1.0	0.10

correlation coefficient for the EC1 method and test results to be 0.83. The method is described in Annex A1. The method has a number of limitations. It is valid in a certain range of enclosure thermal inertia b_{th} and opening factor O . The limits for those parameters correlate well with the limits for practical application. There are also strict limitations of the compartment geometry: compartment floor area $A_{fi} \leq 500 \text{ m}^2$ and compartment height $H \leq 4.0 \text{ m}$. These limitations have more serious impact on the practical applicability. In order to analyse fire gas temperatures for a wider set of cases, more advanced methods must be implemented, for example zone models or CFD based methods. Nowadays, an efficient tool to perform fire temperature analysis of the moderate complexity is OZone software package, based on the combined zone method. The tool is widely used in practice and research. The theory behind the OZone software and the zone methods can be found in [16]. Comparison between the test data and the software output can be found in [16] and [19]. OZone software has built-in possibility for the definition of the design fire load density in accordance with Annex E of the EN 1991-1-2. For both methods (EC1 and OZone) temperature evolution in a steel section is calculated in the similar way – the method of EN 1993-1-2 [20] is implemented as described in Annex A2.

In this work the fire temperature rise model is not applied implicitly in the reliability analysis. Fire simulations are performed in a separate procedure and the generated temperature distributions are imported into the reliability procedure. Monte-Carlo Simulation (MCS) implementing Eurocode Parametric Fire Curve Method (EC1 method) was used for the wide range of the fire compartment configurations. EC1 model was chosen because it is formulated in simple analytical form and can be easily integrated into the MCS procedure. The temperature rise models can be classified as lower and higher precision models. For further reliability studies it would be important to know how the choice of the temperature model influence the results of the reliability analysis. At first it is assumed that the model of higher precision should give lower output variance, which leads to lower failure probability for a given mean value of response. Consequently, if the temperature distributions are generated using lower precision model (EC1 method), the estimation of temperature variance can be expected to be on the safe side. In order to test this assumption, Maximum Entropy Multiplicative Dimensional Reduction Method (ME-MDRM) was used as proposed by Zhang [92]. ME-MDRM was used in combination with the software package OZone. In addition to the ME-MDRM, MCS implementing OZone fire simulator is used to generate and analyse temperature distributions for a limited number of fire parameters. The results for the comparison are presented in 6.5.4.

4.5 Safety concepts

The main aim of structural design is to provide certain level of safety accounting for inherent uncertainties of structural system and actions. In structural analysis concepts for safety control can be distinguished into three major groups: fully-deterministic, semi-probabilistic and fully-probabilistic. In fact, these concepts form an evolutionary chain. The main safety concepts are shortly described as follows.

The fully-deterministic approach to safety is based almost entirely on empirical data, acquired through trial and error experience. The concept is demonstrated in Figure 4.4. Global safety factor γ is used to account for all the uncertainties and is estimated based on the past experience.

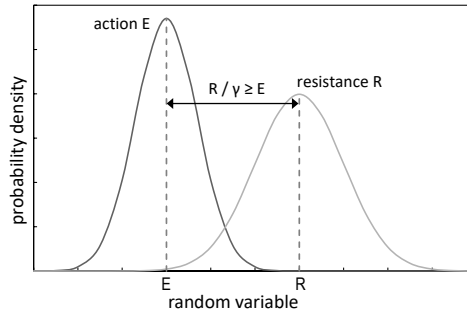


Figure 4.4: Fully-deterministic safety concept

Semi-probabilistic approach is best known for the partial safety factors concept. The approach is demonstrated in Figure 4.5. Two groups of uncertainties are separated: related to action (load) E and related to resistance R , which are represented by the corresponding characteristic values E_k and R_k . The uncertainties are estimated for each group separately and introduced in the form of safety factors: γ_E for the action effect and γ_R for resistance. In addition to the uncertainties of the input variables, safety factors account for the uncertainties of the models [83]. Safety factors are calibrated in order to match the target failure probability p_t . The actual design process is deterministic using the predefined safety factors.

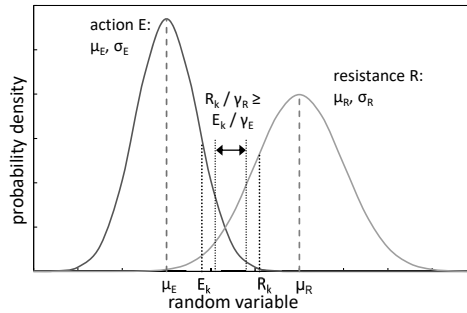


Figure 4.5: Semi-probabilistic safety concept

In the fully-probabilistic approach, the failure probability p_f is calculated directly for a given design configuration accounting for the uncertainties of the input parameters individually and is compared to the target value p_t , as is demonstrated in Figure 4.6.

In the current Eurocode system both semi- and fully-probabilistic approaches are allowed [34]. It is expected that both approaches should lead to the same level of safety. Partial safety factors are assumed to be calibrated by the fully-probabilistic analysis. As in reality this principle is not always followed leading to the scatter of reliability levels [93]. A number of researchers have reported certain inconsistencies in the reliability estimations of structures designed according to Eurocode for ultimate limit state (ULS) [37], [40] and serviceability limit state [41]. In the mentioned works, one of the reasons of reliability misestimations is related to the fraction of the variable load in the total load (factor α formulated as (4-24) in section 4.4.2). In this work failure probability calculations using direct Monte-Carlo simulation were performed in order to demonstrate the aforementioned inconsistencies. Buckling design method of EN 1993-1-1 [57] for the axially loaded column was analysed in ULS. Initially curved element implying first yield criteria was used as the mechanical response model, described in section 2.3.2. Resistance and loading uncertainties were accounted for using data from section 4.4.1

and section 4.4.2. The details of the general scheme of Monte-Carlo simulation is presented further in section 6.5.1. Results are presented in Figure 4.7. Target failure probability for the 50 years reference period and reliability class RC2 (common design problem) is $p_t = 7.235 \times 10^{-5}$ or $\beta_t = 3.8$ as was described in section 4.3. In considerable number of cases the failure probability does not match the target level, which is in line with the results by other researchers [40].

It is assumed that due to the involvement of thermal parameters the task of matching the target probability in case of fire is a more complex comparing to normal temperature conditions. Therefore fully-probabilistic calibration should be implemented. This aspect is one of the main topics of the current research.

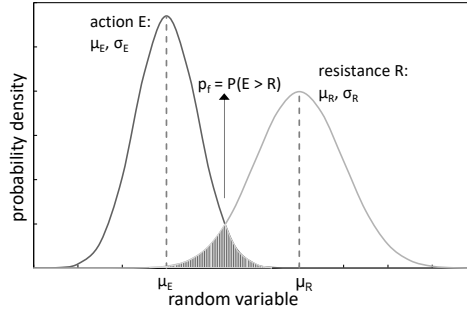


Figure 4.6: Fully-probabilistic safety concept

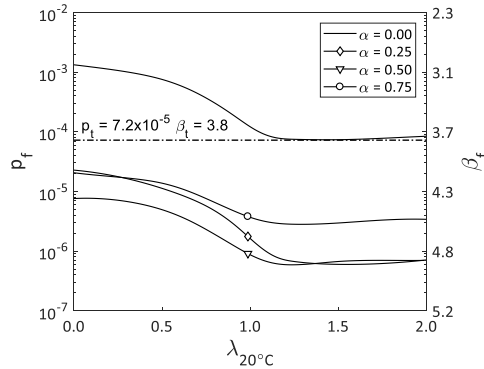


Figure 4.7: Failure probabilities in the ultimate limit state

4.6 Sensitivity analysis

Sensitivity analysis is used in structural modelling to estimate if randomness of input variable should be accounted for or it could be neglected. It is widely used in various fields, where the system output variance as a function of input variables variance is investigated [94]. Sensitivity analysis has been performed for a number of structural design problems [88], [95], [96]. Sensitivity of structural stability problems has been studied by Kala [87].

In this work Sobol's method was used for the sensitivity analysis. Method is only shortly described here according to [97]. $Y = f(X_1, X_2, \dots, X_N)$ is a deterministic model with scalar output, where $X_{1...N}$ are statistically independent model input variables. The variance of Y can be presented in the following form:

$$V(Y) = \sum_i^n V_i + \sum_{i \leq j \leq n}^n V_{ij} \dots + \quad (4-25)$$

$V_i = V(E(Y|X_i))$ is the first order partial variance, $V_{ij} = V(E(Y | X_i, X_j))$ is the second order partial variance etc. Partial variance V_i measures the contribution of variable X_i to the total variance of output $V(Y)$. Partial variance V_{ij} measures the contribution of the interaction between X_i and X_j to the total variance $V(Y)$. Definition of higher partial variances is inductive. Sobol sensitivity indices are obtained by normalizing partial variances:

$$S_i = \frac{V_i}{V(Y)}; S_{ij} = \frac{V_{ij}}{V(Y)}; S_{ijk} = \frac{V_{ijk}}{V(Y)}; \dots \quad (4-26)$$

Total number of Sobol indices is $2^n - 1$ and the sum of all Sobol indices must be 1.0. The variances V_i are estimated using MCS. Sample size was chosen as 10^6 . Computational effort of the Sobol's method for the first and total order sensitivity indices evaluation, is $10^6 \times (2n + 1)$ which is quite demanding. In practice this means that FEM procedure is not efficient enough concerning computational time. Two approaches are used in this work, which will be justified later: polynomial/spline approximation technique and analytical response model. Results of the sensitivity analysis are presented in section 6.2.

4.7 Polynomial and spline approximation

Polynomial approximation is used to optimize the computational time for sensitivity analysis. Buckling capacity of the compressed steel column $N_{Rd,fi,pln}$ is approximated by the polynomial in the form of (4-27) for each fixed column height and temperature value which are two crucial parameters defining axially loaded column mechanics.

$$N_{Rd,fi,pln} = a_0 + \sum_{j=1}^4 \sum_{i=1}^n a_{i+8(j-1)} X_i^j \quad (4-27)$$

, where a_i is the polynomial coefficient and X_i is the input variable (yield limit stress, deformation modulus etc).

Polynomial base is composed of results of 1000 FEM simulations for each column height and temperature values (21 values from 200°C to 900°C). Input variables were chosen using statistical parameters from Table 4-11. Polynomial performance was tested against 1000 cases of randomly generated values of input variables including column height and temperature. Capacity calculate using polynomial $N_{Rd,fi,pln}$ was compared with corresponding capacity calculated using FEM $N_{Rd,fi,FEM}$. Results of the statistical analysis for the comparative factor $N_{Rd,fi,pln}/N_{Rd,fi,FEM}$ are presented in Summary

Methodology of probabilistic analysis was presented in this section. The main ideas of reliability analysis were described. Target reliability levels were addressed. Approach to the estimation of fire probability was reported. Parameter uncertainties for resistance, loading and thermal variables were described. Sobol's method for sensitivity.

In order to account for the temperature influence on the buckling capacity, spline interpolation was used in the following procedure: for each case, solution (4-27) was used to define the capacity values for 21 temperature values (from 200°C to 900°C), forming the spline base; spline interpolation was performed between 21 base values in order to define the column buckling capacity for any temperature.

Spline interpolation technique performance was tested against 1000 cases of randomly generated input variable values including temperature. Capacity calculated using spline NRd.fi.spl was compared with corresponding capacity calculated using FEM. Results of the statistical analysis for the comparative factor $N_{Rd,fi.spl}/N_{Rd,fi.fem}$ of spline and FEM models are presented in Table 4-15.

Table 4-14: Descriptive statistics for the factor $N_{Rd,fi.spl}/N_{Rd,fi.FEM}$

Parameter	Value
Mean	0.999795
Standard Error	0.000473
Standard Deviation	0.010578
Minimum	0.98204
Maximum	1.01795

Table 4-15: Descriptive statistics for the factor $N_{Rd,fi.spl}/N_{Rd,fi.fem}$

Parameter	Value
Mean	0.994705
Standard Error	0.000454
Standard Deviation	0.01435
Minimum	0.97004
Maximum	1.01967

4.8 Summary

Methodology of probabilistic analysis was presented in this section. The main ideas of reliability analysis were described. Target reliability levels were addressed. Approach to the estimation of fire probability was reported. Parameter uncertainties for resistance, loading and thermal variables were described. Sobol's method for sensitivity analysis was described. Polynomial/spline approximation is introduced for the sensitivity analysis to optimize computational time.

Safety concepts of structural systems were described and it was demonstrated. Fully-probabilistic analysis of Eurocode framework reveals that matching the target safety goals is not always achieved even in normal temperature conditions. Due to the involvement of thermal parameters the task of matching the target probability in case of fire is a more complex comparing to normal temperature conditions. There is no comprehensive data about the probabilistic response of steel column fire conditions covering large scope of thermal and mechanical configurations. The objective of the current work is to provide lacking data and propose efficient method for probabilistic evaluation. Results will be presented in the format which enables to apply the proposed method independently of any chosen safety framework, i.e. it can be implemented in combination with Euro code fire safety concept or fire probabilities obtained from other sources of risk analysis.

5 Results of mechanical response

5.1 Overview

Results of the mechanical response of steel column in fire are presented in this section. Numerical program is introduced and results the form of buckling factors for various steel grades, different temperatures and section types are reported. Dependence of bending stiffness on temperature and stress-state is analysed. Distribution of normal stresses at failure for different temperatures and slenderness values is reported. The impact of initial residual stresses on the buckling capacity is demonstrated. Based on the results of numerical simulations an original computationally efficient method for prediction of buckling capacity is proposed and validated.

5.2 Numerical program

In the present work numerical modelling of compression elements at various temperatures was carried out with non-linear FEM procedure described in 3.2.7. The models and methods used were described in sections 2 and 3.3. Program of numerical studies consisted of 24 sections grouped in 4 categories (Table 5-1); 15 slenderness (5-1) values were selected to model columns in 8 temperature ranges (200°C to 900°C); steel grades S235, S355 and S460 were used for all specimens. Total number of models was 8 640.

$$\lambda_{20^{\circ}\text{C}} = \frac{L}{i \pi} \sqrt{\frac{f_{y,20^{\circ}\text{C}}}{E_{20^{\circ}\text{C}}}} \quad (5-1)$$

5.3 Dependence of bending stiffness on stress state

The current Eurocode design method is based on the formulation which assumes constant bending stiffness for both ambient and elevated temperature conditions. In this section bending stiffness dependence on stress-state is analysed.

In Figure 5.1 stiffness reduction curves are presented for various sections in ambient temperature conditions. EI stands for the bending stiffness accounting for material property dependence on stress state, EI_0 is the initial bending stiffness at zero stress state, M is the acting bending moment, $M_{pl,N,rd}$ is the bending moment capacity for certain axial load level. Different curves correspond to different axial load levels. Value of the factor $N/N_{pl,Rd}$, where N is the acting axial load and $N_{pl,Rd}$ is the section axial load capacity is plotted on the curve. It is obvious that the bending stiffness dependence on the stress state is highly non-linear. The bending stiffness remains constant until the moment, where stresses from lateral bending combined with stresses from axial load reach the yield limit stress, which for the ambient temperature conditions coincides with the proportionality limit stress. Starting from this point the bending stiffness drops sharply and the rate with which bending stiffness is reduced depends on the axial load level, section type and section geometrical parameters. Evidently the group of reduction curves for I-section weak axis differs from reduction curve groups for the other section types.

In Figure 5.2 and Figure 5.3 the bending stiffness reduction curves are presented for I-section strong axis and I-section weak axis in variable temperature conditions. EI_{fi} is the

Table 5-1: Sections used for numerical modelling

Section type	Profile	Axis	Description
CHS	CHS48.3x3.0	-----	Circular hollow sections
	CHS127x4.0	-----	
	CHS168.3x5.0	-----	
	CHS219.1x6.0	-----	
	CHS273x8.0	-----	
	CHS323.9x10.0	-----	
RHS	RHS50x3	-----	Rectangular hollow sections
	RHS160x6	-----	
	RHS300x12	-----	
	RHS80x60x4	strong	
	RHS150x100x6	strong	
	RHS300x150x10	strong	
I-Y	HEA100	strong	Hot-rolled I sections
	HEA500	strong	
	HEA1000	strong	
	IPE100	strong	
	IPE300	strong	
	IPE600	strong	
I-Z	HEA100	weak	
	HEA500	weak	
	HEA1000	weak	
	IPE100	weak	
	IPE300	weak	
	IPE600	weak	

bending stiffness in fire accounting for effect of temperature and stress state on material properties, $EI_{fi,0}$ is the bending stiffness in fire accounting effect of temperature on material properties (zero stress state), M is the acting bending moment, $M_{pl,N,rd,fi}$ is the bending moment capacity in fire situation for a certain axial load level. Different curves correspond to the different axial load levels. Value of the factor $N/N_{pl,Rd,fi}$, where N is the acting axial load and $N_{pl,Rd,fi}$ is the section axial load capacity in fire situation is plotted on the curve. It can be observed that the curve shape is strongly dependent on the load level factor $N/N_{pl,Rd,fi}$, i.e. the stress level caused by the axial load. It is visually evident, that curves can be classified into two types. A curve belongs to the first type, if the stress caused by the axial load is lower than the proportionality limit. Initial stiffness reduction factor is equal to 1.0 and starts to decrease, when the total stress from axial load and acting bending moment exceeds the proportionality limit. A curve belongs to the second type in case the stress caused by the axial load only, is higher than the proportionality limit. In this case initial stiffness reduction factor is smaller than 1.0. It can be observed, that for this type of curves the stiffness reduction factor increases together with the

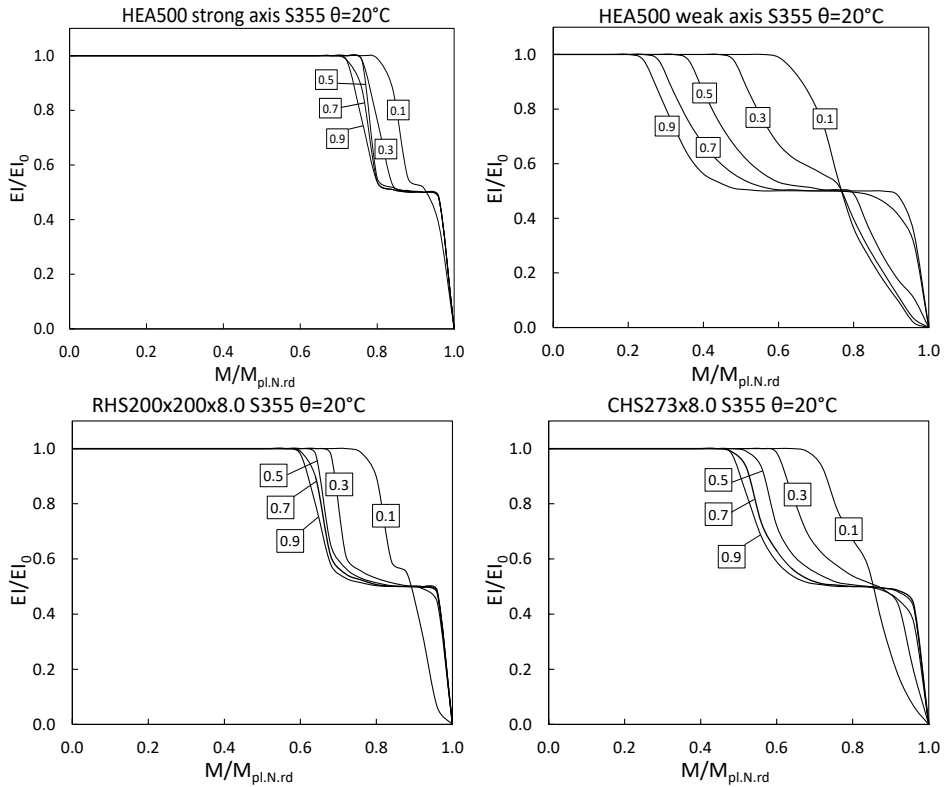


Figure 5.1: Bending stiffness reduction curves for various section S355 in ambient conditions

increasing bending moment. This happens due to the more intense stiffness growth in the unloaded region of the section, compared to the stiffness degradation in the section part experiencing additional loading from bending. Character of the curve depends on the temperature and is quite irregular. Comparing results in Figure 5.2 and Figure 5.3 it is evident that for I-section weak axis the bending stiffness reduction is more intense. Another possible way to analyse bending stiffness reduction is presented in Figure 5.4 and Figure 5.5. Bending stiffness reduction as a function of load value is presented for two states: normal temperature conditions and 500°C temperature conditions. Two curves are presented on each diagram, where continuous line is the bending stiffness in the mid-section of the column (maximum bending moment) and dotted line is the bending stiffness in the top section of the column (zero bending moment). Results presented in Figure 5.4, although visually not impressive, validate the Ayrton-Perry approach in the form of the first-yield criterion 2.3.2. With growing axial load the bending stiffness remains undamaged until the sharp drop in the bending stiffness which takes place simultaneously with the loss of stability. This pattern is valid for all slenderness values. For 500°C temperature the situation is different. For small slenderness values, with growing axial load the bending stiffness remains undamaged. After reaching the proportionality limit the bending stiffness starts to degrade, but this does not lead to immediate loss of stability. For slenderness value $\lambda_{20^\circ\text{C}} = 0.1$ bending stiffness curves in the top section and mid-section are very close to each other. For slenderness value 1.0, the bending stiffness in the top section remains undamaged prior column buckling, but column buckling does not occur immediately after the bending stiffness in the mid-section starts to deteriorate. For slenderness value $\lambda_{20^\circ\text{C}} = 2.0$, the bending stiffness

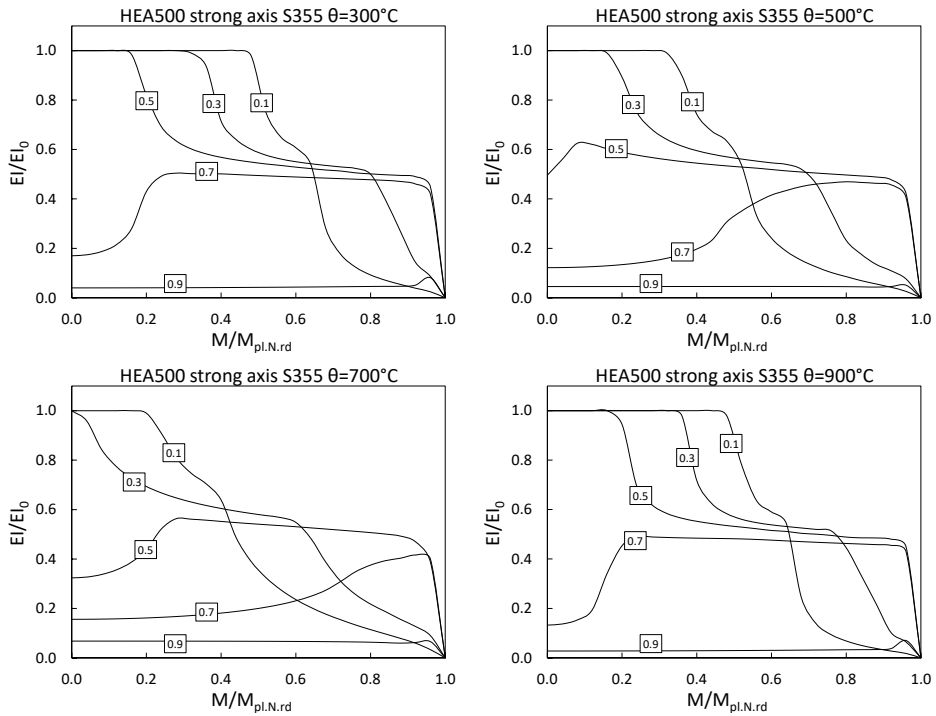


Figure 5.2: Bending stiffness reduction for HEA500 S355 strong axis in elevated temperature conditions

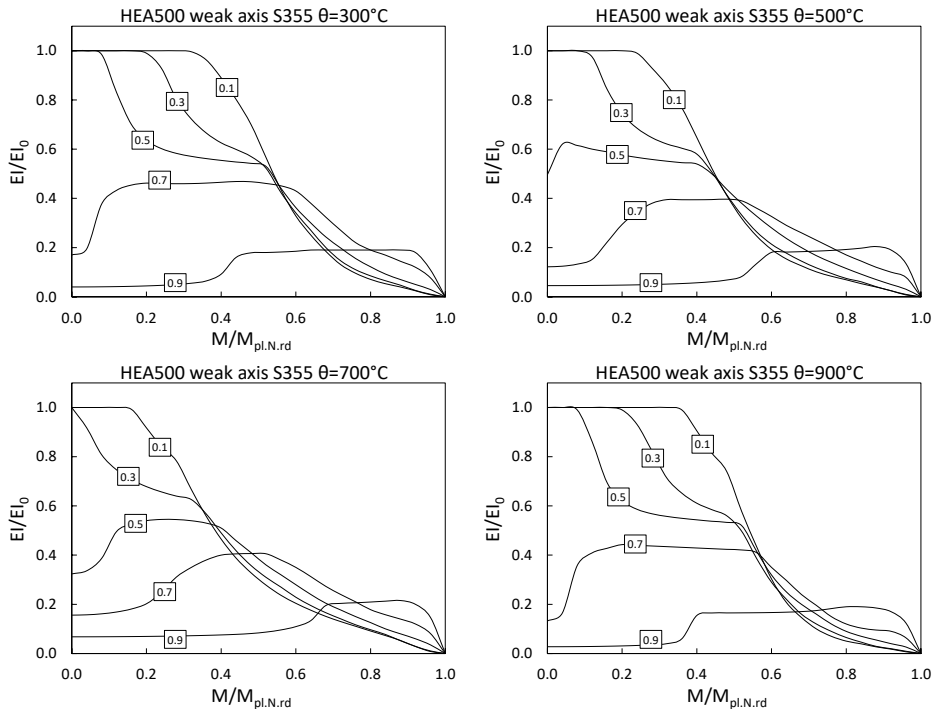


Figure 5.3: Bending stiffness reduction for HEA500 S355 weak axis in elevated temperature conditions

reduction pattern is analogous to the normal temperature conditions. It can be concluded, that in the elevated temperature conditions different mechanisms of buckling take place depending on column slenderness. This issue is to be addressed in the following sections.

Complexity of bending stiffness dependence on stress-state was demonstrated. The Eurocode design method for axially compressed columns is based on the model assuming constant bending stiffness invariant to the stress state and yield-limit stress condition is implied which is adequate for the ideal elasto-plastic material in ambient temperature. Analogous approach is extrapolated for elevated temperature conditions, but as it has been shown the bending stiffness dependence on stress state is more complicated. In addition to that yield-limit stress type criterion cannot be implemented, because at elevated temperature conditions the material model is not ideal elasto-plastic. The dependence of bending stiffness on stress state in elevated conditions motivates the discussion whether Ayrton-Perry type model is the best choice to serve as the basis for the design method.

5.4 Column shape

As it was stated in section 3.2.3, sinusoidal half-wave was used for initial curvature which is a standard practice. Column shape after buckling is analysed in this section.

In Figure 5.6 results of the horizontal displacements u_x along the column length x/L , where x is the coordinate along column and L is the length are presented. Continuous lines correspond to the calculated displacements, while dashed lines correspond to approximation function (sinusoid). From the Figure 5.6 it can be seen, that the shape of the curve for calculated displacements and approximated solution coincide. It is evident that the deformed shape of the initially curved compressed steel element in the variable temperature conditions replicates the shape of the initial curvature. Similar assumption is made in the von Karman buckling model described in section 2.4.

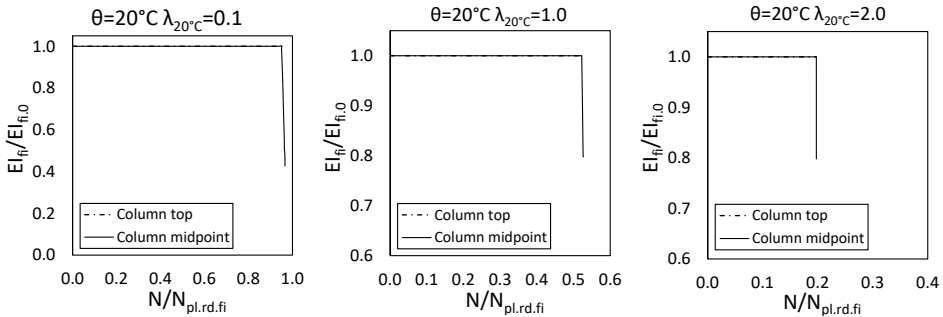


Figure 5.4: Bending stiffness path for S355 HEA500 strong axis 20°C conditions

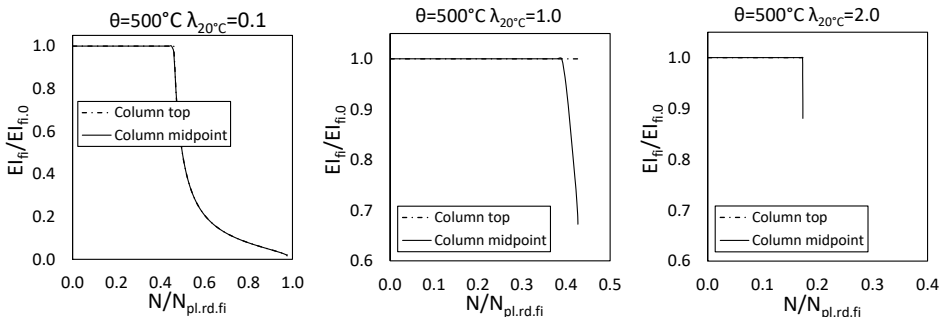


Figure 5.5: Bending stiffness path for S355 HEA500 strong axis 500°C conditions

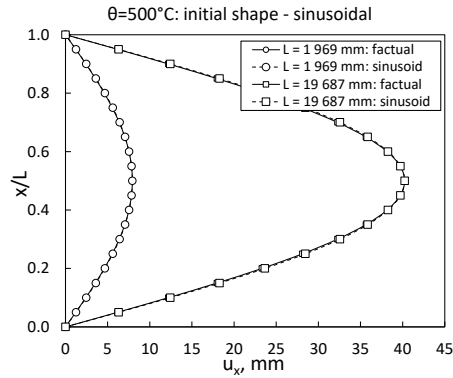


Figure 5.6: Deformed shape prior to buckling of the HEA500 S355 columns

5.5 Stresses

This section is dedicated to the analysis of stresses in the column at buckling. Stress profiles of columns at different conditions are presented in Figure 5.7, Figure 5.8 and Figure 5.9. Stresses along the column length x/L are presented in three section points: point C is located on the axis of the column, point 1 is located on the section edge under tension from lateral bending and point 2 is located on the section edge under additional compression from lateral bending. There are three diagrams for each slenderness and temperature value: axial stresses σ along column length x/L , axial stresses in relation to the yield limit stress at temperature θ $\sigma/f_{y,\theta}$ along column length x/L and axial stresses in relation to the proportionality limit stress at temperature θ $\sigma/f_{p,\theta}$ along column length x/L . Minus sign indicates compression. In case factor $\sigma/f_{y,\theta}$ is greater than 1.0 or smaller than -1.0, stress σ is above the yield limit stress $f_{y,\theta}$. In case factor $\sigma/f_{p,\theta}$ is greater than 1.0 or smaller than -1.0, stress σ is above proportionality limit stress $f_{p,\theta}$.

A number of interesting tendencies can be outlined by visual analysis of the stress diagrams. First, the case for temperature $\theta=200^\circ\text{C}$ and slenderness $\lambda_{20^\circ\text{C}}=0.1$ is considered (Figure 5.7). The buckling stresses are above proportionality limit in each point of the column. Stresses in points 1 and 2 have sinusoidal distribution along the column length. Stresses in point C also have sinusoidal distribution along the column length, but obviously stress distribution forms more than one half-wave. Next slenderness $\lambda_{20^\circ\text{C}}=1.0$ is considered. The stress state at buckling has changed qualitatively. Stresses are above the proportionality limit locally: range between $x/L=0.40$ and $x/L=0.60$ and only for point 2. Stresses at points 1 and 2 have the sinusoidal distribution along the column length, but it is different with stresses in point C: stresses remain constant along the column length in elastic state up to the point where stresses in point 2 exceed the proportionality limit. From the point $x/L=0.40$ along column length up to the point $x/L=0.60$ stresses distribution at point C along becomes sinusoidal, but stresses remain below the proportionality limit. The curve representing stresses at point C along the column length has two diffraction points. The nature of this diffraction is simple and is integrated into the steel material model. At slenderness $\lambda_{20^\circ\text{C}}=2.0$ column buckling occurs when stress in the mid-section of the column at point 2 approaches the proportionality limit. This case is similar to the yield-limit condition at normal temperatures, where ideal elasto-plastic is valid.

In Figure 5.8 diagrams set for temperature $\theta=500^\circ\text{C}$ is presented. General conclusions are similar to the case of $\theta=200^\circ\text{C}$ for slenderness $\lambda_{20^\circ\text{C}}=0.1$ as the stress distribution patterns are similar to $\theta=200^\circ\text{C}$. The same stands for the slenderness $\lambda_{20^\circ\text{C}}=1.0$, with

difference in the length of the zone where stresses at point 2 exceed the proportionality limit. For slenderness $\lambda_{20^\circ\text{C}}=2.0$ the situation is different comparing to $\theta=200^\circ\text{C}$. Stress patterns are more similar to the case of $\theta=200^\circ\text{C}$ $\lambda_{20^\circ\text{C}}=1.0$.

Temperature $\theta=900^\circ\text{C}$ is considered next. Stress distribution patterns at buckling are more similar to $\theta=200^\circ\text{C}$ than to $\theta=500^\circ\text{C}$. The presented diagrams are related to a limited sub-set of the whole set of slenderness values, temperatures and materials. In order to analyse a bigger number of cases Table 5-2, Table 5-3 and Table 5-4 were composed. Tables consists of factor $\sigma/f_{p,\theta}$ values. For each slenderness and temperature value 6 factor value are presented grouped in two rows: first row – stresses in three points 1, C and 2 of the column top section; second row presents stress in three points of column mid-section (maximum bending moment). Minus sign indicates compressive stress. In case the factor is less than -1 stress in the corresponding point is higher than the proportionality limit stress. Bold values in the tables highlight factor values which are less than -1. The tables have one more dimension – data range is divided into zones, depending on the stress state at buckling: TP1, TP2, TP3 and TP4. TP1 is the stress state for which stresses in the top section and the mid-section are above the proportionality limit. TP2 is the stress state for which stresses in the top section are above $f_{p,\theta}$ while due to the bending moment stresses in the mid-section are partially below $f_{p,\theta}$. TP3 is the stress state for which stresses in the top section are below $f_{p,\theta}$, while due to the bending moment stresses in the mid-section are partially above $f_{p,\theta}$. TP4 corresponds to the proportionality limit type buckling.

Stress distribution at failure across the section for different temperature values is presented in Figure 5.10 (strong axis buckling) and Figure 5.11 (weak axis buckling). Presented tables and figures demonstrate the buckling phenomenon complexity. Each type of stress state at buckling can also be referred to as a different type of buckling: for TP4 the proportionality limit model can be used while for TP1 tangent model theory gives good results. The range of slenderness values corresponding to a certain buckling type changes with temperature and material type. The following observations can be made based on Figure 5.10 and Figure 5.11:

- a. Strong axis buckling – for all temperature and slenderness values considered, the stress at point 1 are above proportionality limit.
- b. Strong axis buckling – for certain slenderness ranges (0.1, 0.2, 0.8 – 2.0) stress variation across the section is close to linear, while for the slenderness range 0.3 – 0.8 stress variation across the section is not linear.
- c. Weak axis buckling – for all temperature and slenderness values considered, the stress at point 1 is above proportionality limit.
- d. Weak axis buckling – in some cases the stress at point 2 is above the proportionality limit.
- e. Weak axis buckling – stress variation pattern across the section is significantly different compared to the strong axis buckling.

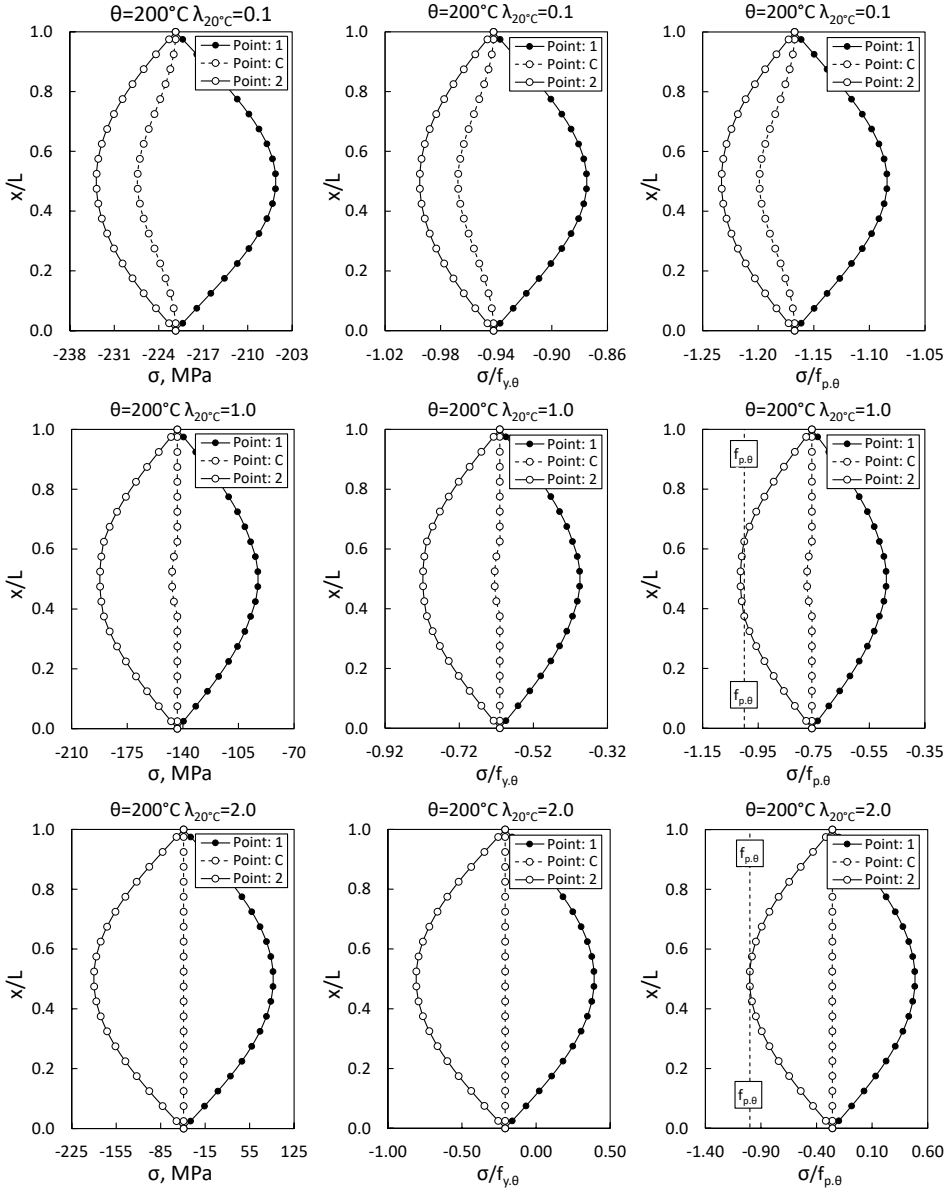


Figure 5.7: Stress profiles along the HEA500 S235 column prior to buckling at $\theta=200^{\circ}\text{C}$

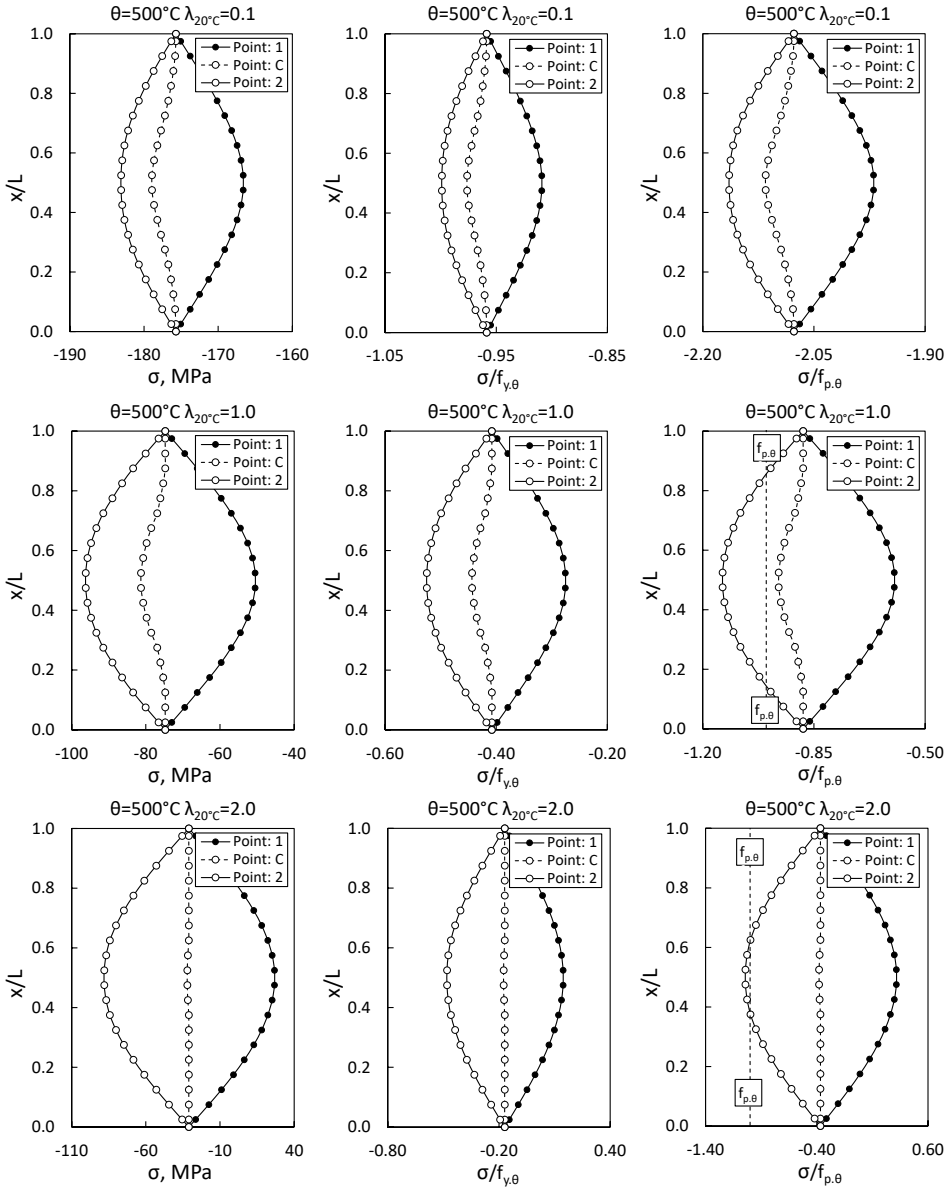


Figure 5.8: Stress profiles along the HEA500 S235 column prior to buckling at $\theta=500^\circ\text{C}$

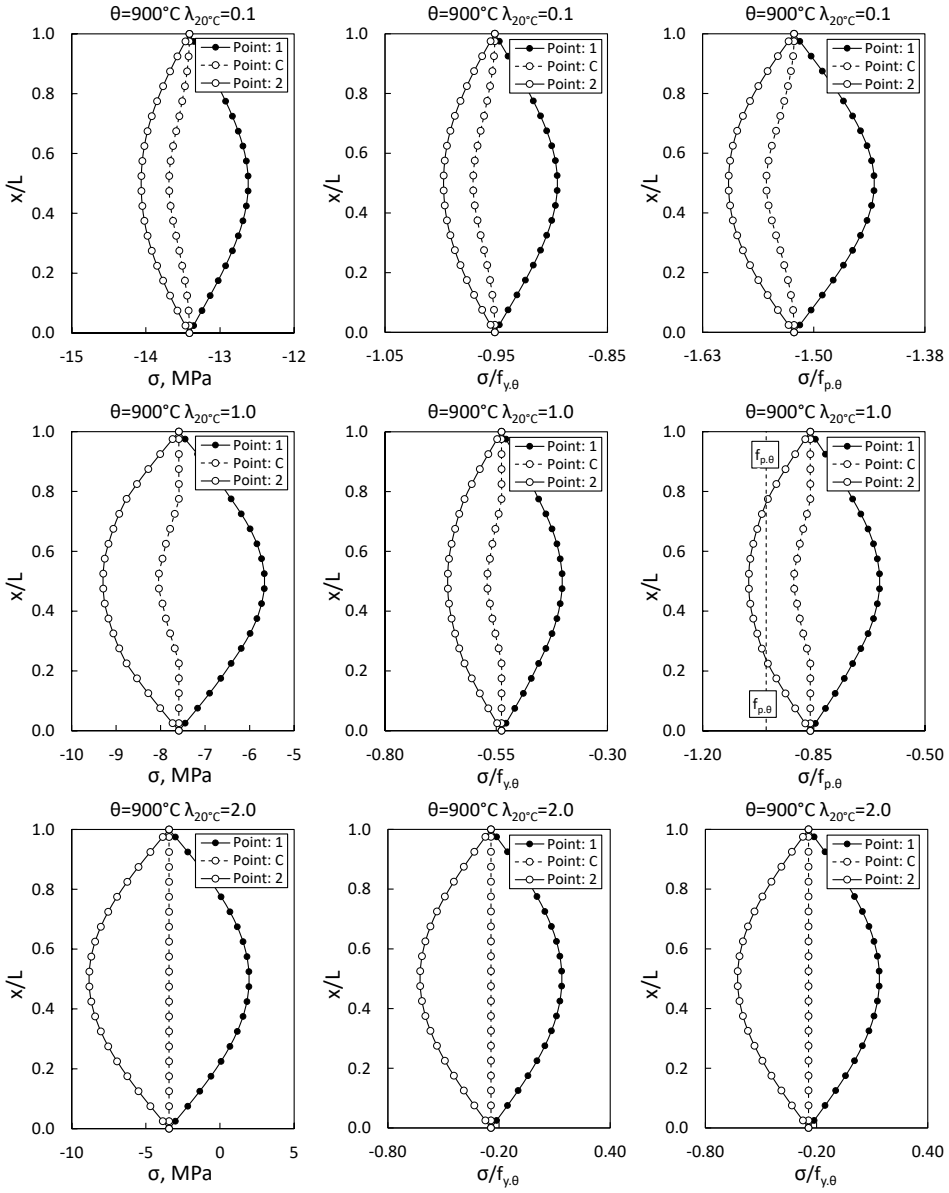


Figure 5.9: Stress profiles along the HEA500 S235 prior to buckling at $\theta=900^{\circ}\text{C}$

Table 5-2: Stress at buckling for S235

		$\theta=200^{\circ}\text{C}$			$\theta=300^{\circ}\text{C}$			$\theta=400^{\circ}\text{C}$			$\theta=500^{\circ}\text{C}$			$\theta=600^{\circ}\text{C}$			$\theta=700^{\circ}\text{C}$			$\theta=800^{\circ}\text{C}$			$\theta=900^{\circ}\text{C}$		
		p	1	p	1	p	1	p	1	p	1	p	1	p	1	p	1	p	1	p	1	p	1	p	1
$\lambda_{200^{\circ}\text{C}}=0.1$	top	-1.17	-1.17	-1.17	-1.55	-1.55	-1.55	-2.29	-2.29	-2.29	-2.08	-2.08	-2.08	-2.51	-2.51	-2.51	-2.95	-2.95	-2.95	-2.11	-2.11	-2.11	-1.52	-1.52	-1.52
	mid	-1.08	-1.20	-1.23	-1.46	-1.59	-1.63	-2.17	-2.33	-2.38	-1.97	-2.12	-2.16	-2.39	-2.55	-2.61	-2.82	-3.00	-3.06	-2.00	-2.15	-2.20	-1.43	-1.55	-1.60
$\lambda_{200^{\circ}\text{C}}=0.2$	top	-1.06	-1.06	-1.06	-1.34	-1.34	-1.34	-1.95	-1.95	-1.95	-1.78	-1.78	-1.78	-2.15	-2.15	-2.15	-2.53	-2.53	-2.53	-1.80	-1.80	-1.80	-1.31	-1.31	-1.31
	mid	-0.93	-1.11	-1.16	-1.05	-1.45	-1.56	-1.51	-2.11	-2.31	-1.36	-1.93	-2.10	-1.65	-2.33	-2.55	-1.94	-2.74	-3.00	-1.38	-1.96	-2.14	-1.03	-1.42	-1.53
$\lambda_{200^{\circ}\text{C}}=0.3$	top	-1.01	-1.01	-1.01	-1.18	-1.18	-1.18	-1.63	-1.63	-1.63	-1.50	-1.50	-1.50	-1.78	-1.78	-1.78	-2.08	-2.08	-2.08	-1.52	-1.52	-1.52	-1.16	-1.16	-1.16
	mid	-0.91	-1.06	-1.09	-0.87	-1.30	-1.42	-0.99	-1.86	-2.13	-0.95	-1.70	-1.92	-1.06	-2.04	-2.35	-1.20	-2.39	-2.78	-0.95	-1.72	-1.96	-0.87	-1.28	-1.39
$\lambda_{200^{\circ}\text{C}}=0.4$	top	-0.99	-0.99	-0.99	-1.09	-1.09	-1.09	-1.41	-1.41	-1.41	-1.31	-1.31	-1.31	-1.52	-1.52	-1.52	-1.75	-1.75	-1.75	-1.33	-1.33	-1.33	-1.08	-1.08	-1.08
	mid	-0.89	-1.03	-1.05	-0.83	-1.19	-1.28	-0.79	-1.63	-1.89	-0.77	-1.51	-1.72	-0.80	-1.77	-2.08	-0.83	-2.06	-2.47	-0.79	-1.53	-1.75	-0.84	-1.18	-1.26
$\lambda_{200^{\circ}\text{C}}=0.5$	top	-0.96	-0.96	-0.96	-1.03	-1.03	-1.03	-1.26	-1.26	-1.26	-1.19	-1.19	-1.19	-1.34	-1.34	-1.34	-1.51	-1.51	-1.51	-1.20	-1.20	-1.20	-1.03	-1.03	-1.03
	mid	-0.86	-1.02	-1.04	-0.83	-1.12	-1.18	-0.72	-1.45	-1.68	-0.75	-1.35	-1.53	-0.69	-1.57	-1.85	-0.67	-1.80	-2.18	-0.74	-1.37	-1.56	-0.83	-1.12	-1.18
$\lambda_{200^{\circ}\text{C}}=0.6$	top	-0.94	-0.94	-0.94	-0.99	-0.99	-0.99	-1.16	-1.16	-1.16	-1.10	-1.10	-1.10	-1.22	-1.22	-1.22	-1.34	-1.34	-1.34	-1.12	-1.12	-1.12	-1.00	-1.00	-1.00
	mid	-0.82	-1.00	-1.03	-0.80	-1.07	-1.13	-0.70	-1.32	-1.51	-0.74	-1.24	-1.39	-0.68	-1.41	-1.64	-0.62	-1.58	-1.92	-0.73	-1.26	-1.41	-0.82	-1.07	-1.13
$\lambda_{200^{\circ}\text{C}}=0.7$	top	-0.91	-0.91	-0.91	-0.95	-0.95	-0.95	-1.08	-1.08	-1.08	-1.04	-1.04	-1.04	-1.12	-1.12	-1.12	-1.22	-1.22	-1.22	-1.05	-1.05	-1.05	-0.96	-0.96	-0.96
	mid	-0.77	-0.94	-1.02	-0.77	-1.03	-1.10	-0.69	-1.22	-1.38	-0.72	-1.16	-1.29	-0.66	-1.29	-1.49	-0.60	-1.42	-1.72	-0.72	-1.18	-1.31	-0.79	-1.04	-1.10
$\lambda_{200^{\circ}\text{C}}=0.8$	top	-0.87	-0.87	-0.87	-0.91	-0.91	-0.91	-1.01	-1.01	-1.01	-0.99	-0.99	-0.99	-1.05	-1.05	-1.05	-1.12	-1.12	-1.12	-1.00	-1.00	-1.00	-0.93	-0.93	-0.93
	mid	-0.70	-0.90	-1.02	-0.71	-0.98	-1.08	-0.68	-1.14	-1.29	-0.70	-1.10	-1.22	-0.65	-1.19	-1.37	-0.60	-1.29	-1.55	-0.71	-1.11	-1.23	-0.75	-1.01	-1.08
$\lambda_{200^{\circ}\text{C}}=0.9$	top	-0.82	-0.82	-0.82	-0.86	-0.86	-0.86	-0.95	-0.95	-0.95	-0.94	-0.94	-0.94	-0.98	-0.98	-0.98	-1.03	-1.03	-1.03	-0.95	-0.95	-0.95	-0.90	-0.90	-0.90
	mid	-0.60	-0.85	-1.02	-0.64	-0.90	-1.06	-0.64	-1.07	-1.23	-0.66	-1.03	-1.17	-0.62	-1.11	-1.29	-0.56	-1.19	-1.44	-0.67	-1.05	-1.18	-0.69	-0.99	-1.07
$\lambda_{200^{\circ}\text{C}}=1.0$	top	-0.76	-0.76	-0.76	-0.81	-0.81	-0.81	-0.90	-0.90	-0.90	-0.88	-0.88	-0.88	-0.92	-0.92	-0.92	-0.96	-0.96	-0.96	-0.90	-0.90	-0.90	-0.86	-0.86	-0.86
	mid	-0.49	-0.77	-1.01	-0.55	-0.84	-1.05	-0.58	-1.00	-1.18	-0.60	-0.96	-1.14	-0.56	-1.03	-1.23	-0.53	-1.08	-1.34	-0.61	-0.99	-1.15	-0.64	-0.91	-1.05
$\lambda_{200^{\circ}\text{C}}=1.2$	top	-0.62	-0.62	-0.62	-0.68	-0.68	-0.68	-0.78	-0.78	-0.78	-0.77	-0.77	-0.77	-0.79	-0.79	-0.79	-0.81	-0.81	-0.81	-0.79	-0.79	-0.79	-0.77	-0.77	-0.77
	mid	-0.22	-0.63	-1.01	-0.29	-0.70	-1.05	-0.39	-0.83	-1.13	-0.41	-0.81	-1.10	-0.40	-0.85	-1.16	-0.34	-0.89	-1.25	-0.45	-0.84	-1.10	-0.46	-0.81	-1.05
$\lambda_{200^{\circ}\text{C}}=1.4$	top	-0.49	-0.49	-0.49	-0.55	-0.55	-0.55	-0.65	-0.65	-0.65	-0.65	-0.65	-0.65	-0.67	-0.67	-0.67	-0.68	-0.68	-0.68	-0.67	-0.67	-0.67	-0.66	-0.66	-0.66
	mid	0.02	-0.49	-1.00	0.06	-0.56	-1.03	-0.18	-0.68	-1.10	-0.19	-0.67	-1.08	-0.18	-0.70	-1.13	-0.15	-0.71	-1.18	-0.23	-0.71	-1.09	-0.29	-0.68	-1.02
$\lambda_{200^{\circ}\text{C}}=1.6$	top	-0.39	-0.39	-0.39	-0.44	-0.44	-0.44	-0.53	-0.53	-0.53	-0.53	-0.53	-0.53	-0.55	-0.55	-0.55	-0.56	-0.56	-0.56	-0.56	-0.56	-0.56	-0.56	-0.56	-0.56
	mid	-0.22	-0.39	-1.00	-0.13	-0.45	-1.01	-0.03	-0.56	-1.09	-0.02	-0.55	-1.07	-0.03	-0.57	-1.11	-0.05	-0.58	-1.15	-0.02	-0.59	-1.08	-0.10	-0.56	-1.01
$\lambda_{200^{\circ}\text{C}}=1.8$	top	-0.31	-0.31	-0.31	-0.36	-0.36	-0.36	-0.44	-0.44	-0.44	-0.44	-0.44	-0.44	-0.45	-0.45	-0.45	-0.46	-0.46	-0.46	-0.47	-0.47	-0.47	-0.46	-0.46	-0.46
	mid	0.37	-0.31	-1.00	0.30	-0.37	-1.01	0.22	-0.46	-1.09	0.17	-0.45	-1.04	0.20	-0.47	-1.10	0.22	-0.48	-1.13	0.11	-0.48	-1.04	0.09	-0.47	-1.01
$\lambda_{200^{\circ}\text{C}}=2.0$	top	-0.26	-0.26	-0.26	-0.30	-0.30	-0.30	-0.37	-0.37	-0.37	-0.37	-0.37	-0.37	-0.38	-0.38	-0.38	-0.38	-0.38	-0.38	-0.39	-0.39	-0.39	-0.39	-0.39	-0.39
	mid	0.48	-0.26	-1.00	0.41	-0.30	-1.00	0.32	-0.38	-1.05	0.32	-0.38	-1.04	0.35	-0.40	-1.10	0.35	-0.40	-1.11	0.27	-0.40	-1.04	0.22	-0.39	-1.00

Table 5-3: Stress at buckling for S355

		$\theta=200^{\circ}\text{C}$			$\theta=300^{\circ}\text{C}$			$\theta=400^{\circ}\text{C}$			$\theta=500^{\circ}\text{C}$			$\theta=600^{\circ}\text{C}$			$\theta=700^{\circ}\text{C}$			$\theta=800^{\circ}\text{C}$			$\theta=900^{\circ}\text{C}$		
		p	1	p	1	p	1	p	1	p	1	p	1	p	1	p	1	p	1	p	1	p	1		
$\lambda_{200^{\circ}\text{C}}=0.1$	TP1	-1.19	-1.19	-1.19	-1.59	-1.59	-1.59	-2.32	-2.32	-2.32	-2.11	-2.11	-2.11	-2.55	-2.55	-2.55	-3.00	-3.00	-3.00	-2.15	-2.15	-2.15	-1.55	-1.55	-1.55
	mid	-1.14	-1.21	-1.24	-1.53	-1.60	-1.63	-2.26	-2.35	-2.38	-2.05	-2.13	-2.17	-2.48	-2.57	-2.61	-2.92	-3.03	-3.07	-2.08	-2.17	-2.20	-1.50	-1.57	-1.60
$\lambda_{200^{\circ}\text{C}}=0.2$	TP1	-1.09	-1.09	-1.09	-1.42	-1.42	-1.42	-2.10	-2.10	-2.10	-1.90	-1.90	-1.90	-2.31	-2.31	-2.31	-2.72	-2.72	-2.72	-1.93	-1.93	-1.93	-1.39	-1.39	-1.39
	mid	-0.96	-1.15	-1.19	-1.19	-1.51	-1.60	-1.78	-2.21	-2.36	-1.61	-2.01	-2.14	-1.96	-2.43	-2.58	-2.33	-2.86	-3.04	-1.63	-2.04	-2.17	-1.16	-1.48	-1.57
$\lambda_{200^{\circ}\text{C}}=0.3$	TP1	-1.03	-1.03	-1.03	-1.26	-1.26	-1.26	-1.80	-1.80	-1.80	-1.64	-1.64	-1.64	-1.98	-1.98	-1.98	-2.32	-2.32	-2.32	-1.67	-1.67	-1.67	-1.24	-1.24	-1.24
	mid	-0.92	-1.08	-1.12	-0.94	-1.38	-1.51	-1.23	-2.01	-2.25	-1.14	-1.82	-2.04	-1.35	-2.20	-2.47	-1.58	-2.58	-2.92	-1.15	-1.85	-2.07	-0.94	-1.35	-1.47
$\lambda_{200^{\circ}\text{C}}=0.4$	TP2	-1.00	-1.00	-1.00	-1.15	-1.15	-1.15	-1.56	-1.56	-1.56	-1.44	-1.44	-1.44	-1.70	-1.70	-1.70	-1.97	-1.97	-1.97	-1.46	-1.46	-1.46	-1.14	-1.14	-1.14
	mid	0.90	-1.05	-1.07	-0.85	-1.26	-1.38	-0.92	-1.78	-2.07	-0.88	-1.64	-1.87	-0.95	-1.96	-2.29	-1.07	-2.28	-2.70	-0.89	-1.66	-1.90	-0.85	-1.25	-1.35
$\lambda_{200^{\circ}\text{C}}=0.5$	TP2	-0.98	-0.98	-0.98	-1.08	-1.08	-1.08	-1.38	-1.38	-1.38	-1.29	-1.29	-1.29	-1.49	-1.49	-1.49	-1.70	-1.70	-1.70	-1.31	-1.31	-1.31	-1.07	-1.07	-1.07
	mid	-0.88	-1.03	-1.05	-0.83	-1.17	-1.26	-0.77	-1.59	-1.87	-0.77	-1.47	-1.69	-0.78	-1.73	-2.06	-0.81	-1.99	-2.42	-0.77	-1.50	-1.73	-0.84	-1.17	-1.25
$\lambda_{200^{\circ}\text{C}}=0.6$	TP2	-0.95	-0.95	-0.95	-1.02	-1.02	-1.02	-1.25	-1.25	-1.25	-1.18	-1.18	-1.18	-1.33	-1.33	-1.33	-1.50	-1.50	-1.50	-1.20	-1.20	-1.20	-1.03	-1.03	-1.03
	mid	0.85	-1.01	-1.04	-0.82	-1.11	-1.19	-0.72	-1.43	-1.68	-0.75	-1.33	-1.53	-0.70	-1.54	-1.84	-0.67	-1.76	-2.18	-0.74	-1.36	-1.56	-0.83	-1.11	-1.18
$\lambda_{200^{\circ}\text{C}}=0.7$	TP3	-0.93	-0.93	-0.93	-0.98	-0.98	-0.98	-1.15	-1.15	-1.15	-1.10	-1.10	-1.10	-1.22	-1.22	-1.22	-1.34	-1.34	-1.34	-1.12	-1.12	-1.12	-0.99	-0.99	-0.99
	mid	-0.81	-0.96	-1.03	-0.80	-1.06	-1.13	-0.71	-1.30	-1.51	-0.73	-1.23	-1.40	-0.67	-1.39	-1.66	-0.62	-1.56	-1.93	-0.73	-1.25	-1.42	-0.81	-1.07	-1.13
$\lambda_{200^{\circ}\text{C}}=0.8$	TP3	-0.89	-0.89	-0.89	-0.94	-0.94	-0.94	-1.08	-1.08	-1.08	-1.04	-1.04	-1.04	-1.12	-1.12	-1.12	-1.22	-1.22	-1.22	-1.05	-1.05	-1.05	-0.96	-0.96	-0.96
	mid	0.74	-0.92	-1.03	-0.75	-1.01	-1.10	-0.70	-1.20	-1.39	-0.72	-1.15	-1.30	-0.66	-1.27	-1.50	-0.59	-1.40	-1.74	-0.72	-1.17	-1.32	-0.78	-1.04	-1.11
$\lambda_{200^{\circ}\text{C}}=0.9$	TP3	-0.84	-0.84	-0.84	-0.89	-0.89	-0.89	-1.01	-1.01	-1.01	-0.98	-0.98	-0.98	-1.04	-1.04	-1.04	-1.11	-1.11	-1.11	-1.00	-1.00	-1.00	-0.93	-0.93	-0.93
	mid	-0.66	-0.86	-1.02	-0.68	-0.94	-1.08	-0.66	-1.12	-1.30	-0.69	-1.08	-1.23	-0.65	-1.17	-1.38	-0.58	-1.26	-1.57	-0.70	-1.10	-1.25	-0.75	-1.00	-1.08
$\lambda_{200^{\circ}\text{C}}=1.0$	TP3	-0.78	-0.78	-0.78	-0.84	-0.84	-0.84	-0.94	-0.94	-0.94	-0.92	-0.92	-0.92	-0.97	-0.97	-0.97	-1.02	-1.02	-1.02	-0.94	-0.94	-0.94	-0.89	-0.89	-0.89
	mid	-0.53	-0.80	-1.02	-0.59	-0.87	-1.07	-0.62	-1.03	-1.24	-0.63	-1.01	-1.18	-0.60	-1.08	-1.30	-0.54	-1.15	-1.45	-0.66	-1.03	-1.19	-0.69	-0.95	-1.07
$\lambda_{200^{\circ}\text{C}}=1.2$	TP3	-0.64	-0.64	-0.64	-0.70	-0.70	-0.70	-0.81	-0.81	-0.81	-0.80	-0.80	-0.80	-0.85	-0.85	-0.85	-0.86	-0.83	-0.86	-0.83	-0.83	-0.83	-0.80	-0.80	-0.80
	mid	-0.26	-0.64	-1.01	-0.35	-0.72	-1.05	-0.43	-0.86	-1.16	-0.46	-0.84	-1.13	-0.60	-1.23	-1.05	-0.38	-0.93	-1.30	-0.49	-0.87	-1.14	-0.53	-0.83	-1.05
$\lambda_{200^{\circ}\text{C}}=1.4$	TP3	-0.50	-0.50	-0.50	-0.56	-0.56	-0.56	-0.67	-0.67	-0.67	-0.67	-0.67	-0.67	-0.69	-0.69	-0.69	-0.71	-0.71	-0.71	-0.70	-0.70	-0.70	-0.69	-0.69	-0.69
	mid	0.00	-0.50	-1.00	-0.08	-0.58	-1.04	-0.21	-0.70	-1.12	-0.23	-0.69	-1.09	-0.22	-0.72	-1.15	-0.17	-0.74	-1.22	-0.29	-0.72	-1.10	-0.32	-0.71	-1.05
$\lambda_{200^{\circ}\text{C}}=1.6$	TP3	-0.40	-0.40	-0.40	-0.45	-0.45	-0.45	-0.55	-0.55	-0.55	-0.55	-0.55	-0.55	-0.57	-0.57	-0.57	-0.57	-0.57	-0.57	-0.58	-0.58	-0.58	-0.57	-0.57	-0.57
	mid	0.21	-0.40	-1.04	-0.14	-0.46	-1.04	-0.01	-0.56	-1.08	-0.01	-0.56	-1.08	0.00	-0.59	-1.12	-0.03	-0.59	-1.17	-0.07	-0.60	-1.08	-0.11	-0.59	-1.03
$\lambda_{200^{\circ}\text{C}}=1.8$	TP3	-0.32	-0.32	-0.32	-0.37	-0.37	-0.37	-0.45	-0.45	-0.45	-0.45	-0.45	-0.45	-0.47	-0.47	-0.47	-0.47	-0.47	-0.47	-0.48	-0.48	-0.48	-0.48	-0.48	-0.48
	mid	0.36	-0.32	-1.00	0.28	-0.37	-1.01	0.19	-0.47	-1.09	0.17	-0.46	-1.07	0.17	-0.48	-1.09	-0.22	-0.49	-1.15	0.12	-0.49	-1.07	0.06	-0.48	-1.01
$\lambda_{200^{\circ}\text{C}}=2.0$	TP3	-0.26	-0.26	-0.26	-0.30	-0.30	-0.30	-0.38	-0.38	-0.38	-0.37	-0.37	-0.37	-0.39	-0.39	-0.39	-0.39	-0.39	-0.39	-0.40	-0.40	-0.40	-0.40	-0.40	-0.40
	mid	0.48	-0.26	-1.00	0.41	-0.31	-1.02	0.32	-0.38	-1.07	0.32	-0.38	-1.06	0.33	-0.40	-1.09	0.36	-0.40	-1.13	0.27	-0.41	-1.07	0.22	-0.40	-1.01

Table 5-4: Stress at buckling for S460

		$\theta=200^{\circ}\text{C}$			$\theta=300^{\circ}\text{C}$			$\theta=400^{\circ}\text{C}$			$\theta=500^{\circ}\text{C}$			$\theta=600^{\circ}\text{C}$			$\theta=700^{\circ}\text{C}$			$\theta=800^{\circ}\text{C}$			$\theta=900^{\circ}\text{C}$			I
		p 1	p C	p 2	p 1	p C	p 2	p 1	p C	p 2	p 1	p C	p 2	p 1	p C	p 2	p 1	p C	p 2	p 1	p C	p 2	p 1	p C	p 2	
$\lambda_{20^{\circ}\text{C}}=0.1$	top	-1.21	-1.21	-1.21	-1.60	-1.60	-1.60	-2.34	-2.34	-2.34	-2.13	-2.13	-2.13	-2.57	-2.57	-2.57	-3.02	-3.02	-3.02	-2.16	-2.16	-2.16	-1.57	-1.57	-1.57	I
	mid	-1.17	-1.22	-1.24	-1.56	-1.61	-1.63	-2.29	-2.36	-2.38	-2.08	-2.14	-2.17	-2.51	-2.58	-2.61	-2.96	-3.04	-3.07	-2.11	-2.18	-2.20	-1.52	-1.58	-1.60	
$\lambda_{20^{\circ}\text{C}}=0.2$	top	-1.11	-1.11	-1.11	-1.47	-1.47	-1.47	-2.17	-2.17	-2.17	-1.97	-1.97	-1.97	-2.39	-2.39	-2.39	-2.81	-2.81	-2.81	-2.00	-2.00	-2.00	-1.44	-1.44	-1.44	I
	mid	-0.99	-1.16	-1.21	-1.29	-1.53	-1.61	-1.93	-2.25	-2.37	-1.74	-2.05	-2.15	-2.12	-2.48	-2.60	-2.53	-2.91	-3.05	-1.77	-2.08	-2.19	-1.26	-1.50	-1.58	
$\lambda_{20^{\circ}\text{C}}=0.3$	top	-1.05	-1.05	-1.05	-1.31	-1.31	-1.31	-1.91	-1.91	-1.91	-1.74	-1.74	-1.74	-2.10	-2.10	-2.10	-2.47	-2.47	-2.47	-1.76	-1.76	-1.76	-1.29	-1.29	-1.29	I
	mid	-0.93	-1.10	-1.14	-1.02	-1.42	-1.55	-1.42	-2.08	-2.30	-1.30	-1.89	-2.09	-1.57	-2.28	-2.53	-1.87	-2.67	-2.97	-1.32	-1.92	-2.12	-1.00	-1.39	-1.51	
$\lambda_{20^{\circ}\text{C}}=0.4$	top	-1.02	-1.02	-1.02	-1.19	-1.19	-1.19	-1.67	-1.67	-1.67	-1.53	-1.53	-1.53	-1.82	-1.82	-1.82	-2.13	-2.13	-2.13	-1.55	-1.55	-1.55	-1.18	-1.18	-1.18	I
	mid	-0.91	-1.06	-1.09	-0.88	-1.31	-1.44	-1.04	-1.88	-2.17	-1.00	-1.71	-1.95	-1.13	-2.06	-2.38	-1.30	-2.40	-2.81	-0.99	-1.75	-1.99	-0.88	-1.29	-1.41	
$\lambda_{20^{\circ}\text{C}}=0.5$	top	-0.99	-0.99	-0.99	-1.11	-1.11	-1.11	-1.47	-1.47	-1.47	-1.36	-1.36	-1.36	-1.60	-1.60	-1.60	-1.84	-1.84	-1.84	-1.38	-1.38	-1.38	-1.11	-1.11	-1.11	I
	mid	-0.89	-1.03	-1.06	-0.84	-1.21	-1.32	-0.83	-1.69	-1.99	-0.82	-1.55	-1.79	-0.88	-1.84	-2.18	-0.94	-2.13	-2.58	-0.82	-1.58	-1.83	-0.85	-1.20	-1.30	
$\lambda_{20^{\circ}\text{C}}=0.6$	top	-0.97	-0.97	-0.97	-1.05	-1.05	-1.05	-1.33	-1.33	-1.33	-1.24	-1.24	-1.24	-1.42	-1.42	-1.42	-1.62	-1.62	-1.62	-1.26	-1.26	-1.26	-1.05	-1.05	-1.05	I
	mid	-0.87	-1.01	-1.04	-0.82	-1.14	-1.23	-0.76	-1.51	-1.79	-0.76	-1.41	-1.63	-0.74	-1.64	-1.98	-0.76	-1.87	-2.32	-0.77	-1.43	-1.65	-0.83	-1.14	-1.22	
$\lambda_{20^{\circ}\text{C}}=0.7$	top	-0.94	-0.94	-0.94	-1.01	-1.01	-1.01	-1.21	-1.21	-1.21	-1.15	-1.15	-1.15	-1.29	-1.29	-1.29	-1.44	-1.44	-1.44	-1.17	-1.17	-1.17	-1.01	-1.01	-1.01	I
	mid	-0.83	-0.98	-1.04	-0.81	-1.08	-1.16	-0.72	-1.37	-1.62	-0.74	-1.29	-1.48	-0.69	-1.47	-1.78	-0.65	-1.66	-2.09	-0.73	-1.31	-1.52	-0.82	-1.09	-1.16	
$\lambda_{20^{\circ}\text{C}}=0.8$	top	-0.90	-0.90	-0.90	-0.96	-0.96	-0.96	-1.12	-1.12	-1.12	-1.08	-1.08	-1.08	-1.18	-1.18	-1.18	-1.29	-1.29	-1.29	-1.09	-1.09	-1.09	-0.98	-0.98	-0.98	I
	mid	-0.77	-0.93	-1.03	-0.77	-1.03	-1.12	-0.69	-1.26	-1.48	-0.72	-1.19	-1.37	-0.66	-1.33	-1.61	-0.60	-1.48	-1.88	-0.72	-1.22	-1.40	-0.80	-1.06	-1.13	
$\lambda_{20^{\circ}\text{C}}=0.9$	top	-0.86	-0.86	-0.86	-0.91	-0.91	-0.91	-1.05	-1.05	-1.05	-1.01	-1.01	-1.01	-1.09	-1.09	-1.09	-1.17	-1.17	-1.17	-1.03	-1.03	-1.03	-0.95	-0.95	-0.95	I
	mid	-0.69	-0.87	-1.02	-0.71	-0.96	-1.10	-0.68	-1.15	-1.36	-0.70	-1.11	-1.28	-0.65	-1.22	-1.47	-0.57	-1.33	-1.70	-0.70	-1.14	-1.31	-0.76	-1.02	-1.10	
$\lambda_{20^{\circ}\text{C}}=1.0$	top	-0.80	-0.80	-0.80	-0.86	-0.86	-0.86	-0.98	-0.98	-0.98	-0.95	-0.95	-0.95	-1.01	-1.01	-1.01	-1.07	-1.07	-1.07	-0.97	-0.97	-0.97	-0.91	-0.91	-0.91	I
	mid	-0.57	-0.81	-1.02	-0.62	-0.89	-1.08	-0.62	-1.07	-1.29	-0.65	-1.04	-1.22	-0.61	-1.12	-1.37	-0.54	-1.19	-1.55	-0.67	-1.06	-1.23	-0.72	-0.96	-1.08	
$\lambda_{20^{\circ}\text{C}}=1.2$	top	-0.65	-0.65	-0.65	-0.72	-0.72	-0.72	-0.83	-0.83	-0.83	-0.82	-0.82	-0.82	-0.86	-0.86	-0.86	-0.89	-0.89	-0.89	-0.85	-0.85	-0.85	-0.82	-0.82	-0.82	I
	mid	-0.28	-0.65	-1.01	-0.36	-0.73	-1.06	-0.46	-0.88	-1.19	-0.49	-0.86	-1.14	-0.45	-0.91	-1.24	-0.40	-0.95	-1.35	-0.51	-0.90	-1.16	-0.57	-0.84	-1.06	
$\lambda_{20^{\circ}\text{C}}=1.4$	top	-0.51	-0.51	-0.51	-0.57	-0.57	-0.57	-0.69	-0.69	-0.69	-0.69	-0.69	-0.69	-0.71	-0.71	-0.71	-0.72	-0.72	-0.72	-0.72	-0.72	-0.72	-0.70	-0.70	-0.70	I
	mid	0.00	-0.51	-1.01	-0.11	-0.58	-1.04	-0.23	-0.71	-1.14	-0.25	-0.71	-1.11	-0.23	-0.74	-1.17	-0.18	-0.75	-1.25	-0.31	-0.74	-1.11	-0.35	-0.72	-1.04	
$\lambda_{20^{\circ}\text{C}}=1.6$	top	-0.40	-0.40	-0.40	-0.46	-0.46	-0.46	-0.56	-0.56	-0.56	-0.56	-0.56	-0.56	-0.58	-0.58	-0.58	-0.59	-0.59	-0.59	-0.59	-0.59	-0.59	-0.59	-0.59	-0.59	I
	mid	0.20	-0.40	-1.00	0.12	-0.46	-1.04	-0.01	-0.58	-1.11	-0.11	-0.57	-1.02	0.00	-0.60	-1.14	0.05	-0.61	-1.21	-0.08	-0.61	-1.09	-0.14	-0.60	-1.03	
$\lambda_{20^{\circ}\text{C}}=1.8$	top	-0.32	-0.32	-0.32	-0.37	-0.37	-0.37	-0.46	-0.46	-0.46	-0.46	-0.46	-0.46	-0.47	-0.47	-0.47	-0.48	-0.48	-0.48	-0.49	-0.49	-0.49	-0.49	-0.49	-0.49	I
	mid	0.36	-0.32	-1.00	0.30	-0.38	-1.04	0.18	-0.47	-1.09	0.16	-0.47	-1.07	0.17	-0.48	-1.11	0.23	-0.49	-1.17	0.10	-0.50	-1.07	-0.04	-0.49	-1.01	
$\lambda_{20^{\circ}\text{C}}=2.0$	top	-0.26	-0.26	-0.26	-0.30	-0.30	-0.30	-0.38	-0.38	-0.38	-0.38	-0.38	-0.38	-0.39	-0.39	-0.39	-0.40	-0.40	-0.40	-0.41	-0.41	-0.41	-0.40	-0.40	-0.40	I
	mid	0.47	-0.26	-1.00	0.41	-0.31	-1.02	0.32	-0.39	-1.07	0.30	-0.38	-1.06	0.33	-0.40	-1.10	0.36	-0.41	-1.14	0.25	-0.41	-1.06	0.21	-0.41	-1.01	

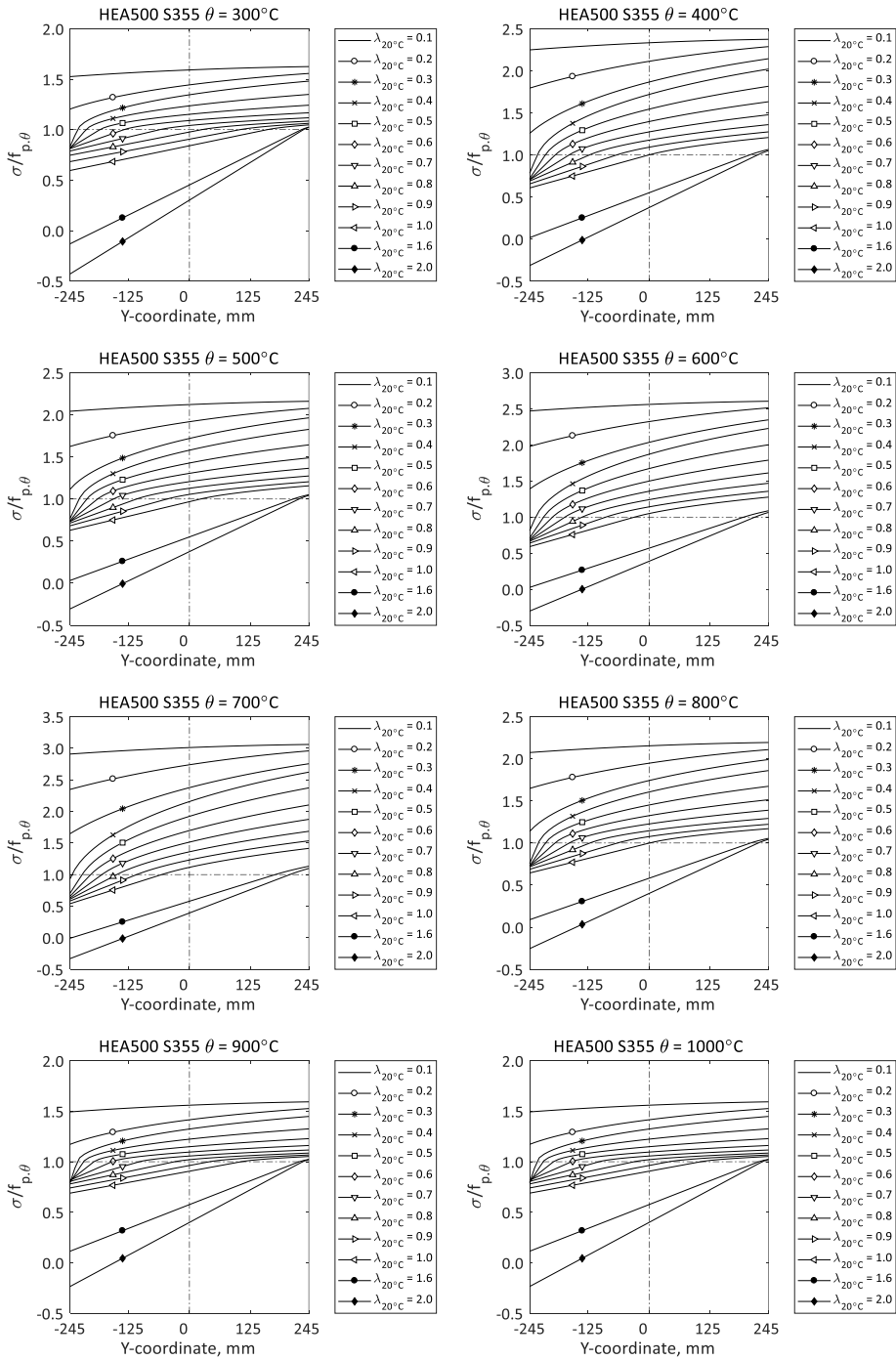


Figure 5.10: Stress distribution inside the mid-section prior to failure for the strong axis buckling of the HEA500 S355 column

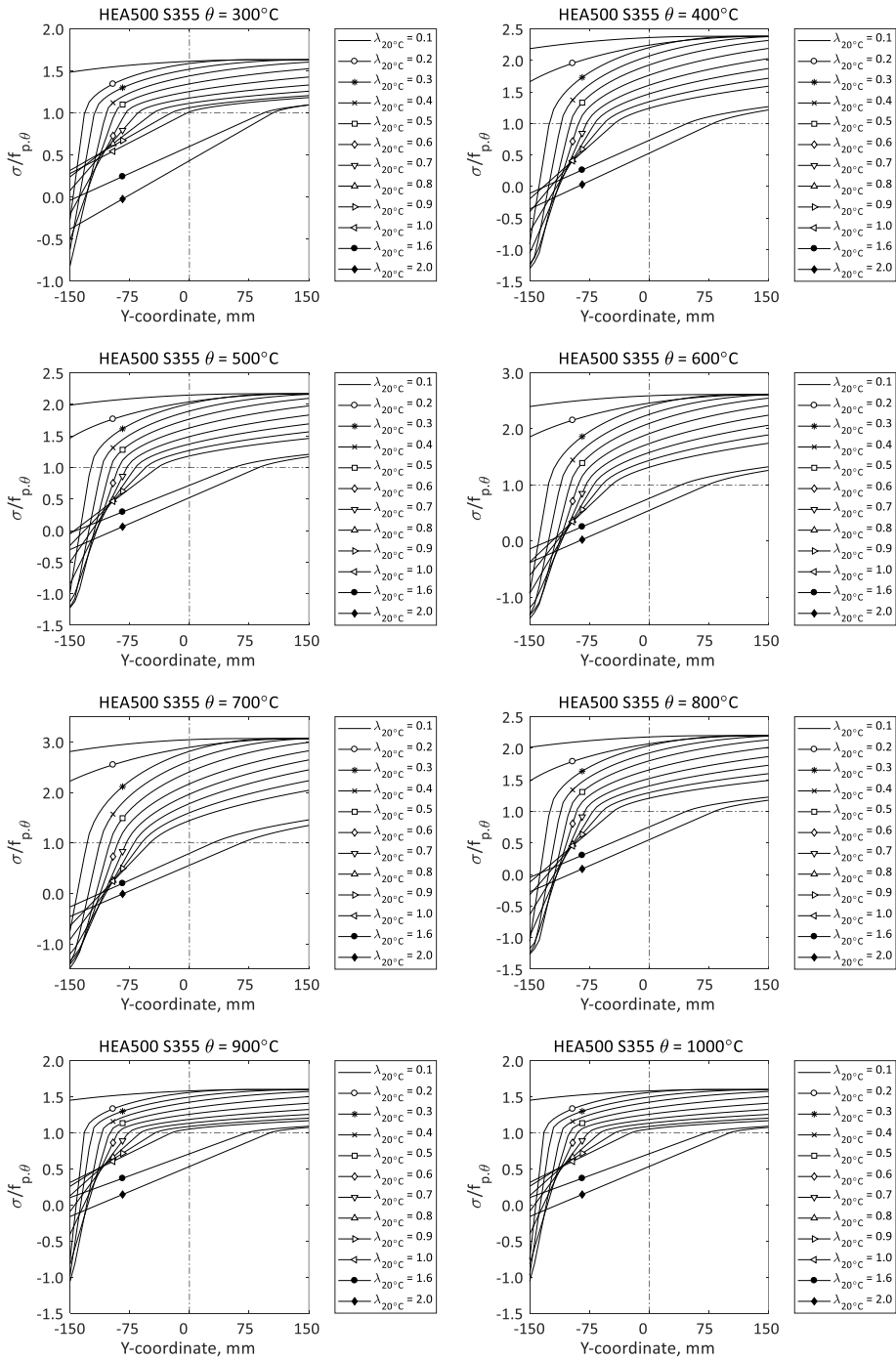


Figure 5.11: Stress distribution inside the mid-section prior to failure for the weak axis buckling of the HEA500 S355 column

5.6 Residual stresses

Residual stress (RS) influences stability of a compressed element mainly through stiffness. Due to residual stresses total stresses in some section points reach proportionality limit earlier and in others with delay. The cumulative outcome is defined by the pattern of the residual stresses and section topology. As it was mentioned in chapter 3.4, the adequacy of residual stress patterns is not in the focus of the current research. The patterns were adopted as presented in Figure 3.21.

First the influence of the residual stresses on the bending stiffness of a section is studied. In Figure 5.12 the bending stiffness reduction curves for various temperatures are presented. Used notation is the same as for Figure 5.2, which is defined in section 5.3. Two sets of curves are presented on each diagram: the continuous line corresponds to the bending stiffness without RS and the dash-dotted line corresponds to the bending stiffness with RS. Curves are presented for different axial load levels $N/N_{pl.Rd,fi}$, where N is the acting axial load and $N_{pl.Rd,fi}$ is the axial load capacity in fire situation. Factor $N/N_{pl.Rd,fi}$ value is specified in the intersection point of the corresponding curve. The diagrams demonstrate that in general RS reduce the bending stiffness, although there are ranges where the influence is opposite. With increasing factor $M/M_{pl.N,rd,fi}$ (approach of section fully plastic state) the influence of RS decreases. It is expected that RS have minor influence on the columns of small slenderness and stronger influence on slender columns. Buckling factor of two model types are compared one including RS and the one ignoring RS. The results are presented in Figure 5.15 – Figure 5.18 by 3 curves as follows: buckling factors as a function of slenderness $\lambda_{20^\circ C}$ for model without the RS (left-hand vertical axis), buckling factors for model with RS (left-hand vertical axis) and difference curve for two model types defined as $(\chi_{fi,noRS} - \chi_{fi,RS}) / \chi_{fi,RS}$ (right-hand vertical axis), where $\chi_{fi,noRS}$ is the buckling factor of model without RS and $\chi_{fi,RS}$ is the buckling factor of model with RS.

The following conclusions can be made. RS have more influence at temperature $\theta=200^\circ C$, because the material model for this temperature is closer to the ideal elasto-plastic model. For section type I-Y (Figure 5.13) and RHS (Figure 5.17) the influence of RS is more significant for $\lambda_{20^\circ C} \geq 1.0$, while for section type I-Z (Figure 5.15, Figure 5.16) the influence of RS is more significant for $\lambda_{20^\circ C} \geq 0.7$. For section type CHS (Figure 5.18) the influence of RS is not significant. The influence of RS is less significant for higher steel grades because chosen RS patterns are defined as a fraction of yield stress limit of 235 MPa irrespective of the factual yield limit stress of the material.

5.7 Buckling factors

This section presents buckling factors for numerical program described in section 5.2. Results presented here form the basis of the proposed design methods.

Results of modelling are presented in Figure 5.19, Annexes A3 and A4. Figures present buckling factors as a function of slenderness $\lambda_{20^\circ C}$ defined as (5-1). Each buckling factor is the average value for a group of sections according to Table 5-1. Results of the statistical analysis for the comparison of individual buckling value to its group average (factor $\chi_i/\chi_{gr,mean}$) are presented in the Table 5-5. Statistical analysis indicate that elements under axial compression behave similarly within their section group. The biggest variation between individual values within one section group emerged in group I-Z (hot-rolled I section weak axis).

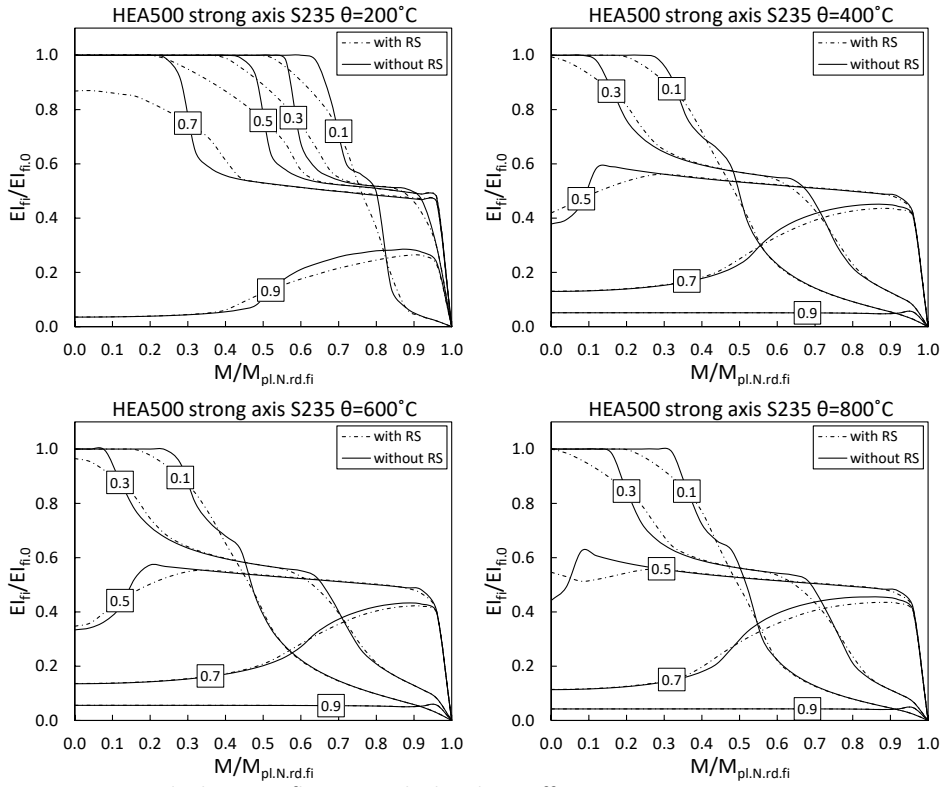


Figure 5.12: Residual stress influence on the bending stiffness

Table 5-5: Descriptive statistics for individual buckling factor χ_i vs. group average buckling factor

$\chi_{gr.mean}$						
Group ID		CHS			RHS	
Steel grade	S235	S355	S460	S235	S355	S460
Mean	1.00018	1.00020	1.00022	1.00008	1.00008	1.00005
Standard Error	0.00001	0.00002	0.00006	0.00010	0.00009	0.00010
Standard Deviation	0.00040	0.00041	0.00056	0.00057	0.00064	0.00066
Minimum	0.99751	0.99878	0.99225	0.99013	0.99203	0.99119
Maximum	1.00588	1.00851	1.00871	1.00986	1.00912	1.00949
Group ID		I-Y			I-Z	
Steel grade	S235	S355	S460	S235	S355	S460
Mean	1.00020	1.00024	1.00021	1.00002	1.00009	1.00011
Standard Error	0.00009	0.00011	0.00008	0.00012	0.00011	0.00011
Standard Deviation	0.00075	0.00069	0.00082	0.00198	0.00156	0.00151
Minimum	0.99387	0.99532	0.99472	0.99161	0.99264	0.98933
Maximum	1.00697	1.00786	1.00926	1.01519	1.01832	1.01129

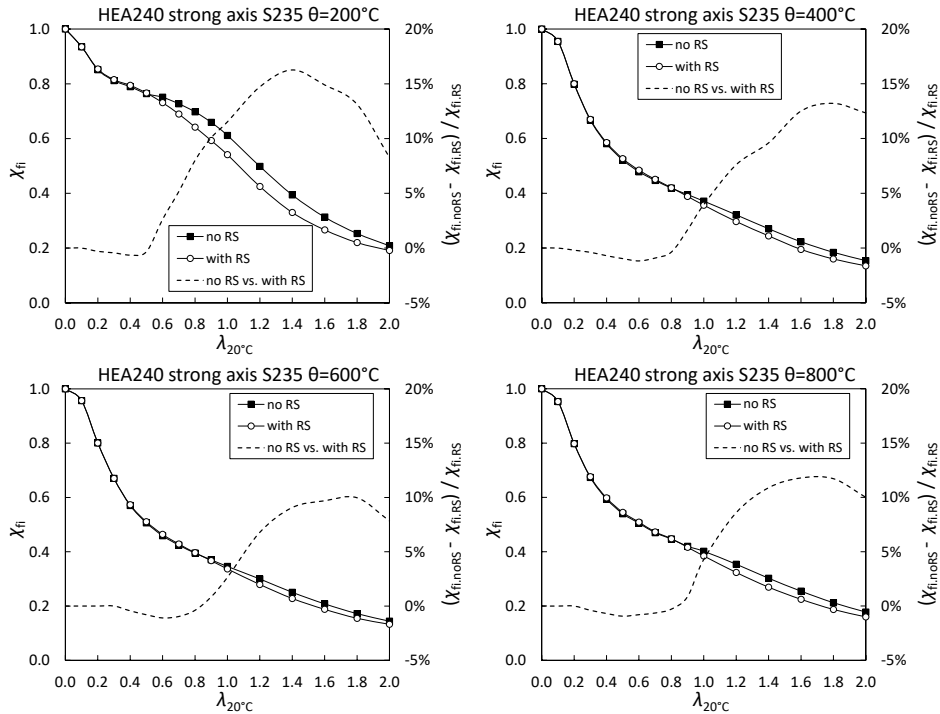


Figure 5.13: Residual stresses influence on the buckling factor for I-type section strong axis (I-Y) in case $h/b \leq 1.2$

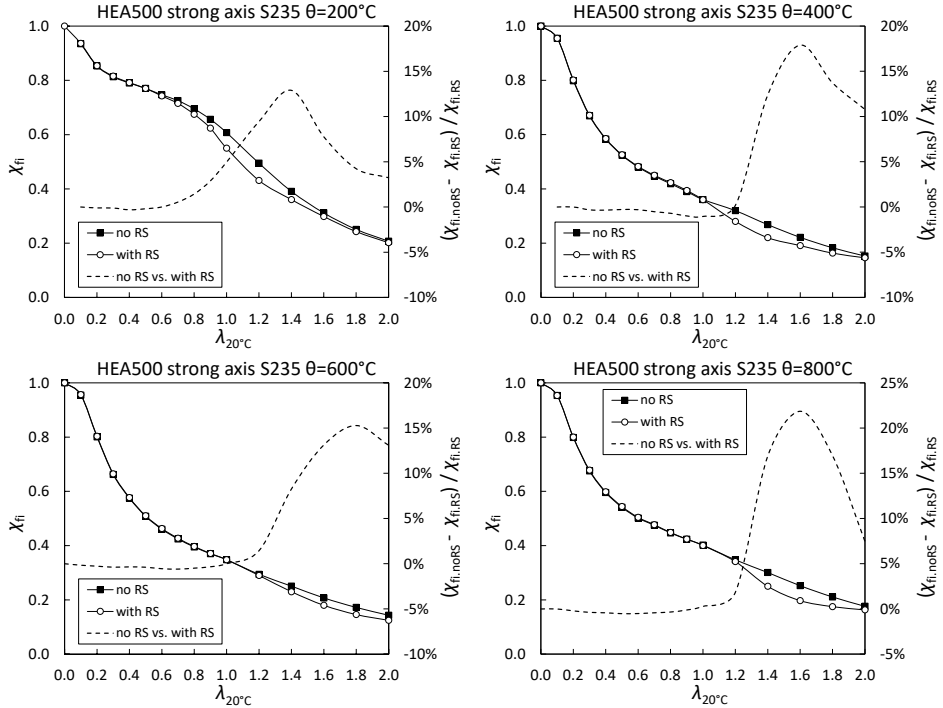


Figure 5.14: Residual stresses influence on the buckling factor for I-type section strong axis (I-Y) in case $h/b > 1.2$

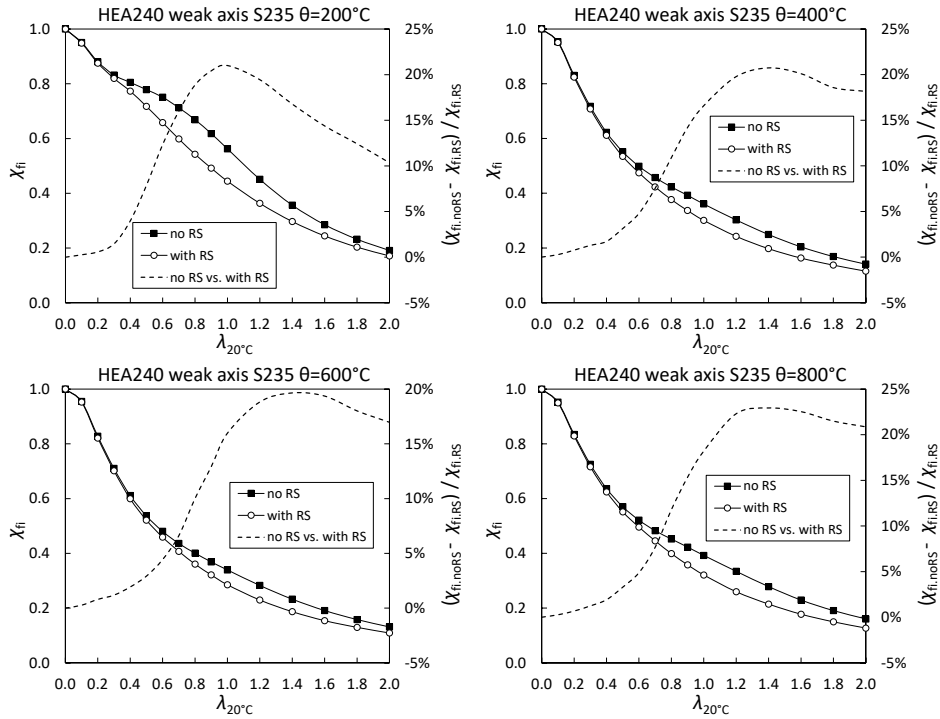


Figure 5.15: Residual stresses influence on the buckling factor for I-type section weak axis (I-Z) in case $h/b \leq 1.2$

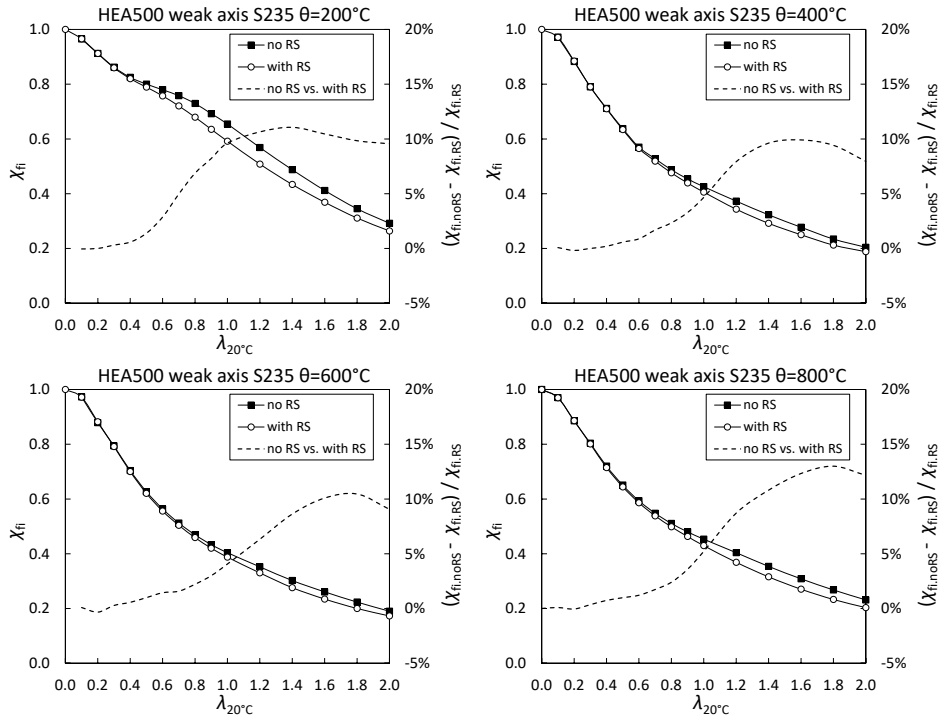


Figure 5.16: Residual stresses influence on the buckling factor for I-type section weak axis (I-Z) in case $h/b > 1.2$

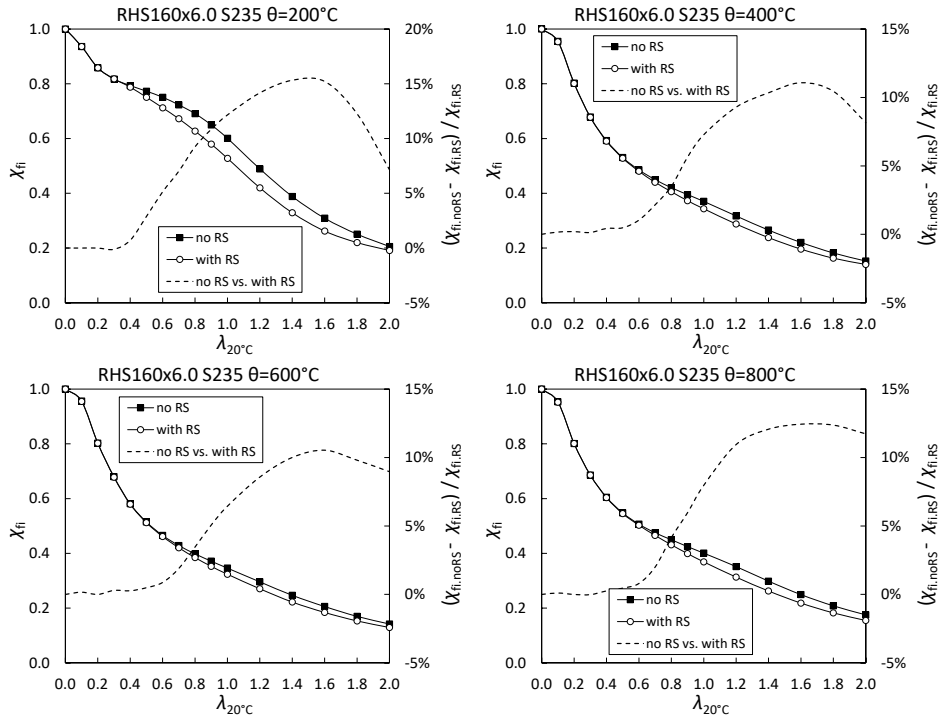


Figure 5.17: Residual stresses influence on the buckling factor for RHS-type section

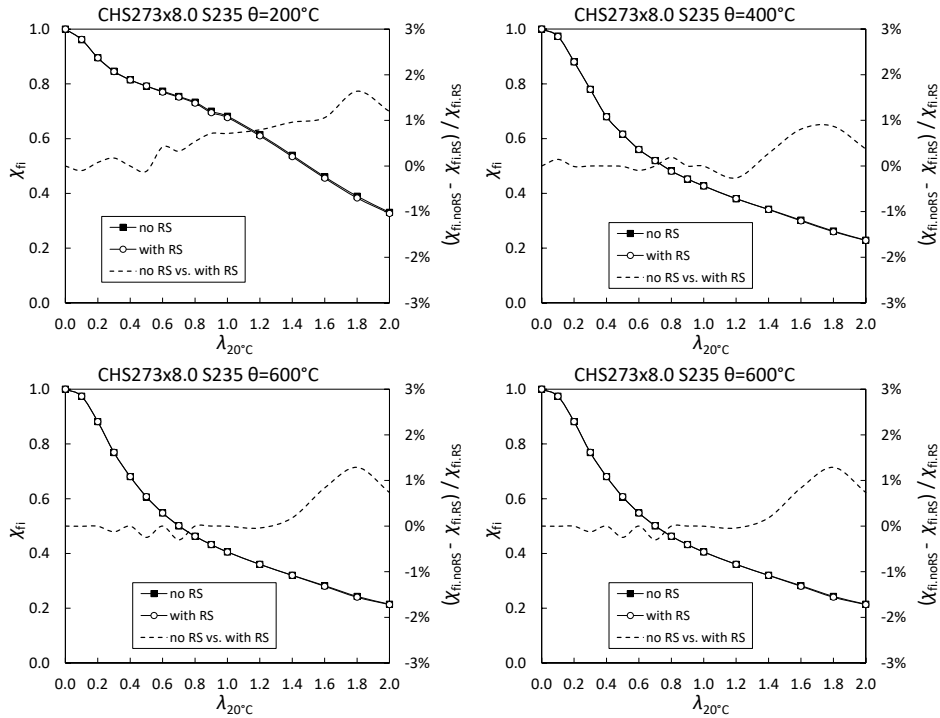


Figure 5.18: Residual stresses influence on the buckling factor for CHS-type section

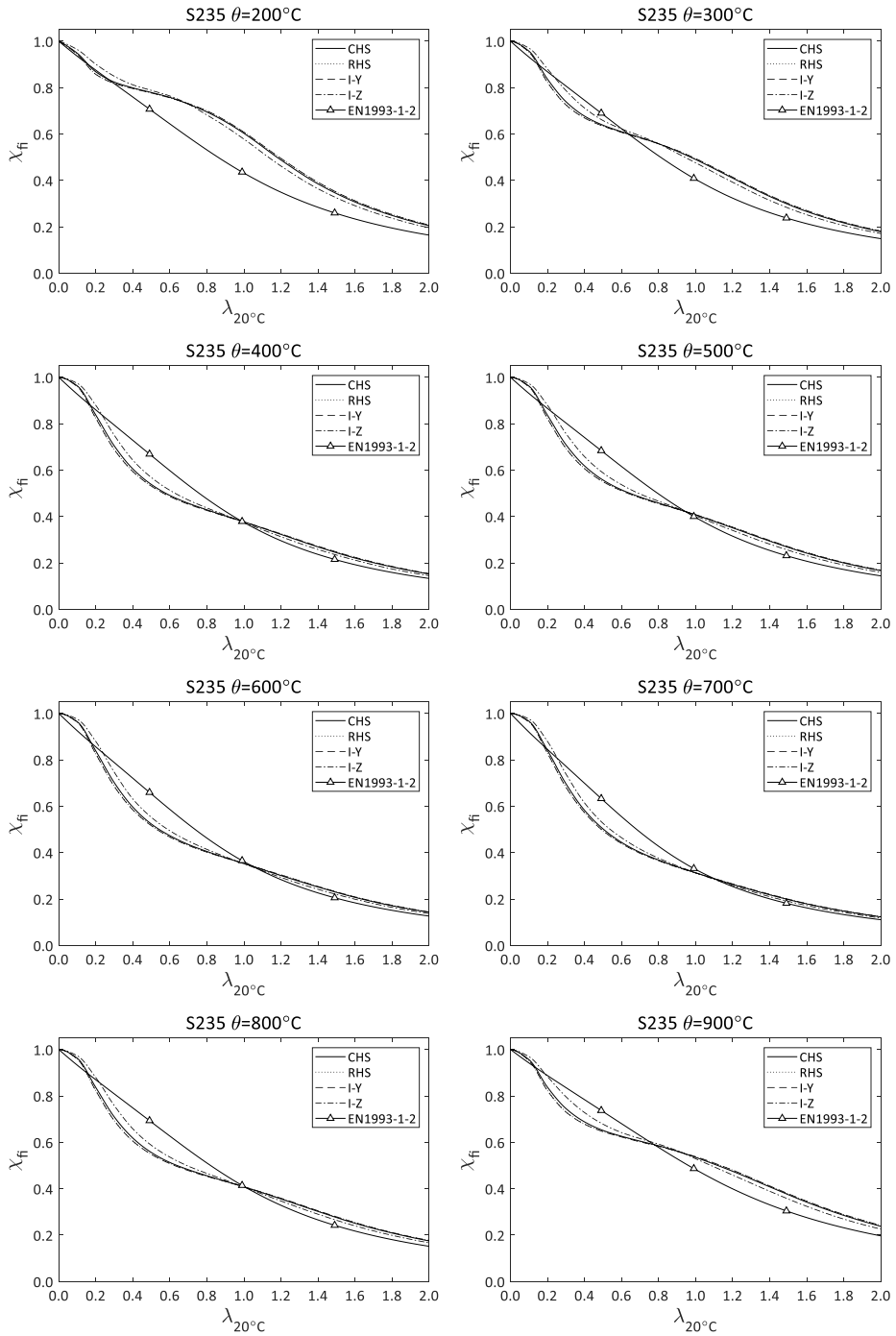


Figure 5.19: Buckling factors according to numeric modelling and EN 1993-1-2: S235

Table 5-6: Buckling factor differences between section groups

		S235			S355			S460		
		CHS vs. RHS	CHS vs. I-Y	CHS vs. I-Z	CHS vs. RHS	CHS vs. I-Y	CHS vs. I-Z	CHS vs. RHS	CHS vs. I-Y	CHS vs. I-Z
$\theta=200^{\circ}\text{C}$	mean	0.8%	0.9%	2.9%	0.7%	0.8%	2.7%	0.7%	0.7%	2.5%
	max	1.8%	1.9%	5.6%	1.6%	1.7%	5.1%	1.5%	1.5%	5.0%
$\theta=300^{\circ}\text{C}$	mean	0.9%	0.9%	3.3%	0.8%	0.8%	3.0%	0.7%	0.7%	2.8%
	max	1.7%	1.8%	6.5%	1.5%	1.6%	5.8%	1.3%	1.4%	5.1%
$\theta=400^{\circ}\text{C}$	mean	0.9%	0.9%	3.5%	0.8%	0.8%	3.1%	0.7%	0.7%	2.8%
	max	2.2%	2.2%	6.6%	1.6%	1.7%	5.7%	1.3%	1.4%	5.2%
$\theta=500^{\circ}\text{C}$	mean	0.9%	0.9%	3.5%	0.8%	0.8%	3.2%	0.7%	0.8%	2.9%
	max	2.2%	2.3%	6.7%	1.7%	1.7%	6.0%	1.4%	1.4%	5.4%
$\theta=600^{\circ}\text{C}$	mean	0.9%	0.9%	3.4%	0.8%	0.8%	3.0%	0.7%	0.7%	2.8%
	max	2.1%	2.2%	6.4%	1.6%	1.6%	5.5%	1.3%	1.3%	5.3%
$\theta=700^{\circ}\text{C}$	mean	0.9%	0.9%	3.2%	0.7%	0.9%	2.7%	0.7%	0.7%	2.3%
	max	2.0%	2.1%	6.1%	1.4%	2.1%	5.1%	1.8%	1.2%	4.4%
$\theta=800^{\circ}\text{C}$	mean	0.9%	1.0%	3.6%	0.8%	0.9%	3.2%	0.7%	0.8%	3.0%
	max	2.3%	2.3%	6.8%	1.7%	1.8%	6.1%	1.5%	1.5%	5.6%
$\theta=900^{\circ}\text{C}$	mean	0.9%	0.9%	3.4%	0.8%	0.8%	3.2%	0.8%	0.8%	3.0%
	max	2.0%	2.0%	6.8%	1.8%	1.8%	6.2%	1.6%	1.6%	5.9%

Visual analysis of the diagrams presented in Figure 5.19, Annexes A3 and A4 allows to make the following conclusion: three groups of sections show quite similar results (*CHS*, *RHS*, *I-Y*) while the results for the group *I-Z* obviously differ from others. To analyse the differences between the two groups, Table 5-6 was composed. In this table for each temperature and material, mean and average factor (5-2) is presented. Results for group *CHS* are chosen as χ_{base} , while stands χ_i for groups *RHS*, *I-Y* and *I-Z*.

$$abs\left(\frac{\chi_{base} - \chi_i}{\chi_{base}}\right) * 100\% \quad (5-2)$$

Behaviour of groups *CHS*, *RHS* and *I-Y* is very similar. Group *I-Z* is obviously different from others for all temperatures and materials. For further buckling study two groups of sections *gr1* (*CHS*, *RHS*, *I-Y*) and *gr2* (*I-Z*) are formed.

In order to analyse steel grade influence on the buckling factor Table 5-7 was composed. Factor (5-2) was used, but this time for χ_{base} results for S235 were used, while for χ_i corresponds to S355 and S460. Table 5-7 demonstrates significant differences for different materials. Differences between elements of different steel grades increase in the temperature range $200^{\circ}\text{C} - 400^{\circ}\text{C}$, differences decrease between 400°C and 600°C , then once again start to increase in the range $600^{\circ}\text{C} - 700^{\circ}\text{C}$ and finally decrease in the range $700^{\circ}\text{C} - 900^{\circ}\text{C}$. Such tendency is explained by Eurocode material model at elevated temperatures (stress-strain relationship curves) as described in 3.3.2.

Table 5-7: Buckling factor differences between materials

		S235 vs S355	S235 vs S460
$\theta=200^{\circ}\text{C}$	mean	2.2%	3.6%
	max	3.6%	5.8%
$\theta=300^{\circ}\text{C}$	mean	3.5%	5.7%
	max	6.6%	11.2%
$\theta=400^{\circ}\text{C}$	mean	5.5%	9.2%
	max	10.8%	18.3%
$\theta=500^{\circ}\text{C}$	mean	5.0%	8.4%
	max	9.6%	16.5%
$\theta=600^{\circ}\text{C}$	mean	6.0%	10.0%
	max	11.7%	19.8%
$\theta=700^{\circ}\text{C}$	mean	6.8%	11.3%
	max	13.0%	22.0%
$\theta=800^{\circ}\text{C}$	mean	5.2%	8.6%
	max	9.8%	16.7%
$\theta=900^{\circ}\text{C}$	mean	3.5%	5.8%
	max	6.2%	10.5%

Finally, the most important issue observed is the performance of EN 1993-1-2 [20] model against fem simulation. Results are presented using once again factor (5-2). For χ_{base} stands for EN 1993-1-2 model, while for χ_i denotes results for FEM modelling. Results for factor (5-2) are presented Table 5-8. Negative factor value means that EN 1993-1-2 method overestimates buckling capacity compared to FEM, while positive factor value means that EN 1993-1-2 method underestimates buckling capacity compared to FEM.

The difference in the results between EN 1993-1-2 model and FEM has been also reported in the earlier works [6], [7]. In the temperature range from 200°C to 300°C results for EN 1993-1-2 model are considered satisfactory, because for most slenderness values EN 1993-1-2 model predicts load-bearing capacity lower than obtained by the FEM. For all other temperatures the situation is more diversified and can be summarized as follows: for slenderness values ≤ 1.0 EN 1993-1-2 overestimates the load-bearing capacity and for values > 1.0 EN 1993-1-2 slightly underestimates the load-bearing capacity with respect to the FEM model. EN 1993-1-2 method for buckling capacity at elevated temperature conditions makes no distinction between sections types which is not corresponding to the results of numerical modelling.

5.8 Proposed design method – Method C

The method for buckling design proposed in this work is referred to as Method C. The method is based on the following assumption: stability of a column is guaranteed in case the equilibrium between the external and internal forces is established. In case of an axially loaded column with pinned supports and sinusoidal initial shape the fulfilment of this condition can be checked only in the mid-section of the column (location of the maximum lateral displacement). In this case the relationship between

Table 5-8: Buckling factor differences between FEM vs. EC3

		S235	S355	S460
$\theta=200^{\circ}\text{C}$	mean	15.6%	13.4%	12.0%
	min	-2.1%	-1.5%	-1.4%
	max	29.5%	26.6%	24.8%
$\theta=300^{\circ}\text{C}$	mean	10.7%	9.1%	8.2%
	min	-11.4%	-10.7%	-9.4%
	max	21.9%	19.3%	18.0%
$\theta=400^{\circ}\text{C}$	mean	10.7%	9.3%	8.3%
	min	-24.9%	-21.3%	-18.9%
	max	13.9%	12.6%	11.0%
$\theta=500^{\circ}\text{C}$	mean	10.6%	9.3%	8.4%
	min	-23.3%	-20.4%	-18.6%
	max	15.3%	13.4%	12.3%
$\theta=600^{\circ}\text{C}$	mean	11.2%	9.5%	8.4%
	min	-26.6%	-22.6%	-19.4%
	max	12.5%	10.9%	10.9%
$\theta=700^{\circ}\text{C}$	mean	11.0%	9.0%	7.5%
	min	-26.7%	-21.7%	-17.5%
	max	10.7%	9.4%	9.4%
$\theta=800^{\circ}\text{C}$	mean	11.1%	10.0%	9.1%
	min	-25.5%	-22.5%	-20.7%
	max	14.5%	12.6%	11.5%
$\theta=900^{\circ}\text{C}$	mean	10.0%	8.9%	8.2%
	min	-15.6%	-14.5%	-14.1%
	max	20.4%	17.9%	16.8%

lateral displacement and mid-section curvature can be established using (2-24). For a steel column in ambient conditions ideal elasto-plastic material model implementation is justified. Then section internal forces can be easily calculated as there is a linear stress distribution across section. As a result the equilibrium control of the internal and external forces is relatively easy procedure. The situation changes for non-linear stress-strain relationship, which is the case for the steel column in fire conditions. Stress distribution across the section is no longer linear and the calculation process of the internal forces becomes much more complex. The destabilizing forces on the other hand can be easily expressed as (2-36). In order to find the maximum load for which the equilibrium between the internal and the external forces is possible, it is essential to know the relationship between the destabilizing (external) bending moment and the stabilizing (internal) bending moment for each axial load value. This general scheme was proposed by Von-Karman [33]. The calculation method for steel columns in fire was proposed by Somaini [26] and was described in section 2.4. The method proposed in this section is also based on the Von-Karman scheme.

Column mid-section under consideration is presented in Figure 5.20. The following initial assumptions are made:

- Navier-Bernoulli hypothesis is valid
- Eurocode material model is valid
- Section point 1 is subjected to additional compression as a result of the lateral displacement; in contrast the point 2 is subjected to unloading as a result of the lateral displacement

The of stresses in the column mid-section at buckling load are presented in Figure 5.10 and Figure 5.11., where stresses in the section wall (buckling around strong axis) and in the section flange (buckling around weak axis) are reported in relation to the proportionality limit stress.

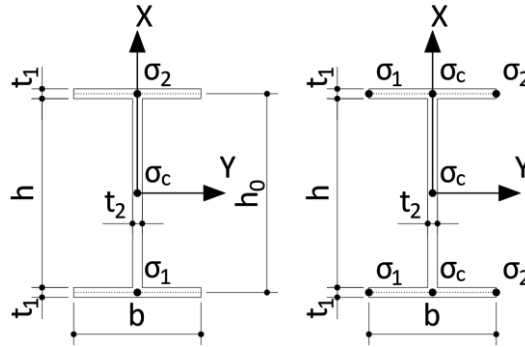


Figure 5.20: Column section scheme for Method C

At first buckling around the strong axis is considered. Internal forces are defined as follows. An important assumption is made (5-3): stress in the section centroid is equal to the mean value of stresses at points 1 and 2. Assumption (5-3) is identical to the assumption of linear stress variation across the section. Section internal axial force N_i can be split into 3 components (5-4): force in the section flanges (5-5) and (5-6), force in the section wall (5-7). For the section wall, Simpson integration scheme is used. Total internal axial force of the section can be written as (5-8). Factors α_1 (5-9) and α_2 (5-10) are introduced and will be explained later. In similar way the internal bending moment is treated in (5-11) – (5-16). Factors β_1 and β_2 are introduced as (5-14). Using the internal and external axial force equilibrium condition, the stress at section point 1 is expressed through the stress at section point 2 (5-17). Stresses at point 2 are assumed to follow Eurocode material model as described in section 3.3.2. (5-17) can then be rewritten into (5-18). For a pin-ended column with sinusoidal initial curvature, the total displacement/eccentricity in the middle of the column can be formulated as a function of the section curvature (5-19) similarly to the approach described in section 2.4. Acting external bending moment for the axially loaded column is expressed as (5-21). Using the internal and external bending moment equilibrium condition, the dependence between stress at point 2 and strain at point 2 from the strain at point 1 is obtained (5-22). At this point one more important assumption is made as (5-23). The stress at point 2 σ_2 is calculated using the secant modulus $E_{s,fi}$, which is itself formulated as follows: in case average stress from the axial load is lower than the proportionality limit stress, the secant modulus is equal to the elasticity modulus for the temperature under consideration (5-24); in case the opposite is true, the secant modulus is calculated using (5-25), where ϵ_{fi} is simply the inverse function to the EN 1993-1-2 stress function in the inelastic range. (5-18) can be updated into (5-26). (5-23) is integrated into (5-22) in order to produce

(5-27), which represents the dependence between the strain at point 2 on the strain at section point 1. Factors $\gamma_0 - \gamma_8$ are introduced in order to simplify symbolic transformations. (5-27) is introduced in the simplified form as (5-32). It is now possible to integrate (5-32) into (5-26) which after some simple transformations will result in a quadratic equation in relation to ε_1 (5-36). The discriminant of this equation is equal to (5-39) and the roots can be found using (5-40). The equation (5-36) can have non-complex roots only in case the discriminant (5-39) is non-negative. (5-39) can be used to check the stability condition: in case (5-39) is positive, column stability is guaranteed; buckling stability limit is reached, when (5-39) is equal to 0. (5-39) can be rewritten using (5-35), (5-37) and (5-38) into (5-41), which can be treated as a simple quadratic equation in relation to γ_4 . The discriminant of the (5-41) is equal to (5-42) and the root with physical meaning is equal to (5-43). By equating (5-33) and (5-43) and performing some transformations it is possible to reach the equation (5-44). The direct solution of (5-44) is not possible, as $E_{s,fi}$ and γ_0 are functions of N_e . Instead, critical force is introduced as (5-45) and the buckling stability criteria is formulated as (5-46). The proposed method is based on the section shape consisting of rectangles (Figure 5.20). Actual section may vary from the idealized (for example chamfered corners of the rolled I-shaped profiles). Idealized section area is denoted by A_i , while actual section by A . In case the design load is denoted by N_{fi} , N_e is defined as (5-47).

$$\sigma_c = \frac{\sigma_1 + \sigma_2}{2} \quad (5-3) \quad N_i = N_{i.1} + N_{i.2} + N_{i.3} \quad (5-4)$$

$$N_{i.1} = \sigma_1 b t_1 \quad (5-5) \quad N_{i.2} = \sigma_2 b t_1 \quad (5-6)$$

$$N_{i.3} = \frac{h t_2}{6} (\sigma_1 + 4\sigma_c + \sigma_2) = \sigma_1 \frac{h t_2}{2} + \sigma_2 \frac{h t_2}{2} \quad (5-7)$$

$$N_i = \sigma_1 \left(b t_1 + \frac{h t_2}{2} \right) + \sigma_2 \left(b t_1 + \frac{h t_2}{2} \right) = \sigma_1 \alpha_1 + \sigma_2 \alpha_2 \quad (5-8)$$

$$\alpha_1 = b t_1 + \frac{h t_2}{2} \quad (5-9) \quad \alpha_2 = b t_1 + \frac{h t_2}{2} \quad (5-10)$$

$$M_i = M_{i.1} + M_{i.2} + M_{i.3} \quad (5-11) \quad M_{i.1} = -\sigma_1 b t_1 \frac{h_0}{2} \quad (5-12)$$

$$M_{i.2} = \sigma_2 b t_1 \frac{h_0}{2} \quad (5-13) \quad \beta_1 = \beta_2 = b t_1 \frac{h_0}{2} + \frac{h^2 t_2}{12} \quad (5-14)$$

$$M_{i.3} = \frac{h t_2}{6} \left(-\sigma_1 \frac{h}{2} + \sigma_2 \frac{h}{2} \right) = \sigma_2 \frac{h^2 t_2}{12} - \sigma_1 \frac{h^2 t_2}{12} \quad (5-15)$$

$$M_i = \sigma_2 \left(\frac{h^2 t_2}{12} + b t_1 \frac{h_0}{2} \right) - \sigma_1 \left(\frac{h^2 t_2}{12} + b t_1 \frac{h_0}{2} \right) = \sigma_2 \beta_2 - \sigma_1 \beta_1 \quad (5-16)$$

$$-N_e = N_i = \sigma_1 \alpha_1 + \sigma_2 \alpha_2 \rightarrow \sigma_1 = -\frac{N_e}{\alpha_1} - \frac{\alpha_2}{\alpha_1} \sigma_2 \quad (5-17)$$

$$-f_{p,\theta} + c_{EC} - \frac{b_{EC}}{a_{EC}} \sqrt{a_{EC}^2 - (\varepsilon_{y,\theta} + \varepsilon_1)^2} = -\frac{N_e}{\alpha_1} - \frac{\alpha_2}{\alpha_1} \sigma_2 \quad (5-18)$$

$$y_{tot} = y_0 + \frac{\varepsilon_2 - \varepsilon_1}{h_0} \left(\frac{L}{\pi} \right)^2 = y_0 + (\varepsilon_2 - \varepsilon_1) \chi_0 \quad (5-19)$$

$$\chi_0 = \frac{1}{h_0} \left(\frac{L}{\pi} \right)^2 \quad (5-20) \quad M_e = N_e y_{tot} \quad (5-21)$$

$$\begin{aligned} M_i = M_e \rightarrow \sigma_2 \beta_2 - \sigma_1 \beta_1 = N_e y_{tot} \rightarrow \frac{\beta_2}{N_e} \left(\sigma_2 + \frac{\beta_1 N_e}{\beta_2 \alpha_1} + \frac{\beta_1 \alpha_2}{\beta_2 \alpha_1} \sigma_2 \right) &= y_{tot} \rightarrow \\ \frac{\beta_2}{N_e} \left[\sigma_2 \left(1 + \frac{\beta_1 \alpha_2}{\beta_2 \alpha_1} \right) + \frac{\beta_1 N_e}{\beta_2 \alpha_1} \right] &= y_0 + (\varepsilon_2 - \varepsilon_1) \chi_0 \rightarrow \\ \sigma_2 \left(\beta_2 + \beta_1 \frac{\alpha_2}{\alpha_1} \right) \frac{1}{N_e} - \varepsilon_2 \chi_0 &= y_0 - \varepsilon_1 \chi_0 - \frac{\beta_1}{\alpha_1} \end{aligned} \quad (5-22)$$

$$\sigma_2 = \varepsilon_2 E_{s,fi} \quad (5-23) \quad \text{if } \frac{N_e}{A_i} < f_{p,\theta} \rightarrow E_{s,fi} = E_{a,\theta} \quad (5-24)$$

$$\text{if } \frac{N_e}{A} > f_{p,\theta} \rightarrow \varepsilon_{fi} = \varepsilon_{y,\theta} - a_{EC} \sqrt{1 - \frac{1}{a_{EC}^2} \left(\frac{N_e}{A_i} + c_{EC} - f_{p,\theta} \right)^2} \rightarrow E_{s,fi} = \frac{N_e}{A \varepsilon_{fi}} \quad (5-25)$$

$$-f_{p,\theta} + c_{EC} - \frac{b_{EC}}{a_{EC}} \sqrt{a_{EC}^2 - (\varepsilon_{y,\theta} + \varepsilon_1)^2} = -\frac{N_e}{\alpha_1} - \frac{\alpha_2}{\alpha_1} E_{s,fi} \varepsilon_2 \rightarrow \quad (5-26)$$

$$\sqrt{a_{EC}^2 - (\varepsilon_{y,\theta} + \varepsilon_1)^2} = \frac{a_{EC}}{b_{EC}} \frac{\alpha_2}{\alpha_1} E_{s,fi} \varepsilon_2 + \frac{a_{EC}}{b_{EC}} \left(\frac{N_e}{\alpha_1} - f_{p,\theta} + c_{EC} \right)$$

$$E_{s,fi} \varepsilon_2 \left(\beta_2 + \beta_1 \frac{\alpha_2}{\alpha_1} \right) \frac{1}{N_e} - \varepsilon_2 \chi_0 = y_0 - \varepsilon_1 \chi_0 - \frac{\beta_1}{\alpha_1} \rightarrow \quad (5-27)$$

$$\varepsilon_2 \left[\left(\beta_2 + \beta_1 \frac{\alpha_2}{\alpha_1} \right) \frac{1}{N_e} E_{s,fi} - \chi_0 \right] = y_0 - \varepsilon_1 \chi_0 - \frac{\beta_1}{\alpha_1} \rightarrow$$

$$\varepsilon_2 = \frac{y_0 - \frac{\beta_1}{\alpha_1}}{\left(\beta_2 + \beta_1 \frac{\alpha_2}{\alpha_1} \right) \frac{1}{N_e} E_{s,fi} - \chi_0} - \varepsilon_1 \frac{\chi_0}{\left(\beta_2 + \beta_1 \frac{\alpha_2}{\alpha_1} \right) \frac{1}{N_e} E_{s,fi} - \chi_0}$$

$$\gamma_0 = \left(\beta_2 + \beta_1 \frac{\alpha_2}{\alpha_1} \right) \frac{1}{N_e} E_{s,fi} - \chi_0 \quad (5-28)$$

$$\gamma_1 = \frac{y_0 - \frac{\beta_1}{\alpha_1}}{\gamma_0} \quad (5-29)$$

$$\gamma_2 = \frac{\chi_0}{\gamma_0} \quad (5-30) \quad \gamma_3 = \frac{a_{EC}}{b_{EC}} \left(\frac{N_e}{\alpha_1} - f_{p,\theta} + c_{EC} \right) \quad (5-31)$$

$$\varepsilon_2 = \gamma_1 - \gamma_2 \varepsilon_1 \quad (5-32) \quad \gamma_4 = \frac{a_{EC}}{b_{EC}} \frac{\alpha_2}{\alpha_1} E_{s,fi} \gamma_1 + \gamma_3 \quad (5-33)$$

$$\gamma_5 = \frac{a_{EC}}{b_{EC}} \frac{\alpha_2}{\alpha_1} E_{s,fi} \gamma_2 \quad (5-34) \quad \gamma_6 = 1 + \gamma_5^2 \quad (5-35)$$

$$\begin{aligned} \sqrt{a_{EC}^2 - (\varepsilon_{y,\theta} + \varepsilon_1)^2} &= \frac{a_{EC}}{b_{EC}} \frac{\alpha_2}{\alpha_1} E_{s,fi} (\gamma_1 - \gamma_2 \varepsilon_1) + \gamma_3 \rightarrow \\ \sqrt{a_{EC}^2 - (\varepsilon_{y,\theta} + \varepsilon_1)^2} &= \frac{a_{EC}}{b_{EC}} \frac{\alpha_2}{\alpha_1} E_{s,fi} \gamma_1 + \gamma_3 - \frac{a_{EC}}{b_{EC}} \frac{\alpha_2}{\alpha_1} E_{s,fi} \gamma_2 \varepsilon_1 \rightarrow \\ \sqrt{a_{EC}^2 - (\varepsilon_{y,\theta} + \varepsilon_1)^2} &= \gamma_4 - \gamma_5 \varepsilon_1 \rightarrow \end{aligned} \quad (5-36)$$

$$\begin{aligned} a_{EC}^2 - \varepsilon_{y,\theta}^2 + 2\varepsilon_{y,\theta} \varepsilon_1 - \varepsilon_1^2 &= \gamma_4^2 - 2\gamma_4 \gamma_5 \varepsilon_1 + \gamma_5^2 \varepsilon_1^2 \rightarrow \\ \varepsilon_1^2 (1 + \gamma_5^2) - \varepsilon_1 (2\gamma_4 \gamma_5 - 2\varepsilon_{y,\theta}) + (\gamma_4^2 - a^2 + \varepsilon_{y,\theta}^2) &= 0 \rightarrow \\ \gamma_6 \varepsilon_1^2 - \gamma_7 \varepsilon_1 + \gamma_8 &= 0 \end{aligned}$$

$$\gamma_7 = 2\gamma_4 \gamma_5 - 2\varepsilon_{y,\theta} \quad (5-37) \quad \gamma_8 = \gamma_4^2 - a^2 + \varepsilon_{y,\theta}^2 \quad (5-38)$$

$$D = \gamma_7^2 - \gamma_6 \gamma_8 \quad (5-39) \quad \varepsilon_{1:1,2} = \frac{\gamma_7 \pm \sqrt{\gamma_7^2 - \gamma_6 \gamma_8}}{2\gamma_6} \quad (5-40)$$

$$\begin{aligned} \gamma_7^2 - 4\gamma_6 \gamma_8 &= 4\gamma_4^2 \gamma_5^2 - 8\gamma_4 \gamma_5 \varepsilon_{y,\theta} + 4\varepsilon_{y,\theta}^2 - 4(1 + \gamma_5^2)(\gamma_4^2 - a_{EC}^2 + \varepsilon_{y,\theta}^2) \rightarrow \\ \gamma_4^2 + 2\gamma_5 \varepsilon_{y,\theta} \gamma_4 + [\gamma_5^2 (\varepsilon_{y,\theta}^2 - a_{EC}^2) - a_{EC}^2] &= 0 \end{aligned} \quad (5-41)$$

$$D = 4\gamma_5^2 a_{EC}^2 + 4a_{EC}^2 \quad (5-42) \quad \gamma_{4:1,2} = -\gamma_5 \varepsilon_{y,\theta} + a_{EC} \sqrt{\gamma_5^2 + 1} \quad (5-43)$$

$$\begin{aligned} \frac{a_{EC}}{b_{EC}} \frac{\alpha_2}{\alpha_1} E_{s,fi} \gamma_1 + \gamma_3 &= -\gamma_5 \varepsilon_{y,\theta} + a_{EC} \sqrt{\gamma_5^2 + 1} \rightarrow \\ \frac{a_{EC}}{b_{EC}} \left(\frac{N_e}{\alpha_1} - f_{p,\theta} + c_{EC} \right) &= -\gamma_5 \varepsilon_{y,\theta} + a_{EC} \sqrt{\gamma_5^2 + 1} - \frac{a_{EC}}{b_{EC}} \frac{\alpha_2}{\alpha_1} E_{s,fi} \gamma_1 \rightarrow \\ N_e &= \alpha_1 \left[\frac{b_{EC}}{a_{EC}} \left(a_{EC} \sqrt{\gamma_5^2 + 1} - \frac{a_{EC}}{b_{EC}} \frac{\alpha_2}{\alpha_1} E_{s,fi} \gamma_1 - \gamma_5 \varepsilon_{y,\theta} \right) + f_{p,\theta} - c_{EC} \right] \rightarrow \\ N_e &= \alpha_1 \left[b_{EC} \sqrt{\left(\frac{a_{EC}}{b_{EC}} \frac{\alpha_2}{\alpha_1} E_{s,fi} \frac{\chi_0}{\gamma_0} \right)^2 + 1} - \frac{\alpha_2}{\alpha_1} E_{s,fi} \varepsilon_{y,\theta} \frac{\chi_0}{\gamma_0} - \frac{\alpha_2}{\alpha_1} E_{s,fi} \frac{y_0 - \frac{\beta_1}{\alpha_1}}{\gamma_0} + f_{p,\theta} - c_{EC} \right] \\ N_{cr,fi} &= \alpha_1 \left[b_{EC} \sqrt{\left(\frac{a_{EC}}{b_{EC}} \frac{\alpha_2}{\alpha_1} E_{s,fi} \frac{\chi_0}{\gamma_0} \right)^2 + 1} - \frac{\alpha_2}{\alpha_1} E_{s,fi} \varepsilon_{y,\theta} \frac{\chi_0}{\gamma_0} - \frac{\alpha_2}{\alpha_1} E_{s,fi} \frac{y_0 - \frac{\beta_1}{\alpha_1}}{\gamma_0} + f_{p,\theta} - c_{EC} \right] \end{aligned} \quad (5-44)$$

$$N_{cr,fi} = \alpha_1 \left[b_{EC} \sqrt{\left(\frac{a_{EC}}{b_{EC}} \frac{\alpha_2}{\alpha_1} E_{s,fi} \frac{\chi_0}{\gamma_0} \right)^2 + 1} - \frac{\alpha_2}{\alpha_1} E_{s,fi} \varepsilon_{y,\theta} \frac{\chi_0}{\gamma_0} - \frac{\alpha_2}{\alpha_1} E_{s,fi} \frac{y_0 - \frac{\beta_1}{\alpha_1}}{\gamma_0} + f_{p,\theta} - c_{EC} \right] \quad (5-45)$$

$$N_e \leq N_{cr,fi} \quad (5-46)$$

$$N_e = N_{fi} \frac{A_i}{A} \quad (5-47)$$

Performance of the proposed method against non-linear FEM is demonstrated in Figure 5.21. and appears to be satisfactory. The method for the buckling capacity around the weak axis is basically the same, with the only difference in the formulation of the internal forces (5-8) and (5-16). Assuming linear stress variation and using Simpson's integration scheme, factors β_1 and β_2 must be reformulated as (5-48). As shown in Figure 5.11, stress variation for the weak axis buckling in the column mid-section at buckling is considerably different from linear. Replacing the linear stress variation by the elliptical stress variation, factors α_1 and α_2 are reformulated as (5-49) and (5-50), while factors β_1 and β_2 are reformulated as (5-51). Performance of Method C for the weak axis buckling is presented in Figure 5.22. In each diagram two curves are presented: 1 – for the linear stress variation across the section; 2 – for the elliptical stress variation. Performance of the Method C for the weak axis buckling is considerably worse compared to the strong axis buckling. For the large slenderness values, method C performance is quite good in case linear stress variance is assumed. On the other hand, for small slenderness values the assumption of elliptical stress variance gives better results.

$$\beta_1 = \beta_2 = \frac{b^2 t_1}{6} \quad (5-48)$$

$$\alpha_1 = 2bt_1 \frac{\pi}{4} + \frac{\sqrt{3}}{2} ht_2 \quad (5-49) \quad \alpha_2 = 2bt_1 \left(1 - \frac{\pi}{4} \right) + \frac{2 - \sqrt{3}}{2} ht_2 \quad (5-50)$$

$$\beta_1 = \beta_2 = b^2 t_1 \frac{3\pi - 8}{12} \quad (5-51)$$

The weak performance of Method C for the weak axis buckling motivates to improve the method. It is proposed to use the curve fitting approach in combination with the initial framework of Method C. At the same time, curve fitting is used to account for the influence of the residual stresses. The base composed of the non-linear FEM simulations presented section 5.7 is used. In the fitting procedure factors α_1 , α_2 , β_1 and β_2 are targeted by introducing control parameters g_1 , g_2 and g_3 and reformulating α_1 , α_2 , β_1 and β_2 as (5-52), (5-53), (5-54) and (5-55) correspondingly. The solution (5-45) is not otherwise modified. The fitting procedure is performed as follows. Parameter g_3 value is chosen in the range 0.3 ... 1.0; for each slenderness $\lambda_{20^\circ\text{C}}$ (5-1) value from 0.1 to 2.0, for each steel class (S235, S355, S460) and for each temperature value from 200°C to 900°C parameters g_1 and g_2 are obtained numerically by minimizing the goal function which is the difference between the corresponding FEM solution and the solution by Method C (5-45). Curve fitting procedure is executed for the parameters g_1 and g_2 in the slenderness domain (Figure 5.23 and Figure 5.24) using 5-th degree polynomial: (5-56) for g_1 and (5-57) for g_2 approximation. Polynomial coefficients are presented in Table 5-9. Optimal values of the parameter g_3 are presented in Table 5-10. Results of the performance of the improved Method C are presented in Figure 5.25 (strong axis buckling) and Figure 5.26 (weak axis buckling) for steel class S355. Results for steel class S235 and S460 are presented in Annexes A5 – A8. Considerable improvement of the performance can be observed, which is especially important for the weak axis buckling as the initial performance of the proposed method was not satisfactory. Still, even after the improvement the difference between the buckling capacity around the weak axis for the temperature of 200°C predicted by Method C and non-linear FEM is up to 8% and on the unsafe side. For other temperatures the difference is below 5%.

Solution for the strong axis buckling can be used for buckling analysis of rectangular hollow core sections by replacing wall thickness t_2 with the hollow core section thickness multiplied by 2. The proposed method has no direct analytical solution. Buckling capacity can be checked using one calculation cycle, but iterative procedure is needed to define the buckling capacity limit. The calculation of maximum buckling capacity definition is computationally efficient demanding on average 2×10^{-5} seconds compared to 2 seconds for non-linear FEM procedure (8 cores 3.6 GHz). Computational efficiency of the proposed method allows to perform large set of reliability calculations for a big number of thermal configurations.

$$\alpha_1 = g_1 A \quad (5-52) \quad \alpha_2 = (1 - g_1) A \quad (5-53)$$

$$\beta_1 = W_{el} g_2 g_3 \quad (5-54) \quad \beta_2 = W_{el} (2 - g_2) g_3 \quad (5-55)$$

$$g_1 = p_1 \lambda_{20^\circ\text{C}}^5 + p_2 \lambda_{20^\circ\text{C}}^4 + p_3 \lambda_{20^\circ\text{C}}^3 + p_4 \lambda_{20^\circ\text{C}}^2 + p_5 \lambda_{20^\circ\text{C}} + p_6 \quad (5-56)$$

$$g_2 = q_1 \lambda_{20^\circ\text{C}}^5 + q_2 \lambda_{20^\circ\text{C}}^4 + q_3 \lambda_{20^\circ\text{C}}^3 + q_4 \lambda_{20^\circ\text{C}}^2 + q_5 \lambda_{20^\circ\text{C}} + q_6 \quad (5-57)$$

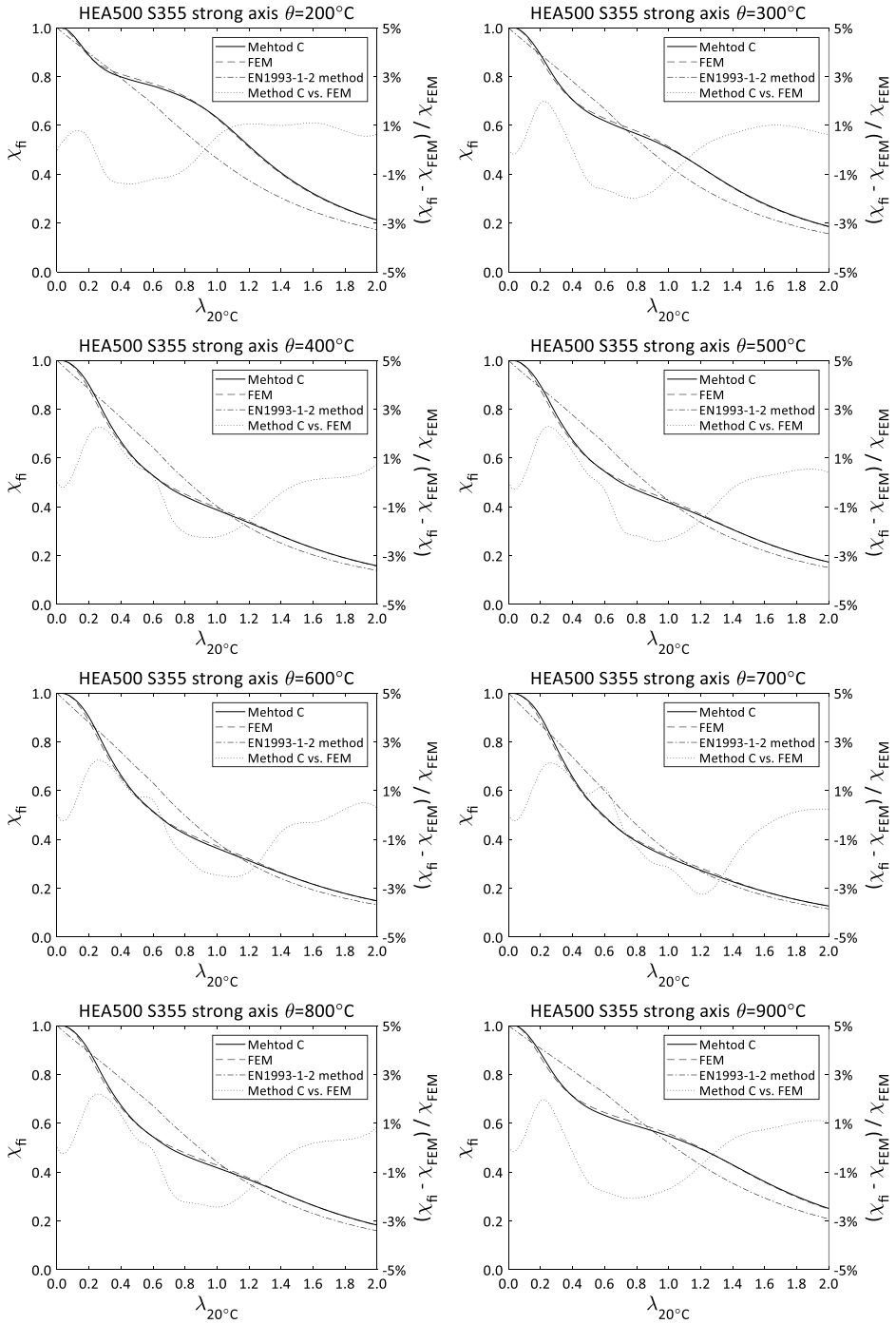


Figure 5.21: Method C performance against non-linear FEM for the strong axis buckling

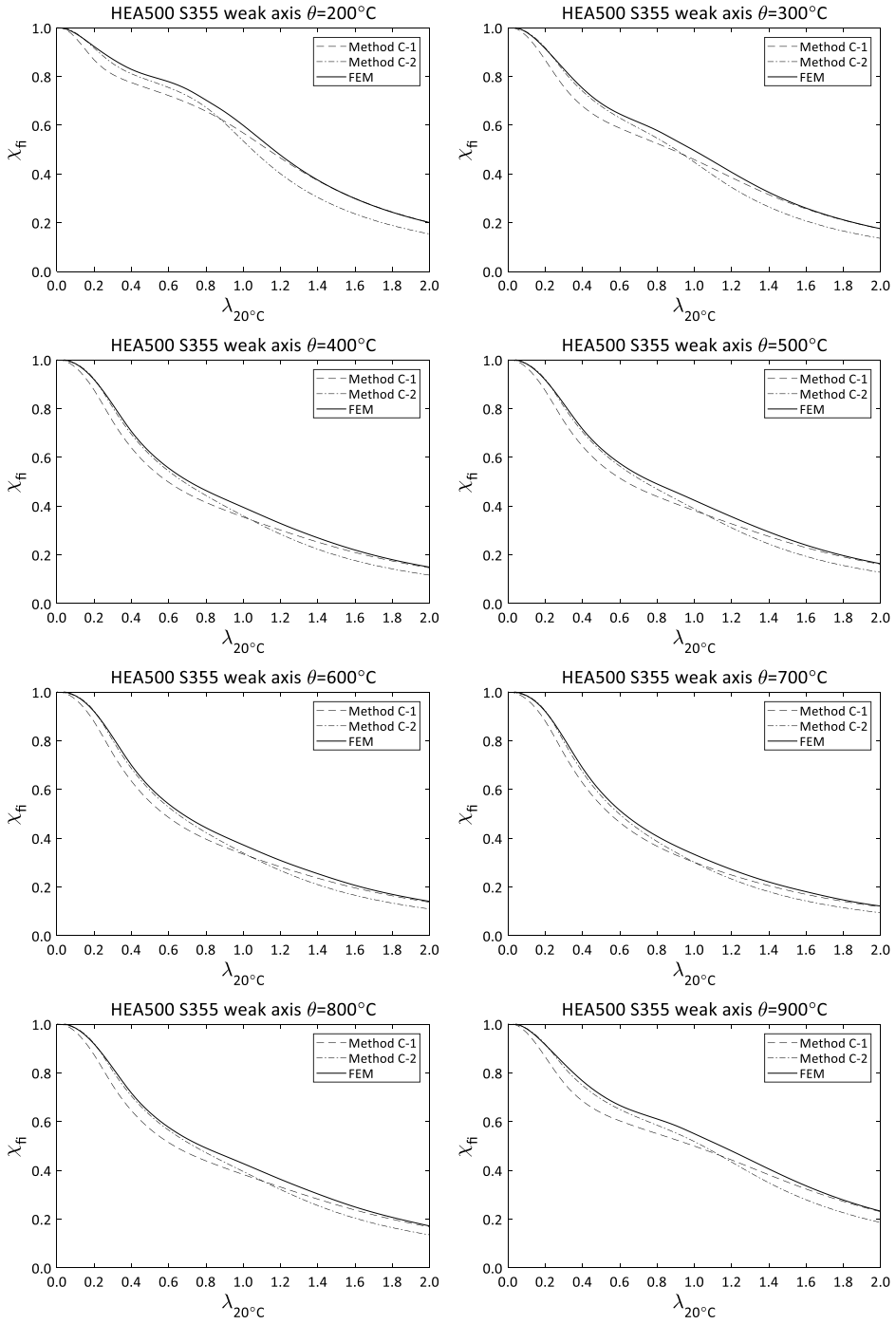


Figure 5.22: Method C performance against non-linear FEM for the weak axis buckling

Table 5-9: Polynomial coefficients for g_1 and g_2

		i=1	i=2	i=3	i=4	i=5	i=6
strong axis	p_i	-0.01818	0.10224	-0.20326	0.16956	-0.04802	0.50328
	q_i	-0.05820	0.33083	-0.66140	0.54747	-0.14433	1.00670
weak axis	p_i	-0.02233	0.12767	-0.25498	0.15452	0.01291	0.49730
	q_i	-0.03406	0.21528	-0.43014	0.20758	0.07611	0.99910

Table 5-10: Control parameter g_3 values

	S235	S355	S460
strong axis		0.510	
weak axis	0.585	0.550	0.535

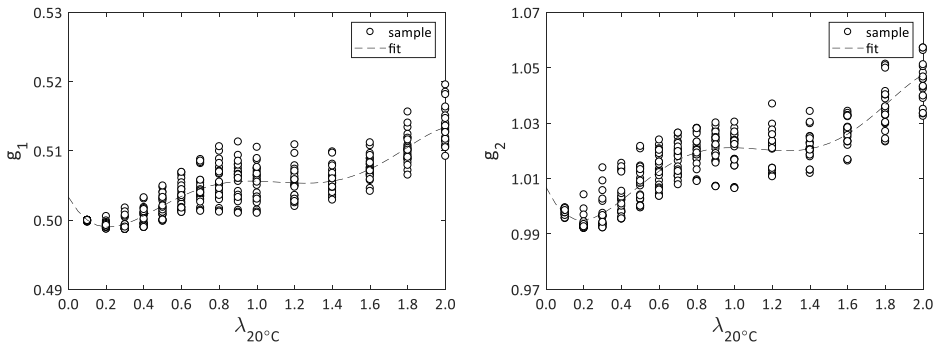


Figure 5.23: Control parameters g_1 and g_2 for the strong axis buckling

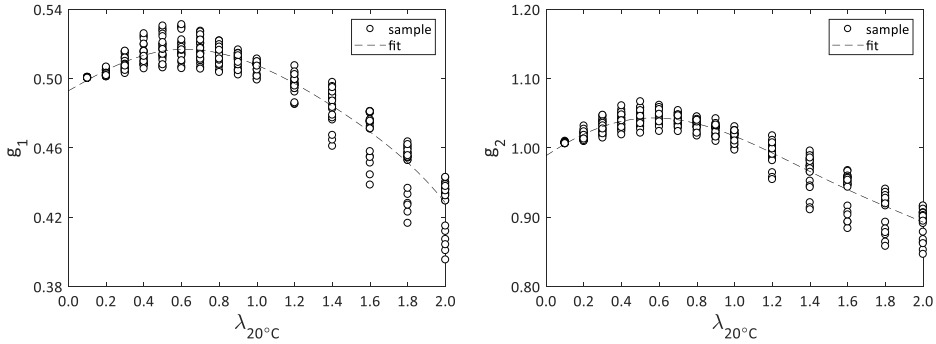


Figure 5.24: Control parameters g_1 and g_2 for the weak axis buckling

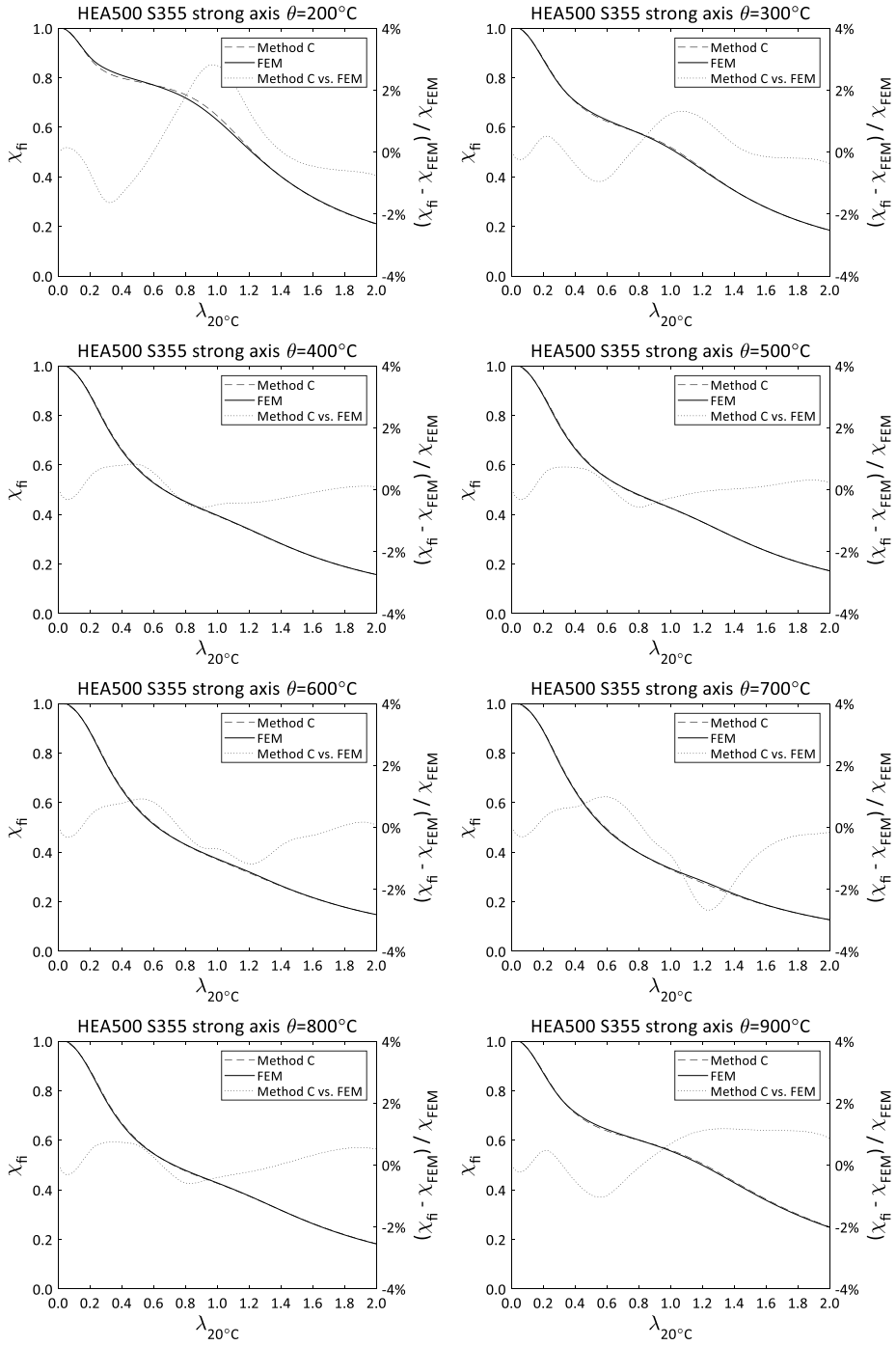


Figure 5.25: Method C performance for the strong axis buckling after model improvement

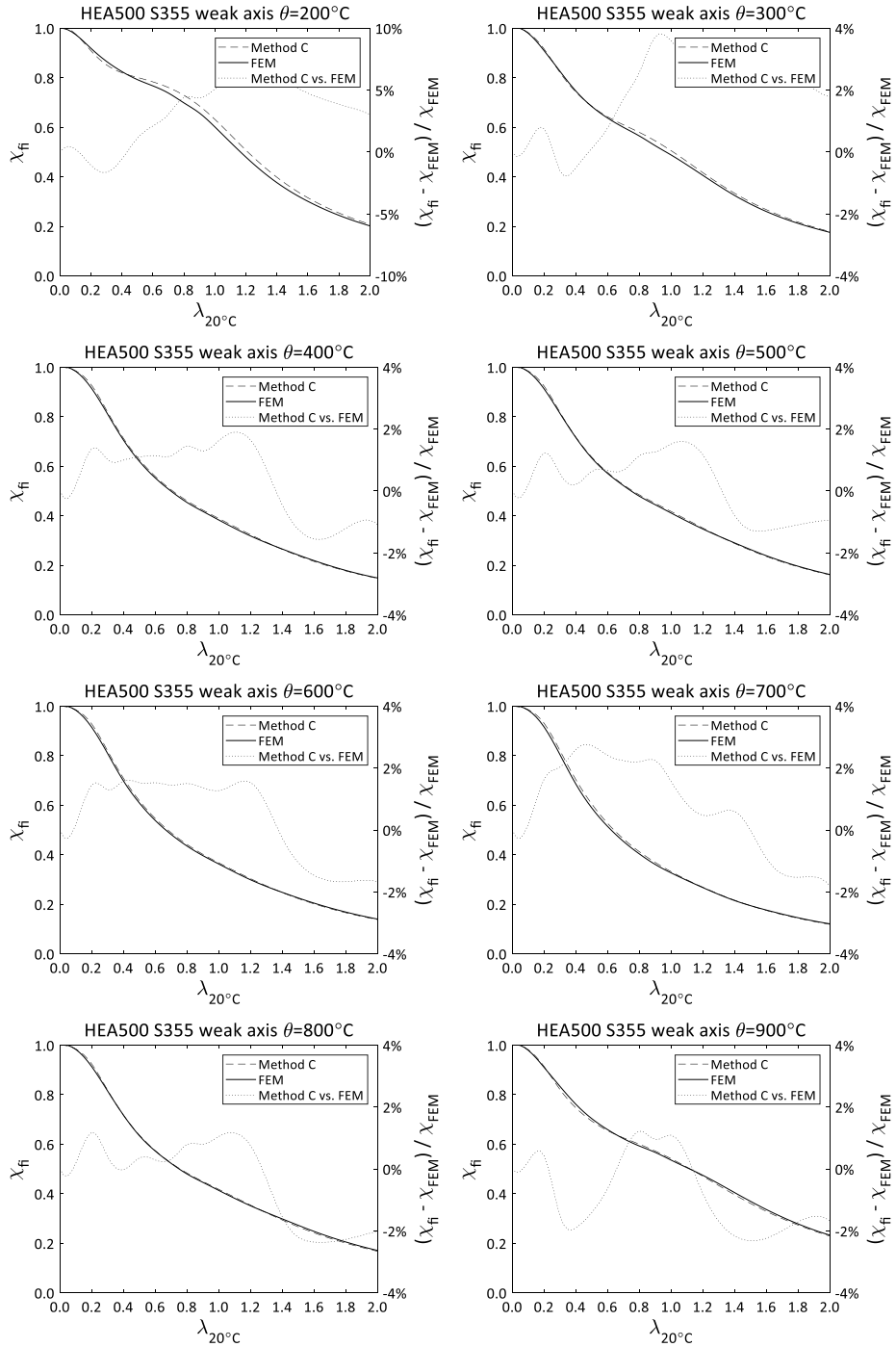


Figure 5.26: Method C performance for the weak axis buckling after model improvement

The method procedure is summarized as follows:

1. Calculate idealized section area A_i , elastic modulus $W_{el,i}$ and initial eccentricity y_0 .
2. Calculate adjusted design load N_e from the design load N_{fi} :

$$N_e = N_{fi} \frac{A_i}{A}$$

3. Calculate parameters g_1 , g_2 and g_3 using data for p_i and q_i from Table 5-9:

$$g_1 = p_1 \lambda_{20^\circ\text{C}}^5 + p_2 \lambda_{20^\circ\text{C}}^4 + p_3 \lambda_{20^\circ\text{C}}^3 + p_4 \lambda_{20^\circ\text{C}}^2 + p_5 \lambda_{20^\circ\text{C}} + p_6$$

$$g_2 = q_1 \lambda_{20^\circ\text{C}}^5 + q_2 \lambda_{20^\circ\text{C}}^4 + q_3 \lambda_{20^\circ\text{C}}^3 + q_4 \lambda_{20^\circ\text{C}}^2 + q_5 \lambda_{20^\circ\text{C}} + q_6$$

$$\text{Strong axis: } g_3 = 0.510$$

$$\text{Weak axis: } S235 \rightarrow g_3 = 0.580 \quad S355 \rightarrow g_3 = 0.550 \quad S460 \rightarrow g_3 = 0.535$$

4. Calculate section parameters:

$$\alpha_1 = g_1 A_i \quad \alpha_2 = (1 - g_1) A_i \quad \beta_1 = W_{el} g_2 g_3 \quad \beta_2 = W_{el} (2 - g_2) g_3$$

5. Calculated secant modulus $E_{s,fi}$:

$$\text{if } \frac{N_e}{A_i} < f_{p,\theta} \rightarrow E_{s,fi} = E_{a,\theta}$$

$$\text{if } \frac{N_e}{A} > f_{p,\theta} \rightarrow \varepsilon_{fi} = \varepsilon_{y,\theta} - a_{EC} \sqrt{1 - \frac{1}{a_{EC}^2} \left(\frac{N_e}{A_i} + c_{EC} - f_{p,\theta} \right)^2} \rightarrow E_{s,fi} = \frac{N_e}{A_i \varepsilon_{fi}}$$

6. Calculated model parameters:

$$\chi_0 = \frac{1}{h_0} \left(\frac{L}{\pi} \right)^2 \quad \gamma_0 = \left(\beta_2 + \beta_1 \frac{\alpha_2}{\alpha_1} \right) \frac{1}{N_e} E_{s,fi} - \chi_0$$

7. Calculated Eurocode material model parameters a_{EC} , b_{EC} and c_{EC} (presented in section 3.3.2).

8. Calculate critical force:

$$N_{cr,fi} = \alpha_1 \left[b_{EC} \sqrt{\left(\frac{a_{EC} \alpha_2}{b_{EC} \alpha_1} E_{s,fi} \frac{\chi_0}{\gamma_0} \right)^2 + 1} - \frac{\alpha_2}{\alpha_1} E_{s,fi} \varepsilon_{y,\theta} \frac{\chi_0}{\gamma_0} - \frac{\alpha_2}{\alpha_1} E_{s,fi} \frac{y_0 - \frac{\beta_1}{\alpha_1}}{\gamma_0} + f_{p,\theta} - c_{EC} \right]$$

9. Buckling capacity can be checked:

$$\text{If } N_e \leq N_{cr,fi} \rightarrow \text{stability guaranteed.}$$

5.9 Example

In order to demonstrate the proposed methods a calculation example is presented.

Section: HEA500 strong axis

Steel grade: S355 $\rightarrow f_y = 355$ MPa; $E = 210\,000$ MPa

Temperature: $\theta = 500^\circ\text{C}$

Effective length: $L_{eff} = 8\,009$ mm

Section parameters: $A = 19\,754$ mm², $I_y = 869\,748\,000$ mm⁴

Axial load: $N_{fi} = 3\,264$ kN

$$k_{y,\theta} = 0.780 \quad k_{p,\theta} = 0.360 \quad k_{E,\theta} = 0.600 \quad \varepsilon_{p,\theta} = 0.0010143 \quad \varepsilon_{y,\theta} = 0.02 \quad f_{y,\theta} = 276.9 \text{ MPa}$$

$$f_{p,\theta} = 127.8 \text{ MPa} \quad E_{a,\theta} = 126\,000 \text{ MPa}$$

$$\bar{\lambda} = \frac{L_{eff}}{\sqrt{\frac{I_y}{A}}\pi} \sqrt{\frac{f_y}{E}} = \frac{8009}{\sqrt{\frac{869748000}{19754}}\pi} \sqrt{\frac{355}{210000}} = 0.500$$

$$\bar{\lambda}_\theta = \bar{\lambda} \sqrt{\frac{k_{y,\theta}}{k_{E,\theta}}} = 0.5 \sqrt{\frac{0.780}{0.600}} = 0.570$$

Eurocode method:

$$\alpha = 0.65 \sqrt{\frac{235}{f_y}} = 0.65 \sqrt{\frac{235}{355}} = 0.529$$

$$\varphi_\theta = \frac{1}{2} [1 + \alpha \bar{\lambda}_\theta + \bar{\lambda}_\theta^2] = \frac{1}{2} [1 + 0.529 * 0.570 + 0.570^2] = 0.813$$

$$\chi_{fi} = \frac{1}{\varphi_\theta + \sqrt{\varphi_\theta^2 - \bar{\lambda}_\theta^2}} = \frac{1}{0.813 + \sqrt{0.813^2 - 0.570^2}} = 0.718$$

$$N_{b,fi,t,Rd,EC} = \chi_{fi} A k_{y,\theta} f_y = 0.718 * 19754 * 0.780 * 355 = 3\,926\,041\,N$$

FEM:

$$N_{b,fi,t,Rd,FEM} = 3\,260\,050\,N$$

Method C:

1. Idealized section area A_i , elastic modulus $W_{el,i}$ and initial eccentricity y_0 :

$$A_i = 2 * 300 * 23 + 444 * 12 = 19\,128\,mm^2$$

$$W_{el,i} = \frac{2 * (300 * 23 * 233.5^2 + \frac{300 * 23^3}{12}) + \frac{12 * 444^3}{12}}{\frac{490}{2}} = 3.431 * 10^6\,mm^3$$

$$y_0 = \frac{L_{eff}}{1\,000} = \frac{8\,009}{1\,000} = 8.009\,mm$$

2. Adjusted design load N_e from the design load N_{fi} :

$$N_e = N_{fi} \frac{A_i}{A} = 3\,264\,000 * \frac{19\,128}{19\,754} = 3\,160\,565\,N$$

3. Parameters g_1 , g_2 and g_3 using data for p_i and q_i from Table 5-9:

$$g_1 = p_1 \lambda_{20^\circ C}^5 + p_2 \lambda_{20^\circ C}^4 + p_3 \lambda_{20^\circ C}^3 + p_4 \lambda_{20^\circ C}^2 + p_5 \lambda_{20^\circ C} + p_6 = -0.01818 * 0.5^5 + \\ + 0.10224 * 0.5^4 - 0.20326 * 0.5^3 + 0.16956 * 0.5^2 - 0.04802 * 0.5 + 0.50328 = \\ = 0.5021$$

$$g_2 = q_1 \lambda_{20^\circ C}^5 + q_2 \lambda_{20^\circ C}^4 + q_3 \lambda_{20^\circ C}^3 + q_4 \lambda_{20^\circ C}^2 + q_5 \lambda_{20^\circ C} + q_6 = -0.0582 * 0.5^5 + \\ + 0.33083 * 0.5^4 - 0.6614 * 0.5^3 + 0.54747 * 0.5^2 - 0.14433 * 0.5 + 1.0067 = \\ = 1.0076$$

$$g_3 = 0.510$$

4. Section parameters:

$$\begin{aligned}\alpha_1 &= g_1 A_i = 0.5021 * 19\,128 = 9\,604\,mm^2 \\ \alpha_2 &= (1 - g_1) A_i = (1 - 0.5021) * 19\,128 = 9\,524\,mm^2 \\ \beta_1 &= W_{el} g_2 g_3 = 3.431 * 10^6 * 1.0076 * 0.510 = 1.763 * 10^6\,mm^3 \\ \beta_2 &= W_{el} (2 - g_2) g_3 = 3.431 * 10^6 * (2 - 1.0076) * 0.510 = 1.736 * 10^6\,mm^3\end{aligned}$$

5. Secant modulus $E_{s,fi}$:

$$\begin{aligned}\sigma_{fi} &= \frac{N_e}{A_i} = \frac{3\,160\,565}{19\,128} = 165.2\,MPa > f_{p,\theta} = 0.360 * 355 = 127.8\,MPa \\ \varepsilon_{fi} &= \varepsilon_{y,\theta} - a_{EC} \sqrt{1 - \frac{1}{b_{EC}^2} \left(\frac{N_e}{A_i} + c_{EC} - f_{p,\theta} \right)^2} = \\ &= 0.02 - 0.019 \sqrt{1 - \frac{1}{159.716^2} \left(\frac{3\,160\,565}{19\,128} + 10.616 - 127.8 \right)^2} = 0.0018802 \\ E_{s,fi} &= \frac{N_e}{A_i \varepsilon_{fi}} = \frac{3\,160\,565}{19\,128 * 0.0018802} = 87\,882\,MPa\end{aligned}$$

6. Calculated model parameters:

$$\begin{aligned}\chi_0 &= \frac{1}{h_0} \left(\frac{L}{\pi} \right)^2 = \frac{1}{467} \left(\frac{8\,009}{\pi} \right)^2 = 13\,917\,mm \\ \gamma_0 &= \left(\beta_2 + \beta_1 \frac{\alpha_2}{\alpha_1} \right) \frac{E_{s,fi}}{N_e} - \chi_0 = \left(1.736 * 10^6 + 1.763 * 10^6 * \frac{9\,524}{9\,604} \right) \frac{87\,882}{3\,160\,565} = \\ &= 82\,982\,mm\end{aligned}$$

7. Eurocode material model parameters a_{EC} , b_{EC} and c_{EC} (presented in section 3.3.2):

$$a_{EC} = 0.019 \quad b_{EC} = 159.716 \quad c_{EC} = 10.616$$

8. Calculate critical force:

$$\begin{aligned}N_{cr,fi} &= \alpha_1 \left[b_{EC} \sqrt{\left(\frac{a_{EC} \alpha_2}{b_{EC} \alpha_1} E_{s,fi} \frac{\chi_0}{\gamma_0} \right)^2 + 1} - \frac{\alpha_2}{\alpha_1} E_{s,fi} \varepsilon_{y,\theta} \frac{\chi_0}{\gamma_0} - \frac{\alpha_2}{\alpha_1} E_{s,fi} \frac{y_0 - \frac{\beta_1}{\alpha_1}}{\gamma_0} + f_{p,\theta} - c_{EC} \right] = \\ &= 9\,604 * (159.716 \sqrt{\left(\frac{0.019}{159.716} * \frac{9\,524}{9\,604} * 87\,882 * \frac{13\,917}{82\,982} \right)^2 + 1} - \\ &\quad - \frac{9\,524}{9\,604} * 87\,882 * 0.02 * \frac{13\,917}{82\,982} - \frac{9\,524}{9\,604} * 87\,882 * \frac{8.009 - \frac{1.763 * 10^6}{9\,604}}{82\,982} + 127.8 - \\ &\quad - 10.616) = 3\,165\,493\,N\end{aligned}$$

9. Buckling capacity check:

$$N_e = 3\,160\,565\,N \leq N_{cr,fi} = 3\,165\,493\,N \rightarrow \text{stability guaranteed.}$$

Buckling capacity can be defined iteratively.

$$N_{e.max} = 3\,173\,919\,N \rightarrow N_{fi.max} = N_{e.max} \frac{A}{A_i} = 3\,173\,919 * \frac{19\,754}{19\,128} = 3\,277\,792\,N$$

The maximum buckling capacity calculated using the proposed method is 3 277 792 N, which is very close to the buckling capacity calculated using non-linear FEM 3 260 050 N (difference is around 0.5%).

5.10 Validation against tests

The methods proposed in this work are based on and are validated by the results obtained by FEM. Results obtained by FEM have been validated by tests from databases: SCOFIDAT [30] and ETHZ [60]. Document [30] is the basic report for the current EN 1993-1-2 [20] design method. Tests from the report are dated back to 1979 – 1994. Tests were performed in different laboratories in Belgium, Germany and France. The report deals with the I-section buckling. Most cases in the report are related to the weak axis buckling. All tests were performed in the temperature domain, i.e. columns were loaded at ambient temperature and then temperature was raised until the column collapsed. Limited data of the material properties has been reported (elastic modulus and yield limit stress), but the data concerning stress-strain relationships is not available.

Tests in ETHZ [60] were performed in 2012 for a smaller number of columns, but including I-section weak and strong axis and RHS sections. Tests were organized in the load domain, i.e. columns were heated uniformly up to a given temperature and then loaded until collapse. The tests were accompanied by the material tests and accurate data regarding stress-strain relationships is available, which is very important in case good validation with the numerical model is expected. Validation results are presented in Figure 5.27, Table 5-11 and Table 5-12.

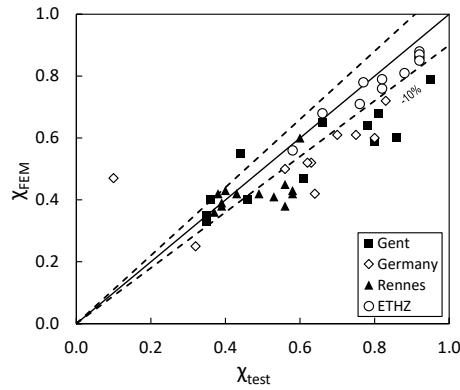


Figure 5.27: Validation against test results

Table 5-11: Validation against test series from SCOFIDAT

ID	Profile	Axis	f_y , MPa	L_{eff} , mm	F_{ult} , kN	$f_{y.fi}$, MPa	χ_{test}	χ_{FEM}	$\frac{\chi_{FEM}}{\chi_{Test}}$	θ_{test} , °C	θ_{FEM} , °C	$\frac{\theta_{FEM}}{\theta_{Test}}$
7	HEB300	weak	271	1 890	2 000	137	1.02	0.79	0.77	588	455	0.77
8	IPE160	weak	271	1 890	106	158	0.35	0.33	0.96	564	573	1.02
9	IPE160	weak	271	1 890	154	226	0.35	0.35	1.00	475	582	1.22
10	IPE200	weak	271	1 890	203	162	0.46	0.40	0.88	559	582	1.04
11	IPE200	weak	271	1 890	267	271	0.36	0.40	1.12	394	506	1.28
12	IPE200	weak	271	1 916	324	271	0.44	0.55	1.26	250	404	1.62
14	HEB120	weak	260	1 890	267	134	0.61	0.47	0.77	585	559	0.96
15	HEB180	weak	275	1 890	603	119	0.80	0.59	0.73	616	553	0.90
16	HEB180	weak	275	1 890	893	163	0.86	0.60	0.70	560	442	0.79
17	HEA200	weak	279	1 890	677	169	0.78	0.64	0.81	556	484	0.87
18	HEA300	weak	269	1 890	1 607	159	0.95	0.79	0.83	561	413	0.74
19	HEA220	weak	252	1 916	972	195	0.81	0.68	0.84	502	354	0.71
20	HEB200	weak	218	1 916	681	137	0.66	0.65	0.98	549	522	0.95
31	HEB120	strong	257	3 800	318	153	0.64	0.42	0.67	560	519	0.93
54	HEB180	strong	267	3 860	891	223	0.63	0.52	0.83	475	414	0.87
55	HEB180	strong	249	3 860	876	224	0.62	0.52	0.84	446	390	0.88
78	HEB240	weak	229	3 700	1 230	216	0.56	0.50	0.89	425	407	0.96
79	HEB240	weak	221	1 860	1 195	140	0.83	0.72	0.87	547	439	0.80
82	HEM100	weak	332	2 860	147	88	0.32	0.25	0.79	685	669	0.98
83	HEM160	weak	247	2 860	141	154	0.10	0.47	4.86	550	799	1.45
96	HEB180	weak	283	1 930	928	209	0.70	0.61	0.87	513	435	0.85
97	HEB180	weak	278	1 930	928	182	0.80	0.60	0.75	540	426	0.79
98	HEB180	weak	277	1 930	938	196	0.75	0.61	0.80	523	418	0.80
103	HEA100	weak	300	1 994	337	300	0.56	0.45	0.80	365	304	0.83
104	HEA100	weak	300	1 994	318	300	0.53	0.41	0.77	400	435	1.09
105	HEA100	weak	300	1 994	260	225	0.58	0.43	0.75	510	438	0.86
106	HEA100	weak	300	1 994	143	188	0.38	0.42	1.10	550	582	1.06
107	HEA100	weak	300	1 994	110	141	0.39	0.39	0.99	600	619	1.03
108	HEA100	weak	300	1 994	61	83	0.37	0.36	0.98	680	690	1.01
109	HEA100	weak	300	1 994	57	51	0.56	0.38	0.67	750	696	0.93
110	HEA100	weak	300	1 994	360	300	0.60	0.60	1.00	235	265	1.13
111	HEA100	weak	300	1 994	320	274	0.58	0.42	0.72	440	435	0.99
112	HEA100	weak	300	1 994	260	267	0.49	0.42	0.87	450	438	0.97
113	HEA100	weak	300	1 994	200	247	0.40	0.43	1.07	480	529	1.10
114	HEA100	weak	300	1 994	48	69	0.35	0.35	0.99	701	729	1.04

Table 5-12: Validation against test series from ETHZ

ID	Profile	Axis	L_{eff} , mm	$f_{y,fi}$, MPa	θ_{test} , °C	F_{ult} , kN	χ_{test}	χ_{FEM}	χ_{FEM} / χ_{Test}
L2	RHS 160x160x5.0	strong	1 981	284	400	760	0.82	0.76	0.93
L5	RHS 160x160x5.0	strong	1 983	155	550	467	0.92	0.86	0.93
L6	RHS 160x160x5.0	strong	1 983	43	700	130	0.92	0.88	0.96
L08	HEA 100	strong	1 921	356	400	608	0.76	0.71	0.94
L07	HEA 100	strong	1 920	198	550	395	0.88	0.81	0.92
L01	HEA 100	strong	1 921	73	700	152	0.92	0.87	0.94
M02	HEA 100	weak	920	356	400	646	0.82	0.79	0.96
M03	HEA 100	weak	920	198	550	405	0.92	0.85	0.92
L16	HEA 100	weak	1 920	356	400	466	0.58	0.56	0.97
L11	HEA 100	weak	1 920	198	550	297	0.66	0.68	1.03
L12	HEA 100	weak	1 920	73	700	128	0.77	0.78	1.01

Table 5-13: Validation against test series – descriptive statistics

	Gent			Germany			Rennes			ETHZ
Mean	0.897	/	0.882	1.215	/	0.828	0.903	/	0.906	0.955
Standard Error	0.045	/	0.036	0.406	/	0.017	0.037	/	0.034	0.011
Standard Deviation	0.163	/	0.119	1.283	/	0.047	0.137	/	0.119	0.037
Minimum	0.698	/	0.730	0.667	/	0.748	0.673	/	0.716	0.916
Maximum	1.262	/	1.119	4.863	/	0.890	1.096	/	1.065	1.028

In tables the following notation is used: ID is the test identifier in the SCOFIDAT database or ETHZ test report; f_y is the factual yield limit stress in ambient conditions; F_{ult} is the ultimate load; σ_c is the stress from axial load; $f_{y,fi}$ is the yield limit stress corresponding to temperature at failure calculated in accordance with EN 1993-1-2 [20]; χ_{test} is the buckling factor according to the test result; χ_{FEM} is the calculated buckling factor; θ_{test} is the average temperature at failure according to test result; θ_{FEM} is the calculated critical temperature.

Relation between buckling factors from tests and FEM were analysed statistically. Corresponding results are presented in Table 5-13. For the tests from SCOFIDAT, two data sets for each laboratory are presented – the whole dataset and reduced data set, where two extreme cases have been excluded.

Analysing the results of the validation it can be concluded, that good correlation with the tests from ETHZ was achieved. Validation results against the test data from SCOFIDAT are less satisfactory, but are in agreement with the results achieved by other authors: [21], [23], [26]. This is probably due to the fact, that the data on actual material behaviour for the test of the ETHZ was more comprehensive comparing to SCOFIDAT report.

5.11 Summary

Extensive numerical simulation program was performed for different temperature values, steel grades and section types. Based on the numerical results, column sections were distinguished into two groups. This allocation is used further for the derivation of buckling method and in the reliability analysis. Bending stiffness is a key parameter characterizing the buckling process. Dependence of the bending stiffness on stress state was presented for ambient and elevated temperature conditions demonstrating more complex reduction path in elevated temperatures compared to the normal temperature conditions. The influence of residual stresses on the bending stiffness and buckling factors was demonstrated. Distribution of stresses at buckling was analysed in detail. Buckling factors were presented and compared with the values calculated using the current Eurocode method. An original analytical design method was proposed and validated against the non-linear FEM and test data. The implementation of the proposed method was demonstrated by an example. The proposed method has very high computational efficiency, which makes it useful for the extensive reliability calculations performed further in this work.

6 Results of probabilistic analysis

6.1 Overview

Results of extensive probabilistic analysis of steel column in fire are reported in this section. The impact of the variability of various input parameters on the stochastic performance is estimated using sensitivity analysis. A large set of temperature distributions is presented depending on the parameters like fire load, fire compartment geometry, passive protection solution etc. Stochastic thermal impact on the distribution of resistance function is demonstrated. Failure probabilities are reported for various steel grades, mean temperatures and slenderness values. Based on the results of the reliability analysis, the method for failure probability prediction is proposed. The proposed method is validated and compared with the current Eurocode methodology. Implementation of the method is demonstrated by an example.

6.2 Results of sensitivity analysis

Sensitivity analysis was used to analyse the stochastic performance of the axially compressed steel element in fire conditions. HEB200 S355 strong axis was investigated. Statistical parameters of variables related to the section geometry and material properties were chosen in accordance with the principles described in 4.4.1 and are summarized in Table 6-1. Statistical parameters of the loading variables were chosen in accordance with the principles described in 4.4.2. Full capacity utilization was assumed and only dead load G was considered. Statistical parameters of the thermal variables were chosen in accordance with the principles described in 4.4.3 and are summarized in Table 6-2. Three configurations of the thermal parameters were investigated. Uncertainty factors for the resistance u_R and loading models u_L were implemented in accordance with the Table 4-11 and Table 4-13 respectively.

Sample size was 10^6 . Computational requirement of the Sobol's method for the evaluation of the first and the total order sensitivity indices is consequently $10^6 \times (2n + 1)$, where n stands for the number of variables. In fact, two analysis types were implemented: the first treating temperature as a deterministic value and the second as a stochastic variable. Sensitivity analysis was performed using polynomial/spline approximation technique as described in section 4.7.

The first set of results (deterministic temperature) is presented in Figure 6.1 showing dependence of the sensitivity indices on the column slenderness $\lambda_{20^\circ\text{C}}$ (5-1) for different temperature values. The second set of results (stochastic temperature) is presented in Table 6-3. Table format was preferred because of the nature of the results – sensitivity indices for the temperature related parameters dominate over other parameters by such a large margin, that it makes no sense to analyse the results in the form of diagrams.

For the analysis with the deterministic temperature variables the following observations are made (Figure 6.1):

1. Material yield limit stress f_y is the dominant variable for relatively low slenderness values representing most of the practical cases. The region where f_y is dominating (highest sensitivity index) is different for different temperature values. Maximum sensitivity index corresponding to the variable f_y lies within is between 0.71 and 0.76.
2. Elasticity modulus E_s becomes dominating for higher slenderness values. The region when E_s is dominating is different for different temperature values. Maximum sensitivity index corresponding to the variable E_s is between 0.32 and 0.52.

3. Initial imperfection e_0 is the third variable which is dominating others for certain slenderness regions. The region is different for different temperatures and lies between f_y and E domination regions. Maximum sensitivity index corresponding to the variable e_0 is between 0.27 and 0.31.
4. Flange thickness t_2 sensitivity index remains relatively stable in both normal and elevated temperature conditions, ranging from 0.16 to 0.27.
5. Residual stresses RS have relatively low sensitivity index values. Sensitivity index peaks are place between the slenderness $\lambda_{20^\circ C}$ values from 1.3 to 1.6.
6. Other input variables from Table 2.1 (h , t_1 , b) have sensitivity index values below 0.06, i.e. contribution of these variables into the buckling capacity variance is minimal.
7. The changes of sensitivity indices curves for variables f_y , E_s , e_0 and RS with temperature as described in points 1, 2, 3 and 5 respectively, can be explained by the differences in stress-strain relationship models for different temperature regimes.

Table 6-1: Resistance related uncertainties: HEB200 S355

ID	Description	Symbol	Density	Unit	Mean value (μ_i)	Std. deviation (σ_i)	Coefficient of variation (COV)
1	section height	h	Normal	mm	200	0.88	0.0044
2	section width	b	Normal	mm	200	1.96	0.0098
3	wall thickness	t_1	Normal	mm	9.0	0.3564	0.0396
4	flange thickness	t_2	Normal	mm	15.0	0.6915	0.0461
5	yield limit stress	f_y	Log-normal	MPa	399.50	27.965	0.0700
6	elasticity modulus	E_s	Normal	MPa	210 000	12 600	0.0300
7	global imperfection	e_0	Normal	mm	0.000611 L	0.000461 L	0.7547
8	maximum residual stress	RS	Normal	MPa	90.0	18.0	0.2000

Table 6-2: Temperature related uncertainties

ID	Description	Symbol	Density	Unit	Mean value (μ_i)	Std. deviation (σ_i)
1	fire load density	q_f	Log-normal	MJ/m ²	520 720 920	156 216 276
2	compartment width	W	Deterministic	m	25.0	--
3	compartment length	L	Deterministic	m	20.0	--
4	compartment height	H	Deterministic	m	4.0	--
5	enclosure thermal inertia	b_{th}	Normal	J/(m ² s ^{0.5} K)	1742 1742 1200	157 157 108
6	opening factor	O	Log-normal	m ^{0.5}	0.04 0.08 0.06	0.14
7	insulation material thermal resistance	d_p/λ_p	Log-normal	m ² sK/J	0.083 0.083 0.063	0.018 0.018 0.014
8	model uncertainty	u_T	Log-normal	--	1.0	0.10

8. For all temperature values and for a given slenderness value, the sensitivity indices sum of all variables remained in the range between 0.981 and 0.988, which gives evidence that the effect of the higher order variable interactions is minimal.

For the analysis with the stochastic temperature variables the following observations are made (Table 6-3):

1. Sensitivity indices for the thermal variables are dominating over other groups (mechanical and loading) of variables for all the analysed configurations and slenderness values.
2. Sensitivity indices for the mechanical response variables are neglectably small and can be ignored in the reliability analysis. It was decided to neglect the variability of the following variables: section geometry variables h , b , t_1 , t_2 and residual stresses RS .
3. Sensitivity index for the loading variable G is relatively moderate.
4. The highest values of the sensitivity indices among the thermal variables group correspond to the properties of thermal insulation material d_p/λ_p and fire load density q_f .
5. Sensitivity indices for the uncertainty factors for models of loading u_L and mechanical response u_R are relatively moderate. Sensitivity index of the thermal model uncertainty u_T is quite high for all the cases considered and in many cases has the maximum value among all variables.
6. Total value of the first order sensitivity indices $\sum S_{i,1}$ lies within the range between 0.67 and 0.93 indicating that in certain cases the impact of the higher order variable interaction may be considerable. Second order sensitivity indices were analysed and the results indicate that only interaction of thermal variables provided considerable input into the total variability. The total $\sum S_{i,1}$ and $\sum S_{i,2}$ lie within the range of 0.93 and 0.99.

The dominating role of thermal variables in the sensitivity analysis was reported earlier by Shcleich et al [18].

6.3 Temperature distributions

Temperature distributions were generated using EC1 method as justified in 4.4.3., where variables and their statistical parameters were presented (Table 4-13). Direct MCS was implemented. The following parameter ranges were investigated: fire load density $q_f = 100 \dots 1500 \text{ MJ/m}^2$; enclosure thermal inertia $b_{th} = 500 \dots 2200 \text{ J/(m}^2\text{s}^{0.5}\text{K)}$; opening factor $O = 0.02 \dots 0.20 \text{ m}^{0.5}$; steel section factor $A_p/V = 50 \dots 250 \text{ m}^{-1}$; relation of thermal insulation thickness to thermal conductivity $d_p/\lambda_p = 0.021 \dots 0.083 \text{ m}^2\text{sK/J}$; fire compartment area $A_{fi} = 10 \dots 500 \text{ m}^2$. The total number of analysed configurations was 3240. The number of simulations per configuration was 10^5 .

Results of the temperature distributions for all 3240 simulations are presented in Figure 6.2. Temperature distributions are grouped by the mean temperature value. Selected temperature distributions are presented in Figure 6.3, Figure 6.4 and Figure 6.5. Distributions presented in Figure 6.3 (cases 1 – 8) with certain level of abstraction can be described as smooth unimodal and to some degree replicating common theoretical distributions.

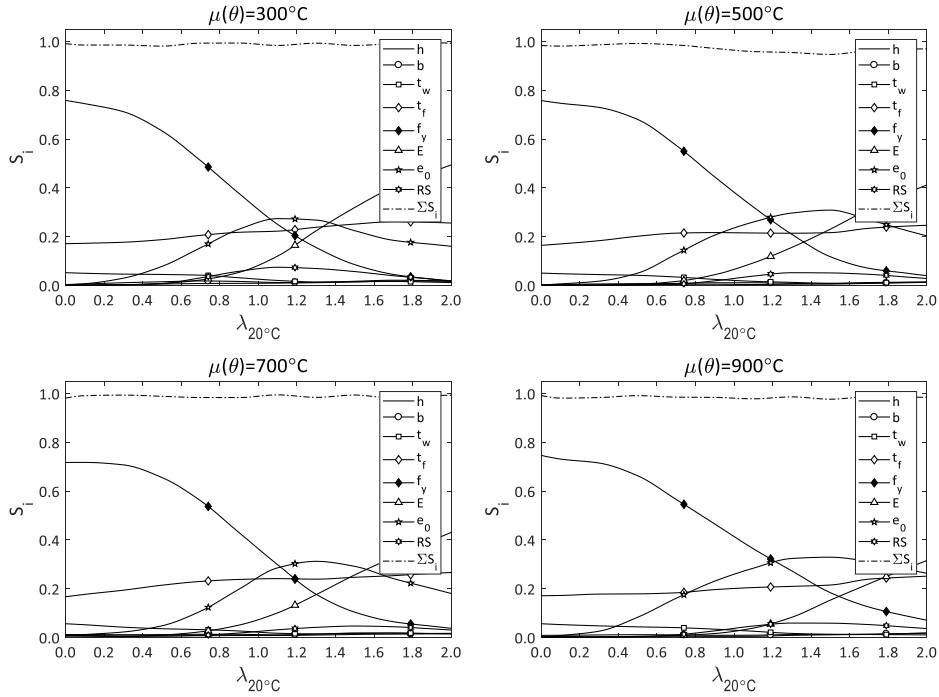


Figure 6.1: Sensitivity analysis results – sensitivity indices S_i in case of the deterministic temperature variable

Distributions presented in Figure 6.4 and Figure 6.5 (cases 9 – 24) are much more complex. Distributions are disrupted by two phenomena:

- density concentration around the temperature value 735°C (peak specific heat value as described in section 3.3.7) – cases 9, 11, 14 and 15;
- distribution bimodality caused by two possibilities of fire development: fuel or ventilation controlled fire (Annex A1) – cases 10, 12, 18, 20, 23;
- temperature distribution shape for the cases 13, 16, 17, 19, 21, 22 and 24 can be explained by the combination of the above described aspects.

An important observation can be made by analysing the relation of the nominal steel temperature θ_{nom} calculated for the nominal thermal property values and the calculated mean temperature $\mu(\theta)$ obtained as a result of the MCS for the same fire configuration. For the cases 1 – 8, θ_{nom} and $\mu(\theta)$ lie relatively close to each other or θ_{nom} is higher than $\mu(\theta)$. The situation for the cases 9 – 24 is much more complex. The “specific heat effect” does not dislocate θ_{nom} from $\mu(\theta)$ considerably. The “bimodality effect” causes considerable difference between θ_{nom} and $\mu(\theta)$.

Obviously the temperature distributions have complex shape and not always correlate well with the theoretical distributions. It is important to study the influence of the temperature distribution shape on the failure probability. This issue will be addressed in section 6.5.

6.4 Resistance distributions

The computational performance of the response function is extremely important for the MCS due to the large number of response function evaluations. Results of the sensitivity

Table 6-3: Sensitivity analysis results – sensitivity indices S_i in case of the stochastic thermal variables

	$\mu(\theta) = 304^\circ\text{C}$					$\mu(\theta) = 646^\circ\text{C}$					$\mu(\theta) = 790^\circ\text{C}$				
	$\lambda_{20^\circ\text{C}} = 0.0$	$\lambda_{20^\circ\text{C}} = 0.5$	$\lambda_{20^\circ\text{C}} = 1.0$	$\lambda_{20^\circ\text{C}} = 1.5$	$\lambda_{20^\circ\text{C}} = 2.0$	$\lambda_{20^\circ\text{C}} = 0.0$	$\lambda_{20^\circ\text{C}} = 0.5$	$\lambda_{20^\circ\text{C}} = 1.0$	$\lambda_{20^\circ\text{C}} = 1.5$	$\lambda_{20^\circ\text{C}} = 2.0$	$\lambda_{20^\circ\text{C}} = 0.0$	$\lambda_{20^\circ\text{C}} = 0.5$	$\lambda_{20^\circ\text{C}} = 1.0$	$\lambda_{20^\circ\text{C}} = 1.5$	$\lambda_{20^\circ\text{C}} = 2.0$
$S_{1,1}$	h	0.000	0.000	0.000	0.000	0.000	0.001	0.000	0.000	0.002	0.000	0.000	0.000	0.001	0.001
	b	0.000	0.000	0.000	0.000	0.000	0.002	0.000	0.000	0.002	0.000	0.000	0.000	0.001	0.001
	t_1	0.000	0.000	0.000	0.000	0.001	0.002	0.000	0.000	0.002	0.000	0.000	0.000	0.001	0.001
	t_2	0.000	0.000	0.001	0.001	0.002	0.004	0.000	0.002	0.003	0.004	0.000	0.000	0.002	0.001
	f_y	0.003	0.002	0.002	0.002	0.002	0.017	0.013	0.006	0.001	0.001	0.001	0.001	0.001	0.001
	E_s	0.000	0.000	0.000	0.000	0.003	0.001	0.000	0.001	0.006	0.010	0.000	0.000	0.002	0.002
	RS	0.000	0.000	0.000	0.000	0.000	0.000	0.000	0.000	0.000	0.000	0.000	0.000	0.000	0.000
	e_0	0.000	0.000	0.001	0.001	0.002	0.001	0.000	0.004	0.004	0.003	0.000	0.000	0.002	0.001
	b_{th}	0.000	0.000	0.000	0.000	0.002	0.001	0.000	0.000	0.000	0.001	0.000	0.000	0.001	0.001
	O	0.089	0.087	0.085	0.083	0.085	0.072	0.068	0.067	0.066	0.069	0.069	0.070	0.068	0.073
	q_f	0.175	0.174	0.169	0.168	0.167	0.151	0.146	0.143	0.143	0.144	0.138	0.137	0.139	0.140
	d_p/λ_p	0.180	0.178	0.173	0.171	0.173	0.260	0.266	0.270	0.260	0.258	0.143	0.145	0.147	0.147
	G	0.036	0.034	0.033	0.035	0.042	0.062	0.065	0.076	0.079	0.081	0.009	0.010	0.011	0.015
	u_R	0.013	0.013	0.015	0.012	0.016	0.071	0.064	0.056	0.059	0.060	0.006	0.006	0.007	0.009
	u_L	0.036	0.033	0.033	0.034	0.041	0.063	0.065	0.076	0.079	0.082	0.009	0.010	0.011	0.015
	u_T	0.293	0.293	0.291	0.286	0.287	0.216	0.220	0.225	0.216	0.213	0.294	0.299	0.309	0.313
$S_{1,2}$	$\sum S_{1,1}$	0.825	0.814	0.803	0.794	0.823	0.925	0.907	0.926	0.916	0.931	0.669	0.675	0.694	0.724
	Oq_f	0.012	0.012	0.011	0.011	0.010	0.005	0.005	0.004	0.004	0.004	0.023	0.022	0.021	0.018
	Od_p/λ_p	0.011	0.010	0.010	0.010	0.010	0.005	0.005	0.004	0.004	0.004	0.024	0.022	0.021	0.019
	$O u_T$	0.015	0.015	0.015	0.014	0.013	0.008	0.008	0.007	0.006	0.006	0.033	0.032	0.029	0.026
	$q_f d_p/\lambda_p$	0.022	0.021	0.019	0.017	0.016	0.009	0.008	0.008	0.008	0.008	0.047	0.047	0.045	0.040
	$q_f u_T$	0.031	0.030	0.027	0.026	0.024	0.012	0.012	0.012	0.010	0.010	0.067	0.062	0.062	0.054
	$d_p/\lambda_p, u_T$	0.034	0.051	0.078	0.094	0.076	0.013	0.039	0.019	0.037	0.025	0.064	0.072	0.057	0.059
	$\sum S_{1,1} + \sum S_{1,2}$	0.951	0.952	0.963	0.966	0.972	0.977	0.983	0.980	0.985	0.988	0.927	0.931	0.928	0.934

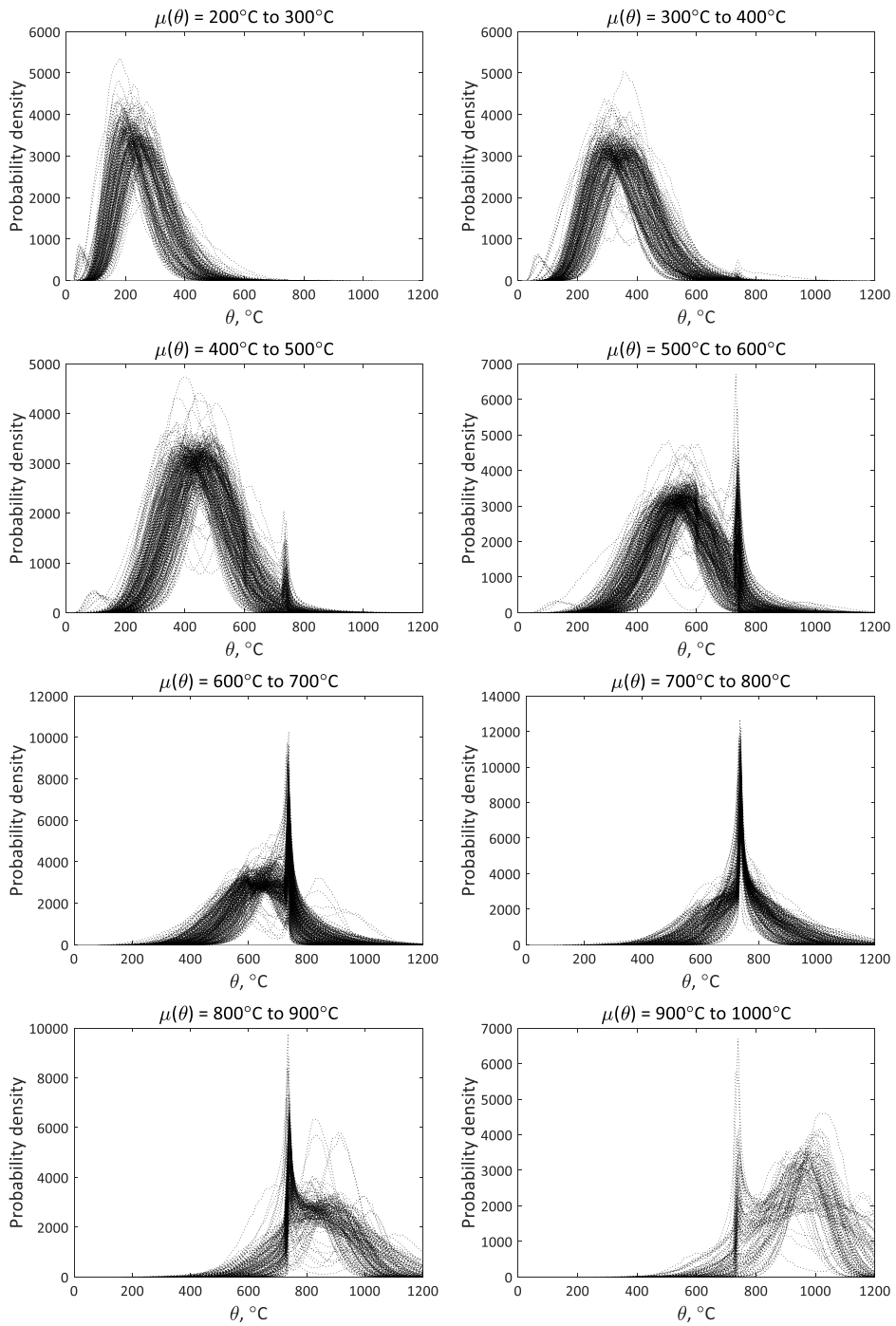


Figure 6.2: pdf for the maximum steel section temperature

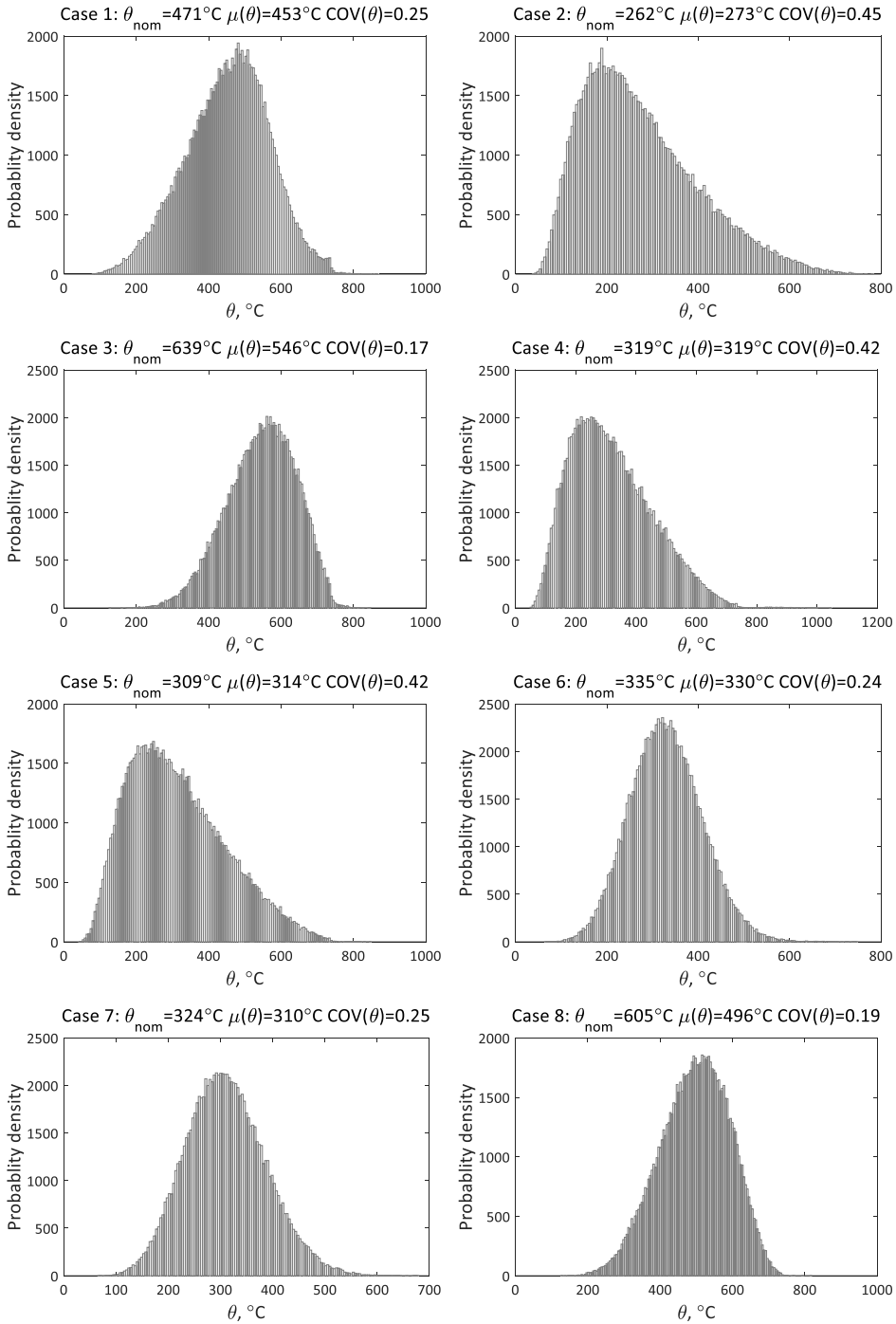


Figure 6.3: Selected pdf for the maximum steel section temperature – part 1

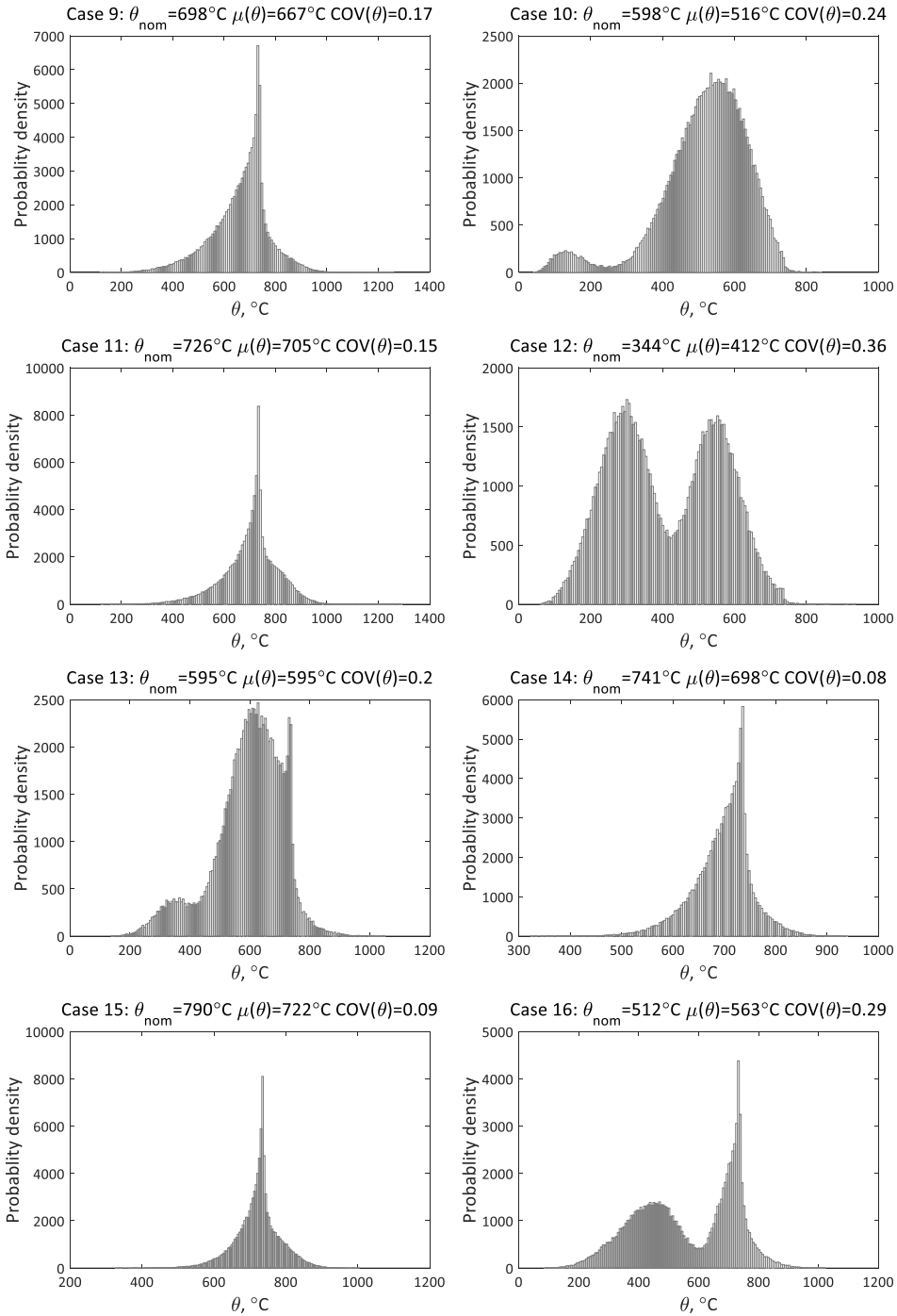


Figure 6.4: Selected pdf for the maximum steel section temperature – part 2

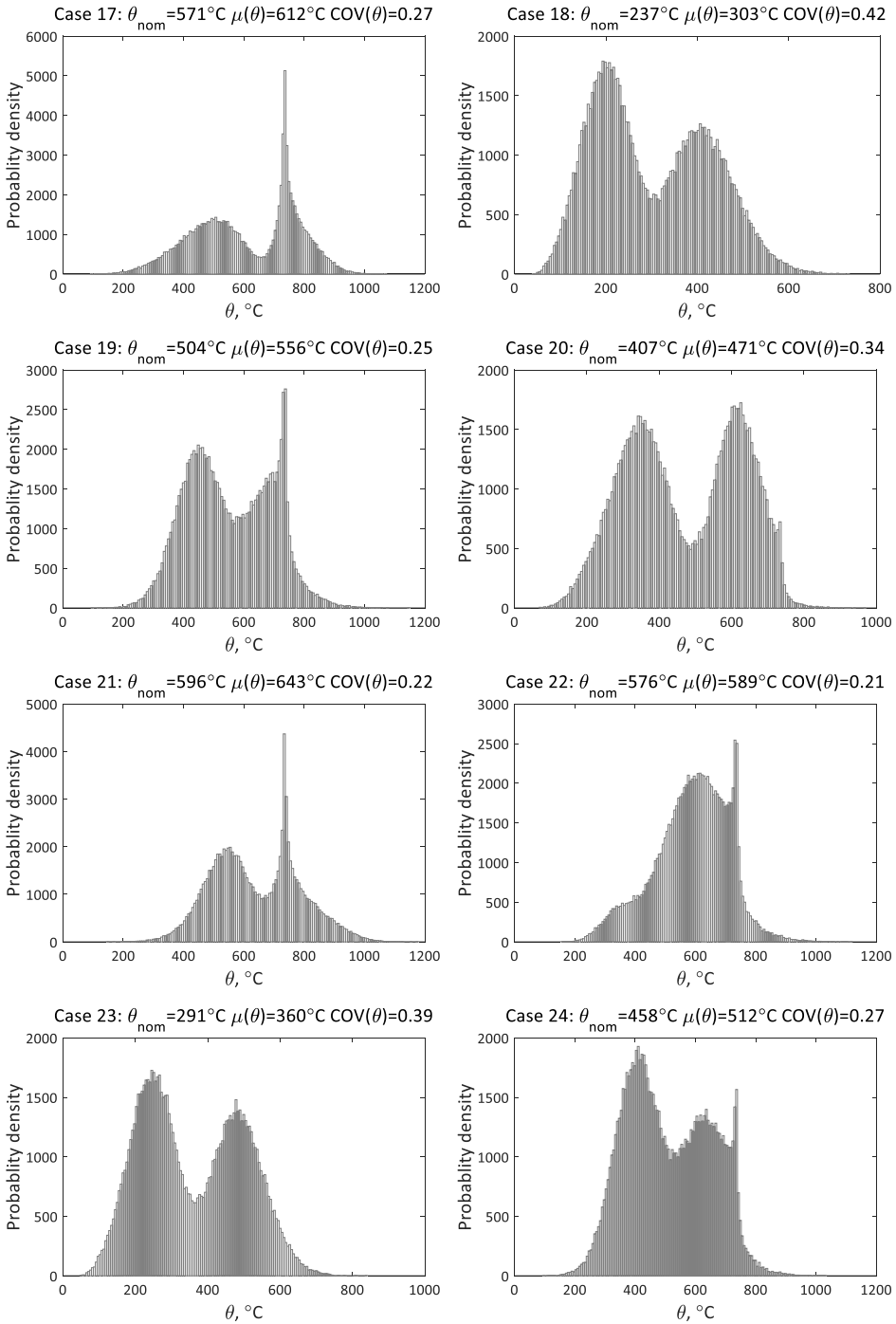


Figure 6.5: Selected pdf for the maximum steel section temperature – part 3

analysis demonstrated that the input of the residual stresses into the variability of the resistance function is small especially when temperature is treated as stochastic. It was decided to perform all the reliability calculations using the Method C model presented in section 5.8. The model of Method C includes residual stresses in implicit form and has no direct analytical solution, i.e. numerical technique must be used but the model has rapid convergence and the solution is usually achieved after 5 evaluations of function (5-45). The average time needed to calculate the buckling capacity using Method C is 2×10^{-5} seconds, using polynomial/spline approximation (section 4.7) 4×10^{-5} seconds, while using the FEM procedure (section 3.2.7) requires 2 seconds. Processor Base Frequency used for the comparison was 3.6 GHz. Parallel processing was implemented for 8 cores. Computational efficiency of the Method C excluded the need to optimize Monte-Carlo simulation process (e.g. Latin Hypercube, Importance Sampling etc).

Data for the section and material statistical parameters was adopted from Table 6-1. Resistance distributions are reported in Figure 6.6, Figure 6.7, Annexes A9 and A10, where histograms of the factor $R_{fi}/R_{fi,nom}$ for various slenderness values and mean temperature values are presented. The factor $R_{fi}/R_{fi,nom}$ can be referred to as the normalized resistance value, where $R_{fi,nom}$ is the resistance calculated for the nominal section and material properties and mean temperature value. In Figure 6.6 two diagrams are presented for each case: left column – temperature is assumed to be normally distributed; right column – temperature is assumed to be deterministic. In case temperature has some kind of distribution (as it should be for the reliability analysis) the distribution of resistance becomes quite complicated and deviate from commonly used theoretical distributions. The resulting resistance distributions can be characterized as random skewed multimodal. The tendency intensifies with increasing mean. The sample distributions are well approximated by the theoretical models. For low slenderness values Lognormal distribution is the best approximation. For slenderness value of 1.0 (Annex A10) Normal distribution is a better approximation.

Resistance distributions were presented with the assumption of the Normal temperature distribution. In Figure 6.7 resistance distributions for the selected temperature distributions from the results of the thermal analysis (Figure 6.3 and Figure 6.4) are presented once again demonstrating complexity of the resistance distribution shape.

It is assumed that the main reason of the complexity of the resistance function distribution is related to the temperature variance. It can be justified as follows: in case temperature is taken as deterministic the distribution resistance function is very close to the Normal or Lognormal (right column of Figure 6.6, Figure 6.7, Annexes A9 and A10).

6.5 Reliability analysis in fire conditions

6.5.1 Reliability analysis scheme

The procedure of reliability analysis is summarized as follows:

1. temperature distribution consisting of 10^5 values is imported from the results of the fire simulations and the corresponding mean temperature is calculated;
2. column height (slenderness) is chosen from 0.0 to 2.0;
3. 10^5 random values of material properties (f_y and E) and initial imperfection (e_0) are generated using data from Table 4-11 and based on the results of the sensitivity analysis (section 6.2) the variability of section geometry and RS is ignored;

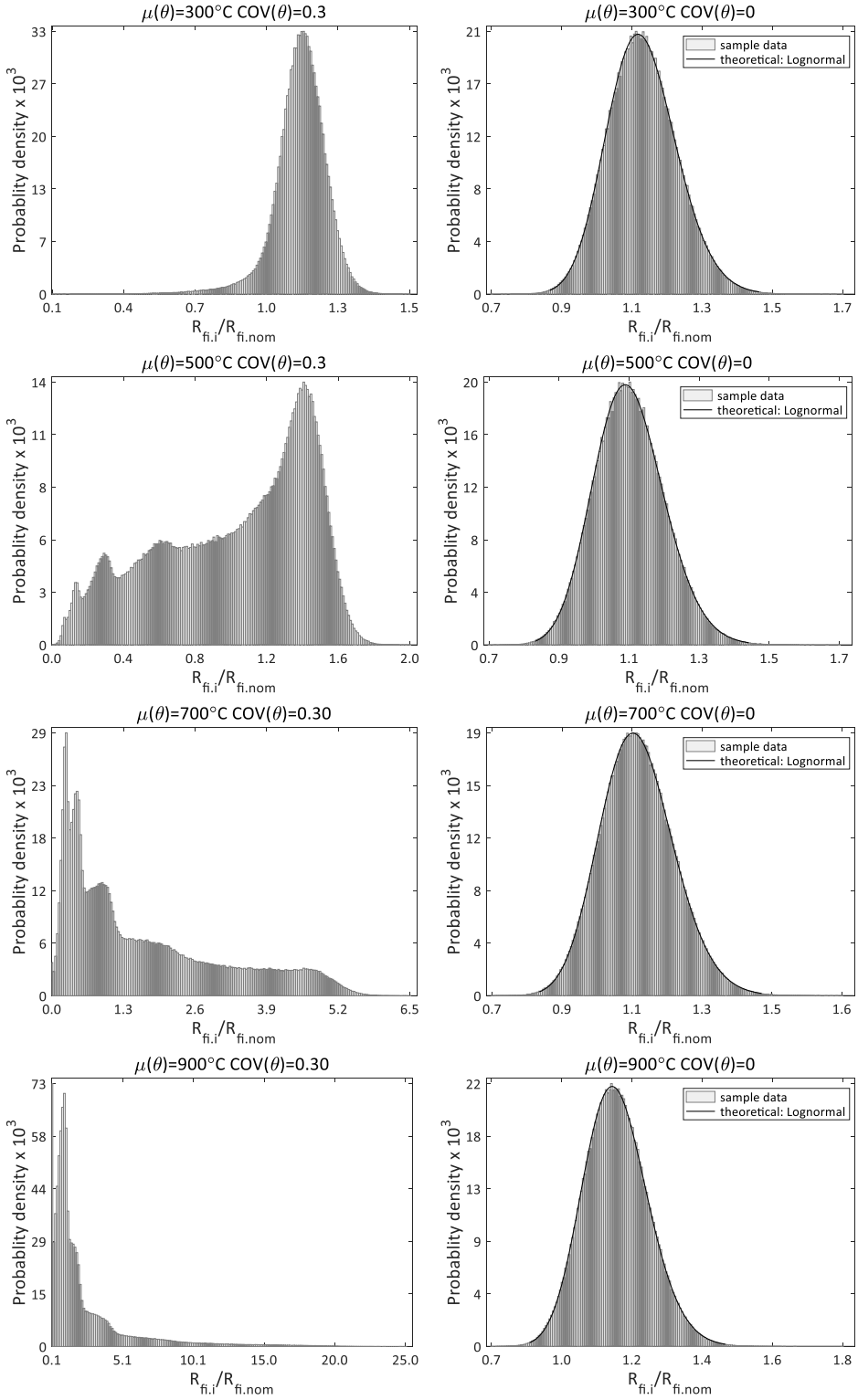


Figure 6.6: Resistance function distributions for slenderness value $\lambda_{20^\circ\text{C}} = 0.0$

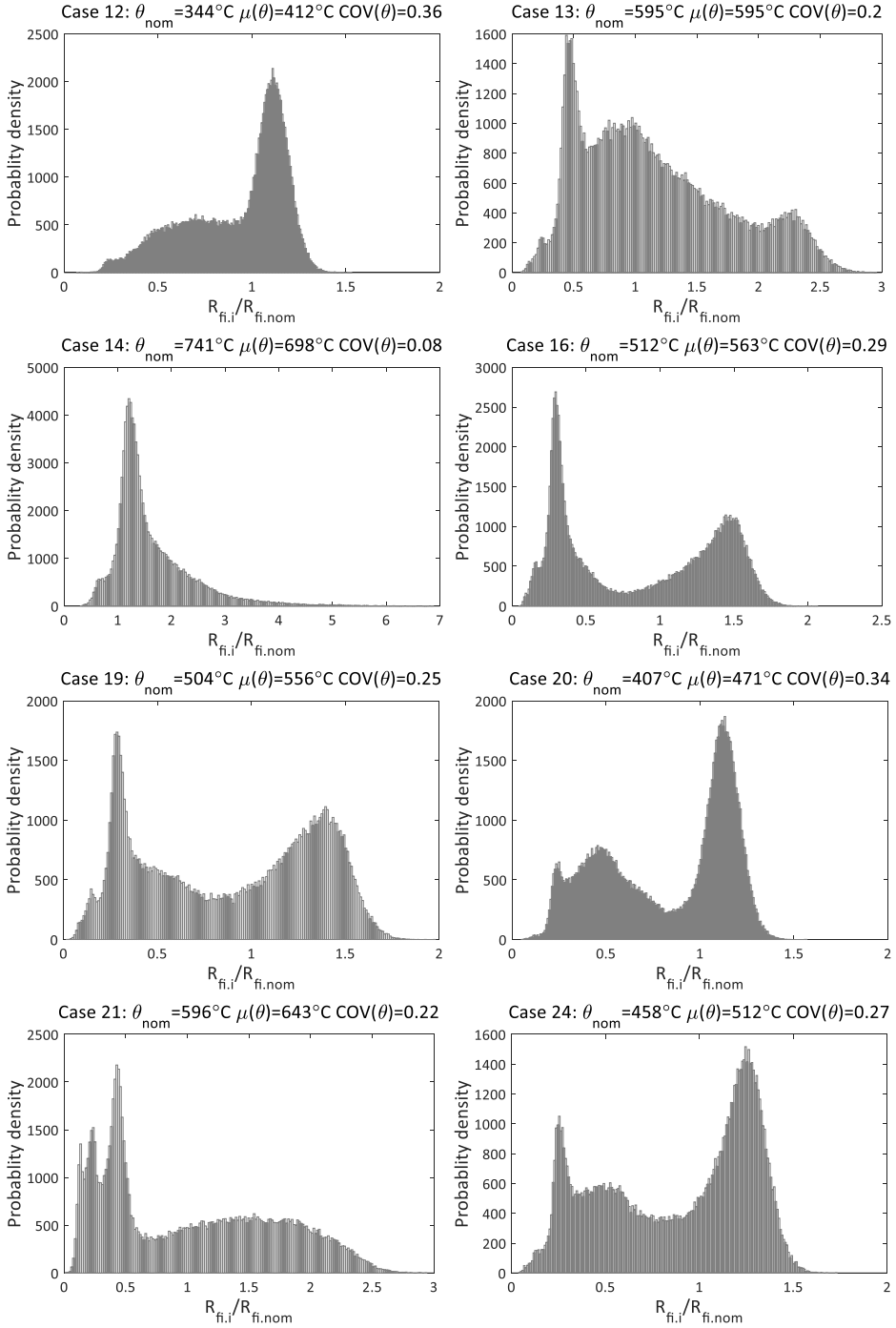


Figure 6.7: Resistance function distributions for the selected temperature distributions and for slenderness value $\lambda_{20^{\circ}\text{C}} = 0.0$

4. column nominal buckling capacity $R_{fi,Nom}$ is defined using Method C (section 5.8) for nominal section and material parameters for the chosen column slenderness and mean temperature value;
5. for each factor α value ranging from 0.00 to 0.75 two load sets (permanent loads set **G** and variable load set **Q**) each consisting of 10^5 values are generated, fulfilling condition: $G_k + Q_k = R_{fi,Nom}$ (full nominal capacity utilization is assumed) and then merged into total the load set **V** = **G** + **Q**
6. load bearing capacity set **R** based on the generated section, material and temperature data sets is calculated using Method C (section 5.8).
7. failure probability in fire $p_{f,fi}$ is calculated for the set **R** – **V**.

The procedure is repeated for all the 3 240 temperature distributions. Result set for S355 $\lambda_{20^\circ C} = 0.0$ $\alpha = 0.0$ (only dead load is assumed) is presented on the left diagram of Figure 6.8. For any chosen mean temperature value the failure probability may vary in a wide range. The variability of the failure probabilities for any chosen mean temperature value is explained by the differences in the temperature distribution shape. As an example on the right diagram of Figure 6.8 the failure probabilities for the mean temperature from 500°C to 510°C are presented. Two cases are highlighted: case 1 corresponding to the minimum failure probability for the temperature range from 500°C to 510°C and case 2 corresponding to the maximum failure probability in the same range. Temperature distributions corresponding to both cases are presented in Figure 6.9. An important observation can be made by analysing the relation between the mean temperature $\mu(\theta)$ and the nominal temperature θ_{nom} (calculated using nominal thermal variable values) for the same distribution. For the case of minimum failure probability (case 1), the mean temperature $\mu(\theta)$ is smaller than the nominal θ_{nom} . The opposite is true for the cases of maximum failure probability (case 2). It is not easy to decide, which failure probability is the most representative for a given temperature subrange. The simple approach is to choose the maximum failure probability as the representative value. This approach can become relatively conservative regarding the difference between the maximum and the minimum failure probability for a given temperature subrange. In order to account for the variability of failure probability ranking approach is introduced further in this section.

In this work, the failure probability is reported as follows. Mean temperature range from 300°C to 900°C is divided into subranges of 10°C: 300°C, 310°C ... 890°C, 900°C. For each subrange, 4 failure probability $p_{f,fi}$ values are defined corresponding to the 25-th, 50-th (mean failure probability value), 75-th and 100-th (maximum failure probability value) percentile values of failure probability $p_{f,fi}$ in the mean temperature subrange under consideration. Resulting failure probability values are assigned to the left border value of the temperature range. For example for the 500°C – 510°C mean temperature subrange, the obtained values of failure probability are assigned to the mean temperature value of 500°C. Ranking is introduced to avoid excessive conservatism in probability prediction and is defined as follows: R1 – is the 25-th percentile $p_{f,fi}$ value; R2, R3 and R4 – to the 50-th, 75-th and 100-th percentile $p_{f,fi}$ values correspondingly. Failure probability values for different slenderness values, variable load type and factor α are presented in the following section. Ranking process is described in section 6.5.3.

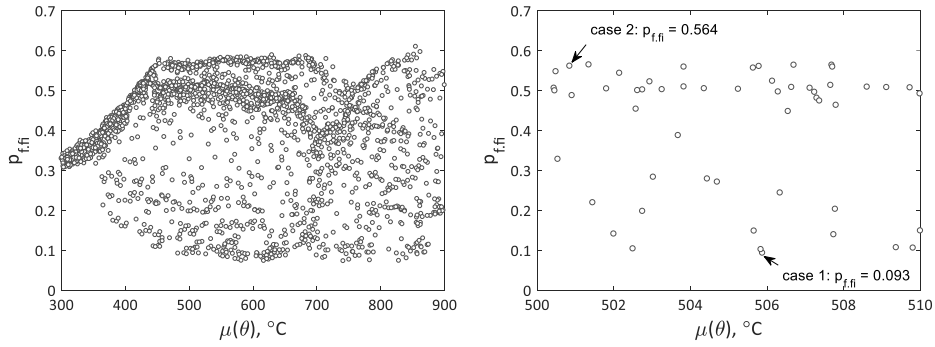


Figure 6.8: Failure probability $p_{f,fi}$ dependence on the mean temperature: S355 $\lambda_{20^\circ\text{C}} = 0.0$ $\alpha = 0.0$

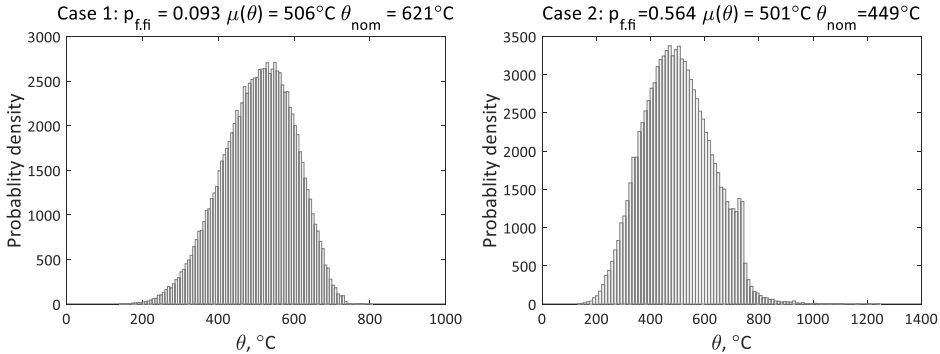


Figure 6.9: Temperature distributions corresponding to the minimum and maximum failure probabilities in the temperature subrange 500 °C – 510 °C

6.5.2 Failure probability in fire conditions

Failure probabilities are calculated using the scheme presented in the previous section. Results of the reliability analysis are presented in Figure 6.10, Figure 6.11, Annexes A11 – A15 for three steel classes S235, S355 and S460, for strong and weak column axes and for imposed variable load Q . For each configuration (steel class, buckling axis and mean temperature), the failure probability $p_{f,fi}$ is presented assuming fire probability p_{fire} being equal to 1.0. There are two diagrams for each configuration: on the left side for the failure probability ranks R1 and R2 and on the right side for the ranks R3 and R4 (ranks were defined in 6.5.1). Each diagram includes several curves corresponding to the different variable load levels, i.e. factor α value (4-24). Calculations for wind W and snow S variable loads were also performed, but are not reported in detail in this work.

For more convenient comparison the results are regrouped and presented in Figure 6.12 and Figure 6.13, where in the diagrams in the left column the influence of the variable load type on the R4 (maximum) failure probability can be analysed for the strong axis buckling of the S355 steel class. In the right column the influence of the steel class and buckling axis (strong / weak) on the R4 (maximum) failure probability can be analysed factor α value of 0.

The following observations can be made:

1. Failure probability is strongly dependent on the factor α (4-24): the smaller the factor α value the higher the failure probability. The difference between the failure probability for $\alpha = 0.00$ (only dead load is applied) and $\alpha = 0.75$ is significant. Similar tendencies were reported for ambient conditions by Kala et al [89].

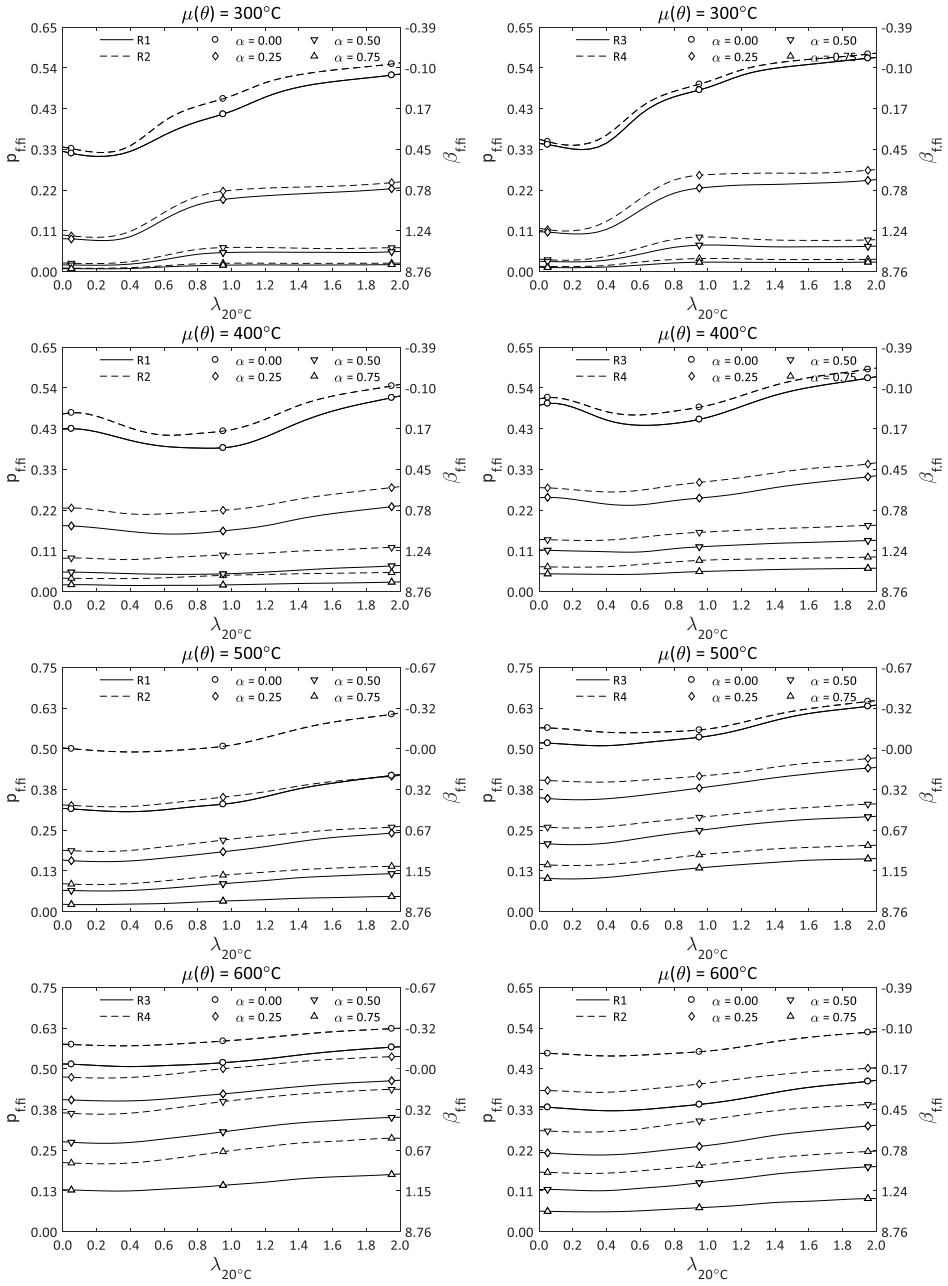


Figure 6.10: Failure probability $p_{f,fi}$ and reliability index $\beta_{f,fi}$ for S355 steel column strong axis in case of the imposed variable load Q – part 1

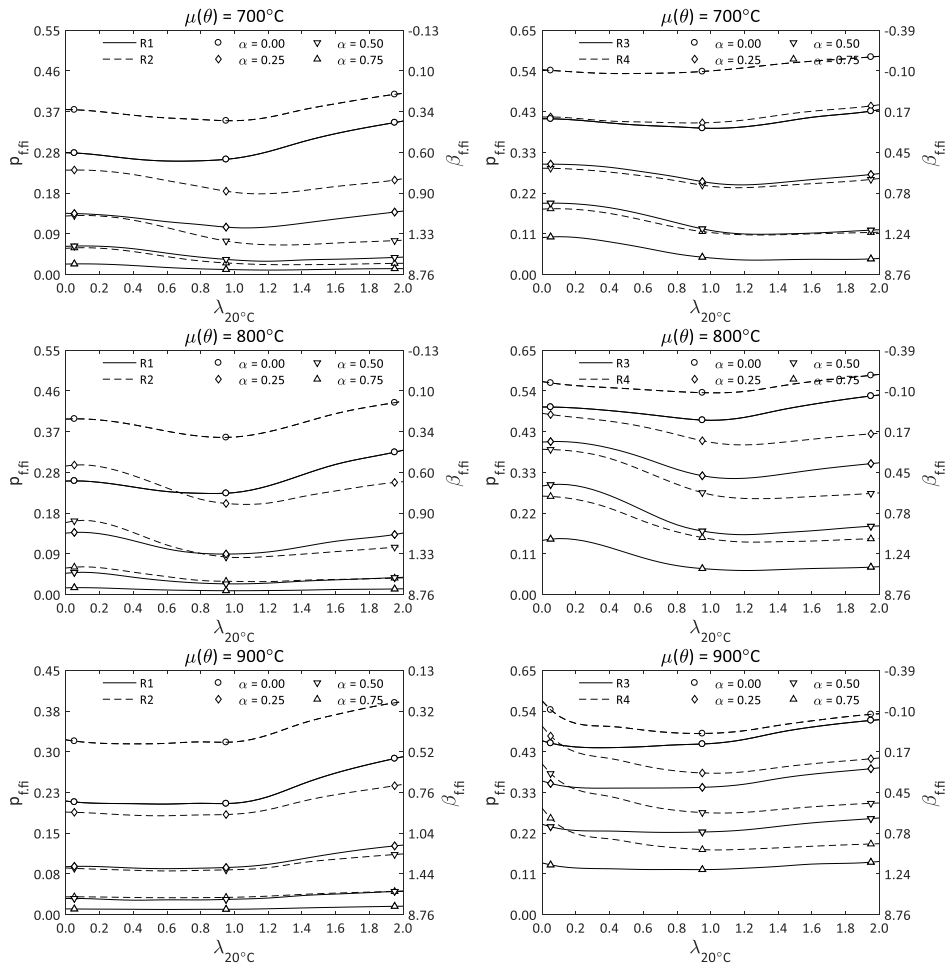


Figure 6.11: Failure probability $p_{f,fi}$ and reliability index $\beta_{f,fi}$ for S355 steel column strong axis in case of the imposed variable load Q – part 2

- The results of the reliability analysis for different imposed load types are significantly different (Figure 6.12, Figure 6.13 – left column). Failure probabilities for imposed variable load Q are smaller comparing to the corresponding results for wind load W ; failure probabilities for wind load W are smaller compared to the corresponding results for snow load S . This tendency can be explained by the relationship of the nominal load to mean load factor: $\mu(Q_k) / Q_k = 0.20$, $\mu(W_k) / W_k = 0.30$, $\mu(S_k) / S_k = 0.35$ (section 4.4.2).
- The influence of the steel class and the buckling axis on the reliability performance of the axially compressed steel column in fire conditions is moderate (Figure 6.12, Figure 6.13 – right column). Although certain differences can be observed the failure probabilities still remain relatively close to each other.

6.5.3 Ranking system of failure probability

Ranking was introduced in section 6.5.1. Results of the failure probabilities corresponding to different ranking values were presented in the previous section. Hereby the aim is to establish the connection between the failure probability rank and some

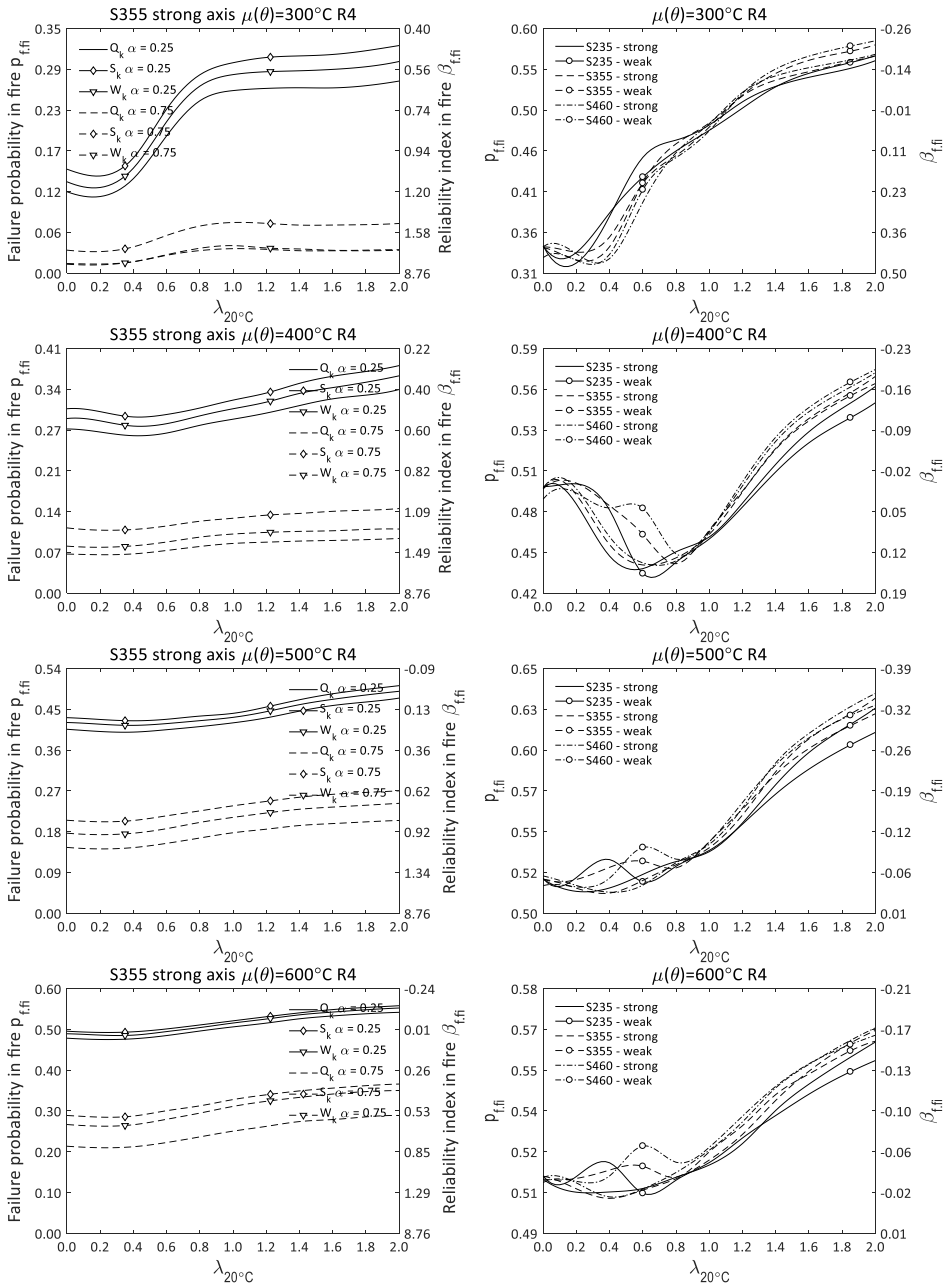


Figure 6.12: Influence of the variable load type (left column) and steel class / buckling axis (right column) on the R4 failure probability – part 1

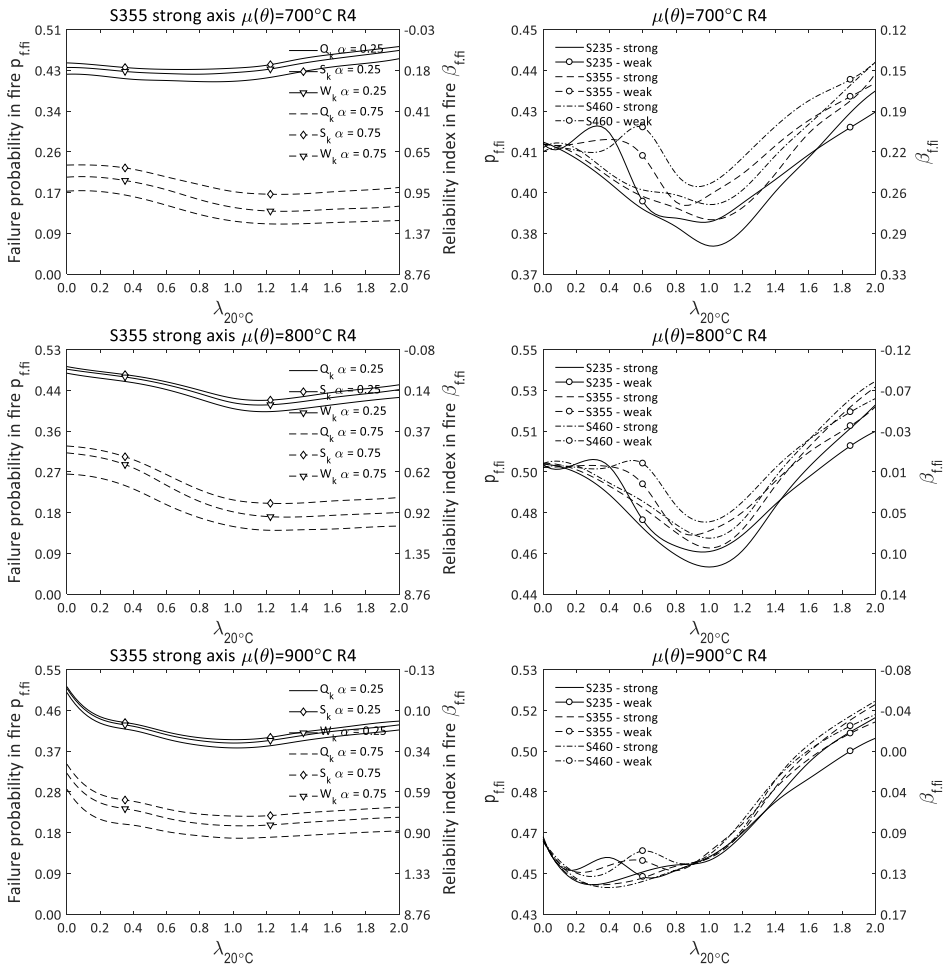


Figure 6.13: Influence of the variable load type (left column) and steel class / buckling axis (right column) on the R4 failure probability – part 2

parameter, which will allow to estimate the rank from the known input values like fire characteristics.

It was demonstrated, that for the elements having similar mean temperature, failure probability may vary in a wide range (right side diagram of Figure 6.8). The reason for vast discrepancies in failure probabilities are related to the differences in the temperature distribution shapes. In Figure 6.9 it was demonstrated, that for the considered cases the factor $\mu(\theta)/\theta_{nom}$ value below 1.0 corresponds to the lower bound failure probability, while the factor value above 1.0 corresponds to the upper bound of the failure probability. The dependence between the failure probability $p_{f,fi}$ and the factor $\mu(\theta)/\theta_{nom}$ is demonstrated in Figure 6.14, where the failure probabilities have been calculated for S355 $\lambda_{20^\circ\text{C}} = 0.0$ $\alpha = 0.0$ (only dead load is assumed) in 3 240 simulated cases of fire (section 6.3). It can be concluded that the higher factor $\mu(\theta)/\theta_{nom}$ value corresponds to the higher failure probability value and higher variation of the failure probability.

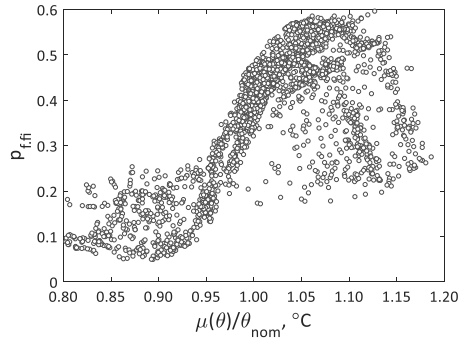


Figure 6.14: Dependence between failure probability $p_{f,fi}$ and factor $\mu(\theta)/\theta_{nom}$

Factor $\mu(\theta)/\theta_{nom}$ cannot be used as the basis for the ranking system, because there is no simple method for the calculation of mean temperature. The basis for the ranking system must be formed of input variables of thermal analysis. For this purpose the following parameter was introduced using trial and error approach:

$$R = \sqrt{\frac{O}{b_{th}}} \quad (6-1)$$

, where O is the opening factor as defined in 4.4.3 and Annex A1; b_{th} is the enclosure thermal inertia as defined in 4.4.3 and Annex A1.

The ranking procedure was performed using MCS according to the scheme summarized as follows:

1. temperature distribution consisting of 10^5 values is imported from the results of fire simulations;
2. the corresponding nominal temperature θ_{nom} and factor R (6-1) are calculated;
3. failure probability $p_{f,fi}$ is calculated and linked to the nominal temperature θ_{nom} and factor R ;
4. the procedure is repeated for all the 3240 simulated temperature distributions;
5. results set consist of the 3240 $\{p_{f,fi} \theta_{nom} R\}$ triplets;
6. nominal temperature range from 300°C to 900°C is divided into subranges of 10°C: 300°C, 310°C ... 890°C, 900°C;
7. for each subrange, the $p_{f,fi}$ dependence on the factor R is analysed as demonstrated in Figure 6.15;
8. the failure probability envelope curve is defined (dashed line in Figure 6.15) and percentile scale for the failure probability is introduced for the analysed subrange (right-hand vertical axis of the diagrams in Figure 6.15);
9. factor R values are defined corresponding to the 25%, 50% and 75% percentile of failure probability (ranks R1, R2 and R3 correspondingly) as shown in Figure 6.15, while factor R higher than R3 limit is ranked R4;
10. the output of the ranking process is a set of factor R - θ_{nom} pairs, as is presented in Figure 6.16;
11. the following rank limits were fixed: R1 limit value – $R = 0.0042$, R2 limit value – $R = 0.0062$, R3 limit value – $R = 0.0082$, factor $R > 0.0082$ corresponds to rank R4 (maximum failure probability).

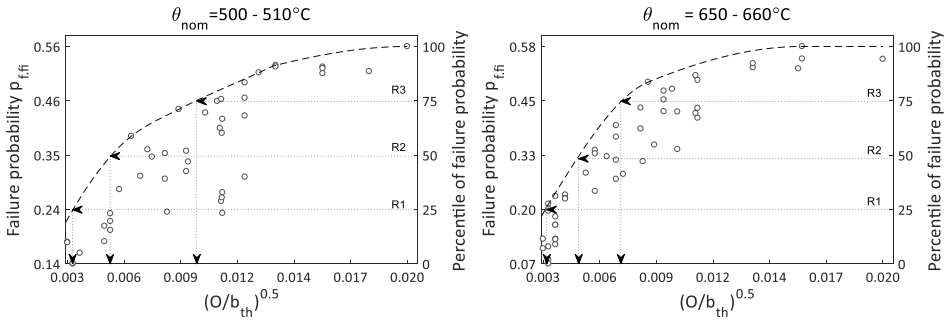


Figure 6.15: Example of the ranking process for temperature subranges 500-510°C and 650-660°C

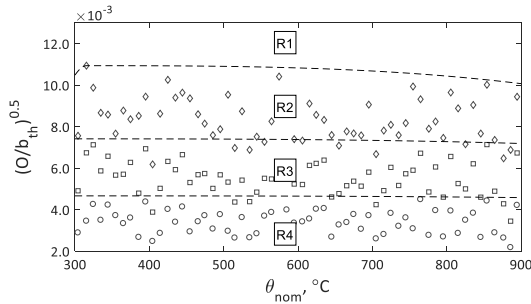


Figure 6.16: Factor R dependence on the θ_{nom} and ranking limits

The simulation was performed for the S355 $\lambda_{20^\circ\text{C}} = 0.0$ $\alpha = 0.0$ (only dead load is assumed) configuration. Calculated failure probabilities were transferred into the percentile domain. As a result of this transformation the precise numeric value of the failure probability for any subrange is of secondary importance. It was assumed that ranking which is based on the failure probabilities for the S355 $\lambda_{20^\circ\text{C}} = 0.0$ $\alpha = 0.0$ can be utilized for other steel grades, slenderness values, variable load types and factor α values. This assumption was tested and the corresponding results are presented in Figure 6.17, where the failure probabilities calculated using MCS (vertical axis) are compared with the predicted failure probabilities (horizontal axis) according to the scheme as follows:

1. temperature distribution was imported from the thermal simulation results (section 6.3);
2. corresponding mean temperature, nominal temperature and factor R values were calculated;
3. steel grade, buckling axis, slenderness, variable load type and factor α were chosen;
4. failure probability $p_{f,fi,MCS}$ was defined for the chosen parameters using MSC according to the scheme described in 6.5.1;
5. failure probability $p_{f,fi,pr}$ was defined for the chosen parameters using ranking system and diagrams in Figure 6.10, Figure 6.11, Annexes A11 – A15.

The procedure was repeated for the steel grades from S235, S355 and S460, slenderness $\lambda_{20^\circ\text{C}}$ values from 0.0 to 2.0, factor α values from 0.0 to 0.75 and all the 3 240 thermal simulations. The total number of cases for the comparison was 281 556. Results indicate that in 97.5% of the cases the predicted failure probability $p_{f,fi,pr}$ does not exceed

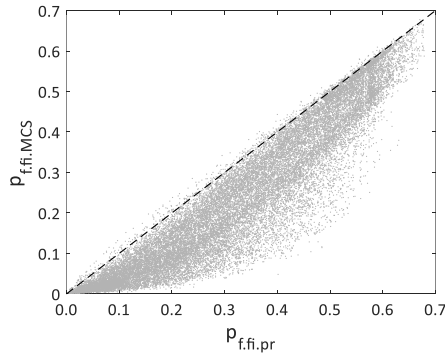


Figure 6.17: Ranking system testing results

the failure probability calculated using direct MCS $p_{f,fi,MCS}$. For the 2.5% of the cases for which $p_{f,fi,pr} < p_{f,fi,MCS}$, the mean value of failure probability misestimation is 5.8% of the $p_{f,fi,MCS}$ value. Based on those results the performance of the ranking system was considered satisfactory.

6.5.4 Influence of the fire temperature model on the failure probability

Eurocode Parameter Fire Curve model (EC1) is used to simulate the fire temperature evolution. Failure probability reported in section 6.5.2 is presented in relation to the mean temperature calculated using the EC1 model. The Design method proposed in section 6.6 is based on the nominal temperature, which was also calculated using the EC1 model. In section 4.4.3 the following question was raised. How the resulting failure probabilities are influenced by the choice of the fire model? The same question can be formulated differently as follows. If the nominal temperature calculations are performed using a thermal model different from EC1, could the design method proposed in this work still be implemented? It is assumed in this work that if the method used for thermal calculations is more advanced than the EC1 model, then it is justified to implement it in combination with the proposed reliability based buckling design method. In order to check the assumption, calculations performed using the EC1 model are compared with the calculations performed by the mixed-zone model implemented in OZone software package (section 4.4.3, [98]).

The mixed-zone model is by definition more complex and presumably more accurate compared to the EC1 model. According to Schleich et al [18] the correlation coefficient for the temperatures predicted by the EC1 method and test results is 0.83. The comparison between test data and the OZone can be found in [16] and [19]. Further in this work the mixed-zone model will be referred to as OZone model. The EC1 model is used in this work as a temperature variability generator. The focus of interest is not so much on the difference of the temperature values calculated using EC1 and OZone, but in the differences in temperature variability instead.

The raised question is approached in two ways. Initially the temperature coefficients of variance (COV) are compared. For the EC1 model, COV is calculated using MCS for 3 240 thermal simulations (section 6.3). For a limited number of configurations the COV of temperature distributions simulated using OZone was calculated. The implementation of MCS in combination with OZone is complicated by the computational demand of the latter. Therefore calculation of the COV for the OZone model was performed by the Maximum Entropy Multiplicative Dimensional Reduction Method (ME-MDRM) as proposed by Zhang [92]. ME-MDRM enables to estimate temperature variance with

relatively low number of model evaluations: $5n + 1$, where n is the number of stochastic variables and 5 is the number of Gauss integration points [92].

Results of the temperature variance of the EC1 model are presented in the form of two diagrams in Figure 6.18. COV dependence on the mean temperature is demonstrated. Diagrams include two types of lines: dot-dashed is the linear trend; dashed is the envelope line covering COV values. For both protected and unprotected steel members COV has a tendency to decrease with growing mean temperature value. Another important observation is related to the fact that the envelope trends for both protected and unprotected sections are similar to each other. ME-MDRM calculations with OZone model were performed for the following set of parameters: fire load density $q_{f,k} = [420, 600, 780] \text{ MJ/m}^2$; enclosure thermal inertia $b = [1\ 000, 1\ 913] \text{ J/(m}^2\text{s}^{0.5}\text{K)}$; opening factor $O = [0.02, 0.11, 0.20] \text{ m}^{0.5}$; steel section factor $A_p/V = 253 \text{ m}^{-1}$ (HEA140); thermal insulation thickness to thermal conductivity relation $d_p/\lambda_p = [0.083, 0.17, 0.25] \text{ m}^2\text{sK/J}$; fire compartment area $A_{fi} = [100, 500, 2\ 500] \text{ m}^2$; compartment height $H = [4.0, 8.0] \text{ m}$. Total number of cases considered was 54. Results are presented in the bottom diagram of Figure 6.18. On the diagram three sets are separated: cases where compartment parameters are within the limits of the EC1 method and temperature calculations are performed using OZone model are denoted by rings; cases where compartment parameters are within the limits of the EC1 method and temperature calculations are performed using EC1 model are denoted by squares; cases where compartment parameters are outside the EC1 limits ($A_{fi} > 500 \text{ m}^2$; $H > 4.0 \text{ m}$) and temperatures calculations are performed using OZone model are denoted by triangles; dashed limit corresponds to the COV envelope line of the protected steel section. From the results it can be seen that for all the cases considered the COV values for the OZone model are below the envelope line of the EC1 model. EC1 model demonstrates higher

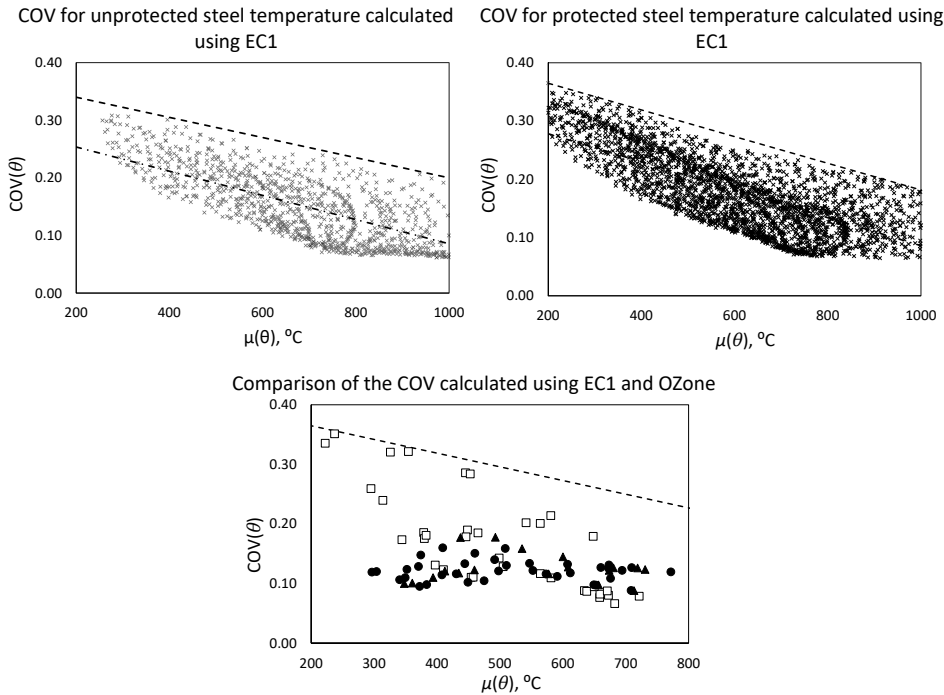


Figure 6.18: COV as a function of mean temperature

variability of the COV. COV values for the OZone model lie in the range from 0.10 to 0.20. COV values for the fire compartments outside the EC1 limits lie close to those within the EC1 model limits.

Comparing the results for two models it is evident that temperature variability for the EC1 model is higher than for the OZone model. Unfortunately, this is not enough for making judgment on the assumption made in the beginning of this section. Results of the COV comparison serve only as an indicator of the tendency and more detailed analysis is needed in order to make final conclusion. The easiest way of analysis, is to perform full reliability analysis for both cases and compare the failure probabilities. Direct MCS reliability analysis with the implementation of OZone is not feasible in reasonable time limits. Results of the sensitivity analysis (section 6.2) indicated, that the variables having the strongest impact on the variability of the output are fire load density $q_{f,k}$ and passive protection d_p/λ_p . d_p/λ_p influences the temperature of steel via method described in Annex A2, which is similar for both cases: the one used in this work in combination with EC1 fire model and the one integrated into OZone software package [98]. Therefore the variability of d_p/λ_p could be ignored, because the impact is similar for both EC1 and OZone models. The problem can be reduced to single variable – fire load density $q_{f,k}$. In this case, for each given configuration the dependence between the fire load density $q_{f,k}$ and maximum steel temperature θ can be established using polynomial. The range of $q_{f,k}$ is divided into 19 sections by 20 nodes. For each node ($q_{f,k}$ value) the steel temperature is calculated and the dependence between is $q_{f,k}$ and θ is established by polynomial as demonstrated on the left diagram of Figure 6.19. Reliability analysis can then be performed in accordance with the scheme presented in section 6.5.1, with the following modification: on step 1, the established polynomial is used to produce temperature distribution from the generated fire load distribution. An example of the produced temperature distribution is presented on the right side diagram of Figure 6.19. The reliability analysis was performed for the S355 $\lambda_{20^\circ\text{C}} = 0.0$ $\alpha = 0.0$ (only dead load is assumed) and 54 thermal cases described in the beginning of this section. In parallel, the reliability calculations were performed for the configurations corresponding to the EC1 model limits in accordance with the scheme presented in section 6.5.1. Failure probability is used as a marker, similarly to the ranking process described in section 2. Results of the marking process are presented in Figure 6.20. In the diagram the failure probabilities are presented as a function of the nominal temperature θ_{nom} .

Results are presented for three sets: EC1 – reliability analysis and nominal temperature were calculated implementing the EC1 fire model; OZone 1 – reliability analysis and nominal temperature were calculated implementing the OZone fire model for the cases corresponding to the EC1 limits; OZone 2 – reliability analysis and nominal temperature were calculated implementing the OZone fire model for the cases outside the EC1 limits. Failure probabilities calculated using the EC1 fire model show higher variability than Ozone model. Failure probabilities calculated using OZone lie relatively close to the trend line. Results of the failure probability marking apparently support the assumption that more advanced fire simulation method generates lower temperature variability comparing to the EC1 model.

The main weakness of the presented arguments is the limited range of parameters (fire compartments, fire load densities and etc.) for the supportive analysis. Both EC1 and OZone models have been used in parallel in the research work resulting in the Natural Fire Safety Concept (NFSC) [18], [99]. NFSC is one of the main background documents for the Eurocode framework for fire induced actions [12] and design of steel structures in

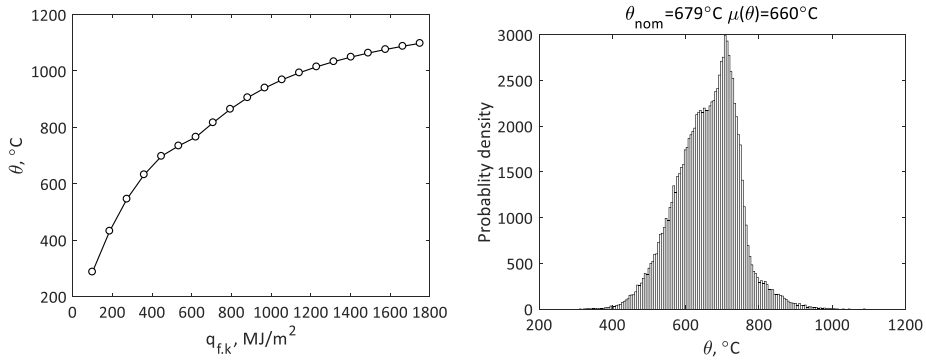


Figure 6.19: Technique for the implementation of the MCS with OZone

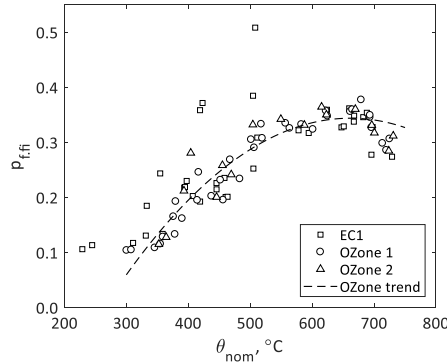


Figure 6.20: Failure probability marking for different fire evolution models

fire conditions [20]. The implementation of both zone-models and EC1 in EN 1991-1-2 [12] is sufficient justification to assume that both methodologies (OZone and EC1) provide similar level of safety and it can be concluded that the stochastic performance of both methods is comparable.

Based on the above argumentation it is concluded that the reliability based method for buckling design proposed in this work can be used not only with the EC1 method for fire temperature simulation, but also in combination with the zone model.

6.6 Reliability based design method

6.6.1 Derivation of the method

Reliability calculation scheme was presented in section 6.5.1, where the failure probability $p_{f,fi}$ was calculated assuming full utilization of buckling capacity $G_k + Q_k = R_{fi,Nom}$. The relationship between the nominal resistance value $R_{fi,Nom}$ and the failure probability $p_{f,fi}$ can be established. For this purpose a factor c_{fi} is introduced as a multiplier to the nominal resistance $R_{fi,nom}$ in the reliability calculations for modification of its value (step 4 in the procedure presented in section 6.5.1). For each factor c_{fi} value from a predefined range (e.g. 0 – 1.2 for 500°C) the reliability calculations were performed according to the scheme of section 6.5.1. The nominal resistance $R_{fi,Nom}$ value in step 4 is multiplied by the factor c_{fi} and failure probability is obtained for each combination of configurations (temperature distribution from the thermal simulations, column slenderness, variable load fraction).

The described procedure resulted in a large array of data – for each material grade, column slenderness, variable load type and variable load fraction (factor α) combination a set of 3 240 $c_{fi}-p_{f,fi}$ curves was generated and ranking was implemented. The whole range of temperatures of interest was divided into subranges with respective values of nominal temperature. The set of $c_{fi}-p_{f,fi}$ curves was grouped on the basis of the corresponding nominal temperature value and for each temperature subrange four curves $c_{fi}-p_{f,fi}$ for ranks R1 ... R4 were fixed. The process is demonstrated in Figure 6.21.

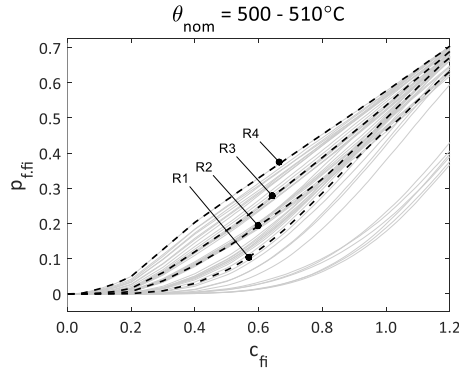


Figure 6.21: Ranking example of $c_{fi} - p_{f,fi}$ curve

In order to give the proposed design method a convenient form and adapt the method to the Eurocode load combination rules the factor χ_{Rel} with the limiting value of $\chi_{20^\circ C}$ (buckling factor in normal temperature conditions) is introduced (6-2) as follows. The product of factor c_{fi} and nominal resistance $R_{fi,Nom}$ is normalized by the section plastic capacity in ambient conditions $Af_{y,20^\circ C}$ and multiplied by the factor from equation (6-5), which transforms the loading from the reliability analysis to the EN 1990 procedure. As the reliability calculations use unfactored characteristic load values (6-3) and the Eurocode system uses factored accidental load combination (6-4), the output buckling capacity of the reliability analysis must be reduced in order to be comparable with the corresponding load of EN 1990 approach. The factor (6-5) is derived by dividing the load combination rule of EN 1990 by the unfactored combination of values accounting also for the variable load fraction (factor α). According to the EN 1990, recommended factor ψ_1 values for the imposed load Q are in the range between 0.5 and 0.9 [34]. Factor ψ_1 value of 0.5 is assumed for the imposed load in this work. The main parameter of the proposed method factor χ_{Rel} is presented in the form of tables. Results for the $\theta_{nom} = 500^\circ C$ S355 strong axis buckling are presented in Table 6-4 as an example. Results for other temperature values, steel grades and buckling axes are presented in Annexes A16 – A21. Results are reported only for the imposed variable load type Q . Design tables present the factor χ_{Rel} as a function of the failure probability $p_{f,fi}$ and the reliability index $\beta_{f,fi}$. The same tables present the dependence between factor χ_{Rel} and the fire probability factor δ_{af} which is valid only in case target failure probability p_t is assumed to be equal to 7.235×10^{-5} (section 4.3). The tables can be used without reference to the EN 1991-1-2 [12] fire safety framework if used in the failure probability $p_{f,fi}$ or the reliability index $\beta_{f,fi}$ domain. When the tables are used in the factor δ_{af} domain, EN 1991-1-2 fire safety framework is implicitly assumed. Four factor χ_{Rel} values are presented in accordance with the introduced ranking system (2).

$$\chi_{Rel} = \min \left\{ \frac{c_{fi} R_{fi,nom}}{A f_{y,20^\circ C}} (1 - \alpha + \alpha \Psi_1); \chi_{20^\circ C} \right\} \quad (6-2)$$

$$G_k + Q_k \quad (6-3) \quad N_{fi,d} = G_k + \Psi_1 Q_k \quad (6-4)$$

$$\frac{G_k + \Psi_1 Q_k}{G_k + Q_k} = \frac{G_k + \Psi_1 \frac{\alpha}{1-\alpha} G_k}{G_k + \frac{\alpha}{1-\alpha} G_k} = \frac{1 - \alpha + \Psi_1 \alpha}{1 - \alpha} \frac{G_k}{G_k} = 1 - \alpha + \alpha \Psi_1 \quad (6-5)$$

In Figure 6.22 the failure probability as a function of the factor c_{fi} is presented when used within the Eurocode framework for the treatment of fire probability. As an example, factor α is assumed to be 0.0 (only dead load is applied). The horizontal dashed lines represent different levels of fire probability. The case of slenderness 0.0 is discussed: for the mean temperature 300°C in case the fire probability p_{fire} is estimated to be equal to 7.235×10^{-3} ($\beta_{f,fi} = 2.33$; $\delta_{af} = 1.56$), the acceptable failure probability $p_{f,fi}$ is equal to 0.01 (meaning: $p_{fire} \times p_{f,fi} = 7.235 \times 10^{-3} \times 0.01 = 7.235 \times 10^{-5}$) – in that case the maximum factor c_{fi} is around 0.51; for the temperature 900°C in case fire probability p_{fire} is estimated to be equal to 1.034×10^{-4} ($\beta_{f,fi} = -0.52$; $\delta_{af} = 0.72$), acceptable failure probability $p_{f,fi}$ is equal to 0.70 (meaning: $p_{fire} \times p_{f,fi} = 1.034 \times 10^{-4} \times 0.70 = 7.235 \times 10^{-5}$) – in that case the maximum factor c_{fi} value is around 1.43. Obviously in case the fire probability p_{fire} is equal or lower than 7.235×10^{-5} the acceptable failure probability $p_{f,fi}$ is equal to 1.0, meaning that theoretically the factor c_{fi} value can be taken as infinite. In other words, in case of low fire probability collapse of the column is tolerated by the Eurocode framework. This aspect has received reiterated attention by the researchers questioning the adequacy of the safety concept in fire of the current Eurocode methodology [47], [49], [50]. As it was already stated, the present work does not discuss the treatment of the fire probability in the present Eurocode system. In case the research community comes to a conclusion that the fire probability concept in the Eurocode system should be revised, the changes in the proposed methodology of the present work can be expected to be moderate – factor δ_{af} will have to be recalibrated.

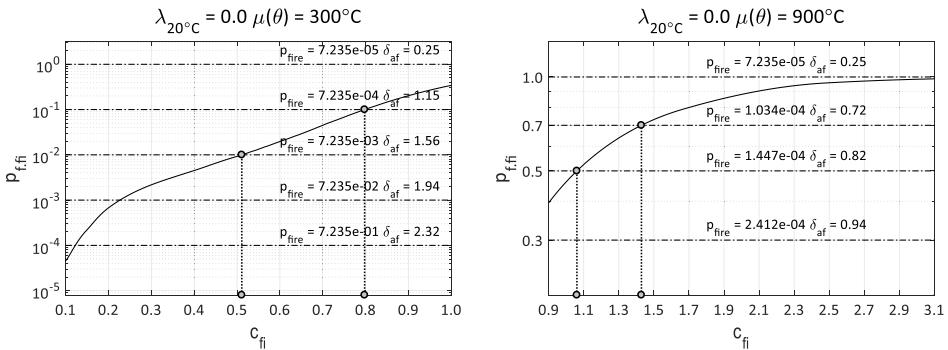


Figure 6.22: Failure probability as a function of factor c_{fi} for different mean temperature values of the S355 column, strong axis buckling

6.6.2 Implementation of the method

The proposed method enables to perform two types of tasks:

- Calculate failure probability as a function of design load with user-friendly effort.
- Obtain buckling capacity value that exhibits improved consistency with the stated target safety level compared to current Eurocode.

The procedure of the method is summarized as follows:

1. Steel column geometry (section area, slenderness) and material are assumed to be known.
2. Steel column temperature is defined. The method for temperature calculation should correspond to the criteria prescribed in EN 1991-1-2 [12]. Temperature calculations must be performed using the mean fire load density values from Table E.4 of EN 1991-1-2 [12] and nominal values of other parameters (opening factor, thermal inertia, protection material properties etc.).
3. Based on the input data of the step 1 and 2, two types of practical tasks can be solved:
 - a. In case the design load in fire conditions $N_{fi,d}$ is known, factor χ_{Rel} can be calculated using (6-6) and Table 6-4 or Annexes A16 – A21 can be used to estimate the failure probability of the column in fire $p_{f,fi}$. Calculated failure probability in fire $p_{f,fi}$ can be used in combination with probability of fire p_{fire} obtained by any risk analysis framework. By varying design load $N_{fi,d}$, different failure probability values can be easily obtained and different scenarios investigated.

$$\chi_{Rel} = \frac{N_{fi,d}}{Af_{y,20^{\circ}C}} \quad (6-6)$$

- b. The proposed method can be used within the current EN 1991-1-2 [12] safety framework for calculating buckling capacity. Then for a given slenderness, nominal temperature and factor δ_{af} value, factor χ_{Rel} is defined using Table 6-4 or Annexes A16 – A21 and the buckling capacity is calculated using equation (6-7). Probabilistic characteristic of the resulting buckling capacity better matches the principle of safety compared to current Eurocode method, as is demonstrated in section 6.6.4 and 3.

$$N_{b,fi,Rd,Rel} = \chi_{Rel} Af_{y,20^{\circ}C} \quad (6-7)$$

The proposed design method was composed based on the analysis of the strong and weak axis of the rolled I sections. According to the results of the mechanical analysis (section 5.7), the buckling curves for hollow core rectangular and hollow core circular sections are very similar to the buckling curves for strong axis buckling of I sections. Results of the sensitivity analysis (section 6.2) showed that temperature variability has crucial impact on the response function variability and consequently on the failure probability. Based on those arguments it was concluded that the proposed method can be used for hollow core sections.

Implementation procedure of the proposed method is demonstrated by an example.

Table 6-4: Factor χ_{Rel} : $\theta_{nom} = 500^{\circ}\text{C}$ S355 strong axis imposed (Q) variable load type

$p_{ffi} \rightarrow$	0.10	0.20	0.30	0.40	0.50	0.60	0.70	0.80	0.90	0.10	0.20	0.30	0.40	0.50	0.60	0.70	0.80	0.90
$\beta_{ffi} \rightarrow$	1.28	0.84	0.52	0.40	0.00	-0.25	-0.52	-0.84	-1.28	1.28	0.84	0.52	0.40	0.00	-0.25	-0.52	-0.84	-1.28
$\delta_{af} \rightarrow$	1.15	1.02	0.94	0.88	0.82	0.77	0.72	0.67	0.60	1.15	1.02	0.94	0.88	0.82	0.77	0.72	0.67	0.60
	$\alpha=0.00$									$\alpha=0.25$								
$\lambda_{20^{\circ}\text{C}}=0.00$	R1	0.422	0.527	0.612	0.694	0.785	0.871	0.963	1.000	1.000	0.457	0.572	0.663	0.753	0.853	0.946	1.000	1.000
	R2	0.330	0.458	0.573	0.666	0.752	0.836	0.927	1.000	1.000	0.356	0.497	0.622	0.723	0.818	0.909	1.000	1.000
	R3	0.276	0.398	0.508	0.612	0.714	0.811	0.912	1.000	1.000	0.298	0.432	0.553	0.666	0.776	0.881	0.992	1.000
	R4	0.217	0.319	0.439	0.557	0.671	0.783	0.897	1.000	1.000	0.237	0.346	0.477	0.605	0.728	0.851	0.975	1.000
$\lambda_{20^{\circ}\text{C}}=0.25$	R1	0.355	0.443	0.513	0.583	0.657	0.731	0.810	0.904	0.993	0.384	0.480	0.557	0.632	0.713	0.796	0.882	0.985
	R2	0.277	0.386	0.480	0.560	0.631	0.702	0.779	0.874	0.993	0.301	0.418	0.520	0.607	0.687	0.763	0.849	0.953
	R3	0.232	0.335	0.427	0.515	0.599	0.681	0.768	0.867	0.993	0.251	0.364	0.463	0.558	0.650	0.739	0.834	0.944
	R4	0.183	0.268	0.371	0.469	0.563	0.657	0.752	0.855	0.988	0.200	0.292	0.401	0.509	0.611	0.714	0.818	0.932
$\lambda_{20^{\circ}\text{C}}=0.50$	R1	0.246	0.309	0.362	0.413	0.468	0.522	0.581	0.647	0.744	0.266	0.336	0.392	0.447	0.507	0.568	0.633	0.705
	R2	0.189	0.267	0.337	0.396	0.449	0.500	0.557	0.626	0.727	0.205	0.289	0.366	0.430	0.488	0.544	0.606	0.682
	R3	0.158	0.230	0.297	0.362	0.425	0.485	0.549	0.620	0.716	0.171	0.250	0.323	0.393	0.462	0.528	0.597	0.676
	R4	0.124	0.183	0.255	0.328	0.398	0.468	0.539	0.610	0.703	0.136	0.199	0.277	0.355	0.432	0.509	0.586	0.664
$\lambda_{20^{\circ}\text{C}}=0.75$	R1	0.188	0.242	0.286	0.330	0.378	0.423	0.471	0.525	0.610	0.204	0.262	0.311	0.359	0.411	0.460	0.512	0.572
	R2	0.142	0.205	0.264	0.315	0.361	0.403	0.450	0.508	0.594	0.154	0.223	0.287	0.342	0.391	0.438	0.490	0.554
	R3	0.117	0.175	0.230	0.285	0.341	0.391	0.444	0.502	0.581	0.127	0.191	0.250	0.310	0.370	0.425	0.483	0.547
	R4	0.094	0.138	0.195	0.255	0.317	0.377	0.436	0.494	0.567	0.102	0.149	0.212	0.277	0.344	0.410	0.474	0.538
$\lambda_{20^{\circ}\text{C}}=1.00$	R1	0.153	0.199	0.239	0.278	0.319	0.357	0.397	0.443	0.515	0.166	0.216	0.259	0.302	0.347	0.388	0.433	0.483
	R2	0.114	0.167	0.219	0.264	0.304	0.341	0.380	0.429	0.501	0.123	0.181	0.238	0.287	0.330	0.371	0.414	0.468
	R3	0.093	0.142	0.189	0.238	0.287	0.330	0.375	0.424	0.490	0.101	0.153	0.205	0.258	0.311	0.359	0.408	0.463
	R4	0.075	0.109	0.158	0.211	0.266	0.318	0.369	0.418	0.479	0.080	0.119	0.172	0.229	0.289	0.346	0.401	0.454
$\lambda_{20^{\circ}\text{C}}=1.50$	R1	0.093	0.121	0.146	0.170	0.195	0.218	0.241	0.268	0.307	0.101	0.132	0.159	0.185	0.212	0.237	0.262	0.293
	R2	0.068	0.101	0.134	0.162	0.186	0.209	0.232	0.260	0.300	0.074	0.110	0.145	0.175	0.202	0.227	0.252	0.284
	R3	0.056	0.085	0.115	0.145	0.175	0.202	0.229	0.257	0.296	0.061	0.093	0.125	0.158	0.191	0.219	0.248	0.280
	R4	0.045	0.065	0.096	0.128	0.163	0.195	0.225	0.254	0.291	0.048	0.071	0.104	0.140	0.177	0.212	0.244	0.276
$\lambda_{20^{\circ}\text{C}}=2.00$	R1	0.056	0.073	0.087	0.102	0.117	0.130	0.144	0.160	0.182	0.060	0.079	0.095	0.110	0.126	0.141	0.156	0.174
	R2	0.041	0.061	0.080	0.097	0.111	0.124	0.138	0.155	0.178	0.044	0.066	0.087	0.105	0.121	0.135	0.151	0.169
	R3	0.034	0.051	0.069	0.087	0.105	0.120	0.136	0.153	0.176	0.036	0.056	0.074	0.094	0.114	0.131	0.148	0.167
	R4	0.027	0.039	0.057	0.077	0.097	0.116	0.134	0.152	0.173	0.029	0.043	0.062	0.084	0.105	0.126	0.146	0.165
	$\alpha=0.50$									$\alpha=0.75$								
$\lambda_{20^{\circ}\text{C}}=0.00$	R1	0.509	0.639	0.747	0.851	0.964	1.000	1.000	1.000	1.000	0.583	0.757	0.904	1.000	1.000	1.000	1.000	1.000
	R2	0.401	0.558	0.699	0.815	0.928	1.000	1.000	1.000	1.000	0.474	0.667	0.844	1.000	1.000	1.000	1.000	1.000
	R3	0.337	0.487	0.621	0.750	0.878	1.000	1.000	1.000	1.000	0.408	0.587	0.756	0.924	1.000	1.000	1.000	1.000
	R4	0.267	0.393	0.539	0.684	0.824	0.966	1.000	1.000	1.000	0.324	0.488	0.659	0.838	1.000	1.000	1.000	1.000
$\lambda_{20^{\circ}\text{C}}=0.25$	R1	0.427	0.537	0.628	0.714	0.806	0.909	0.993	0.993	0.993	0.487	0.634	0.760	0.883	0.993	0.993	0.993	0.993
	R2	0.337	0.467	0.586	0.686	0.779	0.872	0.977	0.993	0.993	0.400	0.561	0.709	0.847	0.978	0.993	0.993	0.993
	R3	0.284	0.409	0.522	0.630	0.736	0.844	0.956	0.993	0.993	0.342	0.493	0.635	0.775	0.921	0.993	0.993	0.993
	R4	0.225	0.331	0.453	0.574	0.691	0.811	0.935	0.993	0.993	0.274	0.411	0.554	0.704	0.857	0.993	0.993	0.993
$\lambda_{20^{\circ}\text{C}}=0.50$	R1	0.296	0.375	0.441	0.505	0.575	0.649	0.726	0.817	0.951	0.341	0.445	0.534	0.623	0.721	0.831	0.951	0.951
	R2	0.230	0.325	0.412	0.485	0.553	0.620	0.695	0.790	0.951	0.275	0.391	0.498	0.596	0.694	0.800	0.918	0.951
	R3	0.193	0.281	0.364	0.444	0.523	0.600	0.683	0.781	0.916	0.234	0.340	0.442	0.544	0.649	0.762	0.893	0.951
	R4	0.154	0.226	0.313	0.401	0.489	0.576	0.670	0.769	0.902	0.187	0.281	0.384	0.493	0.605	0.726	0.866	0.951
$\lambda_{20^{\circ}\text{C}}=0.75$	R1	0.227	0.294	0.350	0.404	0.466	0.523	0.587	0.664	0.780	0.263	0.349	0.424	0.496	0.578	0.674	0.777	0.876
	R2	0.174	0.250	0.323	0.385	0.444	0.500	0.562	0.642	0.759	0.209	0.302	0.392	0.474	0.556	0.642	0.742	0.876
	R3	0.144	0.214	0.282	0.350	0.418	0.482	0.553	0.633	0.746	0.177	0.260	0.345	0.429	0.518	0.614	0.722	0.876
	R4	0.115	0.169	0.239	0.314	0.389	0.465	0.543	0.625	0.728	0.141	0.211	0.294	0.386	0.480	0.582	0.699	0.876
$\lambda_{20^{\circ}\text{C}}=1.00$	R1	0.186	0.243	0.292	0.340	0.392	0.442	0.496	0.562	0.725	0.216	0.289	0.353	0.415	0.486	0.566	0.655	0.725
	R2	0.139	0.205	0.269	0.323	0.374	0.422	0.475	0.542	0.641	0.168	0.247	0.324	0.396	0.468	0.541	0.626	0.725
	R3	0.115	0.173	0.232	0.292	0.351	0.407	0.467	0.534	0.628	0.141	0.211	0.284	0.357	0.433	0.515	0.607	0.725
	R4	0.091	0.135	0.195	0.260	0.326	0.392	0.458	0.527	0.615	0.113	0.170	0.240	0.319	0.401	0.489	0.590	0.725
$\lambda_{20^{\circ}\text{C}}=1.50$	R1	0.112	0.148	0.179	0.208	0.239	0.270	0.302	0.340	0.395	0.131	0.177	0.216	0.254	0.297	0.345	0.395	0.395
	R2	0.083	0.124	0.164	0.197	0.229	0.258	0.290	0.329	0.395	0.101	0.150	0.198	0.242	0.284	0.330	0.395	0.395
	R3	0.069	0.105	0.141	0.178	0.215	0.249	0.285	0.325	0.395	0.085	0.128	0.172	0.217	0.264	0.315	0.395	0.395
	R4	0.055	0.081	0.118	0.158	0.199	0.239	0.279	0.320	0.395	0.068	0.102	0.146	0.194	0.244	0.298	0.359	0.395
$\lambda_{20^{\circ}\text{C}}=2.00$	R1	0.067	0.089	0.107	0.124	0.143	0.161	0.180	0.202	0.232	0.078	0.105	0.129	0.152	0.177	0.206	0.232	0.232
	R2	0.050	0.074	0.098	0.118	0.136	0.154	0.173	0.196	0.232	0.061	0.090	0.118	0.144	0.170	0.197	0.232	0.232
	R3	0.041	0.063	0.084	0.106	0.128	0.148	0.169	0.193	0.232	0.051	0.076	0.103	0.130	0.158	0.187	0.232	0.232
	R4	0.033	0.048	0.071	0.095	0.119	0.143	0.166	0.191	0.232	0.041	0.061	0.087	0.116	0.146	0.177	0.213	0.232

6.6.3 Example

HEB240 S355 steel column buckling capacity around the strong axis must be defined. Calculation results are compared with the current design method: EN 1991-1-2 [12] and EN 1993-1-2 [20]. In addition to that failure probabilities are defined for a given loading set.

Fire compartment parameters

Area: $A_{fi} = 500 \text{ m}^2$; height: $H = 4.0 \text{ m}$; opening factor $O = 0.05 \text{ m}^{0.5}$; enclosure thermal inertia: $b = 1742 \text{ J}/(\text{m}^2\text{s}^{0.5}\text{K})$; rank $R = (0.05 / 1742)^{0.5} = 0.0054 \rightarrow \text{R2}$.

Column geometry

Section area: $A = 1.06 \times 10^4 \text{ mm}^2$; moment of inertia around strong axis $I_y = 1.126 \times 10^8 \text{ mm}^4$; nominal yield limit stress in normal temperature conditions: $f_{y,20^\circ\text{C}} = 355 \text{ MPa}$; nominal deformation modulus in normal temperature conditions: $E_{20^\circ\text{C}} = 210\,000 \text{ MPa}$; column effective length: $L = 3939 \text{ mm}$ (effective length reduction opportunity in fire conditions is ignored); $\lambda_{20^\circ\text{C}} = 0.5$; buckling factor in normal temperature conditions $\chi_{20^\circ\text{C}} = 0.880$; section factor $A/V = 0.131 \text{ mm}^{-1}$.

Fire characteristics

Occupancy type: office; mean fire load density: $q_{f,k, \text{Mean}} = 420 \text{ MJ}/\text{m}^2$; 80% fractile fire load density: $q_{f,k,80} = 511 \text{ MJ}/\text{m}^2$; fire growth rate: medium $t_{lim} = 20 \text{ minutes}$; fire probability: three cases are considered $\delta_{af} = 0.60$, $\delta_{af} = 0.80$, $\delta_{af} = 1.00$.

Column passive protection

Three cases are considered: unprotected column, column protected with 5 mm vermiculite cement layer ($\lambda = 1.2 \text{ J}/\text{msK}$), column protected with 12 mm vermiculite cement layer ($\lambda = 1.2 \text{ J}/\text{msK}$).

Thermal calculations

Eurocode parametric fire method is used [12]. The proposed method assumes the use of the mean value of the fire load density $q_{f,k, \text{mean}}$ for the fire temperature calculations and fire probability is taken into account on the level of capacity calculations. Eurocode temperature calculation method uses design fire load density $q_{f,d}$, which itself is calculated by multiplication of the 80% fractile value of fire load density $q_{f,k,80}$ by the factor δ_{af} and by the combustion factor 0.8. For the Eurocode design method thermal calculations are performed for three factor δ_{af} values: 0.60, 0.80, 1.00. Results of the thermal calculation are presented in Figure 6.23.

Loading

Buckling capacities are defined for the following conditions: factor α value is 0.25; variable load type – imposed load Q_k . Failure probabilities are defined for the following permanent loads: set 1 – $G_k = 500 \text{ kN}$, set 2 – $G_k = 750 \text{ kN}$, set 3 – $G_k = 950 \text{ kN}$; for every load three factor α values are considered 0.25, 0.50, 0.75; combination factor value $\psi_1 = 0.5$.

Results

Results of the buckling resistance using the proposed method $N_{b,fi,Rd,Rel}$ are summarized in Table 6-5. Results are compared with the buckling capacity calculated using the current Eurocode methodology, $N_{b,fi,Rd,EC}$. The results in Table 6-5 indicate that the differences between the current Eurocode design method and the proposed method of the present work can be quite considerable. The differences are not one-sided: in some cases the capacity predicted by the proposed method is higher compared to Eurocode, in other cases the opposite is true. Results of the more extended comparison between the methodologies are presented in section 3.

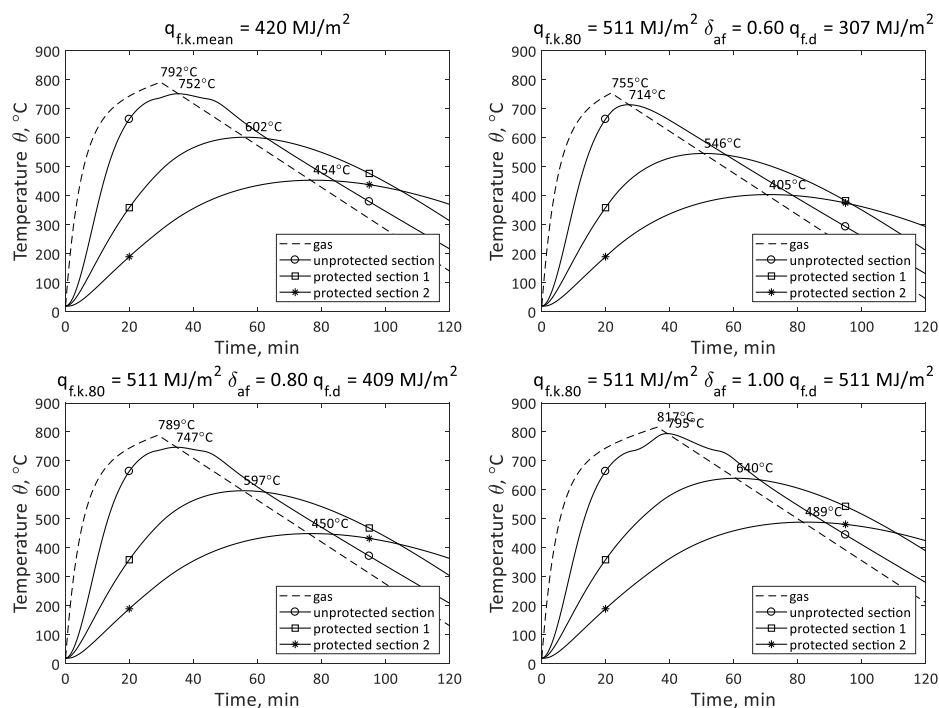


Figure 6.23: Design method example – thermal calculations results

Table 6-5: Design method example – results summary part 1

Description	Eurocode method			Proposed method			$N_{b,fi,Rd,EC} / N_{b,fi,Rd,EC}$
	θ , °C	$N_{b,fi,Rd,EC}$	N	θ_{nom} , °C	χ_{Rel}	$N_{b,fi,Rd,Rel}$	
unprotected section	$\delta_{af} = 0.60$	714	539 991		0.237	891 078	1.65
	$\delta_{af} = 0.80$	747	450 055		0.120	452 689	1.01
	$\delta_{af} = 1.00$	795	315 339		0.068	256 260	0.81
protected section 1	$\delta_{af} = 0.60$	546	1 703 886		0.626	2 357 143	1.38
	$\delta_{af} = 0.80$	597	1 253 832		0.322	1 210 933	0.97
	$\delta_{af} = 1.00$	640	968 220		0.178	670 567	0.69
protected section 2	$\delta_{af} = 0.60$	405	2 620 177		0.859	3 233 922	1.23
	$\delta_{af} = 0.80$	450	2 378 216		0.590	2 219 417	0.93
	$\delta_{af} = 1.00$	489	2 167 112		0.396	1 490 901	0.69

Failure probabilities for the given load sets are reported in Table 6-6. Column $N_{fi,d}$ is the design load in fire conditions in accordance with the EN 1990 [34] load combination rules. The table demonstrates how the proposed method can be used independent of the current Eurocode fire safety concept (section 4.3).

6.6.4 Validation of the proposed method

The method validation is performed using the following scheme:

1. Temperature distribution is imported from the thermal simulation results. Nominal temperature θ_{nom} is fixed, factor α and slenderness $\lambda_{20^\circ\text{C}}$ are chosen.
2. Failure probability $p_{f,fi,Rel}$ is chosen from the range 0.1 to 0.9. Table 6-4 and Annexes A16 – A21 are used to define the factor χ_{Rel} for the given θ_{nom} , α and $\lambda_{20^\circ\text{C}}$.

Table 6-6: Design method example – results summary part 2

Description	$\theta_{nom}, ^\circ\text{C}$	G_k, N	Q_k, N	α	$N_{fi,d}, \text{N}$	χ_{Rel}	$p_{f,fi}$
unprotected section	752	500 000	166 667	0.25	583 333	0.155	0.733
		500 000	500 000	0.50	750 000	0.199	0.793
		500 000	1 500 000	0.75	1 250 000	0.332	0.872
protected section 1	602	750 000	250 000	0.25	875 000	0.233	0.352
		750 000	750 000	0.50	1 125 000	0.299	0.420
		750 000	2 250 000	0.75	1 875 000	0.498	0.578
protected section 2	454	950 000	316 667	0.25	1 108 333	0.295	0.113
		950 000	950 000	0.50	1 425 000	0.379	0.158
		950 000	2 850 000	0.75	2 375 000	0.631	0.328

- Buckling capacity $N_{b,fi,Rd,Rel}$ is defined using factor χ_{Rel} . Reliability calculations are performed using the scheme from section 6.5.1, where the nominal resistance $R_{fi,nom}$ from step 4 is replaced by the $N_{b,fi,Rd,Rel}$. Failure probability $p_{f,fi,MCS}$ is calculated.
- $p_{f,fi,Rel}$ and $p_{f,fi,MCS}$ are compared.

The total number of cases for validation was 298 620. Results of the validation are reported in Figure 6.24 and Figure 6.25. Results are presented for the 5 $p_{f,fi,Rel}$ values. For each $p_{f,fi,Rel}$ value two diagrams are presented: left column – scatter plot for the failure probabilities obtained by performing MCS $p_{f,fi,MCS}$ in relation to the nominal temperature θ_{nom} ; right column – histogram of the $p_{f,fi,MCS}$ values. It is evident, that the calculated failure probabilities $p_{f,fi,MCS}$ in vast majority of cases does not exceed the initially assumed failure probability $p_{f,fi,Rel}$. $p_{f,fi,MCS}$ exceeds $p_{f,fi,Rel}$ in 2.5% of the considered cases. The maximum values of the $p_{f,fi,MCS}$ are presented on the right-hand histogram of Figure 6.24 and Figure 6.25. The maximum error of the failure probability estimation is 0.03 (for the case of $p_{f,fi,Rel} = 0.70$). Based on the presented results it was concluded that the proposed method was successfully validated.

6.6.5 Comparison with the current Eurocode design methodology

Before the comparison of the methodologies, failure probabilities of the current Eurocode methodology are investigated in a procedure similar to the validation process of the proposed methodology presented in the previous section. The analysis is performed using the following scheme:

- Temperature distribution is imported from the thermal simulation results, factor α and slenderness $\lambda_{20^\circ\text{C}}$ are chosen.
- Target failure probability $p_{f,fi,t}$ is chosen from the range 0.1 to 0.9, factor δ_{af} is calculated using Figure 4.3.
- Temperature θ_{EC} is calculated according to the rules of EN 1991-1-2.
- Buckling capacity $N_{b,fi,Rd,EC}$ is calculated using EN 1993-1-2 for temperature θ_{EC} . Reliability calculations are performed using the scheme from section 6.5.1, where the nominal resistance $R_{fi,nom}$ in step 4 is replaced by the $N_{b,fi,Rd,EC}$. Failure probability $p_{f,fi,MCS}$ is calculated.
- $p_{f,fi,t}$ and $p_{f,fi,MCS}$ are compared.

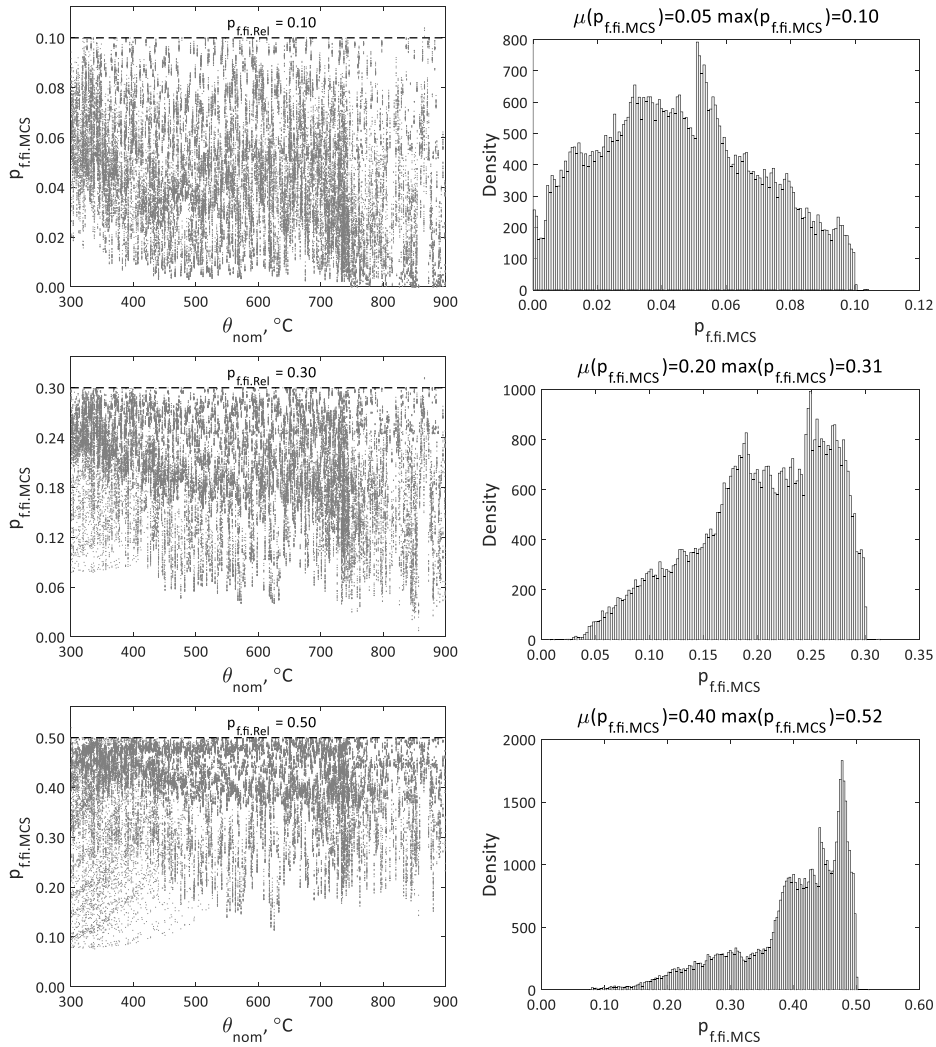


Figure 6.24: Validation of the proposed method – part 1

Results are presented in Figure 6.26 and Figure 6.27: on the left side diagram scatter plot of the failure probabilities is presented; on the right side histogram of failure probabilities is presented. The results reveal that on average the failure probability calculated directly is smaller than the expected target level. For example for the case of $\delta_{af} = 0.94$: $\mu(p_{f,fi,MCS}) = 0.20 \leq p_{f,fi,t} = 0.30$. Still, for a considerable number of cases, the failure probability calculated directly $p_{f,fi,MCS}$ differs from the expected target level $p_{f,fi,t}$. The following tendency is valid. For smaller target failure probability $p_{f,fi,t}$ values, the mean value of calculated failure probabilities $\mu(p_{f,fi,MCS})$ matches the stated target value, but in considerable number of cases the calculated failure probability $p_{f,fi,MCS}$ exceeds the target level $p_{f,fi,t}$. For higher target failure probability $p_{f,fi,t}$ value, the number of cases for which the calculated failure probability $p_{f,fi,MCS}$ is higher than the stated target level $p_{f,fi,t}$ is small, but the mean value of the calculated failure probabilities $\mu(p_{f,fi,MCS})$ is also smaller in relation to the stated target level $p_{f,fi,t}$. Described tendency indicate that target failure probability matching by the Eurocode methodology in fire conditions is weaker compared to the proposed method (Figure 6.24 and Figure 6.25). This result was

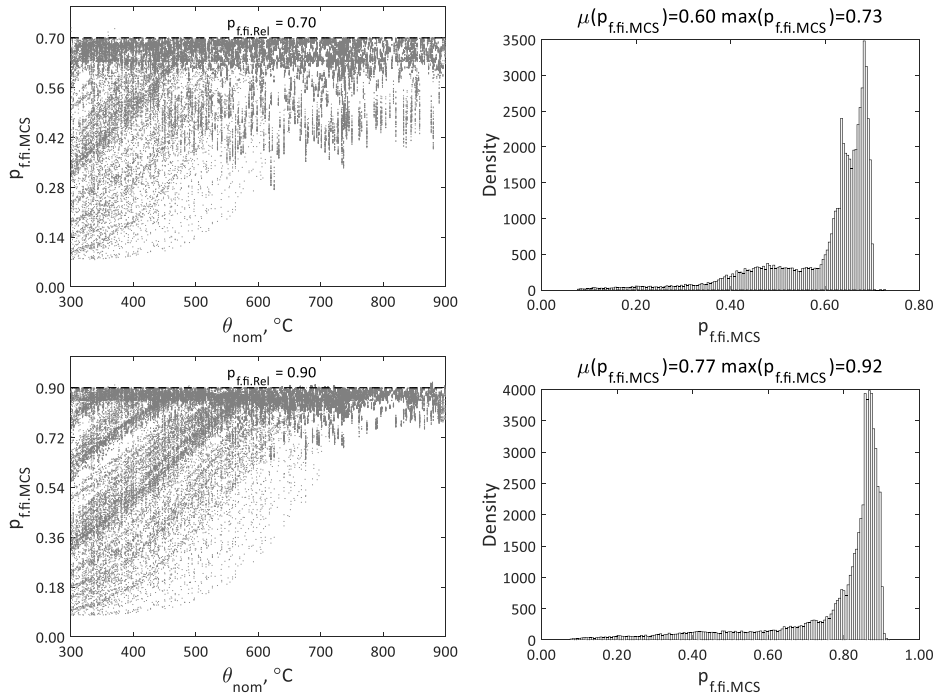


Figure 6.25: Validation of the proposed method – part 2

predicted in the section dedicated to the safety concepts (section 4.5), where similar tendencies for the normal temperature conditions were addressed.

Comparison of the buckling capacities predicted by the proposed method and the current method of EN 1991-1-2 [12] in combination with EN 1993-1-2 [20] (EC method) is reported further. The comparison was performed for the same cases as described in the previous section, i.e. the number of the compared cases was 298 620. The principles of the thermal analysis are the same as presented in the example (section 6.6.3). Comparison is reported using diagrams in Figure 6.28 and Figure 6.29. Left side diagram of Figure 6.28 demonstrates the relation between factor χ_{Rel} and $N_{b.fi.Rd.EC}/(A f_{y,20^\circ C})$, where $N_{b.fi.Rd.EC}$ is the buckling capacity calculated using EC methodology, A is the section area and $f_{y,20^\circ C}$ is the yield limit stress in ambient conditions. In the right side diagram of Figure 6.28 the histogram of the factor $N_{b.fi.Rd.Rel}/N_{b.fi.Rd.EC}$ is presented. The influence of the slenderness $\lambda_{20^\circ C}$ and variable load factor α on the mean value of the $N_{b.fi.Rd.Rel}/N_{b.fi.Rd.EC}$ is presented in Figure 6.29. The mean value of the factor $N_{b.fi.Rd.Rel}/N_{b.fi.Rd.EC}$ for the whole set is 1.18, which means that on average the proposed method predicts 18% higher buckling capacity compared to the EC method. Results presented in Figure 6.29 show that for the low factor α values in the slenderness range $\lambda_{20^\circ C} = 0.3 \dots 1.0$ the EC method on average predicts higher buckling capacity comparing to the proposed method. Regarding this result an important observation can be made referring to the difference between the buckling factors calculated using the EN 1993-1-2 method and the non-linear FEM which were presented in Figure 5.19, Annexes A4 and A5. The biggest differences between buckling factors appear in the slenderness range $\lambda_{20^\circ C} = 0.3 \dots 1.0$. Consequently the value of the factor $\mu(N_{b.fi.Rd.Rel}/N_{b.fi.Rd.EC})$ smaller than 1.0 in the same slenderness range is caused by the differences in the response of the mechanical models. It is evident that the higher factor $\mu(N_{b.fi.Rd.Rel}/N_{b.fi.Rd.EC})$ value corresponds to the higher

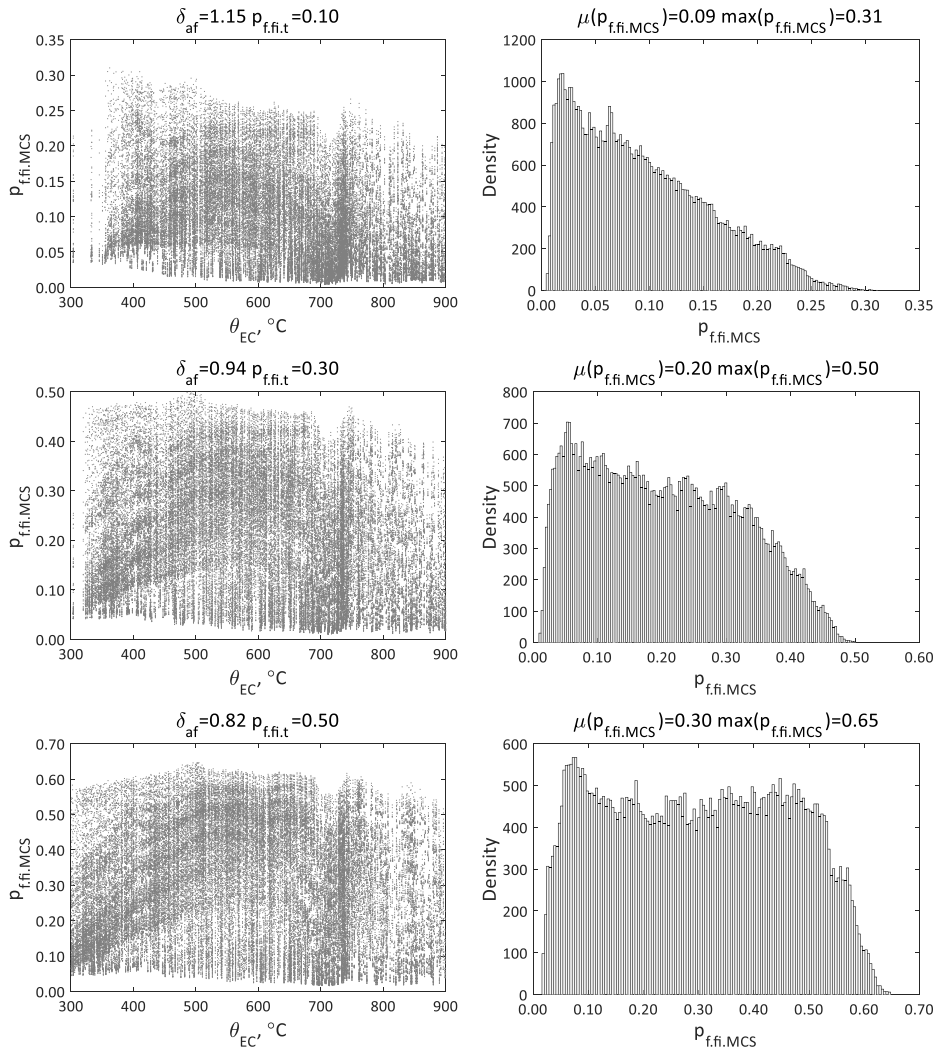


Figure 6.26: Failure probabilities for the current EN methodology – part 1

factor α value, which is in line with the results of the failure probability presented in section 6.5.2.

The performance of the proposed methodology against the current Eurocode methodology is concluded to be satisfactory.

6.7 Summary

Results of the sensitivity analysis were reported and appropriate decisions were made for the reliability analysis. The dominating role of thermal variables (fire load density, passive protection properties) on the stochastic response was demonstrated. Based on those results, the variability of geometrical properties and residual stresses was ignored in the reliability calculations. Results of the extensive thermal simulations were presented and analysed. Large scope of reliability calculations was made possible due to the computationally efficient procedure for prediction of buckling capacity of steel column in fire (Method C). Computational efficiency of the latter allowed to use direct

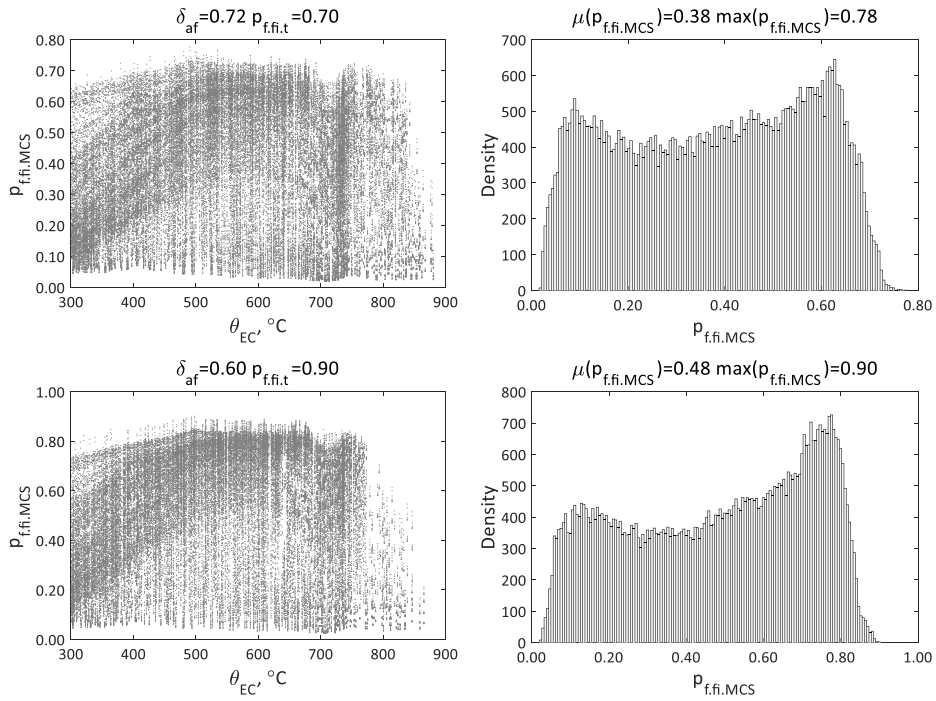


Figure 6.27: Failure probabilities for the current EN methodology – part 2

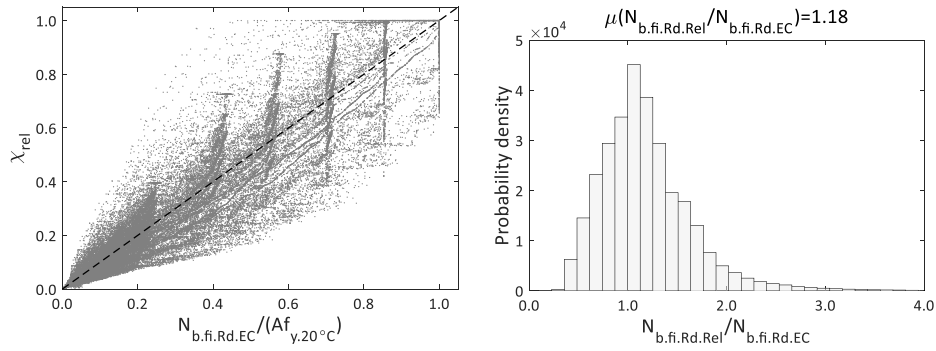


Figure 6.28: Proposed method vs. EC method – part 1

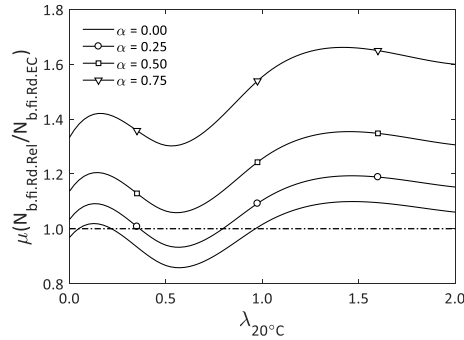


Figure 6.29: Proposed method vs. EC method – part 2

full Monte-Carlo simulation without the need to refer to the optimization techniques (e.g. Latin Hypercube or Importance Sampling). The shape complexity of temperature distributions was demonstrated, which has major impact on the resistance function distribution and consequently on failure probability. Results of the reliability analysis were presented for different steel grades and buckling axes. A special ranking system was introduced in order to differentiate failure probability predictions for practical applications. The influence of the fire model on the failure probability was investigated and it was shown that the proposed method can be used with different fire simulation models. A reliability based design method was proposed and validated. The proposed method allows to calculate efficiently failure probability in fire from a given set of input parameters in minimal time without the need to perform computationally demanding reliability calculations. The implementation of the proposed method was demonstrated by an example. Performance of the proposed method was compared with the current Eurocode methodology. The proposed method demonstrates considerably better matching to the target failure probability compared to the current Eurocode.

7 Conclusions and further research

7.1 Conclusions

The first part of this work is dedicated to the mechanical model of buckling of axially compressed steel column in fire conditions. Steel columns with common section types in fire conditions have been studied. Non-linear FEM procedure was composed for the analysis of the problem and validated against a general purpose FEM software package. Different aspects of modelling of the buckling problem were investigated: finite element types and meshing, initial shape etc. Different material models and their influence on the buckling capacity were studied regarding the nonlinearity of stress-strain relationship. The impact of the residual stresses was estimated. Based on the results of the initial research, an extended numerical study was carried out to form the database serving as the basis for the development of an analytical design method, determination of the necessary parameters and validation of the proposed method. FEM models were validated against the available test data.

An analytical procedure was proposed for calculating the buckling resistance with the aim to provide efficient tool for the resource demanding reliability calculations. Proposed method avoids certain simplifications of the current Eurocode design method, regarding the characteristics of different section types, the effect of nonlinear stress-strain relationship and initial imperfection. Based on the data of the numerical studies the whole range of section types was allocated into two groups according to the column mechanical response in fire. The allocation was applied to the proposed method increasing accuracy of buckling capacity prediction. The method is compatible with the current standard procedures. Computational efficiency of the method was used in the following research of reliability.

Reliability analysis of axially compressed steel columns in fire has been performed in the second part of the work. Monte-Carlo simulation has been applied with uncertainties of the stochastic variables taken into account. Statistical variation data of material properties, element geometry, loading and fire parameters have been obtained from available references. Monte Carlo simulation has been generally accepted as a reliable tool for direct probability calculations but its use for practical tasks is limited due to computational demand. In the current research the computational costs of Monte-Carlo simulations of the column buckling were reduced by implementing computationally efficient procedure from the first part of the work (Method C), which excluded the need to refer to the optimization techniques of Monte Carlo simulation (e.g. Latin Hypercube or Importance Sampling). Thermal simulations have been performed in a separate Monte Carlo procedure implementing the parametric design fire model of EN 1991-1-2 for producing the database of temperature distributions. Sensitivity analysis has been performed, which showed the dominance of the thermal analysis related variables. Extensive reliability analysis was performed for a large set of configurations, demonstrating the impact of temperature distribution shape on the distribution of the resistance function and consequently on the variability of failure probability.

Based on the results of the probabilistic analysis, a reliability based design method has been proposed for buckling of steel columns in fire. While making use of the advantages of Monte Carlo simulations, the disadvantages in practical applications of Monte Carlo method can be avoided in the proposed method, i.e. the large amount of trial calculations is performed only in the preparatory phase of the method producing a set

of parameter values. In practical applications the end-user can execute an easy procedure, linked to the common Eurocode algorithm supplemented by the predefined factors from tables or diagrams for the whole range of practical applications. The proposed design method allows better differentiation of the fire probability in the capacity assessment compared to the existing Eurocode design method. The method provides a convenient tool for evaluation of the safety level of a steel column in fire and comparison design alternatives. It can also be used to estimate the failure probability in fire independent of the target reliability of Eurocode framework as the target safety limits of structures in fire are sometimes argued and not always unequivocally interpreted.

Initially the reliability based buckling design method was developed for strong and weak axes of rolled I sections. In accordance with the results of the mechanical response and sensitivity analysis it was concluded that the solution for the strong axis buckling is applicable for hollow core section type. Although the thermal data for the proposed method was generated using parametric design fire model of EN 1991-1-2 the applicability of the produced method in combination with zone-model has been also demonstrated.

The proposed method was validated against the results of the direct reliability analysis. The performance of the proposed reliability based method was compared with the current Eurocode procedures. The proposed method demonstrates considerably better matching to the target failure probability compared to the current Eurocode.

7.2 Further research

The research presented in this work was dedicated only to the axially compressed steel columns in fire conditions. A number of important aspects were whether excluded or only roughly estimated. The following topics could be proposed for further research:

1. Mechanical buckling model of Method C could be developed to account for the influence of the load eccentricity and the possibility of the first order bending moment variation along the column axis.
2. Reliability analysis of the columns with complex loading conditions (axial force and different first order bending moment configurations) should be performed using computationally efficient mechanical model based on Method C.
3. Stochastic analysis of fire temperatures could be extended. Temperature variance in local fires and the influence of nonuniform heating on the stochastic response could be investigated.
4. Using the proposed methodology, reliability based design methods could be proposed for other problems related to the stability of steel elements in fire conditions.

Annexes

A1 Parametric fire curve (adopted from EN 1991-1-2)

Fire temperature at time t during the growing phase is calculated as following:

$$\theta_g = 20 + 1325(1 - 0.324e^{-0.2t^*} - 0.204e^{-1.7t^*} - 0.472e^{-19t^*})$$

, where:

$$t^* = t\Gamma$$

modified time for ventilation, hours

$$t^* = t\Gamma_{lim}$$

modified time for fuel controlled fire, hours

$$t$$

factual time, hours

$$\Gamma = \left[\frac{O}{b_{th}} \right]^2 / \left[\frac{0.04}{1160} \right]^2$$

$$\Gamma_{lim} = \left[\frac{O_{lim}}{b_{th}} \right]^2 / \left[\frac{0.04}{1160} \right]^2$$

$$100 \leq b_{th} = \sqrt{\rho c \lambda} \leq 2000$$

enclosure thermal inertia, J/(m²s^{0.5}K)

$$\rho$$

density of boundary of enclosure, kg/m³

$$c$$

specific heat of boundary of enclosure, J/kgK

$$\lambda$$

thermal conductivity of boundary of enclosure, W/mK

$$0.02 \leq O = A_v \sqrt{h_{eq}/A_t} \leq 0.20$$

opening factor, m^{0.5}

$$O_{lim} = 0.1 * 10^{-3} \frac{q_{t.d}}{t_{lim}}$$

$$A_v$$

total area of vertical openings on all walls, m²

$$h_{eq}$$

weighted average of window heights on all walls, m

$$A_t$$

total area of enclosure (including openings), m²

$$t_{lim}$$

fire growth rate characterizing time (25 minutes – slow fire growth rate fire; 20 minutes – medium fire growth rate; 15 minutes – fast fire growth rate), h

The maximum temperature is reached (heating phase end) at time moment calculated as following:.

$$t_{max}^* = t_{max}\Gamma$$

, where:

$$t_{max} = \max \left[\frac{0.2 * 10^{-3}}{O} q_{t.d}; t_{lim} \right]$$

fire is ventilation controlled in case $t_{lim} < t_{max}$ and fuel controlled in the opposite case

$$50 \leq q_{t.d} = q_{f.d} \frac{A_f}{A_t} \leq 1000$$

fire load design density load related to the total area of the enclosure (A_t), MJ/m²

$$q_{f.d}$$

fire load design density load related to the floor area (A_f), MJ/m²

In the cooling phase the temperature must be defined as following:

$$\begin{aligned} \text{for } t_{max}^* \leq 0.5 \quad \theta_g &= \theta_{max} - 625(t^* - t_{max}^*) \\ \text{for } 0.5 \leq t_{max}^* \leq 2.0 \quad \theta_g &= \theta_{max} - 250(3 - t_{max}^*)(t^* - t_{max}^*x) \\ \text{for } t_{max}^* \geq 2.0 \quad \theta_g &= \theta_{max} - 250(t^* - t_{max}^*x) \end{aligned}$$

, where:

$$t_{max}^* = \frac{t^* = t\Gamma}{0.2 * 10^{-3} q_{t.d} \Gamma}$$

$$x = 1.0$$

$$x = \frac{t_{lim}\Gamma}{t_{max}^*}$$

for ventilation controlled fire

for fuel controlled fire

A2 Temperature growth in the steel element (adopted from EN 1991-1-2)

For an equivalent uniform temperature distribution in the unprotected cross-section the increase in temperature during the time interval Δt (< 5.0 sec) can be determined using following expressions:

$$\Delta\theta_{a,t} = 0.9k_{sh} \frac{A_p/V}{c_a\rho_a} \dot{h}_{net,d} \Delta t$$

$$\dot{h}_{net,d} = 5.67 * 10^{-8} \phi \varepsilon_{res} \left[(\theta_g + 273)^4 - (\theta_m + 273)^4 \right] + \alpha_c (\theta_g - \theta_m)$$

, where:

k_{sh}	correction factor for shadow effect
A_p/V	section factor, m^{-1}
c_a	specific heat of steel, J/kgK
ρ_a	unit mass of steel, kg/m^3
$\dot{h}_{net,d}$	net heat flux per unit area, W/m^2
$5.67 * 10^{-8}$	Stephan Boltzmann constant
ϕ	geometrical configuration factor
ε_{res}	resultant emissivity
θ_g	gas temperature, $^{\circ}C$
θ_m	steel temperature, $^{\circ}C$

For an equivalent uniform temperature distribution in the protected cross-section the increase in temperature during the time interval Δt (< 5.0 sec) can be determined using following expressions:

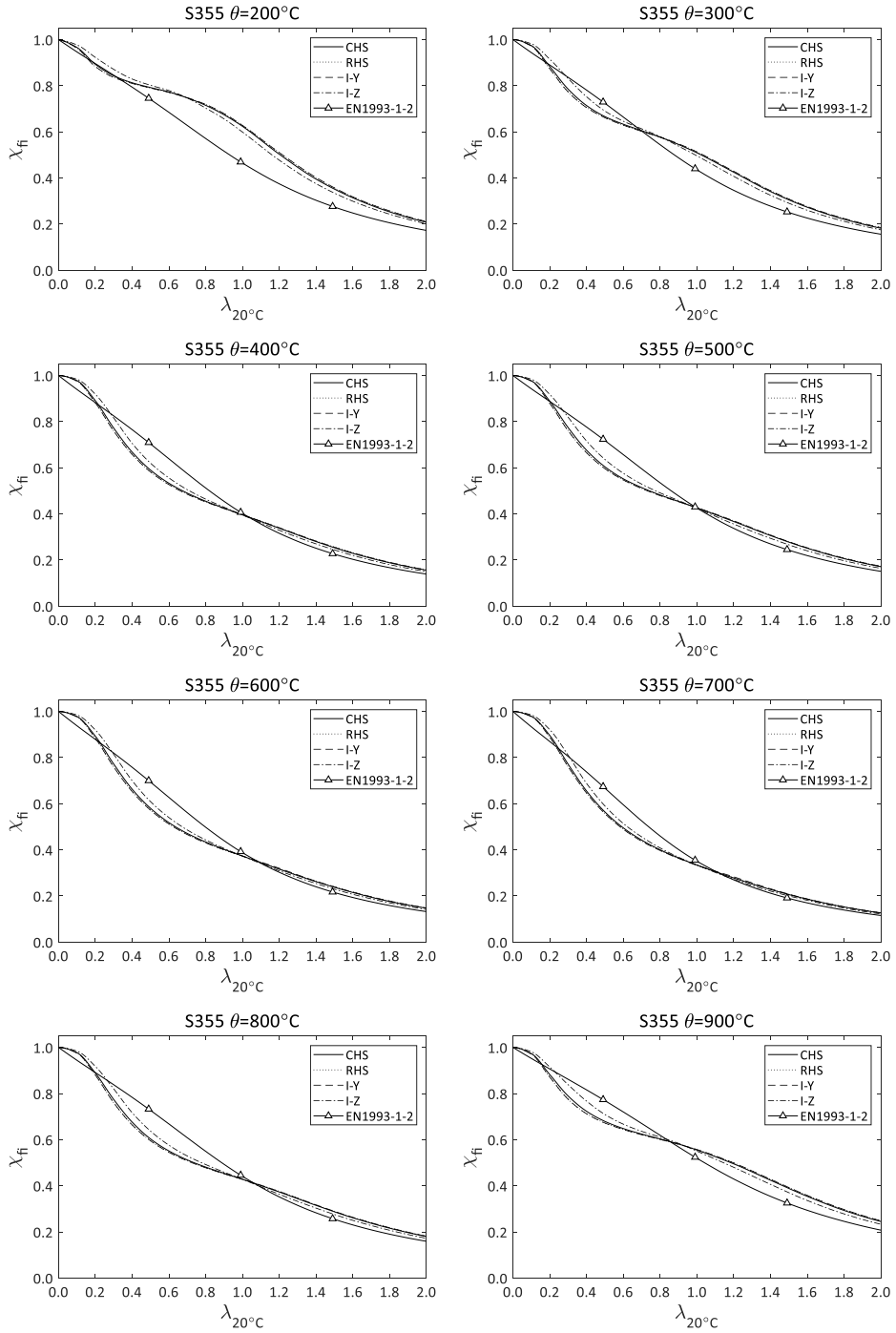
$$\Delta\theta_{a,t} = \frac{\lambda_p A_p/V}{d_p c_a \rho_a} \frac{(\theta_g - \theta_m)}{1 + \phi/3} \Delta t - e^{\phi/10} \Delta\theta_g$$

$$\phi = \frac{c_p \rho_p}{c_a \rho_a} d_p A_p/V$$

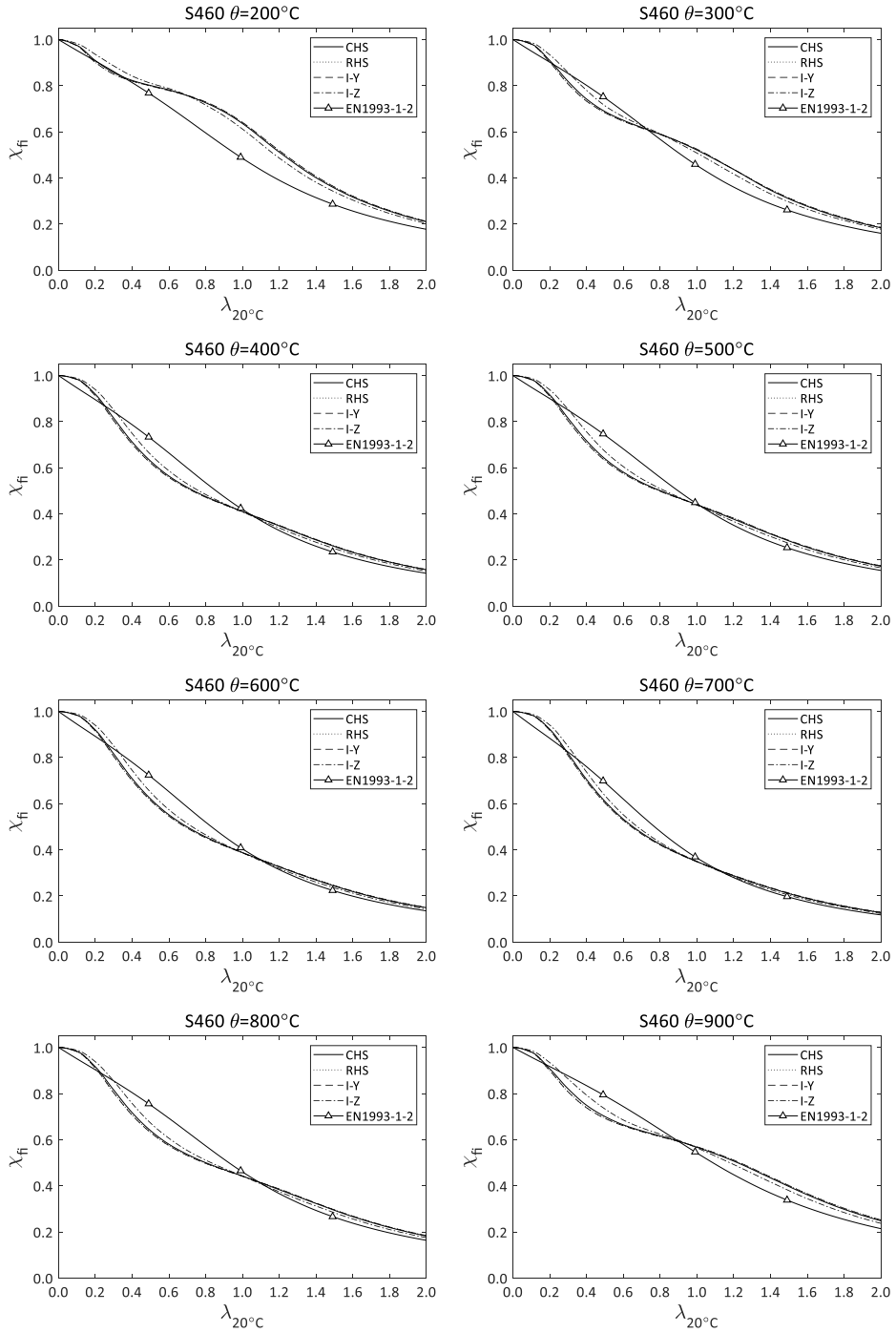
, where:

λ_p	thermal conductivity of the fire protection material, W/mK
A_p/V	insulated section factor, m^{-1}
ϕ	factor
d_p	thickness of the fire protection material, m
c_p	specific heat of fire protection material, J/kgK
ρ_p	unit mass of fire protection material, kg/m^3

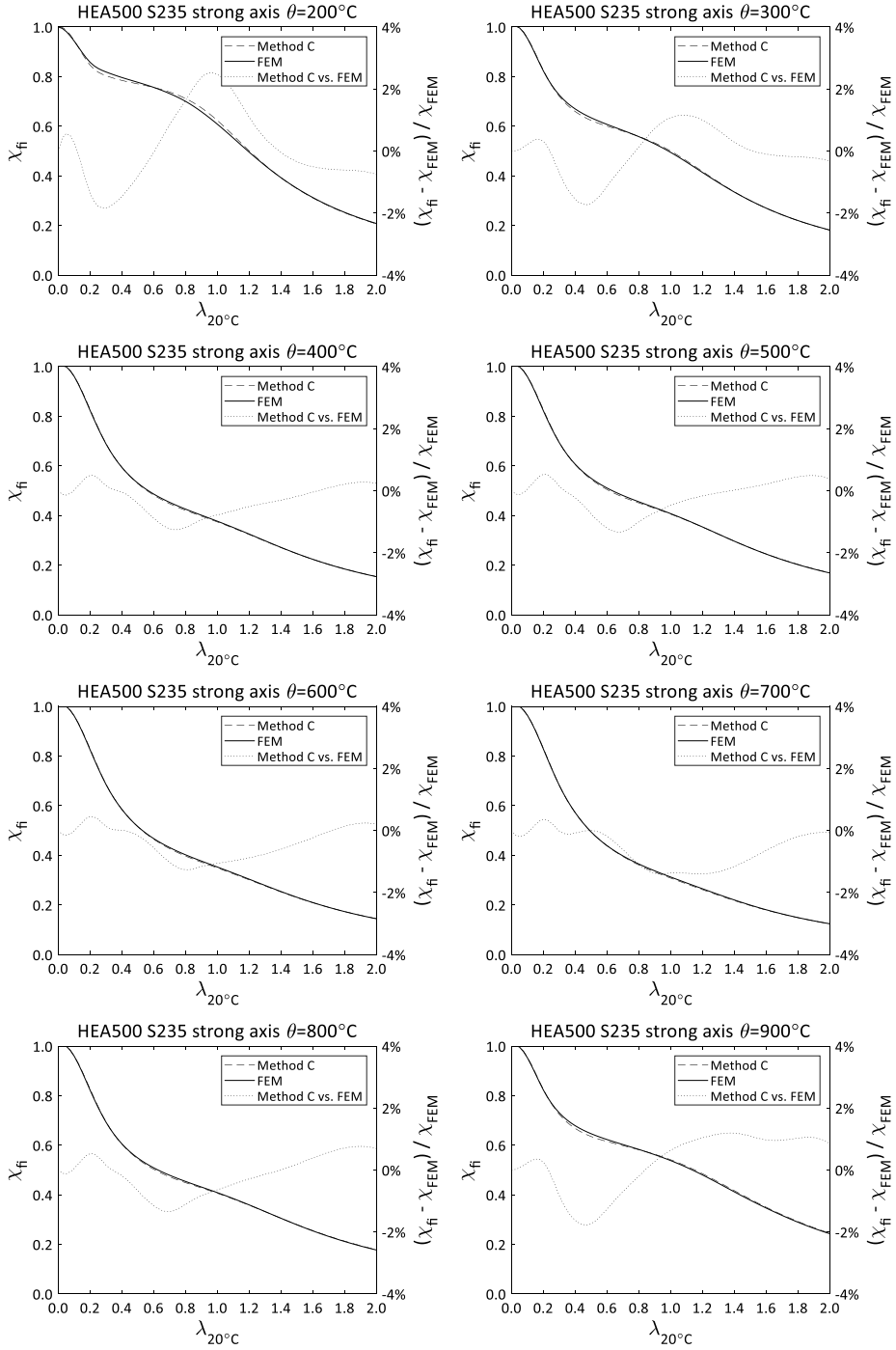
A3 Buckling factors according to modelling and EN 1993-1-2: S355



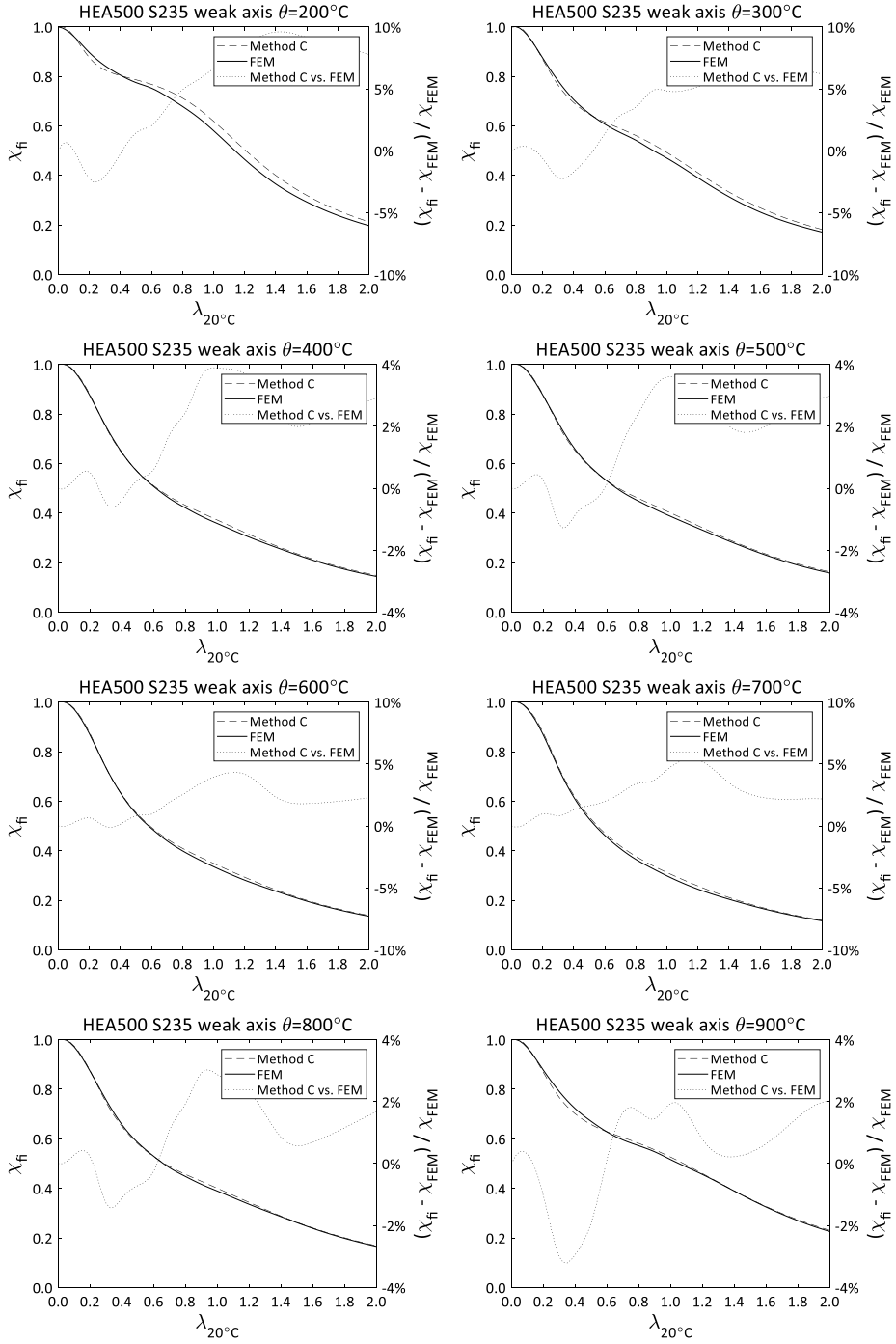
A4 Buckling factors according to modelling and EN 1993-1-2: S460



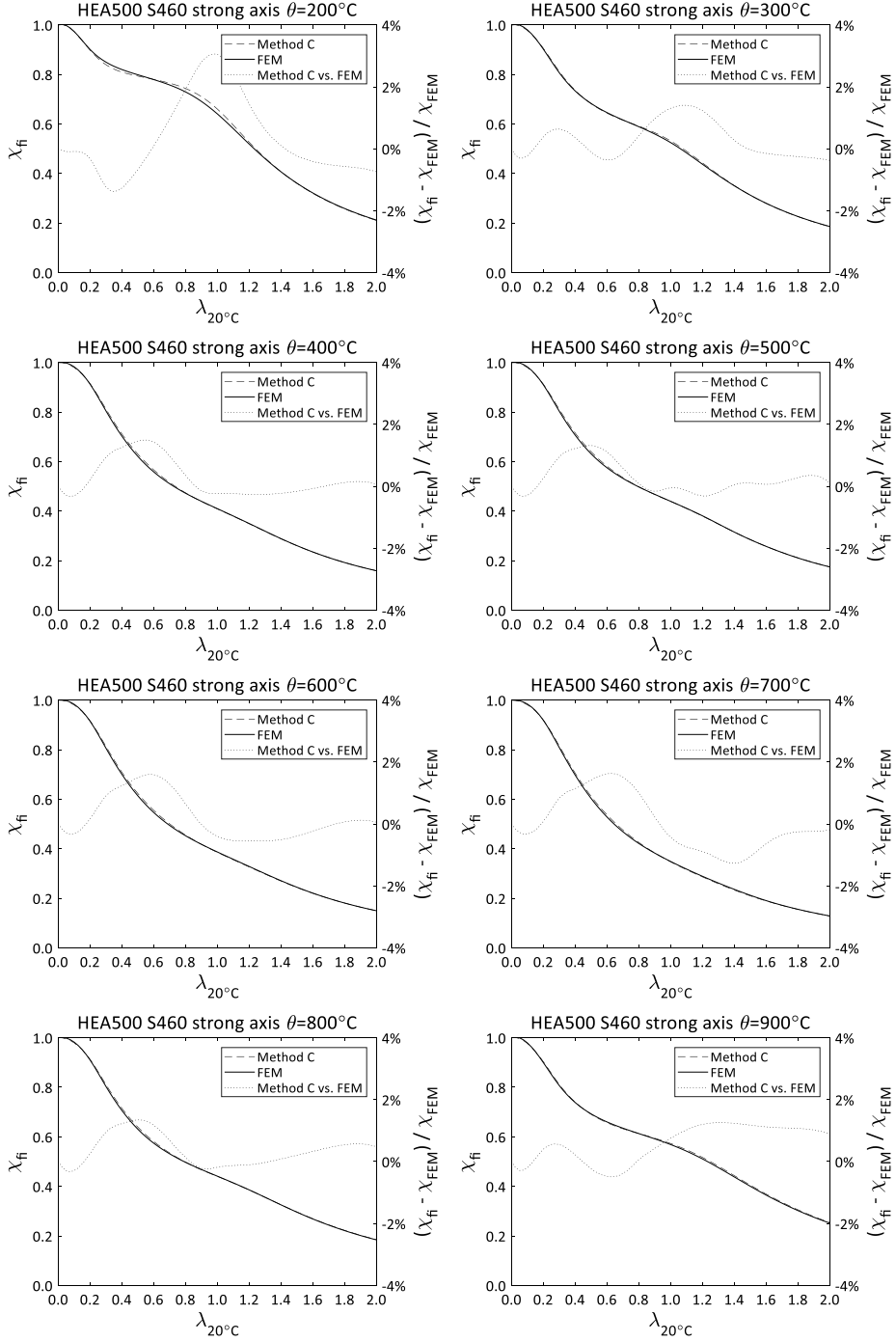
A5 Method C performance for the strong axis buckling and steel class S235



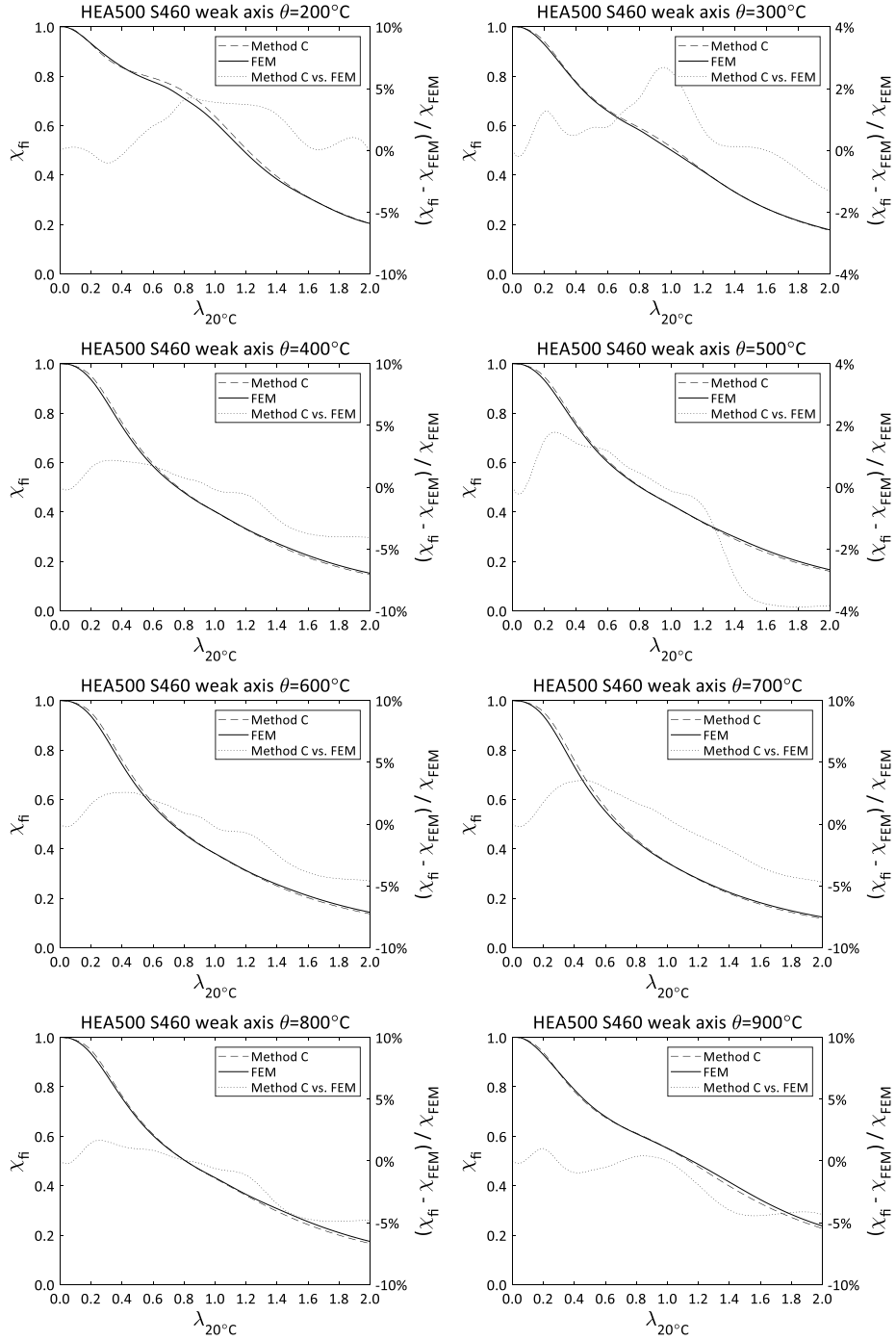
A6 Method C performance for the weak axis buckling and steel class S235



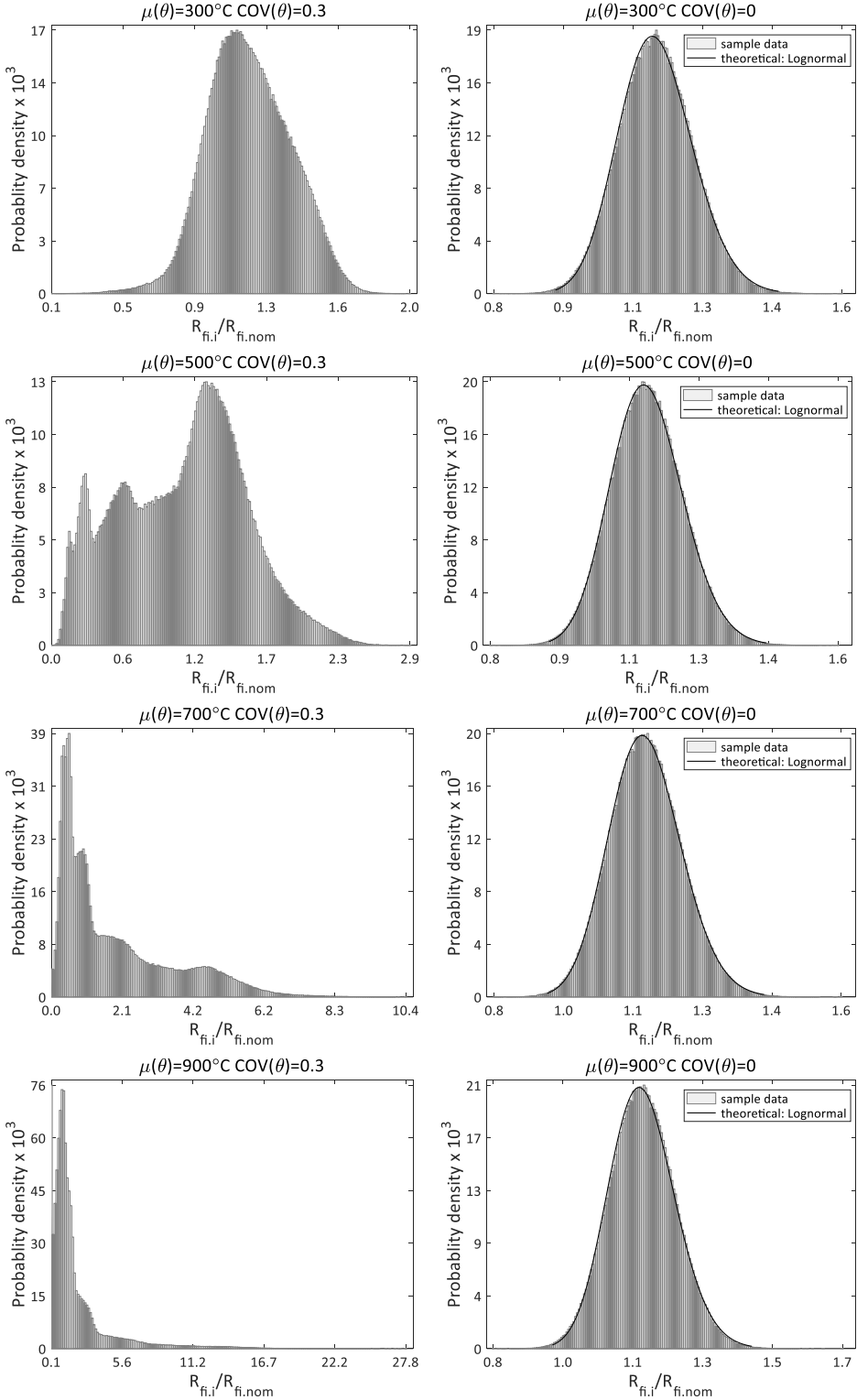
A7 Method C performance for the strong axis buckling and steel class S460



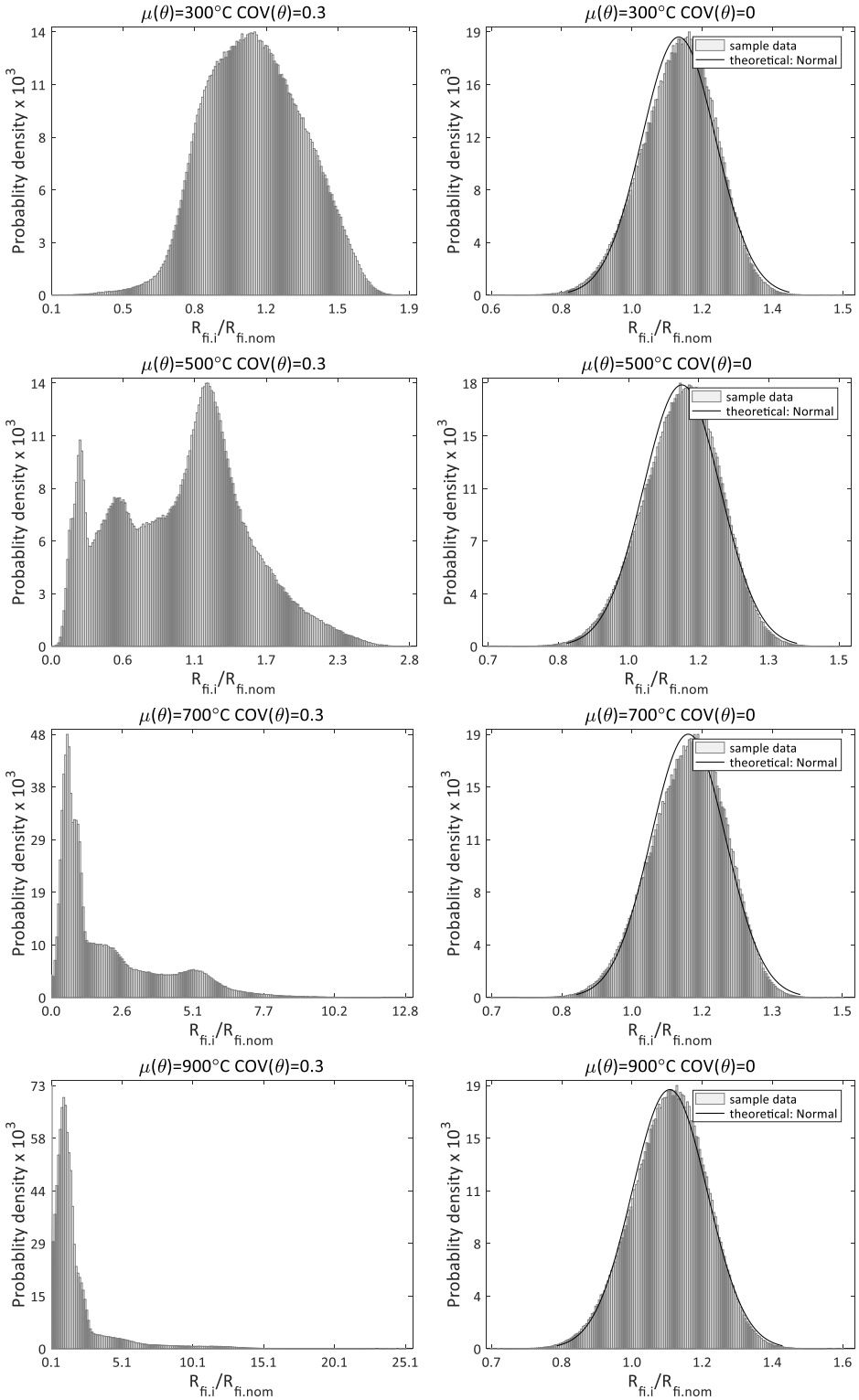
A8 Method C performance for the weak axis buckling and steel class S460



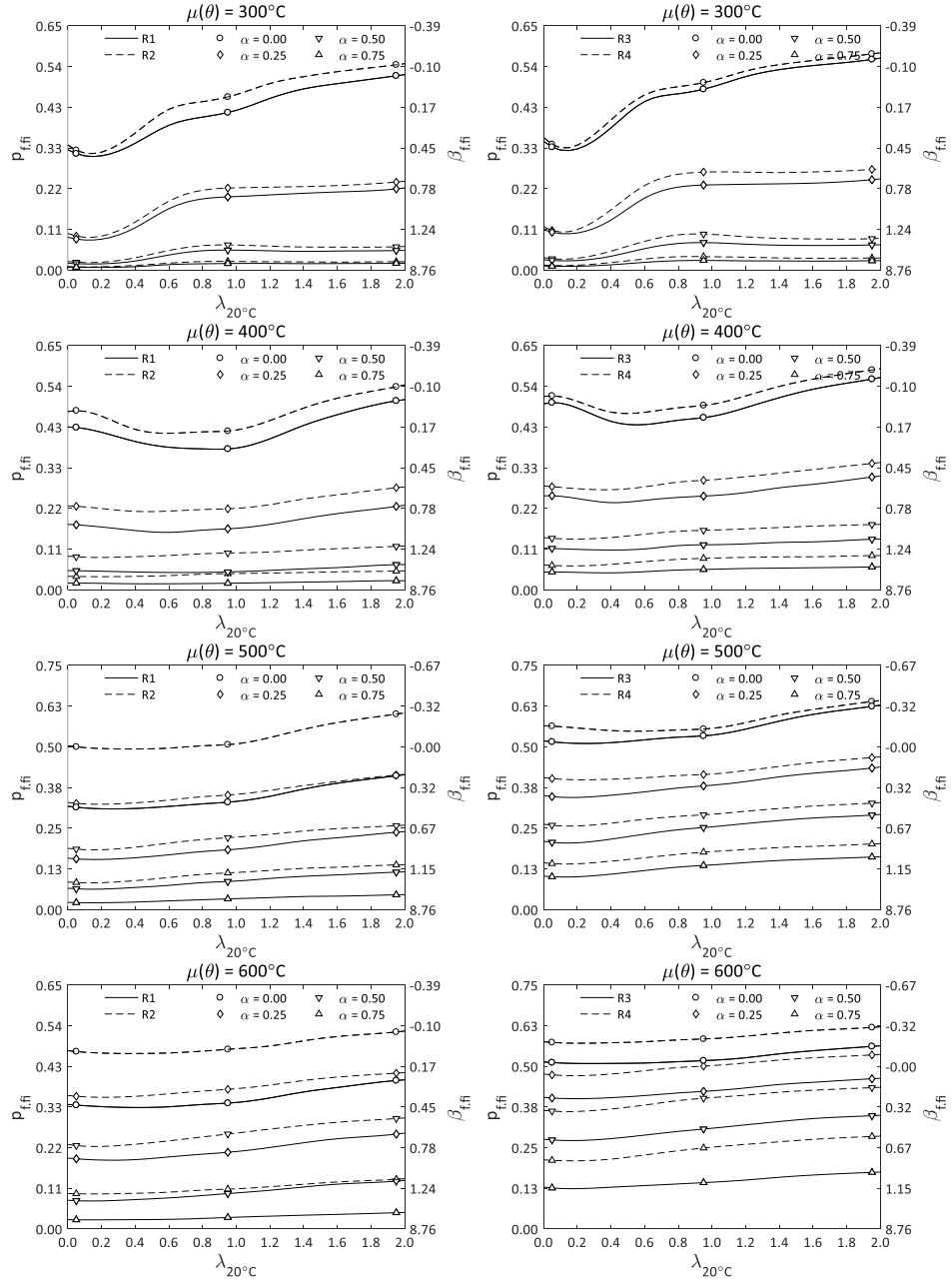
A9 Resistance function distributions for slenderness value $\lambda_{20^\circ\text{C}} = 0.5$

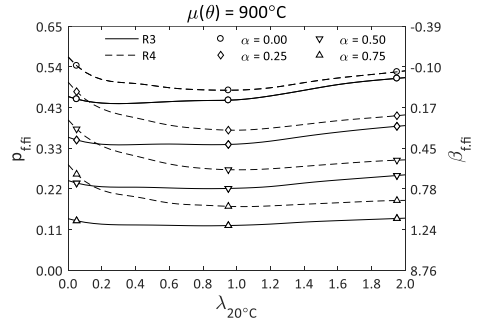
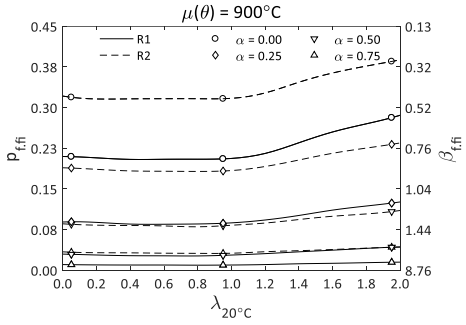
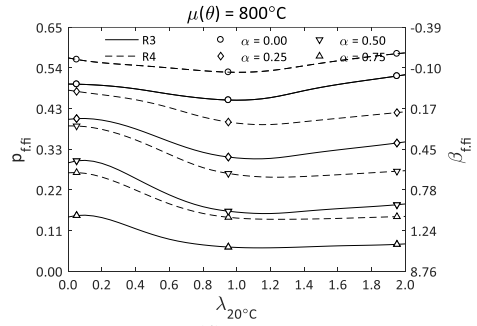
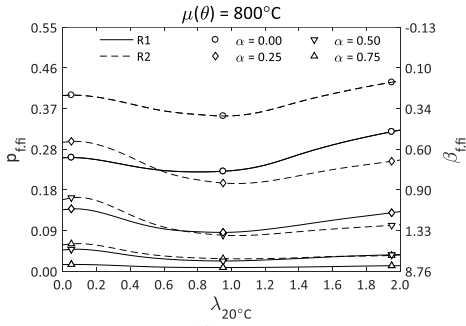
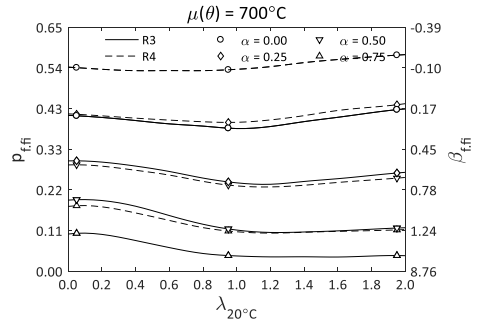
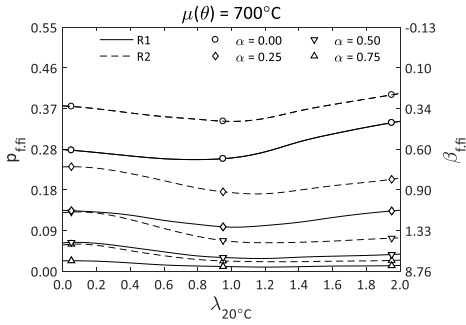


A10 Resistance function distributions for slenderness value $\lambda_{20^\circ\text{C}} = 1.0$

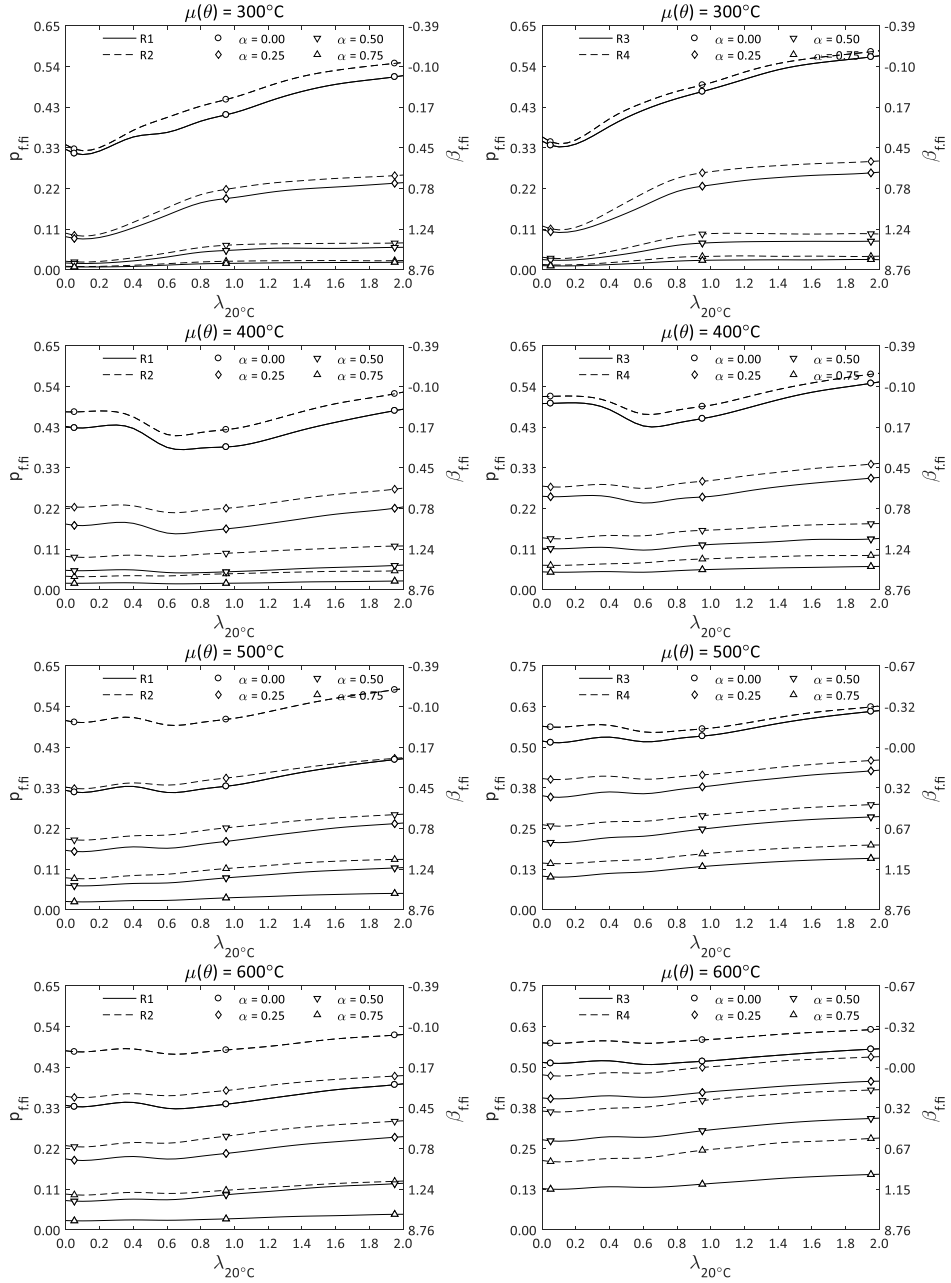


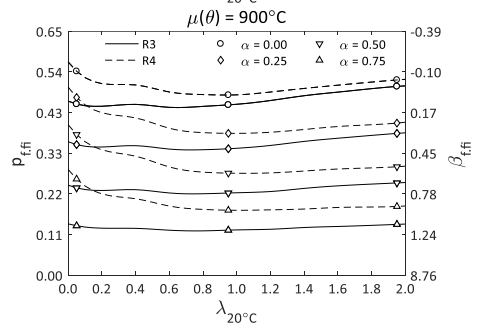
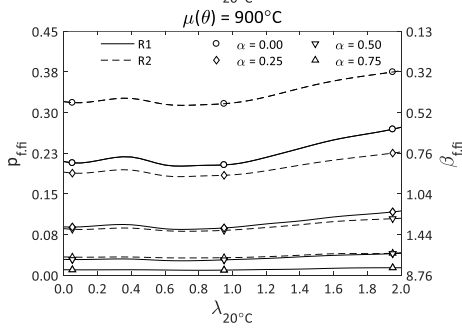
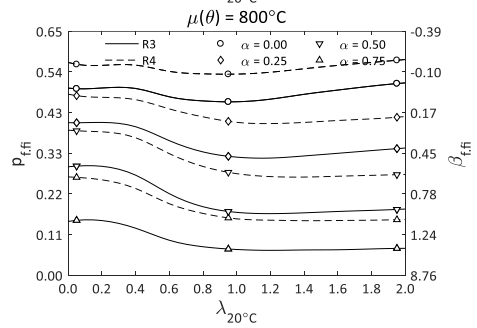
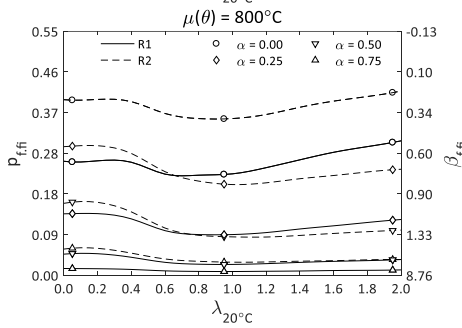
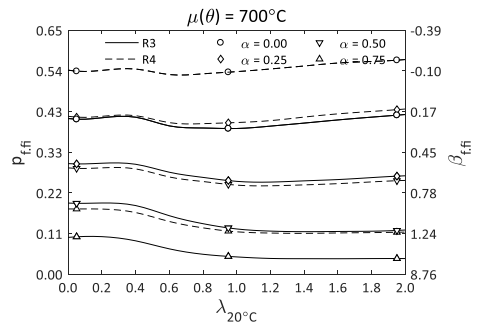
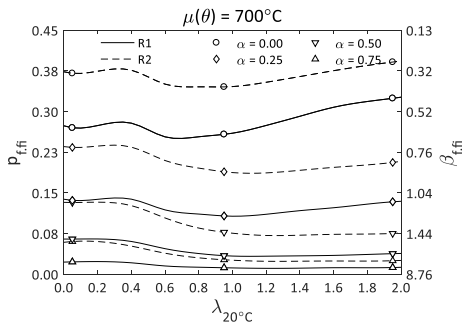
A11 Failure probability for S235 steel column strong axis and imposed (Q) variable load



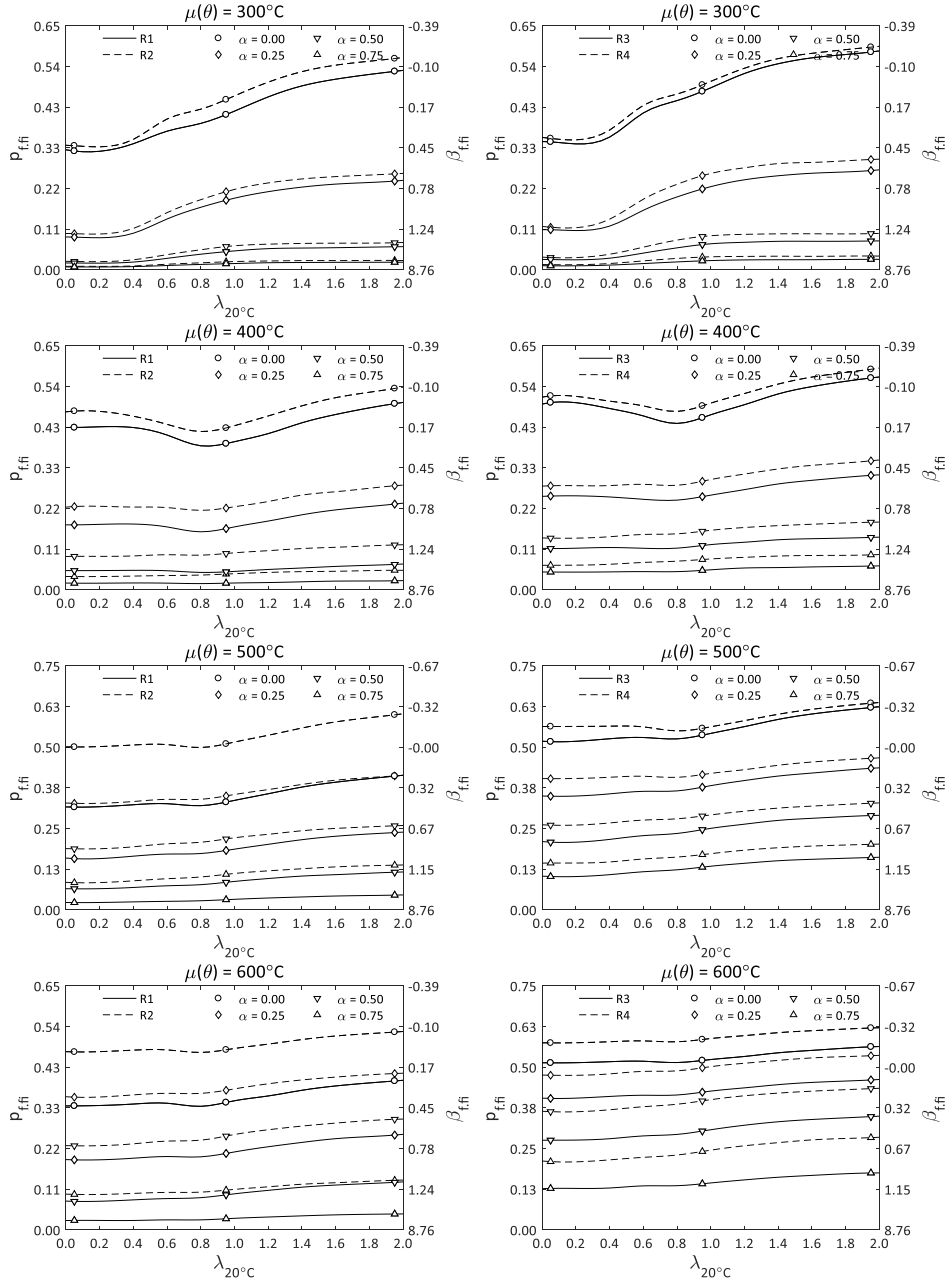


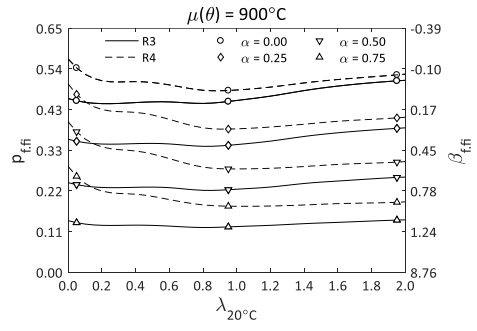
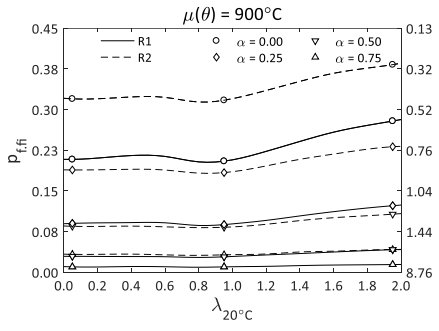
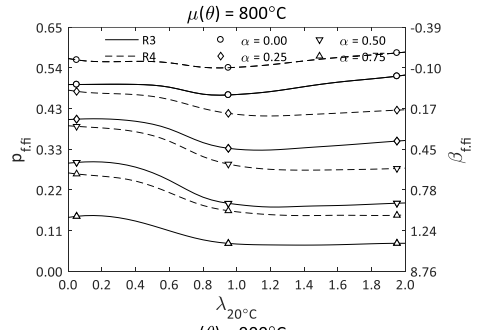
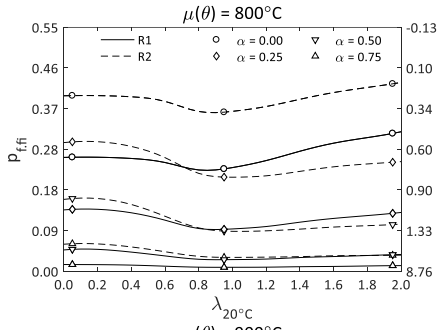
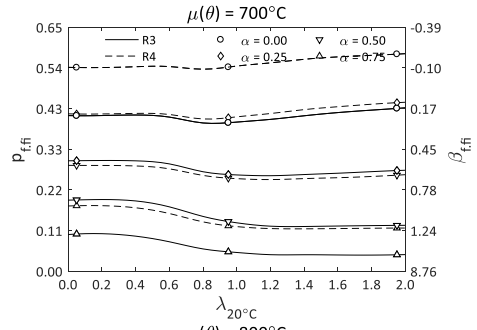
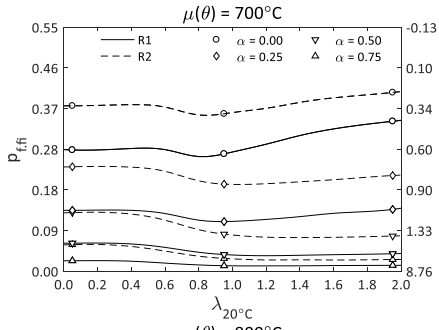
A12 Failure probability for S235 steel column weak axis and imposed (Q) variable load



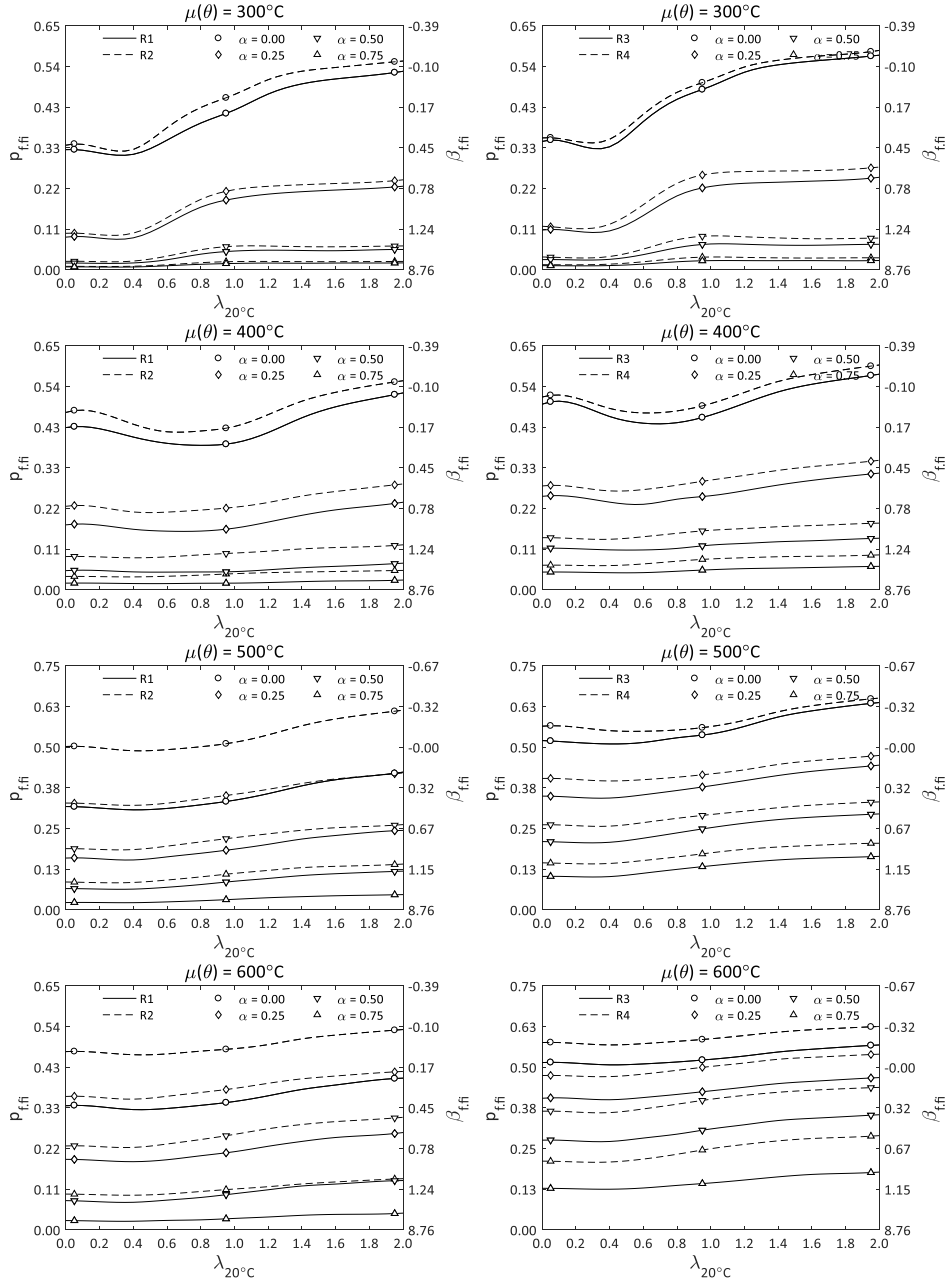


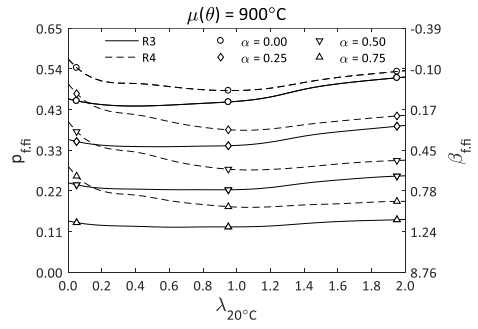
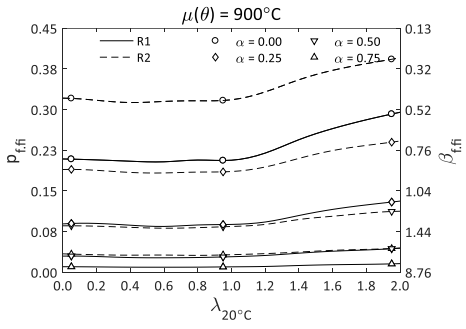
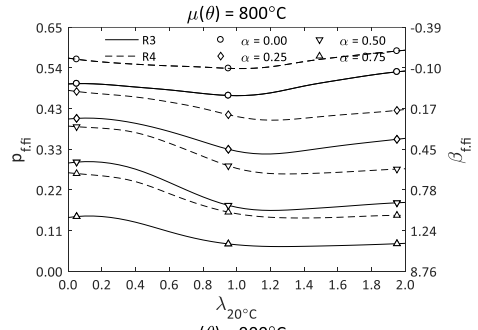
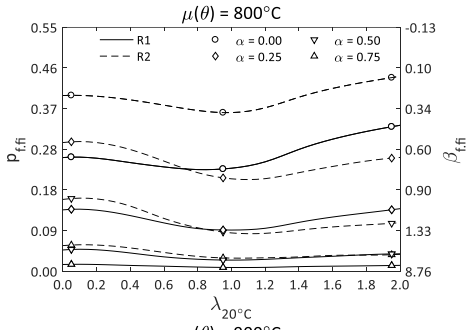
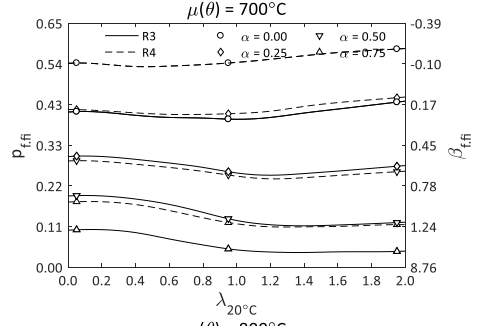
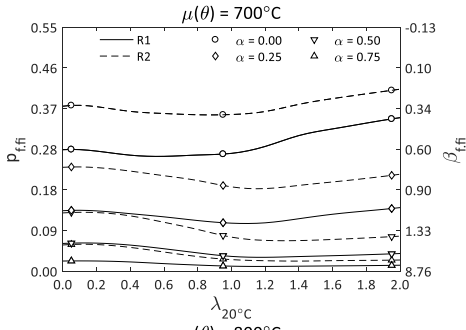
A13 Failure probability for S355 steel column weak axis and imposed (Q) variable load



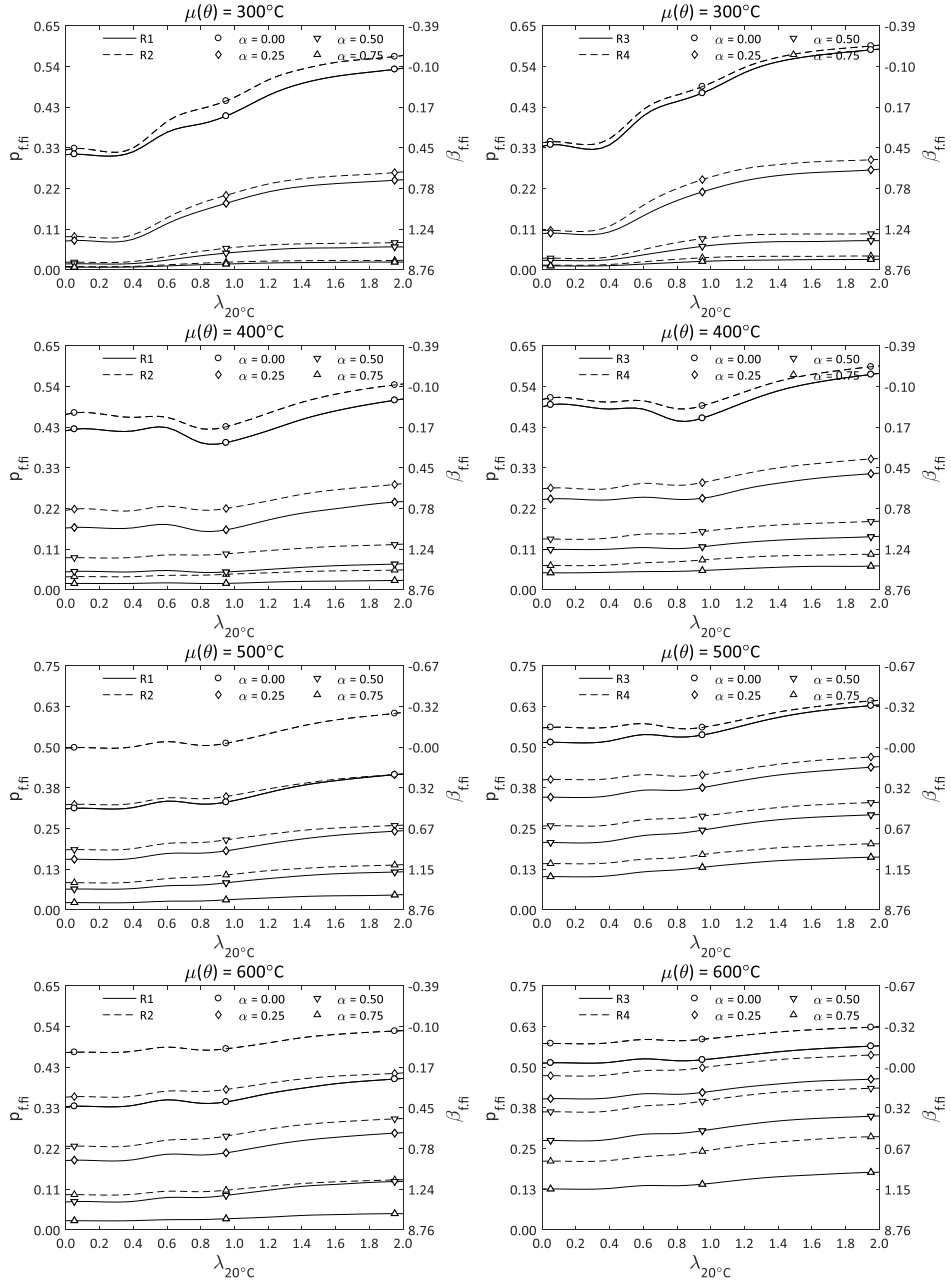


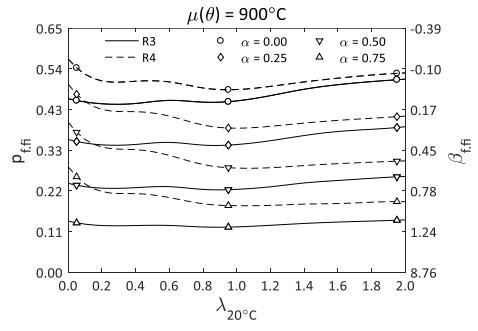
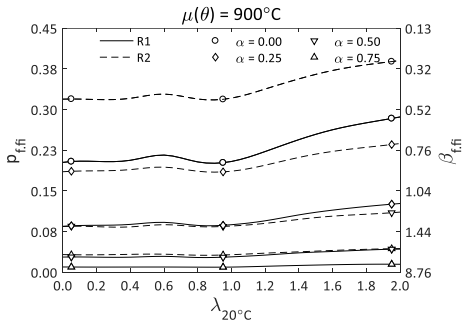
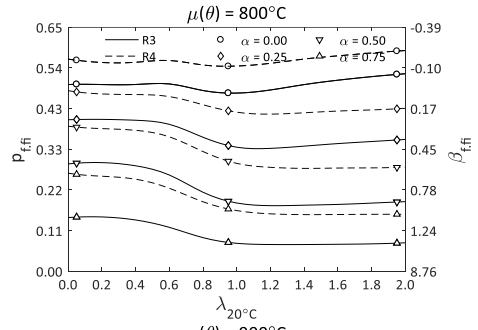
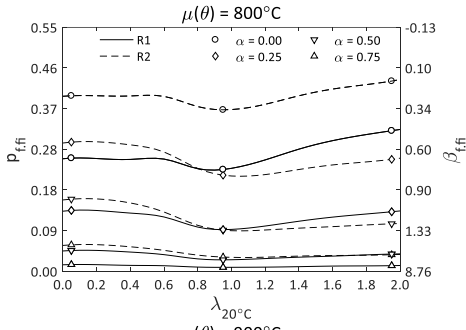
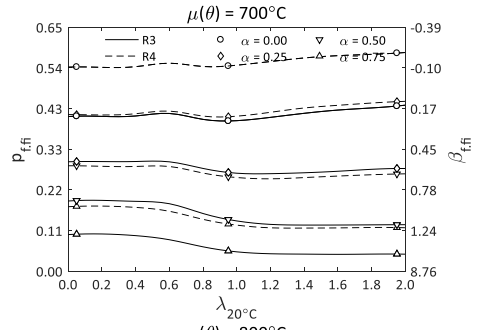
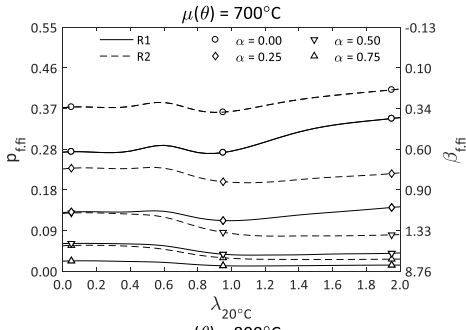
A14 Failure probability for S460 steel column strong axis and imposed (Q) variable load





A15 Failure probability for S460 steel column weak axis and imposed (Q) variable load





A16 Factor χ_{Rel} for S235 strong axis, imposed (Q) variable load type

		$\theta_{nom} = 300^{\circ}\text{C}$																	
$p_{f_{fi}} \rightarrow$	0.10	0.20	0.30	0.40	0.50	0.60	0.70	0.80	0.90	0.10	0.20	0.30	0.40	0.50	0.60	0.70	0.80	0.90	
$\beta_{f_{fi}} \rightarrow$	1.28	0.84	0.52	0.40	0.00	-0.25	-0.52	-0.84	-1.28	1.28	0.84	0.52	0.40	0.00	-0.25	-0.52	-0.84	-1.28	
$\delta_{of} \rightarrow$	1.15	1.02	0.94	0.88	0.82	0.77	0.72	0.67	0.60	1.15	1.02	0.94	0.88	0.82	0.77	0.72	0.67	0.60	
		$\alpha=0.00$									$\alpha=0.25$								
$\lambda_{20^{\circ}\text{C}}=0.00$	R1	0.814	0.906	0.977	1.000	1.000	1.000	1.000	1.000	1.000	0.881	0.982	1.000	1.000	1.000	1.000	1.000	1.000	
	R2	0.793	0.891	0.964	1.000	1.000	1.000	1.000	1.000	1.000	0.855	0.965	1.000	1.000	1.000	1.000	1.000	1.000	
	R3	0.782	0.884	0.959	1.000	1.000	1.000	1.000	1.000	1.000	0.845	0.956	1.000	1.000	1.000	1.000	1.000	1.000	
	R4	0.742	0.856	0.935	1.000	1.000	1.000	1.000	1.000	1.000	0.801	0.926	1.000	1.000	1.000	1.000	1.000	1.000	
$\lambda_{20^{\circ}\text{C}}=0.25$	R1	0.634	0.709	0.767	0.819	0.869	0.923	0.984	0.993	0.993	0.685	0.769	0.833	0.890	0.947	0.993	0.993	0.993	
	R2	0.617	0.696	0.757	0.808	0.859	0.914	0.976	0.993	0.993	0.666	0.754	0.821	0.879	0.936	0.993	0.993	0.993	
	R3	0.609	0.691	0.750	0.803	0.855	0.908	0.970	0.993	0.993	0.657	0.748	0.814	0.873	0.931	0.991	0.993	0.993	
	R4	0.576	0.667	0.731	0.787	0.840	0.895	0.957	0.993	0.993	0.622	0.722	0.793	0.855	0.915	0.978	0.993	0.993	
$\lambda_{20^{\circ}\text{C}}=0.50$	R1	0.473	0.536	0.587	0.637	0.685	0.735	0.792	0.865	0.951	0.511	0.580	0.638	0.692	0.745	0.800	0.864	0.951	
	R2	0.457	0.523	0.575	0.621	0.668	0.717	0.775	0.847	0.951	0.494	0.567	0.624	0.676	0.727	0.781	0.844	0.951	
	R3	0.448	0.515	0.566	0.609	0.653	0.702	0.757	0.827	0.951	0.484	0.558	0.614	0.663	0.710	0.765	0.826	0.903	
	R4	0.416	0.492	0.546	0.594	0.642	0.692	0.747	0.812	0.908	0.450	0.532	0.592	0.646	0.699	0.754	0.815	0.886	
$\lambda_{20^{\circ}\text{C}}=0.75$	R1	0.404	0.463	0.515	0.563	0.610	0.657	0.715	0.787	0.876	0.438	0.503	0.558	0.610	0.663	0.716	0.779	0.876	
	R2	0.387	0.450	0.500	0.546	0.591	0.640	0.696	0.765	0.876	0.420	0.488	0.545	0.595	0.643	0.696	0.758	0.876	
	R3	0.379	0.441	0.491	0.532	0.573	0.622	0.678	0.745	0.876	0.412	0.480	0.534	0.578	0.623	0.677	0.738	0.812	
	R4	0.350	0.417	0.469	0.517	0.563	0.612	0.664	0.726	0.876	0.379	0.454	0.512	0.563	0.613	0.666	0.724	0.793	
$\lambda_{20^{\circ}\text{C}}=1.00$	R1	0.347	0.397	0.440	0.481	0.522	0.561	0.608	0.725	0.725	0.375	0.430	0.478	0.523	0.567	0.611	0.725	0.725	
	R2	0.333	0.386	0.429	0.468	0.506	0.546	0.592	0.650	0.725	0.361	0.418	0.466	0.508	0.550	0.594	0.645	0.725	
	R3	0.327	0.379	0.420	0.455	0.490	0.531	0.578	0.633	0.725	0.354	0.411	0.456	0.495	0.533	0.577	0.630	0.725	
	R4	0.301	0.359	0.403	0.442	0.482	0.523	0.568	0.621	0.725	0.325	0.389	0.437	0.481	0.524	0.568	0.619	0.725	
$\lambda_{20^{\circ}\text{C}}=1.50$	R1	0.209	0.235	0.257	0.277	0.296	0.316	0.338	0.395	0.395	0.226	0.255	0.278	0.300	0.322	0.344	0.395	0.395	
	R2	0.202	0.230	0.252	0.272	0.290	0.310	0.332	0.360	0.395	0.218	0.250	0.274	0.295	0.316	0.338	0.362	0.395	
	R3	0.199	0.227	0.249	0.267	0.285	0.304	0.326	0.354	0.395	0.215	0.246	0.270	0.290	0.310	0.331	0.356	0.395	
	R4	0.185	0.218	0.241	0.261	0.281	0.301	0.323	0.350	0.395	0.200	0.236	0.262	0.284	0.305	0.327	0.352	0.395	
$\lambda_{20^{\circ}\text{C}}=2.00$	R1	0.125	0.140	0.152	0.164	0.175	0.186	0.199	0.215	0.232	0.135	0.152	0.165	0.178	0.190	0.203	0.217	0.232	
	R2	0.121	0.137	0.150	0.161	0.172	0.183	0.196	0.212	0.232	0.131	0.149	0.162	0.175	0.187	0.199	0.213	0.232	
	R3	0.119	0.136	0.148	0.159	0.169	0.180	0.193	0.209	0.232	0.129	0.147	0.161	0.172	0.184	0.196	0.210	0.232	
	R4	0.111	0.130	0.144	0.155	0.166	0.178	0.191	0.207	0.232	0.120	0.141	0.156	0.168	0.181	0.194	0.208	0.232	
		$\alpha=0.50$									$\alpha=0.75$								
$\lambda_{20^{\circ}\text{C}}=0.00$	R1	0.955	1.000	1.000	1.000	1.000	1.000	1.000	1.000	1.000	1.000	1.000	1.000	1.000	1.000	1.000	1.000	1.000	
	R2	0.930	1.000	1.000	1.000	1.000	1.000	1.000	1.000	1.000	1.000	1.000	1.000	1.000	1.000	1.000	1.000	1.000	
	R3	0.917	1.000	1.000	1.000	1.000	1.000	1.000	1.000	1.000	0.991	1.000	1.000	1.000	1.000	1.000	1.000	1.000	
	R4	0.872	1.000	1.000	1.000	1.000	1.000	1.000	1.000	1.000	0.947	1.000	1.000	1.000	1.000	1.000	1.000	1.000	
$\lambda_{20^{\circ}\text{C}}=0.25$	R1	0.745	0.853	0.937	0.993	0.993	0.993	0.993	0.993	0.993	0.803	0.979	0.993	0.993	0.993	0.993	0.993	0.993	
	R2	0.725	0.837	0.922	0.993	0.993	0.993	0.993	0.993	0.993	0.785	0.961	0.993	0.993	0.993	0.993	0.993	0.993	
	R3	0.715	0.829	0.915	0.991	0.993	0.993	0.993	0.993	0.993	0.775	0.952	0.993	0.993	0.993	0.993	0.993	0.993	
	R4	0.675	0.799	0.889	0.968	0.993	0.993	0.993	0.993	0.993	0.736	0.914	0.993	0.993	0.993	0.993	0.993	0.993	
$\lambda_{20^{\circ}\text{C}}=0.50$	R1	0.558	0.647	0.719	0.786	0.854	0.951	0.951	0.951	0.951	0.609	0.750	0.868	0.951	0.951	0.951	0.951	0.951	
	R2	0.540	0.631	0.702	0.768	0.831	0.901	0.951	0.951	0.951	0.591	0.730	0.848	0.951	0.951	0.951	0.951	0.951	
	R3	0.529	0.621	0.690	0.752	0.814	0.881	0.951	0.951	0.951	0.580	0.718	0.834	0.951	0.951	0.951	0.951	0.951	
	R4	0.493	0.590	0.666	0.733	0.799	0.868	0.951	0.951	0.951	0.541	0.684	0.804	0.915	0.951	0.951	0.951	0.951	
$\lambda_{20^{\circ}\text{C}}=0.75$	R1	0.482	0.562	0.629	0.694	0.758	0.876	0.876	0.876	0.876	0.529	0.657	0.765	0.876	0.876	0.876	0.876	0.876	
	R2	0.463	0.546	0.613	0.675	0.734	0.801	0.876	0.876	0.876	0.513	0.638	0.745	0.876	0.876	0.876	0.876	0.876	
	R3	0.452	0.536	0.601	0.657	0.713	0.779	0.876	0.876	0.876	0.500	0.625	0.729	0.876	0.876	0.876	0.876	0.876	
	R4	0.415	0.507	0.576	0.638	0.700	0.765	0.876	0.876	0.876	0.462	0.591	0.697	0.797	0.876	0.876	0.876	0.876	
$\lambda_{20^{\circ}\text{C}}=1.00$	R1	0.413	0.480	0.537	0.592	0.648	0.725	0.725	0.725	0.725	0.452	0.561	0.652	0.725	0.725	0.725	0.725	0.725	
	R2	0.396	0.467	0.525	0.577	0.627	0.725	0.725	0.725	0.725	0.437	0.545	0.636	0.725	0.725	0.725	0.725	0.725	
	R3	0.388	0.458	0.514	0.562	0.610	0.725	0.725	0.725	0.725	0.427	0.534	0.623	0.725	0.725	0.725	0.725	0.725	
	R4	0.358	0.434	0.492	0.545	0.598	0.654	0.725	0.725	0.725	0.396	0.505	0.595	0.725	0.725	0.725	0.725	0.725	
$\lambda_{20^{\circ}\text{C}}=1.50$	R1	0.246	0.284	0.313	0.341	0.395	0.395	0.395	0.395	0.395	0.268	0.327	0.395	0.395	0.395	0.395	0.395	0.395	
	R2	0.239	0.277	0.307	0.334	0.361	0.395	0.395	0.395	0.395	0.259	0.320	0.395	0.395	0.395	0.395	0.395	0.395	
	R3	0.234	0.274	0.303	0.330	0.355	0.395	0.395	0.395	0.395	0.256	0.316	0.365	0.395	0.395	0.395	0.395	0.395	
	R4	0.218	0.262	0.293	0.321	0.348	0.395	0.395	0.395	0.395	0.239	0.301	0.352	0.395	0.395	0.395	0.395	0.395	
$\lambda_{20^{\circ}\text{C}}=2.00$	R1	0.147	0.168	0.186	0.202	0.217	0.232	0.232	0.232	0.232	0.159	0.194	0.232	0.232	0.232	0.232	0.232	0.232	
	R2	0.142	0.165	0.183	0.199	0.214	0.232	0.232	0.232	0.232	0.155	0.190	0.232	0.232	0.232	0.232	0.232	0.232	
	R3	0.141	0.163	0.180	0.196	0.211	0.232	0.232	0.232	0.232	0.152	0.188	0.217	0.232	0.232	0.232	0.232	0.232	
	R4	0.131	0.156	0.175	0.191	0.207	0.232	0.232	0.232	0.232	0.142	0.179	0.209	0.232	0.232	0.232	0.232	0.232	

$\theta_{\text{nom}} = 400^{\circ}\text{C}$

$p_{f,fi} \rightarrow$	0.10	0.20	0.30	0.40	0.50	0.60	0.70	0.80	0.90	0.10	0.20	0.30	0.40	0.50	0.60	0.70	0.80	0.90
$\beta_{f,fi} \rightarrow$	1.28	0.84	0.52	0.40	0.00	-0.25	-0.52	-0.84	-1.28	1.28	0.84	0.52	0.40	0.00	-0.25	-0.52	-0.84	-1.28
$\delta_{af} \rightarrow$	1.15	1.02	0.94	0.88	0.82	0.77	0.72	0.67	0.60	1.15	1.02	0.94	0.88	0.82	0.77	0.72	0.67	0.60
	$\alpha=0.00$									$\alpha=0.25$								
$\lambda_{20^{\circ}\text{C}}=0.00$	R1	0.756	0.854	0.927	0.992	1.000	1.000	1.000	1.000	0.818	0.924	1.000	1.000	1.000	1.000	1.000	1.000	1.000
	R2	0.616	0.742	0.831	0.909	0.984	1.000	1.000	1.000	0.666	0.805	0.901	0.987	1.000	1.000	1.000	1.000	1.000
	R3	0.579	0.726	0.823	0.903	0.975	1.000	1.000	1.000	0.627	0.786	0.892	0.980	1.000	1.000	1.000	1.000	1.000
	R4	0.521	0.680	0.788	0.876	0.954	1.000	1.000	1.000	0.565	0.736	0.855	0.950	1.000	1.000	1.000	1.000	1.000
$\lambda_{20^{\circ}\text{C}}=0.25$	R1	0.584	0.660	0.718	0.769	0.820	0.873	0.934	0.993	0.632	0.715	0.779	0.836	0.892	0.952	0.993	0.993	0.993
	R2	0.475	0.574	0.644	0.705	0.763	0.822	0.887	0.967	0.516	0.622	0.699	0.765	0.830	0.896	0.969	0.993	0.993
	R3	0.447	0.561	0.636	0.699	0.757	0.815	0.880	0.959	0.484	0.607	0.689	0.759	0.823	0.888	0.959	0.993	0.993
	R4	0.401	0.526	0.609	0.678	0.739	0.801	0.868	0.949	0.435	0.568	0.661	0.736	0.805	0.872	0.948	0.993	0.993
$\lambda_{20^{\circ}\text{C}}=0.50$	R1	0.414	0.470	0.513	0.552	0.590	0.630	0.676	0.737	0.448	0.509	0.556	0.599	0.641	0.686	0.737	0.803	0.907
	R2	0.331	0.404	0.456	0.504	0.547	0.591	0.640	0.702	0.358	0.437	0.495	0.546	0.594	0.643	0.698	0.766	0.872
	R3	0.308	0.395	0.451	0.497	0.540	0.583	0.632	0.691	0.334	0.427	0.488	0.539	0.587	0.635	0.689	0.754	0.853
	R4	0.274	0.368	0.431	0.483	0.530	0.574	0.622	0.680	0.297	0.398	0.467	0.524	0.576	0.624	0.677	0.742	0.837
$\lambda_{20^{\circ}\text{C}}=0.75$	R1	0.348	0.396	0.434	0.468	0.502	0.539	0.580	0.637	0.377	0.430	0.471	0.509	0.547	0.587	0.633	0.695	0.798
	R2	0.274	0.338	0.384	0.426	0.465	0.502	0.546	0.605	0.296	0.367	0.417	0.463	0.505	0.547	0.596	0.660	0.764
	R3	0.253	0.330	0.380	0.419	0.457	0.495	0.539	0.592	0.275	0.358	0.412	0.455	0.497	0.539	0.588	0.647	0.737
	R4	0.221	0.306	0.363	0.408	0.449	0.486	0.529	0.580	0.239	0.331	0.393	0.443	0.488	0.529	0.576	0.633	0.721
$\lambda_{20^{\circ}\text{C}}=1.00$	R1	0.298	0.340	0.372	0.401	0.430	0.462	0.498	0.545	0.323	0.368	0.403	0.435	0.468	0.502	0.542	0.595	0.725
	R2	0.234	0.291	0.330	0.365	0.398	0.430	0.468	0.518	0.254	0.314	0.358	0.396	0.433	0.469	0.510	0.565	0.653
	R3	0.215	0.283	0.325	0.359	0.391	0.423	0.462	0.507	0.233	0.307	0.353	0.390	0.426	0.461	0.504	0.554	0.630
	R4	0.188	0.263	0.311	0.350	0.384	0.417	0.452	0.497	0.203	0.284	0.337	0.380	0.418	0.453	0.493	0.541	0.616
$\lambda_{20^{\circ}\text{C}}=1.50$	R1	0.185	0.209	0.227	0.244	0.260	0.277	0.297	0.321	0.200	0.226	0.247	0.265	0.283	0.302	0.324	0.350	0.395
	R2	0.147	0.181	0.204	0.224	0.244	0.261	0.282	0.307	0.159	0.196	0.221	0.244	0.265	0.285	0.307	0.335	0.395
	R3	0.135	0.176	0.201	0.221	0.240	0.258	0.279	0.304	0.146	0.191	0.219	0.240	0.261	0.281	0.304	0.332	0.395
	R4	0.116	0.164	0.192	0.215	0.236	0.255	0.275	0.299	0.127	0.177	0.209	0.234	0.257	0.277	0.299	0.327	0.395
$\lambda_{20^{\circ}\text{C}}=2.00$	R1	0.111	0.126	0.136	0.146	0.156	0.166	0.177	0.191	0.120	0.136	0.148	0.159	0.169	0.180	0.193	0.208	0.232
	R2	0.089	0.109	0.123	0.135	0.146	0.157	0.169	0.183	0.096	0.118	0.133	0.146	0.159	0.171	0.184	0.200	0.232
	R3	0.081	0.106	0.121	0.133	0.144	0.155	0.167	0.181	0.088	0.115	0.132	0.144	0.157	0.169	0.182	0.198	0.232
	R4	0.071	0.099	0.116	0.130	0.142	0.153	0.165	0.179	0.077	0.107	0.126	0.141	0.154	0.166	0.179	0.195	0.232
	$\alpha=0.50$									$\alpha=0.75$								
$\lambda_{20^{\circ}\text{C}}=0.00$	R1	0.891	1.000	1.000	1.000	1.000	1.000	1.000	1.000	0.968	1.000	1.000	1.000	1.000	1.000	1.000	1.000	1.000
	R2	0.732	0.893	1.000	1.000	1.000	1.000	1.000	1.000	0.815	1.000	1.000	1.000	1.000	1.000	1.000	1.000	1.000
	R3	0.692	0.872	0.997	1.000	1.000	1.000	1.000	1.000	0.777	1.000	1.000	1.000	1.000	1.000	1.000	1.000	1.000
	R4	0.625	0.818	0.954	1.000	1.000	1.000	1.000	1.000	0.711	0.944	1.000	1.000	1.000	1.000	1.000	1.000	1.000
$\lambda_{20^{\circ}\text{C}}=0.25$	R1	0.687	0.793	0.875	0.950	0.993	0.993	0.993	0.993	0.747	0.916	0.993	0.993	0.993	0.993	0.993	0.993	0.993
	R2	0.566	0.690	0.782	0.865	0.944	0.993	0.993	0.993	0.627	0.796	0.936	0.993	0.993	0.993	0.993	0.993	0.993
	R3	0.536	0.673	0.771	0.856	0.937	0.993	0.993	0.993	0.599	0.775	0.922	0.993	0.993	0.993	0.993	0.993	0.993
	R4	0.483	0.632	0.738	0.829	0.914	0.993	0.993	0.993	0.549	0.731	0.879	0.993	0.993	0.993	0.993	0.993	0.993
$\lambda_{20^{\circ}\text{C}}=0.50$	R1	0.489	0.565	0.625	0.679	0.733	0.791	0.856	0.951	0.534	0.655	0.757	0.853	0.951	0.951	0.951	0.951	0.951
	R2	0.394	0.486	0.554	0.617	0.679	0.739	0.807	0.893	0.440	0.562	0.663	0.763	0.864	0.951	0.951	0.951	0.951
	R3	0.369	0.474	0.547	0.609	0.668	0.728	0.797	0.880	0.419	0.549	0.655	0.752	0.850	0.951	0.951	0.951	0.951
	R4	0.330	0.441	0.522	0.590	0.654	0.717	0.785	0.866	0.380	0.513	0.623	0.726	0.830	0.951	0.951	0.951	0.951
$\lambda_{20^{\circ}\text{C}}=0.75$	R1	0.412	0.478	0.531	0.579	0.626	0.677	0.735	0.811	0.451	0.555	0.643	0.726	0.811	0.876	0.876	0.876	0.876
	R2	0.326	0.407	0.468	0.524	0.577	0.629	0.690	0.769	0.365	0.472	0.560	0.650	0.738	0.876	0.876	0.876	0.876
	R3	0.304	0.397	0.462	0.515	0.567	0.620	0.681	0.755	0.346	0.461	0.553	0.639	0.723	0.816	0.876	0.876	0.876
	R4	0.268	0.368	0.440	0.500	0.556	0.609	0.668	0.740	0.310	0.430	0.525	0.616	0.708	0.799	0.876	0.876	0.876
$\lambda_{20^{\circ}\text{C}}=1.00$	R1	0.353	0.410	0.454	0.495	0.536	0.579	0.629	0.725	0.387	0.477	0.552	0.622	0.725	0.725	0.725	0.725	0.725
	R2	0.279	0.349	0.401	0.449	0.495	0.538	0.590	0.725	0.313	0.405	0.480	0.555	0.631	0.725	0.725	0.725	0.725
	R3	0.259	0.341	0.396	0.441	0.486	0.530	0.583	0.645	0.295	0.394	0.473	0.546	0.619	0.725	0.725	0.725	0.725
	R4	0.227	0.315	0.377	0.429	0.476	0.522	0.571	0.632	0.263	0.366	0.449	0.527	0.604	0.725	0.725	0.725	0.725
$\lambda_{20^{\circ}\text{C}}=1.50$	R1	0.218	0.252	0.277	0.301	0.324	0.349	0.395	0.395	0.237	0.290	0.334	0.395	0.395	0.395	0.395	0.395	0.395
	R2	0.174	0.217	0.247	0.275	0.302	0.328	0.356	0.395	0.193	0.249	0.295	0.338	0.395	0.395	0.395	0.395	0.395
	R3	0.161	0.212	0.244	0.271	0.297	0.323	0.352	0.395	0.183	0.243	0.291	0.335	0.395	0.395	0.395	0.395	0.395
	R4	0.142	0.196	0.233	0.263	0.291	0.319	0.347	0.395	0.163	0.226	0.276	0.322	0.395	0.395	0.395	0.395	0.395
$\lambda_{20^{\circ}\text{C}}=2.00$	R1	0.131	0.151	0.167	0.180	0.194	0.208	0.232	0.232	0.143	0.174	0.201	0.232	0.232	0.232	0.232	0.232	0.232
	R2	0.105	0.131	0.148	0.165	0.180	0.197	0.213	0.232	0.117	0.150	0.177	0.202	0.232	0.232	0.232	0.232	0.232
	R3	0.097	0.128	0.147	0.163	0.178	0.194	0.210	0.232	0.110	0.146	0.175	0.201	0.232	0.232	0.232	0.232	0.232
	R4	0.086	0.118	0.140	0.158	0.175	0.191	0.208	0.232	0.099	0.135	0.165	0.193	0.232	0.232	0.232	0.232	0.232

$\theta_{\text{nom}} = 500^{\circ}\text{C}$

$p_{f,fi} \rightarrow$	0.10	0.20	0.30	0.40	0.50	0.60	0.70	0.80	0.90	0.10	0.20	0.30	0.40	0.50	0.60	0.70	0.80	0.90
$\beta_{f,fi} \rightarrow$	1.28	0.84	0.52	0.40	0.00	-0.25	-0.52	-0.84	-1.28	1.28	0.84	0.52	0.40	0.00	-0.25	-0.52	-0.84	-1.28
$\delta_{af} \rightarrow$	1.15	1.02	0.94	0.88	0.82	0.77	0.72	0.67	0.60	1.15	1.02	0.94	0.88	0.82	0.77	0.72	0.67	0.60
	$\alpha=0.00$									$\alpha=0.25$								
$\lambda_{20^{\circ}\text{C}}=0.00$	R1	0.420	0.525	0.611	0.692	0.783	0.869	0.961	1.000	1.000	0.456	0.570	0.662	0.752	0.851	0.946	1.000	1.000
	R2	0.329	0.457	0.572	0.665	0.751	0.835	0.926	1.000	1.000	0.357	0.496	0.621	0.722	0.816	0.908	1.000	1.000
	R3	0.276	0.398	0.507	0.612	0.715	0.809	0.912	1.000	1.000	0.298	0.433	0.552	0.665	0.776	0.879	0.992	1.000
	R4	0.216	0.318	0.439	0.557	0.671	0.784	0.897	1.000	1.000	0.236	0.347	0.477	0.605	0.730	0.852	0.975	1.000
$\lambda_{20^{\circ}\text{C}}=0.25$	R1	0.325	0.406	0.471	0.535	0.603	0.673	0.746	0.834	0.958	0.352	0.440	0.512	0.580	0.654	0.732	0.813	0.910
	R2	0.254	0.353	0.441	0.515	0.581	0.646	0.717	0.806	0.935	0.276	0.383	0.478	0.559	0.631	0.704	0.782	0.879
	R3	0.213	0.308	0.392	0.474	0.552	0.628	0.707	0.799	0.928	0.230	0.334	0.426	0.513	0.599	0.682	0.769	0.871
	R4	0.167	0.246	0.340	0.430	0.518	0.607	0.694	0.788	0.914	0.182	0.268	0.368	0.467	0.564	0.659	0.754	0.859
$\lambda_{20^{\circ}\text{C}}=0.50$	R1	0.218	0.277	0.325	0.372	0.422	0.472	0.526	0.588	0.679	0.236	0.300	0.353	0.403	0.458	0.513	0.572	0.640
	R2	0.167	0.237	0.302	0.356	0.405	0.452	0.504	0.568	0.662	0.181	0.257	0.328	0.387	0.440	0.491	0.548	0.618
	R3	0.139	0.205	0.265	0.326	0.384	0.439	0.496	0.562	0.649	0.151	0.222	0.288	0.353	0.417	0.477	0.540	0.613
	R4	0.109	0.162	0.227	0.293	0.359	0.424	0.488	0.552	0.637	0.120	0.176	0.247	0.318	0.390	0.461	0.531	0.602
$\lambda_{20^{\circ}\text{C}}=0.75$	R1	0.173	0.223	0.266	0.308	0.354	0.397	0.442	0.494	0.578	0.187	0.242	0.289	0.335	0.385	0.431	0.481	0.539
	R2	0.130	0.188	0.245	0.294	0.338	0.379	0.423	0.478	0.561	0.141	0.205	0.266	0.319	0.367	0.412	0.460	0.521
	R3	0.107	0.161	0.212	0.266	0.319	0.366	0.417	0.473	0.546	0.116	0.175	0.231	0.289	0.347	0.399	0.453	0.516
	R4	0.085	0.125	0.179	0.236	0.297	0.354	0.410	0.465	0.534	0.092	0.136	0.195	0.257	0.322	0.385	0.446	0.507
$\lambda_{20^{\circ}\text{C}}=1.00$	R1	0.144	0.189	0.227	0.264	0.304	0.341	0.380	0.425	0.495	0.157	0.205	0.246	0.287	0.330	0.371	0.414	0.462
	R2	0.107	0.158	0.208	0.252	0.290	0.326	0.363	0.411	0.481	0.116	0.172	0.226	0.273	0.315	0.354	0.395	0.447
	R3	0.087	0.134	0.179	0.226	0.274	0.315	0.358	0.406	0.468	0.096	0.145	0.194	0.246	0.298	0.342	0.390	0.443
	R4	0.071	0.103	0.150	0.201	0.254	0.304	0.352	0.400	0.458	0.076	0.112	0.163	0.218	0.276	0.331	0.383	0.435
$\lambda_{20^{\circ}\text{C}}=1.50$	R1	0.090	0.118	0.142	0.165	0.190	0.212	0.235	0.262	0.299	0.098	0.128	0.154	0.179	0.206	0.230	0.255	0.285
	R2	0.066	0.098	0.130	0.157	0.181	0.203	0.226	0.254	0.293	0.072	0.107	0.141	0.171	0.197	0.221	0.246	0.276
	R3	0.054	0.083	0.112	0.141	0.171	0.196	0.222	0.251	0.288	0.059	0.090	0.121	0.154	0.186	0.213	0.242	0.273
	R4	0.044	0.063	0.093	0.125	0.158	0.190	0.219	0.247	0.283	0.047	0.069	0.101	0.136	0.172	0.206	0.238	0.269
$\lambda_{20^{\circ}\text{C}}=2.00$	R1	0.054	0.071	0.086	0.100	0.114	0.128	0.141	0.157	0.180	0.059	0.077	0.093	0.108	0.124	0.139	0.154	0.172
	R2	0.040	0.060	0.079	0.095	0.109	0.122	0.136	0.152	0.176	0.043	0.065	0.085	0.103	0.119	0.133	0.148	0.166
	R3	0.033	0.050	0.068	0.086	0.103	0.118	0.134	0.151	0.174	0.036	0.055	0.073	0.093	0.112	0.129	0.146	0.164
	R4	0.026	0.038	0.056	0.076	0.096	0.114	0.132	0.149	0.171	0.029	0.042	0.061	0.082	0.104	0.124	0.143	0.162
	$\alpha=0.50$									$\alpha=0.75$								
$\lambda_{20^{\circ}\text{C}}=0.00$	R1	0.506	0.637	0.746	0.848	0.962	1.000	1.000	1.000	1.000	0.580	0.754	0.904	1.000	1.000	1.000	1.000	1.000
	R2	0.400	0.557	0.697	0.815	0.926	1.000	1.000	1.000	1.000	0.474	0.667	0.845	1.000	1.000	1.000	1.000	1.000
	R3	0.337	0.486	0.622	0.750	0.879	1.000	1.000	1.000	1.000	0.408	0.587	0.757	0.923	1.000	1.000	1.000	1.000
	R4	0.267	0.392	0.538	0.684	0.825	0.967	1.000	1.000	1.000	0.323	0.486	0.657	0.841	1.000	1.000	1.000	1.000
$\lambda_{20^{\circ}\text{C}}=0.25$	R1	0.390	0.492	0.576	0.656	0.741	0.837	0.934	0.993	0.993	0.447	0.581	0.696	0.810	0.934	0.993	0.993	0.993
	R2	0.309	0.430	0.538	0.632	0.716	0.803	0.899	0.993	0.993	0.368	0.516	0.651	0.779	0.901	0.993	0.993	0.993
	R3	0.260	0.375	0.480	0.580	0.678	0.778	0.883	0.993	0.993	0.314	0.451	0.583	0.712	0.847	0.993	0.993	0.993
	R4	0.206	0.303	0.416	0.529	0.637	0.747	0.863	0.993	0.993	0.251	0.375	0.509	0.648	0.792	0.945	0.993	0.993
$\lambda_{20^{\circ}\text{C}}=0.50$	R1	0.263	0.336	0.396	0.455	0.520	0.586	0.657	0.742	0.869	0.303	0.398	0.480	0.560	0.649	0.751	0.868	0.951
	R2	0.204	0.290	0.369	0.436	0.499	0.561	0.629	0.715	0.844	0.244	0.348	0.447	0.537	0.626	0.723	0.832	0.951
	R3	0.170	0.250	0.325	0.399	0.472	0.542	0.618	0.708	0.832	0.208	0.303	0.396	0.489	0.586	0.689	0.807	0.951
	R4	0.135	0.199	0.278	0.360	0.441	0.521	0.606	0.697	0.815	0.165	0.248	0.341	0.441	0.545	0.658	0.785	0.951
$\lambda_{20^{\circ}\text{C}}=0.75$	R1	0.209	0.272	0.325	0.378	0.436	0.493	0.554	0.626	0.738	0.242	0.324	0.394	0.463	0.541	0.631	0.733	0.876
	R2	0.158	0.230	0.301	0.360	0.416	0.470	0.529	0.604	0.717	0.191	0.279	0.364	0.443	0.521	0.603	0.698	0.876
	R3	0.131	0.197	0.261	0.326	0.391	0.453	0.520	0.597	0.702	0.161	0.239	0.319	0.400	0.485	0.575	0.678	0.809
	R4	0.105	0.154	0.220	0.291	0.364	0.437	0.510	0.587	0.686	0.129	0.194	0.271	0.359	0.449	0.547	0.659	0.794
$\lambda_{20^{\circ}\text{C}}=1.00$	R1	0.175	0.230	0.277	0.323	0.374	0.422	0.474	0.538	0.632	0.204	0.275	0.336	0.396	0.463	0.541	0.627	0.725
	R2	0.131	0.193	0.255	0.308	0.356	0.403	0.454	0.518	0.615	0.159	0.235	0.310	0.378	0.444	0.516	0.598	0.725
	R3	0.108	0.164	0.220	0.278	0.335	0.389	0.446	0.513	0.601	0.133	0.200	0.269	0.340	0.413	0.493	0.580	0.725
	R4	0.086	0.127	0.185	0.246	0.311	0.374	0.438	0.504	0.589	0.106	0.160	0.228	0.304	0.383	0.468	0.565	0.725
$\lambda_{20^{\circ}\text{C}}=1.50$	R1	0.109	0.144	0.173	0.202	0.233	0.262	0.293	0.331	0.395	0.127	0.171	0.209	0.246	0.288	0.335	0.395	0.395
	R2	0.081	0.120	0.159	0.192	0.222	0.251	0.282	0.320	0.395	0.098	0.146	0.193	0.235	0.277	0.320	0.395	0.395
	R3	0.067	0.101	0.137	0.173	0.209	0.241	0.277	0.316	0.395	0.083	0.124	0.168	0.211	0.257	0.306	0.359	0.395
	R4	0.054	0.078	0.115	0.153	0.193	0.232	0.271	0.312	0.363	0.066	0.099	0.141	0.189	0.238	0.290	0.349	0.395
$\lambda_{20^{\circ}\text{C}}=2.00$	R1	0.066	0.087	0.105	0.122	0.140	0.158	0.177	0.200	0.232	0.077	0.103	0.127	0.149	0.174	0.202	0.232	0.232
	R2	0.049	0.073	0.096	0.116	0.134	0.152	0.170	0.192	0.232	0.059	0.088	0.116	0.142	0.167	0.194	0.232	0.232
	R3	0.040	0.061	0.083	0.105	0.126	0.146	0.167	0.190	0.232	0.050	0.075	0.102	0.128	0.155	0.184	0.216	0.232
	R4	0.033	0.048	0.070	0.093	0.117	0.141	0.163	0.188	0.232	0.040	0.060	0.085	0.114	0.144	0.175	0.210	0.232

$\theta_{\text{nom}} = 600^{\circ}\text{C}$

$p_{f,fi} \rightarrow$	0.10	0.20	0.30	0.40	0.50	0.60	0.70	0.80	0.90	0.10	0.20	0.30	0.40	0.50	0.60	0.70	0.80	0.90	
$\beta_{f,fi} \rightarrow$	1.28	0.84	0.52	0.40	0.00	-0.25	-0.52	-0.84	-1.28	1.28	0.84	0.52	0.40	0.00	-0.25	-0.52	-0.84	-1.28	
$\delta_{of} \rightarrow$	1.15	1.02	0.94	0.88	0.82	0.77	0.72	0.67	0.60	1.15	1.02	0.94	0.88	0.82	0.77	0.72	0.67	0.60	
	$\alpha=0.00$									$\alpha=0.25$									
$\lambda_{20^{\circ}\text{C}}=0.00$	R1	0.372	0.475	0.558	0.637	0.716	0.799	0.891	0.999	1.000	0.402	0.516	0.606	0.692	0.779	0.868	0.969	1.000	1.000
	R2	0.210	0.270	0.333	0.404	0.480	0.559	0.661	0.783	0.971	0.227	0.293	0.362	0.440	0.521	0.609	0.718	0.852	1.000
	R3	0.194	0.250	0.312	0.385	0.462	0.541	0.629	0.752	0.931	0.210	0.272	0.339	0.418	0.503	0.590	0.685	0.817	1.000
	R4	0.147	0.204	0.252	0.315	0.396	0.488	0.603	0.725	0.876	0.159	0.221	0.274	0.343	0.431	0.531	0.656	0.790	0.957
$\lambda_{20^{\circ}\text{C}}=0.25$	R1	0.287	0.367	0.431	0.493	0.554	0.619	0.690	0.775	0.900	0.310	0.398	0.468	0.534	0.602	0.673	0.751	0.845	0.982
	R2	0.162	0.208	0.258	0.313	0.371	0.434	0.511	0.606	0.753	0.176	0.226	0.279	0.339	0.404	0.473	0.555	0.659	0.821
	R3	0.149	0.193	0.241	0.297	0.357	0.417	0.489	0.579	0.723	0.162	0.210	0.262	0.323	0.388	0.454	0.532	0.631	0.788
	R4	0.113	0.157	0.195	0.244	0.306	0.377	0.464	0.561	0.682	0.124	0.171	0.212	0.265	0.332	0.410	0.505	0.611	0.745
$\lambda_{20^{\circ}\text{C}}=0.50$	R1	0.190	0.247	0.294	0.339	0.385	0.432	0.483	0.543	0.629	0.206	0.268	0.319	0.368	0.418	0.470	0.525	0.592	0.686
	R2	0.106	0.136	0.169	0.208	0.248	0.293	0.349	0.421	0.526	0.115	0.147	0.184	0.226	0.270	0.319	0.379	0.458	0.573
	R3	0.098	0.126	0.158	0.197	0.239	0.282	0.333	0.402	0.504	0.106	0.137	0.171	0.214	0.259	0.307	0.362	0.438	0.550
	R4	0.077	0.104	0.127	0.159	0.203	0.253	0.318	0.386	0.474	0.084	0.112	0.138	0.173	0.220	0.275	0.345	0.421	0.516
$\lambda_{20^{\circ}\text{C}}=0.75$	R1	0.149	0.198	0.239	0.279	0.320	0.362	0.406	0.458	0.530	0.162	0.214	0.259	0.303	0.348	0.393	0.441	0.498	0.579
	R2	0.082	0.105	0.131	0.163	0.198	0.236	0.288	0.352	0.443	0.089	0.114	0.142	0.177	0.215	0.257	0.313	0.383	0.483
	R3	0.076	0.097	0.122	0.154	0.189	0.227	0.270	0.335	0.423	0.083	0.105	0.132	0.167	0.206	0.247	0.294	0.364	0.462
	R4	0.062	0.081	0.098	0.123	0.158	0.202	0.258	0.320	0.397	0.067	0.087	0.107	0.134	0.172	0.219	0.281	0.349	0.433
$\lambda_{20^{\circ}\text{C}}=1.00$	R1	0.124	0.166	0.202	0.238	0.274	0.310	0.348	0.392	0.454	0.135	0.180	0.219	0.258	0.298	0.337	0.379	0.427	0.495
	R2	0.067	0.086	0.108	0.136	0.166	0.199	0.245	0.301	0.380	0.073	0.093	0.118	0.147	0.180	0.217	0.266	0.327	0.414
	R3	0.063	0.080	0.100	0.128	0.158	0.191	0.230	0.286	0.363	0.068	0.086	0.109	0.139	0.172	0.208	0.250	0.312	0.396
	R4	0.052	0.067	0.081	0.101	0.132	0.169	0.219	0.273	0.340	0.057	0.072	0.088	0.110	0.143	0.184	0.238	0.297	0.371
$\lambda_{20^{\circ}\text{C}}=1.50$	R1	0.077	0.103	0.126	0.149	0.171	0.194	0.217	0.243	0.280	0.083	0.112	0.137	0.161	0.186	0.211	0.236	0.266	0.306
	R2	0.042	0.053	0.067	0.084	0.103	0.124	0.153	0.188	0.236	0.045	0.057	0.073	0.091	0.112	0.135	0.166	0.204	0.257
	R3	0.039	0.049	0.062	0.079	0.098	0.119	0.143	0.179	0.227	0.042	0.053	0.067	0.086	0.107	0.129	0.156	0.194	0.247
	R4	0.033	0.041	0.050	0.062	0.082	0.105	0.136	0.170	0.212	0.036	0.045	0.054	0.068	0.089	0.114	0.148	0.185	0.231
$\lambda_{20^{\circ}\text{C}}=2.00$	R1	0.047	0.063	0.076	0.090	0.103	0.117	0.131	0.147	0.168	0.051	0.068	0.083	0.098	0.112	0.127	0.142	0.160	0.184
	R2	0.025	0.032	0.040	0.051	0.062	0.075	0.092	0.114	0.143	0.027	0.035	0.044	0.055	0.068	0.082	0.100	0.123	0.155
	R3	0.024	0.030	0.037	0.048	0.060	0.072	0.087	0.108	0.137	0.026	0.032	0.041	0.052	0.065	0.078	0.094	0.117	0.148
	R4	0.020	0.025	0.030	0.038	0.049	0.063	0.083	0.103	0.128	0.022	0.027	0.033	0.041	0.054	0.069	0.090	0.112	0.139
	$\alpha=0.50$									$\alpha=0.75$									
$\lambda_{20^{\circ}\text{C}}=0.00$	R1	0.449	0.579	0.683	0.783	0.885	0.993	1.000	1.000	1.000	0.524	0.690	0.833	0.974	1.000	1.000	1.000	1.000	1.000
	R2	0.255	0.331	0.410	0.498	0.594	0.696	0.823	0.978	1.000	0.299	0.407	0.510	0.623	0.750	0.896	1.000	1.000	1.000
	R3	0.234	0.309	0.386	0.475	0.572	0.673	0.786	0.938	1.000	0.276	0.382	0.483	0.594	0.722	0.865	1.000	1.000	1.000
	R4	0.178	0.249	0.313	0.391	0.490	0.605	0.749	0.910	1.000	0.206	0.305	0.397	0.499	0.621	0.770	0.962	1.000	1.000
$\lambda_{20^{\circ}\text{C}}=0.25$	R1	0.346	0.447	0.528	0.605	0.685	0.768	0.863	0.981	0.993	0.403	0.533	0.644	0.753	0.868	0.993	0.993	0.993	0.993
	R2	0.196	0.256	0.316	0.385	0.459	0.539	0.635	0.758	0.951	0.231	0.314	0.394	0.481	0.579	0.690	0.822	0.993	0.993
	R3	0.181	0.238	0.298	0.366	0.441	0.519	0.609	0.726	0.916	0.212	0.295	0.373	0.459	0.557	0.667	0.797	0.967	0.993
	R4	0.137	0.192	0.242	0.302	0.378	0.467	0.577	0.704	0.868	0.160	0.235	0.307	0.385	0.480	0.596	0.743	0.939	0.993
$\lambda_{20^{\circ}\text{C}}=0.50$	R1	0.230	0.301	0.360	0.416	0.474	0.535	0.603	0.686	0.804	0.270	0.361	0.440	0.517	0.599	0.690	0.796	0.951	0.951
	R2	0.129	0.167	0.209	0.256	0.307	0.364	0.436	0.526	0.664	0.152	0.207	0.260	0.321	0.389	0.467	0.564	0.695	0.906
	R3	0.119	0.156	0.195	0.243	0.295	0.351	0.414	0.502	0.636	0.140	0.194	0.246	0.305	0.373	0.450	0.541	0.662	0.868
	R4	0.093	0.127	0.158	0.198	0.251	0.314	0.395	0.484	0.600	0.109	0.156	0.202	0.253	0.318	0.400	0.506	0.642	0.828
$\lambda_{20^{\circ}\text{C}}=0.75$	R1	0.181	0.242	0.293	0.343	0.395	0.448	0.507	0.577	0.679	0.215	0.292	0.358	0.426	0.496	0.574	0.666	0.783	0.876
	R2	0.100	0.129	0.162	0.201	0.245	0.294	0.358	0.438	0.561	0.119	0.160	0.203	0.252	0.311	0.378	0.461	0.573	0.760
	R3	0.093	0.120	0.151	0.190	0.235	0.282	0.338	0.417	0.535	0.110	0.150	0.191	0.239	0.297	0.363	0.440	0.545	0.726
	R4	0.075	0.099	0.122	0.153	0.196	0.250	0.321	0.401	0.502	0.088	0.122	0.156	0.197	0.250	0.319	0.410	0.528	0.690
$\lambda_{20^{\circ}\text{C}}=1.00$	R1	0.151	0.203	0.247	0.292	0.337	0.384	0.435	0.495	0.581	0.179	0.245	0.303	0.362	0.424	0.492	0.572	0.725	0.725
	R2	0.082	0.106	0.134	0.167	0.205	0.247	0.305	0.375	0.480	0.098	0.133	0.168	0.210	0.261	0.318	0.391	0.489	0.652
	R3	0.077	0.099	0.124	0.158	0.196	0.238	0.286	0.356	0.459	0.092	0.124	0.158	0.199	0.248	0.305	0.373	0.465	0.622
	R4	0.063	0.082	0.101	0.126	0.163	0.210	0.272	0.341	0.430	0.074	0.102	0.130	0.163	0.207	0.266	0.347	0.448	0.589
$\lambda_{20^{\circ}\text{C}}=1.50$	R1	0.093	0.126	0.155	0.182	0.210	0.239	0.271	0.307	0.359	0.111	0.152	0.189	0.225	0.264	0.306	0.356	0.395	0.395
	R2	0.051	0.065	0.082	0.103	0.127	0.154	0.190	0.234	0.298	0.061	0.082	0.104	0.130	0.161	0.198	0.244	0.304	0.395
	R3	0.048	0.061	0.077	0.098	0.122	0.148	0.178	0.223	0.285	0.057	0.077	0.098	0.123	0.154	0.189	0.232	0.290	0.395
	R4	0.040	0.051	0.062	0.078	0.101	0.130	0.169	0.213	0.268	0.047	0.064	0.081	0.101	0.128	0.166	0.216	0.280	0.395
$\lambda_{20^{\circ}\text{C}}=2.00$	R1	0.057	0.077	0.094	0.110	0.127	0.144	0.163	0.185	0.216	0.067	0.092	0.114	0.136	0.159	0.185	0.214	0.232	0.232
	R2	0.031	0.040	0.050	0.063	0.077	0.093	0.115	0.141	0.180	0.037	0.050	0.063	0.079	0.098	0.120	0.147	0.184	0.232
	R3	0.029	0.037	0.046	0.059	0.074	0.090	0.108	0.134	0.172	0.034	0.047	0.059	0.074	0.093	0.114	0.140	0.175	0.232
	R4	0.024	0.031	0.038	0.047	0.061													

$\theta_{\text{nom}} = 700^{\circ}\text{C}$

$p_{f,fi} \rightarrow$	0.10	0.20	0.30	0.40	0.50	0.60	0.70	0.80	0.90	0.10	0.20	0.30	0.40	0.50	0.60	0.70	0.80	0.90	
$\beta_{f,fi} \rightarrow$	1.28	0.84	0.52	0.40	0.00	-0.25	-0.52	-0.84	-1.28	1.28	0.84	0.52	0.40	0.00	-0.25	-0.52	-0.84	-1.28	
$\delta_{of} \rightarrow$	1.15	1.02	0.94	0.88	0.82	0.77	0.72	0.67	0.60	1.15	1.02	0.94	0.88	0.82	0.77	0.72	0.67	0.60	
	$\alpha=0.00$									$\alpha=0.25$									
$\lambda_{20^{\circ}\text{C}}=0.00$	R1	0.202	0.239	0.276	0.316	0.362	0.414	0.479	0.566	0.735	0.218	0.260	0.299	0.344	0.394	0.451	0.521	0.617	0.801
	R2	0.147	0.185	0.214	0.241	0.274	0.318	0.379	0.472	0.635	0.159	0.201	0.232	0.263	0.298	0.346	0.413	0.515	0.691
	R3	0.113	0.162	0.196	0.225	0.263	0.306	0.361	0.443	0.569	0.123	0.176	0.213	0.245	0.286	0.332	0.392	0.483	0.621
	R4	0.058	0.099	0.143	0.182	0.218	0.262	0.332	0.422	0.525	0.063	0.107	0.156	0.198	0.237	0.285	0.361	0.460	0.572
$\lambda_{20^{\circ}\text{C}}=0.25$	R1	0.155	0.185	0.213	0.244	0.280	0.320	0.370	0.440	0.569	0.168	0.201	0.232	0.265	0.304	0.348	0.403	0.479	0.618
	R2	0.114	0.143	0.165	0.187	0.211	0.247	0.292	0.367	0.496	0.123	0.155	0.179	0.203	0.229	0.270	0.318	0.399	0.541
	R3	0.087	0.125	0.151	0.175	0.202	0.236	0.279	0.343	0.442	0.095	0.136	0.164	0.190	0.220	0.256	0.304	0.374	0.482
	R4	0.047	0.078	0.112	0.142	0.170	0.205	0.259	0.329	0.406	0.051	0.085	0.121	0.154	0.185	0.223	0.282	0.358	0.444
$\lambda_{20^{\circ}\text{C}}=0.50$	R1	0.101	0.120	0.139	0.160	0.184	0.212	0.246	0.294	0.390	0.110	0.130	0.151	0.174	0.200	0.230	0.268	0.321	0.424
	R2	0.077	0.094	0.108	0.122	0.139	0.160	0.192	0.246	0.335	0.083	0.102	0.117	0.132	0.151	0.174	0.210	0.268	0.366
	R3	0.062	0.084	0.100	0.114	0.131	0.154	0.183	0.227	0.296	0.068	0.091	0.108	0.124	0.143	0.168	0.199	0.247	0.322
	R4	0.037	0.057	0.077	0.094	0.111	0.134	0.170	0.215	0.271	0.041	0.062	0.083	0.102	0.121	0.145	0.185	0.234	0.296
$\lambda_{20^{\circ}\text{C}}=0.75$	R1	0.078	0.092	0.106	0.123	0.143	0.166	0.195	0.237	0.323	0.085	0.100	0.116	0.134	0.156	0.181	0.213	0.258	0.352
	R2	0.061	0.074	0.084	0.094	0.106	0.123	0.151	0.196	0.270	0.067	0.080	0.091	0.102	0.116	0.134	0.164	0.214	0.294
	R3	0.052	0.067	0.078	0.088	0.101	0.119	0.142	0.179	0.237	0.057	0.073	0.085	0.096	0.111	0.129	0.155	0.195	0.258
	R4	0.034	0.049	0.062	0.074	0.087	0.103	0.131	0.169	0.215	0.037	0.053	0.068	0.081	0.094	0.112	0.143	0.184	0.234
$\lambda_{20^{\circ}\text{C}}=1.00$	R1	0.064	0.075	0.087	0.101	0.118	0.138	0.163	0.199	0.275	0.070	0.082	0.095	0.110	0.129	0.150	0.177	0.217	0.299
	R2	0.051	0.061	0.069	0.077	0.087	0.101	0.124	0.164	0.229	0.056	0.066	0.075	0.084	0.095	0.110	0.136	0.178	0.248
	R3	0.045	0.056	0.065	0.073	0.084	0.098	0.117	0.149	0.199	0.049	0.061	0.070	0.079	0.091	0.106	0.128	0.161	0.217
	R4	0.031	0.043	0.053	0.062	0.072	0.085	0.108	0.140	0.180	0.034	0.047	0.058	0.068	0.078	0.092	0.118	0.153	0.196
$\lambda_{20^{\circ}\text{C}}=1.50$	R1	0.039	0.046	0.054	0.062	0.073	0.085	0.101	0.124	0.171	0.043	0.050	0.058	0.068	0.079	0.093	0.110	0.134	0.186
	R2	0.032	0.038	0.043	0.047	0.054	0.062	0.077	0.102	0.142	0.035	0.041	0.046	0.052	0.059	0.068	0.084	0.111	0.155
	R3	0.029	0.035	0.040	0.045	0.051	0.060	0.072	0.092	0.124	0.032	0.038	0.044	0.049	0.056	0.065	0.079	0.100	0.135
	R4	0.021	0.028	0.034	0.039	0.045	0.052	0.067	0.087	0.112	0.022	0.030	0.037	0.042	0.049	0.057	0.073	0.094	0.121
$\lambda_{20^{\circ}\text{C}}=2.00$	R1	0.024	0.028	0.032	0.038	0.044	0.052	0.061	0.075	0.104	0.026	0.031	0.035	0.041	0.048	0.056	0.067	0.082	0.113
	R2	0.020	0.023	0.026	0.029	0.033	0.038	0.047	0.062	0.086	0.021	0.025	0.028	0.031	0.035	0.041	0.051	0.067	0.094
	R3	0.018	0.022	0.024	0.027	0.031	0.036	0.044	0.056	0.075	0.019	0.023	0.027	0.030	0.034	0.040	0.048	0.061	0.081
	R4	0.013	0.017	0.021	0.024	0.027	0.032	0.040	0.052	0.067	0.014	0.019	0.022	0.026	0.029	0.035	0.044	0.057	0.074
	$\alpha=0.50$									$\alpha=0.75$									
$\lambda_{20^{\circ}\text{C}}=0.00$	R1	0.242	0.293	0.341	0.393	0.451	0.517	0.601	0.713	0.924	0.278	0.356	0.427	0.500	0.580	0.674	0.792	0.959	1.000
	R2	0.176	0.225	0.263	0.300	0.342	0.398	0.474	0.591	0.801	0.201	0.267	0.324	0.380	0.446	0.523	0.620	0.783	1.000
	R3	0.138	0.196	0.241	0.280	0.328	0.382	0.452	0.555	0.720	0.164	0.235	0.296	0.356	0.426	0.502	0.596	0.739	0.983
	R4	0.072	0.121	0.174	0.224	0.272	0.329	0.415	0.531	0.664	0.088	0.149	0.212	0.277	0.348	0.433	0.544	0.712	0.916
$\lambda_{20^{\circ}\text{C}}=0.25$	R1	0.187	0.226	0.263	0.303	0.348	0.400	0.464	0.554	0.716	0.214	0.274	0.330	0.386	0.448	0.521	0.613	0.743	0.969
	R2	0.135	0.173	0.203	0.233	0.263	0.310	0.365	0.458	0.628	0.155	0.205	0.249	0.294	0.341	0.407	0.478	0.607	0.849
	R3	0.106	0.151	0.185	0.216	0.252	0.295	0.349	0.429	0.559	0.126	0.180	0.228	0.275	0.327	0.388	0.462	0.570	0.765
	R4	0.058	0.096	0.136	0.174	0.211	0.257	0.323	0.412	0.516	0.071	0.117	0.165	0.216	0.272	0.339	0.426	0.546	0.709
$\lambda_{20^{\circ}\text{C}}=0.50$	R1	0.122	0.147	0.172	0.198	0.229	0.264	0.309	0.370	0.490	0.140	0.179	0.216	0.253	0.295	0.345	0.408	0.498	0.659
	R2	0.092	0.114	0.133	0.151	0.174	0.201	0.240	0.308	0.421	0.105	0.136	0.164	0.193	0.226	0.264	0.315	0.405	0.569
	R3	0.076	0.102	0.122	0.142	0.164	0.193	0.228	0.284	0.374	0.089	0.122	0.152	0.180	0.214	0.254	0.303	0.376	0.509
	R4	0.046	0.070	0.093	0.116	0.139	0.168	0.212	0.269	0.343	0.055	0.086	0.114	0.145	0.179	0.221	0.280	0.362	0.472
$\lambda_{20^{\circ}\text{C}}=0.75$	R1	0.094	0.113	0.132	0.153	0.178	0.207	0.244	0.297	0.405	0.108	0.138	0.166	0.196	0.230	0.270	0.322	0.397	0.541
	R2	0.074	0.089	0.103	0.116	0.133	0.155	0.188	0.245	0.340	0.084	0.108	0.128	0.150	0.175	0.205	0.245	0.321	0.462
	R3	0.063	0.081	0.096	0.110	0.128	0.149	0.178	0.223	0.299	0.074	0.098	0.119	0.141	0.167	0.197	0.235	0.296	0.406
	R4	0.042	0.060	0.077	0.092	0.108	0.130	0.164	0.212	0.272	0.049	0.073	0.094	0.116	0.141	0.173	0.217	0.285	0.373
$\lambda_{20^{\circ}\text{C}}=1.00$	R1	0.077	0.093	0.108	0.126	0.147	0.172	0.204	0.250	0.346	0.089	0.114	0.137	0.162	0.189	0.224	0.269	0.333	0.462
	R2	0.062	0.075	0.085	0.096	0.110	0.127	0.155	0.205	0.288	0.070	0.090	0.106	0.123	0.145	0.168	0.204	0.267	0.389
	R3	0.055	0.069	0.080	0.091	0.105	0.122	0.147	0.186	0.250	0.063	0.082	0.099	0.117	0.138	0.163	0.194	0.247	0.341
	R4	0.038	0.053	0.065	0.077	0.090	0.107	0.135	0.176	0.227	0.044	0.063	0.080	0.098	0.118	0.143	0.179	0.236	0.310
$\lambda_{20^{\circ}\text{C}}=1.50$	R1	0.048	0.057	0.067	0.077	0.090	0.106	0.126	0.155	0.216	0.055	0.071	0.085	0.100	0.117	0.138	0.167	0.207	0.287
	R2	0.039	0.046	0.053	0.059	0.068	0.078	0.096	0.127	0.179	0.044	0.056	0.066	0.077	0.090	0.103	0.126	0.166	0.242
	R3	0.035	0.043	0.050	0.056	0.065	0.075	0.090	0.115	0.156	0.040	0.052	0.062	0.073	0.086	0.100	0.120	0.153	0.211
	R4	0.025	0.034	0.041	0.048	0.056	0.066	0.083	0.109	0.141	0.029	0.040	0.051	0.062	0.074	0.089	0.111	0.146	0.192
$\lambda_{20^{\circ}\text{C}}=2.00$	R1	0.029	0.035	0.040	0.047	0.055	0.064	0.077	0.094	0.130	0.033	0.043	0.051	0.060	0.071	0.084	0.101	0.126	0.174
	R2	0.024	0.028	0.032	0.036	0.041	0.047	0.058	0.077	0.108	0.027	0.034	0.040	0.046	0.055	0.063	0.076	0.101	0.146
	R3	0.021	0.026	0.030	0.034	0.039	0.046	0.055	0.070	0.094	0.025	0.032	0.038	0.044	0.052	0.061	0.072	0.092	0.127
	R4	0.015	0.021	0.025	0.029</														

$\theta_{\text{nom}} = 800^{\circ}\text{C}$

$p_{f,fi} \rightarrow$	0.10	0.20	0.30	0.40	0.50	0.60	0.70	0.80	0.90	0.10	0.20	0.30	0.40	0.50	0.60	0.70	0.80	0.90	
$\beta_{f,fi} \rightarrow$	1.28	0.84	0.52	0.40	0.00	-0.25	-0.52	-0.84	-1.28	1.28	0.84	0.52	0.40	0.00	-0.25	-0.52	-0.84	-1.28	
$\delta_{of} \rightarrow$	1.15	1.02	0.94	0.88	0.82	0.77	0.72	0.67	0.60	1.15	1.02	0.94	0.88	0.82	0.77	0.72	0.67	0.60	
$\alpha=0.00$										$\alpha=0.25$									
$\lambda_{20^{\circ}\text{C}}=0.00$	R1	0.070	0.089	0.108	0.127	0.149	0.174	0.200	0.232	0.294	0.076	0.097	0.117	0.138	0.162	0.189	0.218	0.253	0.321
	R2	0.057	0.074	0.094	0.115	0.141	0.167	0.194	0.229	0.284	0.062	0.081	0.102	0.125	0.153	0.182	0.211	0.251	0.310
	R3	0.046	0.061	0.078	0.099	0.124	0.155	0.188	0.223	0.276	0.050	0.067	0.085	0.107	0.135	0.168	0.205	0.243	0.301
	R4	0.027	0.043	0.058	0.075	0.100	0.132	0.171	0.214	0.269	0.030	0.047	0.063	0.082	0.108	0.143	0.187	0.233	0.294
$\lambda_{20^{\circ}\text{C}}=0.25$	R1	0.055	0.069	0.083	0.098	0.115	0.134	0.155	0.180	0.230	0.059	0.075	0.090	0.107	0.125	0.145	0.168	0.197	0.252
	R2	0.045	0.058	0.072	0.089	0.108	0.129	0.150	0.178	0.222	0.049	0.063	0.079	0.097	0.118	0.140	0.164	0.194	0.242
	R3	0.036	0.048	0.061	0.077	0.096	0.119	0.146	0.174	0.215	0.039	0.052	0.066	0.083	0.104	0.130	0.158	0.190	0.234
	R4	0.023	0.036	0.047	0.061	0.080	0.105	0.134	0.166	0.210	0.025	0.039	0.051	0.066	0.087	0.114	0.146	0.181	0.229
$\lambda_{20^{\circ}\text{C}}=0.50$	R1	0.043	0.052	0.060	0.069	0.079	0.090	0.102	0.118	0.150	0.046	0.056	0.066	0.075	0.086	0.098	0.111	0.129	0.164
	R2	0.036	0.045	0.054	0.064	0.075	0.087	0.100	0.117	0.144	0.039	0.049	0.059	0.070	0.082	0.095	0.109	0.127	0.158
	R3	0.030	0.039	0.047	0.057	0.068	0.082	0.097	0.114	0.140	0.032	0.042	0.052	0.062	0.074	0.089	0.106	0.125	0.153
	R4	0.019	0.029	0.038	0.047	0.059	0.073	0.090	0.110	0.136	0.021	0.031	0.041	0.052	0.064	0.080	0.098	0.120	0.148
$\lambda_{20^{\circ}\text{C}}=0.75$	R1	0.038	0.045	0.052	0.058	0.065	0.072	0.080	0.092	0.116	0.041	0.049	0.056	0.063	0.070	0.078	0.088	0.100	0.126
	R2	0.033	0.041	0.048	0.055	0.062	0.070	0.079	0.091	0.112	0.036	0.044	0.052	0.059	0.068	0.076	0.086	0.099	0.121
	R3	0.027	0.035	0.042	0.050	0.058	0.067	0.077	0.089	0.108	0.030	0.038	0.046	0.054	0.063	0.072	0.084	0.097	0.118
	R4	0.018	0.027	0.035	0.042	0.051	0.061	0.072	0.086	0.105	0.019	0.029	0.038	0.046	0.056	0.067	0.079	0.094	0.115
$\lambda_{20^{\circ}\text{C}}=1.00$	R1	0.034	0.040	0.045	0.050	0.055	0.061	0.067	0.076	0.095	0.037	0.044	0.049	0.055	0.060	0.066	0.073	0.083	0.104
	R2	0.030	0.037	0.042	0.048	0.054	0.059	0.066	0.076	0.092	0.033	0.040	0.046	0.052	0.058	0.065	0.072	0.082	0.101
	R3	0.025	0.032	0.038	0.044	0.050	0.057	0.065	0.074	0.089	0.027	0.035	0.041	0.048	0.054	0.062	0.071	0.081	0.097
	R4	0.016	0.024	0.031	0.038	0.045	0.053	0.061	0.072	0.087	0.018	0.027	0.034	0.041	0.049	0.057	0.067	0.078	0.095
$\lambda_{20^{\circ}\text{C}}=1.50$	R1	0.023	0.026	0.029	0.032	0.035	0.038	0.042	0.047	0.059	0.024	0.029	0.032	0.035	0.038	0.042	0.046	0.052	0.064
	R2	0.020	0.024	0.028	0.031	0.034	0.038	0.042	0.047	0.057	0.022	0.026	0.030	0.034	0.037	0.041	0.045	0.051	0.062
	R3	0.017	0.021	0.025	0.029	0.032	0.036	0.041	0.046	0.055	0.018	0.023	0.027	0.031	0.035	0.039	0.044	0.050	0.060
	R4	0.011	0.016	0.021	0.025	0.029	0.034	0.039	0.045	0.054	0.012	0.018	0.023	0.027	0.032	0.037	0.042	0.049	0.059
$\lambda_{20^{\circ}\text{C}}=2.00$	R1	0.014	0.016	0.018	0.020	0.022	0.023	0.026	0.029	0.036	0.015	0.017	0.020	0.021	0.023	0.025	0.028	0.031	0.039
	R2	0.012	0.015	0.017	0.019	0.021	0.023	0.025	0.029	0.034	0.013	0.016	0.018	0.020	0.023	0.025	0.028	0.031	0.038
	R3	0.010	0.013	0.015	0.017	0.020	0.022	0.025	0.028	0.033	0.011	0.014	0.017	0.019	0.021	0.024	0.027	0.031	0.036
	R4	0.007	0.010	0.013	0.015	0.018	0.021	0.024	0.027	0.033	0.007	0.011	0.014	0.017	0.019	0.022	0.026	0.030	0.036
$\alpha=0.50$										$\alpha=0.75$									
$\lambda_{20^{\circ}\text{C}}=0.00$	R1	0.085	0.110	0.133	0.157	0.184	0.215	0.249	0.293	0.373	0.101	0.134	0.165	0.197	0.232	0.273	0.326	0.394	0.519
	R2	0.070	0.092	0.116	0.143	0.174	0.206	0.241	0.291	0.361	0.084	0.114	0.145	0.179	0.219	0.262	0.314	0.390	0.500
	R3	0.056	0.076	0.097	0.122	0.153	0.191	0.234	0.280	0.351	0.067	0.094	0.122	0.155	0.194	0.242	0.302	0.376	0.490
	R4	0.033	0.053	0.071	0.093	0.123	0.163	0.212	0.269	0.344	0.039	0.065	0.090	0.119	0.157	0.206	0.271	0.355	0.480
$\lambda_{20^{\circ}\text{C}}=0.25$	R1	0.066	0.085	0.103	0.121	0.142	0.165	0.193	0.227	0.293	0.078	0.103	0.127	0.152	0.179	0.211	0.251	0.306	0.405
	R2	0.055	0.071	0.089	0.110	0.134	0.160	0.187	0.223	0.283	0.065	0.089	0.112	0.139	0.169	0.203	0.244	0.299	0.393
	R3	0.044	0.059	0.075	0.095	0.118	0.147	0.181	0.219	0.273	0.053	0.073	0.095	0.120	0.150	0.187	0.233	0.293	0.381
	R4	0.029	0.044	0.058	0.075	0.099	0.130	0.166	0.209	0.268	0.034	0.054	0.073	0.096	0.126	0.165	0.213	0.276	0.372
$\lambda_{20^{\circ}\text{C}}=0.50$	R1	0.052	0.063	0.074	0.085	0.098	0.111	0.128	0.149	0.191	0.060	0.077	0.092	0.107	0.124	0.144	0.168	0.201	0.264
	R2	0.044	0.056	0.067	0.079	0.093	0.108	0.125	0.147	0.185	0.052	0.068	0.084	0.100	0.118	0.139	0.163	0.199	0.258
	R3	0.036	0.047	0.059	0.070	0.084	0.101	0.121	0.144	0.179	0.042	0.058	0.073	0.089	0.107	0.129	0.157	0.194	0.249
	R4	0.023	0.035	0.047	0.059	0.073	0.091	0.112	0.138	0.174	0.027	0.043	0.058	0.074	0.093	0.116	0.145	0.184	0.244
$\lambda_{20^{\circ}\text{C}}=0.75$	R1	0.046	0.055	0.064	0.072	0.080	0.090	0.101	0.116	0.148	0.052	0.066	0.079	0.090	0.103	0.117	0.135	0.159	0.206
	R2	0.040	0.050	0.059	0.068	0.077	0.087	0.099	0.115	0.142	0.046	0.060	0.073	0.085	0.099	0.114	0.132	0.157	0.198
	R3	0.033	0.043	0.052	0.061	0.071	0.083	0.097	0.113	0.138	0.038	0.052	0.065	0.077	0.091	0.107	0.127	0.153	0.194
	R4	0.022	0.033	0.043	0.052	0.063	0.076	0.090	0.108	0.135	0.026	0.040	0.052	0.066	0.081	0.098	0.118	0.146	0.190
$\lambda_{20^{\circ}\text{C}}=1.00$	R1	0.041	0.049	0.056	0.062	0.069	0.076	0.085	0.096	0.121	0.046	0.058	0.068	0.078	0.088	0.100	0.114	0.133	0.170
	R2	0.036	0.045	0.052	0.059	0.066	0.074	0.083	0.096	0.117	0.041	0.053	0.064	0.074	0.085	0.097	0.111	0.131	0.164
	R3	0.030	0.039	0.047	0.054	0.062	0.071	0.081	0.094	0.114	0.035	0.047	0.057	0.068	0.079	0.092	0.108	0.129	0.161
	R4	0.020	0.030	0.039	0.047	0.056	0.066	0.077	0.091	0.111	0.023	0.036	0.047	0.058	0.070	0.084	0.101	0.123	0.158
$\lambda_{20^{\circ}\text{C}}=1.50$	R1	0.027	0.032	0.036	0.040	0.044	0.048	0.053	0.060	0.075	0.030	0.038	0.044	0.050	0.056	0.063	0.072	0.083	0.105
	R2	0.024	0.029	0.034	0.038	0.043	0.047	0.052	0.060	0.073	0.027	0.035	0.041	0.048	0.054	0.062	0.070	0.082	0.102
	R3	0.020	0.026	0.031	0.035	0.040	0.045	0.051	0.059	0.071	0.023	0.031	0.037	0.044	0.051	0.059	0.069	0.081	0.100
	R4	0.013	0.020	0.025	0.031	0.036	0.042	0.049	0.057	0.069	0.015	0.024	0.031	0.038	0.046	0.054	0.064	0.078	0.098
$\lambda_{20^{\circ}\text{C}}=2.00$	R1	0.016	0.020	0.022	0.024	0.027	0.029	0.032	0.037	0.046	0.018	0.023	0.027	0.031	0.034	0.039	0.044	0.051	0.064
	R2	0.015	0.018	0.021	0.023	0.026	0.029	0.032	0.036	0.044	0.017	0.021	0.025	0.029	0.033	0.038	0.043	0.050	0.062
	R3	0.012	0.016	0.019	0.021	0.024	0.027	0.031	0.036	0.043	0.014	0.019	0.023	0.027	0.031	0.036	0.042	0.049	0.061
	R4	0.008	0.012	0.016	0.01														

$\theta_{\text{nom}} = 900^{\circ}\text{C}$

$p_{f,fi} \rightarrow$	0.10	0.20	0.30	0.40	0.50	0.60	0.70	0.80	0.90	0.10	0.20	0.30	0.40	0.50	0.60	0.70	0.80	0.90	
$\beta_{f,fi} \rightarrow$	1.28	0.84	0.52	0.40	0.00	-0.25	-0.52	-0.84	-1.28	1.28	0.84	0.52	0.40	0.00	-0.25	-0.52	-0.84	-1.28	
$\delta_{of} \rightarrow$	1.15	1.02	0.94	0.88	0.82	0.77	0.72	0.67	0.60	1.15	1.02	0.94	0.88	0.82	0.77	0.72	0.67	0.60	
	$\alpha=0.00$									$\alpha=0.25$									
$\lambda_{20^{\circ}\text{C}}=0.00$	R1	0.051	0.061	0.070	0.079	0.089	0.101	0.119	0.147	0.211	0.056	0.066	0.076	0.086	0.097	0.110	0.130	0.160	0.230
	R2	0.039	0.049	0.058	0.068	0.081	0.098	0.110	0.145	0.203	0.042	0.053	0.063	0.074	0.088	0.107	0.121	0.158	0.221
	R3	0.025	0.036	0.045	0.055	0.066	0.082	0.107	0.142	0.186	0.027	0.039	0.049	0.059	0.072	0.089	0.115	0.154	0.203
	R4	0.004	0.019	0.031	0.043	0.056	0.073	0.100	0.125	0.152	0.004	0.021	0.034	0.047	0.061	0.079	0.109	0.137	0.165
$\lambda_{20^{\circ}\text{C}}=0.25$	R1	0.040	0.048	0.055	0.062	0.069	0.078	0.093	0.120	0.171	0.044	0.052	0.059	0.067	0.075	0.085	0.101	0.131	0.186
	R2	0.031	0.038	0.045	0.053	0.063	0.075	0.087	0.114	0.158	0.033	0.042	0.049	0.058	0.069	0.082	0.095	0.124	0.174
	R3	0.020	0.029	0.036	0.044	0.054	0.066	0.085	0.110	0.144	0.022	0.031	0.039	0.047	0.059	0.072	0.092	0.120	0.156
	R4	0.013	0.023	0.032	0.042	0.051	0.064	0.082	0.098	0.118	0.014	0.025	0.035	0.045	0.056	0.070	0.089	0.107	0.128
$\lambda_{20^{\circ}\text{C}}=0.50$	R1	0.033	0.038	0.043	0.048	0.052	0.058	0.067	0.082	0.111	0.035	0.042	0.047	0.052	0.057	0.063	0.073	0.089	0.121
	R2	0.025	0.031	0.037	0.042	0.049	0.057	0.064	0.079	0.105	0.027	0.034	0.040	0.046	0.053	0.062	0.069	0.086	0.114
	R3	0.017	0.023	0.030	0.035	0.043	0.051	0.062	0.077	0.097	0.018	0.026	0.032	0.039	0.047	0.055	0.067	0.084	0.106
	R4	0.011	0.019	0.026	0.034	0.041	0.049	0.060	0.070	0.083	0.012	0.020	0.029	0.037	0.044	0.053	0.065	0.077	0.090
$\lambda_{20^{\circ}\text{C}}=0.75$	R1	0.030	0.035	0.039	0.043	0.047	0.051	0.058	0.067	0.087	0.033	0.038	0.043	0.047	0.051	0.056	0.063	0.074	0.095
	R2	0.023	0.029	0.034	0.039	0.044	0.050	0.056	0.066	0.083	0.025	0.031	0.037	0.042	0.048	0.055	0.061	0.071	0.090
	R3	0.015	0.022	0.027	0.033	0.039	0.046	0.054	0.065	0.078	0.017	0.024	0.030	0.036	0.042	0.050	0.059	0.071	0.085
	R4	0.010	0.017	0.024	0.031	0.037	0.044	0.053	0.061	0.070	0.011	0.019	0.026	0.034	0.041	0.048	0.057	0.067	0.077
$\lambda_{20^{\circ}\text{C}}=1.00$	R1	0.027	0.032	0.035	0.038	0.042	0.046	0.051	0.058	0.073	0.030	0.034	0.038	0.042	0.045	0.050	0.055	0.063	0.080
	R2	0.021	0.026	0.031	0.035	0.040	0.044	0.049	0.057	0.070	0.023	0.029	0.033	0.038	0.043	0.048	0.053	0.062	0.076
	R3	0.014	0.020	0.025	0.030	0.036	0.041	0.048	0.056	0.067	0.015	0.022	0.027	0.032	0.039	0.045	0.052	0.061	0.073
	R4	0.009	0.016	0.022	0.028	0.034	0.040	0.047	0.053	0.061	0.010	0.017	0.024	0.031	0.037	0.043	0.051	0.058	0.067
$\lambda_{20^{\circ}\text{C}}=1.50$	R1	0.018	0.021	0.023	0.025	0.027	0.030	0.033	0.037	0.046	0.020	0.023	0.025	0.028	0.030	0.033	0.036	0.041	0.050
	R2	0.014	0.017	0.020	0.023	0.026	0.029	0.032	0.037	0.044	0.015	0.019	0.022	0.025	0.028	0.032	0.035	0.040	0.048
	R3	0.009	0.013	0.017	0.020	0.023	0.027	0.031	0.036	0.042	0.010	0.014	0.018	0.021	0.025	0.029	0.034	0.039	0.046
	R4	0.006	0.011	0.015	0.019	0.022	0.026	0.030	0.035	0.039	0.006	0.011	0.016	0.020	0.024	0.028	0.033	0.038	0.043
$\lambda_{20^{\circ}\text{C}}=2.00$	R1	0.011	0.013	0.014	0.016	0.017	0.018	0.020	0.023	0.028	0.012	0.014	0.016	0.017	0.018	0.020	0.022	0.025	0.031
	R2	0.009	0.011	0.013	0.014	0.016	0.018	0.019	0.022	0.027	0.009	0.012	0.014	0.015	0.017	0.019	0.021	0.024	0.029
	R3	0.006	0.008	0.010	0.012	0.014	0.016	0.019	0.022	0.026	0.006	0.009	0.011	0.013	0.016	0.018	0.021	0.024	0.028
	R4	0.004	0.006	0.009	0.012	0.014	0.016	0.019	0.021	0.024	0.004	0.007	0.010	0.013	0.015	0.017	0.020	0.023	0.026
	$\alpha=0.50$									$\alpha=0.75$									
$\lambda_{20^{\circ}\text{C}}=0.00$	R1	0.062	0.075	0.087	0.098	0.110	0.126	0.149	0.184	0.265	0.071	0.091	0.108	0.124	0.142	0.165	0.198	0.242	0.354
	R2	0.047	0.060	0.071	0.085	0.101	0.123	0.139	0.181	0.255	0.055	0.073	0.091	0.109	0.132	0.160	0.184	0.238	0.339
	R3	0.030	0.044	0.056	0.068	0.082	0.102	0.133	0.178	0.233	0.036	0.053	0.069	0.086	0.106	0.133	0.172	0.230	0.317
	R4	0.005	0.023	0.038	0.053	0.069	0.090	0.125	0.159	0.193	0.006	0.028	0.047	0.066	0.089	0.118	0.161	0.217	0.270
$\lambda_{20^{\circ}\text{C}}=0.25$	R1	0.048	0.059	0.067	0.076	0.086	0.098	0.117	0.148	0.216	0.056	0.071	0.084	0.097	0.111	0.128	0.154	0.193	0.295
	R2	0.037	0.047	0.056	0.066	0.079	0.095	0.110	0.142	0.199	0.043	0.057	0.071	0.085	0.103	0.123	0.146	0.189	0.267
	R3	0.024	0.035	0.044	0.054	0.067	0.083	0.106	0.138	0.181	0.029	0.042	0.055	0.069	0.088	0.108	0.138	0.180	0.246
	R4	0.016	0.028	0.040	0.052	0.064	0.080	0.102	0.124	0.150	0.019	0.034	0.050	0.066	0.084	0.105	0.134	0.171	0.210
$\lambda_{20^{\circ}\text{C}}=0.50$	R1	0.039	0.047	0.053	0.059	0.065	0.073	0.084	0.103	0.141	0.044	0.056	0.065	0.075	0.084	0.096	0.112	0.135	0.194
	R2	0.030	0.038	0.045	0.053	0.061	0.071	0.080	0.099	0.132	0.035	0.046	0.057	0.067	0.079	0.094	0.107	0.132	0.178
	R3	0.020	0.029	0.036	0.044	0.053	0.064	0.078	0.097	0.123	0.024	0.035	0.045	0.055	0.069	0.083	0.102	0.127	0.169
	R4	0.013	0.023	0.032	0.042	0.051	0.061	0.076	0.089	0.106	0.016	0.028	0.040	0.053	0.065	0.080	0.099	0.123	0.149
$\lambda_{20^{\circ}\text{C}}=0.75$	R1	0.036	0.043	0.048	0.053	0.058	0.065	0.073	0.085	0.111	0.040	0.050	0.059	0.067	0.075	0.085	0.098	0.114	0.155
	R2	0.028	0.035	0.042	0.048	0.055	0.063	0.069	0.083	0.105	0.032	0.042	0.052	0.061	0.071	0.083	0.094	0.112	0.144
	R3	0.019	0.027	0.033	0.040	0.048	0.057	0.068	0.081	0.100	0.022	0.032	0.041	0.050	0.062	0.074	0.090	0.109	0.140
	R4	0.012	0.021	0.030	0.038	0.046	0.055	0.066	0.077	0.090	0.014	0.026	0.037	0.048	0.059	0.071	0.087	0.107	0.128
$\lambda_{20^{\circ}\text{C}}=1.00$	R1	0.033	0.038	0.043	0.048	0.052	0.057	0.064	0.073	0.094	0.036	0.045	0.053	0.060	0.067	0.075	0.086	0.099	0.131
	R2	0.026	0.032	0.038	0.043	0.049	0.056	0.061	0.072	0.088	0.030	0.039	0.047	0.055	0.063	0.074	0.083	0.097	0.122
	R3	0.017	0.024	0.030	0.037	0.044	0.051	0.060	0.070	0.085	0.020	0.029	0.037	0.046	0.056	0.066	0.079	0.095	0.120
	R4	0.011	0.019	0.027	0.035	0.042	0.049	0.058	0.068	0.078	0.013	0.023	0.033	0.043	0.053	0.064	0.076	0.094	0.112
$\lambda_{20^{\circ}\text{C}}=1.50$	R1	0.022	0.025	0.029	0.031	0.034	0.037	0.042	0.047	0.059	0.024	0.030	0.035	0.039	0.044	0.049	0.056	0.064	0.083
	R2	0.017	0.021	0.025	0.029	0.032	0.037	0.040	0.046	0.056	0.020	0.026	0.031	0.036	0.041	0.048	0.055	0.063	0.078
	R3	0.011	0.016	0.020	0.024	0.029	0.033	0.039	0.045	0.054	0.013	0.019	0.025	0.030	0.037	0.043	0.051	0.062	0.077
	R4	0.007	0.013	0.018	0.023	0.028	0.032	0.038	0.044	0.051	0.009	0.016	0.022	0.029	0.035	0.042	0.050	0.061	0.073
$\lambda_{20^{\circ}\text{C}}=2.00$	R1	0.013	0.016	0.017	0.019	0.021	0.023	0.025	0.028	0.036	0.015	0.018	0.021	0.024	0.027	0.030	0.034	0.039	0.050
	R2	0.010	0.013	0.015	0.018	0.020	0.022	0.025	0.028	0.034	0.012	0.016	0.019	0.022	0.025	0.029	0.033	0.038	0.048
	R3	0.007	0.010	0.012	0.015	0.018	0.020	0.024	0.028	0.033	0.008	0.012	0.015	0.018	0.023	0.026	0.031	0.038	0.047
	R4	0.004	0.008	0.011	0.014	0.017	0												

A17 Factor χ_{Rel} for S235 weak axis, imposed (Q) variable load type

		$\theta_{\text{nom}} = 300^{\circ}\text{C}$																	
$p_{f,fi} \rightarrow$		0.10	0.20	0.30	0.40	0.50	0.60	0.70	0.80	0.90	0.10	0.20	0.30	0.40	0.50	0.60	0.70	0.80	0.90
$\beta_{f,fi} \rightarrow$		1.28	0.84	0.52	0.40	0.00	-0.25	-0.52	-0.84	-1.28	1.28	0.84	0.52	0.40	0.00	-0.25	-0.52	-0.84	-1.28
$\delta_{of} \rightarrow$		1.15	1.02	0.94	0.88	0.82	0.77	0.72	0.67	0.60	1.15	1.02	0.94	0.88	0.82	0.77	0.72	0.67	0.60
		$\alpha=0.00$									$\alpha=0.25$								
$\lambda_{20^{\circ}\text{C}}=0.00$	R1	0.816	0.908	0.978	1.000	1.000	1.000	1.000	1.000	1.000	0.880	0.984	1.000	1.000	1.000	1.000	1.000	1.000	1.000
	R2	0.792	0.890	0.963	1.000	1.000	1.000	1.000	1.000	1.000	0.857	0.963	1.000	1.000	1.000	1.000	1.000	1.000	1.000
	R3	0.782	0.883	0.958	1.000	1.000	1.000	1.000	1.000	1.000	0.843	0.957	1.000	1.000	1.000	1.000	1.000	1.000	1.000
	R4	0.740	0.854	0.934	1.000	1.000	1.000	1.000	1.000	1.000	0.800	0.926	1.000	1.000	1.000	1.000	1.000	1.000	1.000
$\lambda_{20^{\circ}\text{C}}=0.25$	R1	0.633	0.707	0.765	0.816	0.865	0.918	0.978	0.993	0.993	0.686	0.768	0.830	0.887	0.943	0.993	0.993	0.993	0.993
	R2	0.616	0.694	0.752	0.805	0.856	0.909	0.969	0.993	0.993	0.666	0.752	0.817	0.875	0.932	0.992	0.993	0.993	0.993
	R3	0.607	0.689	0.748	0.800	0.850	0.904	0.964	0.993	0.993	0.657	0.746	0.813	0.870	0.926	0.986	0.993	0.993	0.993
	R4	0.573	0.664	0.728	0.783	0.836	0.891	0.952	0.993	0.993	0.621	0.720	0.791	0.852	0.910	0.972	0.993	0.993	0.993
$\lambda_{20^{\circ}\text{C}}=0.50$	R1	0.500	0.565	0.616	0.666	0.714	0.764	0.821	0.888	0.951	0.540	0.612	0.669	0.723	0.776	0.832	0.951	0.951	0.951
	R2	0.483	0.551	0.603	0.651	0.698	0.748	0.804	0.873	0.951	0.523	0.597	0.655	0.708	0.760	0.814	0.878	0.951	0.951
	R3	0.476	0.544	0.595	0.639	0.683	0.733	0.788	0.858	0.951	0.514	0.589	0.646	0.695	0.744	0.798	0.860	0.951	0.951
	R4	0.442	0.520	0.576	0.625	0.673	0.723	0.779	0.845	0.951	0.477	0.562	0.625	0.679	0.732	0.788	0.849	0.951	0.951
$\lambda_{20^{\circ}\text{C}}=0.75$	R1	0.417	0.478	0.528	0.575	0.622	0.671	0.729	0.876	0.876	0.452	0.519	0.573	0.624	0.676	0.730	0.876	0.876	0.876
	R2	0.401	0.463	0.514	0.560	0.604	0.652	0.708	0.876	0.876	0.434	0.503	0.559	0.609	0.657	0.710	0.876	0.876	0.876
	R3	0.392	0.455	0.505	0.546	0.587	0.635	0.689	0.756	0.876	0.425	0.494	0.548	0.594	0.638	0.691	0.752	0.876	0.876
	R4	0.361	0.430	0.483	0.531	0.577	0.625	0.678	0.740	0.876	0.391	0.468	0.525	0.578	0.628	0.681	0.739	0.876	0.876
$\lambda_{20^{\circ}\text{C}}=1.00$	R1	0.347	0.398	0.441	0.481	0.522	0.564	0.725	0.725	0.725	0.375	0.432	0.478	0.523	0.567	0.725	0.725	0.725	0.725
	R2	0.334	0.386	0.429	0.468	0.507	0.549	0.597	0.725	0.725	0.361	0.418	0.465	0.509	0.551	0.597	0.725	0.725	0.725
	R3	0.326	0.378	0.420	0.455	0.491	0.533	0.581	0.725	0.725	0.352	0.411	0.456	0.496	0.535	0.580	0.725	0.725	0.725
	R4	0.300	0.358	0.402	0.442	0.483	0.524	0.570	0.725	0.725	0.325	0.389	0.436	0.481	0.524	0.570	0.725	0.725	0.725
$\lambda_{20^{\circ}\text{C}}=1.50$	R1	0.210	0.239	0.263	0.284	0.306	0.328	0.395	0.395	0.395	0.227	0.259	0.285	0.309	0.332	0.395	0.395	0.395	0.395
	R2	0.203	0.233	0.257	0.278	0.298	0.320	0.345	0.395	0.395	0.219	0.252	0.278	0.302	0.324	0.349	0.395	0.395	0.395
	R3	0.199	0.229	0.252	0.272	0.292	0.313	0.338	0.395	0.395	0.215	0.248	0.274	0.296	0.317	0.340	0.395	0.395	0.395
	R4	0.184	0.218	0.243	0.265	0.286	0.309	0.334	0.395	0.395	0.199	0.236	0.263	0.288	0.311	0.337	0.395	0.395	0.395
$\lambda_{20^{\circ}\text{C}}=2.00$	R1	0.128	0.145	0.158	0.171	0.183	0.196	0.210	0.232	0.232	0.138	0.157	0.172	0.185	0.199	0.213	0.232	0.232	0.232
	R2	0.124	0.141	0.155	0.167	0.179	0.192	0.206	0.232	0.232	0.134	0.153	0.168	0.182	0.195	0.209	0.232	0.232	0.232
	R3	0.122	0.139	0.153	0.165	0.176	0.188	0.202	0.232	0.232	0.132	0.151	0.166	0.179	0.191	0.204	0.232	0.232	0.232
	R4	0.113	0.133	0.148	0.160	0.173	0.186	0.200	0.232	0.232	0.122	0.144	0.160	0.174	0.188	0.202	0.232	0.232	0.232
		$\alpha=0.50$									$\alpha=0.75$								
$\lambda_{20^{\circ}\text{C}}=0.00$	R1	0.957	1.000	1.000	1.000	1.000	1.000	1.000	1.000	1.000	1.000	1.000	1.000	1.000	1.000	1.000	1.000	1.000	1.000
	R2	0.931	1.000	1.000	1.000	1.000	1.000	1.000	1.000	1.000	1.000	1.000	1.000	1.000	1.000	1.000	1.000	1.000	1.000
	R3	0.918	1.000	1.000	1.000	1.000	1.000	1.000	1.000	1.000	0.989	1.000	1.000	1.000	1.000	1.000	1.000	1.000	1.000
	R4	0.870	1.000	1.000	1.000	1.000	1.000	1.000	1.000	1.000	0.945	1.000	1.000	1.000	1.000	1.000	1.000	1.000	1.000
$\lambda_{20^{\circ}\text{C}}=0.25$	R1	0.744	0.851	0.935	0.993	0.993	0.993	0.											

$\theta_{\text{nom}} = 400^{\circ}\text{C}$

$p_{f,fi} \rightarrow$	0.10	0.20	0.30	0.40	0.50	0.60	0.70	0.80	0.90	0.10	0.20	0.30	0.40	0.50	0.60	0.70	0.80	0.90
$\beta_{f,fi} \rightarrow$	1.28	0.84	0.52	0.40	0.00	-0.25	-0.52	-0.84	-1.28	1.28	0.84	0.52	0.40	0.00	-0.25	-0.52	-0.84	-1.28
$\delta_{af} \rightarrow$	1.15	1.02	0.94	0.88	0.82	0.77	0.72	0.67	0.60	1.15	1.02	0.94	0.88	0.82	0.77	0.72	0.67	0.60
	$\alpha=0.00$									$\alpha=0.25$								
$\lambda_{20^{\circ}\text{C}}=0.00$	R1	0.757	0.853	0.926	0.992	1.000	1.000	1.000	1.000	0.818	0.924	1.000	1.000	1.000	1.000	1.000	1.000	1.000
	R2	0.617	0.744	0.832	0.910	0.984	1.000	1.000	1.000	0.667	0.805	0.903	0.987	1.000	1.000	1.000	1.000	1.000
	R3	0.579	0.727	0.824	0.902	0.975	1.000	1.000	1.000	0.627	0.787	0.892	0.980	1.000	1.000	1.000	1.000	1.000
	R4	0.517	0.678	0.787	0.874	0.954	1.000	1.000	1.000	0.561	0.735	0.854	0.949	1.000	1.000	1.000	1.000	1.000
$\lambda_{20^{\circ}\text{C}}=0.25$	R1	0.583	0.660	0.717	0.768	0.818	0.870	0.929	0.993	0.632	0.716	0.779	0.836	0.891	0.950	0.993	0.993	0.993
	R2	0.475	0.574	0.644	0.704	0.762	0.820	0.883	0.961	0.513	0.622	0.699	0.765	0.829	0.894	0.965	0.993	0.993
	R3	0.446	0.561	0.636	0.698	0.755	0.813	0.877	0.954	0.485	0.608	0.690	0.758	0.822	0.886	0.956	0.993	0.993
	R4	0.400	0.523	0.609	0.677	0.738	0.800	0.866	0.945	0.433	0.568	0.660	0.735	0.803	0.871	0.943	0.993	0.993
$\lambda_{20^{\circ}\text{C}}=0.50$	R1	0.441	0.501	0.546	0.586	0.625	0.667	0.714	0.773	0.477	0.542	0.592	0.636	0.680	0.725	0.778	0.843	0.951
	R2	0.354	0.431	0.486	0.536	0.583	0.628	0.677	0.741	0.383	0.467	0.527	0.581	0.633	0.683	0.739	0.809	0.951
	R3	0.332	0.422	0.481	0.529	0.574	0.619	0.670	0.731	0.359	0.457	0.521	0.574	0.624	0.674	0.729	0.797	0.951
	R4	0.292	0.391	0.459	0.514	0.564	0.610	0.660	0.720	0.318	0.425	0.498	0.558	0.613	0.664	0.719	0.786	0.885
$\lambda_{20^{\circ}\text{C}}=0.75$	R1	0.360	0.410	0.449	0.484	0.519	0.556	0.599	0.655	0.389	0.444	0.487	0.526	0.564	0.606	0.653	0.714	0.876
	R2	0.284	0.351	0.397	0.440	0.481	0.519	0.566	0.625	0.308	0.380	0.431	0.478	0.523	0.565	0.615	0.681	0.876
	R3	0.265	0.342	0.393	0.434	0.472	0.511	0.557	0.612	0.286	0.371	0.426	0.471	0.513	0.557	0.607	0.667	0.758
	R4	0.230	0.316	0.375	0.422	0.464	0.502	0.547	0.600	0.250	0.343	0.407	0.458	0.505	0.547	0.596	0.655	0.745
$\lambda_{20^{\circ}\text{C}}=1.00$	R1	0.298	0.339	0.372	0.401	0.430	0.461	0.497	0.547	0.322	0.368	0.403	0.436	0.468	0.502	0.542	0.596	0.725
	R2	0.234	0.290	0.329	0.365	0.398	0.431	0.469	0.520	0.254	0.314	0.357	0.397	0.433	0.468	0.511	0.568	0.725
	R3	0.217	0.283	0.325	0.359	0.391	0.423	0.462	0.507	0.235	0.307	0.353	0.390	0.426	0.461	0.504	0.553	0.725
	R4	0.187	0.261	0.310	0.349	0.384	0.417	0.453	0.498	0.203	0.283	0.336	0.379	0.418	0.453	0.495	0.543	0.725
$\lambda_{20^{\circ}\text{C}}=1.50$	R1	0.184	0.208	0.227	0.244	0.261	0.279	0.300	0.326	0.198	0.225	0.246	0.265	0.284	0.304	0.327	0.395	0.395
	R2	0.145	0.179	0.202	0.224	0.244	0.262	0.284	0.312	0.157	0.194	0.219	0.243	0.265	0.285	0.309	0.340	0.395
	R3	0.133	0.175	0.200	0.220	0.239	0.258	0.280	0.307	0.145	0.189	0.217	0.239	0.261	0.281	0.306	0.334	0.395
	R4	0.115	0.161	0.191	0.215	0.235	0.254	0.276	0.301	0.125	0.175	0.207	0.233	0.256	0.277	0.301	0.329	0.395
$\lambda_{20^{\circ}\text{C}}=2.00$	R1	0.113	0.128	0.139	0.149	0.159	0.170	0.182	0.198	0.122	0.138	0.151	0.162	0.173	0.185	0.199	0.215	0.232
	R2	0.089	0.110	0.124	0.137	0.149	0.160	0.173	0.189	0.097	0.119	0.135	0.149	0.162	0.174	0.188	0.207	0.232
	R3	0.082	0.108	0.123	0.135	0.147	0.158	0.171	0.187	0.089	0.117	0.133	0.147	0.160	0.172	0.186	0.203	0.232
	R4	0.071	0.099	0.118	0.132	0.144	0.156	0.169	0.184	0.077	0.108	0.127	0.143	0.157	0.170	0.184	0.200	0.232
	$\alpha=0.50$									$\alpha=0.75$								
$\lambda_{20^{\circ}\text{C}}=0.00$	R1	0.890	1.000	1.000	1.000	1.000	1.000	1.000	1.000	0.970	1.000	1.000	1.000	1.000	1.000	1.000	1.000	1.000
	R2	0.733	0.891	1.000	1.000	1.000	1.000	1.000	1.000	0.813	1.000	1.000	1.000	1.000	1.000	1.000	1.000	1.000
	R3	0.693	0.871	0.998	1.000	1.000	1.000	1.000	1.000	0.778	1.000	1.000	1.000	1.000	1.000	1.000	1.000	1.000
	R4	0.623	0.814	0.953	1.000	1.000	1.000	1.000	1.000	0.712	0.944	1.000	1.000	1.000	1.000	1.000	1.000	1.000
$\lambda_{20^{\circ}\text{C}}=0.25$	R1	0.690	0.795	0.877	0.949	0.993	0.993	0.993	0.993	0.750	0.917	0.993	0.993	0.993	0.993	0.993	0.993	0.993
	R2	0.567	0.690	0.782	0.865	0.945	0.993	0.993	0.993	0.631	0.798	0.936	0.993	0.993	0.993	0.993	0.993	0.993
	R3	0.535	0.673	0.772	0.857	0.937	0.993	0.993	0.993	0.600	0.778	0.921	0.993	0.993	0.993	0.993	0.993	0.993
	R4	0.481	0.629	0.737	0.829	0.915	0.993	0.993	0.993	0.548	0.729	0.878	0.993	0.993	0.993	0.993	0.993	0.993
$\lambda_{20^{\circ}\text{C}}=0.50$	R1	0.521	0.602	0.665	0.722	0.778	0.837	0.951	0.951	0.569	0.696	0.802	0.951	0.951	0.951	0.951	0.951	0.951
	R2	0.422	0.518	0.590	0.656	0.721	0.784	0.853	0.951	0.471	0.599	0.706	0.812	0.951	0.951	0.951	0.951	0.951
	R3	0.396	0.506	0.583	0.648	0.710	0.773	0.844	0.951	0.447	0.586	0.696	0.802	0.951	0.951	0.951	0.951	0.951
	R4	0.354	0.472	0.556	0.629	0.697	0.762	0.832	0.951	0.405	0.548	0.664	0.772	0.880	0.951	0.951	0.951	0.951
$\lambda_{20^{\circ}\text{C}}=0.75$	R1	0.427	0.495	0.548	0.598	0.647	0.699	0.758	0.876	0.467	0.573	0.663	0.750	0.876	0.876	0.876	0.876	0.876
	R2	0.340	0.423	0.483	0.541	0.596	0.650	0.712	0.876	0.380	0.489	0.580	0.670	0.761	0.876	0.876	0.876	0.876
	R3	0.317	0.412	0.477	0.533	0.586	0.640	0.702	0.876	0.361	0.478	0.572	0.660	0.749	0.876	0.876	0.876	0.876
	R4	0.280	0.380	0.453	0.517	0.575	0.629	0.689	0.876	0.324	0.444	0.543	0.635	0.728	0.876	0.876	0.876	0.876
$\lambda_{20^{\circ}\text{C}}=1.00$	R1	0.353	0.410	0.454	0.495	0.536	0.579	0.725	0.725	0.386	0.476	0.550	0.725	0.725	0.725	0.725	0.725	0.725
	R2	0.279	0.349	0.400	0.448	0.494	0.538	0.591	0.725	0.313	0.403	0.479	0.556	0.725	0.725	0.725	0.725	0.725
	R3	0.260	0.341	0.395	0.442	0.486	0.530	0.583	0.725	0.294	0.395	0.473	0.546	0.725	0.725	0.725	0.725	0.725
	R4	0.227	0.314	0.376	0.428	0.476	0.521	0.572	0.725	0.264	0.366	0.448	0.526	0.604	0.725	0.725	0.725	0.725
$\lambda_{20^{\circ}\text{C}}=1.50$	R1	0.217	0.251	0.277	0.302	0.325	0.351	0.395	0.395	0.236	0.290	0.335	0.395	0.395	0.395	0.395	0.395	0.395
	R2	0.172	0.215	0.246	0.274	0.302	0.328	0.395	0.395	0.192	0.248	0.294	0.339	0.395	0.395	0.395	0.395	0.395
	R3	0.160	0.210	0.243	0.271	0.297	0.324	0.395	0.395	0.181	0.242	0.289	0.334	0.395	0.395	0.395	0.395	0.395
	R4	0.139	0.194	0.232	0.263	0.292	0.318	0.348	0.395	0.162	0.224	0.274	0.322	0.395	0.395	0.395	0.395	0.395
$\lambda_{20^{\circ}\text{C}}=2.00$	R1	0.133	0.154	0.170	0.184	0.199	0.214	0.232	0.232	0.145	0.178	0.205	0.232	0.232	0.232	0.232	0.232	0.232
	R2	0.106	0.132	0.151	0.168	0.185	0.200	0.232	0.232	0.119	0.152	0.180	0.207	0.232	0.232	0.232	0.232	0.232
	R3	0.099	0.129	0.149	0.166	0.182	0.198	0.232	0.232	0.111	0.148	0.178	0.204	0.232	0.232	0.232	0.232	0.232
	R4	0.086	0.119	0.143	0.161	0.179	0.195	0.213	0.232	0.099	0.137	0.168	0.196	0.232	0.232	0.232	0.232	0.232

$\theta_{\text{nom}} = 500^{\circ}\text{C}$

$p_{f,fi} \rightarrow$	0.10	0.20	0.30	0.40	0.50	0.60	0.70	0.80	0.90	0.10	0.20	0.30	0.40	0.50	0.60	0.70	0.80	0.90
$\beta_{f,fi} \rightarrow$	1.28	0.84	0.52	0.40	0.00	-0.25	-0.52	-0.84	-1.28	1.28	0.84	0.52	0.40	0.00	-0.25	-0.52	-0.84	-1.28
$\delta_{af} \rightarrow$	1.15	1.02	0.94	0.88	0.82	0.77	0.72	0.67	0.60	1.15	1.02	0.94	0.88	0.82	0.77	0.72	0.67	0.60
	$\alpha=0.00$									$\alpha=0.25$								
$\lambda_{20^{\circ}\text{C}}=0.00$	R1	0.421	0.525	0.611	0.693	0.785	0.870	0.962	1.000	1.000	0.456	0.571	0.664	0.752	0.851	0.945	1.000	1.000
	R2	0.329	0.457	0.571	0.665	0.751	0.836	0.927	1.000	1.000	0.357	0.496	0.618	0.721	0.817	0.909	1.000	1.000
	R3	0.276	0.397	0.508	0.612	0.714	0.810	0.913	1.000	1.000	0.299	0.431	0.552	0.665	0.775	0.880	0.993	1.000
	R4	0.217	0.318	0.440	0.556	0.670	0.783	0.897	1.000	1.000	0.237	0.347	0.478	0.604	0.729	0.852	0.976	1.000
$\lambda_{20^{\circ}\text{C}}=0.25$	R1	0.325	0.405	0.471	0.534	0.603	0.672	0.745	0.831	0.952	0.352	0.440	0.512	0.580	0.656	0.731	0.812	0.907
	R2	0.254	0.352	0.440	0.514	0.581	0.645	0.717	0.806	0.931	0.276	0.382	0.478	0.558	0.632	0.702	0.781	0.878
	R3	0.213	0.307	0.392	0.472	0.550	0.626	0.707	0.797	0.921	0.231	0.333	0.425	0.513	0.598	0.681	0.770	0.870
	R4	0.168	0.246	0.340	0.429	0.517	0.605	0.693	0.786	0.907	0.183	0.268	0.368	0.466	0.563	0.658	0.754	0.858
$\lambda_{20^{\circ}\text{C}}=0.50$	R1	0.235	0.297	0.349	0.398	0.452	0.505	0.560	0.626	0.721	0.255	0.322	0.378	0.432	0.491	0.549	0.610	0.682
	R2	0.181	0.255	0.323	0.381	0.433	0.483	0.538	0.606	0.703	0.196	0.277	0.351	0.414	0.470	0.525	0.585	0.660
	R3	0.151	0.220	0.285	0.349	0.411	0.468	0.531	0.599	0.692	0.163	0.239	0.310	0.379	0.446	0.509	0.577	0.652
	R4	0.118	0.175	0.245	0.314	0.384	0.453	0.521	0.590	0.679	0.130	0.190	0.266	0.341	0.417	0.492	0.566	0.643
$\lambda_{20^{\circ}\text{C}}=0.75$	R1	0.182	0.234	0.278	0.320	0.367	0.411	0.458	0.512	0.597	0.198	0.254	0.302	0.348	0.399	0.447	0.499	0.559
	R2	0.138	0.199	0.256	0.306	0.351	0.393	0.439	0.495	0.580	0.150	0.216	0.278	0.332	0.381	0.427	0.477	0.540
	R3	0.114	0.170	0.223	0.277	0.331	0.381	0.433	0.490	0.566	0.124	0.184	0.242	0.302	0.360	0.414	0.471	0.535
	R4	0.091	0.133	0.190	0.248	0.308	0.367	0.425	0.481	0.554	0.099	0.145	0.206	0.269	0.335	0.399	0.462	0.525
$\lambda_{20^{\circ}\text{C}}=1.00$	R1	0.146	0.190	0.228	0.264	0.304	0.341	0.379	0.424	0.495	0.159	0.206	0.248	0.287	0.330	0.370	0.413	0.462
	R2	0.109	0.160	0.209	0.252	0.290	0.325	0.363	0.410	0.480	0.118	0.173	0.227	0.273	0.315	0.354	0.395	0.447
	R3	0.089	0.135	0.180	0.227	0.273	0.315	0.358	0.406	0.469	0.097	0.147	0.196	0.247	0.297	0.342	0.390	0.443
	R4	0.072	0.105	0.152	0.201	0.254	0.304	0.352	0.399	0.458	0.077	0.114	0.165	0.219	0.275	0.330	0.383	0.435
$\lambda_{20^{\circ}\text{C}}=1.50$	R1	0.089	0.117	0.140	0.163	0.188	0.210	0.234	0.260	0.301	0.097	0.127	0.153	0.177	0.204	0.228	0.254	0.284
	R2	0.066	0.097	0.128	0.155	0.179	0.201	0.224	0.252	0.293	0.071	0.106	0.140	0.169	0.194	0.218	0.244	0.275
	R3	0.054	0.082	0.110	0.140	0.169	0.194	0.221	0.250	0.288	0.059	0.089	0.120	0.152	0.183	0.211	0.240	0.272
	R4	0.044	0.063	0.092	0.124	0.157	0.188	0.217	0.246	0.282	0.047	0.069	0.100	0.134	0.170	0.204	0.236	0.268
$\lambda_{20^{\circ}\text{C}}=2.00$	R1	0.055	0.072	0.087	0.101	0.116	0.129	0.143	0.160	0.184	0.060	0.078	0.094	0.109	0.126	0.140	0.156	0.174
	R2	0.040	0.060	0.079	0.096	0.110	0.124	0.138	0.155	0.180	0.044	0.065	0.086	0.104	0.120	0.135	0.150	0.169
	R3	0.033	0.051	0.068	0.086	0.104	0.120	0.136	0.153	0.177	0.036	0.055	0.074	0.094	0.113	0.130	0.148	0.167
	R4	0.027	0.039	0.057	0.076	0.096	0.116	0.134	0.151	0.173	0.029	0.042	0.062	0.083	0.105	0.126	0.145	0.165
	$\alpha=0.50$									$\alpha=0.75$								
$\lambda_{20^{\circ}\text{C}}=0.00$	R1	0.506	0.639	0.747	0.848	0.964	1.000	1.000	1.000	1.000	0.580	0.756	0.905	1.000	1.000	1.000	1.000	1.000
	R2	0.400	0.558	0.697	0.815	0.927	1.000	1.000	1.000	1.000	0.478	0.667	0.844	1.000	1.000	1.000	1.000	1.000
	R3	0.338	0.486	0.621	0.750	0.878	1.000	1.000	1.000	1.000	0.409	0.588	0.755	0.921	1.000	1.000	1.000	1.000
	R4	0.268	0.392	0.539	0.683	0.823	0.966	1.000	1.000	1.000	0.325	0.486	0.659	0.840	1.000	1.000	1.000	1.000
$\lambda_{20^{\circ}\text{C}}=0.25$	R1	0.391	0.493	0.576	0.657	0.742	0.835	0.935	0.993	0.993	0.447	0.582	0.698	0.812	0.935	0.993	0.993	0.993
	R2	0.309	0.430	0.538	0.632	0.717	0.804	0.899	0.993	0.993	0.367	0.514	0.652	0.779	0.904	0.993	0.993	0.993
	R3	0.260	0.374	0.480	0.580	0.678	0.777	0.882	0.993	0.993	0.315	0.452	0.583	0.713	0.848	0.993	0.993	0.993
	R4	0.207	0.304	0.416	0.527	0.636	0.747	0.863	0.993	0.993	0.251	0.376	0.509	0.648	0.791	0.944	0.993	0.993
$\lambda_{20^{\circ}\text{C}}=0.50$	R1	0.284	0.361	0.425	0.487	0.556	0.626	0.701	0.789	0.951	0.327	0.429	0.516	0.601	0.694	0.803	0.951	0.951
	R2	0.220	0.312	0.395	0.467	0.534	0.599	0.672	0.763	0.951	0.264	0.374	0.478	0.575	0.670	0.770	0.887	0.951
	R3	0.185	0.270	0.350	0.427	0.504	0.579	0.661	0.755	0.885	0.225	0.327	0.426	0.524	0.626	0.737	0.861	0.951
	R4	0.147	0.216	0.301	0.387	0.471	0.557	0.647	0.744	0.869	0.179	0.269	0.368	0.475	0.584	0.701	0.837	0.951
$\lambda_{20^{\circ}\text{C}}=0.75$	R1	0.220	0.285	0.339	0.392	0.452	0.509	0.572	0.648	0.876	0.255	0.339	0.411	0.482	0.562	0.653	0.759	0.876
	R2	0.168	0.243	0.313	0.374	0.432	0.488	0.548	0.626	0.742	0.202	0.293	0.380	0.459	0.542	0.624	0.724	0.876
	R3	0.140	0.208	0.273	0.341	0.407	0.469	0.539	0.619	0.725	0.172	0.253	0.334	0.417	0.504	0.597	0.703	0.876
	R4	0.112	0.164	0.233	0.305	0.379	0.453	0.529	0.609	0.711	0.137	0.205	0.286	0.375	0.466	0.568	0.684	0.876
$\lambda_{20^{\circ}\text{C}}=1.00$	R1	0.178	0.232	0.278	0.323	0.373	0.421	0.474	0.536	0.725	0.207	0.277	0.338	0.397	0.463	0.540	0.725	0.725
	R2	0.133	0.195	0.256	0.308	0.357	0.403	0.454	0.518	0.725	0.162	0.237	0.310	0.378	0.446	0.516	0.598	0.725
	R3	0.110	0.166	0.222	0.279	0.336	0.388	0.446	0.512	0.601	0.136	0.203	0.272	0.341	0.415	0.493	0.580	0.725
	R4	0.088	0.129	0.187	0.247	0.311	0.374	0.438	0.504	0.588	0.108	0.163	0.231	0.306	0.383	0.468	0.565	0.725
$\lambda_{20^{\circ}\text{C}}=1.50$	R1	0.108	0.142	0.172	0.200	0.231	0.261	0.292	0.330	0.395	0.126	0.170	0.208	0.245	0.285	0.333	0.395	0.395
	R2	0.080	0.119	0.157	0.190	0.220	0.249	0.280	0.319	0.395	0.097	0.144	0.190	0.232	0.275	0.318	0.395	0.395
	R3	0.066	0.101	0.136	0.171	0.207	0.240	0.275	0.315	0.395	0.082	0.123	0.166	0.210	0.255	0.303	0.395	0.395
	R4	0.053	0.078	0.114	0.152	0.191	0.231	0.269	0.311	0.395	0.066	0.099	0.140	0.187	0.235	0.288	0.347	0.395
$\lambda_{20^{\circ}\text{C}}=2.00$	R1	0.067	0.088	0.106	0.123	0.142	0.160	0.179	0.203	0.232	0.078	0.104	0.128	0.150	0.175	0.205	0.232	0.232
	R2	0.049	0.073	0.097	0.117	0.136	0.153	0.172	0.196	0.232	0.060	0.089	0.117	0.143	0.169	0.196	0.232	0.232
	R3	0.041	0.062	0.084	0.106	0.128	0.148	0.169	0.193	0.232	0.051	0.075	0.102	0.129	0.157	0.187	0.232	0.232
	R4	0.033	0.048	0.070	0.094	0.118	0.142	0.166	0.191	0.232	0.040	0.061	0.086	0.115	0.145	0.177	0.213	0.232

$\theta_{\text{nom}} = 600^{\circ}\text{C}$

$p_{f,fi} \rightarrow$	0.10	0.20	0.30	0.40	0.50	0.60	0.70	0.80	0.90	0.10	0.20	0.30	0.40	0.50	0.60	0.70	0.80	0.90
$\beta_{f,fi} \rightarrow$	1.28	0.84	0.52	0.40	0.00	-0.25	-0.52	-0.84	-1.28	1.28	0.84	0.52	0.40	0.00	-0.25	-0.52	-0.84	-1.28
$\delta_{af} \rightarrow$	1.15	1.02	0.94	0.88	0.82	0.77	0.72	0.67	0.60	1.15	1.02	0.94	0.88	0.82	0.77	0.72	0.67	0.60
	$\alpha=0.00$									$\alpha=0.25$								
$\lambda_{20^{\circ}\text{C}}=0.00$	R1	0.371	0.475	0.558	0.638	0.717	0.800	0.892	1.000	0.402	0.516	0.606	0.694	0.780	0.870	0.970	1.000	1.000
	R2	0.210	0.269	0.333	0.405	0.481	0.560	0.661	0.783	0.227	0.292	0.362	0.439	0.523	0.609	0.719	0.852	1.000
	R3	0.194	0.251	0.312	0.385	0.462	0.542	0.629	0.751	0.210	0.272	0.339	0.419	0.503	0.590	0.684	0.817	1.000
	R4	0.147	0.204	0.252	0.316	0.396	0.490	0.603	0.726	0.160	0.221	0.274	0.343	0.432	0.532	0.654	0.790	0.957
$\lambda_{20^{\circ}\text{C}}=0.25$	R1	0.285	0.366	0.431	0.493	0.554	0.619	0.689	0.774	0.310	0.398	0.468	0.535	0.603	0.674	0.753	0.846	0.979
	R2	0.162	0.208	0.258	0.312	0.371	0.434	0.508	0.605	0.175	0.226	0.280	0.340	0.404	0.472	0.554	0.658	0.819
	R3	0.150	0.193	0.241	0.297	0.357	0.418	0.488	0.580	0.162	0.210	0.262	0.323	0.387	0.454	0.532	0.631	0.785
	R4	0.114	0.158	0.195	0.243	0.306	0.377	0.463	0.559	0.124	0.170	0.212	0.265	0.333	0.411	0.504	0.610	0.743
$\lambda_{20^{\circ}\text{C}}=0.50$	R1	0.205	0.266	0.316	0.364	0.412	0.462	0.516	0.580	0.222	0.289	0.343	0.395	0.447	0.502	0.561	0.632	0.731
	R2	0.115	0.147	0.183	0.225	0.268	0.316	0.375	0.450	0.124	0.160	0.199	0.244	0.292	0.343	0.408	0.490	0.612
	R3	0.106	0.137	0.171	0.213	0.258	0.304	0.357	0.431	0.115	0.149	0.186	0.231	0.280	0.331	0.388	0.469	0.585
	R4	0.083	0.112	0.138	0.173	0.220	0.274	0.341	0.414	0.090	0.122	0.150	0.188	0.239	0.297	0.371	0.451	0.552
$\lambda_{20^{\circ}\text{C}}=0.75$	R1	0.157	0.207	0.250	0.291	0.333	0.375	0.421	0.475	0.171	0.225	0.271	0.316	0.362	0.408	0.458	0.517	0.598
	R2	0.087	0.111	0.140	0.172	0.208	0.248	0.300	0.365	0.094	0.121	0.152	0.187	0.226	0.270	0.326	0.397	0.499
	R3	0.081	0.104	0.130	0.163	0.199	0.239	0.283	0.348	0.088	0.112	0.141	0.177	0.217	0.259	0.308	0.379	0.477
	R4	0.065	0.086	0.105	0.131	0.168	0.213	0.270	0.333	0.071	0.093	0.114	0.143	0.183	0.231	0.293	0.363	0.448
$\lambda_{20^{\circ}\text{C}}=1.00$	R1	0.126	0.167	0.203	0.239	0.274	0.310	0.349	0.393	0.136	0.182	0.221	0.260	0.298	0.337	0.379	0.428	0.495
	R2	0.068	0.087	0.110	0.137	0.167	0.201	0.246	0.301	0.074	0.095	0.120	0.149	0.182	0.219	0.267	0.328	0.414
	R3	0.064	0.081	0.102	0.130	0.160	0.193	0.231	0.286	0.070	0.089	0.111	0.141	0.174	0.210	0.251	0.312	0.395
	R4	0.053	0.068	0.082	0.103	0.134	0.171	0.219	0.274	0.057	0.073	0.089	0.112	0.146	0.186	0.239	0.298	0.371
$\lambda_{20^{\circ}\text{C}}=1.50$	R1	0.076	0.102	0.125	0.147	0.170	0.192	0.215	0.242	0.083	0.111	0.135	0.160	0.184	0.209	0.234	0.264	0.305
	R2	0.041	0.052	0.066	0.083	0.102	0.123	0.151	0.186	0.045	0.057	0.072	0.091	0.111	0.134	0.164	0.203	0.255
	R3	0.039	0.049	0.061	0.079	0.097	0.118	0.142	0.177	0.042	0.053	0.067	0.085	0.106	0.128	0.154	0.193	0.244
	R4	0.033	0.041	0.050	0.062	0.081	0.104	0.135	0.169	0.035	0.045	0.054	0.068	0.088	0.113	0.147	0.184	0.229
$\lambda_{20^{\circ}\text{C}}=2.00$	R1	0.047	0.063	0.077	0.091	0.105	0.118	0.132	0.149	0.051	0.068	0.083	0.099	0.114	0.129	0.144	0.162	0.187
	R2	0.025	0.032	0.041	0.051	0.063	0.076	0.093	0.115	0.027	0.035	0.044	0.056	0.068	0.082	0.101	0.125	0.157
	R3	0.024	0.030	0.038	0.048	0.060	0.073	0.087	0.109	0.026	0.033	0.041	0.053	0.065	0.079	0.095	0.119	0.150
	R4	0.020	0.025	0.031	0.038	0.050	0.064	0.083	0.104	0.022	0.027	0.033	0.042	0.054	0.070	0.090	0.113	0.141
	$\alpha=0.50$									$\alpha=0.75$								
$\lambda_{20^{\circ}\text{C}}=0.00$	R1	0.449	0.579	0.683	0.783	0.887	0.995	1.000	1.000	0.525	0.689	0.832	0.972	1.000	1.000	1.000	1.000	1.000
	R2	0.255	0.331	0.410	0.499	0.595	0.697	0.822	0.979	0.301	0.408	0.510	0.622	0.753	0.896	1.000	1.000	1.000
	R3	0.235	0.309	0.386	0.475	0.571	0.674	0.787	0.940	0.276	0.382	0.484	0.595	0.721	0.863	1.000	1.000	1.000
	R4	0.178	0.250	0.313	0.391	0.491	0.605	0.749	0.911	0.208	0.305	0.396	0.498	0.621	0.773	0.962	1.000	1.000
$\lambda_{20^{\circ}\text{C}}=0.25$	R1	0.345	0.447	0.529	0.606	0.685	0.769	0.865	0.980	0.405	0.534	0.645	0.755	0.871	0.993	0.993	0.993	0.993
	R2	0.196	0.256	0.317	0.385	0.459	0.540	0.634	0.758	0.231	0.314	0.394	0.481	0.581	0.691	0.826	0.993	0.993
	R3	0.181	0.238	0.298	0.366	0.440	0.520	0.610	0.727	0.212	0.295	0.374	0.460	0.557	0.669	0.798	0.966	0.993
	R4	0.138	0.193	0.242	0.302	0.379	0.468	0.577	0.703	0.159	0.235	0.306	0.386	0.481	0.597	0.744	0.940	0.993
$\lambda_{20^{\circ}\text{C}}=0.50$	R1	0.248	0.325	0.387	0.447	0.508	0.573	0.645	0.732	0.292	0.388	0.472	0.555	0.641	0.739	0.852	0.951	0.951
	R2	0.139	0.182	0.226	0.277	0.332	0.392	0.467	0.562	0.165	0.224	0.281	0.346	0.419	0.503	0.605	0.742	0.951
	R3	0.129	0.169	0.212	0.262	0.319	0.378	0.445	0.538	0.152	0.210	0.266	0.330	0.402	0.485	0.582	0.710	0.951
	R4	0.100	0.137	0.172	0.215	0.272	0.339	0.423	0.518	0.117	0.169	0.218	0.275	0.345	0.432	0.544	0.689	0.886
$\lambda_{20^{\circ}\text{C}}=0.75$	R1	0.191	0.254	0.306	0.358	0.410	0.465	0.526	0.598	0.225	0.306	0.375	0.444	0.518	0.598	0.693	0.876	0.876
	R2	0.106	0.137	0.172	0.212	0.258	0.308	0.373	0.455	0.126	0.170	0.214	0.266	0.327	0.396	0.481	0.595	0.876
	R3	0.098	0.128	0.161	0.201	0.247	0.296	0.353	0.433	0.117	0.160	0.203	0.253	0.312	0.380	0.461	0.569	0.754
	R4	0.079	0.105	0.130	0.163	0.208	0.263	0.335	0.417	0.092	0.129	0.166	0.209	0.265	0.336	0.429	0.548	0.715
$\lambda_{20^{\circ}\text{C}}=1.00$	R1	0.153	0.205	0.249	0.293	0.338	0.384	0.436	0.495	0.180	0.247	0.305	0.363	0.424	0.492	0.572	0.725	0.725
	R2	0.083	0.108	0.136	0.169	0.208	0.250	0.306	0.375	0.100	0.135	0.171	0.213	0.263	0.321	0.393	0.488	0.725
	R3	0.078	0.100	0.127	0.161	0.198	0.240	0.288	0.357	0.093	0.126	0.161	0.202	0.251	0.307	0.376	0.467	0.725
	R4	0.064	0.083	0.103	0.128	0.165	0.212	0.272	0.343	0.075	0.103	0.132	0.166	0.211	0.270	0.349	0.451	0.589
$\lambda_{20^{\circ}\text{C}}=1.50$	R1	0.092	0.125	0.153	0.181	0.208	0.237	0.269	0.305	0.109	0.152	0.187	0.223	0.261	0.303	0.395	0.395	0.395
	R2	0.050	0.065	0.082	0.103	0.126	0.153	0.188	0.231	0.060	0.081	0.103	0.129	0.160	0.197	0.242	0.302	0.395
	R3	0.047	0.061	0.076	0.097	0.121	0.147	0.177	0.220	0.056	0.076	0.097	0.122	0.153	0.188	0.230	0.288	0.395
	R4	0.039	0.051	0.062	0.077	0.100	0.129	0.167	0.211	0.046	0.063	0.080	0.100	0.128	0.165	0.214	0.277	0.395
$\lambda_{20^{\circ}\text{C}}=2.00$	R1	0.057	0.077	0.094	0.111	0.129	0.146	0.165	0.188	0.067	0.093	0.115	0.138	0.161	0.187	0.232	0.232	0.232
	R2	0.031	0.040	0.050	0.063	0.078	0.094	0.116	0.143	0.037	0.050	0.063	0.079	0.099	0.121	0.149	0.186	0.232
	R3	0.029	0.037	0.047	0.060	0.074	0.090	0.109	0.136	0.035	0.047	0.060	0.075	0.094	0.115	0.142	0.177	0.232
	R4	0.024	0.031	0.038	0.047	0.062	0.080	0.103	0.130	0.029	0.039	0.049	0.061	0.078	0.101	0.132	0.171	0.232

$\theta_{\text{nom}} = 700^{\circ}\text{C}$

$p_{f,fi} \rightarrow$	0.10	0.20	0.30	0.40	0.50	0.60	0.70	0.80	0.90	0.10	0.20	0.30	0.40	0.50	0.60	0.70	0.80	0.90	
$\beta_{f,fi} \rightarrow$	1.28	0.84	0.52	0.40	0.00	-0.25	-0.52	-0.84	-1.28	1.28	0.84	0.52	0.40	0.00	-0.25	-0.52	-0.84	-1.28	
$\delta_{of} \rightarrow$	1.15	1.02	0.94	0.88	0.82	0.77	0.72	0.67	0.60	1.15	1.02	0.94	0.88	0.82	0.77	0.72	0.67	0.60	
	$\alpha=0.00$									$\alpha=0.25$									
$\lambda_{20^{\circ}\text{C}}=0.00$	R1	0.202	0.239	0.276	0.316	0.362	0.415	0.477	0.566	0.734	0.219	0.260	0.299	0.344	0.394	0.451	0.521	0.617	0.797
	R2	0.148	0.186	0.214	0.242	0.273	0.317	0.380	0.474	0.634	0.159	0.201	0.233	0.263	0.297	0.345	0.414	0.515	0.692
	R3	0.113	0.162	0.196	0.225	0.262	0.306	0.361	0.443	0.569	0.123	0.175	0.213	0.245	0.285	0.333	0.392	0.482	0.619
	R4	0.058	0.099	0.143	0.183	0.218	0.262	0.332	0.422	0.525	0.063	0.107	0.156	0.198	0.237	0.286	0.361	0.460	0.573
$\lambda_{20^{\circ}\text{C}}=0.25$	R1	0.156	0.184	0.212	0.244	0.279	0.320	0.369	0.438	0.568	0.169	0.200	0.231	0.265	0.304	0.349	0.403	0.478	0.620
	R2	0.114	0.143	0.165	0.187	0.212	0.247	0.292	0.369	0.494	0.123	0.155	0.180	0.203	0.230	0.268	0.318	0.402	0.537
	R3	0.087	0.125	0.151	0.174	0.202	0.236	0.279	0.343	0.440	0.095	0.135	0.164	0.190	0.220	0.257	0.304	0.374	0.480
	R4	0.046	0.078	0.112	0.142	0.170	0.205	0.258	0.328	0.406	0.050	0.084	0.121	0.154	0.185	0.223	0.281	0.358	0.443
$\lambda_{20^{\circ}\text{C}}=0.50$	R1	0.110	0.130	0.150	0.173	0.199	0.229	0.266	0.317	0.418	0.119	0.142	0.163	0.188	0.217	0.249	0.290	0.345	0.455
	R2	0.083	0.102	0.117	0.132	0.150	0.174	0.209	0.267	0.359	0.090	0.111	0.127	0.144	0.164	0.189	0.227	0.290	0.391
	R3	0.066	0.090	0.108	0.123	0.143	0.167	0.198	0.246	0.318	0.072	0.098	0.117	0.134	0.155	0.182	0.216	0.267	0.347
	R4	0.039	0.060	0.082	0.102	0.121	0.145	0.184	0.233	0.292	0.042	0.065	0.089	0.111	0.131	0.158	0.200	0.254	0.320
$\lambda_{20^{\circ}\text{C}}=0.75$	R1	0.083	0.098	0.113	0.131	0.152	0.176	0.205	0.248	0.336	0.090	0.107	0.123	0.142	0.165	0.191	0.224	0.270	0.365
	R2	0.065	0.078	0.089	0.100	0.113	0.131	0.159	0.208	0.283	0.070	0.085	0.097	0.109	0.123	0.143	0.173	0.225	0.309
	R3	0.054	0.070	0.083	0.094	0.108	0.126	0.150	0.189	0.248	0.059	0.076	0.090	0.102	0.117	0.138	0.164	0.205	0.270
	R4	0.035	0.051	0.065	0.079	0.092	0.110	0.140	0.178	0.226	0.038	0.055	0.071	0.085	0.100	0.119	0.152	0.194	0.247
$\lambda_{20^{\circ}\text{C}}=1.00$	R1	0.066	0.077	0.089	0.103	0.120	0.140	0.165	0.200	0.275	0.071	0.084	0.097	0.112	0.131	0.152	0.179	0.218	0.300
	R2	0.052	0.062	0.070	0.078	0.089	0.103	0.126	0.166	0.230	0.056	0.067	0.076	0.085	0.097	0.113	0.138	0.181	0.251
	R3	0.045	0.057	0.066	0.074	0.085	0.099	0.119	0.151	0.201	0.049	0.061	0.071	0.081	0.093	0.108	0.130	0.164	0.219
	R4	0.030	0.043	0.053	0.063	0.073	0.086	0.110	0.142	0.182	0.033	0.047	0.058	0.068	0.079	0.094	0.120	0.155	0.198
$\lambda_{20^{\circ}\text{C}}=1.50$	R1	0.039	0.046	0.053	0.062	0.073	0.085	0.100	0.122	0.169	0.043	0.050	0.058	0.067	0.079	0.092	0.109	0.133	0.184
	R2	0.032	0.038	0.042	0.047	0.053	0.062	0.076	0.101	0.141	0.035	0.041	0.046	0.051	0.058	0.068	0.083	0.110	0.153
	R3	0.028	0.035	0.040	0.045	0.051	0.060	0.072	0.091	0.122	0.031	0.038	0.043	0.049	0.056	0.065	0.078	0.099	0.133
	R4	0.020	0.027	0.033	0.038	0.044	0.052	0.066	0.086	0.111	0.022	0.030	0.036	0.042	0.048	0.057	0.072	0.094	0.121
$\lambda_{20^{\circ}\text{C}}=2.00$	R1	0.024	0.028	0.033	0.038	0.045	0.052	0.062	0.075	0.104	0.026	0.031	0.036	0.041	0.048	0.057	0.067	0.082	0.114
	R2	0.020	0.023	0.026	0.029	0.033	0.038	0.047	0.062	0.087	0.022	0.025	0.028	0.032	0.036	0.042	0.051	0.068	0.094
	R3	0.018	0.022	0.025	0.028	0.031	0.037	0.044	0.056	0.075	0.019	0.023	0.027	0.030	0.034	0.040	0.048	0.061	0.082
	R4	0.012	0.017	0.021	0.024	0.027	0.032	0.041	0.053	0.068	0.014	0.019	0.022	0.026	0.030	0.035	0.044	0.058	0.074
	$\alpha=0.50$									$\alpha=0.75$									
$\lambda_{20^{\circ}\text{C}}=0.00$	R1	0.244	0.293	0.341	0.392	0.450	0.517	0.600	0.713	0.925	0.278	0.355	0.426	0.499	0.580	0.674	0.792	0.956	1.000
	R2	0.177	0.226	0.264	0.301	0.342	0.397	0.473	0.591	0.799	0.202	0.268	0.324	0.381	0.445	0.523	0.619	0.780	1.000
	R3	0.137	0.196	0.241	0.280	0.328	0.383	0.452	0.555	0.719	0.163	0.234	0.295	0.355	0.425	0.502	0.596	0.739	0.979
	R4	0.072	0.121	0.175	0.224	0.272	0.328	0.414	0.531	0.667	0.088	0.149	0.213	0.278	0.348	0.432	0.546	0.711	0.913
$\lambda_{20^{\circ}\text{C}}=0.25$	R1	0.187	0.226	0.263	0.302	0.347	0.399	0.463	0.553	0.715	0.214	0.275	0.330	0.386	0.449	0.521	0.613	0.741	0.966
	R2	0.136	0.174	0.203	0.232	0.264	0.309	0.365	0.461	0.626	0.156	0.206	0.251	0.295	0.343	0.405	0.479	0.610	0.847
	R3	0.106	0.151	0.185	0.216	0.252	0.296	0.349	0.430	0.558	0.126	0.181	0.228	0.275	0.328	0.389	0.462	0.572	0.763
	R4	0.057	0.096	0.137	0.174	0.212	0.257	0.323	0.413	0.515	0.070	0.117	0.166	0.216	0.272	0.338	0.425	0.547	0.709
$\lambda_{20^{\circ}\text{C}}=0.50$	R1	0.133	0.160	0.186	0.215	0.247	0.286	0.333	0.400	0.527	0.152	0.195	0.234	0.274	0.320	0.372	0.440	0.536	0.708
	R2	0.099	0.124	0.144	0.164	0.188	0.217	0.260	0.332	0.453	0.113	0.148	0.179	0.209	0.245	0.286	0.341	0.440	0.615
	R3	0.081	0.110	0.133	0.154	0.179	0.209	0.247	0.308	0.403	0.095	0.132	0.164	0.195	0.233	0.275	0.328	0.408	0.548
	R4	0.047	0.074	0.100	0.125	0.151	0.182	0.230	0.292	0.370	0.057	0.091	0.122	0.156	0.194	0.240	0.303	0.392	0.509
$\lambda_{20^{\circ}\text{C}}=0.75$	R1	0.100	0.121	0.140	0.162	0.188	0.219	0.257	0.312	0.422	0.115	0.148	0.177	0.208	0.243	0.285	0.340	0.419	0.566
	R2	0.077	0.095	0.110	0.124	0.142	0.165	0.198	0.259	0.357	0.089	0.114	0.136	0.159	0.185	0.217	0.261	0.339	0.483
	R3	0.066	0.086	0.101	0.117	0.136	0.158	0.189	0.236	0.313	0.077	0.103	0.126	0.149	0.177	0.209	0.250	0.313	0.427
	R4	0.042	0.062	0.080	0.097	0.115	0.138	0.174	0.224	0.287	0.050	0.075	0.098	0.122	0.149	0.183	0.230	0.301	0.393
$\lambda_{20^{\circ}\text{C}}=1.00$	R1	0.079	0.095	0.110	0.128	0.149	0.174	0.206	0.252	0.346	0.091	0.116	0.140	0.165	0.193	0.227	0.272	0.337	0.462
	R2	0.063	0.076	0.087	0.098	0.112	0.130	0.158	0.208	0.290	0.071	0.091	0.108	0.126	0.148	0.171	0.207	0.272	0.393
	R3	0.054	0.069	0.081	0.092	0.107	0.125	0.149	0.189	0.253	0.063	0.083	0.101	0.119	0.140	0.165	0.198	0.251	0.345
	R4	0.037	0.052	0.065	0.078	0.091	0.109	0.138	0.178	0.230	0.043	0.063	0.080	0.098	0.119	0.146	0.183	0.240	0.316
$\lambda_{20^{\circ}\text{C}}=1.50$	R1	0.047	0.057	0.066	0.077	0.090	0.106	0.125	0.153	0.213	0.055	0.070	0.084	0.099	0.116	0.138	0.165	0.205	0.284
	R2	0.038	0.046	0.053	0.059	0.067	0.078	0.095	0.126	0.177	0.043	0.055	0.065	0.076	0.089	0.103	0.125	0.165	0.239
	R3	0.034	0.042	0.049	0.056	0.064	0.075	0.090	0.114	0.154	0.040	0.051	0.061	0.072	0.085	0.099	0.119	0.151	0.209
	R4	0.024	0.033	0.041	0.048	0.055	0.066	0.083	0.108	0.140	0.028	0.040	0.050	0.061	0.073	0.088	0.110	0.145	0.191
$\lambda_{20^{\circ}\text{C}}=2.00$	R1	0.029	0.035	0.041	0.047	0.055	0.065	0.077	0.095	0.131	0.034	0.043	0.052	0.061	0.072	0.085	0.102	0.126	0.175
	R2	0.024	0.028	0.032	0.036	0.041	0.048	0.059	0.078	0.109	0.027	0.034	0.041	0.047	0.055	0.063	0.077	0.102	0.147
	R3	0.021	0.026	0.030	0.034	0.040	0.046	0.055	0.070	0.095	0.025	0.032	0.038	0.044	0.052	0.061	0.073	0.093	0.129
	R4	0.015	0.02																

$\theta_{\text{nom}} = 800^{\circ}\text{C}$

$p_{f,fi} \rightarrow$	0.10	0.20	0.30	0.40	0.50	0.60	0.70	0.80	0.90	0.10	0.20	0.30	0.40	0.50	0.60	0.70	0.80	0.90	
$\beta_{f,fi} \rightarrow$	1.28	0.84	0.52	0.40	0.00	-0.25	-0.52	-0.84	-1.28	1.28	0.84	0.52	0.40	0.00	-0.25	-0.52	-0.84	-1.28	
$\delta_{af} \rightarrow$	1.15	1.02	0.94	0.88	0.82	0.77	0.72	0.67	0.60	1.15	1.02	0.94	0.88	0.82	0.77	0.72	0.67	0.60	
	$\alpha=0.00$									$\alpha=0.25$									
$\lambda_{20^{\circ}\text{C}}=0.00$	R1	0.070	0.089	0.107	0.127	0.149	0.174	0.200	0.232	0.295	0.076	0.097	0.117	0.138	0.162	0.189	0.218	0.253	0.321
	R2	0.057	0.075	0.094	0.116	0.141	0.168	0.195	0.230	0.285	0.062	0.081	0.102	0.126	0.154	0.182	0.212	0.251	0.310
	R3	0.046	0.061	0.078	0.099	0.124	0.155	0.188	0.222	0.277	0.050	0.066	0.085	0.107	0.135	0.168	0.204	0.242	0.301
	R4	0.027	0.043	0.058	0.075	0.100	0.132	0.171	0.214	0.269	0.030	0.047	0.063	0.082	0.108	0.143	0.186	0.233	0.294
$\lambda_{20^{\circ}\text{C}}=0.25$	R1	0.054	0.069	0.083	0.098	0.115	0.134	0.155	0.180	0.230	0.059	0.075	0.090	0.106	0.125	0.145	0.168	0.196	0.251
	R2	0.045	0.058	0.072	0.089	0.109	0.129	0.150	0.178	0.221	0.049	0.063	0.079	0.097	0.118	0.140	0.164	0.193	0.241
	R3	0.036	0.048	0.061	0.076	0.096	0.120	0.146	0.173	0.214	0.039	0.052	0.066	0.083	0.104	0.130	0.159	0.189	0.233
	R4	0.023	0.035	0.046	0.061	0.080	0.105	0.134	0.166	0.208	0.025	0.038	0.051	0.066	0.087	0.114	0.146	0.181	0.227
$\lambda_{20^{\circ}\text{C}}=0.50$	R1	0.044	0.054	0.064	0.074	0.085	0.097	0.111	0.128	0.163	0.048	0.059	0.069	0.080	0.092	0.105	0.120	0.139	0.178
	R2	0.037	0.047	0.057	0.068	0.081	0.094	0.108	0.126	0.157	0.040	0.051	0.062	0.074	0.088	0.102	0.117	0.138	0.171
	R3	0.030	0.040	0.049	0.060	0.072	0.088	0.105	0.124	0.152	0.033	0.043	0.053	0.065	0.079	0.095	0.114	0.135	0.166
	R4	0.020	0.030	0.039	0.049	0.062	0.078	0.097	0.119	0.148	0.021	0.032	0.042	0.053	0.068	0.085	0.106	0.130	0.161
$\lambda_{20^{\circ}\text{C}}=0.75$	R1	0.039	0.046	0.053	0.060	0.067	0.076	0.085	0.097	0.124	0.042	0.050	0.058	0.065	0.073	0.082	0.093	0.106	0.134
	R2	0.034	0.042	0.049	0.057	0.065	0.074	0.083	0.096	0.119	0.036	0.045	0.053	0.062	0.071	0.080	0.090	0.105	0.129
	R3	0.028	0.036	0.043	0.051	0.060	0.069	0.081	0.094	0.115	0.030	0.039	0.047	0.055	0.065	0.076	0.088	0.103	0.126
	R4	0.018	0.027	0.035	0.043	0.053	0.064	0.076	0.091	0.112	0.019	0.029	0.038	0.047	0.057	0.069	0.083	0.099	0.122
$\lambda_{20^{\circ}\text{C}}=1.00$	R1	0.034	0.040	0.045	0.050	0.055	0.061	0.068	0.077	0.097	0.036	0.043	0.049	0.054	0.060	0.067	0.074	0.084	0.106
	R2	0.029	0.036	0.042	0.048	0.054	0.060	0.067	0.077	0.093	0.032	0.039	0.045	0.052	0.058	0.065	0.073	0.084	0.102
	R3	0.024	0.031	0.037	0.043	0.050	0.057	0.065	0.075	0.091	0.026	0.034	0.041	0.047	0.054	0.062	0.071	0.082	0.099
	R4	0.016	0.024	0.031	0.038	0.045	0.053	0.062	0.073	0.088	0.017	0.026	0.033	0.041	0.049	0.057	0.067	0.079	0.096
$\lambda_{20^{\circ}\text{C}}=1.50$	R1	0.022	0.026	0.029	0.032	0.035	0.038	0.042	0.047	0.059	0.024	0.028	0.031	0.034	0.038	0.041	0.046	0.051	0.064
	R2	0.019	0.023	0.027	0.030	0.034	0.037	0.041	0.047	0.056	0.021	0.025	0.029	0.033	0.037	0.040	0.045	0.051	0.062
	R3	0.016	0.020	0.024	0.028	0.031	0.035	0.040	0.046	0.055	0.017	0.022	0.026	0.030	0.034	0.039	0.044	0.050	0.060
	R4	0.010	0.016	0.020	0.024	0.029	0.033	0.038	0.044	0.053	0.011	0.017	0.022	0.026	0.031	0.036	0.041	0.048	0.058
$\lambda_{20^{\circ}\text{C}}=2.00$	R1	0.014	0.016	0.018	0.020	0.021	0.023	0.026	0.029	0.036	0.015	0.017	0.019	0.021	0.023	0.026	0.028	0.032	0.039
	R2	0.012	0.015	0.017	0.019	0.021	0.023	0.025	0.029	0.035	0.013	0.016	0.018	0.020	0.023	0.025	0.028	0.031	0.038
	R3	0.010	0.013	0.015	0.017	0.020	0.022	0.025	0.028	0.034	0.011	0.014	0.016	0.019	0.021	0.024	0.027	0.031	0.037
	R4	0.006	0.010	0.013	0.015	0.018	0.021	0.024	0.027	0.033	0.007	0.011	0.014	0.017	0.019	0.022	0.026	0.030	0.036
	$\alpha=0.50$									$\alpha=0.75$									
$\lambda_{20^{\circ}\text{C}}=0.00$	R1	0.085	0.109	0.132	0.157	0.183	0.215	0.250	0.293	0.374	0.100	0.133	0.164	0.197	0.232	0.273	0.326	0.395	0.519
	R2	0.070	0.092	0.116	0.143	0.174	0.206	0.242	0.291	0.362	0.084	0.114	0.145	0.179	0.219	0.264	0.314	0.390	0.500
	R3	0.056	0.076	0.096	0.122	0.153	0.191	0.234	0.281	0.352	0.067	0.094	0.122	0.154	0.194	0.242	0.301	0.375	0.491
	R4	0.033	0.053	0.071	0.093	0.123	0.163	0.212	0.268	0.344	0.040	0.065	0.090	0.119	0.157	0.206	0.270	0.354	0.479
$\lambda_{20^{\circ}\text{C}}=0.25$	R1	0.066	0.084	0.102	0.121	0.142	0.166	0.193	0.227	0.292	0.078	0.103	0.127	0.152	0.179	0.211	0.252	0.306	0.403
	R2	0.055	0.071	0.089	0.110	0.134	0.159	0.187	0.224	0.281	0.065	0.089	0.112	0.139	0.169	0.204	0.243	0.300	0.390
	R3	0.044	0.059	0.075	0.094	0.118	0.147	0.181	0.218	0.273	0.052	0.073	0.095	0.120	0.150	0.186	0.234	0.293	0.382
	R4	0.028	0.043	0.058	0.075	0.099	0.130	0.166	0.208	0.266	0.034	0.053	0.073	0.096	0.126	0.165	0.212	0.276	0.372
$\lambda_{20^{\circ}\text{C}}=0.50$	R1	0.053	0.067	0.079	0.091	0.104	0.120	0.138	0.161	0.207	0.062	0.081	0.098	0.114	0.133	0.154	0.182	0.218	0.287
	R2	0.045	0.058	0.071	0.084	0.100	0.116	0.134	0.159	0.201	0.054	0.072	0.088	0.106	0.126	0.149	0.176	0.215	0.279
	R3	0.037	0.049	0.061	0.074	0.089	0.108	0.130	0.156	0.194	0.043	0.060	0.077	0.094	0.113	0.138	0.170	0.209	0.271
	R4	0.024	0.036	0.048	0.061	0.077	0.097	0.120	0.149	0.188	0.028	0.044	0.060	0.078	0.098	0.123	0.155	0.199	0.264
$\lambda_{20^{\circ}\text{C}}=0.75$	R1	0.047	0.057	0.066	0.074	0.084	0.094	0.107	0.123	0.157	0.054	0.068	0.081	0.094	0.107	0.122	0.142	0.167	0.218
	R2	0.041	0.051	0.060	0.070	0.081	0.091	0.104	0.122	0.151	0.047	0.062	0.075	0.088	0.103	0.119	0.138	0.166	0.210
	R3	0.033	0.044	0.053	0.063	0.074	0.086	0.101	0.119	0.146	0.039	0.053	0.066	0.079	0.094	0.111	0.134	0.162	0.205
	R4	0.022	0.033	0.043	0.053	0.065	0.079	0.095	0.114	0.143	0.026	0.040	0.053	0.067	0.083	0.101	0.124	0.154	0.201
$\lambda_{20^{\circ}\text{C}}=1.00$	R1	0.040	0.048	0.055	0.062	0.069	0.077	0.086	0.098	0.124	0.046	0.057	0.068	0.078	0.088	0.100	0.115	0.135	0.172
	R2	0.036	0.044	0.051	0.059	0.066	0.075	0.084	0.097	0.120	0.041	0.053	0.063	0.074	0.085	0.098	0.112	0.133	0.167
	R3	0.029	0.038	0.046	0.053	0.062	0.071	0.082	0.095	0.116	0.034	0.046	0.057	0.067	0.079	0.092	0.109	0.130	0.163
	R4	0.019	0.029	0.038	0.046	0.055	0.065	0.077	0.092	0.113	0.023	0.035	0.046	0.058	0.070	0.084	0.101	0.124	0.160
$\lambda_{20^{\circ}\text{C}}=1.50$	R1	0.026	0.031	0.035	0.039	0.043	0.047	0.053	0.060	0.075	0.029	0.037	0.043	0.049	0.055	0.062	0.071	0.082	0.104
	R2	0.023	0.028	0.033	0.037	0.042	0.046	0.052	0.059	0.072	0.026	0.034	0.040	0.047	0.053	0.061	0.069	0.081	0.101
	R3	0.019	0.025	0.030	0.034	0.039	0.044	0.050	0.058	0.070	0.022	0.030	0.036	0.043	0.050	0.057	0.067	0.080	0.099
	R4	0.013	0.019	0.025	0.030	0.035	0.041	0.048	0.056	0.069	0.015	0.023	0.030	0.037	0.045	0.053	0.063	0.076	0.097
$\lambda_{20^{\circ}\text{C}}=2.00$	R1	0.016	0.019	0.022	0.024	0.027	0.029	0.033	0.037	0.046	0.018	0.023	0.027	0.030	0.034	0.039	0.044	0.051	0.064
	R2	0.015	0.018	0.021	0.023	0.026	0.029	0.032	0.037	0.044	0.017	0.021	0.025	0.029	0.033	0.038	0.043	0.050	0.062
	R3	0.012	0.016	0.019	0.021	0.024	0.027	0.031	0.036	0.043	0.014	0.019	0.023	0.027	0.031	0.036	0.042	0.049	0.061
	R4	0.008	0.012	0.01															

$\theta_{\text{nom}} = 900^{\circ}\text{C}$

$p_{f,fi} \rightarrow$	0.10	0.20	0.30	0.40	0.50	0.60	0.70	0.80	0.90	0.10	0.20	0.30	0.40	0.50	0.60	0.70	0.80	0.90	
$\beta_{f,fi} \rightarrow$	1.28	0.84	0.52	0.40	0.00	-0.25	-0.52	-0.84	-1.28	1.28	0.84	0.52	0.40	0.00	-0.25	-0.52	-0.84	-1.28	
$\delta_{of} \rightarrow$	1.15	1.02	0.94	0.88	0.82	0.77	0.72	0.67	0.60	1.15	1.02	0.94	0.88	0.82	0.77	0.72	0.67	0.60	
	$\alpha=0.00$									$\alpha=0.25$									
$\lambda_{20^{\circ}\text{C}}=0.00$	R1	0.052	0.061	0.070	0.079	0.089	0.101	0.119	0.147	0.212	0.056	0.067	0.076	0.086	0.097	0.110	0.130	0.161	0.231
	R2	0.039	0.049	0.058	0.068	0.081	0.098	0.110	0.145	0.203	0.042	0.053	0.063	0.074	0.088	0.107	0.122	0.159	0.221
	R3	0.025	0.036	0.045	0.055	0.066	0.082	0.106	0.142	0.186	0.027	0.039	0.049	0.059	0.072	0.089	0.115	0.155	0.202
	R4	0.004	0.019	0.031	0.043	0.056	0.073	0.100	0.125	0.151	0.004	0.021	0.034	0.047	0.061	0.079	0.109	0.137	0.165
$\lambda_{20^{\circ}\text{C}}=0.25$	R1	0.040	0.048	0.055	0.061	0.069	0.078	0.093	0.121	0.169	0.044	0.052	0.059	0.067	0.075	0.085	0.101	0.131	0.185
	R2	0.030	0.038	0.045	0.053	0.063	0.075	0.087	0.113	0.158	0.033	0.041	0.049	0.058	0.069	0.082	0.095	0.124	0.174
	R3	0.020	0.028	0.036	0.043	0.054	0.066	0.084	0.110	0.143	0.022	0.031	0.039	0.047	0.058	0.072	0.092	0.120	0.156
	R4	0.013	0.023	0.032	0.041	0.051	0.064	0.082	0.097	0.117	0.014	0.025	0.035	0.045	0.056	0.069	0.089	0.106	0.128
$\lambda_{20^{\circ}\text{C}}=0.50$	R1	0.034	0.040	0.045	0.050	0.055	0.062	0.071	0.089	0.120	0.037	0.043	0.049	0.054	0.060	0.067	0.077	0.097	0.131
	R2	0.026	0.032	0.038	0.044	0.052	0.059	0.068	0.084	0.113	0.028	0.035	0.041	0.048	0.056	0.064	0.074	0.092	0.124
	R3	0.017	0.024	0.030	0.036	0.045	0.053	0.066	0.083	0.104	0.018	0.026	0.033	0.040	0.048	0.058	0.071	0.090	0.114
	R4	0.011	0.019	0.027	0.035	0.042	0.051	0.064	0.075	0.088	0.012	0.021	0.029	0.038	0.046	0.056	0.069	0.081	0.096
$\lambda_{20^{\circ}\text{C}}=0.75$	R1	0.030	0.036	0.040	0.044	0.048	0.053	0.059	0.071	0.092	0.033	0.039	0.043	0.048	0.052	0.058	0.065	0.077	0.100
	R2	0.023	0.029	0.034	0.039	0.045	0.051	0.057	0.068	0.088	0.026	0.032	0.037	0.043	0.049	0.056	0.062	0.074	0.095
	R3	0.015	0.022	0.027	0.033	0.040	0.046	0.056	0.067	0.082	0.017	0.024	0.030	0.036	0.043	0.051	0.061	0.073	0.089
	R4	0.010	0.018	0.025	0.031	0.038	0.045	0.054	0.062	0.072	0.011	0.019	0.027	0.034	0.041	0.049	0.059	0.068	0.079
$\lambda_{20^{\circ}\text{C}}=1.00$	R1	0.027	0.031	0.035	0.038	0.041	0.045	0.050	0.058	0.074	0.029	0.034	0.038	0.041	0.045	0.049	0.055	0.063	0.081
	R2	0.021	0.026	0.030	0.034	0.039	0.044	0.049	0.057	0.071	0.023	0.028	0.033	0.037	0.043	0.048	0.053	0.062	0.077
	R3	0.014	0.019	0.024	0.029	0.035	0.040	0.047	0.056	0.067	0.015	0.021	0.026	0.031	0.038	0.044	0.051	0.061	0.073
	R4	0.009	0.015	0.022	0.028	0.033	0.039	0.046	0.053	0.061	0.009	0.017	0.024	0.030	0.036	0.042	0.050	0.058	0.066
$\lambda_{20^{\circ}\text{C}}=1.50$	R1	0.018	0.020	0.023	0.025	0.027	0.029	0.032	0.036	0.045	0.019	0.022	0.025	0.027	0.029	0.032	0.035	0.040	0.050
	R2	0.014	0.017	0.020	0.022	0.025	0.028	0.031	0.036	0.043	0.015	0.018	0.021	0.024	0.028	0.031	0.034	0.039	0.047
	R3	0.009	0.013	0.016	0.019	0.023	0.026	0.030	0.035	0.042	0.010	0.014	0.017	0.021	0.025	0.028	0.033	0.038	0.045
	R4	0.006	0.010	0.014	0.018	0.022	0.025	0.030	0.034	0.038	0.006	0.011	0.015	0.020	0.024	0.028	0.032	0.037	0.042
$\lambda_{20^{\circ}\text{C}}=2.00$	R1	0.011	0.013	0.014	0.015	0.017	0.018	0.020	0.023	0.028	0.012	0.014	0.015	0.017	0.018	0.020	0.022	0.025	0.031
	R2	0.009	0.011	0.012	0.014	0.016	0.018	0.019	0.022	0.027	0.009	0.012	0.013	0.015	0.017	0.019	0.021	0.024	0.029
	R3	0.006	0.008	0.010	0.012	0.014	0.016	0.019	0.022	0.026	0.006	0.009	0.011	0.013	0.015	0.018	0.021	0.024	0.028
	R4	0.004	0.006	0.009	0.011	0.014	0.016	0.019	0.021	0.024	0.004	0.007	0.010	0.012	0.015	0.017	0.020	0.023	0.026
	$\alpha=0.50$									$\alpha=0.75$									
$\lambda_{20^{\circ}\text{C}}=0.00$	R1	0.062	0.075	0.087	0.098	0.110	0.126	0.149	0.184	0.266	0.071	0.091	0.108	0.125	0.142	0.165	0.198	0.242	0.354
	R2	0.047	0.060	0.072	0.085	0.101	0.123	0.139	0.181	0.255	0.055	0.073	0.091	0.110	0.132	0.160	0.185	0.238	0.340
	R3	0.030	0.044	0.056	0.068	0.082	0.102	0.132	0.177	0.234	0.036	0.053	0.070	0.087	0.106	0.133	0.172	0.230	0.318
	R4	0.005	0.023	0.038	0.053	0.069	0.091	0.125	0.158	0.193	0.006	0.028	0.047	0.067	0.089	0.118	0.161	0.217	0.270
$\lambda_{20^{\circ}\text{C}}=0.25$	R1	0.048	0.058	0.067	0.076	0.086	0.098	0.116	0.149	0.214	0.055	0.071	0.084	0.097	0.110	0.128	0.154	0.193	0.293
	R2	0.037	0.047	0.056	0.066	0.079	0.094	0.109	0.142	0.199	0.043	0.057	0.070	0.085	0.102	0.124	0.145	0.187	0.267
	R3	0.024	0.035	0.044	0.053	0.067	0.082	0.106	0.138	0.181	0.029	0.042	0.055	0.068	0.087	0.107	0.138	0.181	0.246
	R4	0.016	0.028	0.040	0.051	0.064	0.080	0.102	0.124	0.149	0.019	0.034	0.049	0.066	0.083	0.104	0.134	0.169	0.209
$\lambda_{20^{\circ}\text{C}}=0.50$	R1	0.040	0.049	0.055	0.062	0.068	0.077	0.089	0.110	0.152	0.046	0.058	0.068	0.078	0.089	0.101	0.119	0.144	0.209
	R2	0.031	0.039	0.047	0.055	0.064	0.075	0.084	0.105	0.143	0.036	0.048	0.059	0.070	0.083	0.099	0.112	0.141	0.192
	R3	0.020	0.030	0.037	0.045	0.055	0.066	0.082	0.103	0.132	0.024	0.036	0.046	0.057	0.072	0.087	0.108	0.136	0.181
	R4	0.013	0.024	0.033	0.043	0.053	0.064	0.080	0.094	0.112	0.016	0.029	0.041	0.054	0.068	0.083	0.104	0.130	0.158
$\lambda_{20^{\circ}\text{C}}=0.75$	R1	0.036	0.043	0.049	0.054	0.059	0.066	0.075	0.089	0.117	0.041	0.051	0.060	0.068	0.077	0.087	0.101	0.118	0.163
	R2	0.028	0.036	0.042	0.049	0.056	0.064	0.071	0.086	0.110	0.033	0.043	0.052	0.062	0.073	0.085	0.096	0.117	0.151
	R3	0.019	0.027	0.034	0.041	0.049	0.058	0.070	0.084	0.104	0.022	0.032	0.042	0.051	0.064	0.076	0.092	0.112	0.145
	R4	0.012	0.021	0.030	0.039	0.047	0.056	0.068	0.079	0.093	0.015	0.026	0.037	0.049	0.060	0.073	0.089	0.110	0.132
$\lambda_{20^{\circ}\text{C}}=1.00$	R1	0.032	0.038	0.042	0.047	0.051	0.057	0.063	0.073	0.094	0.036	0.044	0.052	0.059	0.066	0.074	0.085	0.099	0.132
	R2	0.025	0.031	0.037	0.043	0.049	0.055	0.061	0.072	0.089	0.029	0.038	0.046	0.054	0.063	0.073	0.082	0.098	0.123
	R3	0.016	0.024	0.030	0.036	0.043	0.050	0.059	0.070	0.085	0.019	0.028	0.037	0.045	0.055	0.065	0.078	0.094	0.119
	R4	0.011	0.019	0.027	0.034	0.041	0.049	0.058	0.068	0.078	0.013	0.023	0.033	0.043	0.052	0.063	0.076	0.093	0.111
$\lambda_{20^{\circ}\text{C}}=1.50$	R1	0.021	0.025	0.028	0.030	0.033	0.036	0.040	0.046	0.058	0.023	0.029	0.034	0.038	0.043	0.048	0.054	0.063	0.081
	R2	0.016	0.021	0.024	0.028	0.031	0.036	0.039	0.045	0.055	0.019	0.025	0.030	0.035	0.040	0.047	0.053	0.061	0.076
	R3	0.011	0.016	0.020	0.023	0.028	0.032	0.038	0.044	0.053	0.013	0.019	0.024	0.029	0.036	0.042	0.050	0.060	0.075
	R4	0.007	0.012	0.017	0.022	0.027	0.031	0.037	0.043	0.049	0.008	0.015	0.022	0.028	0.034	0.041	0.049	0.059	0.071
$\lambda_{20^{\circ}\text{C}}=2.00$	R1	0.013	0.015	0.017	0.019	0.021	0.023	0.025	0.028	0.036	0.015	0.018	0.021	0.024	0.027	0.030	0.034	0.039	0.050
	R2	0.010	0.013	0.015	0.017	0.020	0.022	0.024	0.028	0.034	0.012	0.016	0.019	0.022	0.025	0.029	0.033	0.038	0.048
	R3	0.007	0.010	0.012	0.015	0.018	0.020	0.024	0.027	0.033	0.008	0.012	0.015	0.018	0.022	0.026	0.031	0.037	0.047
	R4	0.004	0.008	0.011	0.014	0.017	0												

A18 Factor χ_{Rel} for S355 strong axis, imposed (Q) variable load type

$\theta_{nom} = 300^{\circ}\text{C}$																				
$p_{f,fi} \rightarrow$	0.10	0.20	0.30	0.40	0.50	0.60	0.70	0.80	0.90	0.10	0.20	0.30	0.40	0.50	0.60	0.70	0.80	0.90		
$\beta_{f,fi} \rightarrow$	1.28	0.84	0.52	0.40	0.00	-0.25	-0.52	-0.84	-1.28	1.28	0.84	0.52	0.40	0.00	-0.25	-0.52	-0.84	-1.28		
$\delta_{of} \rightarrow$	1.15	1.02	0.94	0.88	0.82	0.77	0.72	0.67	0.60	1.15	1.02	0.94	0.88	0.82	0.77	0.72	0.67	0.60		
$\alpha=0.00$										$\alpha=0.25$										
$\lambda_{20^{\circ}\text{C}}=0.00$	R1	0.816	0.909	0.980	1.000	1.000	1.000	1.000	1.000	0.881	0.984	1.000	1.000	1.000	1.000	1.000	1.000	1.000		
	R2	0.792	0.892	0.965	1.000	1.000	1.000	1.000	1.000	0.857	0.966	1.000	1.000	1.000	1.000	1.000	1.000	1.000		
	R3	0.782	0.885	0.959	1.000	1.000	1.000	1.000	1.000	0.844	0.957	1.000	1.000	1.000	1.000	1.000	1.000	1.000		
	R4	0.743	0.857	0.936	1.000	1.000	1.000	1.000	1.000	0.803	0.926	1.000	1.000	1.000	1.000	1.000	1.000	1.000		
$\lambda_{20^{\circ}\text{C}}=0.25$	R1	0.683	0.762	0.821	0.876	0.930	0.986	0.993	0.993	0.738	0.825	0.893	0.954	0.993	0.993	0.993	0.993	0.993		
	R2	0.664	0.749	0.812	0.866	0.921	0.977	0.993	0.993	0.718	0.811	0.880	0.942	0.993	0.993	0.993	0.993	0.993		
	R3	0.656	0.742	0.805	0.861	0.915	0.973	0.993	0.993	0.708	0.803	0.873	0.935	0.993	0.993	0.993	0.993	0.993		
	R4	0.622	0.718	0.785	0.844	0.901	0.959	0.993	0.993	0.671	0.776	0.852	0.917	0.981	0.993	0.993	0.993	0.993		
$\lambda_{20^{\circ}\text{C}}=0.50$	R1	0.515	0.580	0.630	0.678	0.726	0.776	0.833	0.904	0.557	0.628	0.683	0.737	0.790	0.845	0.909	0.951	0.951		
	R2	0.499	0.568	0.620	0.667	0.713	0.762	0.817	0.889	0.539	0.614	0.672	0.723	0.775	0.830	0.891	0.951	0.951		
	R3	0.489	0.560	0.612	0.656	0.699	0.749	0.803	0.871	0.528	0.606	0.663	0.712	0.761	0.815	0.876	0.951	0.951		
	R4	0.458	0.537	0.592	0.642	0.688	0.738	0.793	0.858	0.494	0.580	0.643	0.697	0.749	0.804	0.865	0.951	0.951		
$\lambda_{20^{\circ}\text{C}}=0.75$	R1	0.427	0.489	0.539	0.588	0.636	0.685	0.741	0.812	0.463	0.531	0.587	0.640	0.692	0.745	0.808	0.876	0.876		
	R2	0.411	0.475	0.528	0.574	0.618	0.667	0.723	0.794	0.445	0.515	0.574	0.624	0.673	0.726	0.787	0.876	0.876		
	R3	0.402	0.466	0.516	0.559	0.601	0.649	0.704	0.771	0.436	0.506	0.562	0.608	0.654	0.707	0.767	0.876	0.876		
	R4	0.372	0.442	0.495	0.543	0.591	0.640	0.693	0.755	0.402	0.480	0.539	0.591	0.643	0.697	0.755	0.876	0.876		
$\lambda_{20^{\circ}\text{C}}=1.00$	R1	0.364	0.415	0.458	0.499	0.541	0.583	0.630	0.725	0.393	0.450	0.498	0.543	0.588	0.634	0.725	0.725	0.725		
	R2	0.348	0.403	0.448	0.487	0.525	0.567	0.614	0.725	0.378	0.437	0.486	0.530	0.571	0.617	0.725	0.725	0.725		
	R3	0.341	0.396	0.439	0.475	0.510	0.551	0.599	0.657	0.369	0.429	0.476	0.515	0.555	0.600	0.652	0.725	0.725		
	R4	0.315	0.375	0.421	0.461	0.501	0.544	0.589	0.641	0.341	0.407	0.456	0.500	0.545	0.591	0.642	0.725	0.725		
$\lambda_{20^{\circ}\text{C}}=1.50$	R1	0.214	0.241	0.263	0.282	0.302	0.323	0.345	0.395	0.232	0.261	0.285	0.307	0.329	0.351	0.395	0.395	0.395		
	R2	0.208	0.236	0.259	0.278	0.297	0.316	0.339	0.395	0.224	0.256	0.280	0.302	0.323	0.345	0.395	0.395	0.395		
	R3	0.204	0.233	0.255	0.274	0.292	0.310	0.333	0.361	0.221	0.252	0.276	0.297	0.317	0.338	0.363	0.395	0.395		
	R4	0.190	0.223	0.247	0.267	0.286	0.307	0.330	0.357	0.206	0.242	0.267	0.290	0.312	0.334	0.359	0.395	0.395		
$\lambda_{20^{\circ}\text{C}}=2.00$	R1	0.127	0.142	0.155	0.166	0.177	0.189	0.202	0.218	0.137	0.154	0.168	0.180	0.192	0.205	0.232	0.232	0.232		
	R2	0.123	0.139	0.152	0.164	0.174	0.185	0.198	0.214	0.133	0.151	0.165	0.177	0.189	0.202	0.216	0.232	0.232		
	R3	0.121	0.137	0.150	0.161	0.171	0.182	0.195	0.211	0.131	0.149	0.163	0.175	0.186	0.198	0.212	0.232	0.232		
	R4	0.113	0.132	0.146	0.157	0.169	0.180	0.193	0.209	0.122	0.143	0.158	0.171	0.183	0.196	0.210	0.232	0.232		
$\alpha=0.50$										$\alpha=0.75$										
$\lambda_{20^{\circ}\text{C}}=0.00$	R1	0.956	1.000	1.000	1.000	1.000	1.000	1.000	1.000	1.000	1.000	1.000	1.000	1.000	1.000	1.000	1.000	1.000		
	R2	0.931	1.000	1.000	1.000	1.000	1.000	1.000	1.000	1.000	1.000	1.000	1.000	1.000	1.000	1.000	1.000	1.000		
	R3	0.919	1.000	1.000	1.000	1.000	1.000	1.000	1.000	1.000	0.988	1.000	1.000	1.000	1.000	1.000	1.000	1.000		
	R4	0.873	1.000	1.000	1.000	1.000	1.000	1.000	1.000	1.000	0.945	1.000	1.000	1.000	1.000	1.000	1.000	1.000		
$\lambda_{20^{\circ}\text{C}}=0.25$	R1	0.800	0.915	0.993	0.993	0.993	0.993	0.993	0.993	0.864	0.993	0.993	0.993	0.993	0.993	0.993	0.993	0.993		
	R2	0.780	0.898	0.989	0.993	0.993	0.993	0.993	0.993	0.843	0.993	0.993	0.993	0.993	0.993	0.993	0.993	0.993		
	R3	0.770	0.890	0.982	0.993	0.993	0.993	0.993	0.993	0.832	0.993	0.993	0.993	0.993	0.993	0.993	0.993	0.993		
	R4	0.729	0.858	0.954	0.993	0.993	0.993	0.993	0.993	0.786	0.982	0.993	0.993	0.993	0.993	0.993	0.993	0.993		
$\lambda_{20^{\circ}\text{C}}=0.50$	R1	0.607	0.697	0.769	0.837	0.905	0.951	0.951	0.951	0.657	0.803	0.951	0.951	0.951	0.951	0.951	0.951	0.951		
	R2	0.588	0.682	0.755	0.821	0.886	0.951	0.951	0.951	0.640	0.785	0.911	0.951	0.951	0.951	0.951	0.951	0.951		
	R3	0.577	0.673	0.745	0.809	0.871	0.951	0.951	0.951	0.629	0.775	0.897	0.951	0.951	0.951	0.951	0.951	0.951		
	R4	0.539	0.643	0.720	0.788	0.856	0.951	0.951	0.951	0.591	0.740	0.865	0.951	0.951	0.951	0.951	0.951	0.951		
$\lambda_{20^{\circ}\text{C}}=0.75$	R1	0.508	0.593	0.662	0.727	0.792	0.876	0.876	0.876	0.559	0.691	0.803	0.876	0.876	0.876	0.876	0.876	0.876		
	R2	0.490	0.576	0.646	0.710	0.769	0.876	0.876	0.876	0.540	0.669	0.783	0.876	0.876	0.876	0.876	0.876	0.876		
	R3	0.479	0.564	0.633	0.691	0.749	0.812	0.876	0.876	0.528	0.659	0.768	0.876	0.876	0.876	0.876	0.876	0.876		
	R4	0.442	0.534	0.607	0.672	0.736	0.803	0.876	0.876	0.490	0.623	0.734	0.876	0.876	0.876	0.876	0.876	0.876		
$\lambda_{20^{\circ}\text{C}}=1.00$	R1	0.431	0.502	0.561	0.615	0.672	0.725	0.725	0.725	0.472	0.583	0.725	0.725	0.725	0.725	0.725	0.725	0.725		
	R2	0.414	0.487	0.547	0.601	0.652	0.725	0.725	0.725	0.457	0.568	0.725	0.725	0.725	0.725	0.725	0.725	0.725		
	R3	0.405	0.478	0.536	0.586	0.635	0.725	0.725	0.725	0.447	0.558	0.650	0.725	0.725	0.725	0.725	0.725	0.725		
	R4	0.375	0.453	0.513	0.567	0.621	0.725	0.725	0.725	0.415	0.527	0.621	0.725	0.725	0.725	0.725	0.725	0.725		
$\lambda_{20^{\circ}\text{C}}=1.50$	R1	0.253	0.290	0.321	0.348	0.395	0.395	0.395	0.395	0.274	0.335	0.395	0.395	0.395	0.395	0.395	0.395	0.395		
	R2	0.245	0.284	0.315	0.343	0.395	0.395	0.395	0.395	0.266	0.328	0.395	0.395	0.395	0.395	0.395	0.395	0.395		
	R3	0.240	0.280	0.311	0.338	0.363	0.395	0.395	0.395	0.262	0.323	0.395	0.395	0.395	0.395	0.395	0.395	0.395		
	R4	0.224	0.268	0.300	0.328	0.356	0.395	0.395	0.395	0.245	0.308	0.360	0.395	0.395	0.395	0.395	0.395	0.395		
$\lambda_{20^{\circ}\text{C}}=2.00$	R1	0.149	0.171	0.188	0.204	0.232	0.232	0.232	0.232	0.161	0.197	0.232	0.232	0.232	0.232	0.232	0.232	0.232		
	R2	0.144	0.168	0.185	0.201	0.217	0.232	0.232	0.232	0.158	0.193	0.232	0.232	0.232	0.232	0.232	0.232	0.232		
	R3	0.142	0.165	0.183	0.199	0.213	0.232	0.232	0.232	0.155	0.190	0.232	0.232	0.232	0.232	0.232	0.232	0.232		
	R4	0.133	0.158	0.177	0.193	0.209	0.232	0.232	0.232	0.145	0.182	0.212	0.232	0.232	0.232	0.232	0.232	0.232		

$$\theta_{\text{nom}} = 400^{\circ}\text{C}$$

$p_{f,fi} \rightarrow$	0.10	0.20	0.30	0.40	0.50	0.60	0.70	0.80	0.90	0.10	0.20	0.30	0.40	0.50	0.60	0.70	0.80	0.90
$\beta_{f,fi} \rightarrow$	1.28	0.84	0.52	0.40	0.00	-0.25	-0.52	-0.84	-1.28	1.28	0.84	0.52	0.40	0.00	-0.25	-0.52	-0.84	-1.28
$\delta_{af} \rightarrow$	1.15	1.02	0.94	0.88	0.82	0.77	0.72	0.67	0.60	1.15	1.02	0.94	0.88	0.82	0.77	0.72	0.67	0.60
	$\alpha=0.00$									$\alpha=0.25$								
$\lambda_{20^{\circ}\text{C}}=0.00$	R1	0.757	0.854	0.927	0.992	1.000	1.000	1.000	1.000	0.818	0.925	1.000	1.000	1.000	1.000	1.000	1.000	1.000
	R2	0.616	0.743	0.833	0.912	0.986	1.000	1.000	1.000	0.666	0.804	0.904	0.990	1.000	1.000	1.000	1.000	1.000
	R3	0.580	0.726	0.822	0.903	0.976	1.000	1.000	1.000	0.628	0.787	0.892	0.981	1.000	1.000	1.000	1.000	1.000
	R4	0.518	0.679	0.790	0.876	0.956	1.000	1.000	1.000	0.563	0.737	0.857	0.952	1.000	1.000	1.000	1.000	1.000
$\lambda_{20^{\circ}\text{C}}=0.25$	R1	0.634	0.715	0.776	0.832	0.887	0.944	0.993	0.993	0.684	0.774	0.843	0.904	0.964	0.993	0.993	0.993	0.993
	R2	0.518	0.624	0.700	0.764	0.827	0.890	0.958	0.993	0.559	0.675	0.759	0.830	0.899	0.969	0.993	0.993	0.993
	R3	0.486	0.608	0.690	0.757	0.819	0.882	0.952	0.993	0.527	0.659	0.747	0.821	0.890	0.960	0.993	0.993	0.993
	R4	0.435	0.570	0.661	0.735	0.802	0.868	0.939	0.993	0.471	0.617	0.717	0.798	0.872	0.945	0.993	0.993	0.993
$\lambda_{20^{\circ}\text{C}}=0.50$	R1	0.457	0.517	0.563	0.605	0.645	0.688	0.735	0.796	0.494	0.560	0.611	0.656	0.701	0.748	0.802	0.868	0.951
	R2	0.367	0.447	0.504	0.555	0.601	0.648	0.699	0.762	0.397	0.484	0.547	0.602	0.654	0.705	0.764	0.833	0.951
	R3	0.344	0.436	0.497	0.547	0.593	0.640	0.693	0.754	0.372	0.472	0.539	0.594	0.644	0.696	0.754	0.823	0.951
	R4	0.305	0.407	0.476	0.532	0.582	0.631	0.682	0.743	0.330	0.440	0.516	0.577	0.633	0.686	0.744	0.812	0.913
$\lambda_{20^{\circ}\text{C}}=0.75$	R1	0.371	0.421	0.461	0.497	0.532	0.569	0.613	0.672	0.401	0.457	0.500	0.539	0.578	0.620	0.669	0.733	0.876
	R2	0.293	0.360	0.409	0.453	0.493	0.533	0.579	0.639	0.317	0.391	0.444	0.492	0.536	0.579	0.631	0.697	0.803
	R3	0.272	0.352	0.403	0.445	0.485	0.525	0.571	0.625	0.295	0.381	0.438	0.484	0.527	0.572	0.622	0.682	0.775
	R4	0.238	0.327	0.386	0.434	0.476	0.516	0.560	0.614	0.257	0.354	0.419	0.471	0.518	0.562	0.610	0.670	0.761
$\lambda_{20^{\circ}\text{C}}=1.00$	R1	0.312	0.355	0.389	0.419	0.449	0.481	0.518	0.569	0.339	0.385	0.422	0.455	0.488	0.524	0.565	0.620	0.725
	R2	0.246	0.304	0.346	0.383	0.416	0.449	0.489	0.540	0.267	0.329	0.375	0.416	0.452	0.489	0.532	0.589	0.725
	R3	0.227	0.296	0.340	0.376	0.409	0.443	0.482	0.529	0.246	0.322	0.370	0.408	0.445	0.482	0.525	0.577	0.656
	R4	0.196	0.275	0.326	0.366	0.403	0.436	0.473	0.519	0.213	0.298	0.353	0.397	0.437	0.474	0.515	0.566	0.644
$\lambda_{20^{\circ}\text{C}}=1.50$	R1	0.190	0.215	0.233	0.250	0.267	0.284	0.304	0.328	0.205	0.232	0.253	0.272	0.290	0.309	0.331	0.358	0.395
	R2	0.151	0.186	0.210	0.230	0.250	0.268	0.289	0.315	0.163	0.201	0.227	0.250	0.272	0.292	0.314	0.344	0.395
	R3	0.139	0.181	0.207	0.227	0.246	0.265	0.286	0.312	0.150	0.196	0.224	0.247	0.268	0.289	0.311	0.340	0.395
	R4	0.119	0.168	0.198	0.221	0.242	0.261	0.282	0.307	0.129	0.182	0.215	0.240	0.263	0.284	0.307	0.335	0.395
$\lambda_{20^{\circ}\text{C}}=2.00$	R1	0.113	0.127	0.138	0.148	0.158	0.168	0.180	0.194	0.122	0.138	0.150	0.161	0.172	0.183	0.196	0.212	0.232
	R2	0.090	0.111	0.125	0.137	0.148	0.159	0.171	0.186	0.097	0.120	0.135	0.149	0.161	0.173	0.187	0.203	0.232
	R3	0.083	0.108	0.123	0.135	0.146	0.157	0.169	0.184	0.090	0.117	0.133	0.147	0.159	0.171	0.185	0.201	0.232
	R4	0.071	0.100	0.118	0.132	0.144	0.155	0.167	0.182	0.078	0.109	0.128	0.143	0.156	0.169	0.182	0.198	0.232
	$\alpha=0.50$									$\alpha=0.75$								
$\lambda_{20^{\circ}\text{C}}=0.00$	R1	0.892	1.000	1.000	1.000	1.000	1.000	1.000	1.000	0.968	1.000	1.000	1.000	1.000	1.000	1.000	1.000	1.000
	R2	0.733	0.894	1.000	1.000	1.000	1.000	1.000	1.000	0.816	1.000	1.000	1.000	1.000	1.000	1.000	1.000	1.000
	R3	0.693	0.872	0.997	1.000	1.000	1.000	1.000	1.000	0.776	1.000	1.000	1.000	1.000	1.000	1.000	1.000	1.000
	R4	0.624	0.818	0.953	1.000	1.000	1.000	1.000	1.000	0.714	0.947	1.000	1.000	1.000	1.000	1.000	1.000	1.000
$\lambda_{20^{\circ}\text{C}}=0.25$	R1	0.746	0.859	0.946	0.993	0.993	0.993	0.993	0.993	0.812	0.991	0.993	0.993	0.993	0.993	0.993	0.993	0.993
	R2	0.615	0.749	0.848	0.938	0.993	0.993	0.993	0.993	0.682	0.863	0.993	0.993	0.993	0.993	0.993	0.993	0.993
	R3	0.581	0.730	0.836	0.928	0.993	0.993	0.993	0.993	0.653	0.844	0.993	0.993	0.993	0.993	0.993	0.993	0.993
	R4	0.525	0.685	0.800	0.899	0.990	0.993	0.993	0.993	0.595	0.793	0.952	0.993	0.993	0.993	0.993	0.993	0.993
$\lambda_{20^{\circ}\text{C}}=0.50$	R1	0.539	0.622	0.686	0.745	0.803	0.864	0.951	0.951	0.587	0.718	0.829	0.951	0.951	0.951	0.951	0.951	0.951
	R2	0.437	0.537	0.612	0.679	0.746	0.809	0.882	0.951	0.486	0.622	0.730	0.839	0.951	0.951	0.951	0.951	0.951
	R3	0.411	0.524	0.603	0.670	0.735	0.800	0.874	0.951	0.464	0.607	0.721	0.827	0.951	0.951	0.951	0.951	0.951
	R4	0.367	0.489	0.577	0.651	0.720	0.788	0.860	0.951	0.422	0.568	0.688	0.798	0.911	0.951	0.951	0.951	0.951
$\lambda_{20^{\circ}\text{C}}=0.75$	R1	0.438	0.508	0.563	0.613	0.662	0.715	0.776	0.876	0.480	0.590	0.682	0.770	0.876	0.876	0.876	0.876	0.876
	R2	0.349	0.433	0.498	0.557	0.613	0.666	0.731	0.812	0.390	0.502	0.595	0.689	0.782	0.876	0.876	0.876	0.876
	R3	0.326	0.423	0.491	0.546	0.602	0.657	0.720	0.797	0.371	0.491	0.587	0.677	0.766	0.876	0.876	0.876	0.876
	R4	0.288	0.393	0.468	0.531	0.591	0.646	0.707	0.781	0.333	0.457	0.558	0.654	0.748	0.876	0.876	0.876	0.876
$\lambda_{20^{\circ}\text{C}}=1.00$	R1	0.370	0.429	0.475	0.517	0.559	0.604	0.655	0.725	0.405	0.497	0.575	0.648	0.725	0.725	0.725	0.725	0.725
	R2	0.292	0.364	0.419	0.470	0.517	0.563	0.616	0.725	0.329	0.423	0.503	0.582	0.725	0.725	0.725	0.725	0.725
	R3	0.272	0.356	0.414	0.462	0.508	0.555	0.609	0.725	0.309	0.413	0.495	0.572	0.649	0.725	0.725	0.725	0.725
	R4	0.238	0.329	0.395	0.449	0.498	0.545	0.597	0.725	0.275	0.383	0.470	0.552	0.632	0.725	0.725	0.725	0.725
$\lambda_{20^{\circ}\text{C}}=1.50$	R1	0.224	0.258	0.285	0.309	0.332	0.357	0.395	0.395	0.243	0.298	0.343	0.395	0.395	0.395	0.395	0.395	0.395
	R2	0.179	0.223	0.254	0.283	0.309	0.336	0.365	0.395	0.199	0.256	0.303	0.348	0.395	0.395	0.395	0.395	0.395
	R3	0.166	0.217	0.251	0.279	0.305	0.331	0.361	0.395	0.188	0.250	0.298	0.344	0.395	0.395	0.395	0.395	0.395
	R4	0.145	0.201	0.240	0.270	0.299	0.327	0.356	0.395	0.167	0.233	0.284	0.331	0.395	0.395	0.395	0.395	0.395
$\lambda_{20^{\circ}\text{C}}=2.00$	R1	0.133	0.153	0.169	0.183	0.197	0.211	0.232	0.232	0.144	0.177	0.204	0.232	0.232	0.232	0.232	0.232	0.232
	R2	0.107	0.133	0.151	0.168	0.183	0.200	0.216	0.232	0.119	0.152	0.180	0.207	0.232	0.232	0.232	0.232	0.232
	R3	0.099	0.129	0.149	0.166	0.181	0.197	0.214	0.232	0.112	0.148	0.177	0.204	0.232	0.232	0.232	0.232	0.232
	R4	0.087	0.120	0.143	0.161	0.178	0.194	0.211	0.232	0.100	0.138	0.168	0.196	0.232	0.232	0.232	0.232	0.232

$$\theta_{\text{nom}} = 500^{\circ}\text{C}$$

$p_{f,fi} \rightarrow$	0.10	0.20	0.30	0.40	0.50	0.60	0.70	0.80	0.90	0.10	0.20	0.30	0.40	0.50	0.60	0.70	0.80	0.90
$\beta_{f,fi} \rightarrow$	1.28	0.84	0.52	0.40	0.00	-0.25	-0.52	-0.84	-1.28	1.28	0.84	0.52	0.40	0.00	-0.25	-0.52	-0.84	-1.28
$\delta_{af} \rightarrow$	1.15	1.02	0.94	0.88	0.82	0.77	0.72	0.67	0.60	1.15	1.02	0.94	0.88	0.82	0.77	0.72	0.67	0.60
	$\alpha=0.00$									$\alpha=0.25$								
$\lambda_{20^{\circ}\text{C}}=0.00$	R1	0.422	0.527	0.612	0.694	0.785	0.871	0.963	1.000	1.000	0.457	0.572	0.663	0.753	0.853	0.946	1.000	1.000
	R2	0.330	0.458	0.573	0.666	0.752	0.836	0.927	1.000	1.000	0.356	0.497	0.622	0.723	0.818	0.909	1.000	1.000
	R3	0.276	0.398	0.508	0.612	0.714	0.811	0.912	1.000	1.000	0.298	0.432	0.553	0.666	0.776	0.881	0.992	1.000
	R4	0.217	0.319	0.439	0.557	0.671	0.783	0.897	1.000	1.000	0.237	0.346	0.477	0.605	0.728	0.851	0.975	1.000
$\lambda_{20^{\circ}\text{C}}=0.25$	R1	0.355	0.443	0.513	0.583	0.657	0.731	0.810	0.904	0.993	0.384	0.480	0.557	0.632	0.713	0.796	0.882	0.985
	R2	0.277	0.386	0.480	0.560	0.631	0.702	0.779	0.874	0.993	0.301	0.418	0.520	0.607	0.687	0.763	0.849	0.953
	R3	0.232	0.335	0.427	0.515	0.599	0.681	0.768	0.867	0.993	0.251	0.364	0.463	0.558	0.650	0.739	0.834	0.944
	R4	0.183	0.268	0.371	0.469	0.563	0.657	0.752	0.855	0.988	0.200	0.292	0.401	0.509	0.611	0.714	0.818	0.932
$\lambda_{20^{\circ}\text{C}}=0.50$	R1	0.246	0.309	0.362	0.413	0.468	0.522	0.581	0.647	0.744	0.266	0.336	0.392	0.447	0.507	0.568	0.633	0.705
	R2	0.189	0.267	0.337	0.396	0.449	0.500	0.557	0.626	0.727	0.205	0.289	0.366	0.430	0.488	0.544	0.606	0.682
	R3	0.158	0.230	0.297	0.362	0.425	0.485	0.549	0.620	0.716	0.171	0.250	0.323	0.393	0.462	0.528	0.597	0.676
	R4	0.124	0.183	0.255	0.328	0.398	0.468	0.539	0.610	0.703	0.136	0.199	0.277	0.355	0.432	0.509	0.586	0.664
$\lambda_{20^{\circ}\text{C}}=0.75$	R1	0.188	0.242	0.286	0.330	0.378	0.423	0.471	0.525	0.610	0.204	0.262	0.311	0.359	0.411	0.460	0.512	0.572
	R2	0.142	0.205	0.264	0.315	0.361	0.403	0.450	0.508	0.594	0.154	0.223	0.287	0.342	0.391	0.438	0.490	0.554
	R3	0.117	0.175	0.230	0.285	0.341	0.391	0.444	0.502	0.581	0.127	0.191	0.250	0.310	0.370	0.425	0.483	0.547
	R4	0.094	0.138	0.195	0.255	0.317	0.377	0.436	0.494	0.567	0.102	0.149	0.212	0.277	0.344	0.410	0.474	0.538
$\lambda_{20^{\circ}\text{C}}=1.00$	R1	0.153	0.199	0.239	0.278	0.319	0.357	0.397	0.443	0.515	0.166	0.216	0.259	0.302	0.347	0.388	0.433	0.483
	R2	0.114	0.167	0.219	0.264	0.304	0.341	0.380	0.429	0.501	0.123	0.181	0.238	0.287	0.330	0.371	0.414	0.468
	R3	0.093	0.142	0.189	0.238	0.287	0.330	0.375	0.424	0.490	0.101	0.153	0.205	0.258	0.311	0.359	0.408	0.463
	R4	0.075	0.109	0.158	0.211	0.266	0.318	0.369	0.418	0.479	0.080	0.119	0.172	0.229	0.289	0.346	0.401	0.454
$\lambda_{20^{\circ}\text{C}}=1.50$	R1	0.093	0.121	0.146	0.170	0.195	0.218	0.241	0.268	0.307	0.101	0.132	0.159	0.185	0.212	0.237	0.262	0.293
	R2	0.068	0.101	0.134	0.162	0.186	0.209	0.232	0.260	0.300	0.074	0.110	0.145	0.175	0.202	0.227	0.252	0.284
	R3	0.056	0.085	0.115	0.145	0.175	0.202	0.229	0.257	0.296	0.061	0.093	0.125	0.158	0.191	0.219	0.248	0.280
	R4	0.045	0.065	0.096	0.128	0.163	0.195	0.225	0.254	0.291	0.048	0.071	0.104	0.140	0.177	0.212	0.244	0.276
$\lambda_{20^{\circ}\text{C}}=2.00$	R1	0.056	0.073	0.087	0.102	0.117	0.130	0.144	0.160	0.182	0.060	0.079	0.095	0.110	0.126	0.141	0.156	0.174
	R2	0.041	0.061	0.080	0.097	0.111	0.124	0.138	0.155	0.178	0.044	0.066	0.087	0.105	0.121	0.135	0.151	0.169
	R3	0.034	0.051	0.069	0.087	0.105	0.120	0.136	0.153	0.176	0.036	0.056	0.074	0.094	0.114	0.131	0.148	0.167
	R4	0.027	0.039	0.057	0.077	0.097	0.116	0.134	0.152	0.173	0.029	0.043	0.062	0.084	0.105	0.126	0.146	0.165
	$\alpha=0.50$									$\alpha=0.75$								
$\lambda_{20^{\circ}\text{C}}=0.00$	R1	0.509	0.639	0.747	0.851	0.964	1.000	1.000	1.000	1.000	0.583	0.757	0.904	1.000	1.000	1.000	1.000	1.000
	R2	0.401	0.558	0.699	0.815	0.928	1.000	1.000	1.000	1.000	0.474	0.667	0.844	1.000	1.000	1.000	1.000	1.000
	R3	0.337	0.487	0.621	0.750	0.878	1.000	1.000	1.000	1.000	0.408	0.587	0.756	0.924	1.000	1.000	1.000	1.000
	R4	0.267	0.393	0.539	0.684	0.824	0.966	1.000	1.000	1.000	0.324	0.488	0.659	0.838	1.000	1.000	1.000	1.000
$\lambda_{20^{\circ}\text{C}}=0.25$	R1	0.427	0.537	0.628	0.714	0.806	0.909	0.993	0.993	0.993	0.487	0.634	0.760	0.883	0.993	0.993	0.993	0.993
	R2	0.337	0.467	0.586	0.686	0.779	0.872	0.977	0.993	0.993	0.400	0.561	0.709	0.847	0.978	0.993	0.993	0.993
	R3	0.284	0.409	0.522	0.630	0.736	0.844	0.956	0.993	0.993	0.342	0.493	0.635	0.775	0.921	0.993	0.993	0.993
	R4	0.225	0.331	0.453	0.574	0.691	0.811	0.935	0.993	0.993	0.274	0.411	0.554	0.704	0.857	0.993	0.993	0.993
$\lambda_{20^{\circ}\text{C}}=0.50$	R1	0.296	0.375	0.441	0.505	0.575	0.649	0.726	0.817	0.951	0.341	0.445	0.534	0.623	0.721	0.831	0.951	0.951
	R2	0.230	0.325	0.412	0.485	0.553	0.620	0.695	0.790	0.951	0.275	0.391	0.498	0.596	0.694	0.800	0.918	0.951
	R3	0.193	0.281	0.364	0.444	0.523	0.600	0.683	0.781	0.916	0.234	0.340	0.442	0.544	0.649	0.762	0.893	0.951
	R4	0.154	0.226	0.313	0.401	0.489	0.576	0.670	0.769	0.902	0.187	0.281	0.384	0.493	0.605	0.726	0.866	0.951
$\lambda_{20^{\circ}\text{C}}=0.75$	R1	0.227	0.294	0.350	0.404	0.466	0.523	0.587	0.664	0.780	0.263	0.349	0.424	0.496	0.578	0.674	0.777	0.876
	R2	0.174	0.250	0.323	0.385	0.444	0.500	0.562	0.642	0.759	0.209	0.302	0.392	0.474	0.556	0.642	0.742	0.876
	R3	0.144	0.214	0.282	0.350	0.418	0.482	0.553	0.633	0.746	0.177	0.260	0.345	0.429	0.518	0.614	0.722	0.876
	R4	0.115	0.169	0.239	0.314	0.389	0.465	0.543	0.625	0.728	0.141	0.211	0.294	0.386	0.480	0.582	0.699	0.876
$\lambda_{20^{\circ}\text{C}}=1.00$	R1	0.186	0.243	0.292	0.340	0.392	0.442	0.496	0.562	0.725	0.216	0.289	0.353	0.415	0.486	0.566	0.655	0.725
	R2	0.139	0.205	0.269	0.323	0.374	0.422	0.475	0.542	0.641	0.168	0.247	0.324	0.396	0.468	0.541	0.626	0.725
	R3	0.115	0.173	0.232	0.292	0.351	0.407	0.467	0.534	0.628	0.141	0.211	0.284	0.357	0.433	0.515	0.607	0.725
	R4	0.091	0.135	0.195	0.260	0.326	0.392	0.458	0.527	0.615	0.113	0.170	0.240	0.319	0.401	0.489	0.590	0.725
$\lambda_{20^{\circ}\text{C}}=1.50$	R1	0.112	0.148	0.179	0.208	0.239	0.270	0.302	0.340	0.395	0.131	0.177	0.216	0.254	0.297	0.345	0.395	0.395
	R2	0.083	0.124	0.164	0.197	0.229	0.258	0.290	0.329	0.395	0.101	0.150	0.198	0.242	0.284	0.330	0.395	0.395
	R3	0.069	0.105	0.141	0.178	0.215	0.249	0.285	0.325	0.395	0.085	0.128	0.172	0.217	0.264	0.315	0.395	0.395
	R4	0.055	0.081	0.118	0.158	0.199	0.239	0.279	0.320	0.395	0.068	0.102	0.146	0.194	0.244	0.298	0.359	0.395
$\lambda_{20^{\circ}\text{C}}=2.00$	R1	0.067	0.089	0.107	0.124	0.143	0.161	0.180	0.202	0.232	0.078	0.105	0.129	0.152	0.177	0.206	0.232	0.232
	R2	0.050	0.074	0.098	0.118	0.136	0.154	0.173	0.196	0.232	0.061	0.090	0.118	0.144	0.170	0.197	0.232	0.232
	R3	0.041	0.063	0.084	0.106	0.128	0.148	0.169	0.193	0.232	0.051	0.076	0.103	0.130	0.158	0.187	0.232	0.232
	R4	0.033	0.048	0.071	0.095	0.119	0.143	0.166	0.191	0.232	0.041	0.061	0.087	0.116	0.146	0.177	0.213	0.232

$\theta_{\text{nom}} = 600^{\circ}\text{C}$

$p_{f,fi} \rightarrow$	0.10	0.20	0.30	0.40	0.50	0.60	0.70	0.80	0.90	0.10	0.20	0.30	0.40	0.50	0.60	0.70	0.80	0.90	
$\beta_{f,fi} \rightarrow$	1.28	0.84	0.52	0.40	0.00	-0.25	-0.52	-0.84	-1.28	1.28	0.84	0.52	0.40	0.00	-0.25	-0.52	-0.84	-1.28	
$\delta_{of} \rightarrow$	1.15	1.02	0.94	0.88	0.82	0.77	0.72	0.67	0.60	1.15	1.02	0.94	0.88	0.82	0.77	0.72	0.67	0.60	
	$\alpha=0.00$									$\alpha=0.25$									
$\lambda_{20^{\circ}\text{C}}=0.00$	R1	0.371	0.476	0.559	0.639	0.718	0.802	0.892	1.000	1.000	0.402	0.516	0.607	0.693	0.781	0.872	0.971	1.000	1.000
	R2	0.210	0.270	0.334	0.404	0.481	0.560	0.661	0.783	0.971	0.228	0.293	0.363	0.439	0.523	0.609	0.719	0.853	1.000
	R3	0.194	0.250	0.312	0.386	0.463	0.542	0.630	0.753	0.930	0.210	0.272	0.340	0.419	0.503	0.591	0.685	0.818	1.000
	R4	0.147	0.204	0.252	0.315	0.397	0.489	0.602	0.724	0.878	0.160	0.221	0.274	0.343	0.431	0.532	0.656	0.790	0.959
$\lambda_{20^{\circ}\text{C}}=0.25$	R1	0.312	0.400	0.470	0.536	0.603	0.673	0.749	0.842	0.975	0.338	0.434	0.509	0.582	0.655	0.731	0.816	0.919	0.993
	R2	0.177	0.227	0.281	0.341	0.404	0.472	0.555	0.659	0.818	0.191	0.247	0.306	0.370	0.440	0.514	0.602	0.716	0.892
	R3	0.163	0.211	0.263	0.325	0.389	0.455	0.531	0.631	0.782	0.177	0.229	0.286	0.352	0.423	0.494	0.578	0.687	0.853
	R4	0.124	0.172	0.213	0.265	0.333	0.412	0.506	0.609	0.740	0.135	0.186	0.232	0.289	0.363	0.447	0.550	0.664	0.807
$\lambda_{20^{\circ}\text{C}}=0.50$	R1	0.214	0.277	0.329	0.378	0.427	0.478	0.534	0.601	0.694	0.232	0.301	0.356	0.410	0.464	0.520	0.581	0.654	0.759
	R2	0.120	0.154	0.192	0.235	0.279	0.327	0.388	0.467	0.581	0.130	0.167	0.209	0.255	0.304	0.356	0.422	0.508	0.634
	R3	0.111	0.143	0.179	0.222	0.268	0.316	0.371	0.447	0.557	0.121	0.155	0.194	0.241	0.292	0.344	0.404	0.486	0.606
	R4	0.086	0.117	0.144	0.180	0.229	0.284	0.353	0.429	0.524	0.094	0.127	0.157	0.196	0.248	0.309	0.385	0.467	0.572
$\lambda_{20^{\circ}\text{C}}=0.75$	R1	0.163	0.214	0.257	0.300	0.342	0.386	0.432	0.487	0.562	0.176	0.232	0.280	0.326	0.372	0.420	0.470	0.530	0.615
	R2	0.090	0.115	0.144	0.177	0.214	0.255	0.308	0.375	0.472	0.098	0.125	0.156	0.193	0.233	0.277	0.335	0.408	0.513
	R3	0.084	0.107	0.134	0.168	0.205	0.246	0.291	0.357	0.449	0.091	0.116	0.146	0.183	0.223	0.267	0.317	0.389	0.490
	R4	0.067	0.088	0.108	0.135	0.173	0.218	0.277	0.342	0.422	0.073	0.096	0.117	0.147	0.188	0.237	0.302	0.372	0.461
$\lambda_{20^{\circ}\text{C}}=1.00$	R1	0.131	0.175	0.213	0.250	0.288	0.325	0.365	0.411	0.475	0.142	0.190	0.231	0.272	0.312	0.354	0.397	0.448	0.518
	R2	0.071	0.091	0.115	0.143	0.175	0.209	0.257	0.316	0.398	0.077	0.099	0.125	0.155	0.190	0.228	0.279	0.343	0.433
	R3	0.067	0.084	0.106	0.135	0.167	0.202	0.242	0.300	0.380	0.073	0.092	0.116	0.147	0.182	0.220	0.263	0.327	0.414
	R4	0.055	0.071	0.086	0.107	0.139	0.178	0.230	0.286	0.356	0.060	0.077	0.093	0.117	0.152	0.194	0.250	0.311	0.388
$\lambda_{20^{\circ}\text{C}}=1.50$	R1	0.079	0.106	0.130	0.153	0.176	0.199	0.223	0.250	0.288	0.086	0.115	0.141	0.166	0.191	0.216	0.242	0.273	0.314
	R2	0.043	0.054	0.069	0.086	0.106	0.128	0.157	0.193	0.243	0.046	0.059	0.075	0.094	0.115	0.139	0.171	0.211	0.264
	R3	0.040	0.051	0.064	0.082	0.101	0.123	0.147	0.184	0.232	0.044	0.055	0.069	0.089	0.110	0.133	0.160	0.200	0.253
	R4	0.034	0.043	0.051	0.064	0.084	0.108	0.140	0.175	0.218	0.037	0.046	0.056	0.070	0.091	0.117	0.152	0.190	0.238
$\lambda_{20^{\circ}\text{C}}=2.00$	R1	0.047	0.064	0.078	0.092	0.105	0.119	0.133	0.149	0.171	0.051	0.069	0.084	0.099	0.114	0.129	0.145	0.162	0.187
	R2	0.026	0.033	0.041	0.052	0.063	0.076	0.094	0.115	0.145	0.028	0.035	0.045	0.056	0.069	0.083	0.102	0.125	0.158
	R3	0.024	0.030	0.038	0.049	0.061	0.073	0.088	0.110	0.138	0.026	0.033	0.041	0.053	0.066	0.080	0.096	0.119	0.151
	R4	0.021	0.025	0.031	0.038	0.050	0.065	0.084	0.105	0.130	0.022	0.028	0.033	0.042	0.055	0.070	0.091	0.114	0.142
	$\alpha=0.50$									$\alpha=0.75$									
$\lambda_{20^{\circ}\text{C}}=0.00$	R1	0.449	0.580	0.686	0.786	0.887	0.995	1.000	1.000	1.000	0.524	0.691	0.834	0.976	1.000	1.000	1.000	1.000	1.000
	R2	0.255	0.332	0.411	0.497	0.595	0.696	0.823	0.980	1.000	0.300	0.408	0.510	0.623	0.753	0.897	1.000	1.000	1.000
	R3	0.234	0.308	0.387	0.476	0.572	0.673	0.786	0.940	1.000	0.276	0.382	0.484	0.596	0.724	0.865	1.000	1.000	1.000
	R4	0.178	0.250	0.313	0.391	0.491	0.607	0.748	0.910	1.000	0.207	0.304	0.397	0.499	0.622	0.772	0.962	1.000	1.000
$\lambda_{20^{\circ}\text{C}}=0.25$	R1	0.378	0.488	0.576	0.659	0.744	0.836	0.938	0.993	0.993	0.440	0.582	0.702	0.820	0.944	0.993	0.993	0.993	0.993
	R2	0.214	0.279	0.346	0.419	0.500	0.587	0.690	0.823	0.993	0.253	0.343	0.430	0.525	0.634	0.755	0.896	0.993	0.993
	R3	0.198	0.260	0.325	0.399	0.481	0.565	0.663	0.792	0.992	0.231	0.321	0.407	0.501	0.608	0.727	0.867	0.993	0.993
	R4	0.150	0.210	0.264	0.329	0.413	0.510	0.627	0.764	0.942	0.174	0.256	0.334	0.420	0.523	0.649	0.812	0.993	0.993
$\lambda_{20^{\circ}\text{C}}=0.50$	R1	0.259	0.338	0.403	0.465	0.527	0.594	0.668	0.758	0.889	0.304	0.405	0.491	0.577	0.667	0.767	0.884	0.951	0.951
	R2	0.146	0.190	0.236	0.289	0.346	0.406	0.483	0.583	0.736	0.172	0.234	0.294	0.362	0.437	0.523	0.628	0.773	0.951
	R3	0.135	0.177	0.221	0.274	0.332	0.393	0.462	0.558	0.704	0.159	0.219	0.278	0.343	0.419	0.506	0.605	0.736	0.951
	R4	0.104	0.143	0.179	0.224	0.282	0.352	0.440	0.538	0.665	0.121	0.175	0.227	0.286	0.359	0.449	0.565	0.714	0.918
$\lambda_{20^{\circ}\text{C}}=0.75$	R1	0.197	0.262	0.315	0.369	0.422	0.478	0.540	0.614	0.720	0.233	0.315	0.386	0.456	0.530	0.613	0.710	0.876	0.876
	R2	0.109	0.142	0.177	0.219	0.266	0.316	0.384	0.467	0.593	0.129	0.175	0.221	0.274	0.336	0.407	0.493	0.612	0.808
	R3	0.101	0.132	0.165	0.207	0.255	0.305	0.363	0.446	0.567	0.121	0.164	0.209	0.260	0.321	0.390	0.474	0.585	0.774
	R4	0.081	0.108	0.134	0.168	0.214	0.271	0.344	0.428	0.536	0.095	0.133	0.171	0.215	0.271	0.345	0.441	0.563	0.733
$\lambda_{20^{\circ}\text{C}}=1.00$	R1	0.160	0.214	0.261	0.307	0.354	0.403	0.456	0.518	0.607	0.189	0.259	0.320	0.380	0.445	0.516	0.599	0.725	0.725
	R2	0.087	0.113	0.141	0.177	0.217	0.261	0.319	0.393	0.503	0.104	0.141	0.178	0.222	0.275	0.335	0.409	0.512	0.725
	R3	0.081	0.105	0.132	0.167	0.207	0.251	0.301	0.373	0.479	0.097	0.132	0.168	0.210	0.262	0.321	0.391	0.488	0.651
	R4	0.067	0.087	0.107	0.134	0.173	0.221	0.286	0.358	0.450	0.078	0.108	0.137	0.173	0.219	0.282	0.366	0.469	0.617
$\lambda_{20^{\circ}\text{C}}=1.50$	R1	0.096	0.130	0.159	0.188	0.217	0.246	0.278	0.316	0.395	0.114	0.158	0.195	0.233	0.272	0.315	0.365	0.395	0.395
	R2	0.052	0.067	0.085	0.106	0.131	0.159	0.195	0.240	0.306	0.063	0.084	0.107	0.134	0.167	0.204	0.251	0.313	0.395
	R3	0.049	0.063	0.079	0.101	0.125	0.153	0.184	0.229	0.293	0.059	0.079	0.101	0.127	0.159	0.195	0.239	0.298	0.395
	R4	0.041	0.053	0.064	0.080	0.104	0.134	0.174	0.219	0.276	0.048	0.066	0.083	0.104	0.132	0.171	0.222	0.287	0.395
$\lambda_{20^{\circ}\text{C}}=2.00$	R1	0.057	0.078	0.095	0.112	0.129	0.147	0.166	0.188	0.232	0.068	0.094	0.116	0.138	0.162	0.188	0.217	0.232	0.232
	R2	0.031	0.040	0.051	0.064	0.079	0.095	0.117	0.143	0.182	0.038	0.051	0.064	0.080	0.100	0.122	0.149	0.186	0.232
	R3	0.029	0.038	0.047	0.060	0.075	0.091	0.110	0.136	0.174	0.035	0.047	0.060	0.076	0.095	0.117	0.143	0.178	0.232
	R4	0.025	0.032	0															

$$\theta_{\text{nom}} = 700^{\circ}\text{C}$$

$p_{f,fi} \rightarrow$	0.10	0.20	0.30	0.40	0.50	0.60	0.70	0.80	0.90	0.10	0.20	0.30	0.40	0.50	0.60	0.70	0.80	0.90	
$\beta_{f,fi} \rightarrow$	1.28	0.84	0.52	0.40	0.00	-0.25	-0.52	-0.84	-1.28	1.28	0.84	0.52	0.40	0.00	-0.25	-0.52	-0.84	-1.28	
$\delta_{of} \rightarrow$	1.15	1.02	0.94	0.88	0.82	0.77	0.72	0.67	0.60	1.15	1.02	0.94	0.88	0.82	0.77	0.72	0.67	0.60	
	$\alpha=0.00$									$\alpha=0.25$									
$\lambda_{20^{\circ}\text{C}}=0.00$	R1	0.202	0.239	0.276	0.317	0.363	0.414	0.479	0.566	0.731	0.219	0.260	0.300	0.344	0.394	0.452	0.522	0.616	0.797
	R2	0.148	0.186	0.214	0.241	0.275	0.318	0.378	0.473	0.635	0.160	0.201	0.232	0.263	0.299	0.347	0.412	0.515	0.691
	R3	0.113	0.162	0.196	0.225	0.263	0.306	0.362	0.443	0.568	0.123	0.176	0.213	0.245	0.286	0.333	0.393	0.483	0.620
	R4	0.058	0.099	0.144	0.183	0.219	0.263	0.332	0.423	0.526	0.063	0.107	0.156	0.199	0.238	0.286	0.361	0.461	0.574
$\lambda_{20^{\circ}\text{C}}=0.25$	R1	0.170	0.202	0.232	0.267	0.306	0.349	0.403	0.478	0.619	0.184	0.219	0.253	0.290	0.332	0.380	0.440	0.522	0.673
	R2	0.124	0.157	0.180	0.204	0.231	0.270	0.320	0.403	0.538	0.134	0.169	0.196	0.222	0.251	0.293	0.347	0.438	0.586
	R3	0.095	0.137	0.165	0.190	0.221	0.258	0.305	0.376	0.481	0.103	0.148	0.179	0.207	0.241	0.281	0.332	0.409	0.522
	R4	0.050	0.084	0.123	0.156	0.186	0.224	0.282	0.358	0.443	0.054	0.092	0.133	0.169	0.203	0.244	0.307	0.391	0.483
$\lambda_{20^{\circ}\text{C}}=0.50$	R1	0.115	0.136	0.157	0.181	0.208	0.239	0.278	0.330	0.433	0.125	0.148	0.171	0.197	0.226	0.260	0.302	0.359	0.472
	R2	0.086	0.107	0.123	0.138	0.158	0.182	0.217	0.277	0.375	0.093	0.116	0.133	0.150	0.171	0.198	0.236	0.301	0.409
	R3	0.068	0.094	0.113	0.129	0.149	0.174	0.207	0.257	0.332	0.074	0.102	0.122	0.140	0.162	0.190	0.225	0.279	0.362
	R4	0.040	0.062	0.086	0.106	0.126	0.151	0.192	0.243	0.305	0.043	0.067	0.093	0.116	0.137	0.165	0.210	0.264	0.333
$\lambda_{20^{\circ}\text{C}}=0.75$	R1	0.086	0.101	0.117	0.135	0.156	0.181	0.212	0.255	0.343	0.093	0.110	0.127	0.147	0.170	0.197	0.231	0.278	0.375
	R2	0.067	0.081	0.092	0.103	0.117	0.135	0.164	0.213	0.290	0.072	0.087	0.100	0.112	0.127	0.147	0.178	0.232	0.316
	R3	0.056	0.073	0.085	0.096	0.111	0.130	0.155	0.194	0.256	0.061	0.079	0.092	0.105	0.121	0.142	0.169	0.212	0.278
	R4	0.036	0.052	0.068	0.081	0.095	0.113	0.143	0.184	0.233	0.039	0.057	0.073	0.088	0.103	0.123	0.156	0.200	0.254
$\lambda_{20^{\circ}\text{C}}=1.00$	R1	0.068	0.080	0.093	0.108	0.125	0.146	0.172	0.209	0.287	0.074	0.087	0.101	0.117	0.136	0.159	0.187	0.228	0.312
	R2	0.055	0.065	0.073	0.082	0.093	0.108	0.131	0.173	0.240	0.059	0.070	0.079	0.089	0.101	0.117	0.143	0.188	0.262
	R3	0.048	0.059	0.068	0.077	0.089	0.103	0.124	0.157	0.209	0.051	0.064	0.074	0.084	0.097	0.112	0.135	0.171	0.228
	R4	0.032	0.045	0.056	0.066	0.076	0.090	0.115	0.148	0.190	0.035	0.049	0.061	0.072	0.083	0.098	0.125	0.162	0.207
$\lambda_{20^{\circ}\text{C}}=1.50$	R1	0.041	0.048	0.055	0.064	0.075	0.088	0.104	0.127	0.175	0.044	0.052	0.060	0.070	0.082	0.096	0.113	0.138	0.191
	R2	0.034	0.039	0.044	0.049	0.055	0.064	0.079	0.105	0.146	0.036	0.043	0.048	0.053	0.060	0.070	0.086	0.114	0.159
	R3	0.030	0.036	0.041	0.046	0.053	0.062	0.074	0.095	0.127	0.033	0.040	0.045	0.050	0.058	0.067	0.081	0.103	0.138
	R4	0.021	0.029	0.035	0.040	0.046	0.054	0.069	0.089	0.115	0.023	0.031	0.038	0.044	0.050	0.059	0.075	0.097	0.125
$\lambda_{20^{\circ}\text{C}}=2.00$	R1	0.024	0.029	0.033	0.038	0.045	0.053	0.062	0.076	0.105	0.026	0.031	0.036	0.042	0.049	0.057	0.068	0.083	0.115
	R2	0.020	0.023	0.026	0.029	0.033	0.038	0.047	0.063	0.087	0.022	0.026	0.029	0.032	0.036	0.042	0.051	0.068	0.095
	R3	0.018	0.022	0.025	0.028	0.032	0.037	0.045	0.057	0.076	0.020	0.024	0.027	0.030	0.035	0.040	0.048	0.062	0.083
	R4	0.013	0.017	0.021	0.024	0.028	0.032	0.041	0.053	0.069	0.014	0.019	0.023	0.026	0.030	0.035	0.045	0.058	0.075
	$\alpha=0.50$									$\alpha=0.75$									
$\lambda_{20^{\circ}\text{C}}=0.00$	R1	0.243	0.293	0.341	0.393	0.451	0.517	0.600	0.713	0.923	0.278	0.355	0.426	0.499	0.580	0.675	0.793	0.956	1.000
	R2	0.176	0.225	0.263	0.301	0.344	0.399	0.472	0.591	0.803	0.202	0.268	0.324	0.381	0.446	0.525	0.621	0.781	1.000
	R3	0.138	0.197	0.240	0.279	0.328	0.383	0.453	0.557	0.721	0.163	0.234	0.296	0.355	0.426	0.502	0.598	0.739	0.983
	R4	0.072	0.121	0.175	0.225	0.272	0.330	0.415	0.534	0.666	0.088	0.149	0.213	0.277	0.349	0.433	0.547	0.713	0.916
$\lambda_{20^{\circ}\text{C}}=0.25$	R1	0.204	0.247	0.288	0.331	0.380	0.435	0.505	0.602	0.778	0.234	0.300	0.360	0.421	0.489	0.569	0.670	0.809	0.993
	R2	0.148	0.189	0.222	0.254	0.288	0.337	0.398	0.501	0.682	0.169	0.224	0.272	0.321	0.373	0.441	0.520	0.660	0.920
	R3	0.115	0.165	0.202	0.236	0.276	0.322	0.381	0.470	0.606	0.137	0.197	0.248	0.299	0.359	0.423	0.503	0.623	0.831
	R4	0.062	0.103	0.149	0.191	0.231	0.281	0.353	0.450	0.562	0.076	0.127	0.181	0.236	0.297	0.369	0.464	0.595	0.774
$\lambda_{20^{\circ}\text{C}}=0.50$	R1	0.139	0.168	0.195	0.225	0.258	0.298	0.348	0.415	0.545	0.159	0.203	0.244	0.287	0.333	0.389	0.460	0.558	0.736
	R2	0.103	0.129	0.151	0.171	0.197	0.228	0.271	0.345	0.471	0.118	0.154	0.186	0.217	0.256	0.298	0.356	0.456	0.637
	R3	0.083	0.114	0.138	0.160	0.186	0.218	0.259	0.321	0.419	0.098	0.137	0.170	0.204	0.243	0.288	0.343	0.425	0.572
	R4	0.048	0.076	0.104	0.131	0.158	0.190	0.241	0.305	0.387	0.059	0.093	0.127	0.163	0.202	0.251	0.317	0.408	0.532
$\lambda_{20^{\circ}\text{C}}=0.75$	R1	0.103	0.124	0.145	0.167	0.194	0.225	0.265	0.321	0.433	0.118	0.152	0.182	0.214	0.251	0.294	0.350	0.429	0.580
	R2	0.080	0.098	0.113	0.128	0.146	0.169	0.204	0.266	0.367	0.091	0.117	0.140	0.163	0.192	0.223	0.267	0.348	0.498
	R3	0.068	0.088	0.104	0.120	0.139	0.163	0.194	0.243	0.323	0.079	0.106	0.130	0.154	0.183	0.214	0.257	0.323	0.440
	R4	0.043	0.064	0.083	0.100	0.118	0.142	0.180	0.231	0.295	0.052	0.077	0.101	0.126	0.154	0.189	0.237	0.310	0.403
$\lambda_{20^{\circ}\text{C}}=1.00$	R1	0.082	0.099	0.115	0.133	0.156	0.182	0.215	0.263	0.361	0.095	0.121	0.146	0.172	0.201	0.237	0.285	0.353	0.482
	R2	0.065	0.079	0.090	0.102	0.117	0.135	0.164	0.216	0.303	0.074	0.095	0.113	0.131	0.154	0.179	0.215	0.285	0.409
	R3	0.057	0.072	0.084	0.096	0.111	0.130	0.156	0.197	0.264	0.066	0.087	0.105	0.124	0.146	0.172	0.206	0.261	0.359
	R4	0.039	0.055	0.069	0.081	0.095	0.113	0.143	0.186	0.240	0.046	0.066	0.084	0.103	0.125	0.151	0.190	0.250	0.330
$\lambda_{20^{\circ}\text{C}}=1.50$	R1	0.049	0.059	0.069	0.080	0.093	0.110	0.130	0.160	0.221	0.057	0.073	0.087	0.103	0.121	0.143	0.172	0.214	0.295
	R2	0.040	0.048	0.054	0.061	0.070	0.081	0.099	0.131	0.184	0.045	0.057	0.068	0.079	0.093	0.107	0.129	0.172	0.249
	R3	0.036	0.044	0.051	0.058	0.067	0.078	0.093	0.119	0.160	0.042	0.053	0.064	0.075	0.088	0.103	0.124	0.158	0.218
	R4	0.026	0.035	0.043	0.050	0.058	0.068	0.086	0.112	0.145	0.030	0.042	0.053	0.064	0.076	0.091	0.114	0.150	0.198
$\lambda_{20^{\circ}\text{C}}=2.00$	R1	0.030	0.035	0.041	0.048	0.056	0.066	0.078	0.095	0.132	0.034	0.043	0.052	0.062	0.072	0.085	0.103	0.127	0.176
	R2	0.024	0.029	0.033	0.037	0.042	0.048	0.059	0.078	0.110	0.027	0.035	0.041	0.047	0.055	0.064	0.077	0.102	0.149
	R3	0.022	0.027	0.031	0.035	0.040	0.046	0.056	0.071	0.096	0.025	0.032	0.038	0.045	0.053	0.062	0.074	0.094	0.130
	R4	0.016	0.021																

$$\theta_{\text{nom}} = 800^{\circ}\text{C}$$

$p_{f,fi} \rightarrow$	0.10	0.20	0.30	0.40	0.50	0.60	0.70	0.80	0.90	0.10	0.20	0.30	0.40	0.50	0.60	0.70	0.80	0.90	
$\beta_{f,fi} \rightarrow$	1.28	0.84	0.52	0.40	0.00	-0.25	-0.52	-0.84	-1.28	1.28	0.84	0.52	0.40	0.00	-0.25	-0.52	-0.84	-1.28	
$\delta_{of} \rightarrow$	1.15	1.02	0.94	0.88	0.82	0.77	0.72	0.67	0.60	1.15	1.02	0.94	0.88	0.82	0.77	0.72	0.67	0.60	
	$\alpha=0.00$									$\alpha=0.25$									
$\lambda_{20^{\circ}\text{C}}=0.00$	R1	0.070	0.090	0.108	0.127	0.149	0.174	0.201	0.233	0.294	0.076	0.097	0.117	0.138	0.162	0.189	0.218	0.254	0.321
	R2	0.057	0.075	0.094	0.115	0.141	0.167	0.195	0.230	0.285	0.062	0.081	0.102	0.125	0.153	0.182	0.212	0.250	0.310
	R3	0.046	0.061	0.078	0.099	0.124	0.155	0.188	0.223	0.276	0.050	0.067	0.085	0.107	0.135	0.168	0.205	0.243	0.302
	R4	0.027	0.043	0.058	0.075	0.100	0.132	0.171	0.214	0.269	0.030	0.047	0.063	0.082	0.109	0.144	0.187	0.233	0.293
$\lambda_{20^{\circ}\text{C}}=0.25$	R1	0.059	0.075	0.090	0.107	0.125	0.146	0.169	0.197	0.251	0.064	0.081	0.098	0.116	0.136	0.159	0.183	0.214	0.274
	R2	0.048	0.062	0.078	0.096	0.118	0.141	0.164	0.194	0.241	0.052	0.068	0.085	0.105	0.128	0.153	0.178	0.211	0.264
	R3	0.039	0.052	0.066	0.083	0.104	0.130	0.159	0.189	0.234	0.042	0.056	0.071	0.090	0.113	0.142	0.173	0.206	0.255
	R4	0.025	0.038	0.050	0.066	0.087	0.115	0.146	0.181	0.228	0.027	0.041	0.055	0.071	0.095	0.124	0.159	0.198	0.250
$\lambda_{20^{\circ}\text{C}}=0.50$	R1	0.046	0.056	0.066	0.076	0.088	0.101	0.116	0.134	0.171	0.049	0.061	0.072	0.083	0.096	0.110	0.126	0.146	0.186
	R2	0.038	0.048	0.059	0.070	0.084	0.098	0.112	0.132	0.164	0.041	0.053	0.064	0.076	0.091	0.106	0.123	0.144	0.178
	R3	0.031	0.041	0.051	0.062	0.075	0.091	0.109	0.129	0.159	0.034	0.044	0.055	0.067	0.082	0.099	0.119	0.141	0.173
	R4	0.020	0.030	0.040	0.051	0.064	0.081	0.101	0.124	0.154	0.022	0.033	0.043	0.055	0.070	0.088	0.110	0.135	0.168
$\lambda_{20^{\circ}\text{C}}=0.75$	R1	0.040	0.048	0.055	0.062	0.070	0.078	0.088	0.100	0.127	0.043	0.052	0.060	0.067	0.075	0.085	0.095	0.109	0.138
	R2	0.034	0.042	0.050	0.058	0.067	0.076	0.086	0.099	0.122	0.037	0.046	0.055	0.063	0.073	0.083	0.093	0.108	0.134
	R3	0.028	0.037	0.044	0.052	0.061	0.072	0.084	0.097	0.118	0.031	0.040	0.048	0.057	0.067	0.078	0.091	0.106	0.129
	R4	0.018	0.028	0.036	0.044	0.054	0.065	0.078	0.094	0.115	0.020	0.030	0.039	0.048	0.059	0.071	0.085	0.102	0.125
$\lambda_{20^{\circ}\text{C}}=1.00$	R1	0.036	0.042	0.047	0.053	0.058	0.064	0.071	0.081	0.101	0.039	0.046	0.052	0.057	0.063	0.070	0.078	0.088	0.110
	R2	0.031	0.038	0.044	0.050	0.056	0.063	0.070	0.080	0.098	0.034	0.041	0.048	0.054	0.061	0.068	0.076	0.087	0.106
	R3	0.026	0.033	0.040	0.046	0.052	0.060	0.068	0.078	0.094	0.028	0.036	0.043	0.050	0.057	0.065	0.074	0.085	0.103
	R4	0.017	0.025	0.033	0.040	0.047	0.055	0.064	0.076	0.092	0.018	0.027	0.035	0.043	0.051	0.060	0.070	0.083	0.100
$\lambda_{20^{\circ}\text{C}}=1.50$	R1	0.023	0.027	0.030	0.033	0.036	0.040	0.044	0.049	0.061	0.025	0.029	0.033	0.036	0.040	0.043	0.048	0.053	0.066
	R2	0.021	0.025	0.028	0.032	0.035	0.039	0.043	0.048	0.058	0.022	0.027	0.031	0.035	0.038	0.042	0.047	0.053	0.064
	R3	0.017	0.022	0.026	0.029	0.033	0.037	0.042	0.048	0.057	0.019	0.024	0.028	0.032	0.036	0.041	0.046	0.052	0.062
	R4	0.011	0.017	0.022	0.026	0.030	0.035	0.040	0.046	0.055	0.012	0.018	0.023	0.028	0.033	0.038	0.043	0.050	0.061
$\lambda_{20^{\circ}\text{C}}=2.00$	R1	0.014	0.016	0.018	0.020	0.022	0.024	0.026	0.029	0.036	0.015	0.018	0.020	0.022	0.024	0.026	0.029	0.032	0.040
	R2	0.012	0.015	0.017	0.019	0.021	0.023	0.026	0.029	0.035	0.013	0.016	0.019	0.021	0.023	0.025	0.028	0.032	0.038
	R3	0.010	0.013	0.016	0.018	0.020	0.022	0.025	0.029	0.034	0.011	0.014	0.017	0.019	0.022	0.024	0.027	0.031	0.037
	R4	0.007	0.010	0.013	0.016	0.018	0.021	0.024	0.028	0.033	0.007	0.011	0.014	0.017	0.020	0.023	0.026	0.030	0.036
	$\alpha=0.50$									$\alpha=0.75$									
$\lambda_{20^{\circ}\text{C}}=0.00$	R1	0.085	0.109	0.133	0.157	0.184	0.215	0.250	0.293	0.374	0.101	0.134	0.165	0.197	0.232	0.273	0.325	0.394	0.516
	R2	0.070	0.092	0.115	0.143	0.174	0.207	0.242	0.290	0.362	0.084	0.115	0.146	0.180	0.219	0.263	0.314	0.391	0.503
	R3	0.056	0.076	0.097	0.122	0.153	0.191	0.234	0.280	0.352	0.067	0.094	0.122	0.155	0.194	0.242	0.302	0.377	0.491
	R4	0.033	0.053	0.072	0.093	0.124	0.163	0.212	0.268	0.344	0.039	0.065	0.090	0.119	0.157	0.206	0.270	0.354	0.481
$\lambda_{20^{\circ}\text{C}}=0.25$	R1	0.071	0.092	0.111	0.132	0.154	0.180	0.210	0.247	0.319	0.084	0.112	0.138	0.165	0.195	0.230	0.274	0.334	0.443
	R2	0.059	0.077	0.097	0.120	0.146	0.174	0.204	0.244	0.308	0.070	0.096	0.121	0.150	0.183	0.221	0.266	0.327	0.427
	R3	0.047	0.063	0.081	0.103	0.129	0.161	0.198	0.238	0.297	0.056	0.079	0.102	0.130	0.163	0.203	0.254	0.320	0.416
	R4	0.031	0.047	0.062	0.081	0.108	0.142	0.181	0.228	0.291	0.036	0.057	0.079	0.104	0.137	0.179	0.232	0.301	0.406
$\lambda_{20^{\circ}\text{C}}=0.50$	R1	0.055	0.069	0.081	0.094	0.108	0.125	0.144	0.169	0.217	0.064	0.083	0.101	0.118	0.138	0.160	0.189	0.228	0.300
	R2	0.046	0.060	0.072	0.087	0.103	0.121	0.140	0.166	0.209	0.055	0.073	0.090	0.109	0.131	0.155	0.183	0.224	0.292
	R3	0.038	0.050	0.063	0.076	0.093	0.113	0.136	0.163	0.203	0.045	0.062	0.078	0.096	0.118	0.144	0.177	0.218	0.283
	R4	0.024	0.037	0.049	0.063	0.079	0.100	0.125	0.156	0.197	0.029	0.046	0.062	0.080	0.101	0.128	0.161	0.207	0.275
$\lambda_{20^{\circ}\text{C}}=0.75$	R1	0.048	0.059	0.068	0.077	0.086	0.097	0.110	0.126	0.161	0.055	0.070	0.084	0.097	0.110	0.126	0.146	0.172	0.224
	R2	0.041	0.052	0.062	0.072	0.083	0.094	0.107	0.125	0.155	0.048	0.063	0.077	0.091	0.106	0.122	0.142	0.171	0.216
	R3	0.034	0.045	0.055	0.065	0.076	0.089	0.104	0.122	0.151	0.040	0.054	0.068	0.082	0.097	0.115	0.137	0.167	0.211
	R4	0.022	0.034	0.044	0.055	0.067	0.081	0.097	0.118	0.147	0.026	0.041	0.055	0.069	0.085	0.104	0.127	0.158	0.207
$\lambda_{20^{\circ}\text{C}}=1.00$	R1	0.043	0.051	0.058	0.065	0.072	0.080	0.090	0.102	0.129	0.048	0.061	0.071	0.082	0.093	0.105	0.120	0.140	0.180
	R2	0.038	0.046	0.054	0.062	0.070	0.078	0.088	0.101	0.124	0.043	0.056	0.067	0.078	0.089	0.102	0.117	0.138	0.174
	R3	0.031	0.041	0.049	0.056	0.065	0.074	0.086	0.099	0.121	0.036	0.049	0.060	0.071	0.083	0.097	0.114	0.136	0.170
	R4	0.020	0.031	0.040	0.049	0.058	0.069	0.080	0.096	0.118	0.024	0.037	0.049	0.061	0.074	0.089	0.106	0.129	0.167
$\lambda_{20^{\circ}\text{C}}=1.50$	R1	0.028	0.033	0.037	0.041	0.045	0.050	0.055	0.062	0.077	0.031	0.039	0.045	0.052	0.058	0.065	0.074	0.086	0.109
	R2	0.025	0.030	0.035	0.039	0.044	0.049	0.054	0.062	0.075	0.028	0.036	0.043	0.049	0.056	0.064	0.072	0.085	0.105
	R3	0.021	0.027	0.032	0.036	0.041	0.046	0.053	0.060	0.073	0.024	0.032	0.039	0.045	0.053	0.061	0.071	0.083	0.103
	R4	0.013	0.020	0.026	0.032	0.037	0.043	0.050	0.059	0.071	0.016	0.025	0.032	0.040	0.047	0.056	0.066	0.080	0.101
$\lambda_{20^{\circ}\text{C}}=2.00$	R1	0.017	0.020	0.022	0.025	0.027	0.030	0.033	0.037	0.046	0.019	0.023	0.027	0.031	0.035	0.039	0.045	0.052	0.065
	R2	0.015	0.018	0.021	0.024	0.026	0.029	0.032	0.037	0.045	0.017	0.022	0.026	0.030	0.034	0.038	0.044	0.051	0.063
	R3	0.012	0.016	0.019	0.022	0.025	0.028	0.032	0.036	0.043	0.014	0.019	0.023	0.027	0.032	0.037	0.043	0.050	0.062
	R4	0.008	0.012																

$$\theta_{\text{nom}} = 900^{\circ}\text{C}$$

$p_{f,fi} \rightarrow$	0.10	0.20	0.30	0.40	0.50	0.60	0.70	0.80	0.90	0.10	0.20	0.30	0.40	0.50	0.60	0.70	0.80	0.90	
$\beta_{f,fi} \rightarrow$	1.28	0.84	0.52	0.40	0.00	-0.25	-0.52	-0.84	-1.28	1.28	0.84	0.52	0.40	0.00	-0.25	-0.52	-0.84	-1.28	
$\delta_{of} \rightarrow$	1.15	1.02	0.94	0.88	0.82	0.77	0.72	0.67	0.60	1.15	1.02	0.94	0.88	0.82	0.77	0.72	0.67	0.60	
	$\alpha=0.00$									$\alpha=0.25$									
$\lambda_{20^{\circ}\text{C}}=0.00$	R1	0.070	0.090	0.108	0.127	0.149	0.174	0.201	0.233	0.294	0.076	0.097	0.117	0.138	0.162	0.189	0.218	0.254	0.321
	R2	0.057	0.075	0.094	0.115	0.141	0.167	0.195	0.230	0.285	0.062	0.081	0.102	0.125	0.153	0.182	0.212	0.250	0.310
	R3	0.046	0.061	0.078	0.099	0.124	0.155	0.188	0.223	0.276	0.050	0.067	0.085	0.107	0.135	0.168	0.205	0.243	0.302
	R4	0.027	0.043	0.058	0.075	0.100	0.132	0.171	0.214	0.269	0.030	0.047	0.063	0.082	0.109	0.144	0.187	0.233	0.293
$\lambda_{20^{\circ}\text{C}}=0.25$	R1	0.059	0.075	0.090	0.107	0.125	0.146	0.169	0.197	0.251	0.064	0.081	0.098	0.116	0.136	0.159	0.183	0.214	0.274
	R2	0.048	0.062	0.078	0.096	0.118	0.141	0.164	0.194	0.241	0.052	0.068	0.085	0.105	0.128	0.153	0.178	0.211	0.264
	R3	0.039	0.052	0.066	0.083	0.104	0.130	0.159	0.189	0.234	0.042	0.056	0.071	0.090	0.113	0.142	0.173	0.206	0.255
	R4	0.025	0.038	0.050	0.066	0.087	0.115	0.146	0.181	0.228	0.027	0.041	0.055	0.071	0.095	0.124	0.159	0.198	0.250
$\lambda_{20^{\circ}\text{C}}=0.50$	R1	0.046	0.056	0.066	0.076	0.088	0.101	0.116	0.134	0.171	0.049	0.061	0.072	0.083	0.096	0.110	0.126	0.146	0.186
	R2	0.038	0.048	0.059	0.070	0.084	0.098	0.112	0.132	0.164	0.041	0.053	0.064	0.076	0.091	0.106	0.123	0.144	0.178
	R3	0.031	0.041	0.051	0.062	0.075	0.091	0.109	0.129	0.159	0.034	0.044	0.055	0.067	0.082	0.099	0.119	0.141	0.173
	R4	0.020	0.030	0.040	0.051	0.064	0.081	0.101	0.124	0.154	0.022	0.033	0.043	0.055	0.070	0.088	0.110	0.135	0.168
$\lambda_{20^{\circ}\text{C}}=0.75$	R1	0.040	0.048	0.055	0.062	0.070	0.078	0.088	0.100	0.127	0.043	0.052	0.060	0.067	0.075	0.085	0.095	0.109	0.138
	R2	0.034	0.042	0.050	0.058	0.067	0.076	0.086	0.099	0.122	0.037	0.046	0.055	0.063	0.073	0.083	0.093	0.108	0.134
	R3	0.028	0.037	0.044	0.052	0.061	0.072	0.084	0.097	0.118	0.031	0.040	0.048	0.057	0.067	0.078	0.091	0.106	0.129
	R4	0.018	0.028	0.036	0.044	0.054	0.065	0.078	0.094	0.115	0.020	0.030	0.039	0.048	0.059	0.071	0.085	0.102	0.125
$\lambda_{20^{\circ}\text{C}}=1.00$	R1	0.036	0.042	0.047	0.053	0.058	0.064	0.071	0.081	0.101	0.039	0.046	0.052	0.057	0.063	0.070	0.078	0.088	0.110
	R2	0.031	0.038	0.044	0.050	0.056	0.063	0.070	0.080	0.098	0.034	0.041	0.048	0.054	0.061	0.068	0.076	0.087	0.106
	R3	0.026	0.033	0.040	0.046	0.052	0.060	0.068	0.078	0.094	0.028	0.036	0.043	0.050	0.057	0.065	0.074	0.085	0.103
	R4	0.017	0.025	0.033	0.040	0.047	0.055	0.064	0.076	0.092	0.018	0.027	0.035	0.043	0.051	0.060	0.070	0.083	0.100
$\lambda_{20^{\circ}\text{C}}=1.50$	R1	0.023	0.027	0.030	0.033	0.036	0.040	0.044	0.049	0.061	0.025	0.029	0.033	0.036	0.040	0.043	0.048	0.053	0.066
	R2	0.021	0.025	0.028	0.032	0.035	0.039	0.043	0.048	0.058	0.022	0.027	0.031	0.035	0.038	0.042	0.047	0.053	0.064
	R3	0.017	0.022	0.026	0.029	0.033	0.037	0.042	0.048	0.057	0.019	0.024	0.028	0.032	0.036	0.041	0.046	0.052	0.062
	R4	0.011	0.017	0.022	0.026	0.030	0.035	0.040	0.046	0.055	0.012	0.018	0.023	0.028	0.033	0.038	0.043	0.050	0.061
$\lambda_{20^{\circ}\text{C}}=2.00$	R1	0.014	0.016	0.018	0.020	0.022	0.024	0.026	0.029	0.036	0.015	0.018	0.020	0.022	0.024	0.026	0.029	0.032	0.040
	R2	0.012	0.015	0.017	0.019	0.021	0.023	0.026	0.029	0.035	0.013	0.016	0.019	0.021	0.023	0.025	0.028	0.032	0.038
	R3	0.010	0.013	0.016	0.018	0.020	0.022	0.025	0.029	0.034	0.011	0.014	0.017	0.019	0.022	0.024	0.027	0.031	0.037
	R4	0.007	0.010	0.013	0.016	0.018	0.021	0.024	0.028	0.033	0.007	0.011	0.014	0.017	0.020	0.023	0.026	0.030	0.036
	$\alpha=0.50$									$\alpha=0.75$									
$\lambda_{20^{\circ}\text{C}}=0.00$	R1	0.085	0.109	0.133	0.157	0.184	0.215	0.250	0.293	0.374	0.101	0.134	0.165	0.197	0.232	0.273	0.325	0.394	0.516
	R2	0.070	0.092	0.115	0.143	0.174	0.207	0.242	0.290	0.362	0.084	0.115	0.146	0.180	0.219	0.263	0.314	0.391	0.503
	R3	0.056	0.076	0.097	0.122	0.153	0.191	0.234	0.280	0.352	0.067	0.094	0.122	0.155	0.194	0.242	0.302	0.377	0.491
	R4	0.033	0.053	0.072	0.093	0.124	0.163	0.212	0.268	0.344	0.039	0.065	0.090	0.119	0.157	0.206	0.270	0.354	0.481
$\lambda_{20^{\circ}\text{C}}=0.25$	R1	0.071	0.092	0.111	0.132	0.154	0.180	0.210	0.247	0.319	0.084	0.112	0.138	0.165	0.195	0.230	0.274	0.334	0.443
	R2	0.059	0.077	0.097	0.120	0.146	0.174	0.204	0.244	0.308	0.070	0.096	0.121	0.150	0.183	0.221	0.266	0.327	0.427
	R3	0.047	0.063	0.081	0.103	0.129	0.161	0.198	0.238	0.297	0.056	0.079	0.102	0.130	0.163	0.203	0.254	0.320	0.416
	R4	0.031	0.047	0.062	0.081	0.108	0.142	0.181	0.228	0.291	0.036	0.057	0.079	0.104	0.137	0.179	0.232	0.301	0.406
$\lambda_{20^{\circ}\text{C}}=0.50$	R1	0.055	0.069	0.081	0.094	0.108	0.125	0.144	0.169	0.217	0.064	0.083	0.101	0.118	0.138	0.160	0.189	0.228	0.300
	R2	0.046	0.060	0.072	0.087	0.103	0.121	0.140	0.166	0.209	0.055	0.073	0.090	0.109	0.131	0.155	0.183	0.224	0.292
	R3	0.038	0.050	0.063	0.076	0.093	0.113	0.136	0.163	0.203	0.045	0.062	0.078	0.096	0.118	0.144	0.177	0.218	0.283
	R4	0.024	0.037	0.049	0.063	0.079	0.100	0.125	0.156	0.197	0.029	0.046	0.062	0.080	0.101	0.128	0.161	0.207	0.275
$\lambda_{20^{\circ}\text{C}}=0.75$	R1	0.048	0.059	0.068	0.077	0.086	0.097	0.110	0.126	0.161	0.055	0.070	0.084	0.097	0.110	0.126	0.146	0.172	0.224
	R2	0.041	0.052	0.062	0.072	0.083	0.094	0.107	0.125	0.155	0.048	0.063	0.077	0.091	0.106	0.122	0.142	0.171	0.216
	R3	0.034	0.045	0.055	0.065	0.076	0.089	0.104	0.122	0.151	0.040	0.054	0.068	0.082	0.097	0.115	0.137	0.167	0.211
	R4	0.022	0.034	0.044	0.055	0.067	0.081	0.097	0.118	0.147	0.026	0.041	0.055	0.069	0.085	0.104	0.127	0.158	0.207
$\lambda_{20^{\circ}\text{C}}=1.00$	R1	0.043	0.051	0.058	0.065	0.072	0.080	0.090	0.102	0.129	0.048	0.061	0.071	0.082	0.093	0.105	0.120	0.140	0.180
	R2	0.038	0.046	0.054	0.062	0.070	0.078	0.088	0.101	0.124	0.043	0.056	0.067	0.078	0.089	0.102	0.117	0.138	0.174
	R3	0.031	0.041	0.049	0.056	0.065	0.074	0.086	0.099	0.121	0.036	0.049	0.060	0.071	0.083	0.097	0.114	0.136	0.170
	R4	0.020	0.031	0.040	0.049	0.058	0.069	0.080	0.096	0.118	0.024	0.037	0.049	0.061	0.074	0.089	0.106	0.129	0.167
$\lambda_{20^{\circ}\text{C}}=1.50$	R1	0.028	0.033	0.037	0.041	0.045	0.050	0.055	0.062	0.077	0.031	0.039	0.045	0.052	0.058	0.065	0.074	0.086	0.109
	R2	0.025	0.030	0.035	0.039	0.044	0.049	0.054	0.062	0.075	0.028	0.036	0.043	0.049	0.056	0.064	0.072	0.085	0.105
	R3	0.021	0.027	0.032	0.036	0.041	0.046	0.053	0.060	0.073	0.024	0.032	0.039	0.045	0.053	0.061	0.071	0.083	0.103
	R4	0.013	0.020	0.026	0.032	0.037	0.043	0.050	0.059	0.071	0.016	0.025	0.032	0.040	0.047	0.056	0.066	0.080	0.101
$\lambda_{20^{\circ}\text{C}}=2.00$	R1	0.017	0.020	0.022	0.025	0.027	0.030	0.033	0.037	0.046	0.019	0.023	0.027	0.031	0.035	0.039	0.045	0.052	0.065
	R2	0.015	0.018	0.021	0.024	0.026	0.029	0.032	0.037	0.045	0.017	0.022	0.026	0.030	0.034	0.038	0.044	0.051	0.063
	R3	0.012	0.016	0.019	0.022	0.025	0.028	0.032	0.036	0.043	0.014	0.019	0.023	0.027	0.032	0.037	0.043	0.050	0.062
	R4	0.008	0.012	0.01															

A19 Factor χ_{Rel} for S355 weak axis, imposed (Q) variable load type

		$\theta_{\text{nom}} = 300^{\circ}\text{C}$																	
$p_{f,fi} \rightarrow$		0.10	0.20	0.30	0.40	0.50	0.60	0.70	0.80	0.90	0.10	0.20	0.30	0.40	0.50	0.60	0.70	0.80	0.90
$\beta_{f,fi} \rightarrow$		1.28	0.84	0.52	0.40	0.00	-0.25	-0.52	-0.84	-1.28	1.28	0.84	0.52	0.40	0.00	-0.25	-0.52	-0.84	-1.28
$\delta_{of} \rightarrow$		1.15	1.02	0.94	0.88	0.82	0.77	0.72	0.67	0.60	1.15	1.02	0.94	0.88	0.82	0.77	0.72	0.67	0.60
		$\alpha=0.00$									$\alpha=0.25$								
$\lambda_{20^{\circ}\text{C}}=0.00$	R1	0.815	0.909	0.980	1.000	1.000	1.000	1.000	1.000	1.000	0.881	0.985	1.000	1.000	1.000	1.000	1.000	1.000	1.000
	R2	0.792	0.892	0.965	1.000	1.000	1.000	1.000	1.000	1.000	0.856	0.965	1.000	1.000	1.000	1.000	1.000	1.000	1.000
	R3	0.782	0.885	0.959	1.000	1.000	1.000	1.000	1.000	1.000	0.846	0.959	1.000	1.000	1.000	1.000	1.000	1.000	1.000
	R4	0.743	0.857	0.935	1.000	1.000	1.000	1.000	1.000	1.000	0.801	0.927	1.000	1.000	1.000	1.000	1.000	1.000	1.000
$\lambda_{20^{\circ}\text{C}}=0.25$	R1	0.665	0.741	0.800	0.853	0.905	0.959	0.993	0.993	0.993	0.719	0.804	0.869	0.927	0.985	0.993	0.993	0.993	0.993
	R2	0.646	0.727	0.788	0.843	0.895	0.950	0.993	0.993	0.993	0.699	0.789	0.856	0.917	0.975	0.993	0.993	0.993	0.993
	R3	0.638	0.722	0.784	0.838	0.890	0.944	0.993	0.993	0.993	0.690	0.782	0.851	0.911	0.970	0.993	0.993	0.993	0.993
	R4	0.605	0.698	0.764	0.821	0.875	0.933	0.993	0.993	0.993	0.654	0.757	0.829	0.893	0.954	0.993	0.993	0.993	0.993
$\lambda_{20^{\circ}\text{C}}=0.50$	R1	0.531	0.596	0.648	0.696	0.744	0.794	0.851	0.951	0.951	0.573	0.646	0.703	0.756	0.809	0.864	0.951	0.951	0.951
	R2	0.515	0.584	0.636	0.685	0.731	0.780	0.836	0.951	0.951	0.557	0.632	0.691	0.744	0.795	0.850	0.951	0.951	0.951
	R3	0.506	0.576	0.629	0.675	0.720	0.768	0.823	0.951	0.951	0.546	0.624	0.682	0.733	0.783	0.836	0.951	0.951	0.951
	R4	0.474	0.554	0.611	0.661	0.709	0.759	0.814	0.880	0.951	0.512	0.599	0.663	0.718	0.771	0.826	0.887	0.951	0.951
$\lambda_{20^{\circ}\text{C}}=0.75$	R1	0.440	0.501	0.552	0.599	0.647	0.695	0.751	0.876	0.876	0.477	0.545	0.599	0.652	0.704	0.756	0.876	0.876	0.876
	R2	0.425	0.487	0.539	0.586	0.630	0.677	0.733	0.876	0.876	0.459	0.530	0.586	0.637	0.684	0.737	0.876	0.876	0.876
	R3	0.416	0.479	0.530	0.572	0.613	0.661	0.715	0.876	0.876	0.449	0.520	0.576	0.623	0.668	0.719	0.876	0.876	0.876
	R4	0.386	0.457	0.511	0.559	0.605	0.652	0.705	0.876	0.876	0.417	0.496	0.555	0.607	0.658	0.710	0.876	0.876	0.876
$\lambda_{20^{\circ}\text{C}}=1.00$	R1	0.359	0.411	0.454	0.495	0.536	0.577	0.725	0.725	0.725	0.388	0.445	0.492	0.538	0.583	0.725	0.725	0.725	0.725
	R2	0.346	0.399	0.442	0.482	0.520	0.562	0.725	0.725	0.725	0.374	0.432	0.480	0.524	0.565	0.725	0.725	0.725	0.725
	R3	0.337	0.391	0.434	0.470	0.506	0.547	0.594	0.725	0.725	0.365	0.424	0.471	0.511	0.550	0.595	0.725	0.725	0.725
	R4	0.312	0.372	0.417	0.457	0.497	0.538	0.583	0.725	0.725	0.338	0.404	0.453	0.497	0.541	0.586	0.725	0.725	0.725
$\lambda_{20^{\circ}\text{C}}=1.50$	R1	0.210	0.238	0.261	0.282	0.303	0.324	0.348	0.395	0.395	0.227	0.258	0.283	0.306	0.329	0.395	0.395	0.395	0.395
	R2	0.203	0.232	0.255	0.276	0.296	0.317	0.341	0.395	0.395	0.220	0.251	0.277	0.300	0.322	0.345	0.395	0.395	0.395
	R3	0.198	0.228	0.251	0.271	0.289	0.310	0.334	0.395	0.395	0.215	0.247	0.273	0.294	0.315	0.337	0.395	0.395	0.395
	R4	0.185	0.218	0.243	0.264	0.285	0.306	0.330	0.395	0.395	0.200	0.236	0.263	0.287	0.310	0.334	0.395	0.395	0.395
$\lambda_{20^{\circ}\text{C}}=2.00$	R1	0.126	0.142	0.155	0.167	0.179	0.191	0.205	0.232	0.232	0.136	0.154	0.168	0.181	0.195	0.208	0.232	0.232	0.232
	R2	0.122	0.139	0.152	0.164	0.175	0.188	0.201	0.232	0.232	0.132	0.150	0.165	0.178	0.191	0.204	0.232	0.232	0.232
	R3	0.119	0.137	0.150	0.161	0.172	0.183	0.197	0.214	0.232	0.129	0.148	0.162	0.175	0.187	0.200	0.215	0.232	0.232
	R4	0.111	0.131	0.145	0.157	0.169	0.181	0.195	0.212	0.232	0.120	0.142	0.157	0.171	0.184	0.198	0.213	0.232	0.232
		$\alpha=0.50$									$\alpha=0.75$								
$\lambda_{20^{\circ}\text{C}}=0.00$	R1	0.960	1.000	1.000	1.000	1.000	1.000	1.000	1.000	1.000	1.000	1.000	1.000	1.000	1.000	1.000	1.000	1.000	1.000
	R2	0.930	1.000	1.000	1.000	1.000	1.000	1.000	1.000	1.000	1.000	1.000	1.000	1.000	1.000	1.000	1.000	1.000	1.000
	R3	0.919	1.000	1.000	1.000	1.000	1.000	1.000	1.000	1.000	0.993	1.000	1.000	1.000	1.000	1.000	1.000	1.000	1.000
	R4	0.873	1.000	1.000	1.000	1.000	1.000	1.000	1.000	1.000	0.946	1.000	1.000	1.000	1.000	1.000	1.000	1.000	1.000
$\lambda_{20^{\circ}\text{C}}=0.25$	R1	0.781	0.892	0.978	0.993	0.993	0.993	0.993	0.993	0.993	0.843	0.993	0.993	0.993	0.993	0.993	0.993	0.993	0.993
	R2	0.760	0.875	0.963	0.993	0.993	0.993	0.993	0.993	0.993	0.821	0.993	0.993	0.993	0.993	0.993	0.993	0.993	0.993
	R3	0.749	0.867	0.957	0.993	0.993	0.993	0.993	0.993	0.993	0.812	0.993	0.993	0.993	0.993	0.993	0.993	0.993	0.993
	R4	0.712	0.839	0.932	0.993	0.993	0.993	0.993	0.993	0.993	0.773	0.961	0.993	0.993	0.993	0.993	0.993	0.993	0.993
$\lambda_{20^{\circ}\text{C}}=0.50$	R1	0.625	0.717	0.790	0.859	0.951	0.951	0.951	0.951	0.951	0.679	0.827	0.951	0.951	0.951	0.951	0.951	0.951	0.951
	R2	0.607	0.702	0.777	0.844	0.951	0.951	0.951	0.951	0.951	0.660	0.810	0.951	0.951	0.951	0.951	0.951	0.951	0.951
	R3	0.596	0.692	0.767	0.832	0.951	0.951	0.951	0.951	0.951	0.648	0.797	0.951	0.951	0.951	0.951	0.951	0.951	0.951
	R4	0.559	0.665	0.744	0.813	0.881	0.951	0.951	0.951	0.951	0.610	0.763	0.951	0.951	0.951	0.951	0.951	0.951	0.951
$\lambda_{20^{\circ}\text{C}}=0.75$	R1	0.522	0.607	0.675	0.740	0.876	0.876	0.876	0.876	0.876	0.572	0.705	0.876	0.876	0.876	0.876	0.876	0.876	0.876
	R2	0.505	0.591	0.659	0.723	0.876	0.876	0.876	0.876	0.876	0.554	0.687	0.876	0.876	0.876	0.876	0.876	0.876	0.876
	R3	0.492	0.580	0.649	0.707	0.876	0.876	0.876	0.876	0.876	0.541	0.673	0.876	0.876	0.876	0.876	0.876	0.876	0.876
	R4	0.457	0.552	0.624	0.688	0.750	0.876	0.876	0.876	0.876	0.504	0.640	0.754	0.876	0.876	0.876	0.876	0.876	0.876
$\lambda_{20^{\circ}\text{C}}=1.00$	R1	0.426	0.496	0.555	0.725	0.725	0.725	0.725	0.725	0.725	0.468	0.577	0.725	0.725	0.725	0.725	0.725	0.725	0.725
	R2	0.411	0.483	0.541	0.596	0.725	0.725	0.725	0.725	0.725	0.454	0.561	0.725	0.725	0.725	0.725	0.725	0.725	0.725
	R3	0.401	0.473	0.531	0.580	0.725	0.725	0.725	0.725	0.725	0.441	0.551	0.725	0.725	0.725	0.725	0.725	0.725	0.725
	R4	0.371	0.449	0.509	0.564	0.725	0.725	0.725	0.725	0.725	0.410	0.522	0.725	0.725	0.725	0.725	0.725	0.725	0.725
$\lambda_{20^{\circ}\text{C}}=1.50$	R1	0.248	0.286	0.318	0.347	0.395	0.395	0.395	0.395	0.395	0.271	0.332	0.395	0.395	0.395	0.395	0.395	0.395	0.395
	R2	0.240	0.280	0.312	0.340	0.395	0.395	0.395	0.395	0.395	0.263	0.323	0.395	0.395	0.395	0.395	0.395	0.395	0.395
	R3	0.235	0.275	0.306	0.334	0.395	0.395	0.395	0.395	0.395	0.257	0.319	0.395	0.395	0.395	0.395	0.395	0.395	0.395
	R4	0.218	0.263	0.296	0.325	0.395	0.395	0.395	0.395	0.395	0.240	0.303	0.395	0.395	0.395	0.395	0.395	0.395	0.395
$\lambda_{20^{\circ}\text{C}}=2.00$	R1	0.148	0.171	0.189	0.206	0.232	0.232	0.232	0.232	0.232	0.161	0.198	0.232	0.232	0.232	0.232	0.232	0.232	0.232
	R2	0.144	0.167	0.185	0.202	0.232	0.232	0.232	0.232	0.232	0.156	0.193	0.232	0.232	0.232	0.232	0.232	0.232	0.232
	R3	0.141	0.164	0.183	0.199	0.214	0.232	0.232	0.232	0.232	0.153	0.189	0.232	0.232	0.232	0.232	0		

$\theta_{\text{nom}} = 400^{\circ}\text{C}$

$p_{f,fi} \rightarrow$	0.10	0.20	0.30	0.40	0.50	0.60	0.70	0.80	0.90	0.10	0.20	0.30	0.40	0.50	0.60	0.70	0.80	0.90
$\beta_{f,fi} \rightarrow$	1.28	0.84	0.52	0.40	0.00	-0.25	-0.52	-0.84	-1.28	1.28	0.84	0.52	0.40	0.00	-0.25	-0.52	-0.84	-1.28
$\delta_{af} \rightarrow$	1.15	1.02	0.94	0.88	0.82	0.77	0.72	0.67	0.60	1.15	1.02	0.94	0.88	0.82	0.77	0.72	0.67	0.60
	$\alpha=0.00$									$\alpha=0.25$								
$\lambda_{20^{\circ}\text{C}}=0.00$	R1	0.759	0.856	0.928	0.992	1.000	1.000	1.000	1.000	0.821	0.927	1.000	1.000	1.000	1.000	1.000	1.000	1.000
	R2	0.615	0.742	0.833	0.910	0.984	1.000	1.000	1.000	0.667	0.806	0.904	0.988	1.000	1.000	1.000	1.000	1.000
	R3	0.580	0.727	0.823	0.903	0.976	1.000	1.000	1.000	0.629	0.789	0.893	0.981	1.000	1.000	1.000	1.000	1.000
	R4	0.519	0.680	0.790	0.876	0.954	1.000	1.000	1.000	0.564	0.737	0.857	0.952	1.000	1.000	1.000	1.000	1.000
$\lambda_{20^{\circ}\text{C}}=0.25$	R1	0.618	0.697	0.756	0.809	0.861	0.916	0.977	0.993	0.667	0.755	0.821	0.880	0.938	0.993	0.993	0.993	0.993
	R2	0.501	0.605	0.679	0.742	0.802	0.864	0.930	0.993	0.542	0.655	0.737	0.806	0.873	0.941	0.993	0.993	0.993
	R3	0.471	0.592	0.670	0.736	0.796	0.856	0.923	0.993	0.511	0.641	0.728	0.799	0.866	0.933	0.993	0.993	0.993
	R4	0.425	0.553	0.642	0.714	0.779	0.842	0.910	0.993	0.459	0.600	0.697	0.775	0.847	0.917	0.993	0.993	0.993
$\lambda_{20^{\circ}\text{C}}=0.50$	R1	0.476	0.538	0.585	0.627	0.667	0.711	0.759	0.820	0.514	0.583	0.634	0.681	0.726	0.774	0.827	0.951	0.951
	R2	0.381	0.463	0.522	0.574	0.623	0.669	0.721	0.786	0.413	0.502	0.566	0.622	0.678	0.728	0.787	0.858	0.951
	R3	0.357	0.454	0.516	0.567	0.615	0.662	0.715	0.778	0.387	0.491	0.559	0.615	0.668	0.721	0.779	0.850	0.951
	R4	0.319	0.423	0.494	0.551	0.603	0.653	0.706	0.768	0.346	0.458	0.536	0.599	0.656	0.711	0.770	0.838	0.951
$\lambda_{20^{\circ}\text{C}}=0.75$	R1	0.385	0.437	0.477	0.512	0.549	0.587	0.631	0.687	0.416	0.473	0.517	0.557	0.597	0.639	0.687	0.749	0.876
	R2	0.304	0.373	0.422	0.467	0.509	0.549	0.595	0.656	0.330	0.404	0.459	0.507	0.553	0.597	0.649	0.716	0.876
	R3	0.283	0.365	0.418	0.460	0.501	0.542	0.589	0.645	0.307	0.396	0.453	0.500	0.545	0.590	0.642	0.703	0.876
	R4	0.249	0.338	0.399	0.448	0.492	0.532	0.578	0.632	0.270	0.367	0.433	0.486	0.535	0.580	0.630	0.690	0.876
$\lambda_{20^{\circ}\text{C}}=1.00$	R1	0.311	0.353	0.386	0.416	0.445	0.477	0.514	0.563	0.337	0.383	0.419	0.451	0.484	0.519	0.560	0.725	0.725
	R2	0.244	0.301	0.342	0.378	0.412	0.446	0.485	0.535	0.264	0.326	0.371	0.411	0.449	0.485	0.528	0.584	0.725
	R3	0.225	0.295	0.338	0.373	0.406	0.440	0.478	0.524	0.245	0.319	0.366	0.405	0.442	0.479	0.521	0.572	0.725
	R4	0.197	0.272	0.322	0.363	0.398	0.432	0.469	0.514	0.213	0.295	0.350	0.394	0.433	0.470	0.511	0.561	0.725
$\lambda_{20^{\circ}\text{C}}=1.50$	R1	0.184	0.209	0.227	0.244	0.261	0.279	0.298	0.324	0.199	0.226	0.247	0.265	0.284	0.303	0.325	0.395	0.395
	R2	0.145	0.179	0.203	0.224	0.243	0.261	0.283	0.310	0.157	0.194	0.219	0.243	0.264	0.285	0.308	0.338	0.395
	R3	0.133	0.175	0.200	0.220	0.240	0.259	0.280	0.306	0.144	0.190	0.218	0.239	0.260	0.281	0.305	0.334	0.395
	R4	0.116	0.162	0.192	0.215	0.235	0.254	0.275	0.301	0.125	0.176	0.208	0.233	0.256	0.277	0.300	0.328	0.395
$\lambda_{20^{\circ}\text{C}}=2.00$	R1	0.111	0.126	0.137	0.147	0.156	0.167	0.179	0.193	0.120	0.136	0.148	0.160	0.170	0.182	0.195	0.211	0.232
	R2	0.088	0.108	0.122	0.135	0.146	0.157	0.169	0.185	0.095	0.117	0.132	0.146	0.159	0.171	0.185	0.202	0.232
	R3	0.081	0.106	0.121	0.133	0.144	0.155	0.168	0.183	0.088	0.115	0.131	0.144	0.157	0.169	0.183	0.200	0.232
	R4	0.070	0.098	0.116	0.129	0.142	0.153	0.165	0.180	0.076	0.106	0.125	0.140	0.154	0.167	0.180	0.197	0.232
	$\alpha=0.50$									$\alpha=0.75$								
$\lambda_{20^{\circ}\text{C}}=0.00$	R1	0.895	1.000	1.000	1.000	1.000	1.000	1.000	1.000	0.968	1.000	1.000	1.000	1.000	1.000	1.000	1.000	1.000
	R2	0.733	0.893	1.000	1.000	1.000	1.000	1.000	1.000	0.815	1.000	1.000	1.000	1.000	1.000	1.000	1.000	1.000
	R3	0.694	0.872	0.999	1.000	1.000	1.000	1.000	1.000	0.776	1.000	1.000	1.000	1.000	1.000	1.000	1.000	1.000
	R4	0.626	0.818	0.955	1.000	1.000	1.000	1.000	1.000	0.709	0.943	1.000	1.000	1.000	1.000	1.000	1.000	1.000
$\lambda_{20^{\circ}\text{C}}=0.25$	R1	0.729	0.838	0.924	0.993	0.993	0.993	0.993	0.993	0.793	0.969	0.993	0.993	0.993	0.993	0.993	0.993	0.993
	R2	0.596	0.727	0.824	0.911	0.993	0.993	0.993	0.993	0.663	0.841	0.988	0.993	0.993	0.993	0.993	0.993	0.993
	R3	0.565	0.711	0.814	0.904	0.987	0.993	0.993	0.993	0.634	0.820	0.974	0.993	0.993	0.993	0.993	0.993	0.993
	R4	0.510	0.667	0.779	0.874	0.964	0.993	0.993	0.993	0.578	0.771	0.928	0.993	0.993	0.993	0.993	0.993	0.993
$\lambda_{20^{\circ}\text{C}}=0.50$	R1	0.560	0.646	0.713	0.773	0.831	0.951	0.951	0.951	0.611	0.748	0.862	0.951	0.951	0.951	0.951	0.951	0.951
	R2	0.454	0.556	0.633	0.704	0.771	0.838	0.951	0.951	0.506	0.644	0.758	0.867	0.951	0.951	0.951	0.951	0.951
	R3	0.428	0.545	0.626	0.695	0.761	0.827	0.951	0.951	0.482	0.630	0.748	0.857	0.951	0.951	0.951	0.951	0.951
	R4	0.385	0.508	0.598	0.675	0.745	0.814	0.951	0.951	0.439	0.590	0.712	0.825	0.951	0.951	0.951	0.951	0.951
$\lambda_{20^{\circ}\text{C}}=0.75$	R1	0.455	0.526	0.582	0.633	0.683	0.737	0.876	0.876	0.497	0.609	0.704	0.876	0.876	0.876	0.876	0.876	0.876
	R2	0.363	0.449	0.513	0.573	0.631	0.686	0.751	0.876	0.406	0.519	0.614	0.709	0.876	0.876	0.876	0.876	0.876
	R3	0.340	0.439	0.507	0.564	0.621	0.678	0.742	0.876	0.384	0.508	0.606	0.699	0.876	0.876	0.876	0.876	0.876
	R4	0.301	0.407	0.483	0.548	0.609	0.666	0.730	0.876	0.348	0.473	0.576	0.673	0.876	0.876	0.876	0.876	0.876
$\lambda_{20^{\circ}\text{C}}=1.00$	R1	0.367	0.425	0.471	0.513	0.555	0.600	0.725	0.725	0.404	0.496	0.573	0.725	0.725	0.725	0.725	0.725	0.725
	R2	0.291	0.363	0.416	0.465	0.512	0.557	0.725	0.725	0.325	0.420	0.497	0.576	0.725	0.725	0.725	0.725	0.725
	R3	0.271	0.354	0.411	0.458	0.503	0.550	0.603	0.725	0.307	0.410	0.491	0.567	0.725	0.725	0.725	0.725	0.725
	R4	0.238	0.329	0.392	0.444	0.493	0.540	0.591	0.725	0.276	0.381	0.467	0.546	0.725	0.725	0.725	0.725	0.725
$\lambda_{20^{\circ}\text{C}}=1.50$	R1	0.218	0.251	0.277	0.301	0.325	0.350	0.395	0.395	0.237	0.291	0.336	0.395	0.395	0.395	0.395	0.395	0.395
	R2	0.173	0.215	0.246	0.275	0.302	0.327	0.395	0.395	0.193	0.248	0.294	0.338	0.395	0.395	0.395	0.395	0.395
	R3	0.160	0.210	0.243	0.271	0.297	0.323	0.395	0.395	0.182	0.242	0.289	0.334	0.395	0.395	0.395	0.395	0.395
	R4	0.141	0.195	0.232	0.263	0.291	0.318	0.347	0.395	0.162	0.225	0.276	0.322	0.395	0.395	0.395	0.395	0.395
$\lambda_{20^{\circ}\text{C}}=2.00$	R1	0.131	0.151	0.167	0.181	0.195	0.210	0.232	0.232	0.143	0.175	0.202	0.232	0.232	0.232	0.232	0.232	0.232
	R2	0.105	0.130	0.148	0.165	0.181	0.197	0.214	0.232	0.116	0.150	0.177	0.203	0.232	0.232	0.232	0.232	0.232
	R3	0.097	0.127	0.147	0.163	0.178	0.194	0.212	0.232	0.110	0.146	0.175	0.201	0.232	0.232	0.232	0.232	0.232
	R4	0.085	0.117	0.140	0.158	0.175	0.191	0.208	0.232	0.098	0.136	0.165	0.193	0.232	0.232	0.232	0.232	0.232

$\theta_{\text{nom}} = 500^{\circ}\text{C}$

$p_{f,fi} \rightarrow$	0.10	0.20	0.30	0.40	0.50	0.60	0.70	0.80	0.90	0.10	0.20	0.30	0.40	0.50	0.60	0.70	0.80	0.90
$\beta_{f,fi} \rightarrow$	1.28	0.84	0.52	0.40	0.00	-0.25	-0.52	-0.84	-1.28	1.28	0.84	0.52	0.40	0.00	-0.25	-0.52	-0.84	-1.28
$\delta_{af} \rightarrow$	1.15	1.02	0.94	0.88	0.82	0.77	0.72	0.67	0.60	1.15	1.02	0.94	0.88	0.82	0.77	0.72	0.67	0.60
	$\alpha=0.00$									$\alpha=0.25$								
$\lambda_{20^{\circ}\text{C}}=0.00$	R1	0.422	0.527	0.612	0.693	0.784	0.872	0.964	1.000	1.000	0.457	0.571	0.664	0.752	0.851	0.947	1.000	1.000
	R2	0.328	0.458	0.572	0.665	0.753	0.836	0.928	1.000	1.000	0.357	0.497	0.621	0.722	0.818	0.910	1.000	1.000
	R3	0.276	0.398	0.508	0.613	0.716	0.810	0.913	1.000	1.000	0.299	0.432	0.551	0.666	0.778	0.882	0.993	1.000
	R4	0.216	0.319	0.440	0.559	0.672	0.786	0.899	1.000	1.000	0.236	0.347	0.478	0.606	0.729	0.853	0.975	1.000
$\lambda_{20^{\circ}\text{C}}=0.25$	R1	0.344	0.429	0.498	0.563	0.637	0.710	0.786	0.876	0.993	0.372	0.465	0.541	0.613	0.692	0.772	0.856	0.993
	R2	0.268	0.373	0.466	0.543	0.613	0.681	0.756	0.848	0.980	0.291	0.405	0.506	0.590	0.667	0.742	0.823	0.925
	R3	0.225	0.324	0.413	0.500	0.582	0.660	0.745	0.839	0.971	0.244	0.352	0.450	0.543	0.632	0.719	0.811	0.916
	R4	0.176	0.260	0.358	0.454	0.547	0.639	0.731	0.830	0.957	0.193	0.283	0.389	0.494	0.594	0.694	0.796	0.905
$\lambda_{20^{\circ}\text{C}}=0.50$	R1	0.257	0.323	0.377	0.429	0.486	0.542	0.602	0.671	0.770	0.278	0.350	0.409	0.465	0.527	0.590	0.656	0.732
	R2	0.198	0.279	0.351	0.411	0.467	0.519	0.578	0.650	0.751	0.215	0.302	0.381	0.447	0.508	0.565	0.629	0.708
	R3	0.166	0.241	0.310	0.378	0.443	0.504	0.571	0.644	0.741	0.180	0.262	0.336	0.410	0.482	0.549	0.621	0.701
	R4	0.130	0.192	0.268	0.342	0.415	0.488	0.560	0.634	0.729	0.142	0.209	0.291	0.372	0.451	0.530	0.608	0.691
$\lambda_{20^{\circ}\text{C}}=0.75$	R1	0.197	0.252	0.298	0.342	0.391	0.438	0.487	0.543	0.630	0.214	0.274	0.324	0.372	0.424	0.475	0.529	0.591
	R2	0.150	0.215	0.276	0.327	0.374	0.418	0.466	0.526	0.614	0.163	0.234	0.300	0.355	0.406	0.455	0.507	0.573
	R3	0.124	0.184	0.241	0.298	0.354	0.405	0.460	0.520	0.600	0.135	0.200	0.262	0.324	0.384	0.440	0.500	0.567
	R4	0.098	0.145	0.205	0.268	0.330	0.391	0.451	0.512	0.588	0.107	0.157	0.223	0.291	0.358	0.425	0.491	0.558
$\lambda_{20^{\circ}\text{C}}=1.00$	R1	0.154	0.199	0.238	0.275	0.316	0.354	0.394	0.440	0.512	0.167	0.216	0.259	0.299	0.343	0.385	0.429	0.480
	R2	0.115	0.167	0.219	0.262	0.302	0.338	0.377	0.426	0.496	0.124	0.182	0.238	0.285	0.328	0.368	0.410	0.464
	R3	0.094	0.142	0.189	0.237	0.285	0.328	0.372	0.421	0.486	0.103	0.155	0.205	0.258	0.310	0.355	0.405	0.459
	R4	0.076	0.111	0.159	0.211	0.265	0.316	0.365	0.414	0.476	0.082	0.120	0.173	0.230	0.287	0.344	0.398	0.452
$\lambda_{20^{\circ}\text{C}}=1.50$	R1	0.090	0.117	0.141	0.164	0.188	0.211	0.234	0.260	0.300	0.097	0.127	0.153	0.178	0.204	0.229	0.254	0.284
	R2	0.066	0.098	0.129	0.156	0.180	0.201	0.224	0.252	0.293	0.072	0.106	0.140	0.169	0.195	0.219	0.244	0.275
	R3	0.054	0.083	0.111	0.140	0.170	0.195	0.221	0.250	0.287	0.059	0.090	0.120	0.153	0.184	0.212	0.241	0.272
	R4	0.044	0.063	0.093	0.124	0.157	0.188	0.217	0.247	0.282	0.047	0.069	0.101	0.135	0.171	0.204	0.236	0.269
$\lambda_{20^{\circ}\text{C}}=2.00$	R1	0.054	0.071	0.085	0.099	0.114	0.127	0.141	0.157	0.180	0.059	0.077	0.093	0.108	0.124	0.138	0.154	0.171
	R2	0.040	0.059	0.078	0.094	0.109	0.122	0.135	0.152	0.176	0.043	0.064	0.085	0.102	0.118	0.132	0.147	0.166
	R3	0.033	0.050	0.067	0.085	0.103	0.118	0.134	0.151	0.173	0.035	0.054	0.073	0.092	0.111	0.128	0.145	0.164
	R4	0.026	0.038	0.056	0.075	0.095	0.114	0.131	0.149	0.170	0.028	0.042	0.061	0.082	0.103	0.123	0.143	0.162
	$\alpha=0.50$									$\alpha=0.75$								
$\lambda_{20^{\circ}\text{C}}=0.00$	R1	0.508	0.639	0.746	0.850	0.964	1.000	1.000	1.000	1.000	0.583	0.756	0.906	1.000	1.000	1.000	1.000	1.000
	R2	0.400	0.560	0.699	0.816	0.929	1.000	1.000	1.000	1.000	0.477	0.669	0.848	1.000	1.000	1.000	1.000	1.000
	R3	0.337	0.487	0.622	0.752	0.879	1.000	1.000	1.000	1.000	0.408	0.585	0.754	0.921	1.000	1.000	1.000	1.000
	R4	0.267	0.392	0.541	0.686	0.826	0.968	1.000	1.000	1.000	0.324	0.485	0.658	0.839	1.000	1.000	1.000	1.000
$\lambda_{20^{\circ}\text{C}}=0.25$	R1	0.414	0.521	0.609	0.692	0.784	0.880	0.986	0.993	0.993	0.474	0.616	0.738	0.857	0.988	0.993	0.993	0.993
	R2	0.326	0.455	0.569	0.666	0.757	0.847	0.948	0.993	0.993	0.388	0.544	0.689	0.825	0.954	0.993	0.993	0.993
	R3	0.276	0.396	0.507	0.613	0.717	0.819	0.930	0.993	0.993	0.333	0.479	0.617	0.753	0.896	0.993	0.993	0.993
	R4	0.218	0.320	0.440	0.559	0.673	0.789	0.911	0.993	0.993	0.264	0.397	0.537	0.685	0.836	0.993	0.993	0.993
$\lambda_{20^{\circ}\text{C}}=0.50$	R1	0.309	0.392	0.460	0.525	0.598	0.673	0.753	0.848	0.951	0.355	0.465	0.558	0.647	0.747	0.863	0.951	0.951
	R2	0.241	0.341	0.430	0.505	0.575	0.645	0.722	0.819	0.951	0.287	0.408	0.519	0.622	0.723	0.831	0.951	0.951
	R3	0.203	0.294	0.381	0.463	0.544	0.623	0.710	0.811	0.951	0.246	0.356	0.462	0.568	0.678	0.794	0.951	0.951
	R4	0.161	0.236	0.327	0.420	0.509	0.600	0.695	0.801	0.951	0.196	0.294	0.401	0.514	0.631	0.758	0.951	0.951
$\lambda_{20^{\circ}\text{C}}=0.75$	R1	0.239	0.307	0.363	0.419	0.480	0.543	0.608	0.687	0.876	0.276	0.364	0.440	0.515	0.599	0.695	0.876	0.876
	R2	0.183	0.263	0.337	0.400	0.460	0.519	0.582	0.664	0.876	0.220	0.316	0.409	0.493	0.578	0.666	0.876	0.876
	R3	0.153	0.225	0.296	0.365	0.434	0.500	0.572	0.655	0.876	0.187	0.274	0.361	0.447	0.537	0.636	0.746	0.876
	R4	0.121	0.179	0.252	0.329	0.405	0.482	0.561	0.647	0.755	0.148	0.223	0.310	0.405	0.500	0.605	0.725	0.876
$\lambda_{20^{\circ}\text{C}}=1.00$	R1	0.186	0.243	0.290	0.337	0.389	0.438	0.492	0.557	0.725	0.216	0.289	0.352	0.413	0.482	0.561	0.725	0.725
	R2	0.140	0.205	0.268	0.321	0.371	0.419	0.471	0.538	0.725	0.169	0.249	0.325	0.394	0.464	0.537	0.725	0.725
	R3	0.116	0.174	0.232	0.290	0.349	0.404	0.464	0.530	0.725	0.143	0.213	0.284	0.357	0.432	0.512	0.602	0.725
	R4	0.092	0.136	0.196	0.259	0.324	0.389	0.454	0.524	0.725	0.114	0.172	0.242	0.319	0.399	0.486	0.585	0.725
$\lambda_{20^{\circ}\text{C}}=1.50$	R1	0.109	0.143	0.172	0.200	0.231	0.261	0.292	0.330	0.395	0.127	0.170	0.208	0.245	0.286	0.333	0.395	0.395
	R2	0.081	0.120	0.158	0.190	0.221	0.249	0.280	0.318	0.395	0.098	0.145	0.191	0.234	0.275	0.318	0.395	0.395
	R3	0.067	0.101	0.136	0.172	0.208	0.240	0.275	0.314	0.395	0.082	0.123	0.167	0.210	0.256	0.304	0.395	0.395
	R4	0.053	0.079	0.114	0.153	0.192	0.231	0.270	0.310	0.395	0.066	0.099	0.141	0.188	0.236	0.289	0.347	0.395
$\lambda_{20^{\circ}\text{C}}=2.00$	R1	0.066	0.086	0.104	0.121	0.139	0.158	0.176	0.199	0.232	0.077	0.103	0.126	0.148	0.173	0.201	0.232	0.232
	R2	0.049	0.072	0.095	0.115	0.134	0.151	0.169	0.192	0.232	0.059	0.088	0.116	0.141	0.167	0.193	0.232	0.232
	R3	0.040	0.061	0.083	0.104	0.126	0.145	0.166	0.190	0.232	0.050	0.075	0.101	0.127	0.155	0.184	0.232	0.232
	R4	0.032	0.047	0.069	0.092	0.116	0.140	0.163	0.187	0.232	0.040	0.060	0.085	0.114	0.143	0.174	0.209	0.232

$\theta_{\text{nom}} = 600^{\circ}\text{C}$

$p_{f,fi} \rightarrow$	0.10	0.20	0.30	0.40	0.50	0.60	0.70	0.80	0.90	0.10	0.20	0.30	0.40	0.50	0.60	0.70	0.80	0.90
$\beta_{f,fi} \rightarrow$	1.28	0.84	0.52	0.40	0.00	-0.25	-0.52	-0.84	-1.28	1.28	0.84	0.52	0.40	0.00	-0.25	-0.52	-0.84	-1.28
$\delta_{af} \rightarrow$	1.15	1.02	0.94	0.88	0.82	0.77	0.72	0.67	0.60	1.15	1.02	0.94	0.88	0.82	0.77	0.72	0.67	0.60
	$\alpha=0.00$									$\alpha=0.25$								
$\lambda_{20^{\circ}\text{C}}=0.00$	R1	0.372	0.476	0.560	0.639	0.718	0.801	0.892	1.000	1.000	0.403	0.517	0.608	0.694	0.779	0.871	0.970	1.000
	R2	0.210	0.270	0.334	0.404	0.481	0.560	0.662	0.785	0.972	0.227	0.293	0.362	0.439	0.523	0.610	0.721	0.853
	R3	0.194	0.250	0.313	0.385	0.463	0.542	0.630	0.752	0.930	0.210	0.272	0.340	0.418	0.503	0.590	0.686	0.819
	R4	0.147	0.204	0.252	0.316	0.397	0.489	0.603	0.726	0.879	0.160	0.221	0.275	0.343	0.431	0.532	0.656	0.792
$\lambda_{20^{\circ}\text{C}}=0.25$	R1	0.302	0.388	0.456	0.520	0.585	0.653	0.727	0.816	0.943	0.329	0.421	0.495	0.565	0.636	0.709	0.791	0.890
	R2	0.170	0.220	0.272	0.330	0.392	0.458	0.538	0.639	0.792	0.186	0.239	0.296	0.359	0.427	0.498	0.587	0.696
	R3	0.159	0.204	0.255	0.314	0.377	0.442	0.515	0.613	0.758	0.171	0.222	0.277	0.341	0.410	0.481	0.560	0.668
	R4	0.120	0.167	0.206	0.258	0.323	0.399	0.491	0.592	0.717	0.130	0.180	0.224	0.280	0.351	0.434	0.534	0.644
$\lambda_{20^{\circ}\text{C}}=0.50$	R1	0.225	0.290	0.343	0.393	0.444	0.497	0.555	0.623	0.719	0.244	0.315	0.373	0.428	0.483	0.540	0.603	0.679
	R2	0.126	0.162	0.201	0.245	0.292	0.343	0.406	0.485	0.604	0.137	0.176	0.218	0.266	0.317	0.372	0.441	0.528
	R3	0.117	0.150	0.188	0.232	0.281	0.331	0.386	0.465	0.577	0.126	0.163	0.204	0.253	0.305	0.359	0.421	0.506
	R4	0.090	0.123	0.152	0.190	0.240	0.297	0.370	0.447	0.544	0.098	0.133	0.165	0.206	0.260	0.324	0.402	0.487
$\lambda_{20^{\circ}\text{C}}=0.75$	R1	0.171	0.225	0.268	0.312	0.355	0.399	0.447	0.504	0.581	0.186	0.244	0.291	0.338	0.385	0.434	0.486	0.548
	R2	0.095	0.122	0.152	0.187	0.225	0.267	0.321	0.389	0.487	0.103	0.132	0.165	0.203	0.245	0.290	0.340	0.423
	R3	0.088	0.113	0.142	0.177	0.216	0.257	0.303	0.371	0.465	0.096	0.123	0.154	0.192	0.235	0.280	0.330	0.404
	R4	0.070	0.093	0.114	0.143	0.183	0.230	0.289	0.355	0.437	0.076	0.101	0.124	0.155	0.199	0.250	0.315	0.387
$\lambda_{20^{\circ}\text{C}}=1.00$	R1	0.132	0.176	0.213	0.249	0.286	0.323	0.362	0.408	0.471	0.143	0.191	0.231	0.271	0.310	0.350	0.393	0.444
	R2	0.072	0.092	0.116	0.144	0.175	0.210	0.256	0.313	0.394	0.078	0.100	0.126	0.157	0.191	0.229	0.279	0.342
	R3	0.068	0.086	0.108	0.136	0.168	0.202	0.241	0.298	0.376	0.073	0.093	0.117	0.148	0.183	0.220	0.262	0.324
	R4	0.055	0.071	0.087	0.109	0.140	0.179	0.229	0.285	0.353	0.060	0.077	0.094	0.118	0.153	0.195	0.249	0.311
$\lambda_{20^{\circ}\text{C}}=1.50$	R1	0.077	0.103	0.125	0.148	0.170	0.192	0.215	0.242	0.279	0.083	0.112	0.136	0.160	0.185	0.209	0.234	0.264
	R2	0.042	0.053	0.067	0.084	0.102	0.123	0.152	0.186	0.234	0.045	0.057	0.073	0.091	0.111	0.134	0.165	0.203
	R3	0.039	0.049	0.062	0.079	0.098	0.118	0.142	0.177	0.224	0.043	0.053	0.067	0.086	0.106	0.129	0.155	0.193
	R4	0.033	0.041	0.050	0.062	0.081	0.104	0.135	0.169	0.211	0.036	0.045	0.054	0.068	0.089	0.114	0.147	0.184
$\lambda_{20^{\circ}\text{C}}=2.00$	R1	0.046	0.062	0.076	0.089	0.103	0.116	0.130	0.146	0.168	0.050	0.068	0.082	0.097	0.112	0.126	0.142	0.159
	R2	0.025	0.032	0.040	0.050	0.062	0.075	0.092	0.113	0.142	0.027	0.035	0.044	0.055	0.067	0.081	0.100	0.123
	R3	0.024	0.030	0.037	0.048	0.059	0.072	0.086	0.107	0.135	0.026	0.032	0.041	0.052	0.064	0.078	0.094	0.117
	R4	0.020	0.025	0.030	0.038	0.049	0.063	0.082	0.102	0.128	0.022	0.027	0.033	0.041	0.054	0.069	0.089	0.112
	$\alpha=0.50$									$\alpha=0.75$								
$\lambda_{20^{\circ}\text{C}}=0.00$	R1	0.450	0.581	0.685	0.785	0.886	0.994	1.000	1.000	1.000	0.525	0.693	0.836	0.977	1.000	1.000	1.000	1.000
	R2	0.255	0.332	0.411	0.498	0.595	0.696	0.823	0.980	1.000	0.300	0.407	0.511	0.623	0.753	0.896	1.000	1.000
	R3	0.235	0.309	0.387	0.475	0.572	0.674	0.785	0.940	1.000	0.275	0.382	0.484	0.595	0.724	0.864	1.000	1.000
	R4	0.178	0.250	0.314	0.391	0.492	0.606	0.750	0.910	1.000	0.207	0.305	0.398	0.499	0.622	0.772	0.961	1.000
$\lambda_{20^{\circ}\text{C}}=0.25$	R1	0.367	0.474	0.559	0.641	0.724	0.811	0.911	0.993	0.993	0.429	0.564	0.682	0.797	0.918	0.993	0.993	0.993
	R2	0.208	0.271	0.336	0.407	0.485	0.570	0.671	0.800	0.993	0.245	0.333	0.417	0.508	0.614	0.731	0.872	0.993
	R3	0.192	0.252	0.315	0.388	0.467	0.549	0.643	0.769	0.960	0.226	0.312	0.395	0.486	0.589	0.707	0.840	0.993
	R4	0.145	0.203	0.256	0.319	0.400	0.495	0.610	0.743	0.912	0.168	0.248	0.324	0.407	0.507	0.630	0.786	0.989
$\lambda_{20^{\circ}\text{C}}=0.50$	R1	0.272	0.353	0.420	0.484	0.548	0.617	0.693	0.787	0.951	0.318	0.422	0.513	0.601	0.694	0.796	0.951	0.951
	R2	0.153	0.199	0.247	0.302	0.361	0.426	0.506	0.607	0.765	0.180	0.245	0.308	0.378	0.458	0.547	0.656	0.804
	R3	0.142	0.186	0.232	0.287	0.347	0.411	0.482	0.580	0.730	0.167	0.230	0.292	0.359	0.439	0.527	0.631	0.769
	R4	0.109	0.150	0.188	0.235	0.296	0.369	0.460	0.561	0.692	0.127	0.184	0.239	0.301	0.375	0.469	0.589	0.746
$\lambda_{20^{\circ}\text{C}}=0.75$	R1	0.208	0.275	0.329	0.383	0.437	0.494	0.558	0.635	0.744	0.245	0.328	0.401	0.475	0.551	0.636	0.736	0.876
	R2	0.116	0.150	0.187	0.230	0.279	0.331	0.400	0.485	0.617	0.137	0.186	0.234	0.289	0.353	0.425	0.515	0.635
	R3	0.107	0.139	0.175	0.219	0.267	0.319	0.378	0.462	0.587	0.127	0.174	0.221	0.275	0.338	0.410	0.495	0.606
	R4	0.085	0.114	0.142	0.177	0.226	0.284	0.359	0.445	0.553	0.099	0.140	0.181	0.228	0.287	0.363	0.461	0.588
$\lambda_{20^{\circ}\text{C}}=1.00$	R1	0.161	0.215	0.261	0.306	0.352	0.399	0.452	0.515	0.603	0.190	0.259	0.319	0.379	0.441	0.512	0.594	0.725
	R2	0.088	0.114	0.143	0.178	0.217	0.261	0.319	0.390	0.498	0.105	0.142	0.180	0.223	0.276	0.336	0.410	0.511
	R3	0.082	0.106	0.134	0.168	0.208	0.251	0.301	0.372	0.475	0.098	0.133	0.170	0.212	0.263	0.322	0.392	0.487
	R4	0.067	0.087	0.108	0.135	0.174	0.222	0.285	0.356	0.447	0.078	0.108	0.139	0.174	0.221	0.282	0.365	0.468
$\lambda_{20^{\circ}\text{C}}=1.50$	R1	0.093	0.126	0.154	0.181	0.209	0.237	0.268	0.305	0.395	0.110	0.152	0.188	0.224	0.262	0.304	0.395	0.395
	R2	0.051	0.066	0.082	0.103	0.127	0.153	0.189	0.232	0.296	0.061	0.082	0.104	0.129	0.161	0.197	0.242	0.303
	R3	0.048	0.061	0.077	0.097	0.121	0.147	0.177	0.221	0.282	0.057	0.077	0.098	0.123	0.153	0.189	0.231	0.288
	R4	0.040	0.051	0.062	0.078	0.101	0.130	0.168	0.212	0.267	0.046	0.063	0.080	0.101	0.128	0.165	0.215	0.278
$\lambda_{20^{\circ}\text{C}}=2.00$	R1	0.056	0.076	0.093	0.110	0.126	0.144	0.162	0.184	0.216	0.066	0.092	0.114	0.135	0.159	0.184	0.213	0.232
	R2	0.031	0.039	0.050	0.062	0.077	0.093	0.114	0.140	0.179	0.037	0.049	0.062	0.078	0.097	0.119	0.147	0.183
	R3	0.029	0.037	0.046	0.059	0.073	0.089	0.107	0.133	0.170	0.034	0.046	0.059	0.074	0.093	0.114	0.140	0.174
	R4	0.024	0.031	0.038	0.047	0.061	0.078	0.101	0.128	0.161	0.028	0.038	0.049	0.061	0.077	0.100	0.130	0.162

$\theta_{\text{nom}} = 700^{\circ}\text{C}$

$p_{f,fi} \rightarrow$	0.10	0.20	0.30	0.40	0.50	0.60	0.70	0.80	0.90	0.10	0.20	0.30	0.40	0.50	0.60	0.70	0.80	0.90	
$\beta_{f,fi} \rightarrow$	1.28	0.84	0.52	0.40	0.00	-0.25	-0.52	-0.84	1.28	1.28	0.84	0.52	0.40	0.00	-0.25	-0.52	-0.84	-1.28	
$\delta_{of} \rightarrow$	1.15	1.02	0.94	0.88	0.82	0.77	0.72	0.67	0.60	1.15	1.02	0.94	0.88	0.82	0.77	0.72	0.67	0.60	
$\alpha=0.00$										$\alpha=0.25$									
$\lambda_{20^{\circ}\text{C}}=0.00$	R1	0.202	0.239	0.275	0.316	0.362	0.414	0.479	0.565	0.732	0.219	0.259	0.299	0.344	0.394	0.450	0.520	0.617	0.800
	R2	0.148	0.186	0.215	0.242	0.274	0.319	0.380	0.475	0.636	0.160	0.202	0.233	0.263	0.298	0.347	0.414	0.516	0.692
	R3	0.113	0.162	0.196	0.225	0.263	0.306	0.362	0.442	0.571	0.123	0.176	0.213	0.245	0.285	0.333	0.393	0.483	0.621
	R4	0.058	0.099	0.144	0.183	0.218	0.262	0.332	0.423	0.525	0.063	0.107	0.156	0.199	0.238	0.286	0.362	0.462	0.574
$\lambda_{20^{\circ}\text{C}}=0.25$	R1	0.165	0.195	0.225	0.258	0.296	0.338	0.390	0.461	0.599	0.179	0.212	0.244	0.281	0.321	0.368	0.435	0.502	0.652
	R2	0.120	0.152	0.175	0.197	0.223	0.261	0.310	0.391	0.521	0.130	0.164	0.190	0.215	0.243	0.284	0.337	0.426	0.569
	R3	0.092	0.132	0.160	0.184	0.214	0.249	0.296	0.363	0.465	0.100	0.143	0.174	0.200	0.233	0.272	0.322	0.396	0.508
	R4	0.048	0.082	0.118	0.150	0.179	0.217	0.274	0.347	0.430	0.053	0.089	0.128	0.163	0.195	0.236	0.298	0.378	0.468
$\lambda_{20^{\circ}\text{C}}=0.50$	R1	0.121	0.143	0.165	0.190	0.218	0.250	0.290	0.344	0.452	0.131	0.155	0.179	0.206	0.237	0.272	0.315	0.375	0.491
	R2	0.090	0.112	0.129	0.145	0.165	0.191	0.229	0.290	0.390	0.097	0.121	0.140	0.158	0.180	0.208	0.249	0.316	0.424
	R3	0.071	0.098	0.118	0.135	0.157	0.183	0.217	0.269	0.347	0.077	0.107	0.128	0.147	0.171	0.200	0.236	0.292	0.379
	R4	0.040	0.064	0.090	0.111	0.132	0.159	0.202	0.255	0.319	0.044	0.070	0.097	0.121	0.144	0.173	0.220	0.277	0.348
$\lambda_{20^{\circ}\text{C}}=0.75$	R1	0.091	0.107	0.124	0.143	0.165	0.190	0.222	0.267	0.358	0.099	0.116	0.134	0.155	0.179	0.207	0.242	0.291	0.389
	R2	0.070	0.085	0.097	0.109	0.124	0.144	0.174	0.224	0.303	0.076	0.092	0.106	0.119	0.134	0.156	0.189	0.244	0.330
	R3	0.058	0.076	0.090	0.102	0.118	0.138	0.164	0.204	0.268	0.063	0.083	0.097	0.111	0.129	0.150	0.179	0.222	0.292
	R4	0.036	0.054	0.070	0.085	0.100	0.119	0.152	0.194	0.245	0.039	0.058	0.076	0.092	0.109	0.130	0.166	0.212	0.267
$\lambda_{20^{\circ}\text{C}}=1.00$	R1	0.069	0.081	0.094	0.108	0.126	0.147	0.173	0.209	0.286	0.075	0.088	0.102	0.118	0.138	0.160	0.188	0.228	0.312
	R2	0.055	0.065	0.074	0.083	0.094	0.109	0.133	0.174	0.239	0.059	0.071	0.081	0.090	0.102	0.119	0.145	0.190	0.261
	R3	0.047	0.059	0.069	0.078	0.090	0.105	0.126	0.158	0.210	0.051	0.065	0.075	0.085	0.098	0.114	0.137	0.172	0.229
	R4	0.031	0.045	0.056	0.066	0.077	0.091	0.116	0.149	0.190	0.034	0.048	0.061	0.072	0.084	0.099	0.126	0.163	0.208
$\lambda_{20^{\circ}\text{C}}=1.50$	R1	0.040	0.046	0.054	0.062	0.073	0.085	0.100	0.122	0.169	0.043	0.050	0.058	0.068	0.079	0.093	0.109	0.133	0.185
	R2	0.032	0.038	0.043	0.048	0.054	0.063	0.077	0.102	0.141	0.035	0.041	0.046	0.052	0.059	0.068	0.084	0.110	0.154
	R3	0.029	0.035	0.040	0.045	0.051	0.060	0.072	0.092	0.123	0.031	0.038	0.044	0.049	0.056	0.065	0.079	0.100	0.134
	R4	0.020	0.027	0.033	0.039	0.045	0.052	0.067	0.087	0.111	0.022	0.030	0.036	0.042	0.048	0.057	0.073	0.094	0.121
$\lambda_{20^{\circ}\text{C}}=2.00$	R1	0.024	0.028	0.032	0.037	0.044	0.051	0.061	0.074	0.103	0.026	0.030	0.035	0.041	0.048	0.056	0.066	0.081	0.112
	R2	0.020	0.023	0.026	0.029	0.032	0.038	0.046	0.061	0.085	0.021	0.025	0.028	0.031	0.035	0.041	0.050	0.067	0.093
	R3	0.018	0.021	0.024	0.027	0.031	0.036	0.044	0.055	0.075	0.019	0.023	0.026	0.030	0.034	0.039	0.047	0.060	0.081
	R4	0.012	0.017	0.020	0.023	0.027	0.032	0.040	0.052	0.067	0.013	0.018	0.022	0.026	0.029	0.034	0.044	0.057	0.073
$\alpha=0.50$										$\alpha=0.75$									
$\lambda_{20^{\circ}\text{C}}=0.00$	R1	0.243	0.293	0.341	0.392	0.450	0.517	0.599	0.711	0.926	0.277	0.356	0.427	0.499	0.580	0.673	0.793	0.959	1.000
	R2	0.177	0.225	0.264	0.300	0.343	0.399	0.474	0.592	0.803	0.203	0.268	0.325	0.382	0.446	0.523	0.620	0.783	1.000
	R3	0.137	0.196	0.241	0.280	0.328	0.382	0.453	0.555	0.722	0.163	0.235	0.295	0.355	0.427	0.502	0.597	0.740	0.986
	R4	0.072	0.122	0.175	0.224	0.271	0.329	0.416	0.533	0.668	0.088	0.149	0.212	0.278	0.349	0.433	0.546	0.716	0.916
$\lambda_{20^{\circ}\text{C}}=0.25$	R1	0.199	0.239	0.278	0.320	0.367	0.422	0.489	0.580	0.754	0.227	0.290	0.349	0.408	0.473	0.550	0.647	0.782	0.993
	R2	0.144	0.184	0.215	0.245	0.279	0.326	0.386	0.487	0.659	0.166	0.218	0.265	0.311	0.362	0.428	0.506	0.642	0.895
	R3	0.112	0.160	0.196	0.229	0.267	0.312	0.369	0.456	0.588	0.133	0.191	0.241	0.291	0.347	0.411	0.488	0.604	0.806
	R4	0.060	0.101	0.144	0.184	0.223	0.272	0.343	0.437	0.544	0.074	0.123	0.175	0.229	0.287	0.358	0.451	0.579	0.749
$\lambda_{20^{\circ}\text{C}}=0.50$	R1	0.146	0.176	0.204	0.235	0.271	0.312	0.362	0.433	0.567	0.167	0.214	0.257	0.300	0.349	0.407	0.480	0.582	0.763
	R2	0.108	0.136	0.159	0.180	0.207	0.238	0.285	0.363	0.491	0.123	0.161	0.196	0.229	0.268	0.314	0.374	0.477	0.669
	R3	0.087	0.119	0.145	0.168	0.196	0.229	0.272	0.337	0.440	0.102	0.143	0.178	0.213	0.255	0.302	0.359	0.446	0.599
	R4	0.049	0.079	0.109	0.137	0.165	0.199	0.252	0.320	0.403	0.060	0.097	0.132	0.170	0.212	0.263	0.331	0.427	0.554
$\lambda_{20^{\circ}\text{C}}=0.75$	R1	0.110	0.132	0.153	0.177	0.205	0.237	0.278	0.335	0.450	0.126	0.161	0.193	0.226	0.265	0.310	0.368	0.451	0.603
	R2	0.084	0.103	0.120	0.136	0.155	0.180	0.217	0.281	0.383	0.096	0.124	0.149	0.173	0.203	0.237	0.284	0.368	0.518
	R3	0.070	0.092	0.110	0.127	0.148	0.173	0.206	0.257	0.339	0.082	0.111	0.137	0.163	0.193	0.227	0.272	0.340	0.460
	R4	0.044	0.066	0.086	0.105	0.125	0.150	0.190	0.244	0.310	0.053	0.080	0.105	0.132	0.162	0.199	0.251	0.328	0.426
$\lambda_{20^{\circ}\text{C}}=1.00$	R1	0.083	0.100	0.116	0.135	0.157	0.183	0.216	0.263	0.360	0.095	0.122	0.147	0.173	0.203	0.239	0.286	0.352	0.480
	R2	0.066	0.080	0.091	0.103	0.118	0.137	0.166	0.218	0.302	0.075	0.095	0.114	0.132	0.155	0.181	0.218	0.286	0.410
	R3	0.057	0.072	0.085	0.097	0.112	0.131	0.157	0.198	0.265	0.066	0.087	0.106	0.125	0.148	0.174	0.209	0.262	0.359
	R4	0.038	0.054	0.068	0.082	0.096	0.115	0.146	0.188	0.241	0.045	0.065	0.084	0.103	0.125	0.153	0.192	0.252	0.330
$\lambda_{20^{\circ}\text{C}}=1.50$	R1	0.048	0.057	0.067	0.077	0.090	0.106	0.126	0.154	0.213	0.055	0.071	0.085	0.100	0.117	0.138	0.166	0.206	0.283
	R2	0.039	0.046	0.053	0.059	0.068	0.078	0.096	0.127	0.178	0.044	0.056	0.066	0.077	0.090	0.104	0.126	0.166	0.241
	R3	0.034	0.043	0.050	0.056	0.065	0.075	0.090	0.115	0.155	0.040	0.051	0.062	0.073	0.086	0.100	0.120	0.152	0.211
	R4	0.024	0.033	0.041	0.048	0.056	0.066	0.084	0.109	0.141	0.028	0.040	0.050	0.061	0.073	0.089	0.111	0.146	0.192
$\lambda_{20^{\circ}\text{C}}=2.00$	R1	0.029	0.034	0.040	0.047	0.055	0.064	0.076	0.093	0.129	0.033	0.043	0.051	0.060	0.070	0.083	0.100	0.124	0.172
	R2	0.023	0.028	0.032	0.036	0.041	0.047	0.058	0.077	0.108	0.026	0.033	0.040	0.046	0.054	0.			

$$\theta_{\text{nom}} = 800^{\circ}\text{C}$$

$p_{f,fi} \rightarrow$	0.10	0.20	0.30	0.40	0.50	0.60	0.70	0.80	0.90	0.10	0.20	0.30	0.40	0.50	0.60	0.70	0.80	0.90	
$\beta_{f,fi} \rightarrow$	1.28	0.84	0.52	0.40	0.00	-0.25	-0.52	-0.84	-1.28	1.28	0.84	0.52	0.40	0.00	-0.25	-0.52	-0.84	-1.28	
$\delta_{of} \rightarrow$	1.15	1.02	0.94	0.88	0.82	0.77	0.72	0.67	0.60	1.15	1.02	0.94	0.88	0.82	0.77	0.72	0.67	0.60	
	$\alpha=0.00$									$\alpha=0.25$									
$\lambda_{20^{\circ}\text{C}}=0.00$	R1	0.070	0.089	0.107	0.127	0.149	0.174	0.200	0.232	0.294	0.076	0.097	0.117	0.138	0.162	0.189	0.218	0.253	0.320
	R2	0.057	0.075	0.094	0.115	0.141	0.167	0.195	0.230	0.284	0.062	0.081	0.102	0.125	0.153	0.182	0.212	0.251	0.310
	R3	0.046	0.061	0.078	0.099	0.124	0.155	0.188	0.222	0.276	0.050	0.067	0.085	0.107	0.135	0.168	0.205	0.242	0.301
	R4	0.027	0.043	0.058	0.075	0.100	0.132	0.171	0.214	0.269	0.030	0.047	0.063	0.082	0.108	0.143	0.186	0.233	0.294
$\lambda_{20^{\circ}\text{C}}=0.25$	R1	0.057	0.073	0.087	0.103	0.121	0.141	0.163	0.190	0.243	0.062	0.079	0.095	0.112	0.132	0.154	0.178	0.207	0.265
	R2	0.047	0.061	0.076	0.094	0.115	0.136	0.159	0.188	0.232	0.051	0.066	0.083	0.102	0.124	0.148	0.173	0.205	0.254
	R3	0.037	0.050	0.064	0.081	0.101	0.126	0.154	0.183	0.226	0.041	0.054	0.069	0.087	0.110	0.138	0.168	0.199	0.246
	R4	0.024	0.037	0.048	0.063	0.084	0.111	0.142	0.176	0.220	0.026	0.040	0.053	0.069	0.092	0.120	0.154	0.192	0.240
$\lambda_{20^{\circ}\text{C}}=0.50$	R1	0.047	0.058	0.068	0.079	0.092	0.105	0.121	0.140	0.178	0.051	0.063	0.074	0.086	0.100	0.115	0.132	0.153	0.195
	R2	0.039	0.049	0.061	0.073	0.087	0.102	0.118	0.138	0.172	0.042	0.054	0.066	0.079	0.095	0.111	0.128	0.151	0.187
	R3	0.032	0.041	0.052	0.064	0.078	0.095	0.114	0.135	0.166	0.034	0.045	0.056	0.069	0.085	0.103	0.125	0.147	0.181
	R4	0.020	0.031	0.040	0.052	0.066	0.084	0.106	0.130	0.162	0.022	0.033	0.044	0.056	0.072	0.092	0.115	0.141	0.176
$\lambda_{20^{\circ}\text{C}}=0.75$	R1	0.041	0.049	0.057	0.064	0.072	0.082	0.092	0.106	0.134	0.044	0.053	0.061	0.070	0.079	0.089	0.101	0.115	0.147
	R2	0.035	0.043	0.051	0.060	0.069	0.079	0.090	0.105	0.130	0.038	0.047	0.056	0.065	0.075	0.086	0.098	0.115	0.142
	R3	0.029	0.037	0.045	0.054	0.063	0.075	0.088	0.102	0.125	0.031	0.040	0.049	0.058	0.069	0.081	0.095	0.112	0.136
	R4	0.018	0.028	0.036	0.045	0.055	0.068	0.082	0.099	0.122	0.020	0.030	0.039	0.049	0.060	0.074	0.089	0.108	0.133
$\lambda_{20^{\circ}\text{C}}=1.00$	R1	0.035	0.041	0.047	0.052	0.058	0.064	0.072	0.081	0.102	0.038	0.045	0.051	0.057	0.063	0.070	0.078	0.089	0.111
	R2	0.030	0.037	0.043	0.049	0.056	0.063	0.070	0.081	0.099	0.033	0.040	0.047	0.054	0.061	0.068	0.076	0.088	0.107
	R3	0.025	0.032	0.039	0.045	0.052	0.060	0.068	0.079	0.095	0.027	0.035	0.042	0.049	0.056	0.065	0.075	0.086	0.104
	R4	0.016	0.024	0.032	0.039	0.046	0.055	0.064	0.076	0.093	0.018	0.027	0.034	0.042	0.050	0.060	0.070	0.083	0.101
$\lambda_{20^{\circ}\text{C}}=1.50$	R1	0.022	0.026	0.029	0.032	0.035	0.038	0.042	0.047	0.059	0.024	0.028	0.031	0.034	0.038	0.041	0.046	0.051	0.064
	R2	0.019	0.023	0.027	0.030	0.034	0.037	0.041	0.047	0.057	0.021	0.025	0.029	0.033	0.037	0.041	0.045	0.051	0.062
	R3	0.016	0.021	0.024	0.028	0.032	0.036	0.040	0.046	0.055	0.017	0.022	0.026	0.030	0.034	0.039	0.044	0.050	0.060
	R4	0.010	0.016	0.020	0.024	0.029	0.033	0.038	0.044	0.054	0.011	0.017	0.022	0.026	0.031	0.036	0.042	0.049	0.059
$\lambda_{20^{\circ}\text{C}}=2.00$	R1	0.014	0.016	0.018	0.019	0.021	0.023	0.025	0.029	0.035	0.015	0.017	0.019	0.021	0.023	0.025	0.028	0.031	0.039
	R2	0.012	0.014	0.017	0.019	0.021	0.023	0.025	0.028	0.034	0.013	0.016	0.018	0.020	0.022	0.025	0.027	0.031	0.037
	R3	0.010	0.013	0.015	0.017	0.019	0.022	0.025	0.028	0.033	0.011	0.014	0.016	0.019	0.021	0.024	0.027	0.030	0.036
	R4	0.006	0.010	0.012	0.015	0.018	0.020	0.023	0.027	0.032	0.007	0.011	0.014	0.016	0.019	0.022	0.025	0.029	0.036
	$\alpha=0.50$									$\alpha=0.75$									
$\lambda_{20^{\circ}\text{C}}=0.00$	R1	0.085	0.109	0.133	0.157	0.183	0.215	0.249	0.293	0.373	0.100	0.134	0.164	0.196	0.232	0.274	0.326	0.394	0.517
	R2	0.070	0.092	0.115	0.142	0.174	0.207	0.243	0.290	0.361	0.084	0.115	0.145	0.179	0.218	0.263	0.315	0.390	0.502
	R3	0.056	0.076	0.097	0.123	0.154	0.191	0.234	0.280	0.352	0.066	0.094	0.122	0.155	0.194	0.242	0.301	0.375	0.489
	R4	0.033	0.053	0.071	0.093	0.124	0.163	0.211	0.268	0.344	0.039	0.065	0.090	0.119	0.156	0.206	0.270	0.354	0.479
$\lambda_{20^{\circ}\text{C}}=0.25$	R1	0.069	0.089	0.108	0.128	0.149	0.175	0.203	0.239	0.309	0.082	0.108	0.134	0.160	0.189	0.223	0.265	0.323	0.426
	R2	0.057	0.075	0.094	0.116	0.141	0.169	0.198	0.237	0.297	0.068	0.093	0.118	0.146	0.178	0.215	0.258	0.318	0.414
	R3	0.046	0.062	0.078	0.100	0.125	0.156	0.192	0.231	0.288	0.055	0.077	0.100	0.126	0.159	0.198	0.248	0.310	0.404
	R4	0.030	0.045	0.060	0.079	0.104	0.137	0.176	0.220	0.281	0.035	0.056	0.076	0.101	0.132	0.174	0.224	0.292	0.393
$\lambda_{20^{\circ}\text{C}}=0.50$	R1	0.057	0.071	0.084	0.098	0.113	0.130	0.151	0.176	0.227	0.066	0.086	0.104	0.123	0.143	0.168	0.198	0.238	0.315
	R2	0.047	0.061	0.075	0.090	0.107	0.126	0.147	0.174	0.219	0.056	0.075	0.093	0.113	0.136	0.162	0.192	0.235	0.305
	R3	0.038	0.051	0.064	0.079	0.096	0.118	0.142	0.170	0.212	0.045	0.063	0.081	0.100	0.122	0.150	0.184	0.229	0.295
	R4	0.025	0.038	0.050	0.064	0.082	0.104	0.131	0.163	0.207	0.029	0.046	0.063	0.082	0.104	0.132	0.168	0.216	0.289
$\lambda_{20^{\circ}\text{C}}=0.75$	R1	0.049	0.060	0.070	0.079	0.090	0.101	0.116	0.134	0.171	0.056	0.072	0.086	0.100	0.114	0.131	0.153	0.181	0.237
	R2	0.042	0.053	0.063	0.074	0.086	0.099	0.113	0.133	0.165	0.049	0.065	0.079	0.094	0.110	0.128	0.149	0.181	0.228
	R3	0.035	0.045	0.056	0.066	0.079	0.093	0.109	0.129	0.159	0.040	0.055	0.069	0.084	0.100	0.119	0.144	0.175	0.223
	R4	0.022	0.034	0.045	0.056	0.069	0.084	0.102	0.124	0.156	0.027	0.041	0.055	0.070	0.087	0.108	0.132	0.166	0.219
$\lambda_{20^{\circ}\text{C}}=1.00$	R1	0.042	0.050	0.057	0.064	0.072	0.080	0.090	0.103	0.130	0.047	0.060	0.070	0.081	0.092	0.104	0.120	0.141	0.182
	R2	0.037	0.045	0.053	0.061	0.069	0.078	0.088	0.102	0.126	0.042	0.055	0.066	0.077	0.089	0.102	0.117	0.140	0.175
	R3	0.030	0.039	0.047	0.056	0.064	0.074	0.086	0.100	0.122	0.035	0.048	0.059	0.070	0.082	0.096	0.114	0.136	0.171
	R4	0.020	0.030	0.039	0.048	0.057	0.068	0.080	0.096	0.119	0.023	0.036	0.048	0.060	0.073	0.088	0.106	0.130	0.169
$\lambda_{20^{\circ}\text{C}}=1.50$	R1	0.026	0.031	0.035	0.039	0.043	0.048	0.053	0.060	0.075	0.029	0.037	0.043	0.049	0.055	0.062	0.071	0.083	0.105
	R2	0.023	0.028	0.033	0.037	0.042	0.047	0.052	0.060	0.072	0.027	0.034	0.040	0.047	0.054	0.061	0.070	0.082	0.102
	R3	0.019	0.025	0.030	0.034	0.039	0.044	0.051	0.058	0.070	0.022	0.030	0.036	0.043	0.050	0.058	0.068	0.080	0.099
	R4	0.013	0.019	0.025	0.030	0.035	0												

$$\theta_{\text{nom}} = 900^{\circ}\text{C}$$

$p_{f,fi} \rightarrow$	0.10	0.20	0.30	0.40	0.50	0.60	0.70	0.80	0.90	0.10 <td>0.20</td> <td>0.30</td> <td>0.40</td> <td>0.50</td> <td>0.60</td> <td>0.70</td> <td>0.80</td> <td>0.90</td>	0.20	0.30	0.40	0.50	0.60	0.70	0.80	0.90	
$\beta_{f,fi} \rightarrow$	1.28	0.84	0.52	0.40	0.00	-0.25	-0.52	-0.84	-1.28	1.28	0.84	0.52	0.40	0.00	-0.25	-0.52	-0.84	-1.28	
$\delta_{of} \rightarrow$	1.15	1.02	0.94	0.88	0.82	0.77	0.72	0.67	0.60	1.15	1.02	0.94	0.88	0.82	0.77	0.72	0.67	0.60	
$\alpha=0.00$										$\alpha=0.25$									
$\lambda_{20^{\circ}\text{C}}=0.00$	R1	0.052	0.061	0.070	0.079	0.089	0.101	0.119	0.148	0.212	0.056	0.067	0.076	0.086	0.097	0.110	0.130	0.161	0.231
	R2	0.039	0.049	0.058	0.068	0.081	0.098	0.110	0.145	0.203	0.043	0.053	0.063	0.074	0.089	0.107	0.122	0.158	0.220
	R3	0.025	0.036	0.045	0.055	0.066	0.082	0.106	0.142	0.186	0.027	0.039	0.049	0.060	0.072	0.089	0.115	0.155	0.203
	R4	0.004	0.019	0.031	0.043	0.056	0.073	0.100	0.125	0.152	0.004	0.021	0.034	0.047	0.061	0.079	0.109	0.137	0.166
$\lambda_{20^{\circ}\text{C}}=0.25$	R1	0.042	0.050	0.057	0.065	0.072	0.082	0.097	0.128	0.178	0.045	0.054	0.062	0.070	0.079	0.089	0.106	0.139	0.195
	R2	0.032	0.040	0.047	0.055	0.066	0.079	0.091	0.120	0.167	0.035	0.043	0.051	0.060	0.072	0.087	0.099	0.130	0.182
	R3	0.021	0.030	0.037	0.045	0.056	0.069	0.089	0.117	0.151	0.023	0.032	0.041	0.049	0.062	0.075	0.098	0.127	0.165
	R4	0.013	0.024	0.033	0.043	0.053	0.067	0.087	0.102	0.124	0.015	0.026	0.036	0.047	0.058	0.073	0.094	0.112	0.135
$\lambda_{20^{\circ}\text{C}}=0.50$	R1	0.035	0.042	0.047	0.052	0.058	0.065	0.076	0.096	0.131	0.038	0.045	0.051	0.057	0.063	0.071	0.082	0.104	0.143
	R2	0.027	0.034	0.040	0.046	0.054	0.063	0.071	0.091	0.124	0.029	0.036	0.043	0.050	0.059	0.069	0.078	0.099	0.135
	R3	0.018	0.025	0.031	0.038	0.047	0.056	0.070	0.089	0.113	0.019	0.027	0.034	0.041	0.050	0.061	0.076	0.097	0.123
	R4	0.011	0.020	0.028	0.036	0.044	0.054	0.068	0.079	0.095	0.012	0.022	0.031	0.039	0.048	0.058	0.073	0.087	0.103
$\lambda_{20^{\circ}\text{C}}=0.75$	R1	0.031	0.037	0.041	0.045	0.050	0.055	0.063	0.076	0.100	0.034	0.040	0.045	0.049	0.054	0.060	0.068	0.082	0.109
	R2	0.024	0.030	0.035	0.041	0.047	0.053	0.060	0.073	0.095	0.026	0.033	0.038	0.044	0.051	0.058	0.066	0.079	0.103
	R3	0.016	0.023	0.028	0.034	0.042	0.049	0.058	0.071	0.088	0.017	0.025	0.031	0.037	0.045	0.053	0.064	0.078	0.096
	R4	0.010	0.018	0.025	0.032	0.039	0.047	0.057	0.066	0.077	0.011	0.020	0.028	0.035	0.043	0.051	0.062	0.072	0.084
$\lambda_{20^{\circ}\text{C}}=1.00$	R1	0.027	0.032	0.036	0.039	0.042	0.046	0.052	0.061	0.078	0.030	0.035	0.039	0.042	0.046	0.051	0.057	0.066	0.085
	R2	0.021	0.027	0.031	0.035	0.040	0.046	0.050	0.059	0.074	0.023	0.029	0.034	0.038	0.044	0.050	0.055	0.064	0.081
	R3	0.014	0.020	0.025	0.030	0.036	0.042	0.049	0.058	0.070	0.015	0.022	0.027	0.032	0.039	0.045	0.053	0.063	0.076
	R4	0.009	0.016	0.022	0.028	0.034	0.040	0.048	0.055	0.063	0.010	0.017	0.024	0.031	0.037	0.044	0.052	0.060	0.069
$\lambda_{20^{\circ}\text{C}}=1.50$	R1	0.018	0.020	0.023	0.025	0.027	0.029	0.032	0.037	0.046	0.019	0.022	0.025	0.027	0.029	0.032	0.035	0.040	0.050
	R2	0.014	0.017	0.020	0.023	0.025	0.029	0.031	0.036	0.044	0.015	0.018	0.021	0.024	0.028	0.031	0.034	0.039	0.047
	R3	0.009	0.013	0.016	0.019	0.023	0.026	0.030	0.035	0.042	0.010	0.014	0.017	0.021	0.025	0.028	0.033	0.038	0.046
	R4	0.006	0.010	0.014	0.018	0.022	0.025	0.030	0.034	0.039	0.006	0.011	0.015	0.020	0.024	0.028	0.032	0.037	0.042
$\lambda_{20^{\circ}\text{C}}=2.00$	R1	0.011	0.013	0.014	0.015	0.016	0.018	0.020	0.022	0.028	0.012	0.014	0.015	0.017	0.018	0.019	0.022	0.024	0.030
	R2	0.008	0.011	0.012	0.014	0.016	0.018	0.019	0.022	0.026	0.009	0.011	0.013	0.015	0.017	0.019	0.021	0.024	0.029
	R3	0.006	0.008	0.010	0.012	0.014	0.016	0.019	0.021	0.025	0.006	0.009	0.011	0.013	0.015	0.018	0.020	0.023	0.028
	R4	0.004	0.006	0.009	0.011	0.013	0.016	0.018	0.021	0.024	0.004	0.007	0.010	0.012	0.015	0.017	0.020	0.023	0.026
$\alpha=0.50$										$\alpha=0.75$									
$\lambda_{20^{\circ}\text{C}}=0.00$	R1	0.062	0.075	0.087	0.098	0.110	0.126	0.150	0.184	0.266	0.071	0.091	0.108	0.125	0.142	0.165	0.198	0.243	0.355
	R2	0.048	0.060	0.072	0.085	0.101	0.123	0.139	0.182	0.254	0.055	0.073	0.091	0.110	0.132	0.160	0.185	0.239	0.339
	R3	0.030	0.044	0.056	0.068	0.082	0.102	0.133	0.178	0.234	0.035	0.053	0.069	0.086	0.107	0.133	0.172	0.231	0.318
	R4	0.005	0.023	0.038	0.053	0.069	0.091	0.125	0.159	0.194	0.006	0.028	0.047	0.066	0.089	0.118	0.161	0.217	0.270
$\lambda_{20^{\circ}\text{C}}=0.25$	R1	0.050	0.061	0.070	0.080	0.090	0.103	0.122	0.158	0.226	0.058	0.074	0.088	0.101	0.116	0.135	0.162	0.204	0.308
	R2	0.038	0.049	0.058	0.069	0.082	0.099	0.114	0.150	0.210	0.045	0.060	0.074	0.089	0.107	0.131	0.152	0.197	0.282
	R3	0.025	0.036	0.046	0.056	0.070	0.087	0.112	0.146	0.191	0.030	0.044	0.057	0.072	0.092	0.113	0.146	0.191	0.259
	R4	0.016	0.029	0.041	0.054	0.066	0.083	0.108	0.130	0.157	0.020	0.036	0.051	0.068	0.086	0.109	0.141	0.178	0.221
$\lambda_{20^{\circ}\text{C}}=0.50$	R1	0.042	0.051	0.058	0.065	0.072	0.081	0.095	0.119	0.166	0.048	0.061	0.071	0.082	0.093	0.107	0.126	0.155	0.227
	R2	0.032	0.041	0.049	0.057	0.067	0.079	0.090	0.114	0.156	0.038	0.050	0.061	0.073	0.087	0.104	0.119	0.152	0.209
	R3	0.021	0.031	0.039	0.047	0.058	0.070	0.087	0.111	0.143	0.025	0.037	0.048	0.060	0.076	0.091	0.115	0.147	0.195
	R4	0.014	0.024	0.035	0.045	0.055	0.067	0.085	0.101	0.121	0.017	0.030	0.043	0.057	0.071	0.087	0.110	0.138	0.169
$\lambda_{20^{\circ}\text{C}}=0.75$	R1	0.038	0.045	0.051	0.056	0.062	0.069	0.079	0.094	0.127	0.043	0.053	0.062	0.071	0.080	0.092	0.106	0.125	0.175
	R2	0.029	0.037	0.044	0.051	0.058	0.068	0.075	0.091	0.119	0.034	0.045	0.055	0.065	0.076	0.089	0.101	0.124	0.162
	R3	0.019	0.028	0.035	0.042	0.052	0.061	0.074	0.090	0.111	0.023	0.033	0.043	0.053	0.066	0.079	0.097	0.119	0.155
	R4	0.013	0.022	0.031	0.040	0.049	0.058	0.072	0.084	0.098	0.015	0.027	0.038	0.050	0.062	0.076	0.094	0.116	0.140
$\lambda_{20^{\circ}\text{C}}=1.00$	R1	0.033	0.039	0.044	0.048	0.053	0.058	0.066	0.076	0.099	0.037	0.046	0.053	0.061	0.068	0.077	0.088	0.102	0.138
	R2	0.026	0.032	0.038	0.044	0.050	0.057	0.063	0.075	0.094	0.030	0.039	0.047	0.055	0.064	0.075	0.085	0.101	0.129
	R3	0.017	0.024	0.031	0.037	0.044	0.052	0.061	0.073	0.089	0.020	0.029	0.037	0.046	0.057	0.067	0.081	0.098	0.124
	R4	0.011	0.019	0.027	0.035	0.042	0.050	0.060	0.070	0.081	0.013	0.024	0.034	0.044	0.054	0.065	0.079	0.096	0.115
$\lambda_{20^{\circ}\text{C}}=1.50$	R1	0.021	0.025	0.028	0.030	0.033	0.036	0.041	0.046	0.058	0.023	0.029	0.034	0.038	0.043	0.048	0.054	0.063	0.082
	R2	0.016	0.021	0.024	0.028	0.032	0.036	0.039	0.045	0.055	0.019	0.025	0.030	0.035	0.040	0.047	0.053	0.061	0.077
	R3	0.011	0.016	0.020	0.023	0.028	0.033	0.038	0.044	0.053	0.013	0.019	0.024	0.029	0.036	0.042	0.050	0.060	0.076
	R4	0.007	0.012	0.018	0.022	0.027	0.032												

A20 Factor χ_{Rel} for S460 strong axis, imposed (Q) variable load type

		$\theta_{\text{nom}} = 300^{\circ}\text{C}$																	
$p_{f,fi} \rightarrow$		0.10	0.20	0.30	0.40	0.50	0.60	0.70	0.80	0.90	0.10	0.20	0.30	0.40	0.50	0.60	0.70	0.80	0.90
$\beta_{f,fi} \rightarrow$		1.28	0.84	0.52	0.40	0.00	-0.25	-0.52	-0.84	-1.28	1.28	0.84	0.52	0.40	0.00	-0.25	-0.52	-0.84	-1.28
$\delta_{of} \rightarrow$		1.15	1.02	0.94	0.88	0.82	0.77	0.72	0.67	0.60	1.15	1.02	0.94	0.88	0.82	0.77	0.72	0.67	0.60
		$\alpha=0.00$									$\alpha=0.25$								
$\lambda_{20^{\circ}\text{C}}=0.00$	R1	0.816	0.909	0.979	1.000	1.000	1.000	1.000	1.000	1.000	0.882	0.984	1.000	1.000	1.000	1.000	1.000	1.000	1.000
	R2	0.793	0.892	0.965	1.000	1.000	1.000	1.000	1.000	1.000	0.857	0.965	1.000	1.000	1.000	1.000	1.000	1.000	1.000
	R3	0.781	0.884	0.959	1.000	1.000	1.000	1.000	1.000	1.000	0.845	0.958	1.000	1.000	1.000	1.000	1.000	1.000	1.000
	R4	0.742	0.855	0.934	1.000	1.000	1.000	1.000	1.000	1.000	0.800	0.924	1.000	1.000	1.000	1.000	1.000	1.000	1.000
$\lambda_{20^{\circ}\text{C}}=0.25$	R1	0.710	0.790	0.852	0.908	0.963	0.993	0.993	0.993	0.993	0.766	0.855	0.925	0.987	0.993	0.993	0.993	0.993	0.993
	R2	0.691	0.776	0.840	0.898	0.953	0.993	0.993	0.993	0.993	0.746	0.840	0.912	0.976	0.993	0.993	0.993	0.993	0.993
	R3	0.681	0.770	0.836	0.893	0.949	0.993	0.993	0.993	0.993	0.735	0.833	0.906	0.970	0.993	0.993	0.993	0.993	0.993
	R4	0.646	0.744	0.814	0.874	0.933	0.993	0.993	0.993	0.993	0.698	0.806	0.883	0.950	0.993	0.993	0.993	0.993	0.993
$\lambda_{20^{\circ}\text{C}}=0.50$	R1	0.544	0.611	0.663	0.711	0.758	0.808	0.866	0.951	0.951	0.589	0.663	0.719	0.772	0.825	0.880	0.951	0.951	0.951
	R2	0.529	0.600	0.653	0.701	0.746	0.795	0.852	0.951	0.951	0.571	0.648	0.708	0.761	0.812	0.867	0.951	0.951	0.951
	R3	0.519	0.592	0.646	0.691	0.736	0.784	0.840	0.908	0.951	0.561	0.641	0.700	0.751	0.800	0.854	0.916	0.951	0.951
	R4	0.486	0.569	0.626	0.676	0.724	0.774	0.830	0.897	0.951	0.526	0.615	0.678	0.734	0.787	0.842	0.905	0.951	0.951
$\lambda_{20^{\circ}\text{C}}=0.75$	R1	0.445	0.508	0.559	0.608	0.657	0.705	0.761	0.876	0.876	0.482	0.550	0.607	0.661	0.715	0.767	0.876	0.876	0.876
	R2	0.429	0.493	0.546	0.593	0.639	0.688	0.743	0.813	0.876	0.465	0.536	0.593	0.645	0.695	0.750	0.810	0.876	0.876
	R3	0.420	0.485	0.536	0.579	0.622	0.670	0.726	0.792	0.876	0.455	0.527	0.582	0.630	0.676	0.731	0.792	0.876	0.876
	R4	0.389	0.461	0.515	0.563	0.610	0.661	0.715	0.777	0.876	0.421	0.500	0.560	0.612	0.665	0.720	0.780	0.876	0.876
$\lambda_{20^{\circ}\text{C}}=1.00$	R1	0.374	0.426	0.470	0.513	0.555	0.596	0.645	0.725	0.725	0.404	0.462	0.511	0.557	0.603	0.649	0.725	0.725	0.725
	R2	0.360	0.414	0.459	0.499	0.539	0.581	0.629	0.725	0.725	0.389	0.450	0.499	0.543	0.586	0.632	0.725	0.725	0.725
	R3	0.352	0.407	0.451	0.487	0.523	0.565	0.613	0.725	0.725	0.381	0.441	0.489	0.529	0.569	0.614	0.725	0.725	0.725
	R4	0.325	0.386	0.432	0.473	0.514	0.557	0.604	0.725	0.725	0.351	0.418	0.469	0.514	0.558	0.606	0.725	0.725	0.725
$\lambda_{20^{\circ}\text{C}}=1.50$	R1	0.217	0.244	0.266	0.286	0.306	0.327	0.349	0.395	0.395	0.235	0.265	0.289	0.311	0.333	0.356	0.395	0.395	0.395
	R2	0.211	0.239	0.262	0.281	0.301	0.321	0.343	0.395	0.395	0.228	0.259	0.283	0.305	0.327	0.349	0.395	0.395	0.395
	R3	0.207	0.236	0.258	0.277	0.295	0.314	0.337	0.365	0.395	0.224	0.256	0.280	0.301	0.321	0.342	0.395	0.395	0.395
	R4	0.193	0.226	0.250	0.270	0.290	0.311	0.334	0.362	0.395	0.208	0.245	0.271	0.294	0.316	0.338	0.364	0.395	0.395
$\lambda_{20^{\circ}\text{C}}=2.00$	R1	0.128	0.143	0.156	0.167	0.178	0.190	0.203	0.232	0.232	0.138	0.155	0.169	0.181	0.194	0.207	0.232	0.232	0.232
	R2	0.124	0.140	0.153	0.164	0.175	0.187	0.200	0.216	0.232	0.134	0.152	0.166	0.178	0.191	0.203	0.218	0.232	0.232
	R3	0.122	0.139	0.151	0.162	0.173	0.184	0.196	0.213	0.232	0.132	0.150	0.164	0.176	0.188	0.200	0.214	0.232	0.232
	R4	0.114	0.133	0.146	0.158	0.170	0.181	0.195	0.211	0.232	0.123	0.144	0.159	0.172	0.184	0.197	0.212	0.232	0.232
		$\alpha=0.50$									$\alpha=0.75$								
$\lambda_{20^{\circ}\text{C}}=0.00$	R1	0.958	1.000	1.000	1.000	1.000	1.000	1.000	1.000	1.000	1.000	1.000	1.000	1.000	1.000	1.000	1.000	1.000	1.000
	R2	0.930	1.000	1.000	1.000	1.000	1.000	1.000	1.000	1.000	1.000	1.000	1.000	1.000	1.000	1.000	1.000	1.000	1.000
	R3	0.917	1.000	1.000	1.000	1.000	1.000	1.000	1.000	1.000	0.990	1.000	1.000	1.000	1.000	1.000	1.000	1.000	1.000
	R4	0.871	1.000	1.000	1.000	1.000	1.000	1.000	1.000	1.000	0.941	1.000	1.000	1.000	1.000	1.000	1.000	1.000	1.000
$\lambda_{20^{\circ}\text{C}}=0.25$	R1	0.834	0.950	0.993	0.993	0.993	0.993	0.993	0.993	0.993	0.897	0.993	0.993	0.993	0.993	0.993	0.993	0.993	0.993
	R2	0.810	0.930	0.993	0.993	0.993	0.993	0.993	0.993	0.993	0.875	0.993	0.993	0.993	0.993	0.993	0.993	0.993	0.993
	R3	0.800	0.925	0.993	0.993	0.993	0.993	0.993	0.993	0.993	0.864	0.993	0.993	0.993	0.993	0.993	0.993	0.993	0.993
	R4	0.758	0.891	0.990	0.993	0.993	0.993	0.993	0.993	0.993	0.824	0.993	0.993	0.993	0.993	0.993	0.993	0.993	0.993
$\lambda_{20^{\circ}\text{C}}=0.50$	R1	0.640	0.734	0.809	0.876	0.951	0.951	0.951	0.951	0.951	0.694	0.845	0.951	0.951	0.951	0.951	0.951	0.951	0.951
	R2	0.622	0.719	0.794	0.861	0.951	0.951	0.951	0.951	0.951	0.677	0.828	0.951	0.951	0.951	0.951	0.951	0.951	0.951
	R3	0.612	0.711	0.786	0.852	0.916	0.951	0.951	0.951	0.951	0.665	0.817	0.951	0.951	0.951	0.951	0.951	0.951	0.951
	R4	0.573	0.681	0.761	0.831	0.900	0.951	0.951	0.951	0.951	0.627	0.783	0.913	0.951	0.951	0.951	0.951	0.951	0.951
$\lambda_{20^{\circ}\text{C}}=0.75$	R1	0.529	0.615	0.686	0.752	0.876	0.876	0.876	0.876	0.876	0.580	0.714	0.876	0.876	0.876	0.876	0.876	0.876	0.876
	R2	0.511	0.596	0.667	0.733	0.795	0.876	0.876	0.876	0.876	0.562	0.694	0.809	0.876	0.876	0.876	0.876	0.876	0.876
	R3	0.499	0.587	0.656	0.716	0.775	0.876	0.876	0.876	0.876	0.549	0.682	0.795	0.876	0.876	0.876	0.876	0.876	0.876
	R4	0.462	0.558	0.630	0.696	0.760	0.876	0.876	0.876	0.876	0.510	0.647	0.762	0.876	0.876	0.876	0.876	0.876	0.876
$\lambda_{20^{\circ}\text{C}}=1.00$	R1	0.442	0.516	0.575	0.632	0.725	0.725	0.725	0.725	0.725	0.487	0.601	0.725	0.725	0.725	0.725	0.725	0.725	0.725
	R2	0.428	0.500	0.559	0.615	0.725	0.725	0.725	0.725	0.725	0.470	0.582	0.725	0.725	0.725	0.725	0.725	0.725	0.725
	R3	0.418	0.492	0.550	0.601	0.651	0.725	0.725	0.725	0.725	0.459	0.573	0.725	0.725	0.725	0.725	0.725	0.725	0.725
	R4	0.384	0.465	0.527	0.582	0.638	0.725	0.725	0.725	0.725	0.425	0.541	0.637	0.725	0.725	0.725	0.725	0.725	0.725
$\lambda_{20^{\circ}\text{C}}=1.50$	R1	0.256	0.294	0.325	0.353	0.395	0.395	0.395	0.395	0.395	0.278	0.339	0.395	0.395	0.395	0.395	0.395	0.395	0.395
	R2	0.248	0.288	0.319	0.347	0.395	0.395	0.395	0.395	0.395	0.271	0.332	0.395	0.395	0.395	0.395	0.395	0.395	0.395
	R3	0.244	0.284	0.315	0.342	0.395	0.395	0.395	0.395	0.395	0.265	0.327	0.395	0.395	0.395	0.395	0.395	0.395	0.395
	R4	0.227	0.272</																

$\theta_{\text{nom}} = 400^{\circ}\text{C}$

$p_{f,fi} \rightarrow$	0.10	0.20	0.30	0.40	0.50	0.60	0.70	0.80	0.90	0.10	0.20	0.30	0.40	0.50	0.60	0.70	0.80	0.90
$\beta_{f,fi} \rightarrow$	1.28	0.84	0.52	0.40	0.00	-0.25	-0.52	-0.84	-1.28	1.28	0.84	0.52	0.40	0.00	-0.25	-0.52	-0.84	-1.28
$\delta_{af} \rightarrow$	1.15	1.02	0.94	0.88	0.82	0.77	0.72	0.67	0.60	1.15	1.02	0.94	0.88	0.82	0.77	0.72	0.67	0.60
	$\alpha=0.00$									$\alpha=0.25$								
$\lambda_{20^{\circ}\text{C}}=0.00$	R1	0.756	0.854	0.928	0.993	1.000	1.000	1.000	1.000	0.817	0.924	1.000	1.000	1.000	1.000	1.000	1.000	1.000
	R2	0.618	0.744	0.833	0.911	0.984	1.000	1.000	1.000	0.668	0.806	0.903	0.988	1.000	1.000	1.000	1.000	1.000
	R3	0.579	0.726	0.824	0.903	0.976	1.000	1.000	1.000	0.628	0.787	0.893	0.981	1.000	1.000	1.000	1.000	1.000
	R4	0.518	0.680	0.788	0.876	0.956	1.000	1.000	1.000	0.561	0.736	0.855	0.950	1.000	1.000	1.000	1.000	1.000
$\lambda_{20^{\circ}\text{C}}=0.25$	R1	0.659	0.744	0.809	0.866	0.922	0.980	0.993	0.993	0.712	0.805	0.876	0.941	0.993	0.993	0.993	0.993	0.993
	R2	0.538	0.650	0.727	0.795	0.858	0.923	0.993	0.993	0.583	0.703	0.789	0.862	0.933	0.993	0.993	0.993	0.993
	R3	0.506	0.634	0.718	0.789	0.853	0.916	0.987	0.993	0.549	0.687	0.778	0.856	0.927	0.993	0.993	0.993	0.993
	R4	0.454	0.594	0.688	0.764	0.834	0.902	0.975	0.993	0.491	0.642	0.746	0.830	0.907	0.981	0.993	0.993	0.993
$\lambda_{20^{\circ}\text{C}}=0.50$	R1	0.488	0.552	0.601	0.645	0.687	0.732	0.782	0.842	0.527	0.598	0.652	0.700	0.747	0.797	0.853	0.920	0.951
	R2	0.393	0.478	0.538	0.591	0.642	0.689	0.743	0.811	0.426	0.517	0.583	0.641	0.697	0.750	0.810	0.884	0.951
	R3	0.369	0.467	0.532	0.584	0.633	0.682	0.737	0.802	0.400	0.506	0.576	0.634	0.687	0.741	0.803	0.875	0.951
	R4	0.329	0.436	0.509	0.568	0.620	0.672	0.728	0.793	0.356	0.472	0.552	0.616	0.675	0.731	0.793	0.866	0.951
$\lambda_{20^{\circ}\text{C}}=0.75$	R1	0.388	0.441	0.481	0.518	0.554	0.593	0.637	0.695	0.420	0.478	0.523	0.563	0.603	0.646	0.695	0.758	0.876
	R2	0.308	0.378	0.428	0.473	0.516	0.555	0.602	0.663	0.334	0.410	0.464	0.513	0.560	0.605	0.656	0.723	0.876
	R3	0.287	0.370	0.423	0.466	0.507	0.548	0.595	0.651	0.311	0.401	0.459	0.506	0.551	0.595	0.648	0.710	0.805
	R4	0.252	0.343	0.404	0.454	0.498	0.539	0.585	0.639	0.273	0.371	0.438	0.492	0.542	0.587	0.637	0.697	0.790
$\lambda_{20^{\circ}\text{C}}=1.00$	R1	0.323	0.366	0.400	0.431	0.462	0.494	0.532	0.583	0.349	0.397	0.435	0.469	0.502	0.538	0.580	0.635	0.725
	R2	0.254	0.314	0.355	0.393	0.428	0.462	0.503	0.555	0.275	0.340	0.386	0.428	0.466	0.503	0.548	0.606	0.725
	R3	0.235	0.306	0.351	0.387	0.422	0.456	0.496	0.543	0.254	0.332	0.381	0.421	0.458	0.496	0.541	0.592	0.725
	R4	0.203	0.283	0.336	0.377	0.415	0.448	0.487	0.533	0.221	0.306	0.363	0.409	0.450	0.488	0.530	0.582	0.725
$\lambda_{20^{\circ}\text{C}}=1.50$	R1	0.193	0.218	0.237	0.254	0.270	0.288	0.308	0.333	0.209	0.236	0.257	0.276	0.294	0.314	0.336	0.363	0.395
	R2	0.153	0.189	0.212	0.234	0.253	0.272	0.293	0.320	0.166	0.204	0.230	0.254	0.275	0.296	0.319	0.348	0.395
	R3	0.141	0.185	0.211	0.231	0.250	0.269	0.290	0.316	0.153	0.199	0.228	0.250	0.272	0.293	0.316	0.345	0.395
	R4	0.121	0.170	0.201	0.225	0.246	0.265	0.286	0.312	0.132	0.185	0.218	0.244	0.267	0.289	0.312	0.340	0.395
$\lambda_{20^{\circ}\text{C}}=2.00$	R1	0.114	0.129	0.140	0.150	0.159	0.169	0.181	0.195	0.123	0.139	0.152	0.163	0.173	0.184	0.197	0.213	0.232
	R2	0.091	0.112	0.126	0.138	0.149	0.160	0.173	0.187	0.098	0.121	0.136	0.150	0.163	0.175	0.188	0.205	0.232
	R3	0.084	0.109	0.124	0.136	0.147	0.159	0.171	0.186	0.091	0.118	0.135	0.148	0.160	0.172	0.186	0.203	0.232
	R4	0.072	0.101	0.119	0.133	0.145	0.157	0.168	0.184	0.078	0.109	0.129	0.144	0.158	0.170	0.184	0.200	0.232
	$\alpha=0.50$									$\alpha=0.75$								
$\lambda_{20^{\circ}\text{C}}=0.00$	R1	0.892	1.000	1.000	1.000	1.000	1.000	1.000	1.000	0.969	1.000	1.000	1.000	1.000	1.000	1.000	1.000	1.000
	R2	0.735	0.893	1.000	1.000	1.000	1.000	1.000	1.000	0.816	1.000	1.000	1.000	1.000	1.000	1.000	1.000	1.000
	R3	0.693	0.872	0.998	1.000	1.000	1.000	1.000	1.000	0.776	1.000	1.000	1.000	1.000	1.000	1.000	1.000	1.000
	R4	0.623	0.817	0.954	1.000	1.000	1.000	1.000	1.000	0.713	0.945	1.000	1.000	1.000	1.000	1.000	1.000	1.000
$\lambda_{20^{\circ}\text{C}}=0.25$	R1	0.777	0.894	0.985	0.993	0.993	0.993	0.993	0.993	0.843	0.993	0.993	0.993	0.993	0.993	0.993	0.993	0.993
	R2	0.640	0.779	0.883	0.974	0.993	0.993	0.993	0.993	0.712	0.901	0.993	0.993	0.993	0.993	0.993	0.993	0.993
	R3	0.607	0.761	0.872	0.966	0.993	0.993	0.993	0.993	0.681	0.879	0.993	0.993	0.993	0.993	0.993	0.993	0.993
	R4	0.546	0.712	0.833	0.934	0.993	0.993	0.993	0.993	0.620	0.827	0.991	0.993	0.993	0.993	0.993	0.993	0.993
$\lambda_{20^{\circ}\text{C}}=0.50$	R1	0.575	0.664	0.732	0.794	0.855	0.919	0.951	0.951	0.627	0.767	0.884	0.951	0.951	0.951	0.951	0.951	0.951
	R2	0.468	0.574	0.652	0.723	0.793	0.862	0.951	0.951	0.522	0.664	0.780	0.892	0.951	0.951	0.951	0.951	0.951
	R3	0.442	0.561	0.645	0.716	0.783	0.851	0.951	0.951	0.498	0.647	0.769	0.883	0.951	0.951	0.951	0.951	0.951
	R4	0.396	0.523	0.615	0.694	0.767	0.839	0.916	0.951	0.453	0.606	0.733	0.851	0.951	0.951	0.951	0.951	0.951
$\lambda_{20^{\circ}\text{C}}=0.75$	R1	0.460	0.532	0.588	0.639	0.690	0.744	0.807	0.876	0.502	0.616	0.710	0.800	0.876	0.876	0.876	0.876	0.876
	R2	0.368	0.454	0.520	0.581	0.639	0.695	0.759	0.876	0.412	0.527	0.624	0.717	0.812	0.876	0.876	0.876	0.876
	R3	0.344	0.444	0.514	0.572	0.628	0.685	0.750	0.876	0.388	0.515	0.615	0.709	0.802	0.876	0.876	0.876	0.876
	R4	0.303	0.412	0.490	0.555	0.617	0.675	0.737	0.815	0.350	0.479	0.583	0.682	0.780	0.876	0.876	0.876	0.876
$\lambda_{20^{\circ}\text{C}}=1.00$	R1	0.381	0.443	0.489	0.532	0.576	0.621	0.725	0.725	0.418	0.513	0.592	0.725	0.725	0.725	0.725	0.725	0.725
	R2	0.303	0.377	0.433	0.483	0.531	0.578	0.632	0.725	0.338	0.436	0.517	0.598	0.725	0.725	0.725	0.725	0.725
	R3	0.281	0.368	0.427	0.475	0.523	0.571	0.626	0.725	0.319	0.426	0.509	0.588	0.725	0.725	0.725	0.725	0.725
	R4	0.247	0.341	0.407	0.462	0.513	0.561	0.614	0.725	0.285	0.396	0.484	0.567	0.650	0.725	0.725	0.725	0.725
$\lambda_{20^{\circ}\text{C}}=1.50$	R1	0.227	0.262	0.289	0.313	0.336	0.362	0.395	0.395	0.247	0.303	0.348	0.395	0.395	0.395	0.395	0.395	0.395
	R2	0.182	0.226	0.258	0.287	0.314	0.341	0.395	0.395	0.202	0.261	0.307	0.352	0.395	0.395	0.395	0.395	0.395
	R3	0.169	0.220	0.255	0.283	0.310	0.336	0.395	0.395	0.191	0.254	0.303	0.348	0.395	0.395	0.395	0.395	0.395
	R4	0.147	0.204	0.243	0.274	0.303	0.331	0.361	0.395	0.170	0.235	0.287	0.334	0.395	0.395	0.395	0.395	0.395
$\lambda_{20^{\circ}\text{C}}=2.00$	R1	0.134	0.154	0.170	0.184	0.198	0.213	0.232	0.232	0.146	0.178	0.206	0.232	0.232	0.232	0.232	0.232	0.232
	R2	0.108	0.134	0.152	0.169	0.185	0.201	0.218	0.232	0.120	0.154	0.181	0.208	0.232	0.232	0.232	0.232	0.232
	R3	0.100	0.131	0.151	0.167	0.183	0.198	0.215	0.232	0.113	0.150	0.179	0.206	0.232	0.232	0.232	0.232	0.232
	R4	0.088	0.121	0.144	0.162	0.179	0.196	0.213	0.232	0.101	0.139	0.169	0.197	0.232	0.232	0.232	0.232	0.232

$\theta_{\text{nom}} = 500^{\circ}\text{C}$

$p_{f,fi} \rightarrow$	0.10	0.20	0.30	0.40	0.50	0.60	0.70	0.80	0.90	0.10 <td>0.20</td> <td>0.30</td> <td>0.40</td> <td>0.50</td> <td>0.60</td> <td>0.70</td> <td>0.80</td> <td>0.90</td>	0.20	0.30	0.40	0.50	0.60	0.70	0.80	0.90	
$\beta_{f,fi} \rightarrow$	1.28	0.84	0.52	0.40	0.00	-0.25	-0.52	-0.84	-1.28	1.28	0.84	0.52	0.40	0.00	-0.25	-0.52	-0.84	-1.28	
$\delta_{of} \rightarrow$	1.15	1.02	0.94	0.88	0.82	0.77	0.72	0.67	0.60	1.15	1.02	0.94	0.88	0.82	0.77	0.72	0.67	0.60	
$\alpha=0.00$										$\alpha=0.25$									
$\lambda_{20^{\circ}\text{C}}=0.00$	R1	0.423	0.526	0.612	0.695	0.785	0.870	0.963	1.000	1.000	0.458	0.571	0.664	0.753	0.852	0.945	1.000	1.000	1.000
	R2	0.329	0.458	0.573	0.665	0.752	0.836	0.928	1.000	1.000	0.355	0.496	0.621	0.722	0.817	0.910	1.000	1.000	1.000
	R3	0.276	0.397	0.508	0.612	0.716	0.809	0.912	1.000	1.000	0.298	0.432	0.551	0.665	0.777	0.881	0.993	1.000	1.000
	R4	0.217	0.319	0.440	0.557	0.672	0.785	0.897	1.000	1.000	0.237	0.347	0.478	0.603	0.729	0.852	0.975	1.000	1.000
$\lambda_{20^{\circ}\text{C}}=0.25$	R1	0.370	0.461	0.535	0.607	0.685	0.761	0.842	0.940	0.993	0.401	0.500	0.581	0.658	0.742	0.828	0.917	0.993	0.993
	R2	0.288	0.401	0.501	0.581	0.658	0.731	0.811	0.909	0.993	0.313	0.435	0.544	0.632	0.715	0.796	0.883	0.990	0.993
	R3	0.241	0.350	0.444	0.535	0.624	0.708	0.799	0.899	0.993	0.261	0.379	0.483	0.581	0.678	0.770	0.869	0.980	0.993
	R4	0.190	0.280	0.386	0.487	0.587	0.686	0.783	0.889	0.993	0.207	0.305	0.419	0.529	0.638	0.744	0.852	0.970	0.993
$\lambda_{20^{\circ}\text{C}}=0.50$	R1	0.265	0.333	0.389	0.442	0.501	0.558	0.622	0.692	0.795	0.288	0.362	0.422	0.480	0.544	0.607	0.676	0.754	0.868
	R2	0.205	0.288	0.363	0.425	0.482	0.536	0.597	0.670	0.776	0.222	0.313	0.394	0.462	0.523	0.582	0.649	0.730	0.847
	R3	0.172	0.249	0.320	0.389	0.456	0.521	0.586	0.663	0.767	0.186	0.270	0.348	0.422	0.495	0.566	0.638	0.723	0.836
	R4	0.135	0.199	0.276	0.352	0.428	0.503	0.577	0.653	0.753	0.148	0.217	0.300	0.382	0.465	0.546	0.627	0.711	0.822
$\lambda_{20^{\circ}\text{C}}=0.75$	R1	0.200	0.256	0.302	0.347	0.396	0.443	0.492	0.549	0.637	0.218	0.277	0.327	0.377	0.430	0.481	0.536	0.599	0.696
	R2	0.152	0.217	0.280	0.331	0.378	0.423	0.472	0.531	0.621	0.165	0.236	0.303	0.359	0.411	0.460	0.513	0.579	0.677
	R3	0.126	0.187	0.244	0.301	0.358	0.410	0.465	0.527	0.607	0.136	0.202	0.264	0.326	0.389	0.446	0.506	0.573	0.664
	R4	0.100	0.147	0.208	0.270	0.334	0.397	0.457	0.518	0.595	0.109	0.160	0.226	0.293	0.363	0.431	0.496	0.564	0.649
$\lambda_{20^{\circ}\text{C}}=1.00$	R1	0.159	0.206	0.247	0.287	0.329	0.368	0.409	0.457	0.531	0.172	0.224	0.268	0.311	0.357	0.400	0.445	0.497	0.579
	R2	0.118	0.173	0.227	0.272	0.313	0.351	0.392	0.442	0.517	0.128	0.188	0.247	0.295	0.340	0.382	0.426	0.482	0.564
	R3	0.097	0.147	0.195	0.246	0.296	0.340	0.386	0.438	0.504	0.106	0.160	0.212	0.267	0.321	0.370	0.420	0.476	0.551
	R4	0.078	0.114	0.165	0.218	0.274	0.329	0.379	0.430	0.494	0.084	0.124	0.178	0.237	0.298	0.357	0.413	0.469	0.539
$\lambda_{20^{\circ}\text{C}}=1.50$	R1	0.094	0.124	0.148	0.173	0.198	0.221	0.245	0.273	0.312	0.102	0.134	0.161	0.187	0.215	0.240	0.266	0.297	0.340
	R2	0.069	0.103	0.136	0.164	0.189	0.212	0.235	0.264	0.305	0.075	0.112	0.148	0.178	0.205	0.230	0.256	0.288	0.333
	R3	0.057	0.087	0.116	0.148	0.179	0.205	0.232	0.261	0.301	0.062	0.094	0.127	0.161	0.194	0.223	0.252	0.285	0.328
	R4	0.046	0.066	0.098	0.131	0.166	0.198	0.228	0.258	0.295	0.049	0.072	0.106	0.142	0.180	0.215	0.248	0.281	0.322
$\lambda_{20^{\circ}\text{C}}=2.00$	R1	0.056	0.073	0.088	0.103	0.117	0.131	0.145	0.161	0.184	0.061	0.080	0.096	0.111	0.128	0.142	0.158	0.176	0.201
	R2	0.041	0.061	0.081	0.097	0.112	0.125	0.139	0.156	0.180	0.045	0.066	0.088	0.106	0.122	0.136	0.152	0.170	0.197
	R3	0.034	0.051	0.069	0.088	0.106	0.122	0.137	0.155	0.178	0.037	0.056	0.075	0.095	0.115	0.132	0.149	0.168	0.194
	R4	0.027	0.039	0.058	0.078	0.098	0.117	0.135	0.153	0.175	0.029	0.043	0.063	0.084	0.107	0.128	0.147	0.167	0.191
$\alpha=0.50$										$\alpha=0.75$									
$\lambda_{20^{\circ}\text{C}}=0.00$	R1	0.509	0.640	0.747	0.851	0.965	1.000	1.000	1.000	1.000	0.583	0.756	0.905	1.000	1.000	1.000	1.000	1.000	1.000
	R2	0.400	0.558	0.700	0.814	0.928	1.000	1.000	1.000	1.000	0.477	0.667	0.845	1.000	1.000	1.000	1.000	1.000	1.000
	R3	0.337	0.486	0.621	0.750	0.878	1.000	1.000	1.000	1.000	0.407	0.585	0.756	0.922	1.000	1.000	1.000	1.000	1.000
	R4	0.267	0.393	0.539	0.683	0.824	0.967	1.000	1.000	1.000	0.324	0.487	0.660	0.841	1.000	1.000	1.000	1.000	1.000
$\lambda_{20^{\circ}\text{C}}=0.25$	R1	0.445	0.559	0.653	0.743	0.840	0.942	0.993	0.993	0.993	0.510	0.661	0.792	0.919	0.993	0.993	0.993	0.993	0.993
	R2	0.351	0.489	0.611	0.715	0.811	0.909	0.993	0.993	0.993	0.417	0.586	0.740	0.881	0.993	0.993	0.993	0.993	0.993
	R3	0.296	0.427	0.544	0.656	0.766	0.878	0.993	0.993	0.993	0.358	0.512	0.661	0.806	0.956	0.993	0.993	0.993	0.993
	R4	0.234	0.346	0.473	0.599	0.722	0.845	0.974	0.993	0.993	0.286	0.427	0.578	0.734	0.895	0.993	0.993	0.993	0.993
$\lambda_{20^{\circ}\text{C}}=0.50$	R1	0.320	0.404	0.474	0.542	0.616	0.694	0.777	0.873	0.951	0.367	0.480	0.576	0.671	0.773	0.890	0.951	0.951	0.951
	R2	0.250	0.351	0.444	0.521	0.592	0.665	0.745	0.844	0.951	0.298	0.421	0.536	0.640	0.745	0.858	0.951	0.951	0.951
	R3	0.209	0.304	0.392	0.477	0.561	0.643	0.731	0.835	0.951	0.254	0.367	0.476	0.585	0.697	0.819	0.951	0.951	0.951
	R4	0.167	0.246	0.339	0.433	0.526	0.619	0.716	0.824	0.951	0.202	0.304	0.415	0.532	0.650	0.780	0.951	0.951	0.951
$\lambda_{20^{\circ}\text{C}}=0.75$	R1	0.242	0.310	0.367	0.424	0.487	0.549	0.616	0.696	0.814	0.278	0.368	0.446	0.522	0.607	0.704	0.815	0.876	0.876
	R2	0.185	0.266	0.342	0.405	0.466	0.525	0.590	0.671	0.794	0.222	0.319	0.413	0.498	0.583	0.674	0.777	0.876	0.876
	R3	0.154	0.228	0.299	0.369	0.440	0.506	0.580	0.664	0.780	0.189	0.276	0.365	0.453	0.545	0.645	0.755	0.876	0.876
	R4	0.123	0.181	0.255	0.331	0.409	0.488	0.568	0.654	0.762	0.150	0.227	0.313	0.408	0.505	0.613	0.735	0.876	0.876
$\lambda_{20^{\circ}\text{C}}=1.00$	R1	0.193	0.252	0.301	0.350	0.404	0.456	0.511	0.578	0.725	0.224	0.299	0.365	0.428	0.500	0.583	0.725	0.725	0.725
	R2	0.144	0.212	0.278	0.333	0.385	0.436	0.489	0.558	0.725	0.175	0.257	0.337	0.409	0.481	0.557	0.644	0.725	0.725
	R3	0.119	0.180	0.240	0.301	0.363	0.419	0.481	0.551	0.648	0.148	0.219	0.293	0.369	0.447	0.532	0.628	0.725	0.725
	R4	0.095	0.141	0.203	0.268	0.336	0.404	0.472	0.544	0.632	0.118	0.177	0.249	0.332	0.416	0.507	0.609	0.725	0.725
$\lambda_{20^{\circ}\text{C}}=1.50$	R1	0.115	0.151	0.181	0.211	0.243	0.274	0.306	0.345	0.395	0.133	0.179	0.219	0.258	0.300	0.350	0.395	0.395	0.395
	R2	0.085	0.126	0.167	0.200	0.232	0.262	0.294	0.334	0.395	0.103	0.153	0.201	0.245	0.289	0.335	0.395	0.395	0.395
	R3	0.070	0.106	0.143	0.181	0.218	0.252	0.289	0.329	0.395	0.087	0.130	0.175	0.221	0.268	0.320	0.395	0.395	0.395
	R4	0.056	0.082	0.120	0.161	0.202	0.243	0.28											

$$\theta_{\text{nom}} = 600^{\circ}\text{C}$$

$p_{f,fi} \rightarrow$	0.10	0.20	0.30	0.40	0.50	0.60	0.70	0.80	0.90	0.10	0.20	0.30	0.40	0.50	0.60	0.70	0.80	0.90
$\beta_{f,fi} \rightarrow$	1.28	0.84	0.52	0.40	0.00	-0.25	-0.52	-0.84	-1.28	1.28	0.84	0.52	0.40	0.00	-0.25	-0.52	-0.84	-1.28
$\delta_{af} \rightarrow$	1.15	1.02	0.94	0.88	0.82	0.77	0.72	0.67	0.60	1.15	1.02	0.94	0.88	0.82	0.77	0.72	0.67	0.60
	$\alpha=0.00$									$\alpha=0.25$								
$\lambda_{20^{\circ}\text{C}}=0.00$	R1	0.372	0.475	0.559	0.639	0.718	0.801	0.892	1.000	1.000	0.403	0.516	0.607	0.694	0.780	0.871	0.971	1.000
	R2	0.210	0.269	0.334	0.404	0.480	0.560	0.661	0.784	0.969	0.227	0.292	0.363	0.439	0.522	0.609	0.719	0.853
	R3	0.194	0.250	0.313	0.386	0.463	0.542	0.630	0.752	0.929	0.210	0.272	0.340	0.419	0.503	0.589	0.684	0.818
	R4	0.147	0.204	0.252	0.315	0.396	0.489	0.602	0.725	0.880	0.160	0.221	0.274	0.343	0.430	0.531	0.655	0.790
$\lambda_{20^{\circ}\text{C}}=0.25$	R1	0.325	0.417	0.489	0.559	0.628	0.700	0.780	0.874	0.993	0.353	0.452	0.531	0.607	0.683	0.762	0.849	0.953
	R2	0.184	0.236	0.293	0.355	0.421	0.492	0.578	0.686	0.848	0.199	0.257	0.318	0.386	0.458	0.535	0.630	0.746
	R3	0.170	0.220	0.275	0.338	0.405	0.474	0.553	0.656	0.813	0.184	0.239	0.299	0.368	0.440	0.515	0.601	0.715
	R4	0.129	0.179	0.222	0.277	0.347	0.429	0.526	0.634	0.769	0.140	0.194	0.241	0.301	0.377	0.466	0.573	0.692
$\lambda_{20^{\circ}\text{C}}=0.50$	R1	0.232	0.299	0.353	0.406	0.459	0.513	0.573	0.643	0.743	0.252	0.325	0.384	0.441	0.498	0.557	0.623	0.701
	R2	0.130	0.167	0.208	0.254	0.302	0.354	0.418	0.500	0.623	0.141	0.181	0.226	0.276	0.328	0.384	0.454	0.546
	R3	0.121	0.155	0.195	0.241	0.291	0.341	0.400	0.480	0.596	0.131	0.169	0.211	0.262	0.316	0.371	0.435	0.522
	R4	0.093	0.127	0.157	0.196	0.248	0.308	0.381	0.461	0.563	0.101	0.138	0.171	0.213	0.269	0.334	0.414	0.503
$\lambda_{20^{\circ}\text{C}}=0.75$	R1	0.174	0.226	0.271	0.316	0.360	0.405	0.453	0.510	0.587	0.188	0.246	0.295	0.343	0.391	0.440	0.493	0.555
	R2	0.096	0.123	0.154	0.189	0.227	0.269	0.325	0.393	0.493	0.104	0.133	0.167	0.205	0.247	0.293	0.353	0.429
	R3	0.089	0.114	0.143	0.180	0.218	0.260	0.307	0.375	0.471	0.097	0.124	0.156	0.195	0.237	0.282	0.334	0.408
	R4	0.071	0.094	0.115	0.144	0.184	0.232	0.294	0.359	0.443	0.077	0.102	0.125	0.157	0.200	0.252	0.319	0.391
$\lambda_{20^{\circ}\text{C}}=1.00$	R1	0.137	0.181	0.220	0.258	0.297	0.336	0.376	0.423	0.489	0.148	0.197	0.239	0.281	0.322	0.365	0.409	0.461
	R2	0.074	0.095	0.120	0.149	0.181	0.217	0.265	0.326	0.410	0.081	0.103	0.130	0.162	0.197	0.236	0.289	0.354
	R3	0.070	0.088	0.111	0.141	0.173	0.209	0.249	0.309	0.391	0.076	0.096	0.121	0.153	0.189	0.227	0.272	0.336
	R4	0.057	0.074	0.089	0.112	0.145	0.185	0.238	0.295	0.367	0.062	0.080	0.097	0.122	0.158	0.201	0.259	0.322
$\lambda_{20^{\circ}\text{C}}=1.50$	R1	0.081	0.108	0.132	0.156	0.179	0.202	0.226	0.254	0.292	0.087	0.117	0.143	0.169	0.194	0.220	0.246	0.277
	R2	0.043	0.055	0.070	0.088	0.108	0.130	0.160	0.197	0.246	0.047	0.060	0.076	0.096	0.117	0.141	0.173	0.214
	R3	0.041	0.051	0.065	0.083	0.103	0.124	0.150	0.186	0.235	0.045	0.056	0.070	0.090	0.112	0.135	0.163	0.203
	R4	0.035	0.043	0.052	0.065	0.085	0.110	0.143	0.178	0.221	0.038	0.047	0.057	0.071	0.093	0.119	0.155	0.194
$\lambda_{20^{\circ}\text{C}}=2.00$	R1	0.048	0.064	0.078	0.092	0.106	0.120	0.134	0.150	0.173	0.052	0.070	0.085	0.100	0.115	0.130	0.146	0.164
	R2	0.026	0.033	0.042	0.052	0.064	0.077	0.095	0.117	0.146	0.028	0.036	0.045	0.057	0.070	0.084	0.103	0.127
	R3	0.024	0.031	0.039	0.049	0.061	0.074	0.089	0.110	0.140	0.027	0.033	0.042	0.054	0.066	0.080	0.097	0.120
	R4	0.021	0.026	0.031	0.039	0.051	0.065	0.085	0.106	0.131	0.022	0.028	0.034	0.042	0.055	0.071	0.092	0.115
	$\alpha=0.50$									$\alpha=0.75$								
$\lambda_{20^{\circ}\text{C}}=0.00$	R1	0.450	0.579	0.685	0.784	0.887	0.994	1.000	1.000	1.000	0.525	0.692	0.836	0.977	1.000	1.000	1.000	1.000
	R2	0.254	0.331	0.411	0.498	0.595	0.696	0.823	0.979	1.000	0.299	0.407	0.510	0.622	0.751	0.895	1.000	1.000
	R3	0.235	0.308	0.387	0.476	0.572	0.673	0.787	0.938	1.000	0.276	0.382	0.485	0.596	0.724	0.864	1.000	1.000
	R4	0.178	0.250	0.313	0.390	0.490	0.606	0.747	0.909	1.000	0.207	0.304	0.396	0.498	0.621	0.772	0.962	1.000
$\lambda_{20^{\circ}\text{C}}=0.25$	R1	0.394	0.507	0.599	0.686	0.776	0.872	0.978	0.993	0.993	0.461	0.606	0.732	0.855	0.985	0.993	0.993	0.993
	R2	0.224	0.291	0.361	0.437	0.520	0.610	0.719	0.858	0.993	0.263	0.358	0.448	0.547	0.660	0.782	0.934	0.993
	R3	0.206	0.271	0.339	0.417	0.502	0.589	0.689	0.822	0.993	0.242	0.336	0.426	0.522	0.634	0.758	0.902	0.993
	R4	0.156	0.219	0.275	0.343	0.429	0.531	0.655	0.794	0.978	0.181	0.267	0.348	0.438	0.545	0.676	0.845	0.993
$\lambda_{20^{\circ}\text{C}}=0.50$	R1	0.281	0.365	0.434	0.499	0.566	0.637	0.715	0.811	0.951	0.327	0.436	0.529	0.620	0.716	0.823	0.951	0.951
	R2	0.158	0.206	0.256	0.314	0.373	0.439	0.519	0.625	0.788	0.187	0.254	0.319	0.392	0.473	0.564	0.679	0.831
	R3	0.146	0.192	0.240	0.297	0.359	0.425	0.498	0.599	0.754	0.173	0.239	0.302	0.372	0.454	0.545	0.652	0.794
	R4	0.112	0.155	0.195	0.243	0.306	0.381	0.474	0.578	0.714	0.131	0.190	0.247	0.310	0.387	0.484	0.608	0.769
$\lambda_{20^{\circ}\text{C}}=0.75$	R1	0.209	0.277	0.333	0.388	0.443	0.502	0.566	0.643	0.754	0.249	0.333	0.407	0.480	0.558	0.645	0.746	0.876
	R2	0.117	0.152	0.189	0.233	0.282	0.335	0.404	0.491	0.623	0.138	0.187	0.237	0.291	0.356	0.431	0.521	0.643
	R3	0.108	0.141	0.178	0.222	0.270	0.322	0.383	0.468	0.594	0.128	0.176	0.224	0.278	0.342	0.413	0.500	0.616
	R4	0.086	0.115	0.143	0.179	0.228	0.287	0.364	0.450	0.562	0.100	0.142	0.183	0.230	0.289	0.366	0.465	0.595
$\lambda_{20^{\circ}\text{C}}=1.00$	R1	0.166	0.223	0.270	0.317	0.365	0.415	0.469	0.534	0.625	0.196	0.268	0.331	0.393	0.459	0.532	0.616	0.725
	R2	0.091	0.117	0.147	0.184	0.224	0.270	0.331	0.406	0.516	0.108	0.146	0.185	0.230	0.285	0.348	0.424	0.529
	R3	0.085	0.109	0.137	0.174	0.215	0.259	0.311	0.385	0.494	0.101	0.137	0.174	0.219	0.272	0.332	0.406	0.504
	R4	0.069	0.090	0.111	0.139	0.179	0.229	0.294	0.369	0.465	0.081	0.112	0.143	0.179	0.228	0.293	0.378	0.486
$\lambda_{20^{\circ}\text{C}}=1.50$	R1	0.098	0.132	0.162	0.191	0.220	0.250	0.282	0.320	0.395	0.116	0.160	0.198	0.235	0.275	0.320	0.395	0.395
	R2	0.053	0.068	0.086	0.108	0.133	0.161	0.199	0.244	0.311	0.064	0.086	0.109	0.136	0.169	0.207	0.255	0.318
	R3	0.050	0.064	0.080	0.102	0.128	0.155	0.186	0.232	0.297	0.060	0.081	0.102	0.129	0.161	0.198	0.242	0.303
	R4	0.042	0.053	0.065	0.081	0.106	0.136	0.177	0.223	0.280	0.049	0.067	0.084	0.105	0.134	0.174	0.226	0.292
$\lambda_{20^{\circ}\text{C}}=2.00$	R1	0.058	0.079	0.096	0.113	0.130	0.148	0.167	0.190	0.232	0.069	0.095	0.117	0.139	0.163	0.189	0.232	0.232
	R2	0.032	0.041	0.051	0.064	0.079	0.096	0.118	0.145	0.184	0.038	0.051	0.065	0.081	0.100	0.123	0.151	0.188
	R3	0.030	0.038	0.048	0.061	0.076	0.092	0.111	0.138	0.176	0.035	0.048	0.061	0.077	0.096	0.118	0.144	0.179
	R4	0.025	0.032	0.039	0.048	0.062	0.081	0.105	0.132	0.166	0.029	0.040	0.050	0.063	0.080	0.103	0.134	0.173

$$\theta_{\text{nom}} = 700^{\circ}\text{C}$$

$p_{f,fi} \rightarrow$	0.10	0.20	0.30	0.40	0.50	0.60	0.70	0.80	0.90	0.10	0.20	0.30	0.40	0.50	0.60	0.70	0.80	0.90	
$\beta_{f,fi} \rightarrow$	1.28	0.84	0.52	0.40	0.00	-0.25	-0.52	-0.84	-1.28	1.28	0.84	0.52	0.40	0.00	-0.25	-0.52	-0.84	-1.28	
$\delta_{of} \rightarrow$	1.15	1.02	0.94	0.88	0.82	0.77	0.72	0.67	0.60	1.15	1.02	0.94	0.88	0.82	0.77	0.72	0.67	0.60	
	$\alpha=0.00$									$\alpha=0.25$									
$\lambda_{20^{\circ}\text{C}}=0.00$	R1	0.202	0.239	0.276	0.316	0.362	0.414	0.479	0.565	0.732	0.219	0.259	0.300	0.344	0.394	0.451	0.521	0.616	0.799
	R2	0.147	0.185	0.214	0.242	0.274	0.318	0.380	0.475	0.637	0.160	0.201	0.232	0.263	0.298	0.347	0.414	0.516	0.694
	R3	0.113	0.162	0.196	0.225	0.262	0.306	0.362	0.442	0.568	0.123	0.176	0.213	0.245	0.285	0.333	0.394	0.483	0.620
	R4	0.058	0.099	0.144	0.183	0.218	0.262	0.333	0.424	0.526	0.063	0.107	0.156	0.198	0.238	0.285	0.362	0.461	0.574
$\lambda_{20^{\circ}\text{C}}=0.25$	R1	0.177	0.210	0.242	0.278	0.318	0.364	0.419	0.496	0.643	0.192	0.229	0.264	0.302	0.346	0.396	0.457	0.541	0.700
	R2	0.129	0.163	0.188	0.212	0.240	0.280	0.334	0.421	0.559	0.139	0.177	0.204	0.231	0.261	0.305	0.362	0.458	0.608
	R3	0.099	0.142	0.172	0.198	0.230	0.268	0.318	0.390	0.499	0.107	0.154	0.187	0.215	0.250	0.292	0.346	0.425	0.545
	R4	0.052	0.088	0.127	0.162	0.193	0.233	0.295	0.373	0.462	0.056	0.095	0.138	0.175	0.210	0.254	0.321	0.407	0.504
$\lambda_{20^{\circ}\text{C}}=0.50$	R1	0.125	0.148	0.171	0.197	0.226	0.259	0.300	0.356	0.465	0.136	0.161	0.186	0.214	0.245	0.282	0.326	0.388	0.508
	R2	0.093	0.116	0.133	0.150	0.171	0.198	0.237	0.300	0.405	0.100	0.125	0.144	0.163	0.186	0.216	0.257	0.327	0.442
	R3	0.073	0.102	0.122	0.140	0.162	0.189	0.225	0.278	0.359	0.079	0.111	0.133	0.152	0.176	0.207	0.245	0.303	0.392
	R4	0.041	0.066	0.092	0.115	0.137	0.165	0.209	0.263	0.330	0.045	0.072	0.100	0.125	0.149	0.179	0.228	0.286	0.360
$\lambda_{20^{\circ}\text{C}}=0.75$	R1	0.092	0.109	0.125	0.144	0.167	0.193	0.224	0.270	0.362	0.100	0.118	0.136	0.157	0.181	0.210	0.244	0.293	0.394
	R2	0.071	0.086	0.098	0.110	0.125	0.145	0.175	0.226	0.307	0.077	0.093	0.106	0.120	0.136	0.158	0.191	0.246	0.336
	R3	0.059	0.077	0.091	0.103	0.119	0.139	0.166	0.207	0.271	0.064	0.084	0.098	0.112	0.129	0.152	0.181	0.225	0.296
	R4	0.036	0.054	0.071	0.086	0.101	0.121	0.154	0.196	0.248	0.040	0.059	0.077	0.093	0.110	0.132	0.167	0.213	0.270
$\lambda_{20^{\circ}\text{C}}=1.00$	R1	0.071	0.084	0.097	0.112	0.130	0.151	0.179	0.216	0.296	0.077	0.091	0.105	0.122	0.142	0.165	0.195	0.236	0.324
	R2	0.057	0.067	0.076	0.085	0.096	0.112	0.137	0.180	0.248	0.061	0.073	0.083	0.093	0.105	0.122	0.149	0.196	0.271
	R3	0.049	0.062	0.071	0.080	0.092	0.108	0.129	0.163	0.217	0.053	0.067	0.077	0.087	0.100	0.117	0.141	0.178	0.236
	R4	0.033	0.047	0.058	0.068	0.079	0.094	0.119	0.154	0.197	0.036	0.050	0.063	0.074	0.086	0.102	0.130	0.168	0.215
$\lambda_{20^{\circ}\text{C}}=1.50$	R1	0.042	0.049	0.056	0.065	0.076	0.089	0.105	0.129	0.179	0.045	0.053	0.061	0.071	0.083	0.097	0.115	0.141	0.194
	R2	0.034	0.040	0.045	0.050	0.056	0.065	0.081	0.106	0.149	0.037	0.043	0.049	0.054	0.061	0.071	0.088	0.116	0.162
	R3	0.030	0.037	0.042	0.047	0.054	0.063	0.076	0.096	0.129	0.033	0.040	0.046	0.051	0.059	0.068	0.082	0.105	0.141
	R4	0.022	0.029	0.035	0.041	0.047	0.055	0.070	0.091	0.117	0.023	0.032	0.038	0.044	0.051	0.060	0.076	0.099	0.127
$\lambda_{20^{\circ}\text{C}}=2.00$	R1	0.025	0.029	0.033	0.039	0.045	0.053	0.063	0.077	0.106	0.027	0.031	0.036	0.042	0.049	0.058	0.068	0.083	0.115
	R2	0.020	0.024	0.027	0.030	0.034	0.039	0.048	0.063	0.088	0.022	0.026	0.029	0.032	0.036	0.042	0.052	0.069	0.096
	R3	0.018	0.022	0.025	0.028	0.032	0.037	0.045	0.057	0.077	0.020	0.024	0.027	0.031	0.035	0.041	0.049	0.062	0.084
	R4	0.013	0.018	0.021	0.024	0.028	0.033	0.041	0.054	0.069	0.014	0.019	0.023	0.026	0.030	0.036	0.045	0.059	0.076
	$\alpha=0.50$									$\alpha=0.75$									
$\lambda_{20^{\circ}\text{C}}=0.00$	R1	0.243	0.293	0.341	0.393	0.450	0.516	0.598	0.711	0.923	0.278	0.356	0.427	0.500	0.580	0.674	0.793	0.958	1.000
	R2	0.176	0.225	0.263	0.300	0.343	0.398	0.474	0.593	0.803	0.202	0.267	0.324	0.380	0.447	0.525	0.621	0.784	1.000
	R3	0.138	0.197	0.240	0.279	0.328	0.383	0.453	0.556	0.719	0.163	0.235	0.295	0.355	0.425	0.503	0.597	0.739	0.985
	R4	0.071	0.121	0.175	0.224	0.272	0.329	0.415	0.533	0.666	0.088	0.149	0.212	0.277	0.348	0.432	0.547	0.715	0.917
$\lambda_{20^{\circ}\text{C}}=0.25$	R1	0.213	0.257	0.299	0.345	0.395	0.454	0.526	0.626	0.810	0.245	0.312	0.375	0.439	0.509	0.592	0.695	0.837	0.993
	R2	0.155	0.197	0.231	0.263	0.300	0.350	0.415	0.524	0.708	0.177	0.235	0.285	0.335	0.389	0.460	0.544	0.690	0.965
	R3	0.120	0.172	0.211	0.246	0.288	0.336	0.397	0.490	0.632	0.142	0.205	0.259	0.312	0.373	0.441	0.523	0.652	0.863
	R4	0.064	0.108	0.155	0.199	0.241	0.293	0.368	0.469	0.586	0.079	0.132	0.188	0.245	0.309	0.385	0.485	0.620	0.805
$\lambda_{20^{\circ}\text{C}}=0.50$	R1	0.151	0.182	0.212	0.244	0.280	0.323	0.375	0.448	0.586	0.172	0.222	0.266	0.312	0.361	0.421	0.497	0.603	0.793
	R2	0.111	0.140	0.163	0.185	0.214	0.248	0.295	0.375	0.508	0.127	0.166	0.202	0.236	0.278	0.325	0.387	0.494	0.690
	R3	0.089	0.124	0.150	0.174	0.203	0.237	0.281	0.348	0.453	0.104	0.147	0.184	0.221	0.264	0.312	0.372	0.461	0.618
	R4	0.050	0.081	0.112	0.141	0.170	0.206	0.261	0.330	0.419	0.061	0.099	0.137	0.176	0.219	0.272	0.344	0.443	0.575
$\lambda_{20^{\circ}\text{C}}=0.75$	R1	0.111	0.133	0.155	0.179	0.207	0.240	0.281	0.339	0.455	0.127	0.163	0.195	0.229	0.268	0.313	0.372	0.454	0.610
	R2	0.084	0.104	0.120	0.136	0.157	0.181	0.218	0.283	0.388	0.097	0.125	0.150	0.175	0.204	0.239	0.286	0.371	0.524
	R3	0.071	0.094	0.111	0.128	0.149	0.174	0.207	0.259	0.342	0.083	0.113	0.138	0.164	0.195	0.229	0.274	0.343	0.465
	R4	0.044	0.066	0.087	0.106	0.126	0.151	0.192	0.246	0.313	0.053	0.081	0.107	0.133	0.163	0.201	0.253	0.330	0.430
$\lambda_{20^{\circ}\text{C}}=1.00$	R1	0.086	0.103	0.120	0.139	0.162	0.189	0.223	0.272	0.374	0.099	0.126	0.152	0.178	0.209	0.247	0.295	0.364	0.499
	R2	0.068	0.082	0.094	0.106	0.121	0.141	0.171	0.225	0.314	0.077	0.098	0.117	0.137	0.160	0.187	0.224	0.295	0.425
	R3	0.059	0.075	0.087	0.100	0.116	0.135	0.162	0.204	0.275	0.068	0.090	0.109	0.129	0.152	0.179	0.214	0.271	0.372
	R4	0.040	0.057	0.071	0.084	0.099	0.118	0.150	0.193	0.249	0.047	0.068	0.087	0.107	0.129	0.158	0.198	0.260	0.341
$\lambda_{20^{\circ}\text{C}}=1.50$	R1	0.050	0.060	0.070	0.081	0.095	0.111	0.132	0.162	0.225	0.058	0.074	0.089	0.105	0.123	0.145	0.174	0.216	0.300
	R2	0.041	0.049	0.055	0.062	0.071	0.082	0.100	0.133	0.188	0.046	0.058	0.069	0.080	0.094	0.109	0.131	0.174	0.253
	R3	0.037	0.045	0.052	0.059	0.068	0.079	0.095	0.121	0.163	0.042	0.054	0.065	0.077	0.090	0.105	0.125	0.160	0.221
	R4	0.026	0.036	0.043	0.051	0.059	0.069												

$$\theta_{\text{nom}} = 800^{\circ}\text{C}$$

$p_{f,fi} \rightarrow$	0.10	0.20	0.30	0.40	0.50	0.60	0.70	0.80	0.90	0.10	0.20	0.30	0.40	0.50	0.60	0.70	0.80	0.90	
$\beta_{f,fi} \rightarrow$	1.28	0.84	0.52	0.40	0.00	-0.25	-0.52	-0.84	-1.28	1.28	0.84	0.52	0.40	0.00	-0.25	-0.52	-0.84	-1.28	
$\delta_{of} \rightarrow$	1.15	1.02	0.94	0.88	0.82	0.77	0.72	0.67	0.60	1.15	1.02	0.94	0.88	0.82	0.77	0.72	0.67	0.60	
	$\alpha=0.00$									$\alpha=0.25$									
$\lambda_{20^{\circ}\text{C}}=0.00$	R1	0.070	0.090	0.108	0.127	0.149	0.174	0.200	0.233	0.294	0.076	0.097	0.117	0.138	0.162	0.188	0.218	0.254	0.321
	R2	0.057	0.075	0.094	0.115	0.141	0.168	0.195	0.230	0.285	0.062	0.081	0.102	0.125	0.153	0.182	0.212	0.251	0.311
	R3	0.046	0.061	0.078	0.099	0.124	0.155	0.188	0.223	0.276	0.050	0.067	0.085	0.108	0.135	0.168	0.205	0.243	0.301
	R4	0.027	0.043	0.058	0.075	0.100	0.132	0.172	0.214	0.270	0.030	0.047	0.063	0.082	0.108	0.143	0.187	0.233	0.295
$\lambda_{20^{\circ}\text{C}}=0.25$	R1	0.061	0.078	0.094	0.111	0.130	0.152	0.175	0.204	0.262	0.066	0.084	0.102	0.121	0.142	0.165	0.191	0.222	0.286
	R2	0.050	0.065	0.082	0.100	0.123	0.146	0.171	0.202	0.251	0.054	0.070	0.089	0.109	0.134	0.159	0.186	0.221	0.277
	R3	0.040	0.053	0.068	0.086	0.108	0.136	0.166	0.197	0.243	0.044	0.058	0.074	0.094	0.118	0.148	0.181	0.215	0.265
	R4	0.026	0.039	0.052	0.068	0.090	0.119	0.153	0.189	0.237	0.028	0.043	0.057	0.074	0.098	0.130	0.166	0.206	0.259
$\lambda_{20^{\circ}\text{C}}=0.50$	R1	0.048	0.059	0.070	0.082	0.095	0.109	0.125	0.145	0.185	0.052	0.064	0.076	0.089	0.103	0.118	0.136	0.159	0.202
	R2	0.040	0.051	0.062	0.075	0.090	0.106	0.122	0.143	0.178	0.043	0.055	0.067	0.081	0.098	0.115	0.133	0.156	0.194
	R3	0.032	0.042	0.053	0.065	0.080	0.098	0.119	0.140	0.172	0.035	0.046	0.058	0.071	0.087	0.107	0.129	0.152	0.188
	R4	0.021	0.031	0.041	0.053	0.068	0.087	0.109	0.135	0.168	0.022	0.034	0.045	0.058	0.074	0.095	0.119	0.147	0.183
$\lambda_{20^{\circ}\text{C}}=0.75$	R1	0.041	0.050	0.057	0.065	0.073	0.083	0.093	0.107	0.135	0.044	0.054	0.062	0.071	0.080	0.090	0.102	0.117	0.148
	R2	0.035	0.044	0.052	0.061	0.070	0.080	0.091	0.106	0.131	0.038	0.048	0.057	0.066	0.076	0.087	0.099	0.116	0.144
	R3	0.029	0.038	0.046	0.054	0.064	0.076	0.089	0.104	0.126	0.031	0.041	0.050	0.059	0.070	0.082	0.097	0.113	0.138
	R4	0.019	0.028	0.037	0.046	0.056	0.069	0.083	0.100	0.123	0.020	0.031	0.040	0.050	0.061	0.075	0.090	0.109	0.134
$\lambda_{20^{\circ}\text{C}}=1.00$	R1	0.036	0.043	0.049	0.054	0.060	0.066	0.074	0.084	0.105	0.039	0.047	0.053	0.059	0.065	0.072	0.081	0.091	0.115
	R2	0.032	0.039	0.045	0.051	0.058	0.065	0.072	0.083	0.101	0.034	0.042	0.049	0.056	0.063	0.071	0.079	0.091	0.111
	R3	0.026	0.034	0.040	0.047	0.054	0.062	0.071	0.082	0.098	0.029	0.037	0.044	0.051	0.059	0.067	0.077	0.089	0.107
	R4	0.017	0.026	0.033	0.041	0.048	0.057	0.067	0.079	0.096	0.018	0.028	0.036	0.044	0.053	0.062	0.073	0.086	0.105
$\lambda_{20^{\circ}\text{C}}=1.50$	R1	0.024	0.028	0.031	0.034	0.037	0.040	0.044	0.050	0.062	0.026	0.030	0.033	0.037	0.040	0.044	0.048	0.054	0.067
	R2	0.021	0.025	0.029	0.032	0.036	0.040	0.044	0.049	0.060	0.023	0.027	0.031	0.035	0.039	0.043	0.047	0.054	0.065
	R3	0.017	0.022	0.026	0.030	0.034	0.038	0.043	0.048	0.058	0.019	0.024	0.028	0.033	0.037	0.041	0.047	0.053	0.063
	R4	0.011	0.017	0.022	0.026	0.031	0.035	0.041	0.047	0.056	0.012	0.019	0.024	0.029	0.033	0.039	0.044	0.051	0.062
$\lambda_{20^{\circ}\text{C}}=2.00$	R1	0.014	0.017	0.018	0.020	0.022	0.024	0.026	0.030	0.037	0.015	0.018	0.020	0.022	0.024	0.026	0.029	0.032	0.040
	R2	0.013	0.015	0.017	0.019	0.022	0.024	0.026	0.029	0.035	0.014	0.016	0.019	0.021	0.023	0.026	0.028	0.032	0.039
	R3	0.010	0.013	0.016	0.018	0.020	0.023	0.025	0.029	0.034	0.011	0.014	0.017	0.020	0.022	0.025	0.028	0.031	0.038
	R4	0.007	0.010	0.013	0.016	0.018	0.021	0.024	0.028	0.034	0.007	0.011	0.014	0.017	0.020	0.023	0.026	0.031	0.037
	$\alpha=0.50$									$\alpha=0.75$									
$\lambda_{20^{\circ}\text{C}}=0.00$	R1	0.085	0.109	0.132	0.157	0.184	0.214	0.249	0.293	0.374	0.100	0.133	0.165	0.197	0.232	0.273	0.325	0.394	0.519
	R2	0.070	0.092	0.116	0.143	0.174	0.207	0.242	0.290	0.362	0.084	0.114	0.145	0.179	0.219	0.263	0.315	0.391	0.499
	R3	0.056	0.076	0.097	0.122	0.154	0.191	0.234	0.281	0.352	0.067	0.094	0.122	0.154	0.194	0.242	0.302	0.376	0.491
	R4	0.033	0.053	0.071	0.094	0.124	0.163	0.212	0.269	0.344	0.039	0.065	0.090	0.119	0.157	0.206	0.270	0.354	0.480
$\lambda_{20^{\circ}\text{C}}=0.25$	R1	0.074	0.095	0.116	0.137	0.161	0.188	0.219	0.258	0.332	0.088	0.116	0.144	0.172	0.203	0.239	0.285	0.347	0.458
	R2	0.061	0.080	0.101	0.125	0.152	0.181	0.213	0.255	0.319	0.073	0.100	0.127	0.157	0.192	0.231	0.277	0.341	0.444
	R3	0.049	0.066	0.084	0.107	0.134	0.168	0.206	0.249	0.310	0.058	0.082	0.106	0.135	0.169	0.212	0.266	0.333	0.433
	R4	0.032	0.048	0.064	0.085	0.112	0.148	0.189	0.237	0.303	0.038	0.060	0.082	0.108	0.142	0.186	0.241	0.315	0.423
$\lambda_{20^{\circ}\text{C}}=0.50$	R1	0.058	0.072	0.087	0.101	0.117	0.135	0.156	0.183	0.236	0.067	0.088	0.107	0.127	0.148	0.173	0.204	0.246	0.326
	R2	0.049	0.062	0.077	0.093	0.111	0.130	0.152	0.180	0.227	0.058	0.077	0.096	0.117	0.140	0.167	0.198	0.243	0.317
	R3	0.039	0.052	0.066	0.081	0.099	0.121	0.147	0.176	0.220	0.047	0.065	0.082	0.102	0.126	0.154	0.191	0.237	0.307
	R4	0.025	0.039	0.051	0.066	0.084	0.107	0.135	0.169	0.214	0.030	0.048	0.064	0.083	0.107	0.137	0.174	0.224	0.299
$\lambda_{20^{\circ}\text{C}}=0.75$	R1	0.050	0.061	0.071	0.080	0.091	0.102	0.117	0.135	0.173	0.057	0.073	0.087	0.101	0.116	0.133	0.154	0.184	0.240
	R2	0.043	0.054	0.064	0.075	0.087	0.100	0.114	0.134	0.167	0.050	0.066	0.080	0.095	0.111	0.129	0.150	0.181	0.231
	R3	0.035	0.046	0.056	0.067	0.080	0.094	0.111	0.131	0.161	0.041	0.056	0.070	0.085	0.101	0.120	0.145	0.177	0.226
	R4	0.023	0.035	0.045	0.057	0.070	0.085	0.103	0.126	0.158	0.027	0.042	0.056	0.072	0.089	0.109	0.134	0.168	0.222
$\lambda_{20^{\circ}\text{C}}=1.00$	R1	0.044	0.053	0.060	0.067	0.075	0.083	0.093	0.106	0.135	0.050	0.062	0.074	0.084	0.096	0.108	0.124	0.145	0.188
	R2	0.038	0.048	0.056	0.064	0.072	0.081	0.091	0.105	0.130	0.044	0.057	0.068	0.080	0.092	0.106	0.121	0.144	0.181
	R3	0.032	0.041	0.050	0.058	0.067	0.077	0.089	0.103	0.126	0.037	0.050	0.061	0.073	0.085	0.100	0.118	0.141	0.176
	R4	0.021	0.032	0.041	0.050	0.060	0.071	0.083	0.100	0.123	0.025	0.038	0.050	0.063	0.076	0.091	0.110	0.134	0.173
$\lambda_{20^{\circ}\text{C}}=1.50$	R1	0.028	0.033	0.038	0.042	0.046	0.050	0.056	0.063	0.079	0.032	0.040	0.046	0.053	0.059	0.066	0.075	0.087	0.110
	R2	0.025	0.031	0.035	0.040	0.045	0.049	0.055	0.063	0.076	0.029	0.037	0.043	0.050	0.057	0.065	0.074	0.087	0.107
	R3	0.021	0.027	0.032	0.037	0.042	0.												

$\theta_{\text{nom}} = 900^{\circ}\text{C}$

$p_{f,fi} \rightarrow$	0.10	0.20	0.30	0.40	0.50	0.60	0.70	0.80	0.90	0.10	0.20	0.30	0.40	0.50	0.60	0.70	0.80	0.90	
$\beta_{f,fi} \rightarrow$	1.28	0.84	0.52	0.40	0.00	-0.25	-0.52	-0.84	-1.28	1.28	0.84	0.52	0.40	0.00	-0.25	-0.52	-0.84	-1.28	
$\delta_{of} \rightarrow$	1.15	1.02	0.94	0.88	0.82	0.77	0.72	0.67	0.60	1.15	1.02	0.94	0.88	0.82	0.77	0.72	0.67	0.60	
	$\alpha=0.00$									$\alpha=0.25$									
$\lambda_{20^{\circ}\text{C}}=0.00$	R1	0.052	0.061	0.070	0.079	0.089	0.101	0.119	0.148	0.212	0.056	0.067	0.076	0.086	0.097	0.110	0.130	0.161	0.231
	R2	0.039	0.049	0.058	0.068	0.081	0.098	0.110	0.145	0.203	0.042	0.053	0.063	0.074	0.088	0.107	0.122	0.158	0.221
	R3	0.025	0.036	0.045	0.055	0.066	0.082	0.106	0.142	0.186	0.027	0.039	0.049	0.060	0.072	0.089	0.115	0.155	0.203
	R4	0.004	0.019	0.031	0.043	0.056	0.072	0.101	0.125	0.152	0.004	0.021	0.034	0.047	0.061	0.079	0.109	0.137	0.166
$\lambda_{20^{\circ}\text{C}}=0.25$	R1	0.045	0.053	0.061	0.069	0.077	0.088	0.104	0.139	0.192	0.048	0.058	0.066	0.075	0.084	0.096	0.114	0.150	0.209
	R2	0.034	0.042	0.050	0.059	0.071	0.085	0.098	0.129	0.180	0.037	0.046	0.055	0.064	0.077	0.092	0.107	0.140	0.196
	R3	0.022	0.032	0.040	0.048	0.060	0.074	0.096	0.125	0.163	0.024	0.034	0.043	0.052	0.065	0.081	0.104	0.137	0.177
	R4	0.014	0.025	0.036	0.046	0.057	0.071	0.093	0.110	0.133	0.016	0.027	0.039	0.050	0.062	0.078	0.101	0.119	0.145
$\lambda_{20^{\circ}\text{C}}=0.50$	R1	0.036	0.042	0.048	0.053	0.059	0.067	0.078	0.099	0.136	0.039	0.046	0.052	0.058	0.065	0.073	0.085	0.108	0.149
	R2	0.027	0.034	0.040	0.047	0.055	0.065	0.074	0.094	0.128	0.030	0.037	0.044	0.051	0.060	0.070	0.080	0.103	0.139
	R3	0.018	0.025	0.032	0.039	0.048	0.057	0.072	0.092	0.117	0.019	0.028	0.035	0.042	0.051	0.062	0.078	0.100	0.128
	R4	0.012	0.020	0.029	0.037	0.045	0.055	0.069	0.082	0.098	0.013	0.022	0.031	0.040	0.049	0.060	0.075	0.089	0.107
$\lambda_{20^{\circ}\text{C}}=0.75$	R1	0.032	0.038	0.042	0.046	0.051	0.056	0.063	0.077	0.101	0.035	0.041	0.046	0.050	0.055	0.061	0.069	0.083	0.110
	R2	0.024	0.031	0.036	0.041	0.048	0.054	0.061	0.073	0.096	0.027	0.033	0.039	0.045	0.052	0.059	0.066	0.080	0.104
	R3	0.016	0.023	0.029	0.035	0.042	0.049	0.060	0.073	0.089	0.017	0.025	0.031	0.038	0.045	0.054	0.065	0.079	0.097
	R4	0.010	0.018	0.026	0.033	0.040	0.048	0.058	0.067	0.078	0.011	0.020	0.028	0.036	0.043	0.052	0.063	0.073	0.085
$\lambda_{20^{\circ}\text{C}}=1.00$	R1	0.029	0.034	0.038	0.041	0.045	0.049	0.054	0.063	0.080	0.031	0.037	0.041	0.044	0.048	0.053	0.059	0.069	0.088
	R2	0.022	0.028	0.032	0.037	0.042	0.047	0.053	0.061	0.076	0.024	0.030	0.035	0.040	0.046	0.052	0.057	0.067	0.083
	R3	0.015	0.021	0.026	0.032	0.038	0.044	0.051	0.061	0.073	0.016	0.023	0.028	0.034	0.041	0.047	0.055	0.066	0.079
	R4	0.009	0.017	0.023	0.030	0.036	0.042	0.050	0.058	0.066	0.010	0.018	0.025	0.033	0.039	0.046	0.054	0.063	0.072
$\lambda_{20^{\circ}\text{C}}=1.50$	R1	0.019	0.022	0.025	0.027	0.029	0.031	0.034	0.039	0.048	0.021	0.024	0.027	0.029	0.031	0.034	0.038	0.042	0.053
	R2	0.015	0.018	0.021	0.024	0.027	0.030	0.033	0.038	0.046	0.016	0.020	0.023	0.026	0.030	0.033	0.037	0.042	0.050
	R3	0.010	0.014	0.017	0.021	0.024	0.028	0.033	0.038	0.044	0.011	0.015	0.019	0.023	0.027	0.031	0.035	0.041	0.048
	R4	0.006	0.011	0.015	0.020	0.023	0.027	0.032	0.036	0.041	0.007	0.012	0.017	0.021	0.026	0.030	0.035	0.040	0.045
$\lambda_{20^{\circ}\text{C}}=2.00$	R1	0.011	0.013	0.015	0.016	0.017	0.019	0.021	0.023	0.029	0.012	0.014	0.016	0.017	0.019	0.020	0.022	0.025	0.031
	R2	0.009	0.011	0.013	0.015	0.016	0.018	0.020	0.023	0.027	0.010	0.012	0.014	0.016	0.018	0.020	0.022	0.025	0.030
	R3	0.006	0.008	0.010	0.012	0.015	0.017	0.020	0.022	0.027	0.006	0.009	0.011	0.014	0.016	0.018	0.021	0.024	0.029
	R4	0.004	0.007	0.009	0.012	0.014	0.016	0.019	0.022	0.025	0.004	0.007	0.010	0.013	0.015	0.018	0.021	0.024	0.027
	$\alpha=0.50$									$\alpha=0.75$									
$\lambda_{20^{\circ}\text{C}}=0.00$	R1	0.062	0.075	0.087	0.098	0.110	0.126	0.149	0.184	0.265	0.071	0.090	0.107	0.124	0.142	0.165	0.198	0.243	0.355
	R2	0.047	0.060	0.072	0.085	0.101	0.123	0.139	0.181	0.255	0.055	0.073	0.091	0.109	0.132	0.160	0.185	0.239	0.340
	R3	0.030	0.044	0.056	0.068	0.082	0.102	0.132	0.178	0.234	0.036	0.053	0.069	0.086	0.106	0.133	0.172	0.230	0.318
	R4	0.005	0.023	0.039	0.053	0.069	0.091	0.125	0.159	0.194	0.006	0.028	0.047	0.066	0.089	0.118	0.162	0.217	0.270
$\lambda_{20^{\circ}\text{C}}=0.25$	R1	0.054	0.065	0.075	0.085	0.096	0.110	0.131	0.171	0.243	0.062	0.079	0.093	0.108	0.124	0.144	0.174	0.220	0.333
	R2	0.041	0.052	0.062	0.073	0.088	0.107	0.123	0.161	0.226	0.048	0.063	0.078	0.095	0.114	0.140	0.163	0.213	0.302
	R3	0.027	0.039	0.049	0.060	0.075	0.093	0.120	0.157	0.205	0.032	0.047	0.061	0.076	0.098	0.121	0.156	0.206	0.279
	R4	0.018	0.031	0.044	0.057	0.071	0.089	0.116	0.139	0.169	0.021	0.038	0.055	0.073	0.092	0.117	0.152	0.190	0.236
$\lambda_{20^{\circ}\text{C}}=0.50$	R1	0.043	0.052	0.059	0.066	0.074	0.084	0.098	0.123	0.172	0.049	0.062	0.073	0.084	0.095	0.110	0.130	0.160	0.234
	R2	0.033	0.042	0.050	0.058	0.068	0.081	0.093	0.118	0.161	0.038	0.051	0.062	0.075	0.089	0.106	0.122	0.156	0.216
	R3	0.022	0.031	0.039	0.048	0.059	0.071	0.090	0.115	0.148	0.026	0.038	0.049	0.061	0.077	0.093	0.118	0.150	0.202
	R4	0.014	0.025	0.035	0.045	0.056	0.069	0.087	0.104	0.125	0.017	0.030	0.043	0.058	0.072	0.089	0.113	0.142	0.174
$\lambda_{20^{\circ}\text{C}}=0.75$	R1	0.038	0.046	0.052	0.057	0.063	0.070	0.080	0.096	0.128	0.043	0.054	0.063	0.073	0.082	0.092	0.108	0.127	0.177
	R2	0.030	0.037	0.044	0.051	0.060	0.068	0.076	0.093	0.121	0.034	0.045	0.055	0.065	0.077	0.091	0.103	0.126	0.164
	R3	0.020	0.028	0.035	0.043	0.052	0.062	0.074	0.091	0.113	0.023	0.034	0.044	0.054	0.067	0.081	0.098	0.121	0.157
	R4	0.013	0.022	0.031	0.041	0.049	0.060	0.072	0.085	0.100	0.015	0.027	0.039	0.051	0.063	0.078	0.095	0.118	0.141
$\lambda_{20^{\circ}\text{C}}=1.00$	R1	0.035	0.041	0.046	0.051	0.055	0.061	0.068	0.079	0.102	0.039	0.048	0.056	0.064	0.071	0.081	0.092	0.107	0.142
	R2	0.027	0.034	0.040	0.046	0.053	0.060	0.066	0.078	0.097	0.031	0.041	0.049	0.058	0.067	0.078	0.089	0.105	0.134
	R3	0.018	0.026	0.032	0.039	0.047	0.054	0.											

A21 Factor χ_{Rel} for S460 weak axis, imposed (Q) variable load type

		$\theta_{\text{nom}} = 300^{\circ}\text{C}$																	
$p_{f,fi} \rightarrow$		0.10	0.20	0.30	0.40	0.50	0.60	0.70	0.80	0.90	0.10	0.20	0.30	0.40	0.50	0.60	0.70	0.80	0.90
$\beta_{f,fi} \rightarrow$		1.28	0.84	0.52	0.40	0.00	-0.25	-0.52	-0.84	-1.28	1.28	0.84	0.52	0.40	0.00	-0.25	-0.52	-0.84	-1.28
$\delta_{of} \rightarrow$		1.15	1.02	0.94	0.88	0.82	0.77	0.72	0.67	0.60	1.15	1.02	0.94	0.88	0.82	0.77	0.72	0.67	0.60
		$\alpha=0.00$									$\alpha=0.25$								
$\lambda_{20^{\circ}\text{C}}=0.00$	R1	0.829	0.919	0.987	1.000	1.000	1.000	1.000	1.000	1.000	0.895	0.996	1.000	1.000	1.000	1.000	1.000	1.000	1.000
	R2	0.806	0.903	0.974	1.000	1.000	1.000	1.000	1.000	1.000	0.871	0.977	1.000	1.000	1.000	1.000	1.000	1.000	1.000
	R3	0.794	0.895	0.968	1.000	1.000	1.000	1.000	1.000	1.000	0.858	0.969	1.000	1.000	1.000	1.000	1.000	1.000	1.000
	R4	0.753	0.865	0.942	1.000	1.000	1.000	1.000	1.000	1.000	0.814	0.936	1.000	1.000	1.000	1.000	1.000	1.000	1.000
$\lambda_{20^{\circ}\text{C}}=0.25$	R1	0.692	0.768	0.826	0.878	0.928	0.982	0.993	0.993	0.993	0.750	0.834	0.898	0.956	0.993	0.993	0.993	0.993	0.993
	R2	0.672	0.755	0.814	0.867	0.919	0.973	0.993	0.993	0.993	0.726	0.818	0.885	0.944	0.993	0.993	0.993	0.993	0.993
	R3	0.663	0.748	0.809	0.863	0.915	0.967	0.993	0.993	0.993	0.718	0.811	0.879	0.939	0.993	0.993	0.993	0.993	0.993
	R4	0.628	0.723	0.789	0.845	0.899	0.954	0.993	0.993	0.993	0.680	0.785	0.857	0.920	0.979	0.993	0.993	0.993	0.993
$\lambda_{20^{\circ}\text{C}}=0.50$	R1	0.560	0.625	0.675	0.722	0.768	0.815	0.869	0.951	0.951	0.605	0.677	0.732	0.784	0.836	0.951	0.951	0.951	0.951
	R2	0.543	0.613	0.665	0.711	0.756	0.803	0.857	0.951	0.951	0.587	0.663	0.722	0.772	0.823	0.875	0.951	0.951	0.951
	R3	0.535	0.606	0.659	0.703	0.746	0.792	0.845	0.951	0.951	0.577	0.656	0.714	0.763	0.811	0.863	0.951	0.951	0.951
	R4	0.501	0.583	0.640	0.689	0.735	0.783	0.836	0.951	0.951	0.541	0.631	0.694	0.747	0.798	0.852	0.951	0.951	0.951
$\lambda_{20^{\circ}\text{C}}=0.75$	R1	0.459	0.519	0.569	0.615	0.660	0.706	0.760	0.876	0.876	0.495	0.563	0.618	0.668	0.718	0.876	0.876	0.876	0.876
	R2	0.441	0.506	0.556	0.602	0.644	0.690	0.743	0.876	0.876	0.478	0.548	0.604	0.653	0.701	0.752	0.876	0.876	0.876
	R3	0.434	0.498	0.547	0.588	0.629	0.674	0.728	0.876	0.876	0.469	0.540	0.594	0.640	0.684	0.734	0.876	0.876	0.876
	R4	0.401	0.474	0.527	0.574	0.620	0.666	0.716	0.876	0.876	0.434	0.513	0.572	0.623	0.674	0.725	0.876	0.876	0.876
$\lambda_{20^{\circ}\text{C}}=1.00$	R1	0.369	0.421	0.463	0.504	0.545	0.586	0.725	0.725	0.725	0.399	0.456	0.503	0.548	0.593	0.725	0.725	0.725	0.725
	R2	0.355	0.409	0.452	0.491	0.530	0.571	0.725	0.725	0.725	0.384	0.443	0.491	0.534	0.575	0.725	0.725	0.725	0.725
	R3	0.348	0.402	0.444	0.479	0.514	0.555	0.603	0.725	0.725	0.376	0.436	0.482	0.521	0.560	0.604	0.725	0.725	0.725
	R4	0.321	0.382	0.427	0.466	0.506	0.547	0.592	0.725	0.725	0.348	0.414	0.463	0.507	0.550	0.596	0.725	0.725	0.725
$\lambda_{20^{\circ}\text{C}}=1.50$	R1	0.209	0.236	0.258	0.279	0.300	0.321	0.344	0.395	0.395	0.225	0.256	0.281	0.303	0.326	0.349	0.395	0.395	0.395
	R2	0.202	0.231	0.253	0.273	0.293	0.314	0.337	0.395	0.395	0.218	0.250	0.275	0.297	0.318	0.341	0.395	0.395	0.395
	R3	0.198	0.227	0.250	0.268	0.287	0.307	0.331	0.395	0.395	0.214	0.246	0.271	0.291	0.312	0.333	0.395	0.395	0.395
	R4	0.184	0.217	0.241	0.262	0.282	0.303	0.326	0.395	0.395	0.199	0.235	0.261	0.284	0.307	0.330	0.395	0.395	0.395
$\lambda_{20^{\circ}\text{C}}=2.00$	R1	0.124	0.139	0.152	0.164	0.175	0.187	0.201	0.232	0.232	0.134	0.151	0.165	0.178	0.191	0.204	0.232	0.232	0.232
	R2	0.119	0.136	0.149	0.161	0.172	0.184	0.197	0.214	0.232	0.129	0.148	0.162	0.175	0.187	0.200	0.215	0.232	0.232
	R3	0.117	0.134	0.147	0.158	0.169	0.180	0.193	0.210	0.232	0.127	0.146	0.160	0.172	0.183	0.196	0.211	0.232	0.232
	R4	0.109	0.129	0.143	0.154	0.166	0.178	0.191	0.207	0.232	0.118	0.139	0.155	0.168	0.181	0.194	0.209	0.232	0.232
		$\alpha=0.50$									$\alpha=0.75$								
$\lambda_{20^{\circ}\text{C}}=0.00$	R1	0.971	1.000	1.000	1.000	1.000	1.000	1.000	1.000	1.000	1.000	1.000	1.000	1.000	1.000	1.000	1.000	1.000	1.000
	R2	0.943	1.000	1.000	1.000	1.000	1.000	1.000	1.000	1.000	1.000	1.000	1.000	1.000	1.000	1.000	1.000	1.000	1.000
	R3	0.930	1.000	1.000	1.000	1.000	1.000	1.000	1.000	1.000	1.000	1.000	1.000	1.000	1.000	1.000	1.000	1.000	1.000
	R4	0.881	1.000	1.000	1.000	1.000	1.000	1.000	1.000	1.000	0.950	1.000	1.000	1.000	1.000	1.000	1.000	1.000	1.000
$\lambda_{20^{\circ}\text{C}}=0.25$	R1	0.812	0.923	0.993	0.993	0.993	0.993	0.993	0.993	0.993	0.873	0.993	0.993	0.993	0.993	0.993	0.993	0.993	0.993
	R2	0.789	0.906	0.993	0.993	0.993	0.993	0.993	0.993	0.993	0.850	0.993	0.993	0.993	0.993	0.993	0.993	0.993	0.993
	R3	0.778	0.897	0.987	0.993	0.993	0.993	0.993	0.993	0.993	0.839	0.993	0.993	0.993	0.993	0.993	0.993	0.993	0.993
	R4	0.737	0.867	0.961	0.993	0.993	0.993	0.993	0.993	0.993	0.800	0.989	0.993	0.993	0.993	0.993	0.993	0.993	0.993
$\lambda_{20^{\circ}\text{C}}=0.50$	R1	0.656	0.749	0.822	0.951	0.951	0.951	0.951	0.951	0.951	0.707	0.860	0.951	0.951	0.951	0.951	0.951	0.951	0.951
	R2	0.637	0.735	0.810	0.876	0.951	0.951	0.951	0.951	0.951	0.688	0.843	0.951	0.951	0.951	0.951	0.951	0.951	0.951
	R3	0.627	0.726	0.800	0.866	0.951	0.951	0.951	0.951	0.951	0.680	0.834	0.951	0.951	0.951	0.951	0.951	0.951	0.951
	R4	0.589	0.697	0.777	0.846	0.951	0.951	0.951	0.951	0.951	0.639	0.798	0.951	0.951	0.951	0.951	0.951	0.951	0.951
$\lambda_{20^{\circ}\text{C}}=0.75$	R1	0.542	0.627	0.695	0.758	0.876	0.876	0.876	0.876	0.876	0.589	0.726	0.876	0.876	0.876	0.876	0.876	0.876	0.876
	R2	0.522	0.610	0.680	0.742	0.876	0.876	0.876	0.876	0.876	0.573	0.708	0.876	0.876	0.876	0.876	0.876	0.876	0.876
	R3	0.512	0.601	0.669	0.727	0.876	0.876	0.876	0.876	0.876	0.561	0.696	0.876	0.876	0.876	0.876	0.876	0.876	0.876
	R4	0.474	0.571	0.643	0.709	0.876	0.876	0.876	0.876	0.876	0.523	0.661	0.876	0.876	0.876	0.876	0.876	0.876	0.876
$\lambda_{20^{\circ}\text{C}}=1.00$	R1	0.438	0.509	0.567	0.725	0.725	0.725	0.725	0.725	0.725	0.478	0.591	0.725	0.725	0.725	0.725	0.725	0.725	0.725
	R2	0.423	0.493	0.553	0.607	0.725	0.725	0.725	0.725	0.725	0.464	0.575	0.725	0.725	0.725	0.725	0.725		

$$\theta_{\text{nom}} = 400^{\circ}\text{C}$$

$p_{f,fi} \rightarrow$	0.10	0.20	0.30	0.40	0.50	0.60	0.70	0.80	0.90	0.10	0.20	0.30	0.40	0.50	0.60	0.70	0.80	0.90
$\beta_{f,fi} \rightarrow$	1.28	0.84	0.52	0.40	0.00	-0.25	-0.52	-0.84	-1.28	1.28	0.84	0.52	0.40	0.00	-0.25	-0.52	-0.84	-1.28
$\delta_{af} \rightarrow$	1.15	1.02	0.94	0.88	0.82	0.77	0.72	0.67	0.60	1.15	1.02	0.94	0.88	0.82	0.77	0.72	0.67	0.60
	$\alpha=0.00$									$\alpha=0.25$								
$\lambda_{20^{\circ}\text{C}}=0.00$	R1	0.770	0.865	0.936	0.999	1.000	1.000	1.000	1.000	0.832	0.936	1.000	1.000	1.000	1.000	1.000	1.000	1.000
	R2	0.624	0.750	0.840	0.918	0.989	1.000	1.000	1.000	0.675	0.814	0.911	0.997	1.000	1.000	1.000	1.000	1.000
	R3	0.585	0.736	0.831	0.910	0.980	1.000	1.000	1.000	0.635	0.797	0.902	0.988	1.000	1.000	1.000	1.000	1.000
	R4	0.523	0.687	0.798	0.883	0.960	1.000	1.000	1.000	0.568	0.743	0.863	0.956	1.000	1.000	1.000	1.000	1.000
$\lambda_{20^{\circ}\text{C}}=0.25$	R1	0.643	0.722	0.782	0.835	0.887	0.940	0.993	0.993	0.695	0.783	0.849	0.907	0.965	0.993	0.993	0.993	0.993
	R2	0.520	0.627	0.702	0.767	0.828	0.888	0.953	0.993	0.564	0.680	0.762	0.833	0.901	0.968	0.993	0.993	0.993
	R3	0.489	0.614	0.694	0.760	0.820	0.879	0.945	0.993	0.529	0.666	0.754	0.826	0.893	0.959	0.993	0.993	0.993
	R4	0.437	0.574	0.665	0.738	0.803	0.867	0.934	0.993	0.474	0.621	0.721	0.801	0.873	0.944	0.993	0.993	0.993
$\lambda_{20^{\circ}\text{C}}=0.50$	R1	0.505	0.568	0.616	0.659	0.700	0.744	0.791	0.849	0.545	0.615	0.668	0.716	0.762	0.809	0.863	0.951	0.951
	R2	0.405	0.491	0.552	0.604	0.654	0.701	0.753	0.815	0.439	0.532	0.598	0.656	0.711	0.763	0.821	0.951	0.951
	R3	0.379	0.480	0.545	0.597	0.645	0.694	0.746	0.809	0.411	0.520	0.591	0.649	0.702	0.754	0.813	0.882	0.951
	R4	0.338	0.447	0.521	0.581	0.634	0.684	0.738	0.800	0.366	0.485	0.566	0.630	0.689	0.744	0.804	0.873	0.951
$\lambda_{20^{\circ}\text{C}}=0.75$	R1	0.402	0.454	0.494	0.531	0.567	0.604	0.647	0.702	0.434	0.492	0.537	0.577	0.616	0.658	0.704	0.876	0.876
	R2	0.319	0.390	0.440	0.485	0.527	0.567	0.612	0.671	0.345	0.422	0.477	0.527	0.573	0.616	0.667	0.731	0.876
	R3	0.296	0.382	0.435	0.478	0.519	0.559	0.605	0.659	0.321	0.413	0.471	0.519	0.563	0.608	0.660	0.720	0.876
	R4	0.260	0.354	0.415	0.465	0.510	0.550	0.595	0.649	0.283	0.383	0.450	0.505	0.554	0.598	0.649	0.708	0.876
$\lambda_{20^{\circ}\text{C}}=1.00$	R1	0.321	0.364	0.397	0.427	0.456	0.488	0.524	0.573	0.347	0.394	0.431	0.463	0.496	0.531	0.571	0.725	0.725
	R2	0.252	0.311	0.352	0.389	0.424	0.456	0.495	0.546	0.274	0.336	0.382	0.423	0.461	0.497	0.539	0.595	0.725
	R3	0.233	0.304	0.348	0.383	0.417	0.450	0.488	0.534	0.253	0.329	0.377	0.416	0.453	0.489	0.532	0.583	0.725
	R4	0.202	0.281	0.332	0.373	0.409	0.443	0.479	0.525	0.220	0.304	0.360	0.404	0.445	0.481	0.523	0.572	0.725
$\lambda_{20^{\circ}\text{C}}=1.50$	R1	0.184	0.208	0.226	0.243	0.259	0.277	0.297	0.321	0.199	0.225	0.245	0.264	0.282	0.301	0.323	0.351	0.395
	R2	0.145	0.179	0.202	0.223	0.242	0.260	0.281	0.308	0.157	0.194	0.219	0.242	0.263	0.283	0.306	0.335	0.395
	R3	0.134	0.175	0.200	0.220	0.239	0.257	0.278	0.303	0.144	0.189	0.217	0.238	0.259	0.280	0.303	0.331	0.395
	R4	0.115	0.162	0.191	0.214	0.234	0.253	0.274	0.298	0.125	0.175	0.207	0.232	0.255	0.275	0.298	0.326	0.395
$\lambda_{20^{\circ}\text{C}}=2.00$	R1	0.110	0.124	0.134	0.144	0.154	0.164	0.176	0.190	0.118	0.134	0.146	0.157	0.167	0.179	0.191	0.207	0.232
	R2	0.087	0.107	0.121	0.133	0.144	0.155	0.167	0.182	0.094	0.116	0.131	0.144	0.157	0.168	0.182	0.199	0.232
	R3	0.080	0.104	0.119	0.131	0.142	0.153	0.165	0.180	0.087	0.113	0.129	0.142	0.154	0.166	0.180	0.196	0.232
	R4	0.069	0.097	0.114	0.127	0.140	0.150	0.163	0.177	0.075	0.105	0.124	0.138	0.152	0.164	0.177	0.194	0.232
	$\alpha=0.50$									$\alpha=0.75$								
$\lambda_{20^{\circ}\text{C}}=0.00$	R1	0.905	1.000	1.000	1.000	1.000	1.000	1.000	1.000	0.976	1.000	1.000	1.000	1.000	1.000	1.000	1.000	1.000
	R2	0.742	0.902	1.000	1.000	1.000	1.000	1.000	1.000	0.825	1.000	1.000	1.000	1.000	1.000	1.000	1.000	1.000
	R3	0.699	0.881	1.000	1.000	1.000	1.000	1.000	1.000	0.783	1.000	1.000	1.000	1.000	1.000	1.000	1.000	1.000
	R4	0.629	0.823	0.961	1.000	1.000	1.000	1.000	1.000	0.718	0.951	1.000	1.000	1.000	1.000	1.000	1.000	1.000
$\lambda_{20^{\circ}\text{C}}=0.25$	R1	0.757	0.869	0.956	0.993	0.993	0.993	0.993	0.993	0.821	0.993	0.993	0.993	0.993	0.993	0.993	0.993	0.993
	R2	0.620	0.754	0.854	0.941	0.993	0.993	0.993	0.993	0.691	0.871	0.993	0.993	0.993	0.993	0.993	0.993	0.993
	R3	0.586	0.737	0.843	0.933	0.993	0.993	0.993	0.993	0.655	0.848	0.993	0.993	0.993	0.993	0.993	0.993	0.993
	R4	0.527	0.688	0.804	0.903	0.993	0.993	0.993	0.993	0.602	0.798	0.957	0.993	0.993	0.993	0.993	0.993	0.993
$\lambda_{20^{\circ}\text{C}}=0.50$	R1	0.595	0.683	0.751	0.813	0.873	0.951	0.951	0.951	0.644	0.785	0.951	0.951	0.951	0.951	0.951	0.951	0.951
	R2	0.483	0.590	0.669	0.740	0.809	0.877	0.951	0.951	0.536	0.678	0.797	0.951	0.951	0.951	0.951	0.951	0.951
	R3	0.455	0.576	0.661	0.732	0.799	0.866	0.951	0.951	0.511	0.664	0.787	0.951	0.951	0.951	0.951	0.951	0.951
	R4	0.408	0.537	0.631	0.709	0.781	0.853	0.951	0.951	0.466	0.622	0.749	0.868	0.951	0.951	0.951	0.951	0.951
$\lambda_{20^{\circ}\text{C}}=0.75$	R1	0.474	0.547	0.603	0.654	0.705	0.758	0.876	0.876	0.516	0.632	0.729	0.876	0.876	0.876	0.876	0.876	0.876
	R2	0.379	0.467	0.533	0.595	0.652	0.709	0.876	0.876	0.423	0.540	0.638	0.735	0.876	0.876	0.876	0.876	0.876
	R3	0.355	0.457	0.528	0.586	0.642	0.699	0.876	0.876	0.400	0.530	0.629	0.724	0.876	0.876	0.876	0.876	0.876
	R4	0.314	0.424	0.502	0.568	0.629	0.687	0.750	0.876	0.361	0.491	0.597	0.696	0.876	0.876	0.876	0.876	0.876
$\lambda_{20^{\circ}\text{C}}=1.00$	R1	0.379	0.438	0.485	0.527	0.568	0.725	0.725	0.725	0.412	0.507	0.586	0.725	0.725	0.725	0.725	0.725	0.725
	R2	0.301	0.374	0.427	0.478	0.526	0.571	0.725	0.725	0.335	0.430	0.511	0.590	0.725	0.725	0.725	0.725	0.725
	R3	0.280	0.365	0.423	0.470	0.517	0.563	0.725	0.725	0.318	0.423	0.505	0.582	0.725	0.725	0.725	0.725	0.725
	R4	0.245	0.338	0.402	0.456	0.507	0.552	0.606	0.725	0.283	0.391	0.478	0.559	0.725	0.725	0.725	0.725	0.725
$\lambda_{20^{\circ}\text{C}}=1.50$	R1	0.216	0.250	0.276	0.300	0.323	0.347	0.395	0.395	0.236	0.289	0.334	0.395	0.395	0.395	0.395	0.395	0.395
	R2	0.172	0.214	0.245	0.273	0.300	0.326	0.395	0.395	0.193	0.248	0.293	0.337	0.395	0.395	0.395	0.395	0.395
	R3	0.160	0.210	0.242	0.269	0.295	0.321	0.350	0.395	0.181	0.241	0.289	0.333	0.395	0.395	0.395	0.395	0.395
	R4	0.140	0.194	0.231	0.262	0.290	0.316	0.345	0.395	0.162	0.223	0.273	0.320	0.395	0.395	0.395	0.395	0.395
$\lambda_{20^{\circ}\text{C}}=2.00$	R1	0.129	0.149	0.164	0.178	0.192	0.206	0.232	0.232	0.141	0.172	0.199	0.232	0.232	0.232	0.232	0.232	0.232
	R2	0.103	0.128	0.146	0.163	0.178	0.194	0.211	0.232	0.115	0.147	0.174	0.200	0.232	0.232	0.232	0.232	0.232
	R3	0.096	0.125	0.145	0.161	0.176	0.191	0.208	0.232	0.108	0.144	0.172	0.198	0.232	0.232	0.232	0.232	0.232
	R4	0.084	0.116	0.138	0.156	0.172	0.188	0.205	0.232	0.097	0.133	0.163	0.190	0.232	0.232	0.232	0.232	0.232

$\theta_{\text{nom}} = 500^{\circ}\text{C}$

$p_{f,fi} \rightarrow$	0.10	0.20	0.30	0.40	0.50	0.60	0.70	0.80	0.90	0.10	0.20	0.30	0.40	0.50	0.60	0.70	0.80	0.90
$\beta_{f,fi} \rightarrow$	1.28	0.84	0.52	0.40	0.00	-0.25	-0.52	-0.84	-1.28	1.28	0.84	0.52	0.40	0.00	-0.25	-0.52	-0.84	-1.28
$\delta_{af} \rightarrow$	1.15	1.02	0.94	0.88	0.82	0.77	0.72	0.67	0.60	1.15	1.02	0.94	0.88	0.82	0.77	0.72	0.67	0.60
	$\alpha=0.00$									$\alpha=0.25$								
$\lambda_{20^{\circ}\text{C}}=0.00$	R1	0.425	0.530	0.615	0.697	0.788	0.875	0.964	1.000	1.000	0.460	0.575	0.667	0.757	0.855	0.949	1.000	1.000
	R2	0.330	0.459	0.574	0.670	0.756	0.838	0.928	1.000	1.000	0.358	0.499	0.624	0.728	0.821	0.911	1.000	1.000
	R3	0.277	0.400	0.510	0.615	0.719	0.815	0.916	1.000	1.000	0.301	0.434	0.554	0.669	0.781	0.886	0.995	1.000
	R4	0.217	0.320	0.442	0.561	0.676	0.788	0.901	1.000	1.000	0.238	0.348	0.480	0.609	0.735	0.857	0.979	1.000
$\lambda_{20^{\circ}\text{C}}=0.25$	R1	0.356	0.443	0.514	0.582	0.659	0.731	0.807	0.898	0.993	0.386	0.481	0.558	0.632	0.716	0.795	0.880	0.979
	R2	0.276	0.384	0.480	0.560	0.632	0.702	0.778	0.870	0.993	0.300	0.417	0.522	0.609	0.687	0.764	0.847	0.949
	R3	0.232	0.335	0.427	0.515	0.600	0.681	0.765	0.860	0.991	0.251	0.363	0.464	0.560	0.653	0.741	0.834	0.938
	R4	0.183	0.268	0.370	0.469	0.564	0.659	0.754	0.850	0.974	0.199	0.291	0.401	0.510	0.614	0.717	0.819	0.926
$\lambda_{20^{\circ}\text{C}}=0.50$	R1	0.273	0.342	0.399	0.453	0.513	0.571	0.633	0.702	0.800	0.296	0.371	0.432	0.491	0.556	0.621	0.688	0.765
	R2	0.211	0.295	0.371	0.435	0.492	0.547	0.607	0.680	0.784	0.229	0.321	0.403	0.473	0.535	0.594	0.661	0.741
	R3	0.177	0.257	0.329	0.399	0.468	0.532	0.599	0.673	0.774	0.191	0.278	0.357	0.434	0.508	0.578	0.651	0.733
	R4	0.139	0.204	0.283	0.362	0.439	0.514	0.589	0.663	0.759	0.152	0.222	0.308	0.394	0.477	0.559	0.640	0.723
$\lambda_{20^{\circ}\text{C}}=0.75$	R1	0.208	0.264	0.311	0.357	0.406	0.454	0.503	0.560	0.646	0.225	0.287	0.338	0.387	0.441	0.493	0.547	0.610
	R2	0.157	0.225	0.288	0.341	0.388	0.433	0.482	0.542	0.630	0.171	0.244	0.312	0.370	0.422	0.471	0.525	0.591
	R3	0.131	0.193	0.252	0.311	0.369	0.421	0.475	0.536	0.618	0.141	0.210	0.274	0.338	0.401	0.457	0.518	0.584
	R4	0.103	0.153	0.215	0.280	0.344	0.407	0.468	0.528	0.604	0.113	0.165	0.234	0.304	0.374	0.442	0.510	0.575
$\lambda_{20^{\circ}\text{C}}=1.00$	R1	0.159	0.206	0.245	0.284	0.325	0.365	0.404	0.450	0.522	0.172	0.223	0.266	0.308	0.353	0.396	0.440	0.491
	R2	0.119	0.173	0.225	0.270	0.310	0.348	0.387	0.436	0.508	0.129	0.188	0.245	0.294	0.337	0.377	0.421	0.475
	R3	0.098	0.147	0.195	0.244	0.294	0.337	0.382	0.431	0.497	0.107	0.160	0.212	0.265	0.319	0.366	0.416	0.470
	R4	0.078	0.115	0.165	0.218	0.273	0.326	0.376	0.424	0.485	0.085	0.124	0.179	0.237	0.296	0.354	0.408	0.463
$\lambda_{20^{\circ}\text{C}}=1.50$	R1	0.090	0.117	0.141	0.164	0.188	0.210	0.233	0.259	0.298	0.097	0.127	0.153	0.177	0.204	0.228	0.253	0.282
	R2	0.066	0.097	0.129	0.155	0.179	0.201	0.223	0.251	0.291	0.072	0.106	0.140	0.169	0.195	0.218	0.243	0.274
	R3	0.054	0.083	0.111	0.140	0.169	0.195	0.220	0.249	0.287	0.059	0.090	0.120	0.152	0.184	0.211	0.240	0.271
	R4	0.044	0.063	0.093	0.124	0.157	0.188	0.217	0.245	0.281	0.047	0.069	0.101	0.135	0.170	0.204	0.236	0.267
$\lambda_{20^{\circ}\text{C}}=2.00$	R1	0.053	0.070	0.084	0.098	0.112	0.125	0.139	0.155	0.177	0.058	0.076	0.091	0.106	0.122	0.136	0.151	0.169
	R2	0.039	0.058	0.077	0.093	0.107	0.120	0.133	0.150	0.173	0.043	0.063	0.083	0.101	0.116	0.130	0.145	0.163
	R3	0.032	0.049	0.066	0.084	0.101	0.116	0.131	0.148	0.171	0.035	0.053	0.072	0.091	0.110	0.126	0.143	0.162
	R4	0.026	0.038	0.055	0.074	0.094	0.112	0.129	0.146	0.168	0.028	0.041	0.060	0.081	0.102	0.122	0.141	0.160
	$\alpha=0.50$									$\alpha=0.75$								
$\lambda_{20^{\circ}\text{C}}=0.00$	R1	0.511	0.643	0.750	0.854	0.968	1.000	1.000	1.000	1.000	0.586	0.762	0.911	1.000	1.000	1.000	1.000	1.000
	R2	0.402	0.561	0.702	0.820	0.932	1.000	1.000	1.000	1.000	0.477	0.672	0.848	1.000	1.000	1.000	1.000	1.000
	R3	0.339	0.488	0.626	0.756	0.885	1.000	1.000	1.000	1.000	0.409	0.588	0.761	0.928	1.000	1.000	1.000	1.000
	R4	0.269	0.394	0.542	0.689	0.829	0.972	1.000	1.000	1.000	0.326	0.488	0.661	0.842	1.000	1.000	1.000	1.000
$\lambda_{20^{\circ}\text{C}}=0.25$	R1	0.429	0.539	0.628	0.715	0.810	0.908	0.993	0.993	0.993	0.490	0.638	0.763	0.883	0.993	0.993	0.993	0.993
	R2	0.337	0.469	0.587	0.688	0.781	0.872	0.974	0.993	0.993	0.401	0.561	0.711	0.849	0.981	0.993	0.993	0.993
	R3	0.284	0.409	0.524	0.632	0.739	0.844	0.958	0.993	0.993	0.344	0.495	0.637	0.778	0.922	0.993	0.993	0.993
	R4	0.225	0.331	0.455	0.576	0.693	0.813	0.937	0.993	0.993	0.273	0.408	0.555	0.708	0.862	0.993	0.993	0.993
$\lambda_{20^{\circ}\text{C}}=0.50$	R1	0.329	0.415	0.486	0.555	0.630	0.708	0.790	0.886	0.951	0.377	0.492	0.591	0.686	0.788	0.951	0.951	0.951
	R2	0.257	0.361	0.454	0.533	0.607	0.678	0.758	0.858	0.951	0.307	0.432	0.548	0.657	0.762	0.875	0.951	0.951
	R3	0.216	0.313	0.403	0.489	0.575	0.658	0.746	0.850	0.951	0.262	0.379	0.491	0.601	0.714	0.836	0.951	0.951
	R4	0.171	0.252	0.348	0.444	0.539	0.633	0.731	0.839	0.951	0.207	0.313	0.426	0.545	0.667	0.799	0.951	0.951
$\lambda_{20^{\circ}\text{C}}=0.75$	R1	0.251	0.321	0.380	0.435	0.499	0.562	0.629	0.709	0.876	0.290	0.380	0.459	0.535	0.621	0.720	0.876	0.876
	R2	0.192	0.276	0.352	0.417	0.478	0.537	0.602	0.684	0.876	0.230	0.331	0.427	0.514	0.599	0.690	0.876	0.876
	R3	0.161	0.237	0.309	0.381	0.452	0.519	0.591	0.676	0.876	0.196	0.287	0.377	0.466	0.559	0.661	0.876	0.876
	R4	0.127	0.188	0.265	0.343	0.421	0.500	0.581	0.666	0.876	0.156	0.235	0.325	0.422	0.521	0.628	0.751	0.876
$\lambda_{20^{\circ}\text{C}}=1.00$	R1	0.193	0.250	0.299	0.347	0.400	0.450	0.505	0.571	0.725	0.224	0.298	0.363	0.425	0.495	0.576	0.725	0.725
	R2	0.145	0.212	0.276	0.331	0.381	0.431	0.484	0.550	0.725	0.175	0.256	0.334	0.406	0.478	0.552	0.725	0.725
	R3	0.120	0.180	0.239	0.300	0.359	0.415	0.474	0.544	0.725	0.148	0.220	0.293	0.368	0.444	0.527	0.725	0.725
	R4	0.096	0.141	0.203	0.268	0.335	0.400	0.468	0.536	0.725	0.118	0.178	0.250	0.330	0.413	0.501	0.602	0.725
$\lambda_{20^{\circ}\text{C}}=1.50$	R1	0.109	0.143	0.172	0.200	0.231	0.260	0.291	0.328	0.395	0.127	0.170	0.208	0.244	0.285	0.332	0.395	0.395
	R2	0.081	0.120	0.158	0.190	0.220	0.249	0.279	0.317	0.395	0.098	0.145	0.190	0.233	0.274	0.318	0.395	0.395
	R3	0.067	0.101	0.136	0.172	0.207	0.240	0.274	0.313	0.395	0.083	0.124	0.167	0.210	0.255	0.304	0.395	0.395
	R4	0.054	0.079	0.114	0.153	0.192	0.230	0.269	0.309	0.395	0.066	0.099	0.141	0.188	0.236	0.288	0.347	0.395
$\lambda_{20^{\circ}\text{C}}=2.00$	R1	0.065	0.085	0.102	0.120	0.138	0.155	0.174	0.196	0.232	0.076	0.102	0.124	0.146	0.170	0.198	0.232	0.232
	R2	0.048	0.071	0.094	0.114	0.132	0.148	0.167	0.189	0.232	0.058	0.086	0.114	0.139	0.164	0.190	0.232	0.232
	R3	0.040	0.060	0.081	0.103	0.124	0.143	0.164	0.187	0.232	0.049	0.074	0.100	0.126	0.153	0.182	0.213	0.232
	R4	0.032	0.047	0.068	0.091	0.115	0.138	0.160	0.185	0.215	0.039	0.059	0.084	0.112	0.141	0.172	0.207	0.232

$$\theta_{\text{nom}} = 600^{\circ}\text{C}$$

$p_{f,fi} \rightarrow$	0.10	0.20	0.30	0.40	0.50	0.60	0.70	0.80	0.90	0.10	0.20	0.30	0.40	0.50	0.60	0.70	0.80	0.90	
$\beta_{f,fi} \rightarrow$	1.28	0.84	0.52	0.40	0.00	-0.25	-0.52	-0.84	-1.28	1.28	0.84	0.52	0.40	0.00	-0.25	-0.52	-0.84	-1.28	
$\delta_{of} \rightarrow$	1.15	1.02	0.94	0.88	0.82	0.77	0.72	0.67	0.60	1.15	1.02	0.94	0.88	0.82	0.77	0.72	0.67	0.60	
	$\alpha=0.00$									$\alpha=0.25$									
$\lambda_{20^{\circ}\text{C}}=0.00$	R1	0.375	0.480	0.562	0.641	0.720	0.804	0.893	0.999	1.000	0.406	0.521	0.611	0.696	0.784	0.874	0.972	1.000	1.000
	R2	0.211	0.270	0.335	0.407	0.482	0.562	0.663	0.784	0.966	0.229	0.294	0.365	0.442	0.524	0.611	0.720	0.854	1.000
	R3	0.195	0.251	0.314	0.388	0.465	0.545	0.629	0.751	0.927	0.212	0.273	0.341	0.421	0.506	0.592	0.686	0.819	1.000
	R4	0.148	0.205	0.253	0.317	0.397	0.490	0.604	0.725	0.875	0.161	0.222	0.275	0.344	0.433	0.534	0.657	0.790	0.953
$\lambda_{20^{\circ}\text{C}}=0.25$	R1	0.314	0.402	0.471	0.537	0.603	0.672	0.748	0.837	0.961	0.340	0.436	0.512	0.584	0.656	0.732	0.815	0.913	0.993
	R2	0.177	0.227	0.281	0.341	0.404	0.472	0.553	0.656	0.811	0.192	0.246	0.305	0.371	0.439	0.512	0.603	0.715	0.886
	R3	0.164	0.210	0.262	0.324	0.389	0.454	0.528	0.628	0.776	0.177	0.229	0.286	0.353	0.423	0.495	0.575	0.685	0.846
	R4	0.124	0.172	0.212	0.265	0.333	0.411	0.505	0.607	0.732	0.134	0.186	0.230	0.288	0.363	0.447	0.550	0.662	0.798
$\lambda_{20^{\circ}\text{C}}=0.50$	R1	0.240	0.308	0.363	0.416	0.469	0.523	0.583	0.653	0.751	0.260	0.334	0.395	0.452	0.510	0.570	0.634	0.711	0.819
	R2	0.134	0.172	0.214	0.261	0.309	0.362	0.427	0.510	0.632	0.146	0.187	0.232	0.284	0.336	0.394	0.465	0.556	0.688
	R3	0.124	0.160	0.200	0.247	0.298	0.350	0.408	0.489	0.605	0.135	0.174	0.217	0.269	0.324	0.380	0.444	0.532	0.659
	R4	0.096	0.131	0.161	0.201	0.254	0.315	0.390	0.470	0.570	0.104	0.141	0.175	0.219	0.277	0.343	0.424	0.512	0.622
$\lambda_{20^{\circ}\text{C}}=0.75$	R1	0.180	0.236	0.281	0.325	0.369	0.415	0.463	0.520	0.598	0.196	0.256	0.305	0.352	0.401	0.451	0.504	0.566	0.652
	R2	0.100	0.128	0.160	0.196	0.236	0.279	0.334	0.403	0.502	0.108	0.139	0.173	0.214	0.256	0.303	0.363	0.438	0.548
	R3	0.093	0.119	0.149	0.186	0.227	0.269	0.316	0.384	0.480	0.101	0.129	0.162	0.203	0.247	0.293	0.344	0.418	0.523
	R4	0.073	0.098	0.119	0.150	0.192	0.240	0.302	0.369	0.451	0.080	0.106	0.130	0.163	0.208	0.261	0.328	0.401	0.492
$\lambda_{20^{\circ}\text{C}}=1.00$	R1	0.138	0.182	0.219	0.257	0.294	0.332	0.372	0.418	0.481	0.149	0.197	0.238	0.279	0.319	0.360	0.404	0.455	0.525
	R2	0.075	0.096	0.120	0.150	0.181	0.217	0.264	0.322	0.404	0.081	0.104	0.131	0.162	0.197	0.236	0.287	0.350	0.440
	R3	0.070	0.089	0.112	0.141	0.174	0.208	0.248	0.306	0.385	0.076	0.097	0.121	0.154	0.189	0.227	0.270	0.333	0.420
	R4	0.057	0.074	0.090	0.113	0.146	0.185	0.236	0.293	0.362	0.062	0.080	0.097	0.122	0.159	0.201	0.257	0.319	0.395
$\lambda_{20^{\circ}\text{C}}=1.50$	R1	0.077	0.103	0.125	0.147	0.170	0.192	0.215	0.242	0.278	0.083	0.112	0.136	0.160	0.184	0.208	0.234	0.263	0.303
	R2	0.041	0.053	0.067	0.084	0.102	0.123	0.151	0.186	0.234	0.045	0.057	0.073	0.091	0.111	0.134	0.165	0.202	0.255
	R3	0.039	0.049	0.062	0.079	0.098	0.118	0.142	0.177	0.223	0.042	0.054	0.067	0.086	0.107	0.129	0.154	0.192	0.244
	R4	0.033	0.041	0.050	0.063	0.082	0.105	0.135	0.169	0.210	0.036	0.045	0.054	0.068	0.089	0.114	0.147	0.184	0.229
$\lambda_{20^{\circ}\text{C}}=2.00$	R1	0.046	0.061	0.075	0.088	0.101	0.115	0.128	0.144	0.166	0.050	0.067	0.081	0.096	0.110	0.125	0.140	0.157	0.181
	R2	0.025	0.031	0.040	0.050	0.061	0.074	0.090	0.111	0.140	0.027	0.034	0.043	0.054	0.066	0.080	0.098	0.121	0.152
	R3	0.023	0.029	0.037	0.047	0.058	0.071	0.085	0.106	0.133	0.025	0.032	0.040	0.051	0.064	0.077	0.092	0.115	0.145
	R4	0.020	0.025	0.030	0.037	0.049	0.062	0.081	0.101	0.126	0.021	0.027	0.032	0.040	0.053	0.068	0.088	0.110	0.137
	$\alpha=0.50$									$\alpha=0.75$									
$\lambda_{20^{\circ}\text{C}}=0.00$	R1	0.454	0.585	0.688	0.788	0.890	0.998	1.000	1.000	1.000	0.528	0.697	0.840	0.980	1.000	1.000	1.000	1.000	1.000
	R2	0.257	0.333	0.412	0.501	0.596	0.697	0.824	0.980	1.000	0.301	0.409	0.511	0.626	0.754	0.900	1.000	1.000	1.000
	R3	0.236	0.310	0.387	0.477	0.575	0.675	0.787	0.940	1.000	0.277	0.384	0.487	0.598	0.725	0.866	1.000	1.000	1.000
	R4	0.179	0.251	0.314	0.392	0.492	0.608	0.750	0.910	1.000	0.208	0.305	0.397	0.500	0.623	0.773	0.966	1.000	1.000
$\lambda_{20^{\circ}\text{C}}=0.25$	R1	0.381	0.490	0.577	0.660	0.745	0.836	0.936	0.993	0.993	0.444	0.586	0.707	0.825	0.947	0.993	0.993	0.993	0.993
	R2	0.215	0.279	0.346	0.420	0.500	0.585	0.690	0.821	0.993	0.253	0.343	0.430	0.526	0.633	0.753	0.897	0.993	0.993
	R3	0.198	0.260	0.325	0.400	0.482	0.566	0.661	0.787	0.983	0.233	0.322	0.408	0.501	0.609	0.728	0.867	0.993	0.993
	R4	0.150	0.210	0.263	0.329	0.413	0.510	0.629	0.763	0.933	0.174	0.256	0.334	0.419	0.522	0.650	0.809	0.993	0.993
$\lambda_{20^{\circ}\text{C}}=0.50$	R1	0.290	0.375	0.445	0.512	0.579	0.649	0.729	0.825	0.951	0.339	0.448	0.542	0.635	0.732	0.839	0.951	0.951	0.951
	R2	0.163	0.212	0.263	0.321	0.383	0.450	0.533	0.637	0.800	0.192	0.261	0.328	0.402	0.485	0.577	0.691	0.846	0.951
	R3	0.151	0.197	0.247	0.305	0.368	0.434	0.508	0.610	0.765	0.177	0.245	0.310	0.381	0.465	0.558	0.666	0.807	0.951
	R4	0.116	0.160	0.200	0.250	0.314	0.391	0.485	0.590	0.724	0.135	0.195	0.254	0.318	0.398	0.496	0.623	0.784	0.951
$\lambda_{20^{\circ}\text{C}}=0.75$	R1	0.219	0.287	0.344	0.399	0.454	0.514	0.578	0.657	0.876	0.257	0.345	0.419	0.494	0.573	0.660	0.761	0.876	0.876
	R2	0.122	0.158	0.196	0.242	0.292	0.346	0.416	0.501	0.635	0.144	0.195	0.246	0.303	0.369	0.445	0.537	0.659	0.876
	R3	0.113	0.147	0.184	0.230	0.281	0.334	0.394	0.480	0.607	0.133	0.183	0.232	0.288	0.354	0.428	0.515	0.631	0.876
	R4	0.089	0.120	0.149	0.186	0.237	0.298	0.375	0.462	0.571	0.104	0.147	0.190	0.239	0.301	0.380	0.481	0.611	0.876
$\lambda_{20^{\circ}\text{C}}=1.00$	R1	0.167	0.222	0.269	0.316	0.362	0.411	0.464	0.529	0.725	0.197	0.268	0.330	0.391	0.455	0.526	0.725	0.725	0.725
	R2	0.091	0.118	0.148	0.184	0.225	0.269	0.328	0.401	0.510	0.109	0.147	0.186	0.231	0.285	0.346	0.422	0.524	0.725
	R3	0.085	0.110	0.138	0.174	0.216</													

$$\theta_{\text{nom}} = 700^{\circ}\text{C}$$

$p_{f_{fi}} \rightarrow$	0.10	0.20	0.30	0.40	0.50	0.60	0.70	0.80	0.90	0.10	0.20	0.30	0.40	0.50	0.60	0.70	0.80	0.90	
$\beta_{f_{fi}} \rightarrow$	1.28	0.84	0.52	0.40	0.00	-0.25	-0.52	-0.84	-1.28	1.28	0.84	0.52	0.40	0.00	-0.25	-0.52	-0.84	-1.28	
$\delta_{of} \rightarrow$	1.15	1.02	0.94	0.88	0.82	0.77	0.72	0.67	0.60	1.15	1.02	0.94	0.88	0.82	0.77	0.72	0.67	0.60	
	$\alpha=0.00$									$\alpha=0.25$									
$\lambda_{20^{\circ}\text{C}}=0.00$	R1	0.204	0.241	0.276	0.317	0.363	0.415	0.478	0.564	0.732	0.221	0.261	0.301	0.345	0.395	0.452	0.521	0.615	0.798
	R2	0.149	0.187	0.215	0.242	0.274	0.318	0.380	0.474	0.633	0.162	0.203	0.234	0.264	0.298	0.346	0.413	0.515	0.689
	R3	0.113	0.163	0.197	0.226	0.263	0.306	0.361	0.443	0.568	0.123	0.177	0.214	0.246	0.286	0.332	0.393	0.482	0.619
	R4	0.058	0.099	0.145	0.184	0.220	0.262	0.331	0.422	0.524	0.063	0.107	0.157	0.200	0.239	0.285	0.361	0.460	0.571
$\lambda_{20^{\circ}\text{C}}=0.25$	R1	0.171	0.202	0.232	0.266	0.304	0.348	0.401	0.473	0.613	0.185	0.219	0.252	0.290	0.332	0.379	0.437	0.516	0.668
	R2	0.125	0.157	0.181	0.203	0.230	0.267	0.318	0.403	0.532	0.135	0.170	0.196	0.221	0.250	0.292	0.346	0.437	0.579
	R3	0.095	0.137	0.165	0.190	0.220	0.256	0.303	0.373	0.477	0.103	0.148	0.180	0.206	0.240	0.279	0.330	0.405	0.519
	R4	0.050	0.084	0.122	0.156	0.185	0.222	0.281	0.356	0.440	0.054	0.091	0.133	0.169	0.201	0.242	0.306	0.387	0.479
$\lambda_{20^{\circ}\text{C}}=0.50$	R1	0.130	0.153	0.176	0.202	0.231	0.265	0.307	0.363	0.475	0.140	0.166	0.191	0.219	0.252	0.289	0.334	0.395	0.518
	R2	0.096	0.119	0.137	0.154	0.175	0.202	0.243	0.306	0.409	0.104	0.129	0.149	0.168	0.190	0.220	0.263	0.333	0.447
	R3	0.075	0.104	0.126	0.144	0.166	0.194	0.230	0.284	0.365	0.081	0.113	0.136	0.156	0.181	0.212	0.251	0.309	0.399
	R4	0.041	0.067	0.095	0.119	0.141	0.168	0.214	0.270	0.336	0.045	0.073	0.102	0.129	0.153	0.183	0.233	0.294	0.367
$\lambda_{20^{\circ}\text{C}}=0.75$	R1	0.096	0.113	0.130	0.150	0.173	0.200	0.233	0.278	0.371	0.104	0.123	0.141	0.163	0.188	0.218	0.253	0.304	0.403
	R2	0.073	0.090	0.102	0.115	0.129	0.150	0.182	0.234	0.316	0.079	0.097	0.111	0.124	0.141	0.164	0.197	0.255	0.343
	R3	0.060	0.080	0.094	0.107	0.124	0.145	0.172	0.214	0.279	0.065	0.087	0.102	0.116	0.135	0.157	0.187	0.233	0.305
	R4	0.037	0.055	0.073	0.090	0.105	0.125	0.159	0.203	0.256	0.040	0.060	0.080	0.097	0.115	0.136	0.173	0.221	0.279
$\lambda_{20^{\circ}\text{C}}=1.00$	R1	0.072	0.085	0.097	0.113	0.131	0.152	0.178	0.215	0.294	0.078	0.092	0.106	0.123	0.142	0.166	0.194	0.235	0.320
	R2	0.057	0.068	0.077	0.086	0.097	0.113	0.138	0.180	0.247	0.061	0.074	0.083	0.093	0.106	0.123	0.150	0.196	0.269
	R3	0.049	0.062	0.071	0.081	0.093	0.109	0.130	0.164	0.216	0.053	0.067	0.078	0.088	0.101	0.118	0.141	0.178	0.236
	R4	0.032	0.046	0.058	0.069	0.080	0.094	0.120	0.155	0.197	0.035	0.050	0.063	0.075	0.087	0.102	0.130	0.168	0.214
$\lambda_{20^{\circ}\text{C}}=1.50$	R1	0.040	0.047	0.054	0.062	0.073	0.085	0.100	0.122	0.169	0.043	0.051	0.058	0.068	0.079	0.093	0.110	0.133	0.184
	R2	0.032	0.038	0.043	0.048	0.054	0.062	0.077	0.101	0.141	0.035	0.041	0.046	0.052	0.059	0.068	0.084	0.110	0.154
	R3	0.029	0.035	0.040	0.045	0.051	0.060	0.072	0.092	0.123	0.031	0.038	0.044	0.049	0.056	0.065	0.079	0.100	0.134
	R4	0.020	0.027	0.033	0.039	0.045	0.052	0.066	0.087	0.111	0.022	0.030	0.036	0.042	0.049	0.057	0.072	0.094	0.121
$\lambda_{20^{\circ}\text{C}}=2.00$	R1	0.024	0.028	0.032	0.037	0.043	0.051	0.060	0.073	0.101	0.026	0.030	0.035	0.040	0.047	0.055	0.065	0.080	0.110
	R2	0.019	0.023	0.025	0.028	0.032	0.037	0.046	0.060	0.084	0.021	0.025	0.028	0.031	0.035	0.040	0.050	0.066	0.092
	R3	0.017	0.021	0.024	0.027	0.031	0.036	0.043	0.055	0.073	0.019	0.023	0.026	0.029	0.033	0.039	0.047	0.060	0.080
	R4	0.012	0.017	0.020	0.023	0.027	0.031	0.040	0.052	0.066	0.013	0.018	0.022	0.025	0.029	0.034	0.043	0.056	0.072
	$\alpha=0.50$									$\alpha=0.75$									
$\lambda_{20^{\circ}\text{C}}=0.00$	R1	0.246	0.295	0.342	0.393	0.451	0.518	0.599	0.711	0.922	0.280	0.360	0.430	0.502	0.582	0.674	0.792	0.955	1.000
	R2	0.178	0.227	0.265	0.301	0.342	0.398	0.473	0.591	0.799	0.204	0.269	0.326	0.382	0.447	0.522	0.621	0.782	1.000
	R3	0.138	0.198	0.242	0.280	0.328	0.383	0.453	0.555	0.719	0.165	0.237	0.297	0.356	0.427	0.502	0.597	0.737	0.978
	R4	0.072	0.122	0.176	0.226	0.273	0.329	0.414	0.532	0.664	0.089	0.149	0.213	0.278	0.350	0.434	0.546	0.713	0.914
$\lambda_{20^{\circ}\text{C}}=0.25$	R1	0.206	0.248	0.287	0.330	0.378	0.434	0.502	0.595	0.774	0.235	0.301	0.360	0.422	0.488	0.566	0.666	0.803	0.993
	R2	0.149	0.190	0.222	0.253	0.287	0.335	0.397	0.503	0.672	0.170	0.226	0.275	0.321	0.375	0.438	0.520	0.659	0.915
	R3	0.116	0.166	0.202	0.235	0.276	0.321	0.379	0.467	0.603	0.137	0.197	0.248	0.299	0.358	0.422	0.502	0.620	0.825
	R4	0.061	0.103	0.149	0.191	0.231	0.279	0.352	0.448	0.558	0.076	0.127	0.181	0.236	0.296	0.368	0.463	0.594	0.767
$\lambda_{20^{\circ}\text{C}}=0.50$	R1	0.156	0.187	0.218	0.251	0.288	0.331	0.384	0.457	0.596	0.178	0.228	0.273	0.319	0.370	0.430	0.506	0.614	0.805
	R2	0.115	0.145	0.169	0.191	0.220	0.253	0.302	0.383	0.517	0.130	0.172	0.208	0.243	0.285	0.333	0.395	0.505	0.703
	R3	0.091	0.127	0.154	0.178	0.208	0.243	0.288	0.355	0.462	0.107	0.151	0.189	0.227	0.271	0.321	0.381	0.472	0.631
	R4	0.051	0.083	0.115	0.146	0.175	0.211	0.267	0.338	0.427	0.062	0.101	0.140	0.181	0.226	0.279	0.352	0.452	0.586
$\lambda_{20^{\circ}\text{C}}=0.75$	R1	0.116	0.139	0.161	0.186	0.215	0.249	0.291	0.349	0.467	0.133	0.169	0.203	0.238	0.277	0.324	0.385	0.470	0.624
	R2	0.088	0.109	0.126	0.142	0.162	0.188	0.226	0.293	0.399	0.100	0.129	0.155	0.182	0.213	0.249	0.297	0.382	0.542
	R3	0.073	0.097	0.116	0.133	0.155	0.181	0.215	0.268	0.353	0.085	0.116	0.143	0.170	0.203	0.239	0.285	0.356	0.481
	R4	0.045	0.068	0.090	0.110	0.131	0.158	0.199	0.255	0.324	0.054	0.082	0.109	0.138	0.170	0.209	0.263	0.343	0.445
$\lambda_{20^{\circ}\text{C}}=1.00$	R1	0.087	0.104	0.121	0.140	0.163	0.189	0.224	0.272	0.370	0.100	0.127	0.153	0.179	0.210	0.246	0.294	0.363	0.494
	R2	0.068	0.082	0.095	0.107	0.122	0.141	0.171	0.225	0.310	0.077	0.099	0.118	0.137	0.160	0.187	0.225	0.294	0.421
	R3	0.059	0.075	0.088	0.101</														

$$\theta_{\text{nom}} = 800^{\circ}\text{C}$$

$p_{f,fi} \rightarrow$	0.10	0.20	0.30	0.40	0.50	0.60	0.70	0.80	0.90	0.10	0.20	0.30	0.40	0.50	0.60	0.70	0.80	0.90	
$\beta_{f,fi} \rightarrow$	1.28	0.84	0.52	0.40	0.00	-0.25	-0.52	-0.84	-1.28	1.28	0.84	0.52	0.40	0.00	-0.25	-0.52	-0.84	-1.28	
$\delta_{of} \rightarrow$	1.15	1.02	0.94	0.88	0.82	0.77	0.72	0.67	0.60	1.15	1.02	0.94	0.88	0.82	0.77	0.72	0.67	0.60	
$\alpha=0.00$										$\alpha=0.25$									
$\lambda_{20^{\circ}\text{C}}=0.00$	R1	0.071	0.090	0.108	0.127	0.149	0.175	0.201	0.232	0.293	0.076	0.098	0.117	0.139	0.162	0.190	0.218	0.253	0.319
	R2	0.058	0.075	0.094	0.116	0.141	0.169	0.195	0.230	0.283	0.063	0.081	0.102	0.126	0.154	0.183	0.212	0.250	0.309
	R3	0.047	0.061	0.078	0.099	0.124	0.155	0.189	0.222	0.275	0.050	0.067	0.085	0.108	0.135	0.169	0.205	0.242	0.300
	R4	0.028	0.044	0.058	0.075	0.100	0.132	0.172	0.214	0.267	0.030	0.047	0.063	0.082	0.109	0.144	0.187	0.233	0.292
$\lambda_{20^{\circ}\text{C}}=0.25$	R1	0.059	0.075	0.090	0.106	0.125	0.146	0.168	0.195	0.249	0.064	0.081	0.098	0.116	0.136	0.159	0.183	0.213	0.272
	R2	0.048	0.062	0.078	0.096	0.118	0.141	0.164	0.193	0.238	0.052	0.068	0.085	0.105	0.129	0.153	0.178	0.210	0.260
	R3	0.039	0.051	0.065	0.083	0.104	0.130	0.159	0.188	0.230	0.042	0.056	0.071	0.090	0.113	0.142	0.173	0.205	0.252
	R4	0.025	0.038	0.050	0.065	0.086	0.114	0.146	0.181	0.224	0.027	0.041	0.054	0.071	0.094	0.124	0.159	0.197	0.245
$\lambda_{20^{\circ}\text{C}}=0.50$	R1	0.048	0.060	0.071	0.083	0.097	0.112	0.128	0.148	0.189	0.053	0.065	0.078	0.091	0.105	0.122	0.140	0.162	0.206
	R2	0.040	0.051	0.063	0.076	0.092	0.108	0.125	0.147	0.181	0.044	0.056	0.068	0.083	0.100	0.117	0.136	0.160	0.198
	R3	0.033	0.043	0.054	0.066	0.081	0.101	0.121	0.143	0.175	0.035	0.047	0.058	0.072	0.089	0.109	0.132	0.156	0.191
	R4	0.021	0.032	0.042	0.054	0.069	0.089	0.112	0.138	0.170	0.023	0.035	0.045	0.058	0.075	0.096	0.122	0.150	0.186
$\lambda_{20^{\circ}\text{C}}=0.75$	R1	0.042	0.050	0.058	0.067	0.075	0.086	0.097	0.111	0.141	0.045	0.055	0.064	0.072	0.082	0.093	0.105	0.121	0.153
	R2	0.035	0.044	0.053	0.062	0.072	0.083	0.094	0.110	0.135	0.039	0.048	0.057	0.067	0.078	0.090	0.103	0.119	0.148
	R3	0.029	0.038	0.046	0.055	0.066	0.078	0.092	0.107	0.131	0.032	0.041	0.050	0.060	0.071	0.085	0.100	0.117	0.143
	R4	0.019	0.028	0.037	0.046	0.057	0.070	0.086	0.103	0.127	0.020	0.031	0.040	0.050	0.062	0.076	0.093	0.113	0.139
$\lambda_{20^{\circ}\text{C}}=1.00$	R1	0.036	0.042	0.048	0.054	0.060	0.066	0.074	0.084	0.106	0.039	0.046	0.052	0.058	0.065	0.072	0.081	0.092	0.115
	R2	0.031	0.038	0.044	0.051	0.058	0.065	0.073	0.083	0.101	0.034	0.041	0.048	0.055	0.063	0.070	0.079	0.091	0.111
	R3	0.026	0.033	0.039	0.046	0.053	0.061	0.071	0.082	0.099	0.028	0.036	0.043	0.050	0.058	0.067	0.077	0.089	0.108
	R4	0.017	0.025	0.032	0.040	0.047	0.056	0.067	0.079	0.096	0.018	0.027	0.035	0.043	0.052	0.061	0.072	0.086	0.105
$\lambda_{20^{\circ}\text{C}}=1.50$	R1	0.022	0.026	0.029	0.032	0.035	0.038	0.042	0.047	0.059	0.024	0.028	0.031	0.034	0.038	0.041	0.046	0.052	0.064
	R2	0.019	0.023	0.027	0.030	0.034	0.037	0.041	0.047	0.057	0.021	0.025	0.029	0.033	0.037	0.041	0.045	0.051	0.062
	R3	0.016	0.020	0.024	0.028	0.032	0.036	0.040	0.046	0.055	0.017	0.022	0.026	0.030	0.034	0.039	0.044	0.050	0.060
	R4	0.010	0.016	0.020	0.024	0.029	0.033	0.038	0.045	0.054	0.011	0.017	0.022	0.026	0.031	0.036	0.042	0.049	0.059
$\lambda_{20^{\circ}\text{C}}=2.00$	R1	0.013	0.016	0.017	0.019	0.021	0.023	0.025	0.028	0.035	0.014	0.017	0.019	0.021	0.023	0.025	0.027	0.031	0.038
	R2	0.012	0.014	0.016	0.018	0.020	0.022	0.025	0.028	0.034	0.013	0.015	0.018	0.020	0.022	0.024	0.027	0.030	0.037
	R3	0.010	0.013	0.015	0.017	0.019	0.021	0.024	0.027	0.033	0.011	0.014	0.016	0.018	0.021	0.023	0.026	0.030	0.036
	R4	0.006	0.010	0.012	0.015	0.017	0.020	0.023	0.027	0.032	0.007	0.010	0.013	0.016	0.019	0.022	0.025	0.029	0.035
$\alpha=0.50$										$\alpha=0.75$									
$\lambda_{20^{\circ}\text{C}}=0.00$	R1	0.086	0.110	0.133	0.157	0.184	0.215	0.250	0.293	0.372	0.101	0.134	0.166	0.198	0.233	0.274	0.326	0.394	0.518
	R2	0.071	0.092	0.116	0.143	0.175	0.207	0.243	0.290	0.360	0.085	0.115	0.145	0.180	0.219	0.263	0.315	0.390	0.498
	R3	0.057	0.076	0.097	0.122	0.154	0.191	0.234	0.280	0.349	0.067	0.095	0.122	0.155	0.194	0.242	0.302	0.375	0.489
	R4	0.034	0.054	0.072	0.094	0.124	0.164	0.213	0.268	0.341	0.040	0.065	0.091	0.120	0.157	0.206	0.269	0.355	0.477
$\lambda_{20^{\circ}\text{C}}=0.25$	R1	0.071	0.092	0.111	0.131	0.154	0.180	0.210	0.246	0.316	0.084	0.112	0.138	0.165	0.195	0.229	0.274	0.331	0.438
	R2	0.059	0.077	0.096	0.119	0.146	0.174	0.204	0.243	0.304	0.070	0.096	0.121	0.150	0.184	0.221	0.264	0.327	0.425
	R3	0.047	0.063	0.081	0.103	0.129	0.161	0.198	0.237	0.294	0.056	0.079	0.102	0.130	0.163	0.203	0.254	0.318	0.412
	R4	0.030	0.046	0.062	0.081	0.107	0.141	0.181	0.227	0.288	0.036	0.057	0.078	0.103	0.136	0.179	0.231	0.300	0.402
$\lambda_{20^{\circ}\text{C}}=0.50$	R1	0.059	0.074	0.088	0.103	0.119	0.138	0.160	0.187	0.240	0.069	0.090	0.109	0.129	0.151	0.177	0.209	0.253	0.332
	R2	0.049	0.063	0.078	0.094	0.113	0.134	0.155	0.185	0.231	0.058	0.078	0.097	0.119	0.143	0.171	0.203	0.249	0.323
	R3	0.040	0.053	0.066	0.082	0.101	0.124	0.151	0.180	0.224	0.047	0.066	0.084	0.103	0.128	0.157	0.195	0.242	0.313
	R4	0.026	0.039	0.052	0.067	0.085	0.110	0.139	0.173	0.218	0.030	0.048	0.065	0.085	0.108	0.139	0.178	0.229	0.305
$\lambda_{20^{\circ}\text{C}}=0.75$	R1	0.050	0.062	0.072	0.082	0.093	0.106	0.121	0.140	0.179	0.058	0.074	0.089	0.103	0.118	0.137	0.160	0.190	0.248
	R2	0.043	0.054	0.065	0.077	0.089	0.103	0.118	0.138	0.173	0.050	0.067	0.081	0.097	0.114	0.133	0.155	0.188	0.239
	R3	0.035	0.046	0.057	0.068	0.081	0.096	0.115	0.135	0.167	0.041	0.057	0.071	0.086	0.103	0.123	0.150	0.183	0.233
	R4	0.023	0.035	0.046	0.057	0.071	0.087	0.106	0.130	0.162	0.027	0.042	0.057	0.072	0.090	0.111	0.138	0.174	0.229
$\lambda_{20^{\circ}\text{C}}=1.00$	R1	0.043	0.052	0.059	0.066	0.074	0.083	0.093	0.106	0.135	0.048	0.061	0.072	0.083	0.095	0.108	0.124	0.145	0.187
	R2	0.037	0.046	0.054	0.063	0.071	0.081	0.091	0.106	0.130	0.043	0.056	0.067	0.079	0.091	0.105	0.121	0.144	0.182
	R3	0.031	0.040	0.049	0.057	0													

$\theta_{\text{nom}} = 900^{\circ}\text{C}$

$p_{f,fi} \rightarrow$	0.10	0.20	0.30	0.40	0.50	0.60	0.70	0.80	0.90	0.10	0.20	0.30	0.40	0.50	0.60	0.70	0.80	0.90	
$\beta_{f,fi} \rightarrow$	1.28	0.84	0.52	0.40	0.00	-0.25	-0.52	-0.84	-1.28	1.28	0.84	0.52	0.40	0.00	-0.25	-0.52	-0.84	-1.28	
$\delta_{of} \rightarrow$	1.15	1.02	0.94	0.88	0.82	0.77	0.72	0.67	0.60	1.15	1.02	0.94	0.88	0.82	0.77	0.72	0.67	0.60	
	$\alpha=0.00$									$\alpha=0.25$									
$\lambda_{20^{\circ}\text{C}}=0.00$	R1	0.052	0.062	0.071	0.080	0.089	0.101	0.119	0.148	0.212	0.056	0.067	0.077	0.087	0.097	0.110	0.130	0.161	0.230
	R2	0.040	0.049	0.058	0.068	0.081	0.099	0.110	0.146	0.203	0.043	0.053	0.063	0.074	0.089	0.107	0.121	0.159	0.221
	R3	0.025	0.036	0.046	0.055	0.066	0.082	0.106	0.142	0.185	0.027	0.039	0.049	0.060	0.072	0.089	0.115	0.155	0.202
	R4	0.004	0.019	0.032	0.043	0.056	0.073	0.101	0.125	0.151	0.004	0.021	0.034	0.047	0.061	0.079	0.109	0.136	0.165
$\lambda_{20^{\circ}\text{C}}=0.25$	R1	0.043	0.051	0.059	0.066	0.074	0.084	0.100	0.132	0.183	0.047	0.056	0.064	0.072	0.081	0.092	0.108	0.144	0.199
	R2	0.033	0.041	0.048	0.057	0.068	0.082	0.093	0.123	0.172	0.036	0.044	0.052	0.062	0.074	0.090	0.102	0.134	0.187
	R3	0.022	0.031	0.038	0.046	0.057	0.071	0.092	0.120	0.155	0.023	0.033	0.042	0.050	0.063	0.077	0.100	0.131	0.169
	R4	0.014	0.024	0.034	0.044	0.054	0.068	0.089	0.105	0.126	0.015	0.027	0.037	0.048	0.059	0.074	0.097	0.114	0.138
$\lambda_{20^{\circ}\text{C}}=0.50$	R1	0.036	0.043	0.049	0.054	0.060	0.068	0.079	0.102	0.139	0.039	0.047	0.053	0.059	0.065	0.074	0.086	0.111	0.151
	R2	0.028	0.035	0.041	0.047	0.055	0.066	0.075	0.096	0.131	0.030	0.038	0.044	0.051	0.060	0.071	0.081	0.104	0.143
	R3	0.018	0.026	0.032	0.039	0.048	0.058	0.073	0.093	0.119	0.020	0.028	0.035	0.042	0.052	0.063	0.079	0.102	0.130
	R4	0.012	0.021	0.029	0.037	0.045	0.055	0.071	0.083	0.099	0.013	0.022	0.031	0.040	0.049	0.060	0.077	0.090	0.107
$\lambda_{20^{\circ}\text{C}}=0.75$	R1	0.032	0.038	0.042	0.047	0.051	0.057	0.064	0.079	0.104	0.035	0.041	0.046	0.051	0.056	0.062	0.070	0.086	0.114
	R2	0.025	0.031	0.036	0.041	0.048	0.055	0.062	0.075	0.099	0.027	0.033	0.039	0.045	0.052	0.060	0.067	0.082	0.108
	R3	0.016	0.023	0.029	0.035	0.042	0.050	0.060	0.074	0.092	0.018	0.025	0.031	0.038	0.046	0.054	0.065	0.081	0.100
	R4	0.010	0.018	0.026	0.033	0.040	0.048	0.059	0.068	0.079	0.011	0.020	0.028	0.036	0.043	0.052	0.064	0.074	0.086
$\lambda_{20^{\circ}\text{C}}=1.00$	R1	0.028	0.033	0.037	0.040	0.044	0.048	0.053	0.063	0.080	0.030	0.036	0.040	0.043	0.047	0.052	0.058	0.068	0.088
	R2	0.022	0.027	0.032	0.036	0.041	0.047	0.051	0.061	0.076	0.024	0.029	0.034	0.039	0.045	0.051	0.056	0.066	0.083
	R3	0.014	0.020	0.025	0.031	0.036	0.042	0.050	0.060	0.072	0.016	0.022	0.028	0.033	0.040	0.046	0.055	0.065	0.078
	R4	0.009	0.016	0.023	0.029	0.035	0.041	0.049	0.056	0.064	0.010	0.018	0.025	0.032	0.038	0.045	0.054	0.061	0.070
$\lambda_{20^{\circ}\text{C}}=1.50$	R1	0.018	0.020	0.023	0.025	0.027	0.029	0.032	0.037	0.046	0.019	0.022	0.025	0.027	0.029	0.032	0.035	0.040	0.050
	R2	0.014	0.017	0.020	0.022	0.025	0.028	0.031	0.036	0.043	0.015	0.018	0.021	0.024	0.028	0.031	0.034	0.039	0.047
	R3	0.009	0.013	0.016	0.019	0.023	0.026	0.030	0.035	0.042	0.010	0.014	0.017	0.021	0.025	0.028	0.033	0.038	0.046
	R4	0.006	0.010	0.014	0.018	0.022	0.025	0.030	0.034	0.039	0.006	0.011	0.015	0.020	0.024	0.028	0.032	0.037	0.042
$\lambda_{20^{\circ}\text{C}}=2.00$	R1	0.011	0.012	0.014	0.015	0.016	0.018	0.020	0.022	0.027	0.012	0.013	0.015	0.016	0.018	0.019	0.021	0.024	0.030
	R2	0.008	0.010	0.012	0.014	0.015	0.017	0.019	0.022	0.026	0.009	0.011	0.013	0.015	0.017	0.019	0.020	0.024	0.028
	R3	0.005	0.008	0.010	0.012	0.014	0.016	0.018	0.021	0.025	0.006	0.008	0.011	0.013	0.015	0.017	0.020	0.023	0.027
	R4	0.004	0.006	0.009	0.011	0.013	0.015	0.018	0.021	0.023	0.004	0.007	0.009	0.012	0.014	0.017	0.020	0.022	0.025
	$\alpha=0.50$									$\alpha=0.75$									
$\lambda_{20^{\circ}\text{C}}=0.00$	R1	0.063	0.075	0.087	0.099	0.111	0.126	0.149	0.184	0.266	0.072	0.091	0.108	0.125	0.143	0.165	0.199	0.242	0.354
	R2	0.048	0.060	0.072	0.085	0.101	0.123	0.139	0.181	0.254	0.056	0.074	0.091	0.109	0.132	0.161	0.185	0.239	0.338
	R3	0.030	0.044	0.056	0.068	0.082	0.102	0.133	0.178	0.233	0.036	0.053	0.070	0.087	0.107	0.133	0.172	0.231	0.316
	R4	0.005	0.024	0.039	0.053	0.069	0.091	0.125	0.159	0.192	0.006	0.028	0.047	0.067	0.089	0.118	0.161	0.217	0.269
$\lambda_{20^{\circ}\text{C}}=0.25$	R1	0.052	0.063	0.072	0.082	0.092	0.105	0.125	0.163	0.231	0.060	0.076	0.090	0.104	0.119	0.138	0.167	0.210	0.317
	R2	0.040	0.050	0.060	0.071	0.085	0.102	0.117	0.154	0.216	0.046	0.061	0.076	0.091	0.110	0.134	0.155	0.203	0.287
	R3	0.026	0.037	0.047	0.057	0.072	0.088	0.115	0.150	0.195	0.031	0.045	0.059	0.073	0.094	0.116	0.150	0.197	0.266
	R4	0.017	0.030	0.042	0.055	0.068	0.086	0.111	0.133	0.161	0.020	0.037	0.053	0.070	0.089	0.112	0.145	0.182	0.225
$\lambda_{20^{\circ}\text{C}}=0.50$	R1	0.044	0.052	0.060	0.067	0.075	0.085	0.099	0.126	0.175	0.050	0.063	0.074	0.085	0.097	0.111	0.132	0.163	0.240
	R2	0.034	0.042	0.050	0.059	0.069	0.082	0.093	0.119	0.164	0.039	0.052	0.063	0.076	0.090	0.108	0.124	0.158	0.221
	R3	0.022	0.032	0.040	0.048	0.060	0.072	0.091	0.117	0.150	0.026	0.038	0.049	0.061	0.078	0.094	0.119	0.153	0.205
	R4	0.014	0.025	0.036	0.046	0.056	0.069	0.088	0.105	0.126	0.017	0.031	0.044	0.058	0.073	0.090	0.115	0.144	0.177
$\lambda_{20^{\circ}\text{C}}=0.75$	R1	0.039	0.046	0.052	0.058	0.064	0.071	0.081	0.098	0.133	0.043	0.055	0.064	0.073	0.082	0.094	0.109	0.129	0.183
	R2	0.030	0.038	0.044	0.052	0.060	0.069	0.077	0.094	0.125	0.035	0.046	0.055	0.066	0.078	0.091	0.104	0.127	0.169
	R3	0.020	0.028	0.035	0.043	0.053	0.062	0.075	0.093	0.116	0.023	0.034	0.044	0.054	0.067	0.081	0.100	0.123	0.160
	R4	0.013	0.023	0.032	0.041	0.049	0.060	0.073	0.086	0.101	0.015	0.027	0.039	0.051	0.064	0.078	0.096	0.119	0.143
$\lambda_{20^{\circ}\text{C}}=1.00$	R1	0.034	0.040	0.045	0.049	0.054	0.060	0.067	0.078	0.102	0.037	0.047	0.055	0.062	0.070	0.079	0.090	0.105	0.142
	R2	0.026	0.033	0.039	0.045	0.051	0.058	0.064	0.076	0.096	0.030	0.040	0.048	0.057	0.066	0.077	0.087	0.104	0.132
	R3	0.017	0.025	0.031	0.037														

List of figures

Figure 2.1: Column with imperfection	20
Figure 2.2: Graphical representation of the Somaini's methods	23
Figure 2.3: Performance of Somaini method vs. FEM.....	23
Figure 3.1: Meshing density along the column axis	26
Figure 3.2: Section meshing	26
Figure 3.3: Influence of the section mesh density on the buckling factor	27
Figure 3.4: Restraint influence analysis – frame 1	31
Figure 3.5: Restraint influence analysis – frame 2	31
Figure 3.6: Local imperfection according to EN 10034	33
Figure 3.7: Local imperfection according to EN 1991-1-5 Annex C.....	33
Figure 3.8: Local buckling shape example	34
Figure 3.9: Wall imperfections along column length	34
Figure 3.10: Influence of local imperfection on the buckling capacity	35
Figure 3.11: Beam element kinematics.....	36
Figure 3.12: Beam section mesh	36
Figure 3.13: Eurocode 3 material models for carbon steel in elevated temperature conditions.....	38
Figure 3.14: Eurocode 3 reduction coefficients for carbon steel in elevated temperature conditions.....	39
Figure 3.15: ECCS material model for carbon steel in elevated temperature conditions ..	39
Figure 3.16: Lie material model for carbon steel in elevated temperature conditions ..	40
Figure 3.17: Poh material model for carbon steel in elevated temperature conditions	42
Figure 3.18: Variation of reduction coefficients for effective yield strength and elastic modulus	43
Figure 3.19: Comparison of the material models	44
Figure 3.20: Buckling curves for different material models	45
Figure 3.21: Residual stress distribution patterns	46
Figure 4.1: Schematic distributions of action E and resistance R	48
Figure 4.2: Reliability index	49
Figure 4.3: Relation between p_{fire} , $p_{f.fi.t}$, $\beta_{f.fi.t}$ and δ_{af} corresponding to the target failure probability $p_t = 7.235 \times 10^{-5}$	52
Figure 4.4: Fully-deterministic safety concept	58
Figure 4.5: Semi-probabilistic safety concept	58
Figure 4.6: Fully-probabilistic safety concept	59
Figure 4.7: Failure probabilities in the ultimate limit state.....	59
Figure 5.1: Bending stiffness reduction curves for various section S355 in ambient conditions.....	64
Figure 5.2: Bending stiffness reduction for HEA500 S355 strong axis in elevated temperature conditions	65

Figure 5.3: Bending stiffness reduction for HEA500 S355 weak axis in elevated temperature conditions	65
Figure 5.4: Bending stiffness path for S355 HEA500 strong axis 20°C conditions	66
Figure 5.5: Bending stiffness path for S355 HEA500 strong axis 500°C conditions	66
Figure 5.6: Deformed shape prior to buckling of the HEA500 S355 columns	67
Figure 5.7: Stress profiles along the HEA500 S235 column prior to buckling at $\theta=200^{\circ}\text{C}$..	69
Figure 5.8: Stress profiles along the HEA500 S235 column prior to buckling at $\theta=500^{\circ}\text{C}$..	70
Figure 5.9: Stress profiles along the HEA500 S235 prior to buckling at $\theta=900^{\circ}\text{C}$	71
Figure 5.10: Stress distribution inside the mid-section prior to failure for the strong axis buckling of the HEA500 S355 column	74
Figure 5.11: Stress distribution inside the mid-section prior to failure for the weak axis buckling of the HEA500 S355 column	75
Figure 5.12: Residual stress influence on the bending stiffness	77
Figure 5.13: Residual stresses influence on the buckling factor for I-type section strong axis (I-Y) in case $h/b \leq 1.2$	78
Figure 5.14: Residual stresses influence on the buckling factor for I-type section strong axis (I-Y) in case $h/b > 1.2$	78
Figure 5.15: Residual stresses influence on the buckling factor for I-type section weak axis (I-Z) in case $h/b \leq 1.2$	79
Figure 5.16: Residual stresses influence on the buckling factor for I-type section weak axis (I-Z) in case $h/b > 1.2$	79
Figure 5.17: Residual stresses influence on the buckling factor for RHS-type section ...	80
Figure 5.18: Residual stresses influence on the buckling factor for CHS-type section ...	80
Figure 5.19: Buckling factors according to numeric modelling and EN 1993-1-2: S235 .	81
Figure 5.20: Column section scheme for Method C.....	85
Figure 5.21: Method C performance against non-linear FEM for the strong axis buckling .	91
Figure 5.22: Method C performance against non-linear FEM for the weak axis buckling .	92
Figure 5.23: Control parameters g_1 and g_2 for the strong axis buckling	93
Figure 5.24: Control parameters g_1 and g_2 for the weak axis buckling	93
Figure 5.25: Method C performance for the strong axis buckling after model improvement	94
Figure 5.26: Method C performance for the weak axis buckling after model improvement	95
Figure 5.27: Validation against test results.....	99
Figure 6.1: Sensitivity analysis results – sensitivity indices S_i in case of the deterministic temperature variable	106
Figure 6.2: pdf for the maximum steel section temperature.....	108
Figure 6.3: Selected pdf for the maximum steel section temperature – part 1.....	109
Figure 6.4: Selected pdf for the maximum steel section temperature – part 2.....	110
Figure 6.5: Selected pdf for the maximum steel section temperature – part 3.....	111
Figure 6.6: Resistance function distributions for slenderness value $\lambda_{20^{\circ}\text{C}} = 0.0$	113

Figure 6.7: Resistance function distributions for the selected temperature distributions and for slenderness value $\lambda_{20^{\circ}\text{C}} = 0.0$	114
Figure 6.8: Failure probability $p_{f,fi}$ dependence on the mean temperature: S355 $\lambda_{20^{\circ}\text{C}} = 0.0$ $\alpha = 0.0$	116
Figure 6.9: Temperature distributions corresponding to the minimum and maximum failure probabilities in the temperature subrange $500^{\circ}\text{C} - 510^{\circ}\text{C}$	116
Figure 6.10: Failure probability $p_{f,fi}$ and reliability index $\beta_{f,fi}$ for S355 steel column strong axis in case of the imposed variable load Q – part 1.....	117
Figure 6.11: Failure probability $p_{f,fi}$ and reliability index $\beta_{f,fi}$ for S355 steel column strong axis in case of the imposed variable load Q – part 2.....	118
Figure 6.12: Influence of the variable load type (left column) and steel class / buckling axis (right column) on the R4 failure probability – part 1	119
Figure 6.13: Influence of the variable load type (left column) and steel class / buckling axis (right column) on the R4 failure probability – part 2	120
Figure 6.14: Dependence between failure probability $p_{f,fi}$ and factor $\mu(\theta)/\theta_{nom}$	121
Figure 6.15: Example of the ranking process for temperature subranges $500-510^{\circ}\text{C}$ and $650-660^{\circ}\text{C}$	122
Figure 6.16: Factor R dependence on the θ_{nom} and ranking limits	122
Figure 6.17: Ranking system testing results	123
Figure 6.18: COV as a function of mean temperature.....	124
Figure 6.19: Technique for the implementation of the MCS with OZone.....	126
Figure 6.20: Failure probability marking for different fire evolution models	126
Figure 6.21: Ranking example of $c_{fi} - p_{f,fi}$ curve	127
Figure 6.22: Failure probability as a function of factor c_{fi} for different mean temperature values of the S355 column, strong axis buckling.....	128
Figure 6.23: Design method example – thermal calculations results	132
Figure 6.24: Validation of the proposed method – part 1	134
Figure 6.25: Validation of the proposed method – part 2	135
Figure 6.26: Failure probabilities for the current EN methodology – part 1.....	136
Figure 6.27: Failure probabilities for the current EN methodology – part 2.....	137
Figure 6.28: Proposed method vs. EC method – part 1	137
Figure 6.29: Proposed method vs. EC method – part 2	137

List of labels

Table 3-1: Descriptive statistics for beam vs. shell models.....	26
Table 3-2: Influence of loading history (HEA500 S355 strong axis $\theta=500^{\circ}\text{C}$)	28
Table 3-3: Influence of thermal elongation (HEA500 S355 strong axis $\theta=500^{\circ}\text{C}$)	29
Table 3-4: Influence of thermal elongation (HEA500 S355 strong axis $\theta=900^{\circ}\text{C}$)	29
Table 3-5: Influence of the restraint	30
Table 3-6: Section classification – b/t ratio limit values.....	32
Table 3-7: Descriptive statistics for composed procedure vs. ANSYS models	37
Table 3-8: Eurocode 3 material model parameters for carbon steel in elevated temperature conditions	40
Table 3-9: ECCS material model parametrs for carbon steel in elevated temperature conditions.....	40
Table 3-10: Lie material models parametrs for carbon steel in elevated temperature conditions.....	41
Table 3-11: Poh material models parametrs for carbon steel in elevated temperature conditions.....	42
Table 4-1: Target reliability index values according to EN 1990	50
Table 4-2: Probability of severe fire p_1	51
Table 4-3: Reduction factor p_2	51
Table 4-4: Reduction factor p_3	51
Table 4-5: Reduction factor p_4	51
Table 4-6: Probability of ignition p_{ign}	52
Table 4-7: Probability of flashover p_{fi}	52
Table 4-8: Factor δ_{q1}	53
Table 4-9: Factor δ_{q2}	53
Table 4-10: Factor δ_n	53
Table 4-11: Resistance uncertainties summary	55
Table 4-12: Statistical parameters of variable load	56
Table 4-13: Temperature uncertainties summary	56
Table 4-14: Descriptive statistics for the factor $N_{\text{Rd.fi.pln}}/N_{\text{Rd.fi.FEM}}$	61
Table 4-15: Descriptive statistics for the factor $N_{\text{Rd.fi.spl}}/N_{\text{Rd.fi.fem}}$	61
Table 5-1: Sections used for numerical modelling	63
Table 5-2: Stress at buckling for S235	72
Table 5-3: Stress at buckling for S355	72
Table 5-4: Stress at buckling for S460	73
Table 5-5: Descriptive statistics for individual buckling factor χ_i vs. group average buckling factor $\chi_{\text{gr.mean}}$	77
Table 5-6: Buckling factor differences between section groups	82
Table 5-7: Buckling factor differences between materials	83
Table 5-8: Buckling factor differences between FEM vs. EC3	84
Table 5-9: Polynomial coefficients for g_1 and g_2	93

Table 5-10: Control parameter g_3 values	93
Table 5-11: Validation against test series from SCOFIDAT	100
Table 5-12: Validation against test series from ETHZ	101
Table 5-13: Validation against test series – descriptive statistics	101
Table 6-1: Resistance related uncertainties: HEB200 S355	104
Table 6-2: Temperature related uncertainties	104
Table 6-3: Sensitivity analysis results – sensitivity indices S_i in case of the stochastic thermal variables	107
Table 6-4: Factor χ_{Rel} : $\theta_{\text{nom}} = 500^\circ\text{C}$ S355 strong axis imposed (Q) variable load type ..	130
Table 6-5: Design method example – results summary part 1	132
Table 6-6: Design method example – results summary part 2	133

References

- [1] J. Hutchinson, "Plastic Buckling," *Advances in applied mechanics*, vol. 14, pp. 67-144, 1974.
- [2] S. Timoshenko, *History of Strength of Materials*, 1953.
- [3] T. Lin, *Theory of Inelastic Structures*, 1968.
- [4] F. Shanley, "The column paradox," *Journal of Aeronautical Science*, vol. 13(5), p. 678, 1946.
- [5] F. Shanley, "Inelastic Column Theory," *Journal of Aeronautical Science*, vol. 14(5), pp. 261-267, 1947.
- [6] W. Ayrton and J. Perry, "On Struts," *The Engineer*, 1886.
- [7] A. Robertson, "The Strength of Struts," *ICE Selected Engineering Papers*, vol. 28, 1925.
- [8] H. Beer and G. Schulz, "Bases théoriques des courbes européennes de flambement," *Construction métallique*, vol. 3, pp. 35-57, 1970.
- [9] D. Sfintesco, "Fondement expérimental des courbes européennes de flambement," *Construction métallique*, vol. 3, pp. 5-12, 1970.
- [10] J. Strating and H. Vos, "Computer simulation of the ECCS buckling curve using a Monte-Carlo Method," *HERON*, vol. 19, no. 2, 1973.
- [11] O. Vassart, B. Zhao, L. Cajot, F. Robert, U. Meyer and A. Frangi, "Eurocodes: Background ja Applications Structural Fire Design.," *JRC Report*, 2014.
- [12] European committee for standardization, EN1991-1-2: General Actions – Actions on structures exposed to fire, Brussels (Belgium), 2002.
- [13] Society of Fire Protection Engineers, SFPE Handbook of Fire Protection Engineering, Quincy, Massachusetts, 2002.
- [14] O. Pettersson, S. Magnusson and J. Thor, *Fire Engineering Design of Steel Structures*, Sweden, 1976.
- [15] V. Babrauskas, Compf2: a program for calculating post-flashover fire temperatures, 1979.
- [16] J. Cadorin and J. Franssen, "A tool to design steel elements submitted to compartment fires—OZone V2. Part 1: pre-and post-flashover compartment fire model," *Fire Safety Journal*, vol. 38, no. 5, pp. 395-427, 2003.
- [17] K. McGrattan, R. McDermott, S. Hostikka and J. Floyd, *Fire dynamics simulator user's guide*, NIST, 2010.
- [18] J. Schleich and L. Cajot, "Natural fire safety concept – Full scale tests, implementation in the Eurocodes and development of a user-friendly design tool," *ECSC Research 7210-060 1997-2000*, 2003.
- [19] J. Schleich and L. Cajot, "Competitive steel buildings through natural fire safety," *ECSC Research*, 2002.
- [20] European committee for standardization, EN1993-1-2: Design of Steel Structures: General Rules, Structural Fire Design, Brussels (Belgium), 2005.
- [21] D. Talamona, M. Fransen, J. Schelicj and J. Kruppa, "Stability of steel columns in case of fire: Numerical modelling," *Journal of Structural Engineering*, vol. 123, no. 6, pp. 713-720, 1997.
- [22] J. Franssen, D. Talamona, J. Kruppa and L. Cajot, "Stability of steel columns in fire: Experimental Evaluation," *Journal of Structural Engineering*, vol. 124, no. 2, pp. 156-163, 1998.

- [23] M. Knobloch, D. Somaini, J. Pauli and M. Fontana, "Stability of steel columns in fire," *Proceedings of the SDSS'Rio 2010 International Colloquium Stability and Ductility of Steel Structures*, pp. 465-472, 2010.
- [24] P. Vila Real, N. Lopes, L. Simoes da Silva, P. Piloto and F. JM, "Numerical modelling of steel beam-columns in case of fire – comparison with Eurocode 3," *Fire Safety Journal*, vol. 39, pp. 23-39, 2004.
- [25] W. Toh, K. Tan and T. Fung, "Compressive resistance of steel columns in fire: Rankine approach," *Journal of Structural Engineering*, vol. 126, no. 3, pp. 398-405, 2000.
- [26] D. Somaini, M. Knobloch and M. Fontana, "Buckling of steel columns in fire: non-linear behaviour and design proposal," *Steel Construction - Design and Research*, vol. 5, no. 3, pp. 175-182, 2012.
- [27] A. Kervalishvili and I. Talvik, "Alternative approach to buckling of square hollow section steel columns in fire," *Journal of Constructional Steel Research*, vol. 96, pp. 140-150, 2014.
- [28] A. Kervalishvili and I. Talvik, "Modified procedure for buckling of steel columns at elevated temperatures," *Journal of Constructional Steel Research*, vol. 127, pp. 108-119, 2016.
- [29] S. Timoshenko and J. Gere, *Theory of Elastic Stability* (2-nd edition), 1985.
- [30] J. Schleich, L. Gayot, J. Kruppa, D. Talamona, W. Azpizau, J. Unanue, L. Twilt, J. Fellinger, R. Van Foeken and J. Franssen, "Buckling curves of hot rolled H steel sections submitted to fire," *Technical steel research*, 1998.
- [31] I. Neves, J. Valente and J. Rodrigues, "Thermal restraint and fire resistance of columns," *Fire Safety Journal*, vol. 37, no. 8, pp. 753-771, 2002.
- [32] P. Wang, G. Li and Y. Wang, "Behaviour and design of restrained steel column in fire, Part 3: Practical design method," *Journal of Constructional Steel Research*, vol. 66, pp. 1422-1430, 2010.
- [33] T. Karman, "Untersuchungen über Knickfestigkeit," *Forschungshefte des Vereins deutscher Ingenieure*, vol. 81, 1910.
- [34] European committee for standardization, EN1990: Basis of structural design, Brussels (Belgium), 2001.
- [35] W. Liu and W. Bulleit, "Approximate reliability analysis of wood structural systems," *Structural Safety*, vol. 17, no. (2), pp. 59-78, 1995.
- [36] F. Biondini, F. Bontempi and P. Maleraba, "Fuzzy reliability analysis of concrete structures," *Computers & Structures*, vol. 82, no. 13-14, pp. 1033-1052, 2004.
- [37] Z. Kala, "Reliability analysis of the lateral torsional buckling resistance and the ultimate limit state of steel beams with random imperfections," *Journal of Civil Engineering and Management*, vol. 21, no. (7), pp. 902-911, 2015.
- [38] M. Chryssanthopoulos and T. Righiniotis, "Fatigue reliability of welded steel structures," *Journal of Constructional Steel Research*, vol. 62, no. 11, pp. 1199-1209, 2006.
- [39] S. Afshana, P. Francis, N. Baddoo and L. Gardner, "Reliability analysis of structural stainless steel design provisions," *Journal of Constructional Steel Research*, vol. 114, pp. 293-304, 2015.
- [40] N. Meinen and R. Steenbergen, "Reliability levels obtained by Eurocode partial factor design - A discussion on current and future reliability levels," *Heron*, vol. 63, 2018.

- [41] D. Honfi, A. Mårtensson and S. Thelandersson, "Reliability of beams according to Eurocodes in serviceability limit state," *Engineering Structures*, vol. 35, pp. 48-54, 2012.
- [42] O. Magnusson and S. Pettersson, "Rational design methodology for fire exposed load bearing structures," *Fire Safety Journal*, vol. 3, no. 4, pp. 224-241, 1981.
- [43] Q. Guo, K. Shi, Z. Jia and A. Jeffers, "Probabilistic Evaluation of Structural Fire Resistance," *Fire Technology*, vol. 49, pp. 793-811, 2012.
- [44] Q. Guo, Structural reliability assessment under fire, Michigan, 2015.
- [45] C. Zhang, Reliability of Steel Columns Protected by Intumescent Coatings Subjected to Natural Fires, Springer Theses, 2015.
- [46] M. Heidari, F. Robert, D. Lange and G. Rein, "Probabilistic Study of the resistance of a Simply-Supported Reinforced Concrete Slab According to Eurocode Parametric Fire," *Fire Technology*, vol. 55, pp. 1377-1404, 2018.
- [47] R. Van Coile, Reliability-Based Decision Making for Concrete Elements, Gent, 2014.
- [48] S. Devaney, Development of Software for Reliability Based desing of Steel Framed Structures in Fire, Edinburgh, 2014.
- [49] R. Van Coile, D. Hopkin, L. Bisby and R. Caspeelee, "The meaning of Beta: background and applicability of the target reliability index for normal conditions to structural fire engineering," *Procedia Engineering*, vol. 210, pp. 528-536, 2017.
- [50] D. Hopkin, S. Anastasov, K. Swinburne, D. Rush and R. Van Coile, "Applicability of ambient temperature reliability targets for appraising structures exposed to fire," *Proceedings of the Second International Conference on Structural Safety under Fire & Balst - CONFAB 2017*, 2017.
- [51] A. Vrouwenvelder, "Developments towards full probabilistic design codes," *Structural Safety*, vol. 24, pp. 417-432, 2002.
- [52] S. Iqbal and S. Harichandran, "Capacity Reduction and Fire Load Factors for Design of Steel Members Exposed to Fire," *Journal of Structural Engineering*, vol. 136, pp. 1554-1562, 2010.
- [53] ECCS Techinal Comitee 8, Strucutral stability - Manual on Stability 2-nd ed, 1976.
- [54] F. Ali, P. Shepherd, M. Randall, I. Simms, D. O'Connor and I. Burges, "The effect of axial restraint on the fire resistance of steel columns," *Journal of Constructional Steel Research*, vol. 46, pp. 305-306, 1998.
- [55] I. Bennets, C. Poh, A. O'Meagher and J. Thomas, Restraint of compression members in fire, Melbourne: Melbourne Research Lab. Report No. MRL/PSGS/89/002, 1989.
- [56] J. Franssen, "Failure temperature of a system comprising a restrained column submitted to fire," *Fire Safety Journal*, vol. 34, pp. 191-207, 2000.
- [57] European committee for standardization, EN1993-1-1: Design of steel strucutres - General rules and rules for buildings, Brussels (Belgium), 2005.
- [58] European committee for standardization, EN1993-1-5: Plated structural elements, Brussels (Belgium), 2006.
- [59] European committee for standardization, EN10034: Structural steel I and H sections. Tolerances on shape and dimensions, Brussels (Belgium), 1993.
- [60] J. Pauli, The Behaviour of Steel Columns in Fire: Material – Cross-sectional Capacity – Column Buckling, Zürich, 2012.
- [61] E. Maia, C. Couto, P. Vila Real and N. Lopes, "Critical temperatures of class 4 cross-sections," *Journal of Constructional Steel Research*, vol. 121, pp. 370-382, 2016.

- [62] L. Gardner and D. Nethercot, "Numerical modeling of stainless steel structural components - a consistent approach," *Journal of Structural Engineering*, vol. 10, pp. 1586-1601, 2004.
- [63] J. Pauli, D. Somaini, M. Knobloch and M. Fontana, EXPERIMENTS ON STEEL COLUMNS UNDER FIRE CONDITIONS, Zurich, 2012.
- [64] C. Couto, P. L. N. Vila Real and B. Zhao, "Resistance of steel cross-sections with local buckling at elevated temperatures," *Journal of Constructional Steel Research*, vol. 109, pp. 101-114, 2015.
- [65] J. Eaton, D. Bateman, S. Hauberg and R. Wehbring, GNU Octave version 3.8.1 manual: a high-level interactive language for numerical computations, 2014.
- [66] C. Felippa,
["https://www.colorado.edu/engineering/cas/courses.d/NFEM.d/NFEM.Ch11.d/NFEM.Ch11.Slides.d/NFEM.Ch11.Slides.pdf,"](https://www.colorado.edu/engineering/cas/courses.d/NFEM.d/NFEM.Ch11.d/NFEM.Ch11.Slides.d/NFEM.Ch11.Slides.pdf) [Online].
- [67] P. Austrell, O. Dahlblom, J. Lindemann, A. Olsson, K. Olsson, K. Persson, H. Petersson, M. Ristinmaa, G. Sandberg and P. Wernberg, CALFEM A Finite Element toolbox Version 3.4, Lund (Sweden), 2004.
- [68] G. Hu, M. Morovat, J. Lee, E. Schell and M. Engelhardt, "Elevated temperature properties of ASTM A992 steel," *Proceedings of the 2009 Structures Congress - Don't Mess with Structural Engineers*, pp. 1067-1076, 2009.
- [69] K. Poh, Behaviour of Load-Bearing Members in Fire, Victoria (Australia), 1998.
- [70] M. Seif, J. Main, J. Weigand, F. Sadek, L. Choe, C. Zhang, J. Gross, W. Luecke and D. McColskey, NIST Technical Note 1907: Temperature-Dependent Material Modeling for Structural Steels: Formulation and Application, 2016.
- [71] G. Williams-Leir, "Creep of structural-steel in fire - analytical expressions," *Fire and Materials*, vol. 7, pp. 73-78, 1983.
- [72] L. Twilt, "Strength and deformation properties of steel at elevated temperatures: Some practical implications," *Fire Safety Journal*, vol. 13, no. 1, pp. 9-15, 1988.
- [73] A. Buchanan, Structural design for fire safety, New York: Wiley, 2001.
- [74] B. Kirby and R. Preston, "High temperature properties of hot-rolled, structural steels for use in fire engineering design studies," *Fire Safety Journal*, vol. 13, pp. 27-37, 1988.
- [75] L. Twilt, "Stress-strain relationships of structural steel at elevated temperatures: Analysis of various options & European proposal, Part F: mechanical properties," *Report BI-91-015*, 1991.
- [76] ECCS Technical Committee 3, Fire Safety of Steel Structures - Calculation of the fire resistance of load bearing elements and structural assemblies exposed to the standard fire, Brussels, Belgium, 1983.
- [77] T. Lie, Structural Fire Protection: Manual of Practice, ASCE Manuals and Reports of Engineering Practice; no. 78. American Society of Civil Engineers, 1992.
- [78] K. Poh, "General Stress-Strain Equation," *Journal of Materials in Civil Engineering*, vol. 4, no. 9, pp. 214-217, 1997.
- [79] K. Poh, "Stress-strain-temperature relationship for structural steel," *Journal of Materials in Civil Engineering*, vol. 5, no. 13, pp. 371-379, 2001.
- [80] V. Kodur, M. Dwaikat and F. R., "High-Temperature Properties of Steel for Fire Resistance," *Journal of Materials in Civil Engineering*, vol. 22, no. 5, pp. 423-434, 2010.

- [81] J. Franssen, "Residual stresses in steel profiles submitted to the fire: an analogy," *Proceedings of the 3-rd CIB/W14 FSF workshop on modelling*, pp. 103-112, 1996.
- [82] P. Vila Real, R. Cazeli, L. Simoes da Silva, A. Santiago and P. Piloto, "The effect of residual stresses in the lateral-torsional buckling of steel I-beams at elevated temperature," *Journal of Constructional Steel Research*, vol. 60, pp. 783-793, 2004.
- [83] M. Holicky, Reliability analysis for structural design, Stellenbosch: SUM MeDIA, 2009.
- [84] JCSS, "Probabilistic Model Code Part 2: Load Models 2.20 Fire," *JCSS*, 2001.
- [85] J. Melcher, Z. Kala, M. Holicky, M. Fajkus and L. Rozlivka, "Design characteristics of structural steels based on statistical analysis of metallurgical properties," *Journal of Constructional Steel research*, vol. 60, pp. 795-808, 2004.
- [86] JCSS, "Probabilistic Model Code Part 3: Resistance Models 3.02 Structural Steel," *JCSS*, 2000.
- [87] Z. Kala, "Sensitivity assessment of steel members under compression," *Engineering Structures*, vol. 31, no. 6, pp. 1344-1348, 2009.
- [88] Z. Kala and J. Valeš, "Global sensitivity analysis of lateral-torsional buckling resistance based on finite element simulations," *Engineering Structures*, vol. 134, p. 37-47, 2017.
- [89] Z. Kala, "Reliability analysis of the lateral torsional buckling resistance and the ultimate limit state of steel beams with random imperfections," *Journal of Civil Engineering and Management*, vol. 21, no. 7, p. 902-911, 2015.
- [90] JCSS, "Probabilistic Model Code Part 2: Load Models 2.00 General Principles," 2001.
- [91] JCSS, "Probabilistic Model Code Part 3: Resistance Models 3.9 Model uncertainties," *JCSS*, 2000.
- [92] X. Zhang, Efficient Computational Methods for Structural Reliability and Global Sensitivity Analyses, Waterloo, Canada: University of Waterloo, 2013.
- [93] H. Gulvanessian, J. Calgaro and M. Holicky, Designers' Guide to EN 1990 Eurocode: Basis of Structural Design.
- [94] A. Saltelli, S. Tarantola, F. Campolongo and M. Ratto, Sensitivity analysis in practice: A guide to assessing scientific models, John Wiley and Son: New York, 2004.
- [95] G. Soares, "Uncertainty modelling in plate buckling," *Structural Safety*, vol. 5, no. 1, pp. 17-34, 1988.
- [96] Y. Fukumoto, Y. Itoh and M. Kubo, "Strength variation of laterally unsupported beams," *Journal of the Structural Division*, vol. 106, no. 1, pp. 165-181, 1980.
- [97] Z. Kala, "Global sensitivity analysis in stability problems of steel frame structure," *Journal of Civil Engineering and Management*, vol. 22, no. 3, pp. 417-424, 2016.
- [98] J. Cadorin and J. Franssen, "A tool to design steel elements submitted to compartment fires - OZone V2. Part 1: pre- and postflashover compartment fire model," *Fire Safety Journal*, vol. 38, no. 5, pp. 395-427, 2003.
- [99] J. Schleich and L. Cajot, "Competitive steel buildings through natural fire safety," *ECSC Research*, 2002.

Acknowledgements

This acknowledgements section is unconventional. Readers sensitive to the literary ignorance are advised to skip this section.

Undertaking PhD studies has been a literally life-changing experience taking into account the time it took for me to reach this particular moment of writing an acknowledgement section. I must admit that I feel no discomfort in perception of the fact that 13 years have passed since I have entered PhD studies. This is mostly due to the fact that I am satisfied with the outcome of my studies, although the public defines of the thesis has not yet taken place.

Firstly, I would like to express my gratitude to my supervisor Associated Professor Ivar Talvik. Paying tribute to the tradition of writing the acknowledgement section, I have to state the obvious – this work would have never been possible without Ivar's guidance. I would like to add possibly the less obvious – the quality of this work is a result of Ivar's ability to motivate for improvement, his principle of avoiding tokenism and not targeting the minimum requirements. I am fully aware of the risk of explicitly assuming that my thesis is of some quality, but I am being honest and I believe that it is not in contradiction with the concept of writing the acknowledgements section. In case the reader finds this judgement unacceptable, please refer to the first two sentences of this section. In case the reader rates this thesis as being of poor quality, I apologize to Ivar of exposing him to the risk without his consent. I have enjoyed working with Ivar and discussing aspects of different problems dedicated not only to the limited scope of the research.

I would like to thank the staff of School of Engineering of the Department of Civil Engineering and Architecture for being supportive for an abnormally long period of time. I would also like to express my appreciation to the Tallinn University of Technology. The total 19 years that I have spent in TUT/TalTech made it possible for me to see and realize tremendous positive changes that have taken place.

I would like to thank Dr David Lange from The University of Queensland for constructive criticism and valuable comments on the present work.

My sincere thanks go to the official opponents of the work, Professor František Wald from Check Technical University and Professor Mikko Malaska Tampere University of Technology.

I would like to thank all my colleagues from Gravity OÜ, Nordecon Betoon OÜ and Mait Rõõmusaar personally for the sincere support in many aspects of life not limited by the professional interaction.

I would like to thank Professor Mario Fontana from ETHZ and IABSE foundation for supporting my work in the beginning of my PhD studies.

I would like to thank my parents and closest relatives. Unfortunately my farther will not see the end of my PhD studies. He would definitely be proud of me for achieving this long term goal, but I still feel that on a very basic level his attitude to me was invariant to my achievements and mistakes.

The last in sequence, but second in the level of gratitude I would like to thank my wife Regina, my daughter Valerija, sons Timur and David. Thank you all for both direct and unconscious support. You are the meaning of my life.

Abstract

Stability of Compressed Steel Elements in Fire Conditions: a Probabilistic Approach

Considerable effort of the ongoing research in structural engineering is dedicated to fire conditions. Properties of steel deteriorate in fire temperatures leading to resistance reduction of elements. The purpose of structural design is to provide certain level of safety accounting for inherent uncertainties of structural system and actions. Integrity of columns in a structural framework is vital considering progressive collapse of a building. The principal aim of this work is to study the effect of temperature distribution on the probabilistic response of a steel column in fire conditions and propose a user friendly method for estimating the failure probability. The case of axial compression is used to demonstrate the methodology, which can be adopted for other resistance problems of structural steel in fire. According to common approach reliability analysis of structures in fire is usually performed for a limited number of thermal configurations, which is explained by the computational challenges associated with the mechanical response of structures at elevated temperatures. The proposed method enables explicitly estimate the failure probability without tedious calculation cycles and achieve better consistency with the established safety targets compared to the standard procedure.

The first part of this work is dedicated to the mechanical model of buckling of steel column in fire conditions. Non-linear FEM procedure was composed for the analysis of the problem. Effects of aspects like finite element types, meshing, initial shape, loading history and axial restraint on the model behaviour were investigated. Different material models were studied and the effect of residual stresses was estimated. FEM models were validated against the test data from references. On the basis of an extended numerical study, an original analytical procedure was proposed for calculating the buckling resistance. Computational efficiency of the method was used for the following resource demanding reliability calculations.

Reliability analysis of axially compressed steel columns in fire has been performed in the second part of the work applying Monte-Carlo simulations with uncertainties of the stochastic variables taken into account. Statistical variation data of material properties, element geometry, loading and fire parameters have been obtained from available references. In the current research the computational costs of Monte-Carlo simulations of the column buckling were reduced by implementing the computationally efficient procedure developed in the first part of the work, excluding the need for applying optimization techniques to Monte Carlo simulation. Thermal simulations have been performed in a separate procedure and the obtained temperature distributions were used in the following reliability analysis. Sensitivity analysis has been performed to analyse the influence of the variability of individual parameters on the stochastic response of the output function. Extensive reliability analysis was performed for a large set of configurations, demonstrating the effect of the shape of temperature distribution on the distribution of the resistance function and consequently on the variability of failure probability.

Based on the results of the probabilistic analysis, a reliability based design method has been proposed for buckling of steel columns in fire. The method provides a convenient tool for evaluation of the safety level of a steel column in fire and for comparison of design alternatives. The proposed method was compared with the existing safety framework.

Lühikokkuvõte

Surutud teraselementide stabiilsus tulekahju olukorras: tõenäosuslik käsitus

Ehituslike konstruktsioonide uuringutest on tänapäeval suur osa seotud tulekahjuolukorraga. Teraselise elementide omadused temperatuuri tõusmisel muutuvad ning sellest tulenevalt elementide kandevõime väheneb. Konstruktiivse projekteerimise eesmärk on tagada teatud ohutuse tase arvestades karkassi süsteemi omaduste ja koormuste loomuliku määramatusega. Postide kui konstruktsioonisüsteemi elementide kandevõime on väga oluline ehitise progressiivse varingu vältimisel. Käesoleva töö põhieesmärk on uurida temperatuurijaotuste mõju terasposti stohhastilisele käitumisele tulekahju olukorras ja koostada kasutajasõbralik praktiline meetod purunemise tõenäosuse hindamiseks. Metoodika demonstreerimiseks käsitletakse tsentriliselt surutud posti. Meetodit saab laiendada teiste teraskonstruktsioonide kandevõime hindamiseks tulekahju olukorras. Üldlevinud lähenemisviisi kohaselt tehakse stohhastiline analüüs tulekahjuolukorras piiratud arvu konfiguratsioonide jaoks, kuna vajalik arvutuste maht on väga suur. Töös esitatud meetod võimaldab praktilistes ülesannetes määrata purunemise tõenäosus ilma suure hulga arvutustsükkliteta ja saavutada kehtestatud ohutuspiiridega parem kooskõla kui võimaldavad olemasolevad standardikohased protseduurid.

Töö esimeses osas käsitletakse terasposti nõtkekandevõimet tulekahju olukorras. Probleemi lahendamiseks on koostatud mittelineaarne lõplike elementide meetodil põhinev protseduur. Uuritakse erinevaid modelleerimise aspekte, nagu lõplike elementide tüüp ja võrgu tihedus, algkoormus, koormamise ajalugu ja tulekaitse materjalide mõju. Uuritakse ka erinevaid materjalimudeleid ja jääkpingete mõju. Lõplike elementide mudeleid on valideeritud kirjandusest saadud katseandmetega. Mahuka numbrilise analüüsi põhjal on koostatud arvutusmeetod nõtkekandevõime määramiseks. Pakutud meetodi arvutuslikku tõhusust on kasutatud järgnevas töös osas ressursinõudlikes stohhastilistes arvutustes.

Töö teises osas käsitletakse terasposti stohhastilist analüüsi tulekahju olukorras Monte-Carlo simulatsioonide abil muutujate statistilist määramatust arvestades. Materjalide omaduste, elementide geomeetria, koormus- ja tuleparameetrite statistilise varieeruvuse andmed on saadud olemasolevatest allikatest. Käesolevas uurimistöös muudeti Monte-Carlo simulatsioonide ressursivajadust tavapärasest säästlikumaks, rakendades töös esimeses osas välja töötatud arvutuslikult efektiivset protseduuri, mille tõttu ei olnud vaja rakendada Monte-Carlo simulatsiooni optimeerimise meetodeid. Termilised simulatsioonid on teostatud eraldi protseduuris ja saadud temperatuurijaotusi kasutati järgnevas konstruktsioonelemendi stohhastilises analüüsis. Tundlikkuse analüüs tehti üksikute parameetrite varieeruvuse mõju hindamiseks väljundfunktsiooni stohhastilisele käitumisele. Ulatuslik töökindlusanalüüs viidi läbi suure hulga konfiguratsioonide jaoks, mis näitas temperatuuri jaotuskuju mõju vastupanufunktsiooni jaotusele ja sellest tulenevalt varingu tõenäosuse varieeruvusele.

Stohhastilise analüüsi tulemuste põhjal on välja pakutud arvutusmeetod praktikas kasutamiseks. Meetod pakub lihtsat vahendit terasposti ohutustaseme hindamiseks tulekahju olukorras ja alternatiivsete lahenduste võrdlemiseks konstruktsiooni-projekti. Pakutud meetodit on võrreldatud olemasoleva ohutusraamistikuga.

Curriculum vitae

Personal data

Name: Andrei Kervalishvili
Date of birth: 22.12.1981
Place of birth: Tallinn, Estonia
Citizenship: Estonian

Contact data

E-mail: kervalisvili.andrei@gmail.com

Education

2006 – ... TUT – PhD
2004 – 2006 TUT – MSC
2000 – 2004 TUT – BSC
1988 – 2000 Secondary Education

Language competence

English: Fluent
Estonian: Fluent
Russian: Native

Professional employment

2006 – ... Nordecon Betoone OÜ, structural designer
2003 – 2006 Neoprojekt OÜ, structural designer

Elulookirjeldus

Isikuandmed

Nimi: Andrei Kervališvili
Sünniaeg: 22.12.1981
Sünnikoht: Tallinn
Kodakondsus: Eesti

Kontaktandmed

E-post: kervalisvili.andrei@gmail.com

Hariduskäik

2006 – ... Tallinna Tehnikaülikool – PhD
2004 – 2006 Tallinna Tehnikaülikool – MSC
2000 – 2004 Tallinna Tehnikaülikool – BSC
1988 – 2000 Keskkharidus

Keelteoskus

Inglise keel: Kõrgtase
Eesti keel: Kõrgtase
Vene keel: Emakeel

Teenistuskäik

2006 – ... Nordecon Betooni OÜ, ehituskonstrutsioonide projekteerija
2003 – 2006 Neoprojekt OÜ, ehituskonstrutsioonide projekteerija

